Durability of Macromolecular Materials

In Durability of Macromolecular Materials; Eby, R.;
ACS Symposium Series; American Chemical Society: Washington, DC, 1979.

Durability of Macromolecular Materials

R. K. Eby, EDITOR
National Bureau of Standards

Based on a symposium sponsored by the ACS Macromolecular Secretariat, the Society of Plastics Engineers, and the American Physical Society at the 176th Meeting of the American Chemical Society, Miami, Florida, September 11–14, 1978.

ACS SYMPOSIUM SERIES 95

AMERICAN CHEMICAL SOCIETY
WASHINGTON, D. C. 1979

Library of Congress CIP Data

Durability of macromolecular materials.
(ACS symposium series; 95 ISSN 0097-6156)

Includes bibliographies and index.

1. Polymers and polymerization—Deterioration—Congresses.
I. Eby, Ronald Kraft, 1929- . II. American Chemical Society. Macromolecular Secretariat. III. Series: American Chemical Society. ACS symposium series; 95.

TA455.P58D87 620.1'92 78-31777
ISBN 0-8412-0485-3 ASCMC8 95 1–476 1979

PRINTED IN THE UNITED STATES OF AMERICA

ACS Symposium Series

Robert F. Gould, *Editor*

In Durability of Macromolecular Materials; Eby, R.;
ACS Symposium Series; American Chemical Society: Washington, DC, 1979.

FOREWORD

The ACS SYMPOSIUM SERIES was founded in 1974 to provide a medium for publishing symposia quickly in book form. The format of the Series parallels that of the continuing ADVANCES IN CHEMISTRY SERIES except that in order to save time the papers are not typeset but are reproduced as they are submitted by the authors in camera-ready form. Papers are reviewed under the supervision of the Editors with the assistance of the Series Advisory Board and are selected to maintain the integrity of the symposia; however, verbatim reproductions of previously published papers are not accepted. Both reviews and reports of research are acceptable since symposia may embrace both types of presentation.

In Durability of Macromolecular Materials; Eby, R.;
ACS Symposium Series; American Chemical Society: Washington, DC, 1979.

PREFACE

Our field is a remarkable one. Seventy years ago Baekeland made the first commercial synthetic polymer by combining small molecules. Since then these polymers have left little of our culture and technology untouched. The increase in output of the strongly innovative and productive U.S. industry has been impressive, with a compound growth rate of approximately 11 percent between 1951 and 1977. In 1977 production was more than 22 teragrams, corresponding to tens of billions of dollars worth of commerce, hundreds of thousands of jobs, and a favorable balance of trade of approximately two billion dollars.

Synthetic polymers, which represent an outstanding intellectual achievement, serve an overwhelming number of man's needs. They compete in increasingly sophisticated and demanding applications with metals, ceramics, and other materials. In many applications the lifetime under service conditions is critical for reasons of safety, health, security, and protection of capital investment. The list of such critical applications is very long and growing rapidly. High voltage underground power cables require a polyethylene dielectric which should not fail for many years. A most successful orthopaedic prosthesis, the artificial hip, uses polyethylene to replace the acetabular cup. Plastic shipping containers such as 55 gallon drums are used in interstate commerce for hazardous materials. Dentists regularly use composite restoratives with a polymeric matrix that is polymerized in the tooth. Plastic food packaging, which has had a profound role in lowering the rate of spoilage, requires careful control of additive migration during the use life. Structural components of some aircraft are composites with a plastic matrix. Synthetic polymers are used increasingly in automobiles.

The need for fundamental and applied research on lifetime under service conditions is great. As a result, the subjects of dielectric breakdown, fatigue, wear, creep, fracture, oxidation, photodegradation, additive migration, etc., are increasingly important to the effective use of synthetic polymers. The development of a scientific basis for tests that predict accurately the useful service life is a primary need.

In view of the above, it seemed appropriate to select Chemical and Physical Lifetime Limits of Macromolecular Materials as the topic of the Symposium. This provided an opportunity to focus on the lifetime aspect

In Durability of Macromolecular Materials; Eby, R.;
ACS Symposium Series; American Chemical Society: Washington, DC, 1979.

of the problem and to present the results of work in various chemical and physical disciplines in a more unified context. The results of this choice were gratifying. Four divisions of the Macromolecular Secretariat were joined by the Rubber Division of the American Chemical Society, the Division of High Polymer Physics of the American Physical Society, and the Engineering Properties and Structures Division of the Society of Plastics Engineers in arranging and presenting sessions at the Symposium.

On behalf of the Macromolecular Secretariat I thank W. J. MacKnight, S. L. Aggarwal, D. H. Reneker, S. S. Labana, J. M. Dealy, L. E. Smith, and V. T. Stannett who arranged the sessions of the Symposium.

National Bureau of Standards
Washington, D.C.
December 8, 1978

R. K. EBY

In Durability of Macromolecular Materials; Eby, R.;
ACS Symposium Series; American Chemical Society: Washington, DC, 1979.

1

Materials Failure and Materials Research Policy

JOHN D. HOFFMAN

National Measurement Laboratory, National Bureau of Standards,
Washington, DC 20234

The topic of the chemical and physical lifetime limits of macromolecular materials is receiving increased attention throughout that part of the scientific and technical community interested in the effective utilization of materials. This paper outlines some of the trends and scientific challenges in materials utilization that relate to the durability of materials and points out the role of basic materials science in contributing to an effective understanding of materials durability and lifetime prediction. In addition, several topics related to materials research policy are addressed.

Materials are extremely important to our economy. Their utilization is captured in the simplified diagram of the materials cycle in Figure 1. Apart from the service and food sectors, the rest of our economy is primarily concerned with obtaining raw materials, processing them into usable form, transporting them, manufacturing products with them, distributing, and maintaining these products in service, and disposing or recycling discarded products. At every one of these stages, materials science and technology helps determine performance and strongly affects costs. The discussion which follows excludes those parts of the materials cycle that deal with raw materials and with recycling and disposal. These are extremely important areas of concern and merit discussion another time.

There are a number of important trends in materials utilization that bear upon the problems addressed in this symposium. Among these are the use of alternate raw materials, lower energy usage in processing and manufacturing, the stimulation of productivity increases, the use of extreme operating conditions, operation close to design limits, the increasing complexity of engineering materials, and the concerns with health, safety and the environment. Each of these trends places increased performance demands on materials. Each presents a host of scientific challenges that are exciting and demanding. Industry, universities, and government, both individually and in cooperative programs, are addressing these challenges.

In Durability of Macromolecular Materials; Eby, R.;
ACS Symposium Series; American Chemical Society: Washington, DC, 1979.

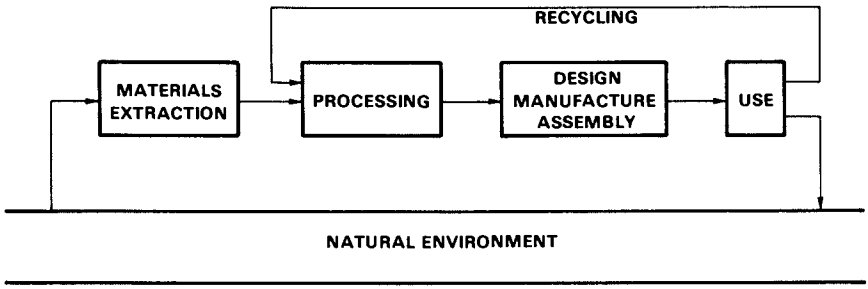

Figure 1. Simplified diagram of the materials cycle. Trends in materials use throughout the cycle place increased performance demands on materials.

In Durability of Macromolecular Materials; Eby, R.;
ACS Symposium Series; American Chemical Society: Washington, DC, 1979.

At the National Bureau of Standards (NBS) these trends are used to help structure research planning in materials science and to directly relate NBS work in processing science, structure/property science, and materials durability science to the materials cycle. The primary focus of this work is measurement and standards because the National Bureau of Standards is charged with providing the National System of Measurement. It is also charged with conducting materials research leading to improved measurements, standards and data about materials needed by industry, commerce, educational institutions and government. Associated with the work in materials science is an important program in nondestructive measurement and evaluation. This program was formally initiated at NBS in 1975 and has grown steadily since then.

The trends indicate, in general, what should be done. They do not specify what can be done. Thus, one has to ask "What are the scientific and technical challenges and what are the practical opportunities?" Let us look specifically at the challenges facing us in materials durability science. Whether we talk about fracture, wear, corrosion, or additive migration in polymers, we are talking about a change in materials properties in service. These changes are a time response to the chemical and physical environment to which the material is subjected in service. This response in turn is a function of the structure and properties of the material. The challenge we all face is to find the specific forms of this function as they relate to particular materials durability problems, and in turn to use this understanding in lifetime prediction.

The economic and social consequences of inadequate lifetime predictions are well documented. It would be reassuring if every kind of material sample or product could be tested to determine expected lifetime under all possible service conditions, but the time and resources required to do so usually makes this approach impractical. Therefore, the results of short-term measurements and tests must be incorporated into most lifetime prediction schemes.

The need for improved prediction capabilities is addressed by (1) investigating the relationship between present properties of a material, the history of these properties, and the future performance of the material; by (2) developing short-term measurement and test methods to forecast the long-term performance of materials, and by (3) constructing basic models for predicting lifetime performance of materials.

The first effort is necessary to gain an understanding of the long-term effects of subcritical failures that occur on a microscopic scale when a material is stressed in a cyclic fashion during use or in proof testing itself. This understanding is necessary in predicting the consequences of conditions as varied as the daily temperature extremes to which a plastic container is subjected as it sits on a loading dock or the variety of stresses

In Durability of Macromolecular Materials; Eby, R.;
ACS Symposium Series; American Chemical Society: Washington, DC, 1979.

placed on artificial hip joints in daily use. The second kind of endeavor is motivated by the need to establish the essential accuracy and reliability in short-term testing that are required if we are to effect a real economy in life tests. The third effort is especially interesting in that it holds even greater promise of economy if predictive physical models can be developed that will furnish the basis of calculating the lifetime performance of a material in a given class of materials without having to measure or test more than a few representative materials in that class.

In all of these efforts to achieve greater predictive capability, the understanding of basic material science is a primary source of innovation. Some aspects of an overall approach to the materials durability/lifetime prediction problem are illustrated in the following examples of on-going research. These happened to be at NBS, but they are typical of work in other laboratories.

In recent years, industry has incorporated a number of developments with regard to plastic containers. Sturdy, chemically resistant, industrial containers in a wide range of styles and sizes are being fabricated. The materials being used have improved impact resistance, stress-crack resistance, and barrier performance. Furthermore, lighter weight plastic containers can offer significant economies in shipping. Thus, plastic containers once regarded as useful only for situations in which metal or glass containers did not provide adequate protection, are being used to satisfy more routine shipping requirements.

New materials placed in new service conditions always raise the question of lifetime performance. In this case, permeation performance, stress-crack resistance, and long-term mechanical integrity are particularly relevant in situations where the plastic containers are expected to be reused. In the case where hazardous materials are transported in plastic containers, regulatory decisions (including the ruling on requests for exemptions) on these containers may be facilitated by using data on the material properties of the polymer.

NBS has been assisting the Office of Hazardous Materials Operation by obtaining and evaluating critical data on these materials as input in formulating performance-oriented specifications. Some of these studies focus on the mechanical and stress-cracking properties of high-molecular-weight polyethylene, initially in uniaxial experiments, and most recently, under biaxial stress conditions. This work addresses the two failure mechanisms represented in Figure 2 which is a generalized plot of time-to-fail versus applied stress for polyethylene. In Region I, where low stresses are applied, crack growth controls the time-to-failure, and in Region II, the high stress region, the visco-elastic nature of the polymer leads to instabilities and failure.

Traditionally, failure tests are made at elevated tempera-

In Durability of Macromolecular Materials; Eby, R.;
ACS Symposium Series; American Chemical Society: Washington, DC, 1979.

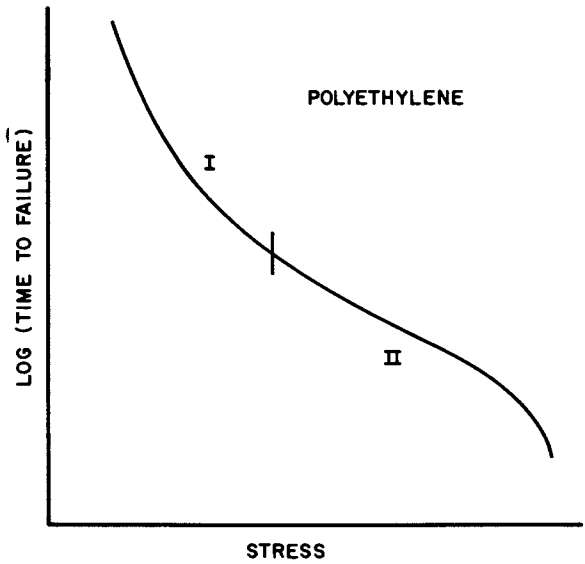

Figure 2. Generalized plot of time-to-fail vs. applied stress for polyethylene. Lifetime prediction is complicated if the two failure mechanisms (Regions I and II) have different activation energies.

In Durability of Macromolecular Materials; Eby, R.;
ACS Symposium Series; American Chemical Society: Washington, DC, 1979.

ture in order to accelerate failure. Time-to-failure under service conditions is then predicted by a superposition of the high temperature results onto the service curve. Our recent results from experiments in uniaxial extension suggest that in some cases no simple time-temperature superposition of the high temperature accelerated test data with operating temperature conditions is possible because the activation energies for the different mechanisms are not the same. Thus, a fundamental understanding of both of these modes of failure is necessary to better estimate the long-term behavior of polymers in service. It should be pointed out that under service conditions materials naturally experience biaxial deformations. Work is currently underway in our laboratory employing a variety of different biaxial stress histories.

Other somewhat parallel cases can be cited to expand the argument that basic science is needed. For example, stress-corrosion is a common mode of failure in ceramics and metals, as well as polymers. The mechanisms are different yet the need for basic understanding is essential in developing practical, reliable predictive measurements and tests.

For ceramics and glasses, an understanding of the mechanisms of subcritical crack growth is necessary for assuring the long-term reliability of these materials in structural applications. The reason that subcritical crack growth is so important for ceramic materials is that they are brittle. The only mechanism of failure for these materials is brittle fracture and associated subcritical crack growth caused by stress corrosion reactions. Studies at the National Bureau of Standards and in other laboratories have shown that crack growth in these materials can be rather complex.

The velocity of crack growth depends on both the environment and the driving force for fracture. At least three mechanisms of fracture have been identified in the case of soda-lime-silicate glass in nitrogen gas environments that contain a small amount of water. At low values of the stress intensity factor, the rate of crack growth is attributed to the rate of the stress enhanced chemical reaction between the water and the glass. At intermediate stress intensities, the reactions between the glass and water continue, but the rate of growth is determined by the rate of transport of water to the crack tip. At larger stress intensities, the rate of crack growth is controlled by the chemical composition and structure of the glass. Temperature and pH have also been shown to affect crack velocities.

Data from crack velocity experiments are used to improve the reliability of ceramic materials. It is particularly useful for the application of proof-testing to structural ceramics, because it leads to an estimate of lifetime under load after the proof test has been used to weed out mechanically defective components. For this purpose, the data in the low crack growth velocity range are of prime importance, because it is, by and large, slow

In Durability of Macromolecular Materials; Eby, R.;
ACS Symposium Series; American Chemical Society: Washington, DC, 1979.

crack growth behavior that determines long-term mechanical behavior of ceramics in structural applications.

Using crack data from the low velocity regime for a given set of service conditions, design diagrams based on proof testing, such as Figure 3, can be constructed. The vertical axis gives the minimum time to the failure while the horizontal axis gives the applied structural load. Each curve represents a different ratio of the proof test load to the service load, so that for a required engineering application (which would characterize the failure-time under stress) the proof test level can be determined. Industry is applying these concepts to assure service life in such areas as glass fibers used for optical communication.

The main point to be emphasized here is that the feasibility of these approaches in assuring the reliability of ceramic materials depends on basic crack growth or strength data that characterize failure mechanisms in these materials. Without these basic data, these techniques of lifetime assurance could not be usefully employed on ceramic materials.

Non-destructive evaluation techniques coupled with predictive models are becoming more important in developing materials performance codes and standards, including those for metals. For example, in 1976, Alyeska Pipeline Service Company requested waivers from the Department of Transportation (DOT) for a number of buried girth welds. The welds contained radiographically detected defects somewhat larger than permitted by DOT regulation. The waiver was based upon a fracture mechanics analysis.

In anticipation of the waiver, DOT requested assistance from NBS in evaluating the fracture mechanics analysis and the non-destructive evaluation methods used to detect and determine the dimensions of specific weld defects. The model used in the waiver request by Alyeska was actually more conservative than others that were generated in the evaluation by NBS scientists.

DOT did eventually conclude that under some circumstances exemptions from existing standards could be granted using fracture mechanics as a basis for the exemption. Thus, more petitions for exemptions can be anticipated. NBS is working with DOT now to establish an even more solid technical framework for ruling on these waiver requests - a framework which need not employ judgment factors unnecessarily nor lead to an overly conservative design approach.

Typical commercial plastics contain a number of low molecular weight additives that develop or maintain particular properties in the plastic. The migration and loss of additives used to prolong the useful life of plastics is a major mode of failure. The migration of these components also raises the possibility of harmful contamination of food by plastic packaging.

Federal responsibility for public safety in this regard lies with the Food and Drug Administration. FDA regulations are

In Durability of Macromolecular Materials; Eby, R.;
ACS Symposium Series; American Chemical Society: Washington, DC, 1979.

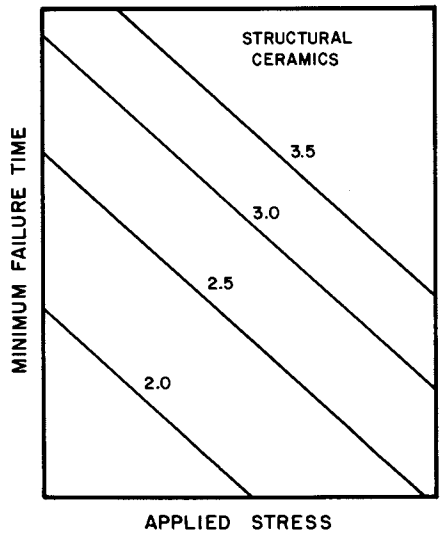

Figure 3. Generalized design diagram used for structural ceramics showing minimum failure time vs. applied structural load. Each curve represents a different ratio of the proof test load to the service load.

In Durability of Macromolecular Materials; Eby, R.;
ACS Symposium Series; American Chemical Society: Washington, DC, 1979.

presently administered on a case-by-case basis. It is an empirical approach which may have been adequate to cope with a small number of materials a few years ago. But today, government, industry and consumer groups alike realize that packaging regulations must be streamlined. NBS will develop the physical models of migration that can be used by FDA in planned revisions of packaging regulations to organize and classify materials on the basis of their migration behavior.

To model migration of minor constituents from a polymeric film to a food-simulating solvent requires knowledge of (1) the equilibrium distribution of a migrant between polymer and solvent phases, i.e., the distribution or partition coefficient (K) and (2) the diffusion coefficient (D) of the migrant in the polymer. This is the minimum amount of information required to describe a polymer/migrant/solvent system. For a polymer at a temperature above its glass transition temperature, knowledge of K and D allows one to calculate migration as a function of time and as a function of temperature if the temperature variation of K and D are also known. Advances made in the last decade in equation-of-state theories for polymer and non-polymer solutions provide a real technical opportunity in developing the general physical models needed to describe this migration.

All of the examples cited above touch upon one portion of the materials picture: materials research and the basic understanding of materials failure. Furthermore, these examples touch upon only one aspect of the national research picture: the role of the Federal Government in materials research. In each case, the understanding developed can be used not only to address a national concern but also to provide the private sector with useful information for product development, productivity increase, and innovation.

It should be recognized that there is a growing national interest in materials problems and materials policy, including materials research policy. For example, the Henniker Conferences, a series of biennial materials policy conferences was started in 1970. At the initial conference, representatives from the private sector and government met (as the conference organizers stated) to " explore the need for a continuing national mechanism in the goverment to recommend, determine, and, as necessary, coordinate policy in the spectrum of issues involving materials." Subsequent conferences have addressed specific issues in the arena of materials policy. The proceedings from these are published, providing insight into both private sector and government roles in the development and internal analysis of materials research policy.

There have been a number of commissions which have addressed some portion of the materials problem. For example, the Paley Commission issued its report, "Resources for Freedom," in 1952. The National Commission on Materials Policy addressed materials needs in the environment in 1973. Most recently, the National

In Durability of Macromolecular Materials; Eby, R.;
ACS Symposium Series; American Chemical Society: Washington, DC, 1979.

Commission on Supplies & Shortages issued its report, "Government and the Nation's Resources." The National Academy of Sciences has issued several reports on materials policy issues. Two important and recent reports are the COSMAT report (of the Committee on the Survey of Materials Science and Engineering) and the COMRATE report (of the Committee on Mineral Resources and the Environment).

The President has asked for a nonfuel minerals policy study in which some materials related issues are being reviewed. A final report is due in the fall of 1979. In addition, there is a growing Congressional interest in a comprehensive National Materials Policy. In 1978, two bills were introduced before the House of Representatives dealing with this. The first bill, HR 10859 - A National Materials Policy, Research and Orgnaization Act of 1978, emphasized the role of basic and applied research in materials science as a central part of a materials policy.

One important feature in recent discussions, thinking, and planning, concerning materials is the recognition of the whole materials cycle. Another characteristic is that most recent discussions emphasize the need to consider materials, energy, and the environment together. Since materials utilization impinges upon a number of national concerns it will certainly receive more attention in the future. Today's processing, design, manufacture, service, maintenance and recycling all depend upon the existing body of materials science and engineering. Tomorrow's sequence of processing through recycling will derive from advances in materials science and engineering coupled with successful product innovation.

One major challenge to industry, academia, and the government is to develop the scientific and technological framework needed for improving the durability of materials. The Scientific aspects of this challenge are addressed in this symposium. The papers which follow underscore the role of basic science in addressing this challenge. The Macromolecular Secretariat, F. E. Bailey, and Ron Eby are to be strongly commended for focusing attention on the problems of materials durability.

RECEIVED December 8, 1978.

2

Physical Factors in Polymer Degradation and Stabilization

F. H. WINSLOW

Bell Laboratories, Murray Hill, NJ 07974

As a rule polymers that contain hydrogen are vulnerable to oxidative degradation at elevated temperatures and during outdoor exposure. A few also fail in ozone and most natural polymers are susceptible to moisture and microorganisms as well. In order to prevent these and other forms of deterioration, nearly all polymers must be protected during processing, and especially during weathering.

Chemical breakdown usually involves oxidative chain reactions that cause embrittlement of semicrystalline polymers and discoloration of poly(vinyl chloride) and polymers with aromatic groups. The reactions are complicated by the presence of transient intermediates and by rates that depend on minute concentrations of molecular defects, impurities and additives. They also depend on several important physical factors outlined in this brief overview of polyolefin degradation. Two of these factors, the transfer of excitation energy and the transport of products and protectants, play a major role in stabilization processes.

Morphology and Reactivity

Early studies of cellulose degradation revealed for the first time that hydrolytic agents selectively attacked the amorphous fraction (1) of the polymer, breaking and reordering accessible chain segments (2). Later work on both poly(ethylene terephthalate) (3,4) and polyethylene (5) confirmed that localized reactions were characteristic of all polymers with impervious crystalline regions.

Oxidative chain scission processes in polyethylene have been described in detail (6). During the course of exhaustive oxidation, the reaction rate subsides as accessible

0-8412-0485-3/79/47-095-011$05.00/0

In Durability of Macromolecular Materials; Eby, R.;
ACS Symposium Series; American Chemical Society: Washington, DC, 1979.

chains are consumed. As might be expected, ultimate oxygen uptake increases in polyethylene as unstable crystallites melt with rising temperature, as shown in Fig. 1. A smaller temperature dependence of cumulative oxygen uptake is observed in rubbers and other polymers fully accessible to oxygen.

The consumption of oxygen also varies with morphology at a given reaction temperature. During prolonged degradation at 100°C, the solution - crystallized polyethylene powder in Fig. 2 reacted with only half as much oxygen as the molded film. Viscosity and gel permeation chromatographic measurements demonstrated that 90% of the chain scissions occurred during an initial oxygen uptake of 10 ml/g. Yet, the $\bar{M}_w$ of the fully oxidized powder was still 20% of the original value (6) and chain fragments with lengths equal to or double the lamellar thickness accounted for less than 10% by weight of the degraded polymer. The results correspond closely to those reported by Peterlin (7) on single crystals of linear polyethylene etched with nitric acid. He concluded that the lamellae had amorphous surface layers. But unlike oxidation in solution, the gaseous reaction forms nonvolatile products which accumulate to form a protective layer over the lamellar surface leaving at least 90% of the chain folds intact.

Evidently the crystallites in poly (4-methylpent-1-ene) are permeable to oxygen. The crystalline and amorphous forms of the polymer have nearly the same densities and oxidation patterns at 100°C (see Fig. 2) and consume tenfold more oxygen than the linear polyethylene.

The ultrahigh molecular weight linear polyethylene in Figs. 3 and 4 has a large weight fraction of tie chains linking adjacent lamellae. When the tie chains break during oxidation the dangling segments realign into denser structures largely inaccessible to oxygen. Though their initial densities and melting points were comparable, the linear polymer in Fig. 3 ultimately reacted with one fifth as much oxygen as the branched sample. The abrupt initial rise in the density of the linear polymer in Fig. 4 resulted more from reordering of tie chains than from an increase in oxygen content. The accessible fraction, remaining after reordering was complete, was tenfold greater in the branched polymer than in the linear polymer.

Oxidation raised the yield stress, increased elongation and reduced the stress at break. Figure 5 shows that the linear polyethylene was brittle at room temperature after an

In Durability of Macromolecular Materials; Eby, R.;
ACS Symposium Series; American Chemical Society: Washington, DC, 1979.

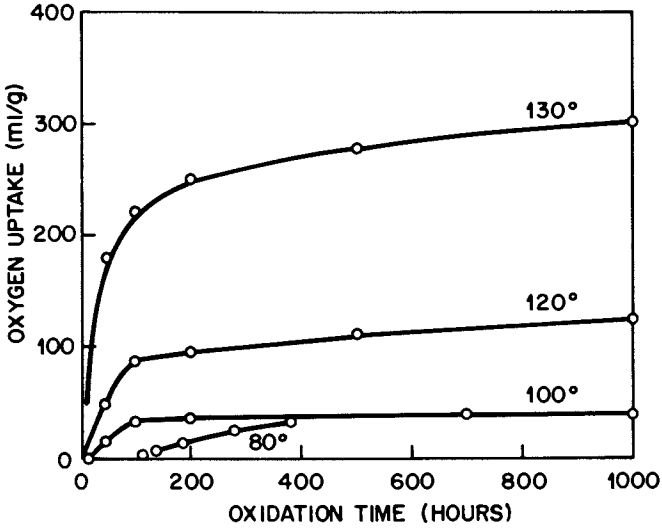

Figure 1. Oxygen consumption by linear polyethylene ($\overline{M}_w > 10^6$) during prolonged reaction at various temperatures

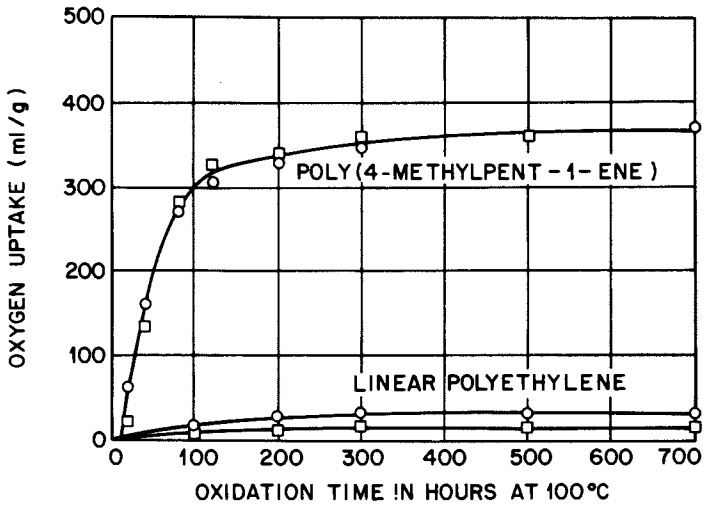

Figure 2. Exhaustive oxidation of molded (○) and solution-crystallized (□) linear polyethylene and poly(4-methylpent-1-ene)

In Durability of Macromolecular Materials; Eby, R.;
ACS Symposium Series; American Chemical Society: Washington, DC, 1979.

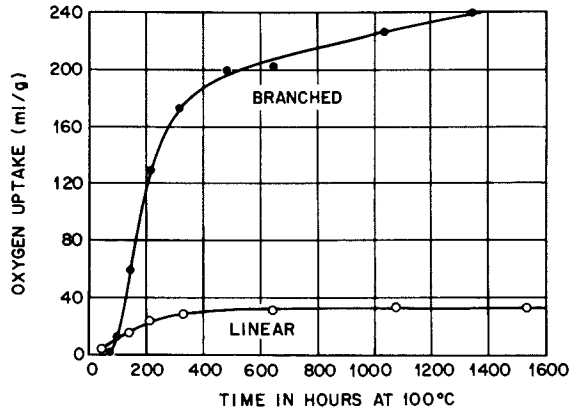

Figure 3. Oxidation patterns of molded linear polyethylene ($\overline{M} > 10^6$) and an ethylene–butene block copolymer

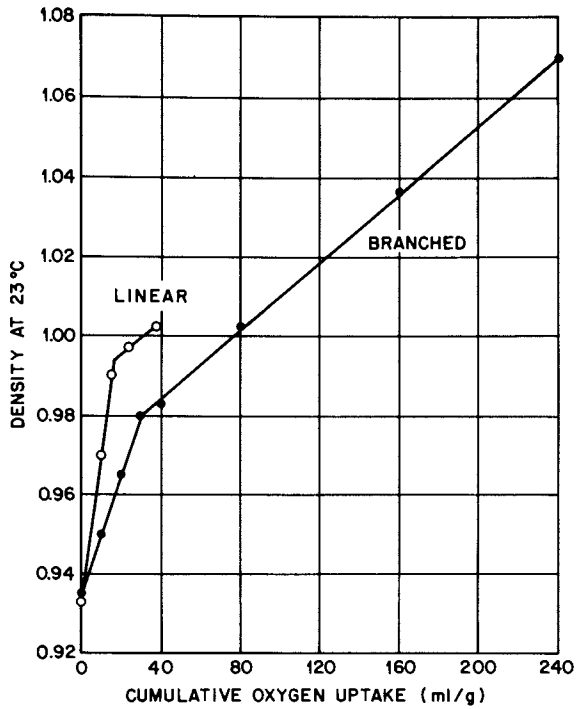

Figure 4. Rise in density with oxygen uptake of the polymers in Figure 3

In Durability of Macromolecular Materials; Eby, R.;
ACS Symposium Series; American Chemical Society: Washington, DC, 1979.

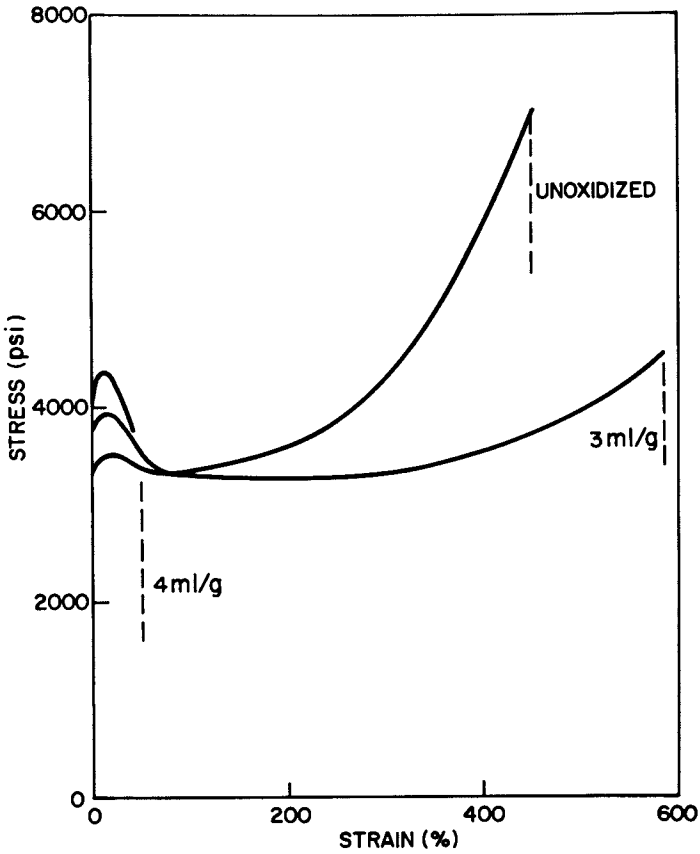

Figure 5. Stress–strain behavior of the linear polyethylene in Figure 3. The yield stress increases with oxidation.

In Durability of Macromolecular Materials; Eby, R.;
ACS Symposium Series; American Chemical Society: Washington, DC, 1979.

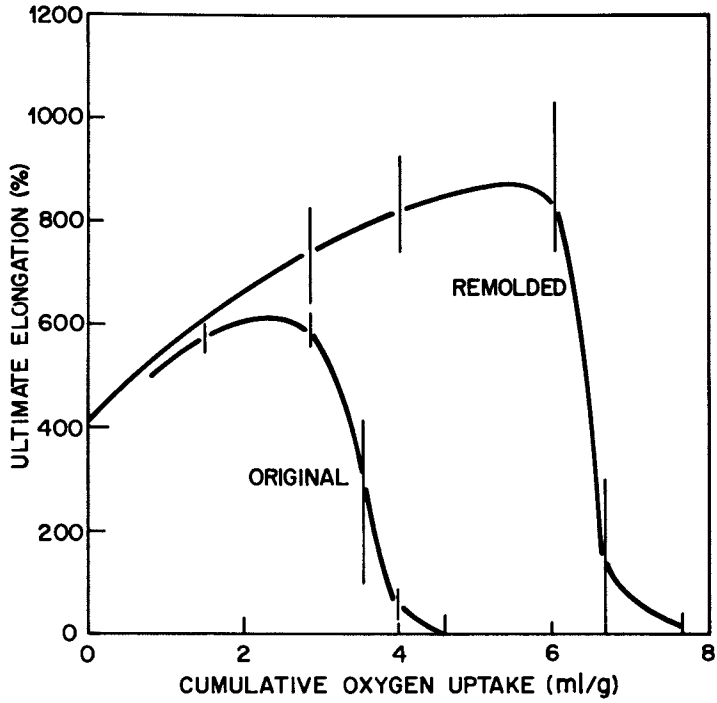

Figure 6. Variation in ultimate elongation with oxygen uptake by original and remolded films of the linear polyethylene in Figure 3. Draw rate was two in./min.

In Durability of Macromolecular Materials; Eby, R.;
ACS Symposium Series; American Chemical Society: Washington, DC, 1979.

oxygen uptake of about 4 ml/g. When the sample was melted and remolded the mechanical strength was restored as Kafavian (8) had reported earlier. In fact, the remolded specimen in Fig. 6 consumed an even greater volume of oxygen before becoming brittle once again. In the absence of any protection, brittle failure occurs after much less oxidation in linear polyethylene than in the branched polymer. Nevertheless, it has been reported (9) that stabilized linear polymers are more durable because they retain stabilizers better than branched types.

Antioxidant Activity and Mobility

For full protection against oxidation, polyolefins require a combination of radical chain terminators, peroxide decomposers and metal deactivators. Maximum effectiveness depends on retention, a prime problem with polyolefins in which volatile protectants are virtually insoluble. During cooling from the melt, the mobile stabilizers concentrate in amorphous regions where they are needed most. Unfortunately their solubility is usually so low that the more volatile compounds migrate rapidly out of the polymer and are lost. As a result superior antioxidants for long-term use generally have molecular weights higher than 500. Their volatility and diffusion rates are low but still sufficient for the stabilizer to readily reach reactive sites. It is also possible to incorporate stabilizing groups into a polymer chain but the resulting bound antioxidants are inherently more expensive and less effective.

Some carbon blacks and other pigments act as immobile antioxidants (10). The antioxidant action of carbon black varies inversely with particle size and directly with concentration, degree of dispersion, and quantity of bound oxygen or sulfur as indicated in Fig. 7. The sulfurized blacks are more effective, most likely because they form sulfur dioxide which is free to migrate through the polymer decomposing hydroperoxides. On the other hand, the oxidative chain reaction and its volatile products must move over an average distance of 20nm or more to reach the surface of an oxidized carbon black particle and be terminated. As a result the mobile aromatic amines and phenols are more efficient antioxidants than carbon blacks. But, unlike the volatile types, the immobile carbon blacks are more effective in solid than in molten polyethylene (see Fig. 6).

Carbon blacks interact synergistically with some antioxidants and antagonistically with others. The reduction in activity of aromatic amines as inhibitors in the

In Durability of Macromolecular Materials; Eby, R.;
ACS Symposium Series; American Chemical Society: Washington, DC, 1979.

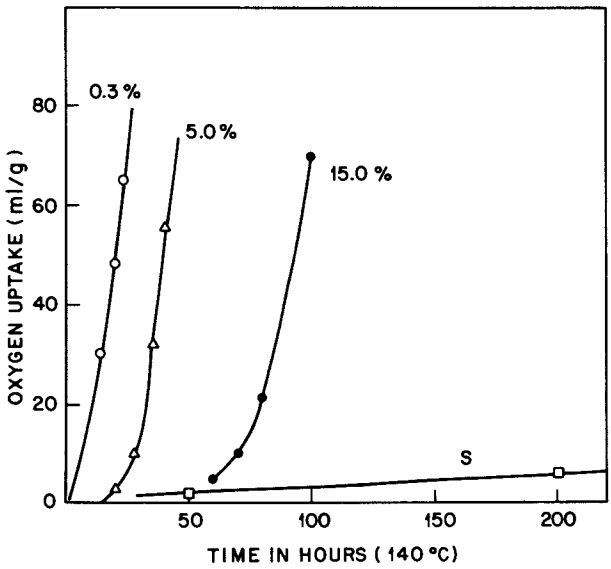

Figure 7. Stabilization of branched polyethylene by activated carbons (3 wt %) with an average particle size of 20 nm. Numbers indicate oxygen contents. S corresponds to a carbon black with a sulfur content of 9%.

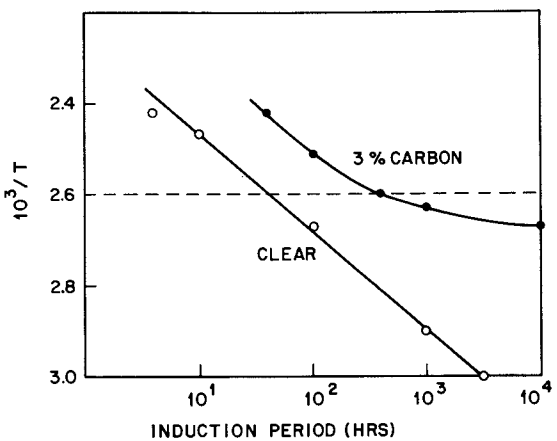

Figure 8. Relationship of morphology to the effectiveness of carbon black as a stabilizer for branched polyethylene: (– – –), indicates the melting temperature of the polymer. Effectiveness of molecular antioxidants does not depend on morphology.

In Durability of Macromolecular Materials; Eby, R.;
ACS Symposium Series; American Chemical Society: Washington, DC, 1979.

presence of carbon has been attributed both to induced decomposition of the amine (11) and to its adsorption and immobilization on the carbon surface (12). The adverse action of carbon black on most aromatic amines and phenols is illustrated in Fig. 9. Thiobisphenols are noteworthy exceptions since they form synergistic combinations with carbon which behave as radical scavengers and peroxide decomposers. Also, oxidized blacks greatly improve the retention of thiobisphenols in polyethylene (13) without impairing their activity as antioxidants.

Radiation Effects

During oxidative degradation, a concentration gradient always develops at a film surface. Inasmuch as the depth profile depends on permeabilities and reaction rates, the effect is more noticeable in photooxidations than in thermal oxidations. An unusually marked skin effect observed in photooxidized polypropylene has been ascribed (14) to the action of chromophores located at or near the surface.

Deterioration outdoors is initiated by ultraviolet radiation of wavelengths greater than 290nm. In addition to chemical structure and impurities, the reaction rate depends on temperature, ultraviolet energy and film thickness. It varies more than tenfold during the year, reaching a maximum about one month after the summer solstice in the northern temperate zone (6).

Since pure hydrocarbons only absorb at wavelengths well below 290nm, it has been suggested (15) that various contaminates and adventitious chromophores act as photosensitizers for polyethylene weathering. Yet, absorption by the polymer above 300nm is weak even after the extensive oxidation shown in Fig. 10. Chromophores such as carbonyl groups and hydroperoxides formed during processing or outdoor reactions with ozone are practically unavoidable. Besides functioning as initiators, the groups are responsible for two types of chain scission reactions (16) in polyethylene.

In Durability of Macromolecular Materials; Eby, R.;
ACS Symposium Series; American Chemical Society: Washington, DC, 1979.

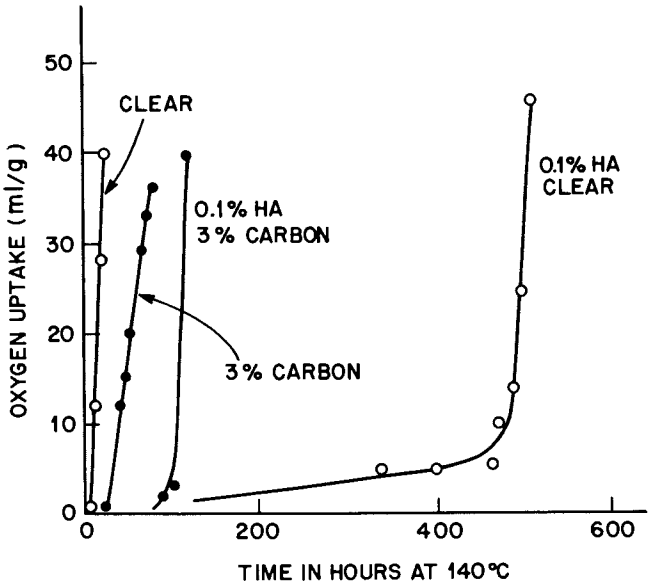

Figure 9. Reduction in effectiveness of N,N′*-diphenyl-*p*-phenylenediamine HA in the presence of carbon black*

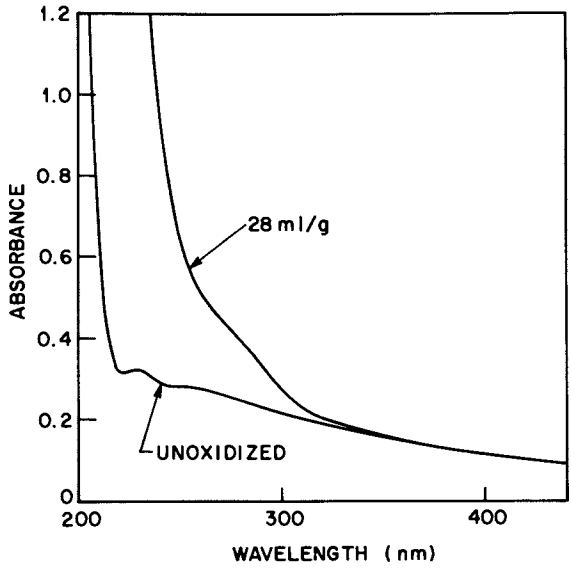

Figure 10. UV absorbance of polyethylene before and after photooxidation

In Durability of Macromolecular Materials; Eby, R.;
ACS Symposium Series; American Chemical Society: Washington, DC, 1979.

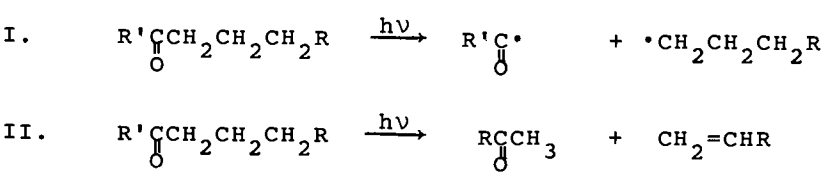

Mechanism II, which accounts for most of the chain scission, is essentially independent of temperature above -25°C. It was also postulated that singlet oxygen molecules formed by quenching of triplet carbonyl groups may play a role in the initiation of photooxidation. Once formed they would perhaps react with vinyl groups from reaction II, producing hydroperoxides which, in turn, would induce oxidative chain reactions. Recent evidence for (17) and against (18) the singlet oxygen mechanism has left its status in weathering processes still in doubt. The details of some photostabilization processes are also controversial.

Mechanisms of Photostabilization

There is ample energy in 290nm radiation to break most bonds in hydrocarbon polymers, but both the absorbance rates and quantum yields are low. Photoreactions begin with the electronic excitation of a molecule. The excited species, A*, may immediately emit its excess energy in the form of radiation

1. Excitation A -> A*
2. Emission A* -> A + light or heat
3. Degradation A* -> decomposition products
4. Deactivation A* + D -> A + D*

and return to the ground state, A, without undergoing degradation. However, if A* has a relatively long lifetime, it has a greater probability of either decomposing (process 3) or of transferring its excess energy to a deactivating molecule, D. Stabilization, of course, occurs when the rate of deactivation is faster than the degradation process.

Photostabilizers suppress the degradation rate by absorbing, quenching or screening out most of the damaging excitation energy. Surface coatings are seldom used for

In Durability of Macromolecular Materials; Eby, R.;
ACS Symposium Series; American Chemical Society: Washington, DC, 1979.

protecting polymers other than wood. Instead, fine dispersions of pigments such as carbon black are ordinarily preferred. The blacks are highly effective. Well-dispersed particles with an average size of 20nm in concentrations as low as 1% have prevented any significant change in the mechanical properties of a polyethylene exposed to weathering in Florida for nearly 50 years. The results in Fig 11 imply that carbon acts primarily as a light screen since the black film oxidized faster than the underlying polyethylene film containing no additive. However, the carbon black altered the course of oxidation in the polymer. After the same oxygen uptake the polymer containing carbon had fewer vinyl groups (i.e., had undergone less Type II chain scission) and a significantly higher hydroperoxide content. Also, the distribution of carbonyl products formed in the black polymer resembled that found in thermal oxidations (17). However, a thiobisphenol reduced the rate of hydroperoxide buildup in both clear and black films and in combination with carbon black showed synergistic behavior in inhibiting the photooxidation of polyethylene (17).

In contrast, the o-hydroxybenzophenone had no noticeable effect on the decomposition chemistry. Though it has been commonly referred to as an ultraviolet absorber, it actually behaves more like a deactivator since the screen film containing it had a lower oxidation rate in Fig. 11 than the underlying clear film devoid of additives. Absorption can hardly account for the protective action of the stabilizer in thin films which are almost completely transparent to 300nm radiation. Neither can the hydroxybenzophenone be an important terminator of radical chain reactions because it is much less effective than other hindered phenols in inhibiting oxidation in the dark.

Until recently the nickel dialkyldithiocarbamates and piperidene derivatives were regarded as deactivators of singlet oxygen and other excited species. But Scott (19) has reported that the nickel compound acts mainly as a light screen, radical chain terminator and peroxide decomposer while others (18) have noted that the piperidene derivatives, though not stabilizers themselves, convert to nitroxyl radicals that are antioxidants. Regular phenolic and aromatic amine antioxidants are inefficient photostabilizers (15). The amines darken rapidly and some phenols act as sensitizers. Synergism has be been observed with combinations of antioxidants and ultraviolet absorbers, though the effect is not as marked as that of the thiobisphenols in the presence of carbon black.

In Durability of Macromolecular Materials; Eby, R.;
ACS Symposium Series; American Chemical Society: Washington, DC, 1979.

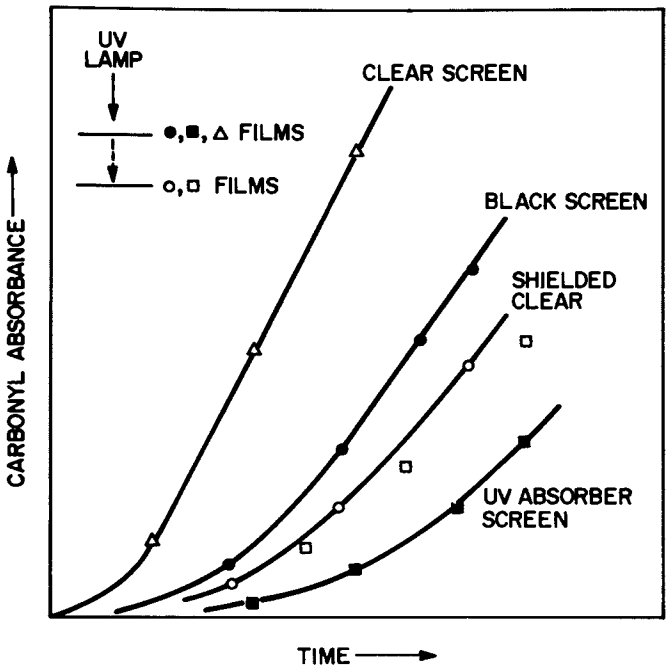

Figure 11. Photooxidation rate of branched polyethylene films containing 0.1% Neotex 150 carbon black (●) and 0.1% substituted o-hydroxybenzophenone (■). Also shown are the rates of unprotected films exposed to direct radiation (△), to radiation transmitted by the black screen (○), and by the film containing the UV absorber (□).

In Durability of Macromolecular Materials; Eby, R.;
ACS Symposium Series; American Chemical Society: Washington, DC, 1979.

TABLE 1

Relative Resistance of Rubbers to Ozone Cracking

High	Ethylene-propylene terpolymers
	Poly(2-chloro-1,3-butadiene)
Medium	Butyl rubber (∿1% isoprene)
	Hydrogenated polybutadiene
Low	Styrene-butadiene rubber
	Polyisoprene

In Durability of Macromolecular Materials; Eby, R.;
ACS Symposium Series; American Chemical Society: Washington, DC, 1979.

Many dyes and pigments such as titanium and zinc oxides function as photosensitizers forming singlet oxygen and hydrogen peroxide (20). However, a relatively large concentration (5-10%) of zinc oxide in combination with zinc dialkyldithiocarbamate is a highly effective protectant system for polyolefins exposed out-of-doors (21).

Ozone Cracking

Reactions of ozone with polyolefins at room temperature produce oxidized surface layers that act as physical barriers to further attack. The layers are too thin (<100nm thick) to affect mechanical properties but the products are capable of initiating thermal and photooxidations.

However, under special circumstances, the reaction with related polymers creates new surface more rapidly than it produces a protective layer. Polyisoprene represents a classic example. When ozone combines with vinylene groups on the polymer surface under a critical stress of >5%, the ozonized chains break and separate, exposing more underlying unsaturation to the gas. Cracks develop and grow in a direction normal to the applied stress. The growth rate of cracks in the elastomer varies directly with the modulus and inversely with crosslink density. Intrinsic stress alone is more than enough to cause crack growth in unvulcanized gutta percha, the plastic or trans form of polyisoprene. Elastomers representing a range of ozone resistance are listed in Table 1.

Antiozonant Action

Two types of stabilizers inhibit crack growth in rubbers: microcrystalline waxes and alkylated phenylene diamines. A small quantity of the wax milled into a rubber will gradually diffuse to the surface where it will serve as a barrier impervious to ozone. A combination of wax and alkylated phenylene diamine antiozonant is generally used for optimum protection. The exact function of antiozonant is still obscure but it is possible that it accelerates scission processes on the polymer surface producing a protective film of viscous products.

Cracks also form in the final stages of thermal and photooxidation of polyolefins. Like those in polycarbonates (22), their growth seems to be associated with repeated temperature and humidity cycles. Otherwise moisture either alone or in combination with microorganisms has no significant effect on the service life of polyolefins.

Acknowledgement

The author thanks F. A. Bovey for helpful discussions.

In Durability of Macromolecular Materials; Eby, R.;
ACS Symposium Series; American Chemical Society: Washington, DC, 1979.

REFERENCES

(1) Nickerson, R. F. Ind. Eng. Chem. 1941, 33, 1022.

(2). Ingersoll, H. G., J. Appl. Phys. 1946, 17, 924.

(3) McMahon, W.; Birdsall, H. A.; Johnson, G. R.; Camilli, C.T., J. Chem. Eng. Data 1959, 4, 57.

(4) Ravens, D. A. S., Polymer 1960, 1, 375.

(5) Winslow, F. H.; Aloisio, C. J.; Hawkins, W. L.; Matreyek, W.; Matsuoka, S., Chem. Ind. (London) 1963, 533 and 1465.

(6) Winslow, F. H. "Treatise on Materials Science and Technology", Schultz, J. M., Ed.; Academic Press Inc.: New York, 1977; Vol. 10, Part B, p 741-773.

(7) Peterlin, A.; Meinel, G., J. Polym Sci. B 1965, 3, 1059.

(8) Kafavian, G., Polym. Sci. 1957, 24, 499.

(9) Gilroy, H.M. "Proceedings of the 23rd International Wire and Cable Symposium"; National Technical Information Service, Springfield, Va., 1974; p 42.

(10) Hawkins, W. L.; Matreyek, W; Winslow, F. H. J. Appl. Polym. Sci. 1961, 5, S15.

(11) Hawkins, W. L.; Worthington, Mrs. M. A. J. Polym. Sci., 1962, 62, S106.

(12) Kuzminskii, A. S.; Lyubschanskyaya, L. I; Khitrava, N. G.; Bass, S. I. Rubber Chem. Technol. 1953, 26, 858.

(13) Hawkins, W. L.; Worthington, Mrs. M. A.; Matreyek, W. J. Appl. Polym. Sci. 1960, 3, 277.

(14) Carlsson, D. J.; Wiles, D. M. Macromolecules 1971, 4, 179.

(15) Burgess, A. R. Natl. Bur. Standards (U.S.) Circ. 525, 1953, 149.

In Durability of Macromolecular Materials; Eby, R.;
ACS Symposium Series; American Chemical Society: Washington, DC, 1979.

(16) Hartley, G. H.; Guillet, J. E. Macromolecules 1968, 1, 165.

(17) Winslow, F. H. Pure Appl. Chem. 1977, 49, 495.

(18) Ivanov, V. B.; Shlyapintakh, V. Ya. J. Polym. Sci., Polym. Chem. Ed. 1978, 16, 899.

(19) Ranaweera, R. P. B.; Scott, G. J. Polym. Sci., Polym. Lett. Ed. 1975, 13, 71.

(20) Pappas, S. P.; Fischer, R. M. J. Paint Tech. 1974, 46(599), 65.

(21) Baum, B. Polym. Eng. Sci. 1974, 14, 206.

(22) Blaga, A.; Yamasaki, R. S. J. Mater. Sci. 1976, 11, 1513.

RECEIVED December 8, 1978.

3

Polymer Film Photodegradation: Optical Density Effects

ALLAN R. SHULTZ

General Electric Corporate Research and Development, P. O. Box 8, Schenectady, NY 12301

Aging of polymer films involves a complex variety of contributing chemical and physical factors. This is especially true of weathering in which sun, rain, air, temperature variation, and various mechanical conditioning effects play individual and interactive roles. Chemical reactions initiated by visible and near-ultraviolet light are major sources of polymer film property alterations. The light absorption characteristics of a given film are the initial determining factors in photochemical change of its properties. Homogeneous, multi-phase, or layered structures in polymer films will influence the amount and location of light absorption.

An obvious division of polymer films into transparent (to visible light), translucent, and opaque categories is convenient in considering photodegradative response. Opaque films may derive their opacity from reflective pigments, absorptive pigments, absorptive dyes, or to combinations of such additives. In some cases opacity, or translucency, may be due to the morphology or chemical structure of a polymer without additives. Thus spherulitic crystallinity or strong chromophores in a polymer can yield obscurance, respectively, by light scattering and reflection, or by absorption. Transparent films may be colorless, having very small extinction coefficients for all light wavelengths in the visible region, or colored, having some differential extinction in the visible region.

It is the intent of the present work to examine the role of light intensity distribution within polymer films upon the nature of their photodegradative aging. Although the term "films" will be used exclusively throughout the presentation, dimensionally thick films, customarily called "sheets", are the structures of most interest. Emphasis will be placed on polymer chain scission by the absorbed light. Ultimately the failure criteria employed will determine whether failure is related only to the average cumulative energy absorption by a film or is also related to the spatial distribution of the energy absorption within the film.

The present paper will first briefly review the development

0-8412-0485-3/79/47-095-029$05.00/0

In Durability of Macromolecular Materials; Eby, R.;
ACS Symposium Series; American Chemical Society: Washington, DC, 1979.

of relationships permitting more quantitative analyses of photodegradation of polymer films having appreciable optical density. Next, the differing light intensity distributions and resultant photodegradation distributions will be indicated for polymer films of equal thickness: film A containing a UV absorber, film B having the UV absorber contained in a topcoat layer, and film C having no UV absorber. To make obvious the salient features of optical density effects, greatly simplifying assumptions will be made and stated. Finally, the polymer films' qualifications under various failure criteria will be inferred.

Scission and Crosslink Enumeration

A very modest amount of publication has appeared treating optical density effects upon polymer photodegradation. Mathematical relations have been derived which permit evaluation of quantum yields for polymer scission and crosslinking by normally-incident, monochromatic light irradiation of polymer films (1-4). Number- and weight-average molecular weight change, solution viscosity change, and/or gel content build or decrease were the physical properties considered. These derivations were based on the assumption that the initial polymer molecular weight distribution was satisfactorily approximated by a "most probable" distribution. Explicit molecular weight distribution functions for such photodegraded films were subsequently published (5). Molecular weight distributions and average molecular weights of an initially monodisperse polymer after pure photoscission of chains in a film have also been computed (6).

Optical density effects on photodegradation in films have been considered in studies on cellulose (2), poly(methyl isopropenyl ketone) (7), poly(ethylene terephthalate) (8), and poly(methyl methacrylate) (3,9). More recently an attempt was made to analyze the photosensitized gelation of poly(vinyl butyral) with correction for optical density effects (10).

Photodegradation of polymer films by polychromatic light introduces further complexity into mathematical treatments. This problem has been approached experimentally by using spectrally-dispersed light from a continuum light source and determining an "activation spectrum" for chromophore production (11,12,13). In this case a number-averaged property was treated. The "most active wavelength region" for net chain scission of poly(ethylene terephthalate) by polychromatic light irradiation was determined by exposing a stack of thin films and analyzing intrinsic viscosity (a weight-averaged property) as a function of stack position (8). Both of these experimental approaches can yield insight into the somewhat complex interplay of film optical density, incident light intensity, and quantum yields as functions of wavelength.

For better analyses of photodegradation of polymer films it will be necessary to derive expressions handling the common occurrence in which the extinction coefficient for the active

In Durability of Macromolecular Materials; Eby, R.;
ACS Symposium Series; American Chemical Society: Washington, DC, 1979.

wavelength of light changes with the extent of reaction. Treatment of the photolysis of a solute in a well-stirred solution has been published which can handle this problem for polymer solutions (14). In such a system the extinction coefficient is conversion (time)-dependent, but not position-dependent. The kinetics of photobleaching in rigid media has been treated mathematically (15). It would appear that generalization and extension of the method used therein could be a profitable approach to improved analyses of polymer film photodegradation.

Various aspects of polymer photodegradation have been reviewed recently (16).

Spatial Distribution of Photodegradation in Polymer Films

Let us consider three polymer films of equal thickness, L(cm) (cf. Figure 1 schematic). Film A contains a uniformly-dispersed ultraviolet light absorber (UV absorber). Film B contains the same UV absorber in a topcoat layer having a UV transparent matrix. Film C has no added UV absorber either dispersed or in a topcoat. The polymer will be referred to as component 1 and the UV absorber as component 2. The following assumptions are made: a) Irradiation is by monochromatic light at normal incidence to the "upper" film surface. b) Light absorptions by the polymer and by the UV absorber obey the Lambert-Beer relation. c) The specific absorption coefficient ε_2 ($cm^2 gm^{-1}$) of the UV absorber is much greater than that, ε_1, of the polymer. d) Change in the absorption coefficients at the activating wavelength is negligible throughout the irradiation period. e) The UV absorber functions only as a light absorber and affects polymer degradation in no other manner. f) Chemical changes in the polymer (chain scission, crosslinking, chromophore production) are proportional to the light absorbed by the polymer. g) The polymer has initially a most probable distribution of molecular weight.

Assumptions a and b provide simple geometry and light intensity relationships. Assumption c permits neglect of the UV absorber contribution to the system volume and film specific volume. Assumption d eliminates the complication of conversion-dependent optical properties. Assumptions e, f, and g lead to mathematically simple relations between integrated light flux and polymer structure alteration. We further state that I_o is the light intensity in the upper film (or topcoat) surface and that $I_o e^{-(k_1+k_2)L}$, $FI_o e^{-k,L}$, and $I_o e^{-k,L}$ are the "forward" intensities reaching the lower surfaces. Consideration of the approximately 5% reflection at the upper air-film interface is then not necessary. The comparable reflection at the lower film-air interface will be ignored.

With the above specifications it is possible to calculate (1) the changes in average molecular weights, molecular weight distribution, gel content (when crosslinking predominates), and new chromophore content as functions of total light flux, quantum

In Durability of Macromolecular Materials; Eby, R.;
ACS Symposium Series; American Chemical Society: Washington, DC, 1979.

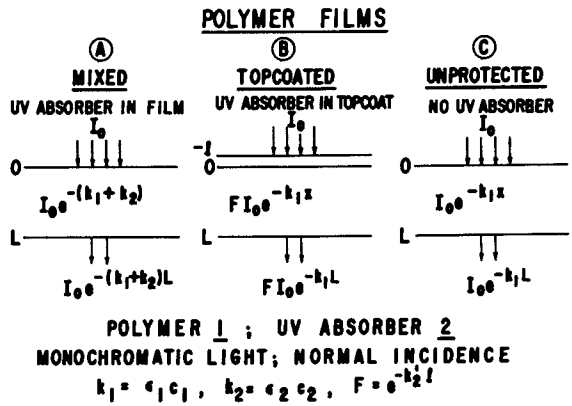

Figure 1. Schematic of polymer films undergoing irradiation by UV light

In Durability of Macromolecular Materials; Eby, R.;
ACS Symposium Series; American Chemical Society: Washington, DC, 1979.

yields, film composition, and film dimensions. In addition, the spatial distribution of these functions between the upper and lower film surfaces can be described.

To illustrate optical density effects on photodegradation we will confine our attention to the simple situation of chain scission and new chromophore production. (Crosslinking will not be considered as occurring. Treatment of concurrent scission and crosslinking can be done with minor increase in mathematical complexity (1).) UV absorber amounts are chosen so that the total light energy absorbed by the polymer in a given exposure is the same in mixed film A and topcoated film B. In terms of average polymer exposure to light we may then say that "equal protection" is provided the polymer in films A and B.

Random Chain Scission and Chromophore Production. Equal Energy Absorption by Polymer in Film A and Film B.

A. Relative Amounts of UV Absorber Required Per Unit Area for Mixed Film A and Topcoated Film B. The amount of UV absorber required in the topcoat of film B to give the polymer "protection equal to" that provided by a given concentration of UV absorber in film A is readily calculated. Referring to the light intensity relations depicted in Figure 1, the average number of photons absorbed per gram by the polymer in films A and B are:

$$\text{Film A:}\quad (R_1)_A = R_{10}L^{-1}\int_o^L e^{-(k_1+k_2)x}dx$$

$$= R_{10}[(k_1+k_2)L]^{-1}(1-e^{-(k_1+k_2)L}) \qquad (1)$$

$$\text{Film B:}\quad (R_1)_B = FR_{10}L^{-1}\int_o^L e^{-k_1x}dx$$

$$= FR_{10}(k_1L)^{-1}(1-e^{-k_1L}) \qquad (2)$$

$$R_{10} = I_o t k_1 \bar{v}_1 \qquad (3)$$

$$F = e^{-k_2'\ell} \qquad (4)$$

$$k_1 = \varepsilon_1 c_1 \qquad (5)$$

$$k_2 = \varepsilon_2 c_2 \qquad (6)$$

$$k_2' = \varepsilon_2 c_2' \qquad (7)$$

I_o (photons $cm^{-2}sec^{-1}$) incident light intensity; t(sec) irradiation time; ε_1, ε_2 (cm^2gm^{-1}) specific absorption coefficients; c_1, c_2 ($gm\ cm^{-3}$) concentrations in film A; $\bar{v}_1$ (cm^3gm^{-1}) specific volume of the polymer.

R_{10} is the number of photons absorbed by polymer per gram of

In Durability of Macromolecular Materials; Eby, R.;
ACS Symposium Series; American Chemical Society: Washington, DC, 1979.

polymer in the upper surface of films A and C. F is the factor by which the light intensity entering film B has been reduced by the UV absorber in its topcoat.

Equal energy absorption by polymer in films A and B requires that $(R_1)_A = (R_1)_B$. Equating these energy absorptions and solving for F gives

$$F = (1+\frac{k_2}{k_1})^{-1} \ (1-e^{-[(1+\frac{k_2}{k_1})k_1L]})(1-e^{-k_1L})^{-1} \tag{8}$$

F is therefore a function of the optical density of the unprotected film C

$$(O.D.)_C = k_1L/2.303 \tag{9}$$

and of the ratio of linear attenuation decrements in the mixed film A

$$k_2/k_1 = \varepsilon_2 c_2 / \varepsilon_1 c_1 \tag{10}$$

The topcoat thickness, ℓ, (cf. Figure 1 and Eq. 4) is unspecified. In practice ℓ will be dictated by considerations of the UV absorber solubility limit in the topcoat matrix material, by the topcoat thickness required to provide other beneficial effects (e.g., abrasion resistance, erosion resistance), by available topcoat application techniques, and by economics. However, we can construct a hypothetical topcoat of thickness L equal to that of the polymer films. Then

$$F = e^{-k''_2 L} \tag{4a}$$

$$C''_2/C_2 = (-\ell nF)/k_2 L \tag{11}$$

The ratio C''_2/C_2 is equal to the ratio of the amount of UV absorber per unit area in film B to the amount of UV absorber per unit area in film A needed to provide equal energy absorption by polymer in the two films. Figure 2 presents this ratio as a function of unprotected film C optical density for two ratios, k_2/k_1, of the linear attenuation decrements. A maximum of one-half as much UV absorber is required in the topcoated construction for very low optical density films. For an unprotected film O.D. = 1.0 and $k_2/k_1 = 10$ only one-tenth the absorber used in film A is needed for film B to provide "equal protection" for the polymer.

B. Average Molecular Weights. Assuming the polymer chains in a laminus are cut at random in direct proportion to the number of photons absorbed by the polymer in the laminus, a convenient degradation variable is

In Durability of Macromolecular Materials; Eby, R.;
ACS Symposium Series; American Chemical Society: Washington, DC, 1979.

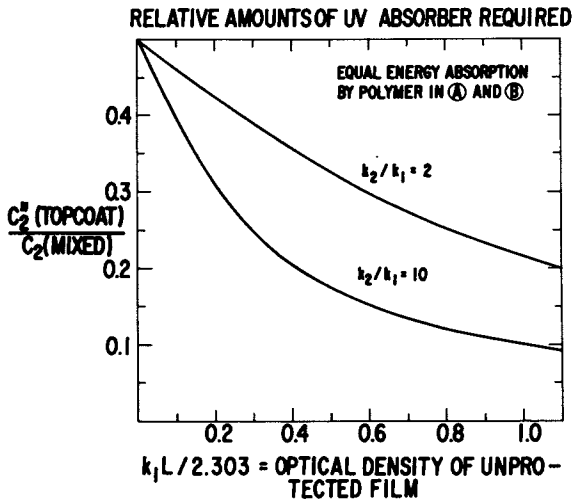

Figure 2. Ratio of amounts of UV absorber per unit area required for film B to that required for film A to give equal energy absorptions by the polymer vs. optical density of unprotected film

In Durability of Macromolecular Materials; Eby, R.;
ACS Symposium Series; American Chemical Society: Washington, DC, 1979.

$$S = \phi_d I_o t k_1 \bar{v}_1 M_n^o \bar{N}^{-1} \quad (12)$$

where ϕ_d (scissions per photon absorbed by polymer) is the scission quantum yield. M_n^o is the initial number-average molecular weight of the polymer, and $\bar{N}$ is Avogadro's number. S is the number of scissions in the upper surface laminus per original polymer molecule in the surface laminus.

By integration of the laminar average molecular weights from the upper surface to the lower surface of the films the number-average and weight-average molecular weights of the UV-irradiated films are found to be (1)

Films A and B

$$M_n = M_n^o / [1 + \frac{S}{(k_1+k_2)L}(1-e^{-(k_1+k_2)L})] \quad (13)$$

Film C

$$M_n = M_n^o / [1 + \frac{S}{k_1 L}(1-e^{-k_1 L})] \quad (14)$$

Film A

$$M_w = M_w^o \; [1+((k_1+k_2)1)^{-1} \ln \frac{(1+Se^{-(k_1+k_2)L})}{(1+S)}] \quad (15)$$

Film B

$$M_w = M_w^o \; [1+(k_1 L)^{-1} \ln \frac{(1+FSe^{-k_1 L})}{(1+FS)}] \quad (16)$$

Film C

$$M_w = M_w^o \; [1+(k_1 L)^{-1} \ln \frac{(1+Se^{-k_1 L})}{(1+S)}] \quad (17)$$

Figures 3 and 4 present, respectively, M_n/M_n^o and M_w/M_w^o for the three film constructions as functions of S when $k_1 L/2.303=0.5$ and $k_2/k_1=10$. Since the same number of new molecules is produced by scission in films A and B for a given total irradiation their M_n/M_n^o are identical for all S. The lowering in weight-average molecular weight for the two films differs, however, due to the nature of the weight-averaging of molecular weights. A superficial reading of Figure 4 would suggest that the polymer in film A is better protected than in film B. This is indeed true if the physical property of concern depends only on M_w for the total film. If, however, the failure criterion is sensitive to regions of highly-degraded polymer, film A will fail sooner than film B. This dictates examination of the distribution of degradation from the upper surface to the lower surface of each film.

C. Average Molecular Weight as a Function of Depth in UV-Irradiated Films. Random scission of polymer chains within a laminus at depth x lowers the average molecular weight but perpetuates the most probable distribution of molecular weight within the laminus. Thus, $(M_w^S)_x = 2(M_n^S)_x$ for all S. Here the superscript S is intended to mean "at irradiation degree yielding S" as the superscript o previously and subsequently used means "original" or "at zero irradiation degree." The Lambert-Beer light intensity

In Durability of Macromolecular Materials; Eby, R.;
ACS Symposium Series; American Chemical Society: Washington, DC, 1979.

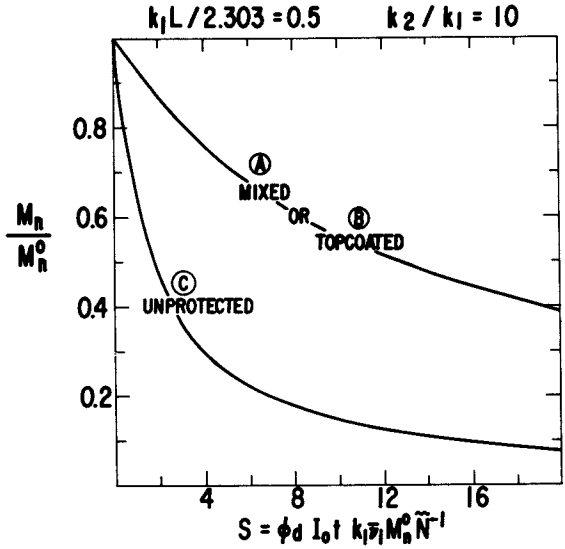

Figure 3. Fraction of original $\overline{M}_n$ retained vs. number of scissions per original molecule in upper surface of film A

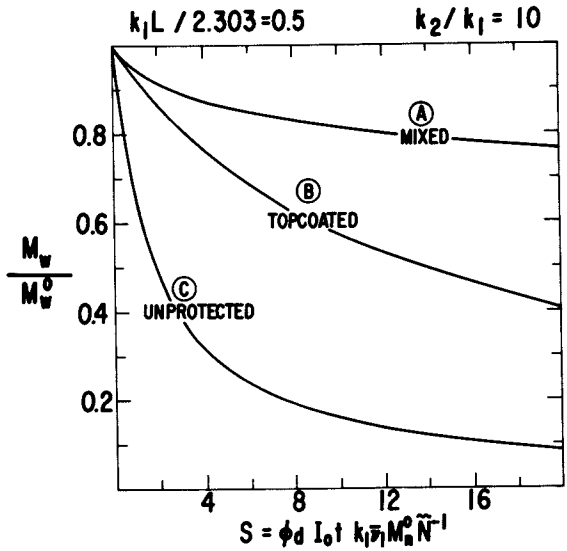

Figure 4. Fraction of original $\overline{M}_w$ retained vs. number of scissions per original molecule in upper surface of film A

In Durability of Macromolecular Materials; Eby, R.;
ACS Symposium Series; American Chemical Society: Washington, DC, 1979.

relation leads to the following laminar molecular weight relations which were used in the integrations leading to Eqs. (13) to (17):

$$\text{Film A} \qquad M^S_{x/L}/M^o = [1+Se^{-(k_1+k_2)L\cdot\frac{x}{L}}]^{-1} \tag{18}$$

$$\text{Film B} \qquad M^S_{x/L}/M^o = [1+FSe^{-k_1L\cdot\frac{x}{L}}]^{-1} \tag{19}$$

$$\text{Film C} \qquad M^S_{x/L}/M^o = [1+Se^{-k_1L\cdot\frac{x}{L}}]^{-1} \tag{20}$$

The ratios $M^S_{x/L}/M^o$ are intended to represent M^S_w/M^o_w or M^S_n/M^o_n (which are equal) in the laminus at fractional depth x/L.

Figures 5 and 6 illustrate for the three films having $k_1L/2.303 = 0.5$ and $k_2/k_1 = 10$ the variation of average molecular weight with depth when the surface scission levels are S = 1 and S = 7, respectively. The molecular weight averages as functions of depth are strikingly different for films A and B. When S = 1 the average molecular weights in film A range from $0.5M^o$ at the upper surface to essentially M^o at the lower surface. The variation is only from $0.88M^o$ to $0.96M^o$ in film B. When S = 7 film A upper surface molecules are at $0.125M^o$ and about 15% by weight of the film is at average $M<0.5M^o$. In film B the average molecular weights are reduced to $0.52M^o$ at the upper surface and to $0.77M^o$ at the lower surface.

D. Concept of a Critical $M^S_{x/L}/M^o$ Ratio. We now postulate that there is a critical value for $M^S_{x/L}/M^o$ below which the polymer in a given film fails to meet a strength criterion at x/L. Let the critical $M^S_{x/L}/M^o$ ratio be Y-1. Then from Eqs. (18) to (20) the polymer reaches this critical ratio at x/L of

$$\text{Film A} \qquad x_c/L = ((k_1+k_2)L)^{-1}\ln[S/(Y-1)] \tag{21}$$

$$\text{Film B} \qquad x_c/L = (k_1L)^{-1}\ln[FS/(Y-1)] \tag{22}$$

$$\text{Film C} \qquad x_c/L = (k_1L)^{-1}\ln[S/(Y-1)] \tag{23}$$

To illustrate these relations we assume that $Y^{-1}=0.5$ is the critical ratio for a given criterion and the polymer films have $k_1L/2.303=0.5$ and $k_2/k_1=2$ or 10. Figure 7 plots the intrusion and fractional penetration of the critical molecular weight ratio for the three films against S. Specifying that $Y^{-1}=0.5$ dictates that intrusion occurs for films A and C when S=Y-1=1 regardless of the k_2/k_1 ratio. For the topcoated film B the critical molecular weight ratio intrusion into the upper surface does not occur until $S=(Y-1)/F = 2.12$ when $k_2/k_1=2$ or S=7.52 when $k_2/k_1=10$. The exposure time to intrusion of the critical molecular weight ratio into film B is 1/F times the exposure time to its intrusion into films A and C irrespective of the value of the critical ratio Y^{-1}. The

In Durability of Macromolecular Materials; Eby, R.;
ACS Symposium Series; American Chemical Society: Washington, DC, 1979.

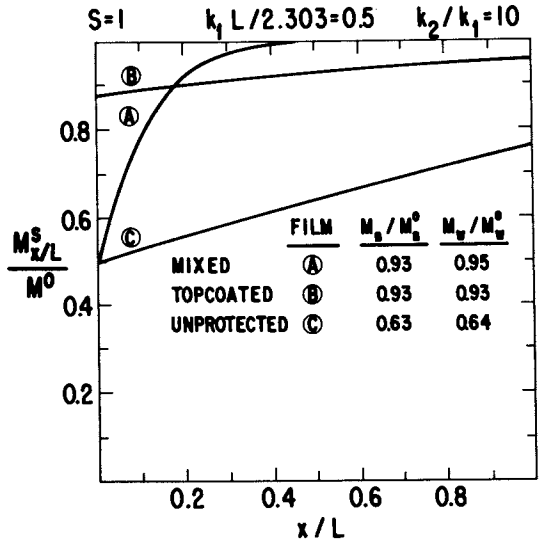

Figure 5. Ratio of av mol wt at fractional depth x/L to original av mol wt after one scission per original molecule in upper surface of film A vs. the fractional depth

In Durability of Macromolecular Materials; Eby, R.;
ACS Symposium Series; American Chemical Society: Washington, DC, 1979.

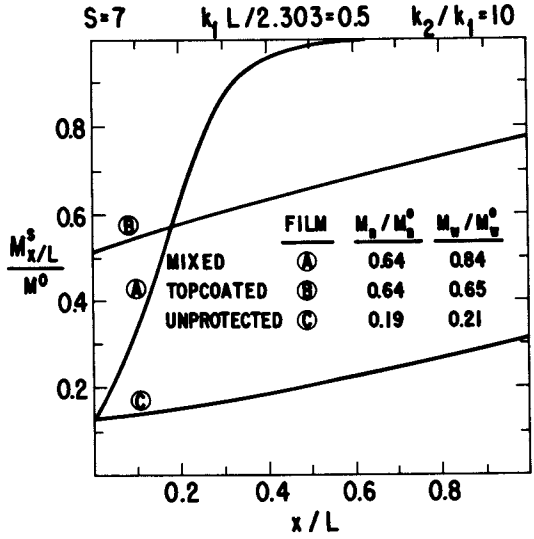

Figure 6. Ratio of av mol wt at fractional depth x/L to original av mol wt after seven scissions per original molecule in upper surface of film A vs. the fractional depth

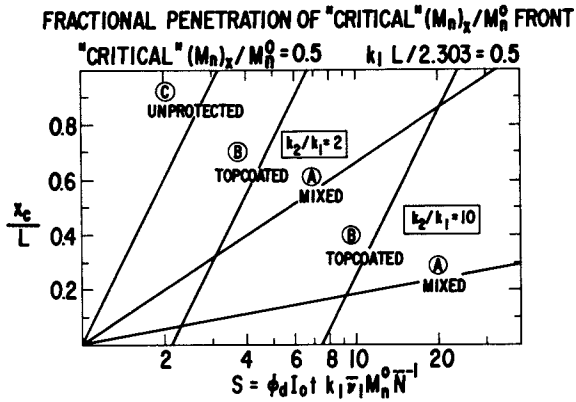

Figure 7. Location of critical molecular weight ratio as a function of S, protection mode, and light absorption decrement ratios

In Durability of Macromolecular Materials; Eby, R.;
ACS Symposium Series; American Chemical Society: Washington, DC, 1979.

fractional penetration of the critical $M^S_{x/L}/M^o$ front through film A proceeds more slowly with irradiation time after intrusion than does the front in films B or C since the slope of the semi-logarithmic plot in Figure 7 is $[(k_1+k_2)L]^{-1}$ for film A and $(k_1L)^{-1}$ for films B and C.

E. Chromophore Production. Assume a new chromophore is produced with a quantum yield ϕ_f at random sites within a polymer chain in direct proportion to the activating light absorbed by the chain. The number of new chromophore units per gram of polymer at depth x is

Film A $$G_x = \phi_f R_{10} e^{-(k_1+k_2)x} \quad (24)$$

Film B $$G_x = \phi_f F R_{10} e^{-k_1 x} \quad (25)$$

Film C $$G_x = \phi_f R_{10} e^{-k_1 x} \quad (26)$$

where, as above, $R_{10} = I_o t k_1 \bar{v}_1$.

Integration through the films from x=0 to x=L gives the average number of new chromophore groups per gram of polymer

Films A and B $$G = \frac{\phi_f R_{10}}{(k_1+k_2)L}(1-e^{-(k_1+k_2)L}) \quad (27)$$

Film C $$G = \frac{\phi_f R_{10}}{k_1 L}(1-e^{-k_1 L}) \quad (28)$$

Films A and B will be "colored to the same extent" as judged by transmitted light.

Discussion

The foregoing sections present average molecular weight, molecular weight positional distribution, critical $M^S_{x/L}/M^o$ ratio, and chromophore production for simple model homogeneous, topcoated, and unprotected polymer films during photodegradation. Oversimplification has been used to allow an overview of salient features regarding geometric and light absorption effects on film photodegradative response. The single novel concept introduced is the concept of a critical molecular weight ratio, or critical molecular weight, intrusion and penetration through the films as degradation proceeds. The critical aspect has been allowed to remain vague to this point. Let us now give somewhat more substance to this concept.

Crazing and fracture are failure modes which are quite sensitive to average molecular weight in most amorphous thermoplastics. High molecular weight polymeric glasses may have considerable toughness and craze resistance. The same polymers at low molecular weight craze readily and/or undergo brittle fracture at very

In Durability of Macromolecular Materials; Eby, R.;
ACS Symposium Series; American Chemical Society: Washington, DC, 1979.

low strains. Although there is not a unique average molecular weight below which craze resistance or toughness suddenly vanishes, these attributes deteriorate rapidly with molecular weight decrease in a rather narrow range of average molecular weight. One can approximately designate a critical average molecular weight for a given thermoplastic below which it will fail a given crazing or brittle fracture test. Since in our formulation a critical ratio $M^S_{X/L}/M^o = Y^{-1}$ is employed, it is apparent that Y is directly proportional to the initial average molecular weight, M^o, of a given film.

In addition to the intrusion and presence of a region of polymer having an inadequate strength, the location and thickness of this region relative to a given applied stress field is important. Mechanical failure will occur most readily if the stress field produces maximum tensile forces in the weakened region. If failure is principally initiation-limited, a very low x_c/L depth can lead to catastrophic failure. If, on the other hand, propagation of failure demands considerable energy in less-degraded regions of the film, a large gradient of degradation with depth can provide stabilization of a partially-failed film. As mentioned above and exemplified by Figure 7, intrusion of the critical $M^S_{X/L}/M^o$ front into film A is to be expected at lower total irradiations than into film B. Surface crazing or microfracture should occur sooner in film A. However, after intrusion has occurred the penetration of the critical $M^S_{X/L}/M^o$ front into the film is much more rapid in film B. Propagation-limited failure can then proceed through film B more readily than through film A.

When using films protected from photodegradation by a marginally adequate amount of UV absorber it is important to consider the geometry of the protection and the mechanics of anticipated failures to assure satisfactory use lifetimes.

Appendix

Reference 1 contains the most extensive mathematical treatment of polymer scission and crosslinking by light. Two text errors in that publication require correction.

Equation (9b) reference 1 should read

$$\bar{M}_w = \bar{M}_{wo} \ln\left[\frac{(R_o/R_L)-(R_o/R^*)}{1-(R_o/R^*)}\right]/\ln(R_o/R_L) \qquad (9b)$$

Equation (12) reference 1 should read

$$[\eta] = Q(kL)^{-1}\bar{M}^a_{wo}\left[\sum_{n=o,1,2,--}(a+n)^{-1}\left(1-\frac{R_o}{R^*}y\right)^{-(a+n)}\right]_{y=1}^{y=e^{-kL}} \qquad (12)$$

In Durability of Macromolecular Materials; Eby, R.;
ACS Symposium Series; American Chemical Society: Washington, DC, 1979.

Literature Cited

1. Shultz, A.R., J. Chem. Phys., (1958), 29, 200.
2. Flynn, J.H., J. Polym. Sci., (1958), 27, 83.
3. Charlesby, A., and Thomas, D.K., Proc. Roy. Soc. (London), (1962), A269, 104.
4. Maxim, L.D., and Kuist, C.H., Official Digest, (1964), 36, 723.
5. Shultz, A.R., J. Appl. Polym. Sci., (1966), 10, 353.
6. Jellinek, H.H.G., J. Polym. Sci., (1962), 62, 281.
7. Shultz, A.R., J. Polym. Sci., (1960), 47, 267.
8. Shultz, A.R., and Leahy, S.M., J. Appl. Polym. Sci., (1961), 5, 64.
9. Shultz, A.R., J. Phys. Chem., (1961), 65, 967.
10. Hippe, Z., "Ultraviolet Light Induced Reactions in Polymers, ACS Symposium Series Vol. 25", S.S. Labana, Ed., pp. 62-63, ACS, Washington, D.C., 1976.
11. Hirt, R.C., Searle, N.Z., Schmitt, R.G., SPE Transactions, (1961), 1, 21.
12. Mullen, P.A. and Searle, N.Z., J. Appl. Polym. Sci., (1970), 11, 765.
13. Hirt, R.C., and Searle, N.Z., "Wavelength Sensitivity or Activation Spectra of Polymers," Preprint SPE RETC,(1964), Washington, D.C.
14. Shultz, A.R., J. Polym. Sci., Part C (1968), 25, 115.
15. Kessler, H.C., Jr., J. Phys. Chem., (1967), 71, 2736.
16. Ranby, B., and Rabek, J.F., "Photodegradation, Photooxidation, and Photostabilization of Polymers," John Wiley and Sons, New York, NY, 1975.

RECEIVED December 8, 1978.

4

The Course of Thermooxidative Degradation of LD- and HD- Polyethylene under Accelerated Testing Conditions

ARNE HOLMSTRÖM

The Polymer Group, Chalmers University of Technology, Fack, 402 20 Gothenburg, Sweden[1]

The search for accelerated testing procedures to predict the useful service life for polyethylene (PE) compositions has been the main incentive for numerous studies on the thermo-oxidative degradation of PE in oxygen-rich atmospheres below 200 °C (1).

The basic requirement for reliable accelerated ageing is that the course of degradation is identical at the service and test conditions. Surprisingly enough, in spite of the many studies and the great technical and economical importance in being able to predict the useful service life for PE products, the information about the dependence of the most common accelerating factor on the structural changes during thermo-oxidative degradation is rather scarce. This is due to the fact that most publications concern measurements of only one structure parameter at a single temperature level. Furthermore, the PEs under investigation have mostly been sparsely characterized, especially with regard to additives and catalyst residues.

In a series of investigations (2, 3, 4, 5, 6, 7) we have studied the temperature dependence of the structural changes occurring in well defined PEs and PE compositions when heated at temperatures between 70 °C and 180 °C in air. Our aim has been to cover the commonly employed accelerated testing conditions under which service life-time predictions of PE are made.

The structural changes have been studied with a series of methods including gel chromatography (GPC), viscometry, IR, differential scanning calorimetry (DSC) and gravimetric measurements.

Experimental

Further experimental details are given in references (2, 3, 4)

Materials and Heat Treatment. The LDPE used, Unifos DFDS 6600, is a high pressure product produced in a tubular reactor. Unifos has reported the LDPE to be free from additives. It had

[1] Current address: Statens provningsanstalt, Laboratory for polymeric materials, Box 857, S-501 15 Borås, Sweden

0-8412-0485-3/79/47-095-045$05.00/0

MI = 0.31 g/10 min, density = 923 kg/m^3, $\bar{M}_n = 29 \cdot 10^3$, $\bar{M}_w = 159 \cdot 10^3$ and degree of long chain branching (LCB) = $1.5 \cdot 10^{-4}$. The HDPE resin, Marlex 6001, was produced by N.V. Polyolefins, Belgium according to the Philips process. Since this resin contained unspecified additives, it was purified by dissolution in p-xylene, filtration, and precipitation in methanol (8). After this treatment no traces of antioxidants or other additives could be detected by IR or UV. The sample contained ~ 1 ppm chromium both before and after the reprecipitation, however, as determined by atomic absorption spectrometry (8). It had MI = 0.10 g/10 min, density = 960 kg/m^3, $\bar{M}_n = 16 \cdot 10^3$, $\bar{M}_w = 150 \cdot 10^3$ and $\lambda = 0.07 \cdot 10^4$.

Compounding LDPE with TiO_2 and carbon black (CB) was performed in a Brabender Plastograph® for 10 min at 90 rpm under nitrogen. The mixing chamber volume was 60 ml and the oil bath temperature 160 °C. The antioxidants (AO) were incorporated by dry blending of 25 kg LDPE with AO and then extrusion and granulation 3-5 times on a Luigi Bandera SRL extruder.

0.25 mm thick films were moulded at 130 °C for LDPE and at 150 °C for HDPE between aluminium foils or reinforced polytetrafluoroethylene films. The degradation experiments were performed on 20x40 mm strips cut from these films.

The n-$C_{44}H_{90}$ was obtained from Fluka AG, Switzerland as puriss quality. No irregular structures such as tertiary carbon-atoms, olefinic or carbonyl groups could be detected by IR and NMR.

The samples were placed on thoroughly cleaned microscope cover glasses and heated in an air oven at temperatures from 70 to 180 °C. The temperature constancy was better than ±1 °C. The heating times ranged from 3936 h at 70 °C to 4 h at 180 °C.

Structural characterization. The content of insoluble material (gel) was determined by soxhlet extraction with p-xylene for 20 h under nitrogen.

Details of the GPC-analysis have been given (9, 10). A Waters Associates GPC Model 200, operating at 135 °C with 1,2,4-trichlorobenzene (TCB) as solvent, was used. The column combination consisted of five Styragel® columns with permeabilities ranging from 10^3 to 10^7 Å, which gave good separation in the MW range of interest.

To calculate the molecular-weight distribution (MWD), average MWs, and degree of long-chain branching (LCB) from GPC and viscosity measurements the computer program devised by Drott (11) was used; LCB is given as $\lambda = n_w/M$, where n_w is the weight-average number of trifunctional branch points per molecule. Because of the difficulties in determining $\bar{M}_w < 20 \cdot 10^3$ (by light scattering), the relation between intrinsic viscosity (I.V.) and $\bar{M}_w$ is hard to establish, which makes Drott's method unapplicable. Samples with $\bar{M}_w < 20 \cdot 10^3$ have been calculated as if they contained only linear molecules. The calibration curve for linear PE was obtained via the universal calibration curve (9).

In Durability of Macromolecular Materials; Eby, R.;
ACS Symposium Series; American Chemical Society: Washington, DC, 1979.

Determination of I.V. was carried out in p-xylene at 105 °C ±0.01 °C by using Ubbelohde viscometers with flow times for pure solvent greater than 100 sec. Like Drott (11) we had found (9) that p-xylene at 105 °C and TCB at 135 °C give the same I.V. for PE. Smooth curves were drawn to fit the experimental points in the plots of I.V. against heating time. In the GPC data treatment the curve values were then used.

The samples (~0.2g) were weighed before and after heat treatment on a Mettler analytical balance S-6 to better than ±0.01 mg.

The melting behavior and determination of crystalline content were studied with a Perkin-Elmer DSC-1 differential scanning calorimeter. The heating rate was 8 °C/min, the sample size, 12.0 mg for LDPE and 3.0 mg for HDPE, and n-$C_{44}H_{90}$. The runs were performed in a nitrogen atmosphere. Before analysis all samples were given the same thermal treatment by heating to 150 °C and cooling down to room temperature in a controlled manner.

In the determination of the crystalline content in PE dotriacontane (n-$C_{32}H_{66}$) was used as a 100 % crystalline calibration material according to common practice (12). It was found that this method resulted in a crystallinity of n-$C_{44}H_{90}$ higher than 100 %, in spite of which the common method was retained for the PE samples, thus allowing for comparison with published results. T_m was the maximum temperature.

IR-spectra were recorded on a Beckman IR-9 and a Perkin-Elmer IR-80 IR spectrophotometer with film 0.20 mm thick. Bruker 270 MHz Fourier Transform NMR equipment was used to obtain NMR spectra.

Results and Discussion.

Gravimetric and IR-Analysis. All the PE-compositions showed a similar pattern of weight changes at all temperature levels (cf. Fig. 1 for additive free LDPE). After an eventual induction period the weight increases initially until a maximum is reached. The weight may remain on this level or turn over into a decrease. The difference between different temperature levels is mainly a matter of time scale and the maximum value reached.

Several workers have reported on the changes in IR spectra with heating time during termo-oxidative degradation (13). No report on the temperature dependence could be found, however. Our results on this question demonstrated an almost identical pattern of changes in both the hydroxyl-, carbonyl- and ether-absorption bands from 70 to 180 °C. Only the time necessary for a certain change differed.

The composition of the carbonyl compounds contributing to the broad IR absorption band for severely oxidized samples have been investigated in some detail by others (14, 15). In these studies, no explicit information is given concerning the composition as a function of the degree of degradation, however. We saponified

In Durability of Macromolecular Materials; Eby, R.;
ACS Symposium Series; American Chemical Society: Washington, DC, 1979.

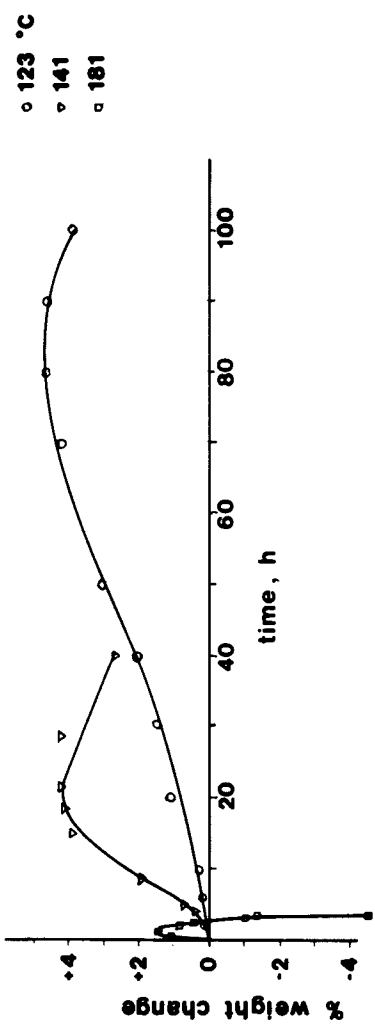

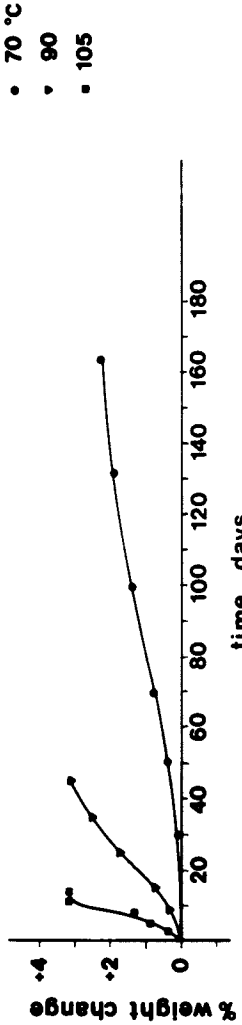

Figure 1. Weight changes for additive-free LDPE heated in air

In Durability of Macromolecular Materials; Eby, R.;
ACS Symposium Series; American Chemical Society: Washington, DC, 1979.

several series of samples with KOH in isopropanol according to Adams (15) and found, as could be expected, that the relative amount of ketones decreased while the relative amount of acids and esters increased with heating time. Evidently this will checkmate all attempts to use the raw carbonyl absorption band as a quantitative measure of the extent of degradation because the absorption coefficients for the different carbonyl compounds differ widely (15).

The results from the gravimetric and IR-analysis did consequently not indicate more than minor differences in the degradation course at different temperature levels.

Measures Related to Molecular Size. Although the I.V. depend on both MW and the degree of LCB and thus not by its own will be especially suitable as a measure of molecular size (10), the results permit comparison with earlier work (16, 17). Results for additive free LDPE which by and large also are representative for HDPE are shown in Fig. 2. (Notice the different time scales.) At 70 and 141 °C the I.V. is continuously reduced down to low levels. After a minimum has been reached a slight increase is observed at 141 °C.

At 181 °C the changes are more complicated which is the case also for 160 °C. After a reduction to about half the initial value the I.V. increases and passes a maximum. Meltzer and coworkers (16, 17) also obtained similar results after hot milling LDPE in air at 160 °C. They suggested this behaviour to be a result of a sequence of stages where chain scission, cross linking and chain scission again should dominate.

Besides the pronounced differences between the I.V. changes at temperatures below and above 150 °C, the mechanical properties were also rather different. No sample heated above 150 °C showed any tendency to brittleness, while the samples heated at lower temperatures became increasingly brittle with heating time.

In Fig. 3 the changes in MWD for additive free LDPE at 70 °C, 141 °C and 181 °C are illustrated. At 70 and 141 °C MWD undergoes a marked narrowing and dramatic shifts toward low MWs are observed up to relatively long heating times. In accordance with the result from I.V., samples heated longer than 30 h at 141 °C show a shift back toward higher MWs. If the heating is prolonged to some weeks, the material turns completely insoluble. In accordance with the results obtained by Husemann et al. (18) for HDPE, we found that the gel may be made completely soluble in TCB by hydrolyzing with KOH in isopropanol. This indicates that the cross-links were due to ester bonds.

The changes in molecular size below 150 °C include not only a marked shift of the MWD toward lower MWs, but also a rapid decrease of the degree of LCB to zero. These facts demonstrate that molecular diminishing is heavily dominating initially. After some time when oxidation products have accumulated, molecular enlargement reactions start, however, and gradually become dominating.

In Durability of Macromolecular Materials; Eby, R.;
ACS Symposium Series; American Chemical Society: Washington, DC, 1979.

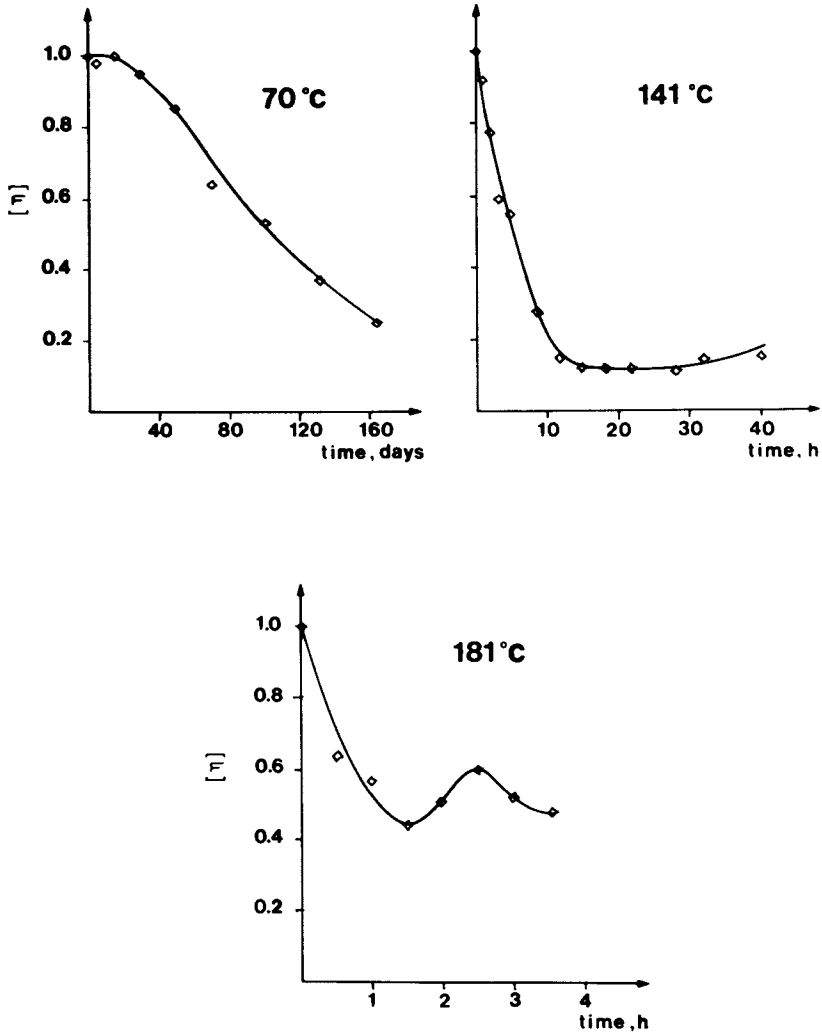

Figure 2. Change in intrinsic viscosity for additive-free LDPE heated in air

In Durability of Macromolecular Materials; Eby, R.;
ACS Symposium Series; American Chemical Society: Washington, DC, 1979.

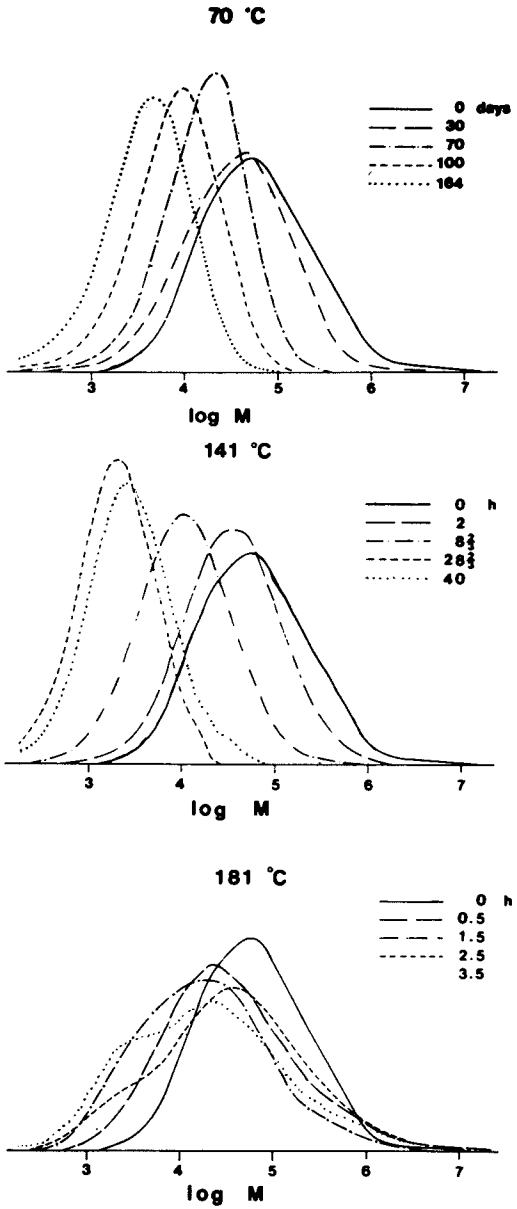

Figure 3. MWD changes for additive-free LDPE heated at 70°, 141°, and 181°C in air

In Durability of Macromolecular Materials; Eby, R.;
ACS Symposium Series; American Chemical Society: Washington, DC, 1979.

The situation is quite different above 150 °C, as exemplified by the MWDs from 181 °C in Fig. 3. Here the changes are much more complex. No narrowing is observed, instead very broad MWDs form rapidly. Already after 0.5 h, the bulk of the MWD is shifted considerably towards lower MWs because of extensive molecular diminishing. The high MW tail increases after 0.5 h, decreases after 1.5 h and increases again after longer heating times. At the same time the degree of LCB increases to twice its original value and after 1 h insoluble material has been formed. The transference of material in insoluble form is the reason for the oscillating behaviour of the I.V. observed above 150 °C, Fig. 2. If it had been possible to take the contribution of the rapidly increasing amount of insoluble material into account, the last drop would for example never had been observed. Evidently, above 150 °C molecular enlargement reactions occur from the very beginning concurrently with the molecular diminishing reactions.

As illustrated in Fig. 4, the course of changes in MWD for the additive free HDPE are very similar to those for LDPE at temperatures above its melting range. This is also the case for both the degree of LCB and the formation of insoluble material. However, compared to LDPE the formation of low MW material is more rapid for HDPE. This might be due to catalyst residues, influencing the way of decomposition of hydroperoxide groups.

The pattern changes markedly below its melting range, exemplified by 123 °C in Fig. 4. Initially the MWDs are shifted towards lower MWs in the same manner as at 141 °C. Beyond 20 h of heating the shift is retarded considerably compared with at 141 °C and a second peak develops. The reason for these differences below and above the melting range should be due to the restricted availability of oxygen in the crystalline regions in the solid HDPE. As is well known (19, 20) only the amorphous parts in the material are attacked. The narrow multimodal shape of the MWDs should reflect the molecular dimensions in the crystalline structure. The result is in accordance with the results obtained by other workers who oxidized HDPE with very strong oxidizing agents such as oxygen under high pressure in combination with catalysts (21), ozone (22) and HNO_3 (23).

Contrary to the gravimetric and IR-analysis which indicated no or only slight dependence of the degradation course with temperature the results from the measurements of molecular size indicate that considerable differences may be encountered. Two transition regions have been found. Above 150 °C both molecular diminishing and enlargement occur concurrently from the very beginning, while below 150 °C molecular enlargement is not observed until after rather long exposure times. HDPE showed furthermore distinct differences between the degradation course in the liquid and solid states. The measures of the changes in molecular size for LDPE did not show a corresponding sensivity for this phase transition, however.

In Durability of Macromolecular Materials; Eby, R.;
ACS Symposium Series; American Chemical Society: Washington, DC, 1979.

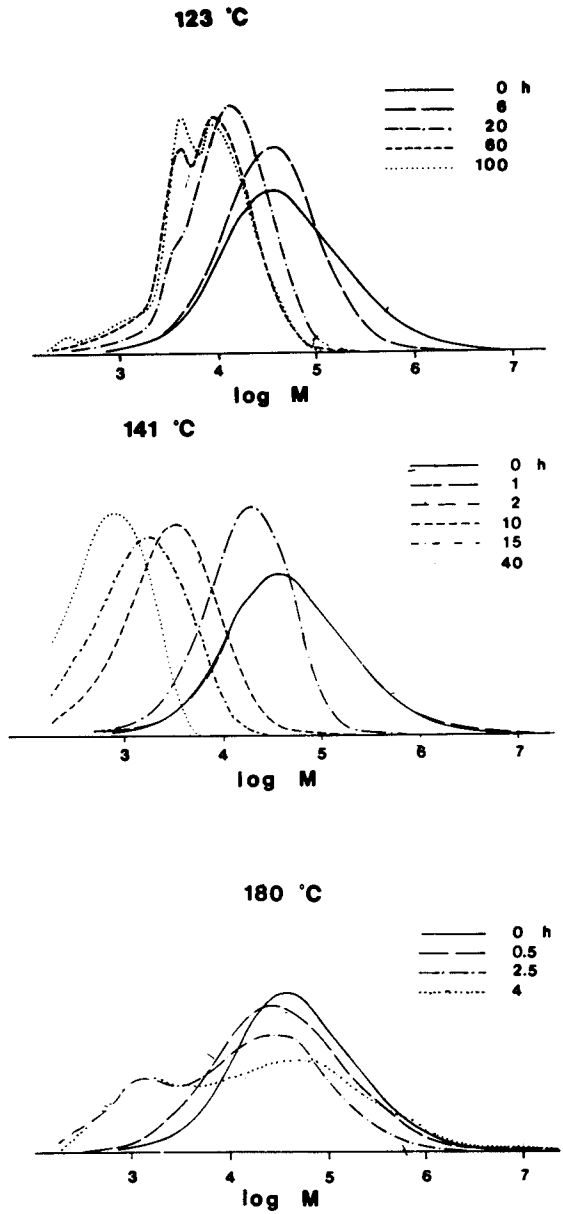

Figure 4. MWD changes for reprecipitated HDPE heated at 123°, 141°, and 180°C in air

In Durability of Macromolecular Materials; Eby, R.;
ACS Symposium Series; American Chemical Society: Washington, DC, 1979.

DSC-Analysis. The necessity of utilizing several complementary methods of analysis when investigating polymer degradation cannot be over-emphasized. As can be seen from Fig. 5, the crystalline melting behaviour of additive free LDPE heated at 123 °C hardly changes up to 20 h of heating. At the same time the $\bar{M}_w$-value was in fact reduced to about one fifth of its original value. On the other hand, a comparison of the DSC thermograms from 105 and 123 °C reveal differences in the degradation course for LDPE not detectable by measuring either weight changes, IR-spectra or molecular size.

The crystalline structure hence the melting behaviour, is governed by the size of the molecules and the amount of irregular structures as discussed in some detail in ref. 2. When degraded in the liquid state (123 °C, LDPE), the PE will be attacked rather randomly along the main chain. As discussed above for HDPE, at temperatures below T_m (105 °C, LDPE) degradation will be confined to the parts of the chains present in the amorphous phase only. The "chemi-crystallization" phenomenon observed under these conditions has been discussed by Winslow and coworkers in a series of papers (24, 25, 26, 27). In effect, the close-packing ability increases for the LDPE, Fig. 5 and more well-ordered crystalline regions form with a higher T_m.

Degradation Reaction Mechanisms. A detailed discussion of a large number of reactions believed to take part in the thermo-oxidative degradation of PE at the temperatures and oxygen concentrations encountered is given in ref. 2. In the following, only some main lines will be reviewed.

At all temperatures used, hydroperoxides should be the key substances and formed according to the classical chain mechanism, reactions (A) and (B).

$$R\cdot + O_2 \rightarrow RO_2\cdot \quad (A)$$

$$RO_2\cdot + RH \rightarrow ROOH + R\cdot \quad (B)$$

$$ROOH \rightarrow RO\cdot + \cdot OH \quad (C)$$

$$RO\cdot + RH \rightarrow ROH + R\cdot \quad (D)$$

$$HO\cdot + RH \rightarrow H_2O + R\cdot \quad (E)$$

$$R\cdot + R\cdot \rightarrow R{-}R \quad (F)$$

Molecular enlargement

$$RO_2\cdot + RO_2\cdot \rightarrow 2RO\cdot + O_2 \quad (G)$$

At temperatures above 150 °C homolytic cleavage of the hydroperoxide is likely to occur rapidly, reaction (C). The alkoxy and hydroxy radicals formed may then as one possibility undergo hydrogen abstraction, reactions (D) and (E). Hereby two neighbouring alkyl radicals are created which in the absence of oxygen may combine and result in molecular enlargement, reaction (F). This reaction sequence should be a parallel to ordinary peroxide curing of PE and may account for the immediate molecular enlargement observed above 150 °C. The C-C-bonds formed should not be susceptible to hydrolysis.

In Durability of Macromolecular Materials; Eby, R.;
ACS Symposium Series; American Chemical Society: Washington, DC, 1979.

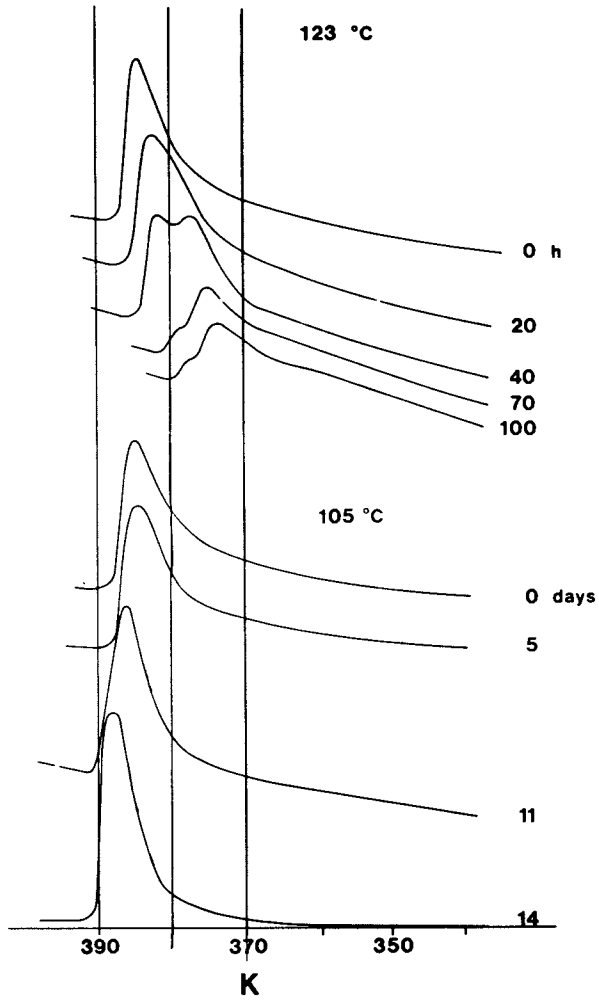

Figure 5. DSC thermograms for additive- free LDPE heated at 105° and 123°C in air

In Durability of Macromolecular Materials; Eby, R.;
ACS Symposium Series; American Chemical Society: Washington, DC, 1979.

The molecular diminishing observed, as well as the majority of the oxygen containing groups formed, (alcohols, acids, esters and ketones) is due to a variety of reactions undergone by the alkoxy radicals.

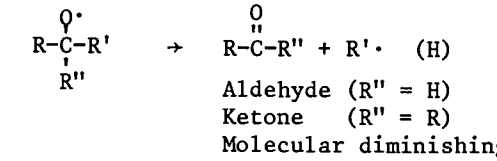

Reaction (D) will for example provide one possible route to alcoholic groups, while an alternative reaction, β-scission of a secondary alkoxy radical, will give aldehyde, reaction (H), which rapidly oxidizes further to peracid. β-scission of a tertiary alkoxy radical result in ketones. Aldehydes and ketones may react further with peracid to give acid and ester groups.

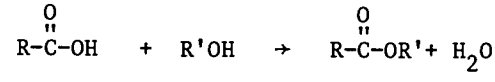

Because of the accumulation of acid and alcoholic groups, reaction (I) becomes increasingly frequent. The formation of ester linkages provides another route to molecular enlargement besides the "peroxide curing". The ester bonds should be prone to hydrolysis, however.

The mechanisms discussed above provide the basis for a reasonable explanation to the observed differences in the degradation course above and below 150 °C. Above 150 °C "peroxide curing" will give immediate molecular enlargement. Later on, when degradation products have accumulated, ester formation should also contribute to the extensive molecular enlargement observed. Molecular diminishing should mainly be due to reaction (H). Below 150 °C no "peroxide curing" seems to occur. Instead, molecular diminishing, reaction (H), will dominate for a long time until the necessary build-up of acid and alcoholic groups has been accomplished to enable ester formation.

The difference in sensitivity to hydrolysis between the C-C-bonds formed by "peroxide curing" and the ester bonds made it possible to test the suggested scheme. n-$C_{44}H_{90}$ was used as a model substance. The results from GPC-analysis are shown in Fig. 6. Hydrolysis by KOH in isopropanol at 50 °C for 1 week of the material heated at 123 °C show that ester formation is the only molecular enlargement reaction operating at this temperature. At 180 °C, on the other hand, it is evident that esterification is only partly responsible for the molecular enlargement, as there are significant amounts of enlarged material not affected by the KOH treatment. The loss of low MW material for the hydrolyzed samples is due to its solubility in the isopropanol.

In Durability of Macromolecular Materials; Eby, R.;
ACS Symposium Series; American Chemical Society: Washington, DC, 1979.

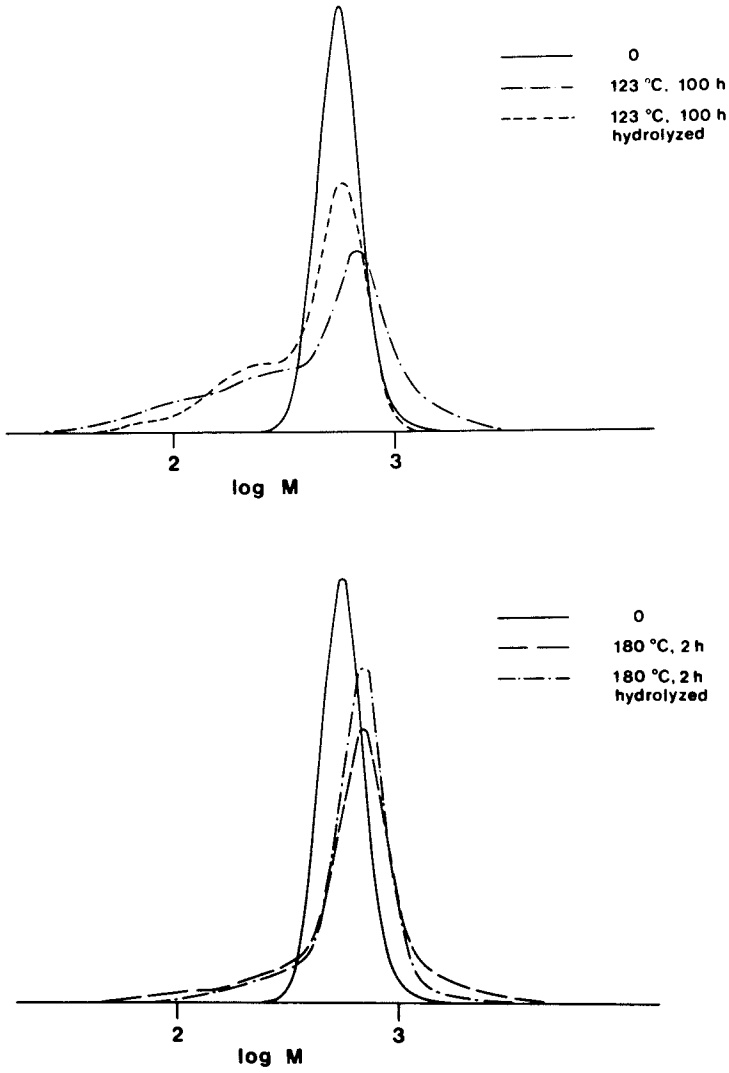

Figure 6. Normalized GPC chromatograms for n-$C_{44}H_{90}$ *samples heated in air at 123° and 180°C before and after hydrolysis*

In Durability of Macromolecular Materials; Eby, R.;
ACS Symposium Series; American Chemical Society: Washington, DC, 1979.

There may be several reasons for the disappearance of the "peroxide curing" below 150 °C. One important factor is the increasing availability of oxygen with decreasing temperature and reaction rates. This should make it more difficult for two alkyl radicals to survive long enough to undergo reaction (F). Instead they will more probably form peroxy radicals according to reaction (A) and end up in alkoxy radicals according to reaction (G) or hydroperoxides, reaction (B). Another important factor may be that the probability for the formation of a pair of alkyl radicals will decrease heavily because of the fact that reaction (C) becomes less favoured for the transformation of hydroperoxides, as recently emphasized by Hiatt (28) and Benson (29). Instead, assisted decomposition by oxygen containing structures or radical attack on the hydroperoxides are more likely to occur.

Influence of additives on the degradation course

Antioxidants. A number of AO-systems have been investigated at different temperature levels concerning their influence on the degradation course of LDPE, Table I. In all cases 0.1 % of each AO was used.

Table I
Antioxidant Systems Used

Compound	Temperature °C			
	105	123	150	180
2,4-tert.-butyl-6-methyl-phenol(BHT)	x	x	x	x
4,4'-thiobis(3-methyl-6-tert.butyl-phenol), (Santonox R)	x			
1,1,3-tri(2-methyl-4-hydroxy-5-tert.-butyl-phenyl) butane (Topanol CA)	x	x	x	x
tetrakis[methylene-3(3',5'-di-tert.-butyl-4'-hydroxylphenyl) propionate] methane, (Irganox 1010)	x	x	x	x
di-lauryl-di-thio-propionate (DLTP)	x	x	x	x
BHT + DLTP		x	x	x
Topanol CA + DLTP		x	x	x
Irganox 1010 + DLTP		x	x	x

These AO-systems showed, as expected, considerable differences in their stabilizing efficiency, but none of them showed any marked influence on either the rate or the course of degradation after the induction period (5). This result was somewhat surprising, as we observed marked effects on the degradation course by an unidentified AO-system in an HDPE (Marlex 6001) at 150 and 160 °C previously (2).

In Durability of Macromolecular Materials; Eby, R.;
ACS Symposium Series; American Chemical Society: Washington, DC, 1979.

Titanium Dioxide Pigments. The influence of all commonly used types of TiO_2 pigments was tested at 150 °C, Table II (3) with 40 % loading, corresponding to a master-batch composition.

Table II
TiO_2 Pigments Used

Designation		Type	Modified with	TiO_2-content %
Kronos	D5[1]	rutile	-	99
"	RN45[1]	"	Al coating	95
"	RN47[1]	"	Al, Si coating, Zn	89
"	RNCX[1]	"	Al, Si, organic coating, Zn	92.5
"	RNCX-P[1]	"	Al, Si, silicone, organic coating	92.5
"	CL220[1]	"	" " " " "	92.5
Finntitan	RFU[2]	"	Zn	98
Kronos	A[1]	anatase	-	99
"	AV[1]	"	Al, Si coating	96

1 TiO_2 produced by Kronos Titan A/S, Norway
2 " " " " Kemira Oy, Finland

The uncoated pigments promoted degradation while the coated qualities exerted a stabilizing action, increasing with the degree and complexity of the coating. Uncoated TiO_2-pigments also caused a pronounced yellowing of LDPE containing phenolic AO, already during the mixing operation. No effects on the degradation course were observed, however.

Carbon Black Pigments. A series of CB-pigments, Table III were also studied at 2 % load (7). They include the types recommended by the suppliers as UV-shielding pigments for polyolefins. The heating temperature was 105 °C.

Table III
Carbon Blacks Used

Designation	Nigrometer Index[1]	DBP absorption[1] ml/100g	Av.Particle Size[1] Å	Surface Area[1] m^2/g	Volatiles[2] wt %	pH[1]
Flamruss 101[3]	102	100	950	21	1.0	7
Corax P[3]	87	-	190	120	1.0	9
Printex 60[3]	87	115	210	115	2.2	9
Printex V[3]	83	120	250	110	7.8	4
Monarch 700[4]	78	127		200	6.6	
" 800[4]	74	75		210	1.4	
" 880[4]	74	115		220	8.4	
" 900[4]	69	75		230	7.8	
" 1100[4]	65	70		240	7.3	

1 Values given by the producer as typical for the product.
2 Determined by heating at 950 °C for 10 min. under nitrogen in a Perkin-Elmer TGS-2 thermogravimetric equipment.
3 CB produced by Degussa, Frankfurt, W. Germany.
4 CB produced by Cabot Corporation, Boston, Mass., USA.

In Durability of Macromolecular Materials; Eby, R.;
ACS Symposium Series; American Chemical Society: Washington, DC, 1979.

At the concentration used, the different types of CB showed large differences in stabilizing effect (7). The extremes being Flamruss 101 at the low efficiency end and Printex V and Monarch 1100 on the other.

Besides this, CB also influences the degradation course. In the initial stages after the induction period, no effects are observed. At this stage, as is the case for the undegraded material, the CB can be filtered off from a 135 °C TCB-solution of the sample, without any detectable loss of PE. Later on the CBs cause the main part of the samples to be insoluble, however, presumably by forming a "carbon gel" (30). This is supported by the fact that it was not possible to extract any further material from the "gel" by increasing the temperature of the TCB to 180 °C and keep it for 5 h or to treat the "gel" with KOH in isopropanol which otherwise completely hydrolyze LDPE crosslinked by oxidation in this temperature range, as discussed above. The presence of "carbon gel" also influences the mechanical properties of the degraded samples, making them considerably less brittle than comparable samples of LDPE free from additives or containing AOs or TiO_2 pigments.

Conclusions

LDPE, HDPE and n-$C_{44}H_{90}$ follow the same course of thermo-oxidative degradation when they are free from additives and present in the liquid state. The same course is also followed by LDPE compositions containing several different AO-systems and TiO_2 pigments. The CB-pigments tested caused the formation of significant amounts of insoluble and non-hydrolyzable material ("carbon gel"), however, which markedly influenced the structural changes and the mechanical properties of the degraded LDPE.

Two large discontinuities in the relation between degradation course and temperature were found. One at 150 °C and the other at T_m for the PE. Extrapolation of accelerated testing results obtained at temperatures above T_m to predict service lifetimes under commonly employed conditions for PE therefore seems highly inaccurate. This is also in accordance with the findings of for example Howard and coworkers at Bell (31), who have reached their conclusions on quite other evidence, however.

Acknowledgement

Financial support from the Swedish Board for Technical Development is gratefully acknowledged. The author also wish to thank Dr. E. Sörvik for the close co-operation and encouragement during the work.

In Durability of Macromolecular Materials; Eby, R.;
ACS Symposium Series; American Chemical Society: Washington, DC, 1979.

Literature Cited

1. See e.g. Reich L. and Stivala S.S. "Autoxidation of Hydrocarbons and Polyolefins" Marcel Dekker Inc., New York, 1969 and Hawkins W.L. (Ed.), "Polymer Stabilization", Wiley-Interscience, 1972.
2. Holmström A. and Sörvik E.M., J. Polym. Sci. Polym. Chem. Ed., In press.
3. Holmström A., Andersson A. and Sörvik E.M. Europ. Polym. J., (1977) 13 483.
4. Holmström A. and Sörvik E.M., Polym. Eng. Sci., (1977) 17 700.
5. Söderqvist G. and Ulfenborg B., Diploma works, Chalmers University of Technology, Gothenburg, Sweden (1976) and (1977).
6. Gustafsson I., Diploma work, Åbo Akademi, Åbo, Finland (1977)
7. Holmström A., Unpublished results.
8. Holmström A. and Sörvik E.M., J. Polym. Sci. Polym. Symp. Ed. (1976) 57 33.
9. Holmström A. and Sörvik E.M., J. Chromatog., (1970) 53 95.
10. Holmström A. and Sörvik E.M., J. Appl. Polym. Sci., (1974) 18 761.
11. Drott E.E. and Mendelson R.A., J. Polym. Sci., A-2, (1970) 8 1361 and 1373.
12. Ke B., J. Polym. Sci., (1960) 42 15.
13. See e.g. Beachell H.C. and Tarbet G.W., J. Polym. Sci., (1960) 45 451.
14. Luongo J.P., J. Polym. Sci., (1960) 42 139.
15. Adams J.H., J. Polym. Sci., A-1., (1970) 8 1077 and 1269.
16. Melzer T.H. and Goldey R.N., SPE Trans., (1962) 2 (1) 11.
17. Melzer T.H. and Supnik R.S., J. Appl. Polym. Sci., (1964) 8 89.
18. Grafmüller F. and Husemann E., Makromol. Chem., (1960) 40 161 and 172.
19. Kavafian G., J. Polym. Sci., (1957) 24 499.
20. Hawkins W.L., Matreyek W. and Winslow F.H., J. Polym. Sci., (1959) 41 1.
21. Ballard D.G.H. and Dawkins J.V., Europ. Polym. J., (1974) 10 829.
22. Keller A., Martuscelli E., Priest D.J. and Udagawa Y., J. Polym. Sci., A-2, (1971) 9 1807.
23. Winslow F.H., Hellmann M.Y., Matreyek W. and Salovey R., Am. Chem. Soc. Polym Prep., (1967) 8 (1) 131.
24. Winslow F.H., Aloisio C.J., Hawkins W.L., Matreyek W. and Matsuoka S., Chem. Ind., (1963) 1465.
25. Winslow F.H., Aloisio C.J. and Hawkins W.L. Am. Chem. Soc. Polym. Prep., (1963) 4 (2) 706.
26. Winslow F.H. and Matreyek W., Am. Chem. Soc. Polym. Prep. (1966) 7 (2) 540.
27. Winslow F.H., Hellmann M.Y., Matreyek W. and Salovey R. Am. Chem. Soc. Polym. Prep., (1967) 8 (1) 131.

In Durability of Macromolecular Materials; Eby, R.;
ACS Symposium Series; American Chemical Society: Washington, DC, 1979.

28. Hiatt R. in Swern D. (Ed.) "Organic Peroxides Vol. 2" p.1., Wiley-Interscience, New York, 1971.
29. Benson S.W. and Shaw R. in Swern D. (Ed.) "Organic Peroxides Vol. 1". p. 105. Wiley-Interscience. New York, 1970.
30. See e.g. Donnet J.-B. and Voet A. "Carbon Black. Physics, Chemistry and Elastomer Reinforcement", p. 276, Marcel Dekker Inc., New York and Basel, 1976.
31. Howard J.B. and Gilroy H.M., Polym. Eng. Sci., (1975) 15 268.

RECEIVED December 8, 1978.

5

Long-Term Photo-and Thermal Oxidation of Polyethylene

H. M. GILROY

Bell Laboratories, Murray Hill, NJ 07974

In this work, the expression "long term" requires defining. For photo-oxidation it refers to natural outdoor exposure up to 38 year duration and artificial accelerated weathering up to two years. In the case of thermal oxidation samples have been maintained at constant temperature for up to seven years.

PHOTO-OXIDATION

The materials examined in this study include both low density polyethylene (LDPE) and high density polyethylene (HDPE) protected by carbon black. These polyethylenes represent several different generations of polymers exposed at various times, the greater bulk of the samples having been exposed from 1946 through 1951. The very early work on the photo-oxidation of polyethylene was carried out in accelerated weathering machines and the compounds selected for outdoor exposure were generally based on the results obtained from accelerated weathering.

In 1950 Wallder, et al.(1) established that 100 hours accelerated weathering was equivalent to one year of natural outdoor exposure for LDPE containing 1% or more of a well dispersed carbon black. Longer exposures outdoors have shown,(2) however, that the relationship is not linear due to a complex relationship between the photo-initiated and thermal degradation processes that occur under two different sets of conditions.

EXPERIMENTAL

The compounds examined in this work contained channel carbon blacks varying in size from 9 to 28 mμ and furnace blacks from 20 to 78 mμ. The polyethylenes used represented the best commercial material available at any given time for cable jacket use.

Outdoor samples were exposed at three locations in the United States; New Jersey, Florida and Arizona at a 45° elevation facing due south.

Accelerated weathering was carried out in a modified X1A

0-8412-0485-3/79/47-095-063$05.00/0

In Durability of Macromolecular Materials; Eby, R.;
ACS Symposium Series; American Chemical Society: Washington, DC, 1979.

Atlas Weather-Ometer described in reference 2. Samples were exposed 50 cm from a bare carbon arc (no filters) and with a 90° sector immediately preceeding the water spray blocked off by a metal baffle to simulate night conditions.

Evaluation of mechanical damage due to photo-oxidation was monitored by changes in low-temperature brittleness per ASTM D746 and by decrease in percent elongation as determined in a standard tensile strength test. Selected samples were examined for changes in bulk oxidative stability by thermal analysis where a specimen is heated in an oxygen atmosphere and the time to onset of the exotherm due to oxidation measured.

The development of surface oxidation was monitored in several materials by internal reflectance infra-red techniques described in reference 3.

Melt Index measurements were made per ASTM D1238, Condition E.

Thermal analysis measurements were made using a duPont 990 Thermal Analyzer using aluminum pans and a heating rate of 10°C/min. Melting endotherms were determined in the presence of helium. Oxidative induction times were measured isothermally at 200°C in the presence of oxygen. A detailed description of this technique is given in reference 4.

WEATHERING RESULTS

Low-Density Polyethylene. The data from outdoor weathering are summarized in Figure 1. The low-temperature brittleness (LTB) measurements show that a well-dispersed carbon black of > 1% concentration and < 35 millimicrons (mμ) particle size is necessary for maximum resistance to photo-oxidation. The results from elongation measurements agree with those found for LTB, as would be expected, since both measurements reflect the notch sensitivity of polyethylene to micro cracks caused by photo-oxidation. Accelerated weathering studies on these compounds have been reported previously (2) and indicate the same ranking as found in outdoor exposure.

The data shown in Figure 1 are representative of many samples containing channel or furnace type carbon blacks and for a given particle size above 1% concentration both blacks afford equal protection.

Examination of the surface of these well protected weathered polyethylenes by internal reflectance infrared spectroscopy (3) shows that surface oxidation, as measured by carbonyl formation, occurs within a few months, but after about a year of outdoor exposure further increase in surface carbonyl is very slight.

However, although rapid oxidation is essentially confined to the surface other changes do occur in the bulk material as time of exposure increases. The melt index of the polyethylene decreases, indicating that crosslinking is occurring (Table I). This is a result of thermal oxidation of the bulk material, as

In Durability of Macromolecular Materials; Eby, R.;
ACS Symposium Series; American Chemical Society: Washington, DC, 1979.

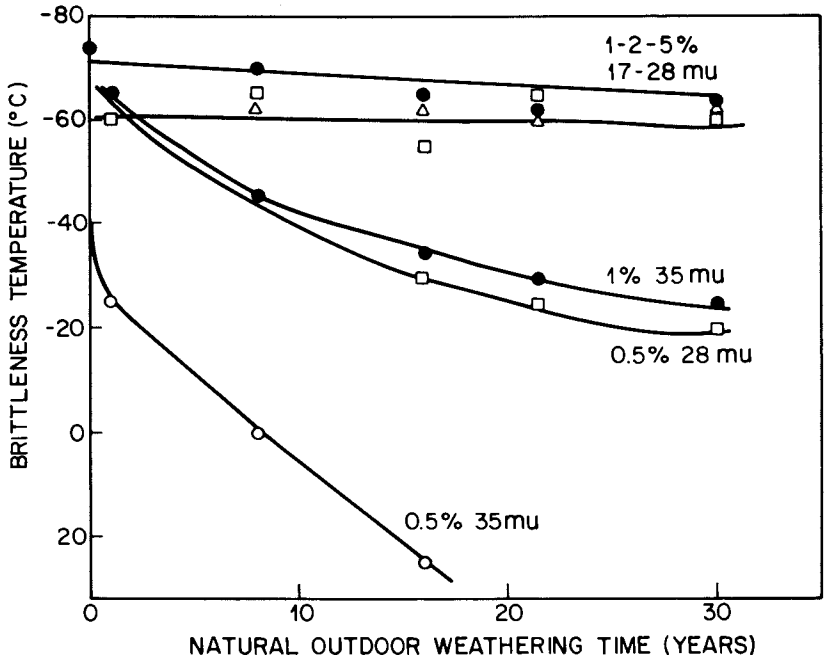

Figure 1. Change in low-temperature brittleness for low-density polyethylene protected by various carbon blacks

In Durability of Macromolecular Materials; Eby, R.;
ACS Symposium Series; American Chemical Society: Washington, DC, 1979.

the black polyethylene heats up outdoors (polymer temperatures up to 70°C have been recorded(5)).

TABLE I

Melt Index Change Produced by Outdoor Weathering
LDPE with 2.5% Channel Carbon Black

Year Exposure Outdoor, Arizona	Melt Index
0	2.0
2	1.7
6	1.6
10	1.3
15	1.1

Annealing effects due to this heating on exposure also occur, and can be seen in LDPE as a form of secondary crystallization when examined by thermal analysis. Figure 2 shows the presence of a large shoulder on the melting endotherm, representing material that has recrystallized during outdoor exposure.

The exposed compounds also show a slow decrease in resistance to thermal oxidation at elevated temperatures, when measured by conventional techniques of oxygen uptake or thermal analysis. Table II shows typical thermal analysis data on samples weathered in New Jersey for 10 years. Similar measurements on compounds exposed for 30 years show that some thermal oxidative stability still remains in the bulk material.

TABLE II

Decrease in Thermal Oxidative Stability
During Outdoor Weathering of LDPE
With 2.5% Channel Carbon Black

Outdoor Exposure, N.J. Years	Oxidative Induction Time(1) Minutes at 200°C (2)	(3)
0	66	-
6	50	-
10	25	-
22	-	11
30	-	8

(1) Measured by Differential Scanning Calorimetry

(2) Stabilized with 0.1% phenolic antioxidant

(3) Stabilized with 0.2% amine antioxidant

High Density Polyethylene. Extrusion grades of high-density polyethylene protected by 2.5% channel type black of 19 mμ particle size were exposed in a Weather-O-Meter for 10,000 hours without any evidence of serious mechanical damage, as measured by low temperature brittleness and elongation tests. This represents the useful limit in our accelerated weathering test, since as described in an earlier paper,(2) film-like deposits form on

In Durability of Macromolecular Materials; Eby, R.;
ACS Symposium Series; American Chemical Society: Washington, DC, 1979.

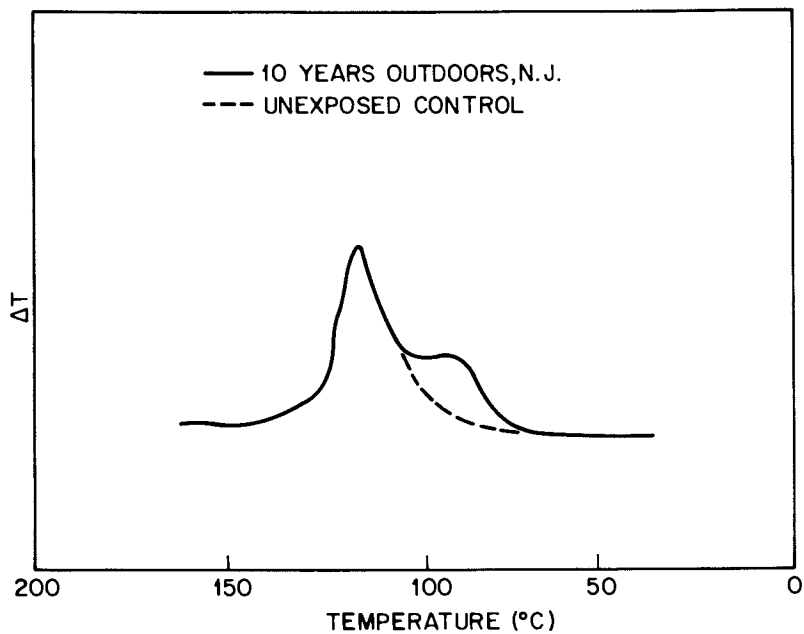

Figure 2. Annealing of low-density polyethylene after ten years outdoors in New Jersey. Thermal analysis heating rate of 10°C/min.

In Durability of Macromolecular Materials; Eby, R.;
ACS Symposium Series; American Chemical Society: Washington, DC, 1979.

the surface and after about 8000 hours weathering effectiveness is lost. However, if we apply the correlation obtained between accelerated and natural outdoor exposure of low-density polyethylene(2) to high-density polyethylene then these high-density polyethylenes will resist photo-oxidation for well in excess of forty years.

Outdoor exposure of these high-density samples for the last 18 years caused no substantial change due to surface oxidation. Bulk changes similar to those found in low-density polyethylene were also found in these high density materials. The melt index slowly decreases and the overall thermal stability measured at high temperature by thermal analysis decreases. However, the secondary crystallization seen in low-density polyethylene was not detected in these high density compounds.

Thermal Oxidation. The majority of materials tested in this phase of the program were in the form of wire insulation (22-26 AWG) but the factors involved in the thermal oxidation of wire insulation have been shown to be the same as those that occur in films and sheets, etc. That is, the polymers rapidly lose stabilizer, oxidize and mechanical failure occurs.

Extensive studies of polyolefin thermal oxidation at elevated temperatures (above the melt) have been reported, but extrapolation of these data to lower temperatures (below the melt) have led to over optimistic estimates of the life-time of these polyolefins.(4) In order to obtain more realistic values for polyolefin lifetimes, samples were tested at temperatures from 110°C to 40°C at 10°C intervals. Small, individual static air ovens were used to isolate individual types of samples and prevent cross contamination.

Samples were maintained at constant temperature and monitored until mechanical failure due to thermal oxidation occurred. Decrease in oxidative stability was followed by thermal analysis and initiation of oxidation by infrared detection of carbonyl species. Failure was defined as the appearance of cracks produced by periodic mechanical stressing.

The time to mechanical failure due to thermal oxidation for several non-black samples is shown in Figure 3. Here it is seen that the high-density polyethylene is more resistant to thermal oxidation than the low-density material. This can be related to the rate of loss of antioxidant, which is lost more slowly from the high density polyethylene. Since these are wire insulation samples in contact with copper, the addition of a metal deactivator would further increase their longevity.

In actual use, the catalytic oxidative degradation of polyolefins is controlled, to a large extent, by the additives and contaminants present in the polymer. Although the stability of polyethylene is related initially to the antioxidant concentration and type, upon aging the critical factor is the rate of loss of the antioxidant. Figure 4 shows typical examples of effective stabilizer loss, due to migration on aging. The samples, shown

In Durability of Macromolecular Materials; Eby, R.;
ACS Symposium Series; American Chemical Society: Washington, DC, 1979.

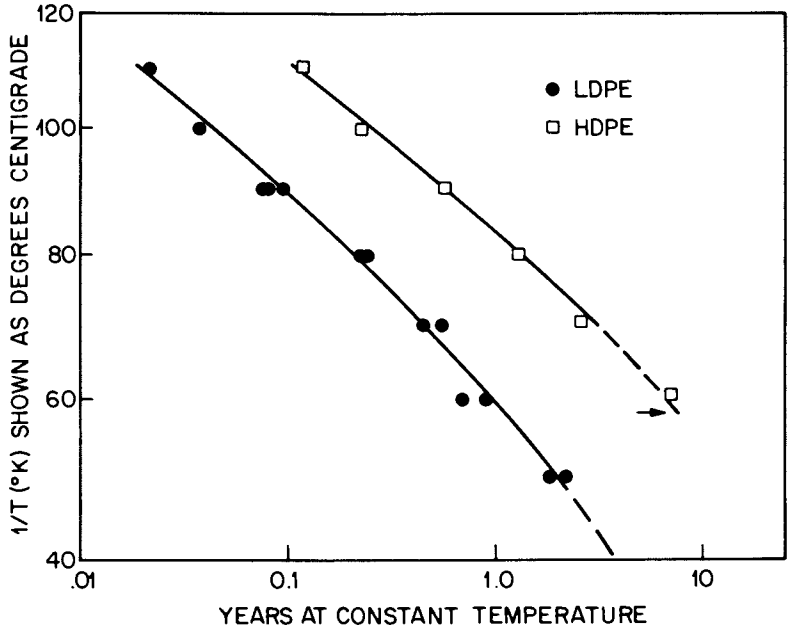

Figure 3. Mechanical failure caused by thermal oxidation. Both samples stabilized with 0.1% phenolic antioxidant.

In Durability of Macromolecular Materials; Eby, R.;
ACS Symposium Series; American Chemical Society: Washington, DC, 1979.

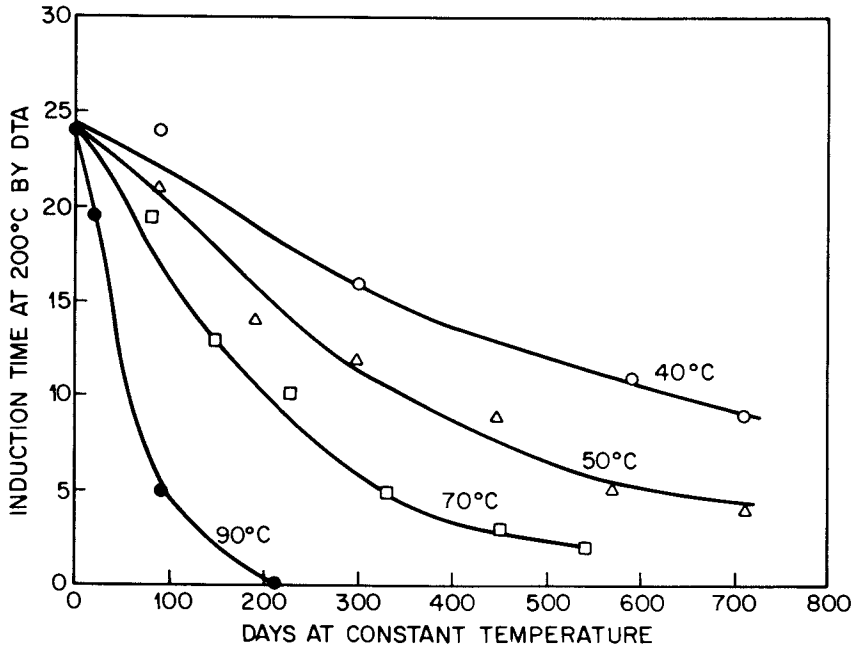

Figure 4. Loss of effective stabilization in low-density polyethylene. Induction time measured by differential scanning calorimetry.

In Durability of Macromolecular Materials; Eby, R.;
ACS Symposium Series; American Chemical Society: Washington, DC, 1979.

in Figure 4, are low density polyethylene wire insulation heated in static air ovens. They contained an initial concentration of 0.1% phenolic antioxidant and 0.1% metal deactivator.

The loss of effective stabilization is predominantly physical, not chemical, as identification of stabilizer on the surface of aged polyolefins has shown.(6,7) The concentration of antioxidant dissolved in the polymer and the resulting oxidative stability decrease with time and approach equilibrium for the temperature of concern. The entire process is complex, with stabilizer solubility only a few parts per million at room temperature(8) and diffusion of stabilizer from the polymer rapid. At higher temperatures (40-70C) both solubility and diffusion increase with opposite effects on stabilizer retention and more rapid loss in oxidative stability.

Impurities and contaminants can also affect the lifetime of polyolefins, generally in an adverse manner. The adverse effect of copper on the long-term stability of polyolefins is well known.(9,10) Other active metals have also been shown to accelerate the oxidation process.(11, 12)

Additives can also affect the longevity of polyethylene. Processing aids, such as polypropylene or low molecular weight polyethylene decrease the long-term stability of wire insulation. Pigments can also be detrimental. Titanium dioxide has been shown to interact with phenolic type antioxidants(13) and several investigators(14,15) have shown titanium dioxide and some red pigments(16) to be inferior to other colors, insofar as long term thermal oxidative stability is concerned.

One additive that improves both long-term photo and thermal stability of polyethylene is carbon black. The ability of carbon black to retard destructive thermal oxidation in polyethylenes at elevated temperatures is well known(17) and, as was seen in the earlier section of this paper on photo oxidation, it is effective at lower temperatures also. Our studies of the thermal oxidation of low-density polyethylene show black samples to be outstanding, even in the presence of copper. For example black low-density polyethylene wire insulation is still intact after 7 years at 80°C while all other colors, including unpigmented, failed mechanically due to oxidation after only about 3 months.

Mechanical failure during the thermal oxidation of non-black polyethylene changes during the oxidative process. Samples oxidize slowly with little change in mechanical properties until the onset of autocatalytic oxidation. During the early part of this rapid oxidation both scission and crosslinking occur and mechanical failure of the material can be induced by strain or impact. As thermal oxidation progresses, crosslinking predominates and mechanical properties improve until, as the material approaches 30-50% gel (as measured by extration in boiling xylene) the polymer becomes highly resistant to mechanical failure. Upon further oxidation the gel content nears 70-80% and

In Durability of Macromolecular Materials; Eby, R.;
ACS Symposium Series; American Chemical Society: Washington, DC, 1979.

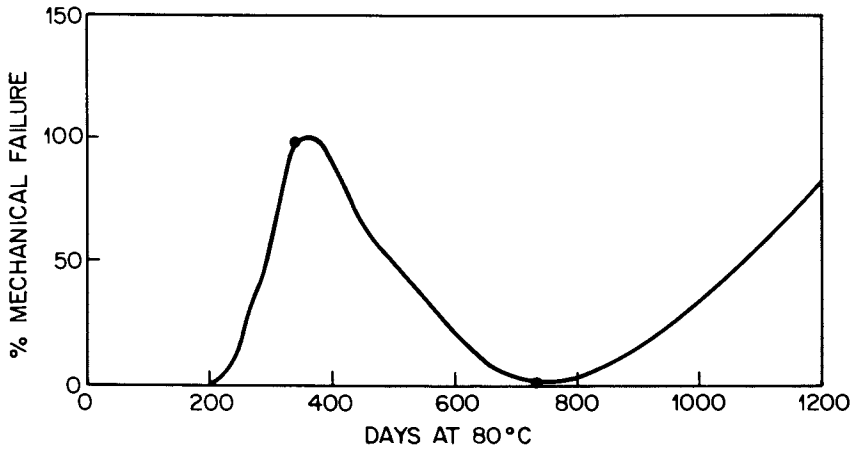

Figure 5. Mechanical failure during thermal oxidation of wire insulation at 80°C

In Durability of Macromolecular Materials; Eby, R.;
ACS Symposium Series; American Chemical Society: Washington, DC, 1979.

crosslinking stops. Then scission again predominates since there are very few sites left to crosslink and mechanical failure again occurs.

Data for this sequence of events for wire insulation at 80°C is shown in Figure 5. The entire process is faster at higher temperatures and slower at lower temperatures.

Black low density polyethylenes have been found to behave differently during thermal oxidation at low temperatures (80 to 40°C). The black samples oxidize and crosslink but they do not fail mechanically, as does non-black LDPE. Hawkins(17) has shown the greater thermal stability of black polyethylene as compared to non-black polyethylene in the solid state. Other investigators (18,19) have demonstrated the activity of carbon black as a free radical trap and others (20) have suggested that polymer radicals form carbon-polymer bonds with the carbon black. The exact reason why the black samples do not fail mechanically even though they oxidize and crosslink is not clear and any one, or a combination of all the above factors could be the cause. It appears that the lack of mechanical failure after oxidation indicates very little or no scission during the oxidative process and finally no further oxidation after the development of the ∿ 70% gel found in oxidized samples.

ACKNOWLEDGMENTS

In a study as extended as the one reported here many individuals are necessarily involved. The author gratefully acknowledges all who contributed, and particularly G. F. Brown, M. G. Chan, J. B. DeCoste, L. Dorrance, C. R. Glenn, J. B. Howard, L. Johnson, V. J. Kuck, L. G. Rainhart and V. T. Wallder.

LITERATURE CITED

1. Wallder, V. T., Clarke, W. J., DeCoste, J. B. and Howard, J. B., Ind. Eng. Chem., (1950), 42, 2320.
2. Howard, J. B. and Gilroy, H. M., Poly. Eng. & Sci., (1969), 9, (No. 4), 286.
3. Chan, M. G., and Hawkins, W. L., Poly. Preprints, (1968) 9, (No. 2), 1938.
4. Howard, J. B., Poly. Eng. & Sci., (1973), 13, (No. 6), 429,
5. Gardner, B. L. and Papillo, P. J., Ind. Eng. Chem. Prod. Res. Dev., (1962), 1, 249.
6. Heyward, I. P., Chan, M. G., Lewis, L., 35th ANTEC, Soc. Plast. Eng., Montreal, (1977).
7. Bair, H. E., Poly. Eng. & Sci., (1973), 13, 435.
8. Roe, R. J. Bair, H. E., & Gieniewski, C., J. Appl. Poly. Sci., (1974), 18, 843.
9. Hansen, R. H., Russell, C. A., DeBenedictis, T., Martin, W. H. & Pascale, J. V., paper presented at 139th Meeting of ACS, 1961.
10. Hawkins, W. L. & Winslow, F. H., Plast, Inst. (London) Trans. (1961), 29, 82.

11. Shelton, J. R., J. Appl. Poly. Sci. (1959, 2, 345.
12. Tobolsky, A. V. & Mesroliam, R. B., "Organic Ploxides" p. 101, Interscience, New York, 1954.
13. Holtzen, D. A., Soc. Plast. Eng. Tech., Papers, (1976) 22, 488.
14. Pusey, B., Chen, M. and Roberts, W., Proc. 20th Int. Wire and Cable Symp., (1971), 209.
15. Howard, J. B., Proc. 21st Int. Wire and Cable Symp. (1972)
16. Gilroy, H. M., Proc. 23, Int. Wire and Cable Symp., (1974), 42.
17. Hawkins, W. L. "Polymer Stabilization", p. 91, Wiley-Interscience, New York, 1972.
18. Donnet, J. B. and Henrich, G., Compt. Re., (1955) 246, 3230.
19. Watson, W. F., Ind. Eng. Chem., (1955), 47, 1281.
20. Szware, M., J. Poly. Sci., (1955), 16, 367.

RECEIVED December 8, 1978.

6

Fourier Transform IR Studies of the Uninhibited Autoxidation of Elastomers

J. R. SHELTON, R. L. PECSOK, and J. L. KOENIG

Department of Macromolecular Science, Case Western Reserve University, Cleveland, OH 44106

The oxidative degradation of elastomers is an autocatalytic process and is termed autoxidation. A plot of time versus the oxygen consumed during the degradation results in an S-shaped curve which is characteristic of autocatalysis. The autoxidation of hydrocarbons is a chain reaction of free radicals and can be represented in general form by the following set of equations (1, 2):

Initiation:

$$ROOH \rightarrow RO\cdot + \cdot OH$$

$$2ROOH \xrightarrow{k_i} RO\cdot + ROO\cdot + H_2O$$

Propagation:

$$RO_2\cdot + RH \xrightarrow{k_p} ROOH + R\cdot$$

$$R\cdot + O_2 \xrightarrow{fast} RO_2\cdot$$

Termination:

$$2R\cdot \rightarrow R\text{-}R$$

$$R\cdot + ROO\cdot \rightarrow ROOR$$

$$2RO_2\cdot \xrightarrow{k_t} \text{nonradical products} + O_2$$

The autocatalytic process can be initiated by thermal, photo, chemical, or mechanical means. It usually begins by the decomposition of small amounts of hydroperoxides which were formed during the preparation and fabrication of the polymer. The decomposition may occur either uni- or bimolecularly to form alkoxy and peroxy radicals. These oxy radicals abstract a labile hydrogen from the hydrocarbon to produce either an alcohol or a hydroperoxide. The alkyl radical thus formed readily adds oxygen to reform a peroxy radical, and the process continues. When the autoxidation occurs in the absence of an antioxidant, the termination of the kinetic chain occurs chiefly by the combination of two peroxy radicals. This termination is a source of alkoxy radicals which can undergo chain scission and give rise to volatile products and carbonyl groups.

0-8412-0485-3/79/47-095-075$05.50/0

The rate of oxidation increases autocatalytically as the newly formed hydroperoxides decompose and initiate new kinetic chains. As the hydroperoxide concentration builds, the rate of initiation becomes essentially controlled by the bimolecular process, k_i (3,4). At normal temperatures, the concentration of R· is negligible with respect to ROO· because of its swift reaction with oxygen. The rate of propagation, then, is governed by the hydrogen abstraction reaction, k_p. Termination via k_t is more likely than crosslinking because of the low concentration of R· radicals.

The early investigations of autoxidation were performed on low molecular weight compounds or involved chemical analysis of the volatile products released from the polymer because the analytical methods consisted of primarily wet chemistry techniques.

In the thermal oxidation of squalene, which is an oligomer of polyisoprene, possible evidence for the occurence of a six-member cyclic dialkyl peroxide was found by Bolland and Hughes (5). One of the isolated products identified was a squalene compound which contained a hydroperoxide and a dialkyl peroxide. Upon reduction, a triol resulted with two of the hydroxyl groups adjacent to each other. This prompted Bolland and Hughes to invoke the following structure in the mechanism of oxidation for polyisoprene:

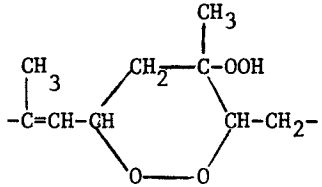

Direct observation of this structure has never been achieved, but its decomposition might yield a product of 2,5-hexanedione as suggested by Tobolsky and Mercurio (6).

Bevilacqua (7, 8, 9, 10) studied the change in molecular weight and the volatile products in the thermal oxidation of synthetic and natural polyisoprene. At 90°C it appeared that every mole of chain scission was accompanied by one mole of a volatile carbonyl compound. Bevilacqua suspected this compound was levulinaldehyde, and this has been substantiated by Percy (11) and Houseman (12) in the oxidation of purified sol rubber at 75°C. Levulinaldehyde could result from the chain scission of a cyclic peroxide structure similar to the Bolland structure:

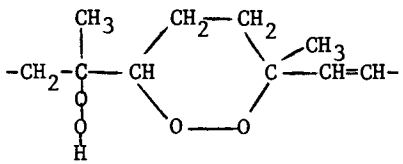

In Durability of Macromolecular Materials; Eby, R.;
ACS Symposium Series; American Chemical Society: Washington, DC, 1979.

Bevilacqua's proposed structure differs from Bolland's by the placement of the hydroperoxide group outside of the peroxy ring. Both of these cyclic peroxy structures are considered to be formed by similar mechanisms. Barnard, Cain, Cunneen, and Houseman (13) have proposed a mechanism for the free radical decomposition of the Bevilacqua structure.

In 1976, Pecsok, Painter, Shelton, and Koenig (14) developed a mechanism for the thermal oxidation of cis-1,4-polybutadiene which incorporated both the Bolland and Bevilacqua structures. Using Fourier transform infrared spectroscopy, the initial oxidative changes in the polymer were obtained for the temperature range of 25-60°C. An oxidative cis/trans conversion was observed as well as formation of di-alkyl peroxide, unsaturated aldehyde, and saturated aldehyde.

Very recently (in 1977), Morand (15) has advanced a mechanism for the oxidation of polyisoprene in the temperature range of 100-140°C which accounts for levulinaldehyde, methyl vinyl ketone, and methacrolein, plus four newly identified volatile products. Using an improved version of Bevilacqua's experimental techniques, six new less volatile products were detected and four of these compounds were identified. Morand's mechanism involves the β-scission of an alkoxy radical (I) to form an unsaturated aldehyde (II) and an alyllic radical (III) which reacts further to produce the observed volatile products.

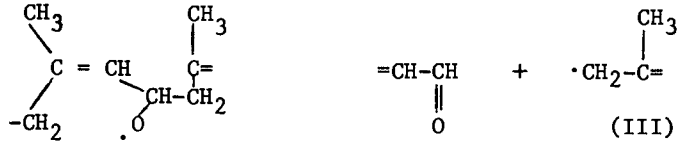

(I) (II) (III) further reaction

Golub (16) found, using ir and NMR, that functional groups of epoxide and alcohol are mainly formed in the oxidation of polybutadiene in the temperature range of 90-180°C. These two products suggest the addition of the peroxy radical to the double bond to form an alkoxy radical and an epoxide group:

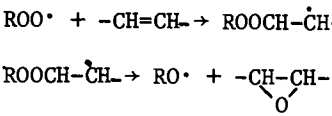

The alkoxy radical is converted to an alcohol by abstraction of hydrogen. The detection of equal amounts of alcohol and epoxide supports this reaction scheme.

Low amounts of dialkyl peroxide were observed in polybutadiene; however, in the oxidation of polyisoprene (17) in the

temperature range of 55-150°C, the peroxides were found to be of nearly the same level as the epoxide and alcohol. Golub attributes the formation of peroxide groups to the following reaction which competes with the epoxidation reaction:

$$ROOCH-\dot{C}H- + O_2 \rightarrow ROOCH-\dot{C}H-OO\cdot$$

Atmospheric oxygen could add to the alkyl radical before the formation of epoxide, resulting in a dialkyl peroxide and a peroxy radical.

Kuzminskii, Degteva, and Lapteva (18) have observed volatile products which vary considerably with the temperature and stage of oxidation. Thus, despite many years of investigation, the autoxidation of elastomers is only partially understood. Many mechanisms of oxidation have been proposed, none are completely consistent with all of the observed oxidation products.

Considerable research in this field has employed spectroscopic techniques -- in particular, infrared spectroscopy. The basis for utilization of this method is the detection of chemical groups such as -OH and C=O formed as a result of oxidation. However, using conventional infrared techniques, it is often difficult to resolve bands of the oxidation products from those of the polymer. This problem is acute in both the initial and final stages of the reaction. In the former case, the low concentration of oxidation products results in extremely weak absorbances and such bands are difficult to detect, whereas in the latter stages of the reaction, only broad, poorly-resolved bands are observed as a consequence of the overlap of polymer bands with those from the diverse products of oxidative attack.

The advent of Fourier transform infrared spectroscopy (FTIR) with its enhanced sensitivity and computer-controlled data handling prompts the re-examination of elastomer autoxidation by infrared spectroscopy. The theory, operation, and capability of FTIR are reviewed by Griffiths (19) and Antoon and Koenig (20). Fourier transform spectroscopy enables increased energy throughout and decreased scan time, greatly reducing the limitations inherent in conventional, dispersive spectrometers. Digital subtraction of spectra performed by an on-line computer depicts the formation of initial products of oxidation which had previously eluded detection.

Experimental

Sample Origin and Preparation. The elastomers listed below were examined. Purification of the polymers from antioxidants was achieved by successive precipitation in methanol from a benzene solution. Following purification, samples were immediately subjected to infrared experimentation. Exposure to light was minimal.

In Durability of Macromolecular Materials; Eby, R.;
ACS Symposium Series; American Chemical Society: Washington, DC, 1979.

Elastomer	Source
cis-1,4-polybutadiene (BR)	The B. F. Goodrich Chemical Co., (CB220), D. Witenhafer
d_4-1,1,4,4,-cis-polybutadiene (d_4BR)	The B. F. Goodrich Chemical Co., C. E. Wilkes
cis-1,4-polyisoprene (IR)	The B. F. Goodrich Chemical Co., (Ameripol)
trans-1,4-polychloroprene (CR)	M. M. Coleman (21), Case Western Reserve University

Fourier Transform Infrared Spectroscopy (FTIR). Films were cast on salt windows from a CS_2 solution. The infrared data were obtained on a Digilab FTS-14 spectrometer which was constantly purged with dry air. High-temperature data was obtained using a thermal cell in the sample chamber. The thermal cell was purged with dry N_2 during the first sampling interval to ensure an unoxidized base spectra. Oxidations at room temperature and at 0°C involved sample storage in a light-free dessicator.

FTIR employs a computer, enabling the mathematical manipulation of digitally-stored spectra. Progressive spectral changes due to oxidation were determined by subtraction of the unoxidized spectra. The ratio of subtraction is variable:

$$k_o(\text{oxidized spectra}) - k_u(\text{unox. spectra}) = \text{difference spectra}$$

where k_o and k_u are variable and can be used to compensate for differences in thickness, etc. For a 1/1 ratio, $k_o = k_u = 1$.

Results and Discussion

Mechanism of Low Temperature Oxidation in BR. A mechanism of oxidation for BR was developed by us (14) previously, consistent with the observed spectral changes. It accounted for the observed oxygen induced conversion of cis to trans, and included the formation of cyclic structures of both the Bolland and Bevilacqua types. The mechanism is expanded in Figure 1 to also include the possible formation of analogous five-membered rings.

Small amounts of peroxide groups initially formed during the preparation and fabrication of the polymers are present in BR and decompose to form oxy radicals. Abstraction of α-methylenic hydrogen by ROO· results in an alyllic radical which can be represented by resonance structures (XI) and (XII). Atmospheric oxygen adds readily to the resonance hybrid of (XI) and (XII) to produce the two peroxy radicals, (XIII) and (XIV). Preserving the double bond minimizes the activation energy of the oxygen addition reaction and the structure may be either cis or trans depending upon which carbon adds oxygen. This cis configuration of the original double bond is retained in (XIII) but the structure in (XIV) could be either cis or trans. It is shown as trans because the preferred conformation of the single bond in the

In Durability of Macromolecular Materials; Eby, R.;
ACS Symposium Series; American Chemical Society: Washington, DC, 1979.

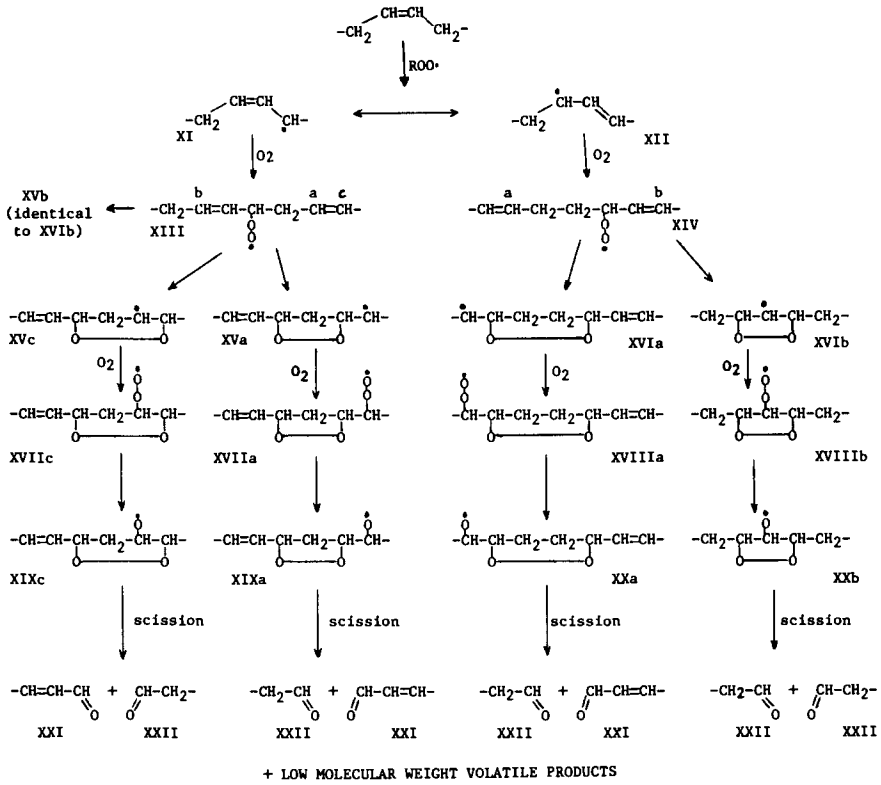

Figure 1. Basic mechanism of thermal oxidation in BR

In Durability of Macromolecular Materials; Eby, R.;
ACS Symposium Series; American Chemical Society: Washington, DC, 1979.

original cis structure is mainly trans for steric reasons and would also be trans in the resonance hybrid. This is consistent with the observed decrease in cis and increase in trans double bonds with time of oxidation.

Peroxy radicals (XIII) and (XIV) can abstract a hydrogen forming hydroperoxide, or add to a neighboring double bond. The preference of hydrogen abstraction to double bond addition is temperature dependent and is discussed later. Intramolecular addition of peroxy radicals (XIII) and (XIV) to an adjacent double bond would result in cyclic peroxy radical structures(XVa), (XVb), (XVc), (XVIa), and (XVIb), depending upon which alkene carbon, a, b, or c, is attacked. Note that (XVb) and (XVIb) are identical structures. Five-membered rings are included where possible because they have the greatest rate of formation in hydrocarbon and alkoxy-hydrocarbon systems (22). Intramolecular addition is favored over intermolecular addition because of the proximity of the two adjacent monomer units. The alkyl radical structures readily scavenge atmospheric oxygen to yield peroxy radicals (XVIIa), (XVIIc), (XVIIIa), and (XVIIIb). Upon hydrogen abstraction, the corresponding hydroperoxides are produced. Alkoxy radicals (XIXa), (XIXc), (XXa), and (XXb) arise from hydroperoxide decomposition and stimulate decomposition of the cyclic peroxide unit via β-scission of the alkoxy radical and cleavage of the O-O bond. Low molecular weight products volatize and escape detection by FTIR.

Saturated aldehyde (XXII) and α,β - unsaturated aldehyde (XXI) groups are produced upon decomposition of the monocyclic-peroxide structures and are depicted in the ir spectra by bands at 1725 and 1700 cm^{-1}, respectively. Structures (XVa), (XVc), and (XVIa) lead to the saturated and unsaturated pairs, while (XVb) and (XVIb) would yield only saturated aldehydes. In the temperature range of 60-120°C, unsaturated and saturated aldehydes detected are of comparable intensity, consistent with formation of (XVa), (XVc), and (XVIa). The formation of (XVb) and (XVIb) is not indicated by these observations and is unlikely since the alkyl radical would be located within a five-membered ring. The alkyl radical projects bond angles of 120° and would be considerably strained if incorporated in a pentagonal ring which normally projects 108° bond angles. The Bevilacqua structure, (XXa), from peroxy structure (XIV), accounts for levulinaldehyde formation. Both the Bolland structure (XIXc) and the five-membered ring (XIXa) would be formed from peroxy structure (XIII) with (XIXa) favored for kinetic reasons as inferred earlier.

The mechanism of Figure 1 is considered to be the basic route of low temperature oxidation. Basic, in the sense that deviations of the mechanism occur which are temperature dependent.

In Figure 2, the spectrum from 2000 to 450 cm^{-1} of unoxidized BR is shown with two difference spectra of oxidized BR minus the unoxidized, scaled to eliminate the BR bands. The center difference spectrum is of a BR sample, aged in air for 1 month at

In Durability of Macromolecular Materials; Eby, R.;
ACS Symposium Series; American Chemical Society: Washington, DC, 1979.

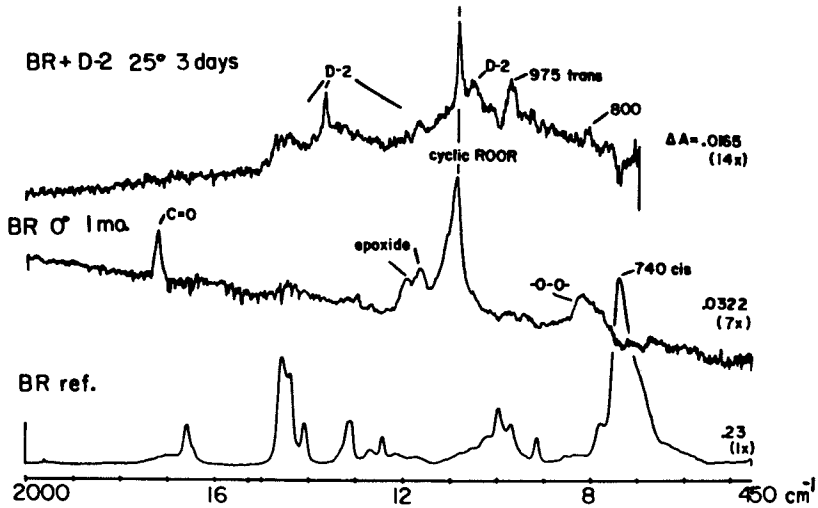

Figure 2. FTIR difference spectra (normalized to band at 1655 cm^{-1}) obtained for BR oxidized under different conditions: (A) BR + di-tert-butylsulfoxide (5 wt %) 3 days at 25°C; (B) BR oxidized at 0°C for one month minus unoxidized BR; and (C) BR unoxidized.

In Durability of Macromolecular Materials; Eby, R.;
ACS Symposium Series; American Chemical Society: Washington, DC, 1979.

0°C in the absence of light and moisture. The strongest band in the spectrum is at 1080 cm^{-1}, corresponding to the C-O band observed in a previous study (14). The absorbance at 820 cm^{-1} is due to O-O stretching and indicates that the C-O band, at least in part, may be due to peroxy. No hydroxyl groups are seen, so the 1080 cm^{-1} band is presumably dialkyl peroxide. The sharpness of the 1080 cm^{-1} band suggests that it is a sterically constrained peroxide, or rather, a cyclic dialkyl peroxide. The bands at 1192 and 1164 cm^{-1} might be attributed to the cyclic peroxide or epoxide.

In oxidations at higher temperatures, the formation of trans methine was observed at 975 cm^{-1} as were saturated and unsaturated aldehydes at 1727 and 1700 cm^{-1}, respectively. In the oxidation at 0°C after one month, saturated aldehyde at 1725 cm^{-1} is detected but there is a lack of trans and an unsaturated aldehyde. This behavior is evidence of a deviation from the mechanism presented in Figure 1.

The proposed cyclic peroxide bands are also observed in BR containing about 5 percent by weight of a peroxide-decomposing antioxidant (D-2), di-t-butyl sulfoxide, shown in the top difference spectrum of Figure 2. The sulfoxide functions by thermal decomposition to products which destroy hydroperoxides (1, 23, 24),but it does not do so at 25°C. After three days at room temperature, stabilized BR exhibited trans methine at 975 cm^{-1} as well as cyclic peroxide at 1080 and 820 cm^{-1}. Apparently, the cyclic peroxide was not decomposed in the presence of the sulfoxide and must be fairly stable at 25°C since no carbonyls were detected.

The FTIR spectrum of the oxidation at 0°C presented in Figure 2 suggests a modified version of the basic mechanism and is shown in Figure 3. Structures (XVIIa) and (XVIIIa) of Figure 1 are presumed to participate predominately in the oxidation mechanism for kinetic reasons previously discussed. Proceeding from the Bevilacqua-type structure (XVIIIa) where a peroxy radical is located outside of the ring, addition of the peroxy radical to a neighboring double bond leads to an alkyl radical site adjacent to a dicyclic peroxide structure (XXIV). A polycyclic peroxide structure develops from further attack by atmospheric oxygen and cyclization. Cyclization propagates along the chain until the peroxy radical: adds to a non-neighboring double bond (intra- or intermolecular); undergoes epoxidation (XXIX); or abstracts a hydrogen, forming hydroperoxide (XXVI).

The peroxy radical of structure (XVIIa) can add to a neighboring double bond forming (XXIII). Further polycyclic peroxidation can occur and hydrogenation (XXV), epoxidation (XXVIII), or addition of the peroxy radical to a non-neighboring double bond terminates cyclization along the chain. Decomposition of a monocyclicperoxy hydroperoxide structure results in an unsaturated and a saturated aldehyde as shown in Figure 1, whereas polycyclicperoxy hydroperoxide structures (XXV) and (XXVI) yield only

In Durability of Macromolecular Materials; Eby, R.;
ACS Symposium Series; American Chemical Society: Washington, DC, 1979.

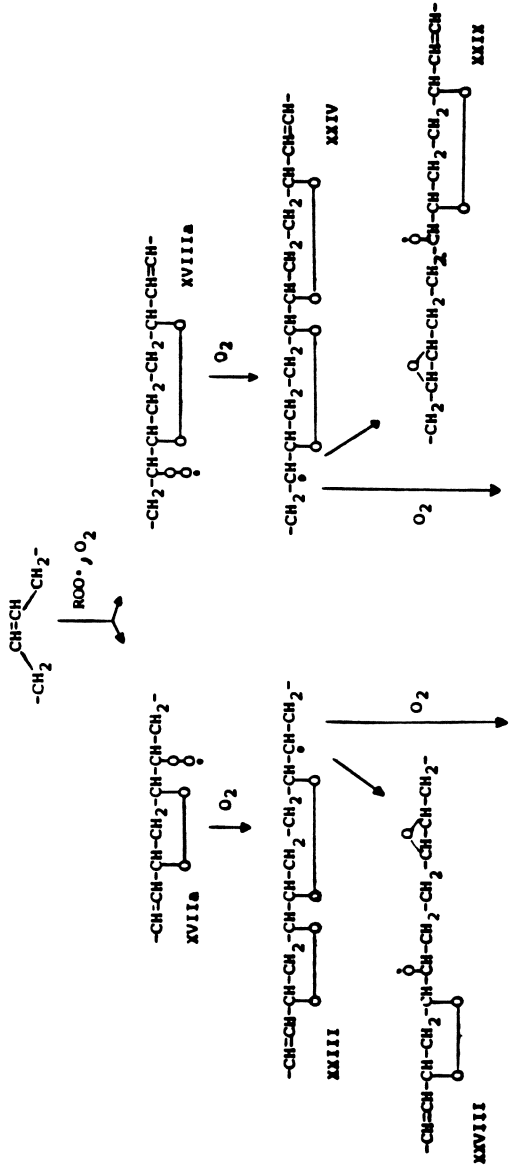

Figure 3. Modified mechanism of thermal oxidation for BR at low temperatures showing polycyclic peroxide formation

saturated aldehyde (in addition to low molecular weight volatile products). Alkoxy radicals in the epoxide structures (XXVIII) and (XXIX) either form an alcohol (16) or undergo β-scission (15).

Propagation of peroxy radicals in autoxidation involves hydrogen abstraction, epoxidation, and addition reactions:

$$ROO\cdot + RH \xrightarrow{k_p} ROO\cdot + R\cdot \qquad \text{hydrogen abstraction}$$

$$R\cdot + O_2 \xrightarrow{\text{fast}} ROO\cdot$$

$$ROO\cdot + C{=}C \xrightarrow{k_e} RO\cdot + \underset{O}{C\text{-}C} \qquad \text{epoxidation}$$

$$ROO\cdot + C{=}C \xrightarrow{k_a} ROO\text{-}C\text{-}\overset{\cdot}{C}\text{-} \qquad \text{addition}$$

Epoxidation and addition can be either intra or intermolecular but, as noted earlier, cyclization involves intramolecular addition. Low oxygen concentration favors epoxide formation because O_2 traps the adduct radical, and high temperature might also, since Gemmer and Golub (16) observed a higher amount of epoxide than dialkyl peroxide in the oxidation of BR from 100° to 150°C. The infrared spectrum of oxidation at 0°C (Figure 2) exhibits the opposite: a large amount of cyclic peroxide (band at 1080 cm^{-1}) and little, if any, epoxide. The temperature behavior is consistent with a lower activation energy for addition than for the corresponding epoxidation reaction in BR.

Existence of polycyclicperoxy structures in elastomer degradation was originally suggested by Mayo (25) and evidence is presented in Figure 2. Dialkyl peroxide bands are present at 1080 and 820 cm^{-1} and no hydroxyl groups are detected. The decomposition product, saturated aldehyde, is evident at 0°C. Absence of trans methine (975 cm^{-1}) implies a large kinetic chain length of addition and very little occurrence of hydrogen abstraction.

Low temperature oxidations typically display the saturated aldehyde but not the unsaturated aldehyde in the initial stages which corresponds to decomposition of the polycyclicperoxy structure. At high temperatures, however, the saturated and unsaturated pair are observed indicating decomposition of monocyclicperoxy structure. This temperature behavior is consistent with a lower activation energy for addition than for hydrogen abstraction. Bevilacqua (26) found that scission efficiency (number of scissions per mole of oxygen absorbed) increases with temperature, also indicating greater participation of hydrogen abstraction at higher temperatures. Polycyclization was also observed in 1,1,4,4,-d_4-cis-polybutadiene (deuterated methylene groups) at higher temperatures than in BR because the deuterium isotope effect impairs hydrogen abstraction.

Addition reactions, both intra and intermolecular, introduce considerable order into the polymer system and would eventually

In Durability of Macromolecular Materials; Eby, R.;
ACS Symposium Series; American Chemical Society: Washington, DC, 1979.

be hampered by steric restrictions. At such a point, peroxy radicals would be more likely to abstract hydrogen. It should be noted that rate constants k_e and k_a are presumably not constant in the polymer oxidation as they fluctuate with changes in the extent of order in the system. Both would be expected to decrease with increasing order because of less chain flexibility and less segmental mobility. Clearly, the degree of order varies with oxidation since crosslinking and chain scission occur. With increasing degradation, elastomers generally become more rigid and thus impede cyclization.

Oxidation Mechanism of IR. The oxidation of cis-1,4-polyisoprene (IR) was examined and the effect of the methyl substituent on the double bond assessed.

Figure 4 shows the 1/1 difference spectra of oxidized IR minus the initial unoxidized IR for 100, 140, and 300 mins. at 80°C. Oxidative changes in the spectra are encountered similar to those found in BR (14). Intensity of the IR bands decreases with time of oxidation, particularly the bands in the 3100-2800 cm^{-1} region and at 838 cm^{-1}. Oxidation products are observed at 100 mins. by the two carbonyl bands at 1720 and 1700 cm^{-1} and the absorbance in the 1100-1060 cm^{-1} region due to C-O groups. After 300 mins., formation of hydroxyl and trans methine groups are denoted by the bands at 3450 and 970 cm^{-1}, respectively. The 2000-450 cm^{-1} region exhibits the hammock effect (27) where the broad absorbances result from the presence of many different oxidation products.

The band at 838 cm^{-1} is of strong intensity and assigned to deformation of the cis methylene group (28). Decrease of the IR bands represents loss of the methylene and cis olefin groups due to oxidation. The 1720 and 1700 cm^{-1} bands are assigned to saturated ketone and α,β-unsaturated aldehyde groups, respectively. Ketones intrinsically absorb more strongly and conjugation lowers the intensity of the aldehyde (29) which explains the stronger intensity of the band at 1720 cm^{-1} compared with the band at 1700 cm^{-1}. Presence of absorbtion in the 1100-1060 cm^{-1} region suggests that the methyl substituent on the double bond enhances the stability of the C-O groups. In contrast, in the oxidation of BR at 60°C (14), very little absorbance of C-O was detected in the initial stages owing to decomposition of C-O groups to carbonyls.

A mechanism of oxidation which is consistent with the spectral changes is presented in Figure 5. Similar to the mechanism proposed for BR in Figures 1 and 3, IR undergoes a process involving hydrogen abstraction, cyclization, and chain scission. Two carbonyls are detected at 80°C, implying decomposition of a monocylicperoxy hydroperoxide. Only a saturated ketone at 1720 cm^{-1} is observed during the early stages of oxidation at room temperature, corresponding to decomposition of polycyclicperoxy hydroperoxide.

In Durability of Macromolecular Materials; Eby, R.;
ACS Symposium Series; American Chemical Society: Washington, DC, 1979.

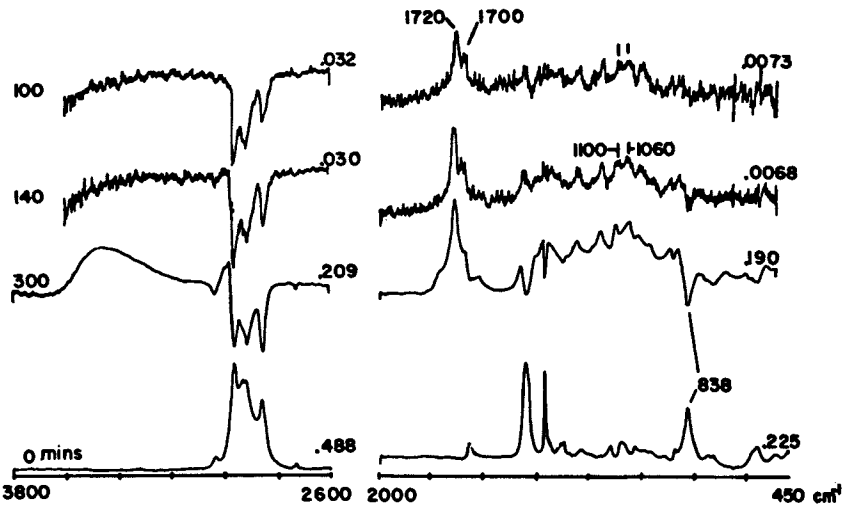

Figure 4. FTIR difference spectra representing the oxidation of IR at 80°C: oxidized IR minus unoxidized IR (ratioed 1/1) after 100, 140, and 300 min.

In Durability of Macromolecular Materials; Eby, R.;
ACS Symposium Series; American Chemical Society: Washington, DC, 1979.

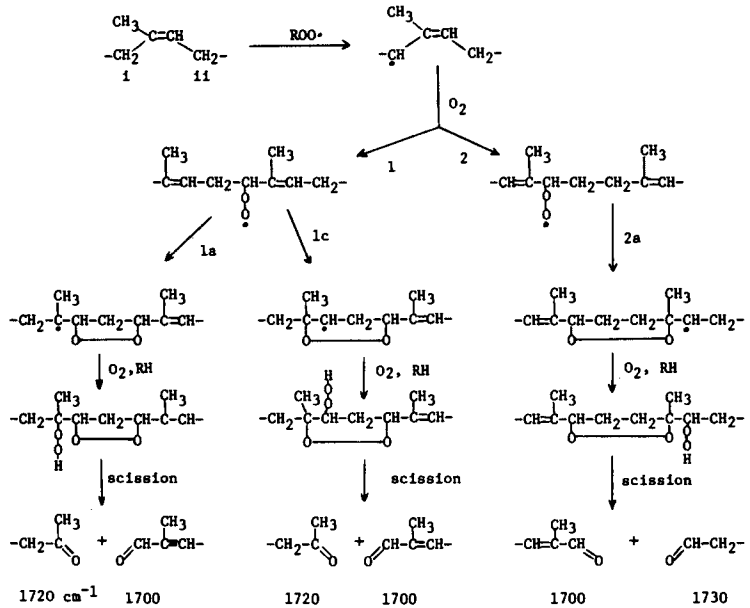

Figure 5a. Basic mechanism of thermal oxidation of IR

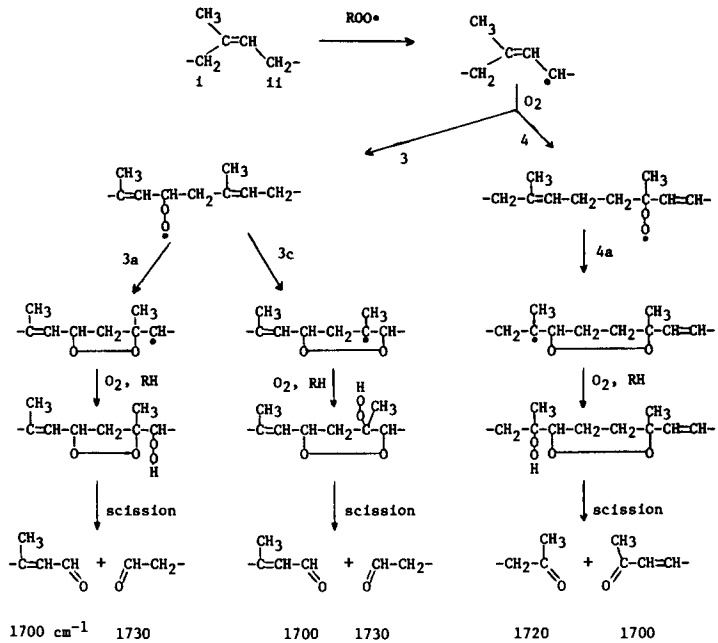

Figure 5b. Basic mechanism of thermal oxidation of IR

In Durability of Macromolecular Materials; Eby, R.;
ACS Symposium Series; American Chemical Society: Washington, DC, 1979.

The methylene groups i and ii of the IR monomer unit have different reactivities because of the methyl substituent on the double bond. The question as to which methylene group is more susceptible to oxidation has been controversial. Bolland (30) predicted that methylene ii is more reactive from structural analysis of the products in the oxidation of 1-methylcyclohexene at 55°C and methyl oleate at 75°C.

As illustrated in Figure 5, hydrogen abstraction by ROO· could occur on either of the two methylene groups, resulting in two pairs of resonance structures. Thus, there are many different reaction paths possible, depending upon where hydrogen abstraction occurs and where oxygen adds on the resonance hybrid of the radical formed. Hydrogen abstraction can occur at methylene group i (paths 1 and 2) or methylene group ii (paths 3 and 4). Paths 1 thru 4 designate where atmospheric oxygen adds to the IR radical after hydrogen abstraction; a and c designate which neighboring alkene carbon is attacked by the peroxy radical. Reaction paths 2a, 3a, and 3c, are not predominant because their decomposition products include a saturated aldehyde (1730 cm^{-1}) in the early stages of oxidation. The same argument excludes the cyclic structures which would form if initial hydrogen abstraction occurred at the methyl carbon. Paths 1a, 1c, and 4a produce pairs of saturated ketone and unsaturated aldehyde/ketone which are observed. The resonance structure preceeding path 1 is identical to that of path 2. However, products of path 2 are not observed which suggests that 1a and 1c are not the principle paths since the rate of path 2a should be comparable. It appears that path 4a is followed preferentially indicating that hydrogen abstraction occurs more readily on methylene group ii in agreement with Bolland's prediction, while localization is favored on the tertiary carbon with cyclization to the structure proposed by Bevilacqua.

Higher reactivity of methylene ii is reasonable because the methyl substituent stabilizes the allylic radical formed during the initial hydrogen abstraction step. The ir absorbance of the C-O groups is greater in IR (Figure 4) than in BR (14) during the initial stages at higher temperatures, possibly because the methyl substituent enhances the stability of the attached oxy groups, such as in the cyclic peroxy structure.

Oxidation Mechanism of CR. A chlorine substituent on the double bond introduces considerable complexity in the degradation of trans-1,4-polychloroprene (CR). CR is more resistant to oxidation than BR and IR, but is subject to dehydrochlorination (32, 33, 34).

Figure 6 shows the initial spectrum of CR at 80°C (top) and the difference spectrum (bottom) of CR after 3 hrs. in air at 80°C minus the initially unoxidized CR. Performing the experiment at 80°C renders CR amorphous and eliminates crystallization effects in the spectra. The difference spectrum represents an early

In Durability of Macromolecular Materials; Eby, R.;
ACS Symposium Series; American Chemical Society: Washington, DC, 1979.

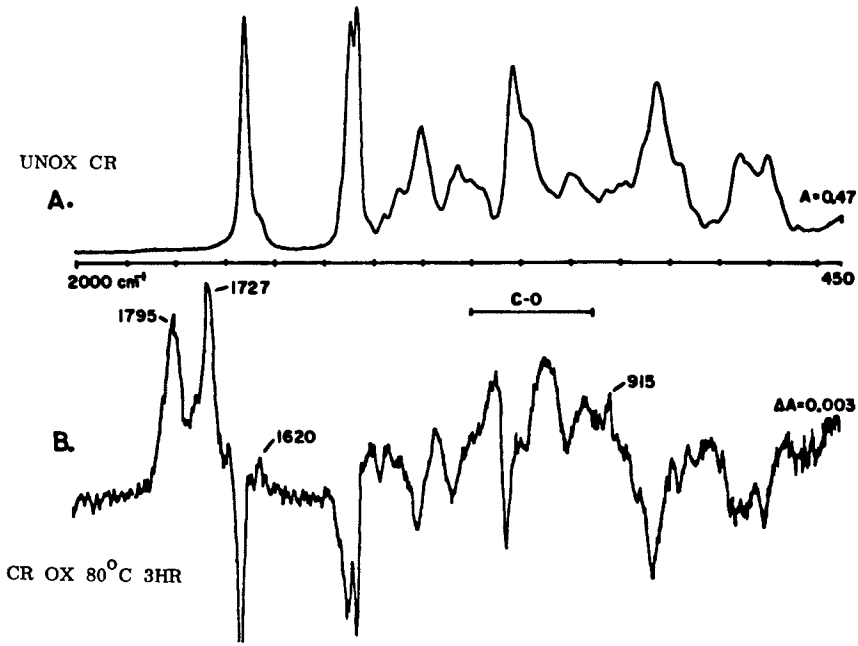

Figure 6. FTIR spectra representing early stage of oxidation in CR: (A) spectrum of unoxidized CR (80°C) and (B) difference spectrum of CR oxidized in air at 80°C for 3 hr minus unoxidized CR (ratioed 1/1).

In Durability of Macromolecular Materials; Eby, R.;
ACS Symposium Series; American Chemical Society: Washington, DC, 1979.

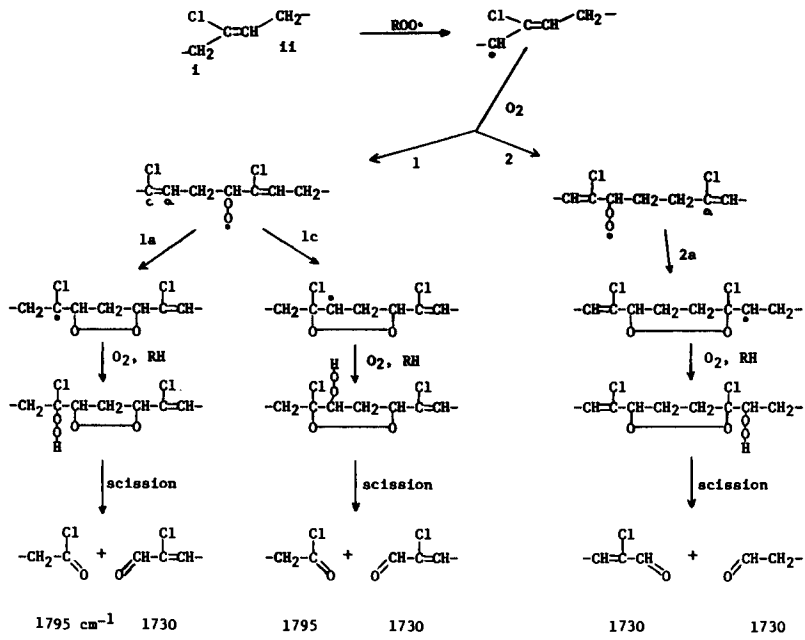

Figure 7a. Basic mechanism of thermal oxidation of CR

In Durability of Macromolecular Materials; Eby, R.;
ACS Symposium Series; American Chemical Society: Washington, DC, 1979.

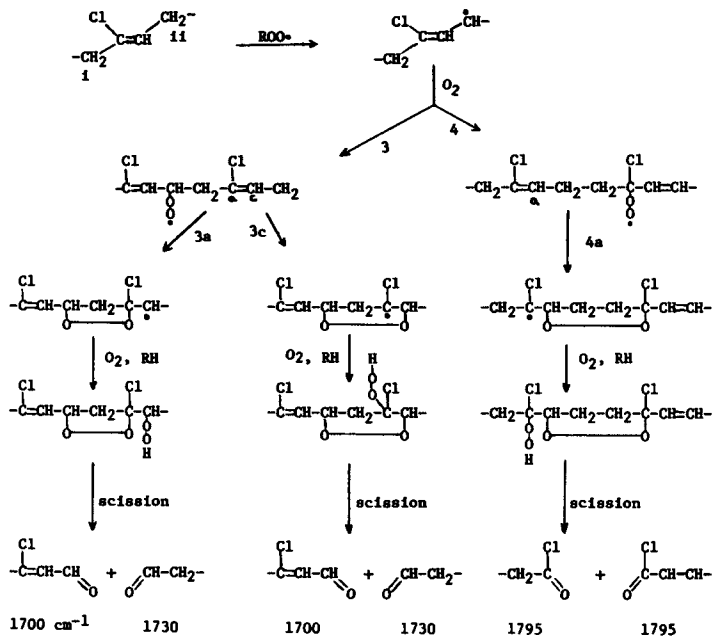

Figure 7b. Basic mechanism of thermal oxidation of CR

In Durability of Macromolecular Materials; Eby, R.;
ACS Symposium Series; American Chemical Society: Washington, DC, 1979.

stage in the oxidation before autocatalysis. Loss of functional groups in CR due to degradation is denoted by negative absorbances of CR bands. Formation of degradation products is observed by the appearance of bands at 1795, 1727, 1620, 915 cm^{-1} and in the region of 1200-950 cm^{-1}.

Increased absorbance in the 1200-950 cm^{-1} region is primarily due to the production of C-O groups (29), but specific assignments are ambiguous. The apparent bands at 1150, 1040, and 960 cm^{-1} are artifacts of the spectral subtraction because they result from negative CR bands superimposed upon a broad C-O band. At 80°C, a very broad absorption of C-O groups is detected, whereas in BR and IR (ref. 14 and Figure 4) the band is narrower and less intense since the C-O intermediates react swiftly to form carbonyls. The difference may be due to the following: 1) many side reactions actively occur in CR producing a wide range of oxygenated products; and/or 2) reaction intermediates are more stable in CR and are present in larger quantities for detection.

The bands at 1795 and 1727 cm^{-1} designate acid chloride and saturated aldehyde groups (29), respectively, and may arise from a mechanism of chain scission similar to BR and IR.

Figure 7 shows a mechanism which has many available routes to chain scission. Paths 1 thru 4 designate where atmospheric oxygen may add to the CR radical after hydrogen abstraction. Hydrogen abstraction can occur at methylene group i (paths 1 and 2) or at methylene group ii (paths 3 and4). Paths 3a and 3c can be excluded on the basis that they do not account for the formation of the observed acid chloride.

Hydrogen abstraction probably occurs more readily at methylene group ii (paths 3 and 4) than at i (paths 1 and 2) because the chlorine affords stabilization of the allylic radical formed. Since path 3 can be excluded as noted previously, path 4a appears to be the major choice for cyclization. Path 4a produces only acid chlorides and these absorb strongly in the ir (29). This is inconsistent with the observation of a comparable absorbtion of saturated aldehyde (Figure 6). Observation of saturated aldehyde might be an indication that the initial peroxy radical in path 4 abstracts hydrogen more readily than it adds to form the cyclic peroxide. Decomposition of the hydroperoxide and β-scission of the corresponding alkoxy radical could account for the formation of both the acid chloride and saturated aldehyde observed in the FTIR spectra:

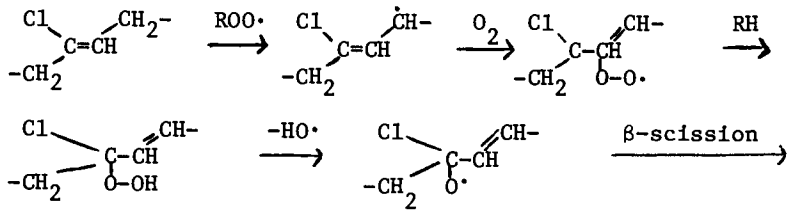

In Durability of Macromolecular Materials; Eby, R.;
ACS Symposium Series; American Chemical Society: Washington, DC, 1979.

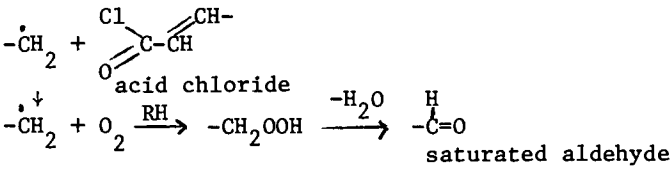

Paths 1c, 2a, and 3a might account, in part, for the observed evolution of hydrogen chloride gas. In these routes, a radical is formed, β to a chlorine substituted carbon, which may promote scission of the C-Cl bond to yield an olefin and a Cl· radical. Bands observed at 1620 and 915 cm^{-1} could be ascribed respectively to ν(C=C) and δ(CH) absorbances of such an olefin. The chlorine radical would abstract a hydrogen, forming hydrogen chloride. This reaction is analogous to many of those proposed for the dehydrochlorination of poly(vinyl chloride) (35, 36, 37) and is offered merely as a possibility. Futher investigations are necessary to establish the mechanism of dehydrochlorination in CR and poly(vinyl chloride).

Conclusions

The uninhibited autoxidation of cis-1,4-polybutadiene, in the temperature range of 0-100°C, was studied primarily by Fourier transform infrared spectroscopy. A mechanism is presented to account for the spectral changes observed in early stages before autocatalysis. Infrared data indicates the formation of both mono and polycyclic peroxide structures by addition of the peroxy radical to a neighboring double bond. Scission of these cyclic peroxides accounts for the observed carbonyl products. Polycyclization is favored at low temperatures while hydrogen abstraction and epoxidation are favored at higher temperatures.

Spectral changes observed in the early oxidation stages of polyisoprene and polychloroprene indicate similar mechanisms are operative. The methylene group adjacent to the methine carbon is found to be most susceptible to oxidation in both polyisoprene and polychloroprene.

Literature Cited

1. Shelton, J. R., Rubber Chem. Tech., (1972), 45 (2), 359.
2. Cunneen, J. I., Rubber Chem. Tech., (1968), 41, 182.
3. Boland, J. L., Quart. Rcv. (London), (1949), 3, 1.
4. Bateman, L., Quart. Rev. (London), (1954), 8, 147.
5. Bolland, J. L., and Hughes, H., J. Chem. Soc., (1949), 492.
6. Tobolsky, A. V., and Mercurio, A., J. Am. Chem. Soc., (1959), 5535.
7. Bevilacqua, E. M., J. Am. Chem. Soc.,(1955), 77, 5394.
8. Bevilacqua, E. M., Rubber Age (N. Y.), (1956), 80, 271.

In Durability of Macromolecular Materials; Eby, R.;
ACS Symposium Series; American Chemical Society: Washington, DC, 1979.

9. Bevilacqua, E. M., J. Am. Chem. Soc.,(1957), 79, 2915.
10. Bevilacqua, E. M., J. Polym. Sci., (1961), 49, 495.
11. Percy, E. J., Ph.D. Thesis, University of London, 1964.
12. Houseman, T. H., Ph.D. Thesis, University of London, 1964.
13. Barnard, D., Cain, M. E., Cunneen, J. L., and Houseman, T.H., Rubber Chem. Tech., (1972), 45, 381.
14. Pecsok, R. L., Painter, P. C., Shelton, J. R., and Koenig, J. L., Rubber Chem. Tech., (1976), 49 (4), 1010.
15. Morand, J. L., Rubber Chem. Tech., (1977), 50, 374.
16. Gemmer, R. V. and Golub, M. A., Polymer Prepr.,(1976), 17 (2), 676.
17. Golub, M. A., Hsu, M. S., and Wilson, L. A., Rubber Chem. Tech., (1975), 48, 953.
18. Kuzminskii, A. S., Degteva, T. G., and Lapteva, K. A., Rubber Chem. Tech, (1956), 29 , 573.
19. Griffiths, P. R., "Chemical Infrared Fourier Transform Spectroscopy," John Wiley and Sons, New York, 1975.
20. Antoon, M. K. and Koenig, J. L., Applied Optics (1978), in press.
21. Tabb, D. L., Koenig, J. L., and Coleman, M. M., J. Polym. Sci., Phys. Ed., (1975), 13, 1145.
22. Odian, G., "Principles of Polymerization," McGraw-Hill, New York, 1970.
23. Shelton, J. R., Rubber Chem. Tech., (1974), 47(4), 949.
24. Kulich, D. M. and Shelton, J. R., Polym. Prepr., (1977), 18(1), 447.
25. Mayo, F. R., J. Am. Chem. Soc., (1958), 80, 2497.
26. Bevilacqua, E. M., Rubber Chem. Tech., (1956), 29, 583.
27. Golub, M. A., Seminar presented at Case Western Reserve University, Cleveland, Ohio, 1976.
28. Hampton, R. R., Rubber Chem. Tech., (1972), 45, 546.
29. Bellamy, L. J., "The Infrared Spectra of Complex Molecules," third ed., Chapman and Hall, London, 1975.
30. Bolland, J. L., Trans. Faraday Soc.,(1950), 46, 358.
31. Farmer, E. H., Bloomfield, G. F., Sundralingham, A., and Sutton, D. A., Trans. Faraday Soc., (1948), 38, 348.
32. Shelton, J. R., Chapter in "Polymer Stabilization," W. L. Hawkins, ed., Wiley, New York, 1972.
33. Geddes, W. C., Rubber Chem. Tech., (1967), 40, 177.
34. Engelman, E., J. Inst. Rubber Ind.,(1969), 3(2), 77.
35. Mayer, Z., J. Macromol. Sci., Revs. Macromol. Chem., (1974), C10, 263.
36. Mitani, K., Ogata, T., Awaya, H., and Tomari, Y., J. Polym. Sci., Chem. Ed.,(1975), 13, 2813.
37. Ayrey, G., Head, B. C., and Poller, R. C., J. Polym. Sci., Macromol. Rev., (1974), 8, 1.

RECEIVED December 8, 1978.

7

Application of New Kinetic Techniques to the Lifetime Prediction of Polymers from Weight-Loss Data

JOSEPH H. FLYNN and BRIAN DICKENS

Polymer Science and Standards Division, National Bureau of Standards, Washington, DC 20234

As more and more polymeric materials are used both in the replacement of other materials and by the creation of new applications, the study of their expected lifetimes assumes greater and greater importance. It is more economical to plan for replacement of defective parts than to suffer an unexpected failure which may occur under inhospitable, inconvenient or even dangerous conditions. Philosophies of how to assess lifetimes fall into several schools. These include: evaluation of experience with the materials under actual service conditions, acceleration of the aging process by increasing one or more degradation factors above their normal levels and assessing the degradation rate by monitoring the first appearances of degradation under service-like conditions.

We have chosen to examine the applicability to lifetime prediction of four methods of thermogravimetry. Although one can argue that many useful properties of polymers may disappear before weight loss occurs, it is worthwhile to examine the role of thermogravimetry in lifetime prediction because the technique can be applied to any condensed phase sample, soluble or not, in almost any geometric form. Further, thermogravimetry is simple, convenient, and, in some modes of application, fairly fast. The hardware is rugged, reliable and stable. Finally, the process which results in the volatilization of small fragments is often closely related to the process which results in the loss of desired properties.

The four methods of thermogravimetry which we discuss here are complementary. No one method is all-encompassing. All provide relevant information. The methods are:

I. Factor-jump Thermogravimetry
II. Isoconversional Diagnostic Plots
III. Varied Heating Rate Analysis
IV. Analysis at Low Conversion

Method I consists of a series of isothermals; the temperature is increased continuously in Methods II, III and IV.

In Durability of Macromolecular Materials; Eby, R.;
ACS Symposium Series; American Chemical Society: Washington, DC, 1979.

I. Factor-jump Thermogravimetry

In its usual application, the factor-jump method (1) consists of imposing a series of temperature plateaus on a sample while recording its weight. The rates of weight-loss and the temperatures at adjacent isothermals are extrapolated to halfway between the plateaus in terms of time or in terms of the associated parameter, extent of reaction. The activation energy, E, is then estimated from the Arrhenius equation

$$E = \frac{RT_1T_2}{\Delta T} \ln \frac{r_2}{r_1} \qquad (1)$$

where R is the gas constant, r's and T's are extrapolated rates and temperatures from two adjacent plateaus and $\Delta T = T_2 - T_1$. Because both rates and both temperatures are estimated at the same extent of reaction, the term containing the extent of reaction and other temperature-independent factors cancel out [see ref. (1)]. The factor-jump method, in our implementation, is automated (2, 3, 4, 5, 6) and computer controlled.

The strong points of the method are as follows:

i) Activation energies are determined using only one sample. (In multi-sample techniques, one must assume that thermal histories are unimportant.)

ii) The model, Eq. (1), is simple and contains no complicating extent of reaction terms.

iii) The experiment is conducted over a narrow range of rates of weight-loss. Thus the concentrations of reactants within and products above the sample are roughly constant.

iv) The quantities used to calculate the activation energy are obtained from a small (6-10°C) temperature range. We may assume that the Arrhenius equation is valid and the pre-exponential factor is independent of temperature over this small interval.

The weakest points of the method are:

i) The initial activation energy cannot be determined because the first determination is made between the first and second isothermal plateaus. This is usually at 5-10% weight-loss.

ii) The method is not computationally robust. It requires that the weight-time trend be fitted to a polynomial which is then differentiated and extrapolated ∿ 15% beyond the range of data. The loss of weight during the degradation of many polymers results from bursting of bubbles. In a derivative-calculating method such as this one, only slight perturbations in the sample weight are needed to mitigate the successful calculation of the derivative. This is because "wild" values can have enormous effects (proportional to the square of their wildness) on the least squares curve fitting which tries to minimize the sum of squared deviations.

In Durability of Macromolecular Materials; Eby, R.;
ACS Symposium Series; American Chemical Society: Washington, DC, 1979.

II. Isoconversional Diagnostic Plots

This method, together with methods III and IV, is a treatment of weight-loss/temperature data obtained in constant heating rate thermogravimetric experiments. Provided we assume that the Arrhenius equation is valid and that the same form, $F(\alpha)$, of the dependence of rate on extent of reaction, α, maintains throughout all the runs at a constant heating rate, β, we can formulate (7, 8), for a given extent of reaction, the equation

$$\Delta \log \beta = - 0.457(E/R)\, \Delta(1/T). \qquad (2)$$
$$(\alpha = \text{constant})$$

E can be estimated from the slope of a plot of log β vs. 1/T at a given extent of reaction from runs at several different heating rates. This can be extended to give E for several extents of reaction, typically every 10%.

The advantages of this method are:

i) The form of the dependence of rate on extent of reaction need not be known or guessed at.

ii) A wide temperature range can be covered.

iii) The method is computationally robust--weight-loss curves are utilized directly.

iv) The change in conditions (usually only the temperature) is constant and can be automated with little need for sophistication.

v) Parallel lines on the plot show in an obvious fashion the consistency of activation energy throughout the range of reaction and throughout a wide temperature range.

The method is not without its disadvantages:

i) As with all integral methods, the effects of errors are cumulative--early errors are passed on to later results.

ii) One must use more than one sample and must assume that the weight-loss kinetics are independent of the differing physical character and thermal histories of the samples. This means that, regardless of the thermal history of the sample, regardless of the temperature and regardless of the effects of degradation, the dependence of rate of weight-loss on the extent of reaction is the same in all samples for a given extent of reaction.

iii) As is the case with all dynamic heating experiments, the temperature may not be able to "equilibrate" at the faster heating rates.

III. Varied Heating Rate Analysis

This method is based on examining the shift with heating rate of peaks in the plots of $d\alpha/dT$ vs. T. Theoretical considerations (9) show that peaks corresponding to independent reactions with widely differing activation energies can be

In Durability of Macromolecular Materials; Eby, R.;
ACS Symposium Series; American Chemical Society: Washington, DC, 1979.

resolved at some attainable heating rate. For competitive reactions, one peak or the other will dominate as the heating rate is changed.

The advantages of the method are:

i) One can resolve whether the weight-loss process is simple or complex in favorable cases.

ii) Likewise, one can resolve whether any complication arises from competing or independent reactions.

iii) As in II, the conditions may include a wide range of temperatures and heating rates and the complete range of the degradation reaction is examined.

iv) From experiments at very slow heating rates, one can better predict which reaction will dominate at service conditions.

The disadvantages are:

i) The difference in activation energies must be rather large ($\sim$ 20 kcal/mole) to obtain good resolution since one can obtain only a factor of $\sim 10^4$ in heating rates. It is probably rather rare that such large differences in activation energy are found in reactions occurring at the same temperature range and as alternatives to one another.

ii) The method requires very slow heating rates with the result that the duration of the experiment may become excessive.

iii) It may be that very fast heating rates are required where the transfer of heat to the specimen becomes a limiting factor.

IV. Analysis at Low Conversion

The heart of this method (10, 11) is to plot $T^2 d\alpha/dT$ against α to obtain a slope of $E/R + 2T$ at low extent of reaction ($\alpha \leq .05$). This can be done simply from a single thermogravimetric trace of weight against time or temperature.

The advantages are:

i) Only one sample is required, thus circumventing all problems arising from differing sample histories.

ii) Because the extent of reaction is always small, the form of the dependence of rate of reaction on extent of reaction may be safely ignored.

iii) One can estimate other aspects of the kinetics from the change in slope as α increases. If the slope increases with increasing α, then the dependence on weight-loss has an autocatalytic character as in the random degradation of polymers. When the slope decreases with increasing α, the kinetics behave as a positive order reaction. A slope independent of α implies zero order kinetics.

The disadvantages are:

i) The extent of conversion enters into both quantities plotted, therefore, one must be more than usually consistent in picking the beginning of the polymer degradation.

ii) The initial rates of weight-loss are especially sensitive

In Durability of Macromolecular Materials; Eby, R.;
ACS Symposium Series; American Chemical Society: Washington, DC, 1979.

to volatile contaminants including monomer, solvent, plasticizer, etc. Their effects often must be minimized by pretreatment.

iii) Chemical effects from residual catalysts, antioxidants, stabilizers, etc. and labile linkages introduced during synthesis and storage may affect the initial kinetics.

Important Parameters in Lifetime Prediction

The four methods just described determine the apparent activation energy, E, rather than the dependence of rate of reaction on extent of reaction, $f(\alpha)$. In fact, they specifically avoid having to estimate the latter term. This is especially appropriate in lifetime prediction where temperature is the only accelerating factor between test and service conditions. The functional form of $f(\alpha)$ affects only the shape of the kinetic curve and not its time-temperature positioning. In any event, for these complex condensed phase reactions, $f(\alpha)$ cannot be separated from the pre-exponential factor of the Arrhenius equation and other factors related to the physical properties of the sample without composing a detailed kinetic model. Such models are often simplistic in their construction and their use can introduce gross errors in the determination of E (1, 12). The omission of any temperature dependence of the pre-exponential factor will be partially compensated for in the calculation of apparent activation energy. These errors should have considerably less effect than errors in E itself which are promulgated exponentially.

Because activation energy represents the temperature dependence of a process, it is important to estimate the precision in the activation energy needed to provide useful estimates of service life after extrapolation of the rates to service temperatures. We may estimate the effects of error, σ, in the activation energy, E, from the Arrhenius equation written in the form

$$\frac{r(T_2)}{r(T_1)} = e^{(E+\sigma)\Delta T/RT_1T_2} = e^{E\Delta T/RT_1T_2}\, e^{\sigma\Delta T/RT_1T_2} \qquad (3)$$

This gives the relationship between rates at temperatures T_1 and T_2 where $T_2 - T_1 = \Delta T$. The temperature scaling factor for the reaction rate is $\exp(E\Delta T/RT_1T_2)$. The term $\exp(\sigma\Delta T/RT_1T_2)$ transmits the error in the activation energy into the ratio of rates. It should be noted that this is a multiplicative exponential effect; in other words, a small amount of error has a large effect. Note that the effect of the error is independent of the activation energy, which is often determined to a percentage of error. Thus at first sight it may appear that processes with large activation energies may, because of the larger error in the value assigned to the activation energy, have greater uncertainty

In Durability of Macromolecular Materials; Eby, R.;
ACS Symposium Series; American Chemical Society: Washington, DC, 1979.

in their extrapolated rates. However, the size of ΔT necessary to accelerate the process is inversely proportional to the activation energy so that for high activation energy reactions the ΔT will be relatively small. If the error in activation energy determinations is anywhere near constant, processes with large activation energies may give more reliable extrapolations than those with low activation energies.

It is illuminating to consider the effects of errors in activation energy on scaled tests. As an illustration, we draw on recent results for the oxidation of polystyrene (13). Table I shows the error in activation energy (σ) at test temperatures of 100, 200, 300, 400 and 500°C which will result in errors in rates of 1, 5, 10, 25, 50, 100 and 250% at service conditions of 25°C.

Table I

Effect of Error in Activation Energy on Accelerated Rate Tests

Service Temp = 25°C

% Error in Rate*	Error($\pm\sigma$) in Activation Energy in kcal/mole				
Test Temp °C =	100	200	300	400	500
1	0.03	0.02	0.01	0.01	0.01
5	0.15	0.08	0.06	0.05	0.05
10	0.28	0.15	0.12	0.10	0.09
25	0.66	0.36	0.28	0.24	0.22
50	1.20	0.65	0.50	0.43	0.39
100	2.05	1.11	0.86	0.74	0.67
250	3.71	2.01	1.56	1.34	1.22

*Calculated at service temperature from rate observed at test temperature by means of Equation (3).

The greater the temperature difference between service life and accelerated test, the smaller the error in activation energy must be for a given error in scaled rate. In the oxidation of polystyrene between 225°C and 275°C, the final averaged activation energy is 21.5 ± 0.2 kcal/mole. Using an error value of 2σ = 0.4 kcal/mole for a 95% confidence level, we estimate by interpolation in Table I that an error of 31% would be introduced into the calculated rate if the rates observed at ∿ 225°C were scaled to room temperature.

The above analysis suggests that extrapolation to lower temperatures of results obtained in accelerated tests at higher temperatures requires activation energies which are known to

In Durability of Macromolecular Materials; Eby, R.;
ACS Symposium Series; American Chemical Society: Washington, DC, 1979.

great accuracy, i.e., to within 0.1 kcal/mole in some cases. Such high precision will be rarely attained even using an average of a large number, N, values from many runs to give a factor of $\sqrt{N}$ in the denominator of the estimated standard deviation. Uncertainties in the continuity of the processes themselves over the extrapolated range further cloud the issue. In cases where such precision is required, the accelerated test will have to be conducted under extremely modest temperature acceleration. However, such a procedure limits the number of values for determining an average activation energy and may require experiments of impracticably long duration. If the rates of weight-loss processes are not sufficiently fast under those conditions, one must look to the analysis of rates of production of minute amounts of products or changes in physical properties of the material as alternate methods of lifetime prediction.

The extrapolation of typical rates of degradation from the temperature at which E is determined to service conditions will change the rates by a factor of 10^{-7} to 10^{-20} due to the large ΔT involved. Therefore, extrapolated rates using $E + 2\sigma$ and $E - 2\sigma$ will probably differ by at least 50%. This all reinforces the conclusion that the temperatures at which ordinary thermogravimetric methods determine E are too high to permit meaningful aging prediction. For example, in Ref. (13), the activation energy for polystyrene oxidation was determined to be $21.5 \pm .2$ kcal/mole above 280°C. For extrapolation to 25°C, a unit rate at 280°C is transformed to a rate of 0.54×10^{-7}, i.e., a process occurring in 30 minutes at 280°C takes 1057 years at 25°C. If we proprogate the $\pm 2\sigma$ errors in the activation energy, the reaction would take between 770 and 1427 years at service conditions.

Thus, the philosophy of lifetime prediction using temperature-accelerated tests is as follows:

1) Determine the activation energy of the degradation process at the lowest possible temperature to the best possible precision ($\sim$ 0.2 kcal/mole in thermogravimetry).

2) Consider the accuracy of this measurement and compare it with other estimates of the activation energy made using other techniques and the measurements of other experimental factors.

3) Assess the desired lengths of time for the accelerated test and service life. Assuming E from 1) is applicable, compute ΔT between service and test conditions and try to prove that the same kinetic processes are going on at the test and service temperatures. Some of the latter techniques in this paper are useful in this connection.

4) Compute, using the error in E, the maximum change in temperature between service and use conditions which will still give the extrapolated rates within the desired bounds and compute the error in these rates using these temperatures. Then attempt

In Durability of Macromolecular Materials; Eby, R.;
ACS Symposium Series; American Chemical Society: Washington, DC, 1979.

to devise a test which uses this highest permissible temperature and still gives changes in the sample which are well characterized and measurable to considerable precision. It may be necessary to accelerate other factors such as oxygen concentration, pressure, etc., to lower the test temperature. Unfortunately, an increase in the intensity of these other factors may introduce errors in their extrapolation to use conditions similar to those resulting from temperature extrapolation.

We will now illustrate these points very briefly using our results (13) for the oxidation of polystyrene:

1) The activation energy for the oxidation of polystyrene is 21.5 ±.2 kcal/mole.

2) This value, obtained by the factor-jump method of thermogravimetry, appears to be realistically precise, i.e., different runs agree well. There seem to be no other studies of comparable precision from which to assess accuracy. For the moment, we will assume the reported value is accurate as well as precise.

3) A typical service life requirement is > 20 years at 25°C. Suppose that the test can be made safely in 3 hours or with marginal confidence in 30 minutes. (Problems arise with short test times in equilibrating the specimen to its test temperature and performing meaningful measurements in the allotted time.) The acceleration factors, A_i, for the two cases are thus 20 yrs./3 hrs. = 58,400 and 20 yrs./30 min. = 350,400. Using $A_i = \exp(21500\ \Delta T/RT_1T_2)$ we find the test temperature for these accelerations to be respectively, 154°C and 186°C.

4) We will consider the limits imposed by the error, σ, in the activation energy, E. If the percentage error allowed is 100 P_E, then Equation (4)

$$\frac{(1 - P_E)}{1} = \frac{\exp[(E - n\sigma)\ \Delta T/(RT_1T_2)]}{\exp[E\Delta T/RT_1T_2]} \qquad (4)$$

specifies that the test temperature, T_2, be such that the effect of $n\sigma$ in scaling ΔT between T_2 and the service temperature, T_1, is to impart 100 P_E% of error. Thus the rearranged form, $\ln(1 - P_E) = - n\sigma\ \Delta T/(RT_1T_2)$, can be used to provide an estimate of T_2. Since E measures the temperature dependence of the process, if we use a value for E which is too high, we obtain inflated values for the estimated service life. If we use an E which is too low, we obtain an underestimate of the service life and will waste effort on needless improvements. Whether both limits apply or whether a one-tailed test (e.g., 95% of all components should exceed 20 years in service) is appropriate depends on the particular application. In either case it is important to use a good estimate of E.

For 2σ = 0.4 kcal/mole, to estimate a rate which is within 5% of the true rate at a service temperature of 25°C, the test

In Durability of Macromolecular Materials; Eby, R.;
ACS Symposium Series; American Chemical Society: Washington, DC, 1979.

temperature would have to be no higher than 50°C. For an allowed error of 10%, the test temperature could be as high as 80°C, and for an error of 25%, it could be as high as 245°C. Therefore, depending on the desired precision and degree of extrapolation it may be necessary to aim for a service life well over the required value to fit within the limits of error.

The above considerations show that although estimate of service life is not straightforward, our methods of thermogravimetry can provide useful information in the form of activation energies and, at least qualitatively, about reaction kinetics.

However, it is obvious that conflicts will often occur between the predictive criteria and the accelerated weight-loss experimental data. The three techniques which we described in Sections II, III and IV are being directed toward two serious problems which remain even for cases in which accelerated weight-loss measurement is a valid criteria for predicting aging at service conditions. These problems are: a) the great length of the temperature range of extrapolation which may render aging predictions too uncertain to be useful, and b) any hidden changes in the rate-limiting step of the degradation in the extrapolated region which will invalidate the use of Arrhenius parameter, E, determined at accelerated conditions, for prediction.

The consequences of these problems may be lessened by a) extending the constant heating rate measurements to as slow a heating rate and, as a result, to as low a temperature as practical, and b) conducting experiments over as wide a range of heating rates (and temperatures) (14) as will give meaningful weight-loss measurements so as to better detect any trends in the degradation kinetics and to interpret these trends to predict which of competing processes may dominate at service conditions.

The heating rates are limited at the fast end of the range by the lags in thermal and mass flow in the sample and time constants of the apparatus and measurement sensors. It is difficult to obtain unperturbed weight-loss measurements at heating rates above 10^{-1} deg/sec(6 deg/min) without specially designed thermogravimetric apparatus. The limit at slow heating rates is entirely up to the experimenter's patience and longevity, as many modern electrobalances exhibit excellent long term base line stability. It requires three and a half days to cover a 300° temperature range at 10^{-3} deg/sec (4 deg/hr), a month at 10^{-4} deg/sec (9 deg/day) and the better part of a year at 10^{-5} deg/sec. If only initial rates are of interest the duration of the experiment can be reduced considerably. Also, non-linear temperature programming, e.g., $dT/dt = aT^2$, will further reduce the length of the experiment.

For E = 40 kcal/mole, a factor of 10^4 in heating rate will result in a 150° shift in temperature at constant extent of reaction (14). This same heating rate factor, 10^4, also brings about a fairly good resolution of two competing independent

In Durability of Macromolecular Materials; Eby, R.;
ACS Symposium Series; American Chemical Society: Washington, DC, 1979.

reactions with respective activation energies of 40 and 60 kcal/mole (14).

Therefore, by examining the weight-loss kinetics over a wide range of heating rates, especially down to very slow rates and low temperatures, one will be able to 1) shorten the temperature extrapolation to service conditions, and 2) infer which of competing reactions will be rate limiting at service conditions. Using techniques in which experiments at different partial pressures of gaseous atmospheres, e.g., water vapor and oxygen, are compared will assist in selecting dominant low temperature processes.

Polyurethanes

The factor-jump method when applied to polyurethane provides information which is interesting for its qualitative trends rather than for the actual numerical quantities estimated for the activation energies. For example, Figure 1 shows the sequence of events during the degradation in vacuum of a methylene diphenyl diisocyanate-polyethylene adipate diol-butanediol polyurethane. The runs produced extensive char of the sample: the best method of sample presentation may be the evaporation of a solution of the polymer directly in the sample pan to produce an extensive thin film. Three methods of sample preparation were used in the experiments summarized in Figure 1a. However, the essential features are common to all three curves. The activation energy data indicate that an early process terminates at between 30 and 40% weight-loss and the residue decomposes further to produce a final char involatile in vacuum below 500°C and amounting to about 30% of the final weight. Comparison of Figures 1a and and 1b indicates that the plateau at 45% to 70% conversion may arise from the decomposition or vaporization of polyester. Thus, the early stages may be inferred to be the weight-loss of methylene diphenyl diisocyanate (MDI) from the sample, apparently with an activation energy of 40-45 kcal/mole. However, this method is not suited to examine the first five percent extent of reaction. The activation energy of the first process falls off with increasing conversion to 24 to 31 kcal/mole, depending on the sample, suggesting that diffusional processes are increasing in importance. A reasonable explanation is that a crust is formed on the samples but cracks as the degradation proceeds.

The activation energies calculated during the in vacuo degradation of three samples of a methylene diphenyl diisocyanate-polytetramethylene oxide-butanediol polyurethane are shown in Figure 2. The gaps indicate regions where the activation energy could not be calculated reliably because the rates of weight-loss become too low. In these regions the temperature was increased by the computer program in several steps to force the rate of weight-loss of the sample above the minimum allowed

In Durability of Macromolecular Materials; Eby, R.;
ACS Symposium Series; American Chemical Society: Washington, DC, 1979.

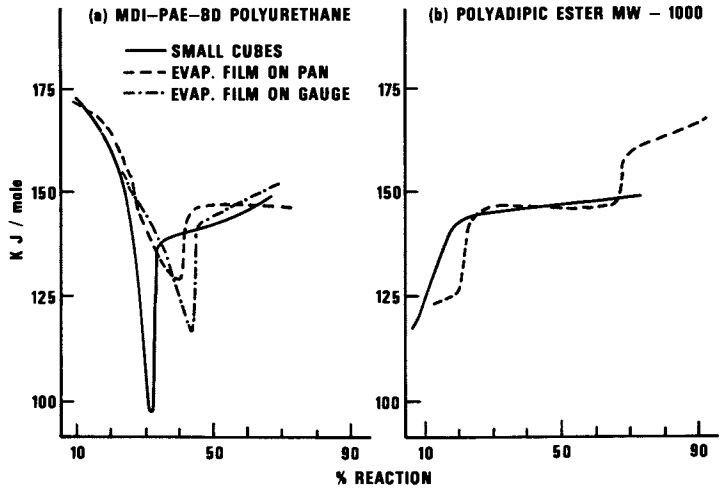

Figure 1. Activation enregy vs. extent of reaction of (a) MDI/polyester polyurethane; (b) polyester: (——), small cubes; (– – –), evaporated film on pan; (— ● —), evaporated film on gauge.

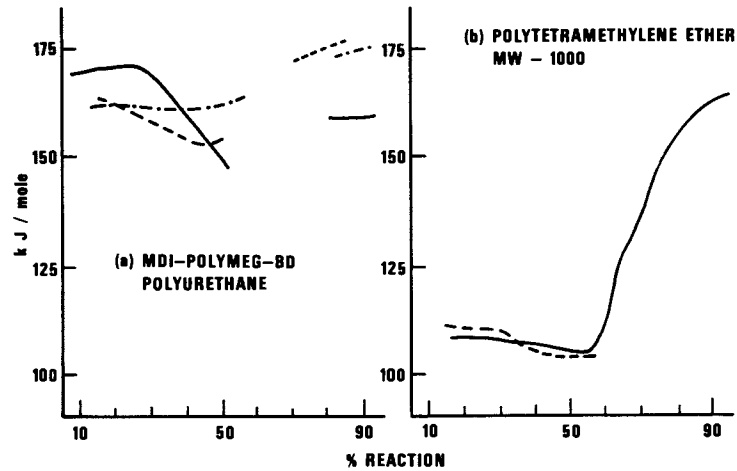

Figure 2. Activation energy vs. extent of reaction for (a) MDI/polyether polyurethane; (b) polyether: (——), small cubes; (– – –), evaporated film on pan; (— ● —), evaporated film on gauge.

In Durability of Macromolecular Materials; Eby, R.;
ACS Symposium Series; American Chemical Society: Washington, DC, 1979.

limits. These results imply that a change in the degradation process occurs at about 50% weight-loss. Comparison of Figure 2a with 2b shows that degradation of the polyether alone is not a dominant process in the in vacuo degradation of the MDI/polyether polyurethanes. MDI-related fragments probably escape from polyether-based polyurethanes during the first part of the weight-loss process just as they do from polyester-based polyurethanes. Figure 2a suggests that there is a complex interplay between the MDI and polyester weight-loss reactions as the activation energy remains at around 35-40 kcal/mole--considerably higher than the 26 kcal/mole, characteristic of the polyether degradation shown in Figure 2b.

In the degradation of polyurethanes, the dominant process changes markedly during the course of the reaction. The activation energy vs. extent of reaction plots provide useful information on the effects of sample geometry (Fig. 1a), the dominant processes (Fig. 1a vs. Fig. 1b) and the extent to which processes are (Fig. 1a), or are not (Fig. 2a) separated. However, as the initial activation energy is not determined by the factor jump method, it provides little information of value for use in extrapolating from test to service conditions.

The second technique for analyzing weight-loss data is illustrated in Figure 3 for an MDI-polytetramethylene oxide-butanediol polymer. The logarithm of the heating rate is plotted against the reciprocal of the temperature necessary to reach 0.02, 0.04, 0.06, 0.08, 0.10, 0.20, 0.30, 0.40, 0.50, 0.60, 0.70, 0.80 and 0.90 fractional weight-loss at heating rates of 10^{-1}, 10^{-2}, 10^{-3} and 10^{-4} degrees per second and covers a temperature range from 175 to 400°C.

The nearly parallel straight lines for the first 10% weight-loss yield, by means of Equation 2, activation energies from 35 to 40 kcal/mole. This suggests that a single process may be operative over this early range of weight-loss between temperatures of 175 and 300°C. However, at greater than ten percent conversion, the curves deviate from linearity at temperature below 300°C, indicating complexities in the kinetics. At faster rates and higher temperatures, the activation energies from the slopes increase from 40 to 62 kcal/mole for 30-50% weight-loss. Cumulative effects from competing processes do not allow any reasonable interpretation of data for greater than 50% weight-loss.

The indication of a single kinetic process in the initial phases of weight-loss from Figure 3 is encouraging. However, the change that occurs at the slowest heating rate at 10% conversion bodes ill for the extrapolation of kinetic parameters for even this initial process to lower temperatures.

A plot of rate of weight-loss ($d\alpha/dT$) vs. temperature for the same experimental data (curves for heating rates of 10^{-1}, 10^{-2}, 10^{-3} and 10^{-4} deg/sec) is illustrated in Figure 4. If one

In Durability of Macromolecular Materials; Eby, R.;
ACS Symposium Series; American Chemical Society: Washington, DC, 1979.

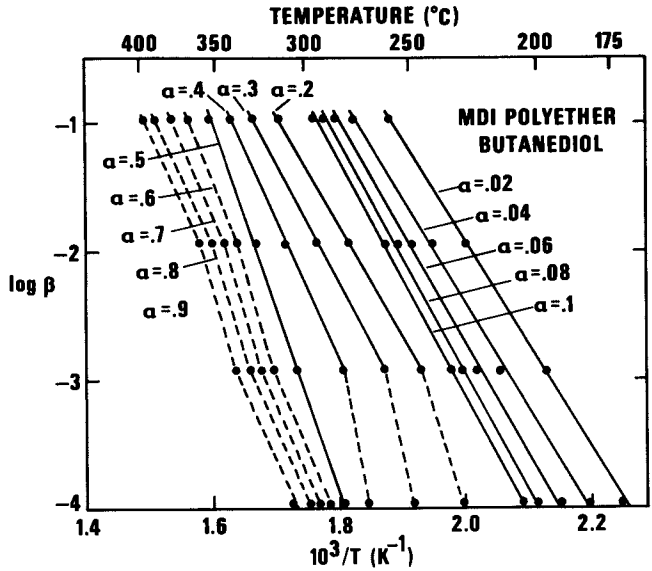

Figure 3. Logarithm of heating rate vs. reciprocal absolute temperature. MDI/polyether polyurethane in vacuum: curves for α = 0.02, 0.04, 0.06, 0.08, 0.10, 0.20, 0.30, 0.40, 0.50, 0.60, 0.70, 0.80, and 0.90.

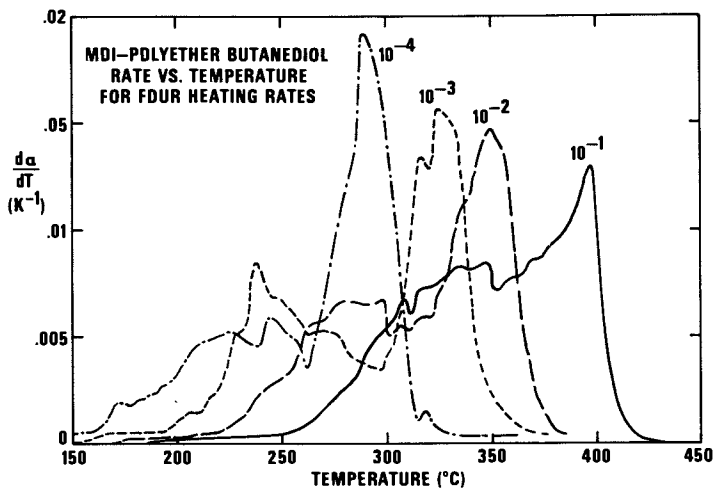

Figure 4. The dα/dT vs. temperature plot for an MDI/polyether polyurethane in vacuum: (——), 0.107 deg/sec; (— —), 0.0119 deg/sec; (– – –), 0.00119 deg/sec; (— • —), 0.000110 deg/sec.

In Durability of Macromolecular Materials; Eby, R.;
ACS Symposium Series; American Chemical Society: Washington, DC, 1979.

ignores the minor irregulatities which often occur during polyurethane degradation, there appears to be a sharpening of the higher temperature, higher conversion process and its gradual encroachment upon the lower temperature, initial process as the heating rate is slowed and the curves are shifted to lower temperatures.

Initial rates for a number of polyurethanes which were synthesized in our laboratories are being investigated in detail (11). A plot of $T^2(d\alpha/dT)$ vs. α is shown in Figure 5 for an MDI-polytetramethylene oxide-butanediol polymer. The activation energy calculated from the slope for the first 5% weight-loss is about 35 kcal/mole. This value is typical for initial activation energies for the weight-loss of MDI polyurethanes in nitrogen atmosphere. These experiments yield values in the range 33-37 kcal/mole for 1-3% conversion (12). On the other hand toluene diisocyanate (TDI) polyurethanes gave consistently lower activation energies (28-31 kcal/mole) in the same conversion range. Therefore, it appears that the early kinetics are dominated by the particular diisocyanate group in these polyurethanes.

The TDI polyurethanes begin to decompose at lower temperatures as well as with lower activation energies than MDI polyurethanes do. This difference in stability of the two types of polyurethanes becomes pronounced upon extrapolation to room temperature.

However, factors other than temperature affect the degradation of polyurethanes. Oxygen appears to have little effect upon the degradation process at high temperatures; however, experiments at slow heating rates and low temperatures (9) suggest that degradation at service conditions may be greatly affected by oxidation processes of low activation energy. Also, the presence of water vapor may cause a catastrophic shortening of the service life of polyurethanes (15).

Therefore, more experimentation to determine the effects of water and oxygen upon the initial weight loss kinetics at low temperatures is necessary before we will be able to decide if weight loss thermal analysis is a viable technique to apply to the predicting of the service life of polyurethanes.

Polystyrene

The factor-jump method provides precise results for the degradation of polystyrene because the process of degradation is unchanged during the fulk of the reaction. An extensive study has been reported (13), therefore we summarize the results. The activation energy of polystyrene degrading in vacuum > 350°C was found to be 44.7 $\pm$ 0.6 kcal/mole. This result is based on polystyrene from several sources which included both thermally polymerized and anionically prepared monodisperse samples. Measurements in the early part of the degradation have poor precision because bursting bubbles in the sample cause the sample weight to follow an erratic course. Nonetheless, it appears that the

In Durability of Macromolecular Materials; Eby, R.;
ACS Symposium Series; American Chemical Society: Washington, DC, 1979.

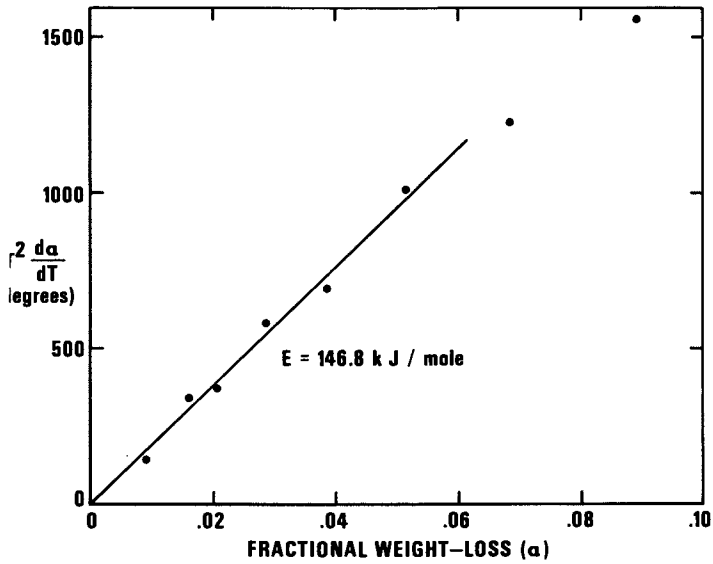

Figure 5. $T^2(d\alpha/dT)$ *vs.* α *for an MDI/polyether polyurethane in nitrogen: heating rate, 2.16 deg/min.*

same activation energy pertains throughout the degradation (10 to 90% weight-loss). The degradation in flowing 99.995% pure nitrogen has an activation energy of 44.9 ± 0.2 kcal/mole which is not significantly different from and is considerably more precise than the value obtained for degradation in vacuum.

Many reports have been made of the activation energy of polystyrene degradation from measurements of a variety of properties and using different techniques of analysis of the kinetics. The closest to that determined by factor-jump thermogravimetry is 44.7 kcal/mole reported by Jellinek (16). The value, 44.9 kcal/mole is far from a widely accepted value of 55 kcal/mole reported by Madorsky and Wall (17, 18). It falls between the values of ∿ 42 kcal/mole (19, 20) and ∿ 49 kcal/mole (21) viewed favorably by Cameron and MacCallum in their review (22). The degree of ubiquity of 44.9 ± 0.2 kcal/mole as the activation energy of thermally degrading polystyrene is not yet well defined. Thermogravimetric methods including method II (see below), Reference (13) and work reported by Still and Whitehead (23) suggest 43-47 kcal/mole; the high value of 55 reported in Refs. (17) and (18) remains an exception. The work which provided 42 and 49 kcal/mole used quite different measurement techniques.

In the oxidation of polystyrene in flowing 50% O_2/50% N_2, it appears that the rate-determining process is extremely well behaved and the activation energy was easily determined by the factor-jump method to be 21.5 ± 0.2 kcal/mole. The sample degrades to a black char at ∿ 80-90% of reaction. Experiments using a ready access of air also gave a value of 21.5 ± 0.2. When the sample is starved of O_2, the apparent activation energy is between 21 and 30 kcal/mole for oxygen partial pressures greater than 4 mm Hg. The actual values observed depend on the thermal history of the sample and are not completely consistent from run to run. The details are given in Ref. (13).

The second technique for analyzing weight-loss data was applied to the degradation of a thermally polymerized polystyrene (NBS-SRM 706). The results are illustrated in Figure 6 where the logarithm of the heating rate is plotted against the reciprocal of the temperature necessary to reach 0.1, 0.2, 0.3, 0.4, 0.5, 0.6, 0.7, 0.8 and 0.9 fractional weight-loss at heating rates of 10^{-1}, 10^{-2}, 10^{-3} and 10^{-4} deg/sec. The nearly parallel lines which cover a range of temperatures from 280 to 420°C yield activation energies between 47.3 and 47.8 kcal/mole. Therefore it appears that the same rate-limiting kinetics are operative over this broad temperature range and from 10 to 90% conversion. It is worthwhile to point out that the 47.5 kcal/mole activation energy obtained independently here further weakens the case for the more or less accepted "high" value of 55 kcal/mole.

The rate of weight-loss vs. temperature spectra is shown in Figure 7 for the same data and conditions as in Figure 6. The sharpening of the single peak with decrease in heating rate

In Durability of Macromolecular Materials; Eby, R.;
ACS Symposium Series; American Chemical Society: Washington, DC, 1979.

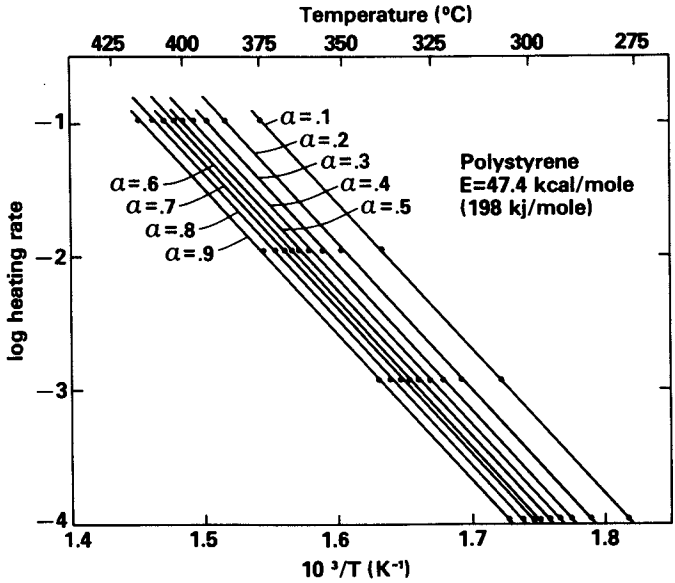

Figure 6. Logarithm of heating rate vs. reciprocal absolute temperature. Polystyrene in vacuum: curves for α = 0.1, 0.2, 0.3, 0.4, 0.5, 0.6, 0.7, 0.8, and 0.9.

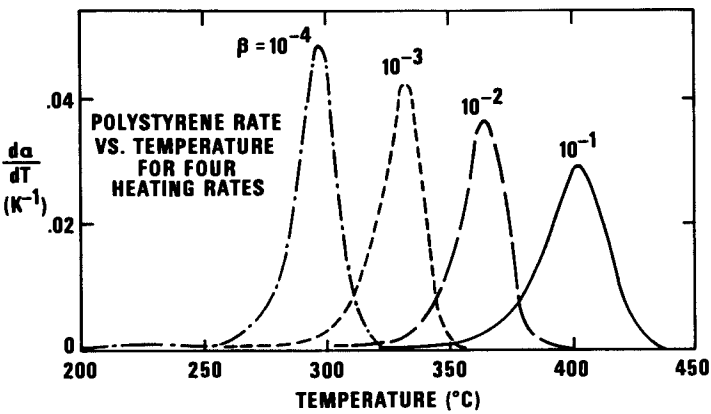

Figure 7. The dα/dT vs. temperature plot for polystyrene in vacuum: (——), 0.105 deg/sec; (— —), 0.0106 deg/sec; (– – –), 0.00116 deg/sec; (— ● —), 0.000107 deg/sec.

In Durability of Macromolecular Materials; Eby, R.;
ACS Symposium Series; American Chemical Society: Washington, DC, 1979.

is normal for a single noncompetitive reaction schema. However, at slow heating rates, a peak of low activation energy separates from the main reaction peak at the initial phases of weight-loss. This diffuse peak is barely discernible in the 200-250°C region of the 10^{-4} deg/sec heating rate curve in Figure 7. It amounts to only about 2% of the total weight-loss. Attempts to analyze the initial kinetics in detail have produced erratic results. Further investigation will be necessary to determine if this early peak can be associated with the breaking of "weak links" which has been postulated since 1947 as occurring in the initial phases of polystyrene degradation (24). This initial peak should not be present in the degradation of anionically polymerized polystyrene where "weak links" are reported to be absent (25).

In any event, oxidative reactions which extrapolate to much faster rates at room temperature, are undoubtedly much more relevant to aging prediction for this polymer.

Conclusions

An analysis of error propagation demonstrates that either activation energies must be measured extremely precisely or the temperature extrapolation to service conditions must be over an extremely modest range if life-time prediction from accelerated weight-loss experiments is to be meaningful.

Of the four methods which are described and illustrated by examples from polystyrene and polyurethane degradation, the factor-jump method attacks the problem of attaining high precision. This method determines values for the activation energy which are independent of one another and of sample history. As a result of automation, a large number of values may be calculated and averaged to obtain a small enough standard deviation so that extrapolation to service conditions may give usefully precise results.

The other three methods, when used over a wide range of heating rates and down to very slow heating rates and correspondingly low temperatures, not only have the advantage of reducing the severity of the temperature extrapolation, but also of allowing a detailed kinetic analysis of the important initial phases of the reaction and of permitting, from the kinetic interplay under different atmospheres and at different heating rates, the prediction of which one or combination of thermal, oxidative and hydrolytic reactions will be the primary agent for the deterioration of properties of the polymer at service conditions.

Acknowledgements

The partial support of this work by the Naval Air Systems Command and the Office of Naval Research is gratefully acknowledged.

Literature Cited

1. Flynn, J. H. and Dickens, B., Thermochim. Acta (1976) 15, 1.
2. Dickens, B., Pummer, W. J. and Flynn, J. H., in "Analytical Pyrolysis," pp. 383-391, C. E. R. Jones and C. A. Cramers, Eds., Elsevier, Amsterdam, 1977.
3. Dickens, B. and Flynn, J. H., in "Proceedings of the First European Symposium on Thermal Analysis," pp. 15-18, D. Dollimore, Ed., Heyden, London, 1976.
4. Dickens, B., Thermochim. Acta, in press (1978).
5. Dickens, B., Thermochim. Acta, in press (1978).
6. Dickens, B., Thermochim. Acta, in press (1978).
7. Ozawa, T., Bull. Chem. Soc. Japan (1965) 38, 7883.
8. Flynn, J. H. and Wall, L. A., Polym. Lett. (1966) 4, 323.
9. Flynn, J. H., unpublished.
10. Flynn, J. H. and Wall, L. A., Polym. Lett. (1967) 5, 192.
11. Flynn, J. H., Pummer, W. J. and Smith, L. E., ACS Polym. Preprints (1977) 18 (1) 757.
12. Flynn, J. H., in "Aspects of Degradation and Stabilization of Polymers," Chapter 12, pp. 573-603, H. H. G. Jellinek, Ed., Elsevier, Amsterdam, 1978.
13. Dickens, B., submitted to J. Poly. Sci. (1978).
14. Flynn, J. H., in "Thermal Methods in Polymer Analysis," pp. 163-186, S. W. Shalaby, Ed., Franklin Institute Press, Philadelphia, 1978.
15. Brown, D. W., Lowry, R. E. and Smith, L. E., ACS Polym. Preprints (1978) 19 (2) 822.
16. Jellinek, H. H. G., J. Polym. Sci. (1949) 4, 13.
17. Madorsky. S. L., "Thermal Degradation of Organic Polymers," p. 61, Interscience, NY, 1964.
18. Wall, L. A., Straus, S., Flynn, J. H., McIntyre, D. and Simha, R., J. Phys. Chem. (1966) 70, 53.
19. Boon, J. and Challa, G., Makromol. Chem. (1965) 84, 25.
20. Nakajima, A., Hamada, F. and Shimizu, T., Makromol. Chem. (1966) 90, 229.
21. Wegner, J. and Patat, F., J. Appl. Polym. Sci. (1970) C31, 121.
22. Cameron, G. G. and MacCallum, J. R., J. Macromol. Sci.-Revs. Macromol. Chem. (1967) C1, 327.
23. Still, R. H. and Whitehead, A., J. Appl. Polym. Sci. (1976) 20, 627.
24. Jellinek, H. H. G., "Degradation of Vinyl Polymers," Academic Press, New York, 1955.
25. Cameron, G. G., private communication.

RECEIVED December 8, 1978.

Literature Cited

1. Flynn, J. H. and Dickens, B., Thermochim. Acta (1976) 15, 1.
2. Dickens, B., Pummer, W. J. and Flynn, J. H., in "Analytical Pyrolysis," pp. 383-391, C. E. R. Jones and C. A. Cramers, Eds., Elsevier, Amsterdam, 1977.
3. Dickens, B. and Flynn, J. H., in "Proceedings of the First European Symposium on Thermal Analysis," pp. 15-18, D. Dollimore, Ed., Heyden, London, 1976.
4. Dickens, B., Thermochim. Acta, in press (1978).
5. Dickens, B., Thermochim. Acta, in press (1978).
6. Dickens, B., Thermochim. Acta, in press (1978).
7. Ozawa, T., Bull. Chem. Soc. Japan (1965) 38, 7883.
8. Flynn, J. H. and Wall, L. A., Polym. Lett. (1966) 4, 323.
9. Flynn, J. H., unpublished.
10. Flynn, J. H. and Wall, L. A., Polym. Lett. (1967) 5, 192.
11. Flynn, J. H., Pummer, W. J. and Smith, L. E., ACS Polym. Preprints (1977) 18 (1) 757.
12. Flynn, J. H., in "Aspects of Degradation and Stabilization of Polymers," Chapter 12, pp. 573-603, H. H. G. Jellinek, Ed., Elsevier, Amsterdam, 1978.
13. Dickens, B., submitted to J. Poly. Sci. (1978).
14. Flynn, J. H., in "Thermal Methods in Polymer Analysis," pp. 163-186, S. W. Shalaby, Ed., Franklin Institute Press, Philadelphia, 1978.
15. Brown, D. W., Lowry, R. E. and Smith, L. E., ACS Polym. Preprints (1978) 19 (2) 822.
16. Jellinek, H. H. G., J. Polym. Sci. (1949) 4, 13.
17. Madorsky. S. L., "Thermal Degradation of Organic Polymers," p. 61, Interscience, NY, 1964.
18. Wall, L. A., Straus, S., Flynn, J. H., McIntyre, D. and Simha, R., J. Phys. Chem. (1966) 70, 53.
19. Boon, J. and Challa, G., Makromol. Chem. (1965) 84, 25.
20. Nakajima, A., Hamada, F. and Shimizu, T., Makromol. Chem. (1966) 90, 229.
21. Wegner, J. and Patat, F., J. Appl. Polym. Sci. (1970) C31, 121.
22. Cameron, G. G. and MacCallum, J. R., J. Macromol. Sci.-Revs. Macromol. Chem. (1967) C1, 327.
23. Still, R. H. and Whitehead, A., J. Appl. Polym. Sci. (1976) 20, 627.
24. Jellinek, H. H. G., "Degradation of Vinyl Polymers," Academic Press, New York, 1955.
25. Cameron, G. G., private communication.

RECEIVED December 8, 1978.

The Use of Chemiluminescence in the Study of Paper Permanence

G. B. KELLY and J. C. WILLIAMS
The Library of Congress, Washington, DC 20540

G. D. MENDENHALL and C. A. OGLE
Battelle's Columbus Laboratories, 505 King Avenue, Columbus, OH 43201

The chemiluminescence maxima from several samples of paper placed in a preheated oven at constant humidities was shown to obey a linear Arrhenius relationship between about 40 C and 90 C. Cycling between dry and moist air at 70 C increased the chemiluminescence from the paper temporarily after each change. The light emission from the paper was ascribed to radicals produced by bond breakage, thermally in the one case and by humidity-induced swelling and contracting in the other.

The humble papermaker of the Middle Ages made paper which survives today, much of it in good condition. The more scientific papermakers of the last 150 years have made reams of paper which have already crumbled to dust. Many librarians with collections of brittle, unusable books have a natural interest in forecasting the life of paper, which will be less than 50 years for many of the books which they receive today.

Forecasting the life of even poor paper is a problem, since paper that lasts half a century is degrading very slowly from the standpoint of an experimental determination at room temperature. The Arrhenius equation,

$$\log_{10} (k_2/k_1) = \frac{-E_a}{2.303 \times R} \left(\frac{1}{T_2} - \frac{1}{T_1}\right) \qquad (1)$$

where k_n is a specific reaction rate constant at T_n, E_a is the activation energy of the reaction, R is the gas constant, 1.9872 cal/deg/mole, and T is the absolute temperature, applies in principle to the individual rate processes which collectively govern the loss in paper quality. The most important of these reactions are presumably those involving chain scission in an amorphous region of the cellulose fiber. Broken cellulose chains are free to crystallize; the increase in degree of crystallinity

0-8412-0485-3/79/47-095-117$05.00/0

In Durability of Macromolecular Materials; Eby, R.;
ACS Symposium Series; American Chemical Society: Washington, DC, 1979.

results in a decrease in plasticizing water and an increase in brittleness. At higher temperatures, cross-linking of cellulose chains with the concommitant elimination of water may give the same result.

The life of paper is commonly predicted by subjecting the paper to accelerated aging at temperatures ranging from 60-100 C, and measuring the decrease of folding endurance at several aging times. Extrapolation of a linear Arrhenius plot of the data to the value of $1/T_{abs}$ corresponding to room temperature then allows one to estimate the rate of loss of folding endurance under ambient conditions. There are difficulties in the use of accelerated aging and the Arrhenius method which have been described in detail by Browning and Wink (1) and by Gray (2).

The faint chemiluminescence emission from many organic materials has been shown to be a rapid, precise, and empirically useful tool for their characterization, (3) even though the actual nature of the emission is usually obscure. The light is usually ascribed to excited states that are generated in the termination step of the autoxidation process, although other, physical processes may also give rise to such emission in the solid state. It was thought that the chemiluminescence emission from paper at series of temperatures could potentially give infomation that would bear on the question of continuity of oxidation processes over the entire temperature range of interest. The degradation of paper is normally caused by both oxidative and acid hydrolytic reactions, so that the results were expected to pertain to the aging alkaline papers in which the contribution of the hydrolytic mechanism is minimized. Barrow (4) has already demonstrated that acid papers degrade rapidly and that by treatment with an alkaline earth metal hydroxide, the rate of degradation is greatly reduced.

In the work being reported here, chemiluminescence measurements were made at Battelle Memorial Institute in Columbus over the 25-90 C range on papers prepared and supplied by the Library of Congress R&T Laboratory, while oven-aging and classical endurance studies were made on the same papers in the R&T Laboratory over the 70-100 C range. The latter results will be reported elsewhere. Various treatments were given to the kraft paper selected, in order to broaden the scope of the investigation. The paper was washed to bring the pH to neutral. Then samples were alkalized with magnesium bicarbonate and with a sequence of calcium bicarbonate and calcium hydroxide. Copper acetate was added to several samples to provide an oxidation catalyst (5).

Experimental. The paper used was taken from one roll of bleached kraft. The composition and properties of this paper are shown in Table I.

In Durability of Macromolecular Materials; Eby, R.;
ACS Symposium Series; American Chemical Society: Washington, DC, 1979.

TABLE I. KRAFT PAPER

Basic weight (25 x 38 - 500)		70 lbs.
Thickness		0.006 in.
Tensile, 15 mm strip	MD	10.2 kg
	CD	5.3 kg
Elongation at break	MD	1.73%
	CD	3.21%
Elmendorf tear (single sheet)	MD	127 g
	CD	120 g
Brightness		75.2
pH (Cold)		4.8
Titration		24 meq/kg
Fiber		90% Southern Pine
		10% Hardwood
Filler		8%, which includes 3% TiO_2
Rosin Size		0.5%
Magnesium		9 ppm
Copper		3 ppm
Iron		123
Cobalt		1 ppm

Sheets of the paper were soaked briefly in denatured alcohol in order to assist wetting. The paper was then washed in running tap water for three hours, and then air-dried on a nonwoven fabric.

Six groups of paper were subjected to the following treatments: Paper A - this paper was washed as described; Paper B - the washed papers were soaked in $Mg(HCO_3)_2$ for one-half hour and dried; Paper C - the washed papers were soaked in 0.02 g/l copper acetate solution for 30 minutes and air-dried. They were then soaked for 30 minutes in the magnesium bicarbonate solution and air-dried. This paper showed 86 ppm copper by atomic adsorption analysis; Paper D - washed papers were soaked in 0.0159 g/l copper acetate solution for 30 minutes and air-dried. They were soaked in calcium hydroxide solution for 15 minutes, then calcium bicarbonate solution for 15 minutes and air-dried. This paper showed 64 ppm copper by analysis; Paper E - washed papers were soaked in 0.0089 g/l copper acetate solution for 60 minutes and air-dried. Analysis indicated 59 ppm copper; Paper F - washed papers were soaked in calcium hydroxide solution for 15 minutes, then in calcium bicarbonate solution for 15 minutes and air-dried.

Chemiluminescence. The paper samples were cut into squares 3" on a side (area 9.0 ± 0.6 $in.^2$). The samples were placed into a small, circular aluminum oven with an inner chamber 4.5" in diameter and 1.75" deep. The paper rested at the bottom of an inverted, aluminum weighing cup 2" in diameter at the base and 0.65" high (to insure equilibrium with air temperature). The temperature of the paper was measured with an iron-constantan thermocouple and a Fluke digital thermometer. The oven was

In Durability of Macromolecular Materials; Eby, R.;
ACS Symposium Series; American Chemical Society: Washington, DC, 1979.

maintained at a constant temperature with heating tape and a Foxboro Co. proportional controller. The atmosphere in the oven was dry air (Columbus Oxygen, 2 ppm water), or air-humidified in accord with the procedure of Gray (2). For the humidification procedure, the air was diverted through a glass frit immersed in about 30 ml of water in a test tube (6" long and 1" in diameter). The tube was immersed in a constant temperature bath (Lauda Model K2/RD) that contained water at the appropriate temperature for the experiment. The aluminum tubing that carried the humidified air was maintained with heating tape at a temperature between that of the sample oven and the constant-temperature bath.

The small oven containing the paper was placed in a large aluminum box measuring approximately 12" on a side, with the photomultiplier mounted on top. Light from the sample passed through a glass plate on the top of the oven and into the photomultiplier system. The unfiltered chemiluminescence emission from the paper was measured with an RCA 4501-V4 12-stage photomultiplier with an HP 5300 series measuring system, frequency counter, and digital-to-analog converter. The maximum sensitivity of the photomultiplier tube is in the region 400-600 nm. The counter was set to average signals over a 10-second period (to detect large spurious signals), and the counts were monitored continuously as a step function on a strip-chart recorder. Activation energies were derived from the maxima at 40-90 C only.

Results and Discussion. At oven temperature above about 40 C the chemiluminescence emission from the paper samples rose to a maximum in a few minutes and then declined over a period of hours to an emission near the background level. The time to rise to the maximum was longer than the time required to bring the paper to the oven temperature. The maximum counting rates are given in Table II, and the associated activation energies are given in Table III. Although additional information about the chemiluminescent process may be obtained from the decaying portion of the curve, and from the spectral distribution of the emitted light, in this study only the emission maxima were analyzed.

The observed rates of chemiluminescence below 40 C were usually lower than predicted by extrapolation of the Arrhenius plots (e.g., Figure 1). This is a reasonable result in view of the curve shape at higher temperatures, which shows a decline in emission with time. Since the samples were stored at 25 C, they have been under examination conditions since the time of fabrication, and would in effect already be in this post-maximum region at the time of observation.

There was observed a striking effect of the chemiluminescence on cycling papers between moist and dry atmospheres (Figure 2). With each change there is an increase in chemiluminescence intensity. Its magnitude decreases slightly with successive cycles, indicating the slow exhaustion of some component or configuration of the paper structure. The rate of change in chemiluminescence

In Durability of Macromolecular Materials; Eby, R.;
ACS Symposium Series; American Chemical Society: Washington, DC, 1979.

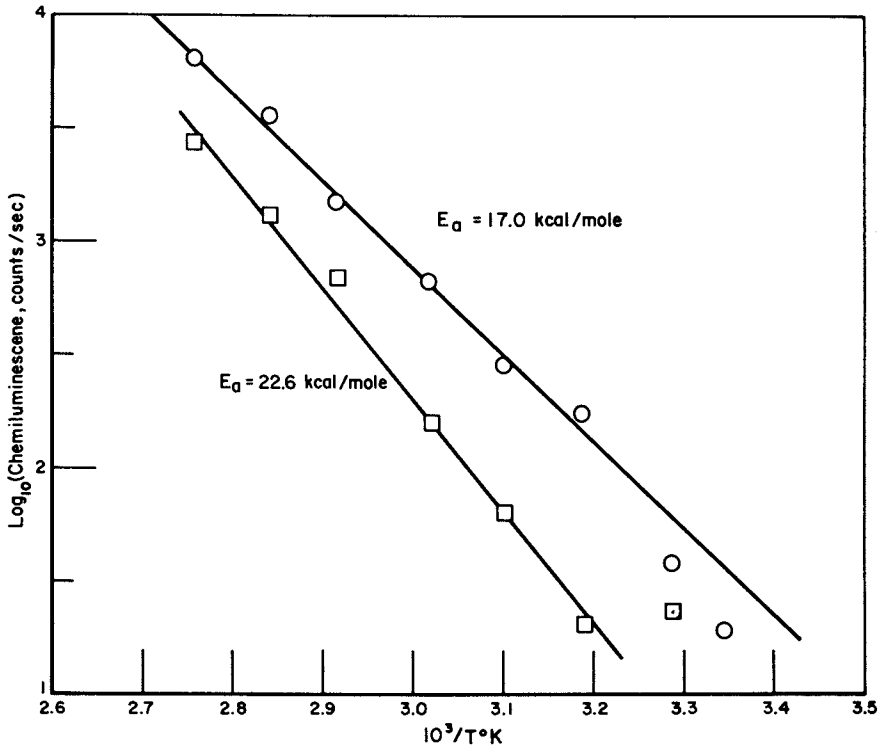

Figure 1. Arrhenius plots of chemiluminescence maxima from paper A (□) in humid air and paper C (○) in dry air

In Durability of Macromolecular Materials; Eby, R.;
ACS Symposium Series; American Chemical Society: Washington, DC, 1979.

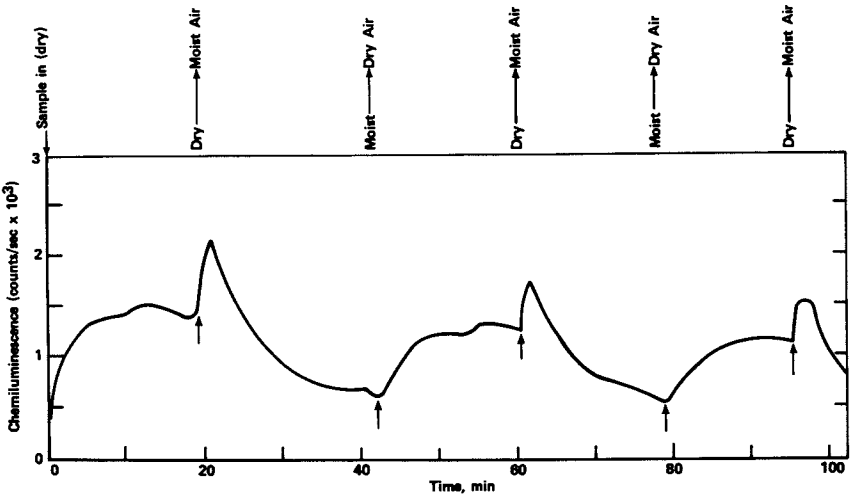

Figure 2. Effects of cycling moist and dry air on chemiluminescence from paper (Sample F, 70 ± 0.4°C)

In Durability of Macromolecular Materials; Eby, R.;
ACS Symposium Series; American Chemical Society: Washington, DC, 1979.

TABLE II. MAXIMUM CHEMILUMINESCENCE FROM PAPER SAMPLES IN AIR AT DIFFERENT TEMPERATURES

Paper	A		B		C		D		E		F	
C	dry	wet	dry	wet	dry	wet	dry	wet	dry	wet	dry	wet
25[a]	4.9,2.8		22,4.5		19,12		12,2.9		6.2,2.3		3.7,3.9	
30[b]	18,24		28,52		38,55		8.8,39		5.0,25		11,30	
40	135,21		170,62		180,29		150,17		72,17		180,24	
50	230,65		370,75		285,75		295,50		175,30		410,65	
60	530,160		840,300		650,285		550,250		385,90		800,195	
70	1260,690		2000,1000		1480,850		1300,700		920,300		1430,880	
80	2300,1300		3800,2110		3650,2110		2900,1350		2050,650		3550,1120	
90	4420,2750		7720,4600		6380,3800		5080,2520		4770,1600		2950,3600	

[a]Bath temperature 7 ± 1 C.

[b]Bath temperature 17 ± 1 C.

TABLE III. ACTIVATION ENERGIES OF CHEMILUMINESCENCE MAXIMA FOR KRAFT PAPER SAMPLES[a]

Paper	Dry Aging E_a	Humid Aging E_a
Washed	16.3 0.99	22.6 0.99
Washed $MgCO_3$	17.4 1.0	21.1 0.97
Washed $CaCO_3$	15.9 1.0	22.7 0.98
Washed Copper	18.9 1.0	21.4 0.99
Washed Copper-$MgCO_3$	17.0 0.99	23.0 0.99
Washed Copper-$CaCO_3$	16.4 0.99	23.3 0.98

[a]E_a (kcal/mole)/r^2.

In Durability of Macromolecular Materials; Eby, R.;
ACS Symposium Series; American Chemical Society: Washington, DC, 1979.

on cycling is faster on changing from a dry to a moist atmosphere than from a moist to dry one. This is possibly associated with lower rates of diffusion of water in the cellulose phase than in the vapor phase, so that moistening of the paper is faster than its drying.

At temperatures of 40 C and above the chemiluminescence from a paper in a moist atmosphere was always observed to be smaller than in a dry atmosphere. Possibly the moisture allows the macromolecular segments in the paper to slide past each other more easily, so that less bond scission occurs. Other explanations, however, are possible in terms of an effect of moisture on the efficiencies of excited state production, or an increased mobility of excited state quenchers. Below 40 C, on the other hand, the maximum emission from samples in moist air was larger in many cases than in dry air, and we may be dealing with an effect involving an increased emission due to the change of atmosphere from the laboratory air to that in the humidified oven (cf. Figure 2).

Both the shape of the chemiluminescence versus time curves and the cycling effect can be accommodated by the hypothesis that heat or humidity changes introduce mechanical strains in the paper which cause homolytic rupture of chemical bonds (Scheme 1).

Scheme 1:

$$\text{Cellulose} \xrightarrow{\text{Stress}} \text{R}\cdot$$

$$\text{R}\cdot + \text{O}_2 \longrightarrow \text{RO}_2\cdot$$

$$\text{RO}_2\cdot + \text{Cell-H} \longrightarrow \text{Cell}\cdot + \text{RO}_2\text{H}$$

$$2\text{RO}_2\cdot \longrightarrow \text{termination}$$

$$\longrightarrow \text{light (minor)}$$

The free radicals thus produced combine with oxygen in the sample and enter into propagation and termination reactions accompanied by the production of light (3). The effect has been previously noted by Williams (6), who used the free radicals so produced to initiate graft polymerization. We note no distinct breaks in the Arrhenius plots of the maxima, which often indicate mechanistic discontinuities in other systems. (3)

Conclusions. A commonly held rule of thumb is that aging paper for 72 hours at 100 C is equivalent to 25 years at room temperature. For a first-order process, this corresponds to an activation energy of 21.8 kcal/mole (1). We note that the chemiluminescence maxima show activation energies close to this value (Table II). Although this observation is interesting, the mechanisms associated with the degradation process and with chemiluminescence are not known with sufficient detail at the molecular level for us to give this result more than empirical significance.

In Durability of Macromolecular Materials; Eby, R.;
ACS Symposium Series; American Chemical Society: Washington, DC, 1979.

The striking increase in chemiluminescence intensity from paper when the humidity is altered supports an earlier suggestion that damage may result from such cyclic treatment (1), and is consistent with the familiar lore that preservation of books and other materials is best achieved under conditions of constant humidity.

Acknowledgement. The authors at Battelle-Columbus are grateful for a grant from the Library of Congress in support of this work.

Reference List

(1) Browning, B. L. and Wink, W. A. (1968), TAPPI, 51, No. 4, 156.
(2) Gray, G. C. (1977), Advances in Chemistry Series, 164, 286.
(3) Mendenhall, G. D., Ang. Chem. Int. Ed., 16, 225 (1977).
(4) Barrow, W. J., "Permanence/Durability of the Book", W. J. Barrow Research Laboratory (1963).
(5) Williams, J. C., Fowler, C. S., Lyon, M. S., and Merrill, T. L. (1977) Advances in Chemistry Series, 164, 37 (1977).
(6) Williams, J. L., Verna, G.S.P., and Stannett, V. T., Ind. Eng. Chem. Prod. Res. Develop., 11, 211 (1972).

RECEIVED December 8, 1978.

Degradation of Chlorinated Polyethylene: Effect of Cross-Linking on Dehydrochlorination

ISMAT A. ABU-ISA

Polymers Department, General Motors Research Laboratories, Warren, MI 48090

Chlorinated polyethylene (CPE) polymers used in this study are made from high density polyethylene and chlorine gas. Several thermoplastic and elastomeric grades of the polymer are available, having different molecular weights and chlorine content. The elastomeric grades of the polymer contain 36 to 48% chlorine and have only a slight residual crystallinity.

The degradation of the polymers prior to crosslinking has been studied by dehydrochlorination and oxygen absorption techniques [1,2]. The effects of crosslinking and compounding ingredients on the stability of the elastomers have been reported, but only in terms of changes in mechanical and oil swell properties [3]. This report deals with the effects of chemical and radiation crosslinking on the rates of dehydrochlorination of CPE with and without stabilizers.

Experimental

The apparatus used for measuring the rates of dehydrochlorination of CPE has been described elsewhere [1]. It allows for the volumetric measurement of HCl evolved from the polymer with time at a constant temperature.

The CPE material used in this study is CM 0342 supplied by The Dow Chemical Company. This CPE grade has a specific gravity of 1.25, a chlorine content of 42 percent, an average Mooney Viscosity [ML1+4(100°C)] of 65 and a residual crystallinity of less than 2 percent. Molded slabs of the pure and compounded polymer were used. Molding was conducted at 163°C for ten minutes which for most compounds is an optimum cure condition. Samples molded under other conditions will be so noted in the text. For dehydrochlorination measurements the samples were cut into about 2 mm cubes.

All chemical crosslinking agents were used as received from the suppliers. These include 2-mercaptoimidazoline (NA-22 Dupont), N,N'-m-phenylenedimaleimide (HVA-2, Dupont), trimethylolpropane trimethacrylate (TMPT, Sartomer), dicumyl peroxide, 40%

0-8412-0485-3/79/47-095-127$05.00/0

In Durability of Macromolecular Materials; Eby, R.;
ACS Symposium Series; American Chemical Society: Washington, DC, 1979.

on Burgess clay (Dicup 40KE, Hercules), α,α'-bis(t-butyl peroxy)-diisopropylbenzene, 40% on Burgess clay (Vulcup 40KE, Hercules) and ethyl-3,3-di (t-butyl peroxy) butyrate (R233, Lucidol). Antioxidants used in the study include tetrakis[methylene-3-(3',5'-di-t-butyl-4'-hydroxyphenyl) propionate]methane (Irganox 1010, Ciba Geigy) and distearylthiodipropionate (NONOX DSTDP,ICI). All other chemicals were reagent grade chemicals used without further purification.

The radiation curing was performed using a 1.5 MEV electron beam accelerator made by Radiation Dynamics with a maximum current capacity of 15 ma. The CPE slabs were irradiated by placing them on a motorized cart which ran past the exit slit of the accelerator. The total radiation exposure was controlled by varying the cart speed, the current, and the number of passes. Generally the samples were irradiated at a current of 15 ma, and a cart speed of 400 mm per second, to a total dose of either 10 or 20 megarads (Mrad). Samples were irradiated in air or nitrogen atmospheres.

Results

Investigation of Crosslinking Systems. Crosslinking of chlorinated polyethylene was attempted with several conventional and novel systems. These include radiation curing with and without added crosslinking coagents such as TMPT, peroxide curing systems with and without crosslinking coagents, and other crosslinking systems such as: alicyclic amines, polyalcohols, metal oxides, metal salts, 2-mercaptoimidazoline, and dipentamethylenethiuram hexasulfide. Most of the above systems were eliminated from further study, because they either degraded the CPE or did not effect sufficient curing of the polymer. The only crosslinking systems that were investigated and will be discussed in this report are the radiation crosslinking and crosslinking by peroxides and NA-22.

Dehydrochlorination Measurements During Crosslinking. In production, CPE is normally crosslinked (i.e., cured) at a temperature around 175°C in either a closed compression mold or in a high pressure steam autoclave. In order to simulate a study of the degradation of the polymer under the above conditions, CPE was degraded in a glass apparatus at 175°C in a nitrogen atmosphere. The rates of dehydrochlorination of the pure polymer and the polymer containing the chemical crosslinking agents, i.e., peroxides and NA-22, were determined. Rates of dehydrochlorination during radiation curing were not measured.

The results of this study are shown in Figure 1. Pure CPE, which under above conditions underwent degradation reactions and very little crosslinking resulted in a maximum rate of dehydrochlorination of 0.117 mg. eq. HCl/g. polymer-hour. Most of the weight loss from the sample after degradation can be accounted

In Durability of Macromolecular Materials; Eby, R.;
ACS Symposium Series; American Chemical Society: Washington, DC, 1979.

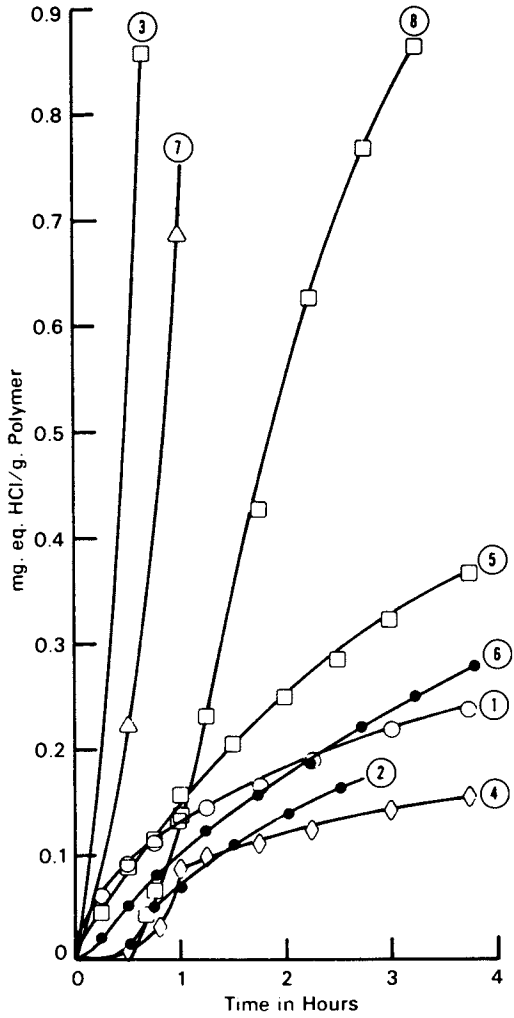

Figure 1. Dehydrochlorination (175°C, N_2) during cross-linking of CPE compounds containing: (1) control; (2) 5 phr Dicup; (3) 5 phr Dicup + 2 phr ZnO; (4) 5 phr Dicup + 6 phr TMPT; (5) phr Dicup + 3 phr HVA-2; (6) 3 phr R233 + 3 phr HVA-2; (7) 8 phr NA-22; and (8) 8 phr NA-22 + 2 phr ZnO.

In Durability of Macromolecular Materials; Eby, R.;
ACS Symposium Series; American Chemical Society: Washington, DC, 1979.

for by the loss of HCl. Addition of Dicup peroxide or R233 peroxide with or without coagents TMPT and HVA-2 resulted only in minor modifications of the rate of dehydrochlorination of the CPE, thus yielding rates that varied between 0.108 and 0.182 mg. eq. HCl/g. polymer-hour. Addition of ZnO to a CPE compound containing Dicup resulted in a very high rate of dehydrochlorination, 6.00 mg. eq. HCl/g. polymer-hour.

Using NA-22 as a crosslinking agent, the rate of dehydrochlorination during crosslinking was higher, 0.817 mg. eq. HCl/g. polymer-hour, than when peroxides were the crosslinking agents. Addition of ZnO to CPE containing NA-22 resulted in this case in a lower rate of dehydrochlorination, than when NA-22 alone was present.

Dehydrochlorination of Peroxide Crosslinked CPE at 180°C in Oxygen. The effects of peroxide crosslinking on the rates of dehydrochlorination of CPE are shown in Table I. The crosslinking coagents trimethylolpropane trimethacrylate (TMPT) and N,N'-m-phenylenedimaleimide (HVA-2) are used for curing CPE and lead to a higher crosslink density of the polymer when used in peroxide curing systems. As seen from Table I crosslinking of the CPE using Dicup alone or Dicup, Vulcup, or R233 with coagents invariably leads to decreased maximum rates of dehydrochlorination. However, the overall rate of dehydrochlorination as can be calculated from the total HCl evolved divided by the total time of degradation is comparable for the uncrosslinked polymer (0.07 mg. eq. HCl/g. polymer-hour) and the crosslinked polymers (0.06 - 0.12 mg. eq. HCl/g. polymer-hour).

Effects of Antioxidants and Stabilizers on Dehydrochlorination of Chemically Crosslinked CPE at 150°C in Nitrogen. The antioxidant system investigated is a synergistic system composed of a phenol, namely, tetrakis[methylene 3-(3',5'-di-t-butyl-4'-hydroxyphenyl)propionate]methane (Irganox 1010) and a sulfur compound, namely, distearylthiodipropionate (DSTDP), both added at 0.5 phr to the CPE. The dehydrochlorination stabilizers consisted of a bisphenol A epoxy resin (DER331) added at 4 phr concentration and PbO added at 5 phr concentration. The effects of these systems on the dehydrochlorination rates of peroxide crosslinked CPE and 2-mercaptoimidazoline crosslinked CPE are shown in Figure 2.

Since the dehydrochlorination was conducted in nitrogen, the antioxidant system alone had no effect on the dehydrochlorination rate. However, the combined antioxidant and stabilizer system had an appreciable effect on peroxide crosslinked CPE, giving rise to an induction period of 105 hours when Dicup was used for crosslinking and 90 hours when Dicup and TMPT were combined to crosslink the polymer. The maximum rate of dehydrochlorination was also appreciably reduced from 55×10^{-3} to 3.1×10^{-3} mg. eq. HCl/g. polymer-hour due to the incorporation of the stabilizer

In Durability of Macromolecular Materials; Eby, R.;
ACS Symposium Series; American Chemical Society: Washington, DC, 1979.

Table I

Dehydrochlorination of CPE
Crosslinked with Peroxides and
2-Mercaptoimidazoline, Measured at 180°C in Oxygen

Crosslinking System	Rates of Dehydrochlorination mg. eq. HCl/g Polymer-Hour	
	Maximum	Overall
None	0.27	0.070
6 phr Dicup	0.16	0.065
6 phr Dicup + 5 phr TMPT	0.084	0.059
6 phr Dicup + 3 phr HVA-2	0.12	0.11
6 phr Vulcup + 3 phr HVA-2	0.10	0.075
3 phr R233 + 3 phr HVA-2	0.18	0.12

In Durability of Macromolecular Materials; Eby, R.;
ACS Symposium Series; American Chemical Society: Washington, DC, 1979.

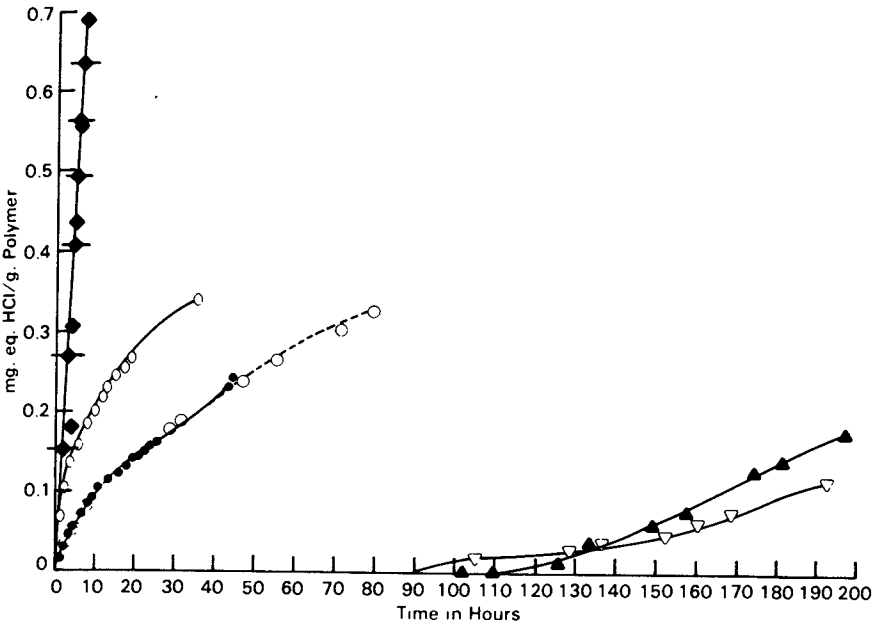

Figure 2. Effects of antioxidants and stabilizers on dehydrochlorination (150°C, N_2) of chemically cross-linked CPE containing: (●), uncross-linked control; (○), uncross-linked control + 0.5 phr DSTDP + 0.5 phr Irganox 1010; (0), 6 phr Dicup; (▲), 6 phr Dicup + 0.5 phr DSTDP + 0.5 phr Irganox 1010 + 4 phr DER + 5 phr PbO; (▽), same as ▲ + TMPT; (–♦–), 8 phr NA-22; (♦), 8 phr NA-22 + 0.5 phr DSTDP + 0.5 phr Irganox 1010 + 4 phr DER + 5 phr PbO.

In Durability of Macromolecular Materials; Eby, R.;
ACS Symposium Series; American Chemical Society: Washington, DC, 1979.

and antioxidant systems.

The beneficial effects of these systems were not observed for the NA-22 crosslinked CPE. Without the stabilizers and antioxidants a high maximum rate of dehydrochlorination of 140×10^{-3} mg. eq. HCl/g. polymer-hour was measured and with these stabilizing additives the maximum rate of dehydrochlorination rose to a higher value namely 150×10^{-3}. It is apparent that this mixed system is ineffective in stabilizing NA-22 crosslinked CPE.

Effects of Antioxidants and Stabilizers on Dehydrochlorination of Chemically Crosslinked CPE at 180°C in Oxygen. The effectiveness of the combined antioxidant (Irganox + DSTDP) and dehydrochlorination stabilizers (DER + PbO) is dramatic in reducing the rate of dehydrochlorination and giving rise to a long induction period in uncured CPE as seen in Figure 3. The maximum rate of dehydrochlorination is reduced from 0.27 to 0.031 mg. eq. HCl/g. polymer-hour and an induction period of 22 hours is observed due to the addition of the combined antioxidant stabilizer system. The system is less effective in stabilizing the peroxide crosslinked polymer. Thus only a marginal reduction from 0.084 to 0.071 in the maximum rate of dehydrochlorination and an induction period of 6 hours are observed when the stabilizer systems are incorporated into the polymer crosslinked by Dicup and TMPT. The maximum rate of dehydrochlorination of NA-22 crosslinked CPE containing the stabilizers continues to be very high (0.60 mg. eq. HCl/g. polymer-hour) under the above degradation conditions.

Effects of Radiation Crosslinking on Dehydrochlorination of CPE at 180°C in Oxygen. Four CPE compounds were chosen for radiation curing and subsequent dehydrochlorination experiments. The first compound (Rad 1) was pure CPE, the second (Rad 2) contained 8 phr TMPT, the third (Rad 3) contained 8 phr TMPT and 0.5 phr of each of the antioxidants, Irganox 1010 and DSTDP, whereas the fourth (Rad 4) contained the dehydrochlorination stabilizers DER 331 (4 phr) and PbO (5 phr) in addition to TMPT, Irganox 1010 and DSTDP. Radiation curing of these compounds was conducted at two dose levels, namely, 10 Mrad and 20 Mrad. Irradiation at each dose level was also carried out in an air and in a nitrogen atmosphere. In order to estimate the level of crosslinking after irradiation, the compounds were immersed for one week in toluene and the percent swell and soluble fractions were measured and compared to chemically cured compounds of CPE (Table II). Except for pure CPE the same level of crosslinking is observed in nitrogen and in air if samples are exposed to the same dose. Addition of TMPT as expected enhances the degree of crosslinking. Addition of the antioxidant system or the dehydrochlorination stabilizer system does not hinder crosslinking by radiation. By comparing with chemically crosslinked systems it can be deduced that CPE in the presence of TMPT requires less

In Durability of Macromolecular Materials; Eby, R.;
ACS Symposium Series; American Chemical Society: Washington, DC, 1979.

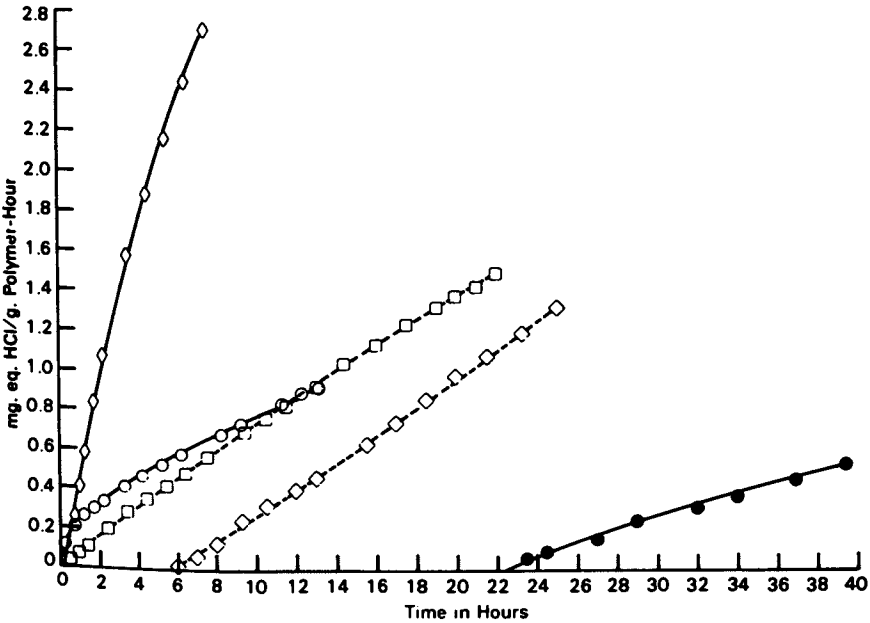

Figure 3. Effects of antioxidants and stabilizers on dehydrochlorination (180°C, O_2) of chemically cross-linked CPE containing: (○), uncross-linked control; (●), uncross-linked control + 0.5 phr DSTDP + 0.5 phr Irganox 1010 + 4 phr DER + 5 phr PbO; (□), 5 phr TMPT + 6 phr Dicup; (◇), 5 phr TMPT + 6 phr Dicup + 0.5 phr DSTDP + 0.5 phr Irganox 1010 + 5 phr PbO + 4 phr DER; (◇), 8 phr NA-22 + 0.5 phr DSTDP + 0.5 phr Irganox 1010 + 5 phr PbO + 4 phr DER.

In Durability of Macromolecular Materials; Eby, R.;
ACS Symposium Series; American Chemical Society: Washington, DC, 1979.

Table II

Toluene Swell Characteristics of Radiation and Chemically Crosslinked CPE

A - Radiation Crosslinked

Polymer	% Volume Swell after Irradiation at (Dose Mrad/Atmosphere)				% Soluble Fraction after Irradiation at (Dose Mrad/Atmos.)			
	10/N_2	10/Air	20/N_2	20/Air	10/N_2	10/Air	20/N_2	20/Air
Rad 1 (CPE)	615	613	478	358	27.6	28.0	20.1	12.9
Rad 2 (CPE + TMPT)	273	270	205	201	15.8	16.8	9.3	7.7
Rad 3 (CPE + TMPT + Irganox + DSTDP)	216	193	173	168	13.7	11.1	7.5	7.7
Rad 4 (CPE + TMPT + Irganox + DSTDP + DER + PbO)	199	207	179	179	14.0	14.6	10.5	10.7

B - Chemically Crosslinked	% Volume Swell	% Soluble Fraction
CPE + NA-22 + Irganox + DSTDP + DER + PbO	316	8.8
CPE + Dicup + Irganox + DSTDP + DER + PbO	466	18.2
CPE + Dicup + TMPT + Irganox + DSTDP + DER + PbO	352	18.6
CPE + Dicup + HVA-2	304	14.2
CPE + Vulcup + HVA-2	358	16.3
CPE + R233 + HVA-2	341	16.2

In Durability of Macromolecular Materials; Eby, R.; ACS Symposium Series; American Chemical Society: Washington, DC, 1979.

than 10 Mrad of radiation for proper cure. This is further verified by tensile property measurements shown in Table III.

Dehydrochlorination measurements of the radiation cured compounds were conducted at 180°C in oxygen (Table IV). Radiation crosslinking of pure CPE reduces the maximum rate of dehydrochlorination from 0.27 for the uncrosslinked polymer to 0.17 - 0.20 mg. eq. HCl/g. polymer-hour. The overall rate of dehydrochlorination is similar for the uncured and radiation cured CPE. Addition of TMPT to the polymer enhances the overall rate of dehydrochlorination from 0.070 to 0.14 - 0.16 mg. eq. HCl/g. polymer-hour. Addition of the antioxidant system reduced the overall rate back to 0.069 - 0.079. When the dehydrochlorination stabilizers are added along with the antioxidants an induction period is produced but the rate of dehydrochlorination remains similar to that observed in the case of antioxidants alone. At 10 Mrad dose the induction period lasts for 10 hours, whereas at 20 Mrad dose it is reduced to 5 hours. The dose level and the irradiation atmosphere do not have a marked influence on the rate of dehydrochlorination as seen in Table IV.

Discussion

Of about twenty different crosslinking systems tried in CPE only three were considered for the dehydrochlorination studies. These are the radiation, the peroxide and the 2-mercaptoimidazoline systems. The others were eliminated from further consideration because they either severely degraded the polymer or did not induce sufficient crosslinking. The suggested mechanisms of crosslinking of the three systems studied will now be discussed.

Two mechanisms are suggested in the literature for the crosslinking of chlorinated polymers by 2-mercaptoimidazoline: when the compound is used alone, and when ZnO is used with it. Csaszar and Galinsky [4] proposed the following mechanism of crosslinking CPE by NA-22:

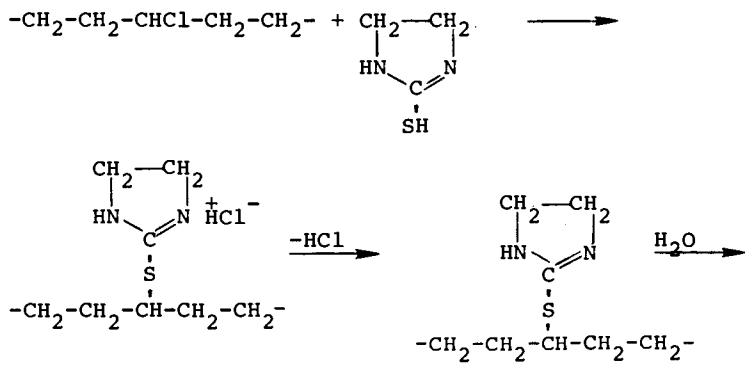

Table III

Mechanical Properties of Radiation Crosslinked CPE

Polymer	Dose Mrad Atmosphere	Tensile Strength MPa	100% Modulus MPa	Elongation %	Tear N/M	Hardness, Durometer Points
Rad 1	0	10.27	2.48	505	25.0	77
Rad 1	10/Air	13.51	2.21	470	22.2	72
Rad 1	$10/N_2$	15.44	2.41	470	23.1	73
Rad 1	20/Air	16.82	2.41	415	23.6	70
Rad 1	$20/N_2$	12.20	2.34	425	22.6	72
Rad 2	0	12.13	7.58	405	40.4	75
Rad 2	10/Air	17.10	9.93	300	30.2	65
Rad 2	$10/N_2$	16.82	9.17	312	29.4	73
Rad 2	20/Air	18.96	10.20	230	25.9	72
Rad 2	$20/N_2$	19.17	9.65	230	28.7	76
Rad 3	0	9.79	1.24	600	16.6	62
Rad 3	10/Air	17.51	8.41	377	42.7	90
Rad 3	$10/N_2$	17.17	8.41	315	41.7	91
Rad 3	20/Air	17.10	10.27	200	30.8	75
Rad 3	$20/N_2$	18.41	10.43	210	35.2	91
Rad 4	0	5.24	0.90	560	14.4	52
Rad 4	10/Air	12.48	7.79	270	39.9	88
Rad 4	$10/N_2$	12.96	7.72	260	40.4	88
Rad 4	20/Air	11.72	8.96	190	37.5	90
Rad 4	$20/N_2$	15.38	9.45	230	39.0	88

In Durability of Macromolecular Materials; Eby, R.;
ACS Symposium Series; American Chemical Society: Washington, DC, 1979.

Table IV

Dehydrochlorination of
Radiation Crosslinked CPE at 180°C in Oxygen

Polymer	Dose, Mrad/ Atmosphere	Rates of Dehydrochlorination mg.eq. HCl/g polymer-hour		Induction Period Hours
		Maximum	Overall	
Rad 1	0	0.27	0.070	0
Rad 1	10/N_2	0.17	0.092	0
Rad 2	10/N_2	0.27	0.14	0
Rad 3	10/N_2	0.18	0.079	0
Rad 4	10/N_2	0.12	0.060	10.5
Rad 1	10/Air	0.20	0.089	0
Rad 2	10/Air	0.22	0.14	0
Rad 3	10/Air	0.086	0.069	0
Rad 4	10/Air	0.12	0.076	10.5
Rad 2	20/N_2	0.24	0.16	0
Rad 4	20/N_2	0.15	0.097	5.0
Rad 1	20/Air	0.18	0.11	0
Rad 4	20/Air	0.15	0.10	5.0

In Durability of Macromolecular Materials; Eby, R.;
ACS Symposium Series; American Chemical Society: Washington, DC, 1979.

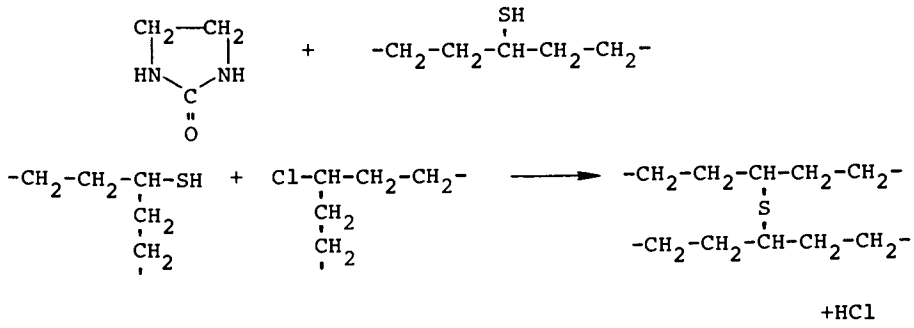

When NA-22 is used in chlorinated elastomer with ZnO the following crosslinking mechanism is suggested by Pariser [5]:

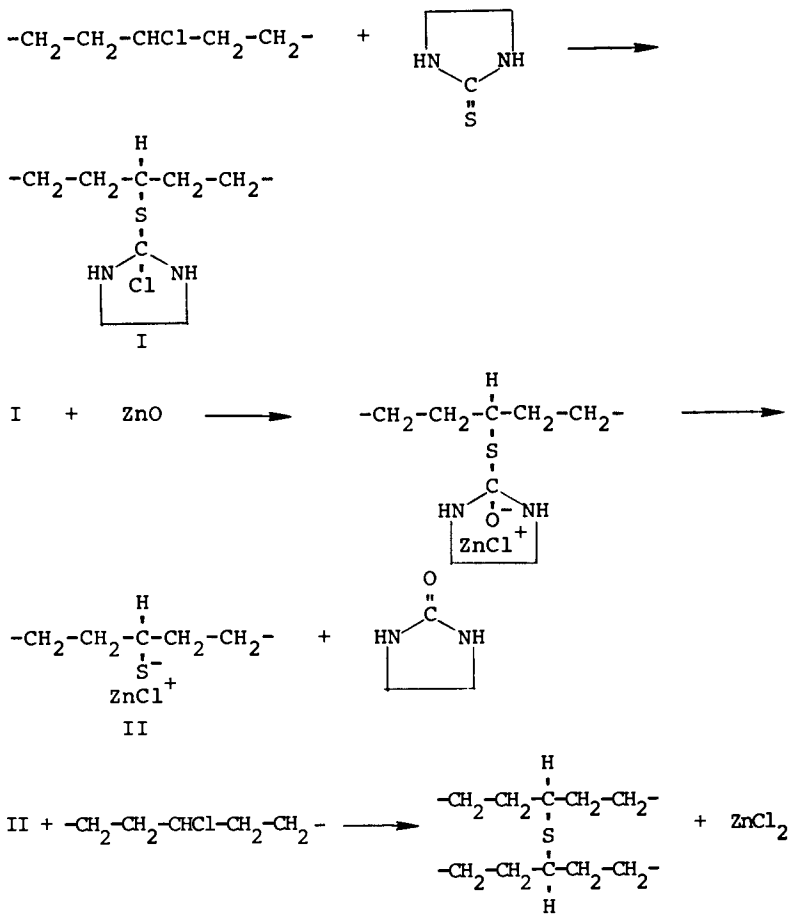

In the case of peroxide crosslinking or radiation crosslinking the mechanism is free radical. The two mechanisms are similar except that the source of the initial free radical is different. A proposed mechanism [4,6] of peroxide crosslinking can be presented as follows:

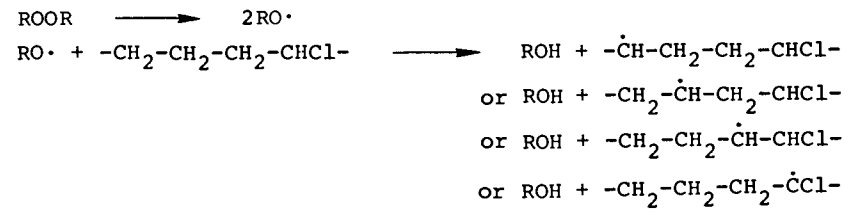

Crosslinking occurs through combinations of the CPE radicals on different chains. To enhance crosslinking by peroxide or by radiation reactive multifunctional monomers are added which are more mobile than the polymer chains and hence act as bridges to crosslink different chains of the polymer. Kovacic and Hein [7] suggested a mechanism for crosslinking of natural rubber with peroxides and dimaleimides which will be adapted here to illustrate the crosslinking of CPE with radiation or peroxide in the presence of a monomer. N,N'-m-phenylenedimaleimide (HVA-2) will be used as the crosslinking monomer.

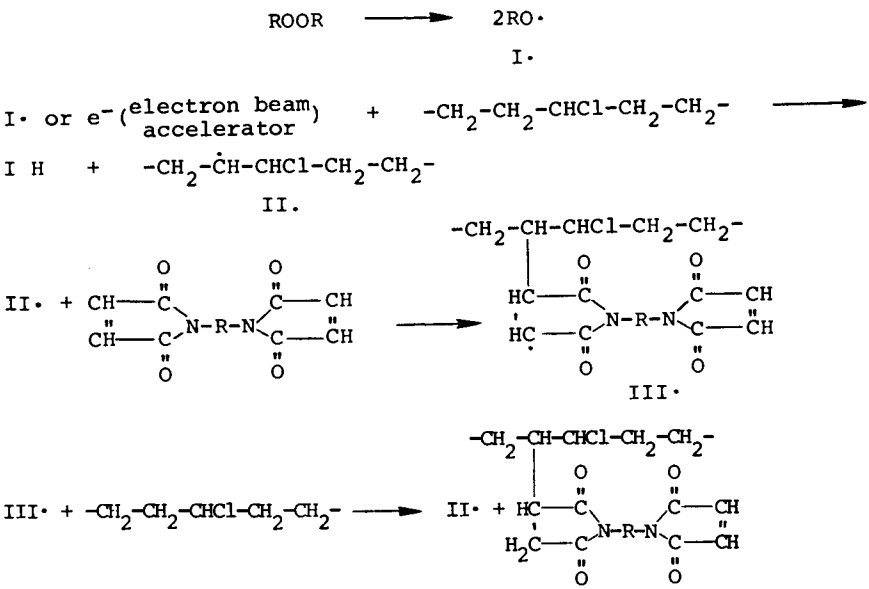

In Durability of Macromolecular Materials; Eby, R.;
ACS Symposium Series; American Chemical Society: Washington, DC, 1979.

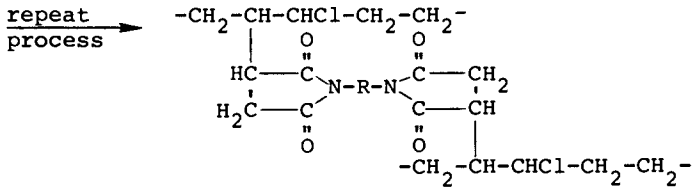

A similar reaction occurs in the case where trimethylolpropane trimethacrylate (TMPT) is used as the crosslinking monomer except that the TMPT can homopolymerize by heat or free radicals. This is evidenced by the high 100% modulus value of the CPE containing the TMPT (Table III, column 4) even prior to irradiation. Evidently the TMPT has polymerized under heat during molding of the polymer into slabs and increased the modulus of the CPE to 7.58 MPa as compared to 2.48 MPa for the CPE without TMPT. Although Rad 3 and Rad 4 compounds contain TMPT, polymerization of the monomer during molding did not occur because of the presence of the antioxidants in the compounds. In all cases toluene swell measurements showed that crosslinking of the CPE did not occur prior to irradiation. Hence, the increase in modulus of the Rad 2 compound could only be attributed to homopolymerization of the TMPT during processing.

The above suggested mechanisms will now be employed to discuss the degradation of CPE data during and after crosslinking with the 2-mercaptoimidazoline systems, with the peroxides, and with radiation crosslinking systems. As seen in Figure 1 the use of 2-mercaptoimidazoline (NA-22) with or without ZnO enhances the rate of dehydrochlorination during crosslinking at 175°C in a nitrogen atmosphere. The use of NA-22 leads to an increase in the maximum dehydrochlorination rate from 0.117 for the pure polymer to 0.817 mg. eq. HCl/g. polymer-hour. This increase could be partly explained on the basis that the crosslinking reaction involving NA-22 gives rise to HCl as a byproduct. Beyond that the two amine groups on the molecule of the NA-22 evidently accelerate the dehydrochlorination by abstracting and eventually releasing HCl from the CPE due to heat. Addition of ZnO with NA-22 reduces the maximum rate of dehydrochlorination to 0.390 mg. eq. HCl/g. polymer-hour. In this case ZnO as shown above takes part in the crosslinking reaction and ends up as $ZnCl_2$ thus absorbing two molecules of HCl.

After crosslinking, the NA-22 present as ethylene urea continues to accelerate the rate of dehydrochlorination. Thus the rate of dehydrochlorination of CPE at 150°C in a nitrogen atmosphere is 16 times faster when crosslinked with NA-22 (Figure 2). Even in the presence of the antioxidants and dehydrochlorination stabilizers, the rate is eight times faster than that of uncrossed polymer at 150°C in nitrogen and three times faster at 180°C in oxygen (Figure 3).

In Durability of Macromolecular Materials; Eby, R.;
ACS Symposium Series; American Chemical Society: Washington, DC, 1979.

Peroxide crosslinking of CPE occurs by combination of radicals on different chains. As shown earlier the radicals are generated by hydrogen abstraction from the polymer by the RO· from peroxides. Crosslinking occurs through C-C linkage of the chain if the monomer is absent or through bridging of the monomer when the latter is present with the peroxide. During crosslinking with peroxides, with or without monomer, Figure 1 shows that the rate of dehydrochlorination is similar to that of pure CPE. This is true even when different peroxides or different monomers are used. Hence the peroxides in this case are not contributing to the dehydrochlorination of CPE. In one case when ZnO was added with Dicup, the rate of dehydrochlorination was appreciably increased. This is to be expected [8] when ZnO is not consumed in the crosslinking reaction and is free to react with HCl to form the Friedel-Crafts catalyst, $ZnCl_2$, which appreciably accelerates dehydrochlorination.

Dehydrochlorination rates of peroxide crosslinked polymers at 180°C in oxygen are slightly lower than the uncrosslinked polymer as shown in Table I. The decrease in the rate of dehydrochlorination is a result of crosslinking which retards oxygen penetration into the polymer. At 150°C and in the absence of oxygen the overall rate of dehydrochlorination of the crosslinked polymer is 0.0096 as compared to 0.0052 mg. eq. HCl/g. polymer-hour for the uncrosslinked polymer (Figure 2). This is possibly the result of generation of more labile tertiary chlorines upon crosslinking.

The influence of the antioxidants and the dehydrochlorination stabilizers on peroxide cured CPE is studied in nitrogen and in oxygen atmospheres. In nitrogen the addition of the antioxidant system to uncrosslinked CPE, as expected, does not influence the rate of dehydrochlorination. However, the incorporation of antioxidants and dehydrochlorination stabilizers into crosslinked CPE appreciably reduces the overall rate of dehydrochlorination by 10 to 13 fold and gives rise to an induction period of 90-105 hours (see Figure 2). In oxygen and at 180°C the effects of the antioxidant system and the dehydrochlorination stabilizer system on the rates of dehydrochlorination are shown in Figure 3. If the polymer is not crosslinked, the antioxidant - stabilizer systems have an appreciable effect in reducing the rate of dehydrochlorination and giving rise to a long induction period. However, the systems are less effective after crosslinking with peroxides with or without the monomer. It is evident that during crosslinking with peroxides the antioxidant - stabilizer systems are partially destroyed. This is to be expected since the antioxidants Irganox 1010 and DSTDP provide oxidation protection to polymers by sacrificially reacting with and decomposing peroxides generated during oxidation.

Irradiation of CPE was carried out on four compounds. These are CPE (Rad 1), CPE with TMPT (Rad 2), CPE with TMPT and antioxidants Irganox 1010 and DSTDP (Rad 3), CPE with TMPT, the

In Durability of Macromolecular Materials; Eby, R.;
ACS Symposium Series; American Chemical Society: Washington, DC, 1979.

antioxidants, and the dehydrochlorination stabilizers DER 331 and PbO (Rad 4). Irradiation was conducted at two dose levels, 10 and 20 Mrad and in two atmospheres, nitrogen and air. The results of the toluene swell measurements, shown in Table II, indicate that a similar level of crosslinking is obtained at the same dose for all compounds except Rad 1. It is also evident that again with the exception of Rad 1 all compounds reach optimum crosslink density comparable to chemically crosslinked CPE at a radiation dose of less than 10 Mrad.

The tensile strength, modulus, elongation, tear and hardness properties of the radiation crosslinked CPE compounds are shown in Table III. In general excellent properties are developed with radiation curing. In Rad 4 it is evident that the addition of dehydrochlorination stabilizers leads to slight degradation in the mechanical properties of the polymer.

Dehydrochlorination measurements of these compounds were conducted at 180°C in oxygen atmosphere (Table IV). The rates of dehydrochlorination of the unstabilized crosslinked polymers are similar to those of the uncrosslinked polymer regardless of dose level or whether the irradiation was conducted in nitrogen or air. Addition of TMPT to the polymer enhances, but only slightly, the overall dehydrochlorination rate from 0.070 for the pure uncrosslinked polymer to 0.14 - 0.16 mg. eq. HCl/g. polymer-hour for the radiation crosslinked polymer containing TMPT.

The influence of the antioxidant system and the dehydrochlorination stabilizer system are shown in Table IV. The largest effect is exhibited in the Rad 4 compound. In this case an induction period of 10.5 hours is generated when Rad 4 is exposed to 10 Mrad radiation and 5 hours when the radiation dose is 20 Mrad. Slight reduction of dehydrochlorination rates are also observed for Rad 3 and Rad 4. Comparing the effect of the stabilizers in the radiation cured systems to that of uncrosslinked polymer it is obvious that both the antioxidant system and the dehydrochlorination stabilizer system are partially consumed during crosslinking and hence lose some of their effectiveness in protecting the crosslinked polymer.

In conclusion this investigation shows:

1. 2-Mercaptoimidazoline curing systems are effective in curing the CPE but result in thermally less stable polymer.

2. Peroxide curing with monomers such as HVA-2 and TMPT is an effective system for producing thermally stable and properly cured CPE.

3. Radiation curing is very effective in crosslinking CPE in the presence of a monomer and results in a thermally stable polymer.

In Durability of Macromolecular Materials; Eby, R.;
ACS Symposium Series; American Chemical Society: Washington, DC, 1979.

4. Although the dehydrochlorination stabilizers (PbO and DER) and the antioxidants (Irganox and DSTDP) are very effective in protecting the uncrosslinked polymer against thermal oxidation, they lose some of their effectiveness when the polymer is crosslinked by radiation or peroxide and are ineffective when the crosslinking agent is 2-mercaptoimidazoline.

Acknowledgments

The author wishes to acknowledge the technical assistance of John A. Krohn who conducted most of the experimental work of this investigation. Technical assistance by Grady Rorie, Cara C. Jackson and T. J. Nakic is also acknowledged.

References

1. Abu-Isa, I. A., J. Polym. Sci., (1972) 10, A-1, 881.

2. Abu-Isa, I. A., Polym. Eng. Sci., (1975), 15(4), 299.

3. Amar, V. R. and Solberger, L. E., paper presented at SAE meeting, Detroit, Michigan, Oct. 13-17, 1975.

4. Csaszar, F. C. and Galinsky, N. M., Polymer Age, Feb. (1968), pp. 49-61.

5. Pariser, R., Kunststoffe, (1960) 50, 623.

6. Farmer, E. H. and Moore, C. G., Chemical Society Journal (1951), pp. 131-148.

7. Kovacic, P. and Hein, R. W., J. Am. Chem. Soc., (1959), 81, 1190.

This is the fourth part of a series.

RECEIVED December 8, 1978.

10

Crystallinity in Hydrolytically Aged Polyester Polyurethane Elastomers

DANIEL W. BROWN, ROBERT E. LOWRY, and LESLIE E. SMITH

National Bureau of Standards, Washington, DC 20234

Polyester polyurethanes degrade in humid environments. The expected lifetime of five years for the best polyester polyurethanes at 25° C [1] is frequently not achieved [2,3]. The ordinary degradation is due to hydrolysis of the polyester component [4]. Acid produced catalyzes additional hydrolysis, thus increasing the rate autocatalytically [5]. Larger acid numbers in the polyester diol from which the polyurethane is made increase the degradation rate of the polyurethane [5]. Polyester polyurethanes can also be attacked by fungi [2].

We have found that aged polyester polyurethanes can be more crystallizable than their unaged counterparts. The crystallinity affects the modulus, whose change has been used to estimate the lifetime [1].

Experimental

Polyurethanes were prepared by both prepolymer and oneshot methods. Our polymers were molded at about 190° C into 0.3 mm sheets. A commercial supplier provided 0.25 mm sheets of polyester based and polyether based polyurethanes. These were used as received, except for cutting.

Strips were aged in sealed tubes containing 1 atmosphere of air (at 25° C) above liquid water. The tubes were placed in thermostatted water baths or in a circulating air oven. Our polymers were aged for 10 days at 24° C, 11 days at 35° C, 13 days at 42° C, 14 days at 50° C, and 35 days at 58° C. Then the tubes were opened and the samples kept at 25° C and 50% relative humidity for 60 days before further processing. The commercial polyurethanes were aged for 19 days at 42° C, 22 days at 50° C, 113 days at 58° C, and 60 days at 25° C. Then the tubes were opened and the samples kept at 25° C and 50% relative humidity for 3 days before further processing. The complex sequential agings were done as part of a study of creep which will not be presented at this time.

In Durability of Macromolecular Materials; Eby, R.;
ACS Symposium Series; American Chemical Society: Washington, DC, 1979.

When the tubes were opened the gasses above the polymers were analyzed for O_2, N_2, and CO_2. The analyses were not significantly different from that of laboratory air. The stress-strain curves of the polymer samples were run to 300% elongation at 25° C and 60° C (on different specimens). Gage marks were initially 2.5 cm apart, jaws were 7.5 cm apart, and crosshead speed was 5 cm/min, unless specified. Sol fractions of insoluble polymers were determined by extraction with tetrahydrofuran at 25° C. Intrinsic viscosities [η], of soluble polymers were determined, also in tetrahydrofuran at 25° C. A differential scanning calorimeter was used to measure the heat of fusion, ΔH_F. Scans were at 10° C/min on 10-20 mg of polymer that had not been subjected to the stress-strain measurements. Samples were rescanned immediately after the first scan, at least 30 days later, and sometimes at intermediate times.

Soluble polymers were run through a gel permeation chromatograph. Polystyrene fractions of known molecular weight were run also and their intrinsic viscosities were measured. The universal calibration technique was used in conjunction with a computer program to calculate the number average molecular weight, M_n, of the polyurethane.

Results and Discussion

Figure 1 shows stress-strain curves for the commercial polyether polyurethane and for PU-13, made from methane diphenyl diisocyanate (MDI), butane diol (BD), and polytetramethylene oxide diol of molecular weight, 2000 (PTMO 2000). There is little difference in stress values for aged and unaged polymers. At 60° C, stress values are about 25 - 35% less than at 25° C.

Figure 2 shows stress-strain curves for the commercial polyester polyurethane and for PU-16, made from MDI, BD, and a polycaprolactone diol of molecular weight 2000 (PCL 2000). At 25° C the stress values for each aged polymer are higher than for the corresponding unaged polymer. The aged commercial polymer broke when drawn at the usual rate so a four-fold slower draw rate was used with all the commercial polyester polyurethane samples. At 60° C even with the slower draw rate the aged sample stretched only 50% before breaking; at 20 and 50% strain the stresses are about half those of the unaged polymer. PU 16 has nearly the same stress values at 60° C, whether aged or unaged. Thus, raising the temperature from 25 to 60° C lowered the stress-strain curves more for aged, than for unaged samples.

Results qualitatively similar to those in Figure 2 were obtained with polyurethanes made from toluene diisocyanate (TDI), BD, and: 1) PCL 2000 2) a polycaprolactone diol of molecular weight 1220 (PCL 1220) 3) a polyethyleneadipate diol of molecular weight 2000 (PEAD 2000). However, all TDI based polymers had very low stress values at 60° C.

In Durability of Macromolecular Materials; Eby, R.;
ACS Symposium Series; American Chemical Society: Washington, DC, 1979.

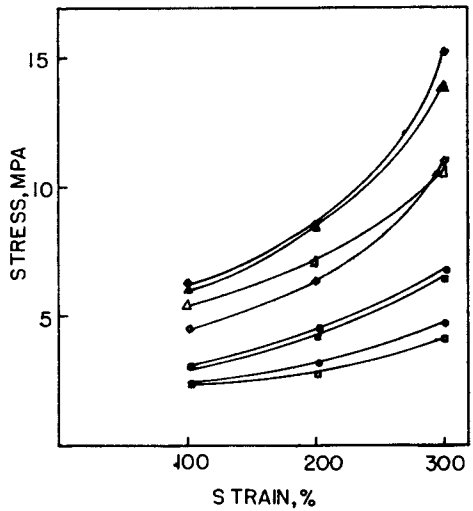

Figure 1. Stress vs. strain at 25° and 60°C for polyether polyurethanes: filled symbols at 25°C; unfilled symbols 60°C. Commercial polymer: (♦, ◇), unaged; (▲, △), aged wet. PU 13: (●, ○), unaged; (■, □) aged wet.

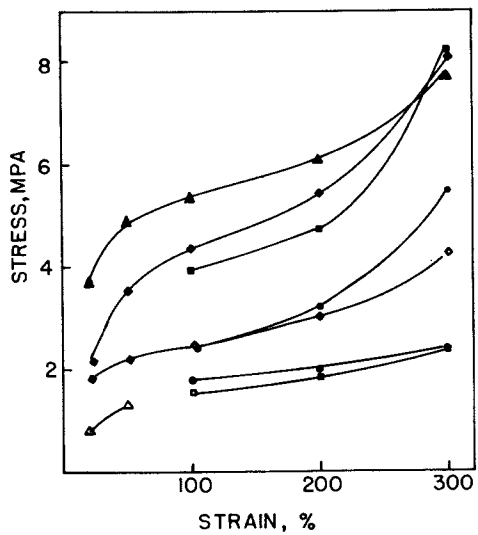

Figure 2. Stress vs. strain at 25 and 60°C for polyester polyurethanes. Filled symbols 25°C, unfilled symbols 60°C. Commercial polymer (stretched 1.25cm/min) (♦, ◇), unaged; (▲, △), aged wet. Pu 16: (●, ○), unaged; (■, □), aged wet.

In Durability of Macromolecular Materials; Eby, R.;
ACS Symposium Series; American Chemical Society: Washington, DC, 1979.

Wide angle X-ray patterns of the aged and unaged polyester are in Figure 3. Sharp lines, indicative of crystallinity, occur in the pattern from the former polymer; these are absent from the pattern from the unaged polymer.

When samples were run in a differential scanning calorimeter none of the polyether polyurethanes showed evidence of crystallinity. All the aged polyester polyurethanes showed melting peaks generally with maxima near 42° C. In all cases melting appeared complete below 51° C. Figure 4 shows the calorimeter plots for the aged commercial polyester based polymer as observed initially and three times thereafter. Recrystallization occurs over a period of days at 25° C. The unaged commercial polyester type did not show a melting transition. Our polyester polyurethanes behaved somewhat differently in that aged and unaged samples both showed melting transitions; those of the aged polymer took up more heat. In addition, for as long as 16 hours after being scanned no melt transitions were detectable in our polymers.

Table 1 lists the heats of fusion found initially and also after the samples had been at 25° C and 50% relative humidity for at least 30 days after the first measurement. Also included in the table are results of solution studies of the polymers - their sol fractions, if not completely soluble, or their intrinsic viscosities.

Our polymers were crosslinked. On molding, sol fractions increased and on aging increased still further, indicating that chain scissions occurred. PU 9 and the commercial polyester type were soluble and showed substantial drops in intrinsic viscosity on aging. The last two polymers in Table 1 are polyether based; for these less scission is indicated by the changes in sol fractions and intrinsic viscosity.

Values of M_n calculated from gel chromatograms of the commercial polymers are: polyester type, Unaged 42400, Aged 11800; polyether type, Unaged 44900, Aged 35800. The difference of the reciprocals of the M_n for aged and unaged samples is the mol of scissions per gram. Values are 6×10^{-5} and 0.6×10^{-5} for the polyester and polyether types, respectively. Thus in our study the overall scission rate of the polyester polyurethane was about 10 times greater than that of the polyether polyurethane.

No crystallinity is detectable in a polymer of MDI, BD, and PCL 1220, that was aged until its M_n had decreased from 64000 to 49000. Thus it appears that it is the molecular weight reached, not the degradation process *per se*, that results in crystallization.

In table 2 are shown data relating molecular weight and crystalline content of unaged polymers. These were prepared by using an excess of OH or NCO functionality. If the functionality not in excess is used up, the theoretical M_n (listed) is the weight charged divided by the excess number of mols. Intrinsic viscosities found show that the desired effect was achieved.

In Durability of Macromolecular Materials; Eby, R.;
ACS Symposium Series; American Chemical Society: Washington, DC, 1979.

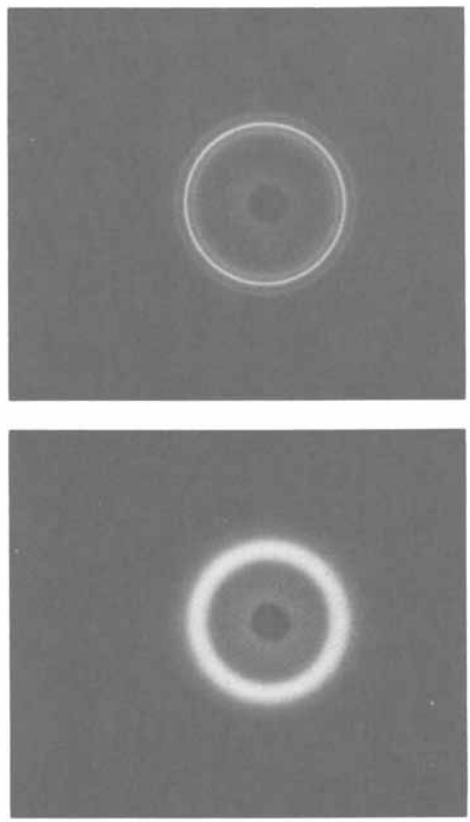

Figure 3. X-ray photographs for commercial polyester polyurethane (Lower, *unaged;* Upper, *aged wet)*

In Durability of Macromolecular Materials; Eby, R.;
ACS Symposium Series; American Chemical Society: Washington, DC, 1979.

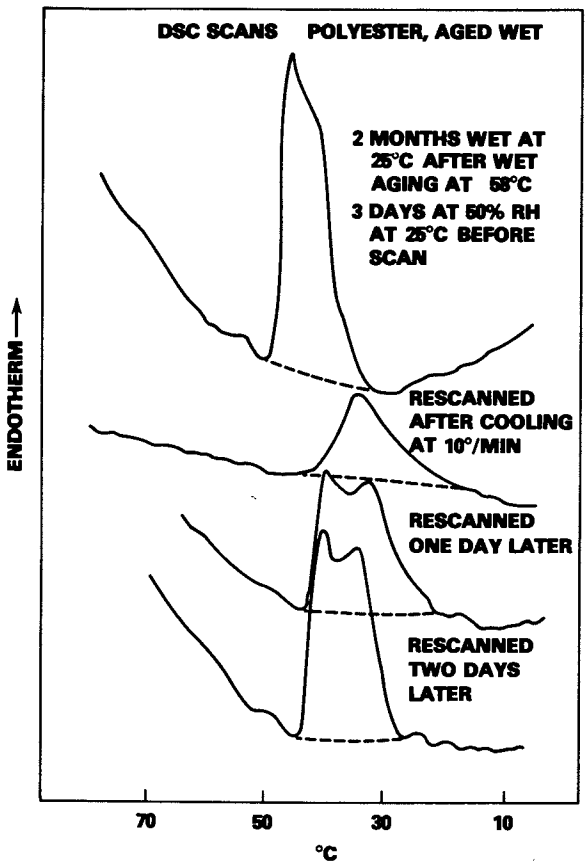

Figure 4. DSC scans, commercial polyester polyurethane, aged wet

In Durability of Macromolecular Materials; Eby, R.;
ACS Symposium Series; American Chemical Society: Washington, DC, 1979.

Table I

Melting and Solution Behavior of Polyurethanes

Polymer and Treatment	ΔH_F J/g	Sol wt%	[η] Dl/g
PU 9, TDI : 1 PEAD 2000: 0.95 BD			
Before molding		58	
After molding, unaged	28,29	100	1.15
Aged wet	42,40	100	0.17
PU 15, 2TDI: 1 PCL 2000: 1 BD			
Before molding		4	
After molding, unaged	36,32	26	
Aged wet	41,39	97	
PU 17, S TDI: 1 PCL 1220, 1 BD			
Before molding		2	
After molding, unaged	6,5	30	
Aged wet	25,21	90	
PU 16, MDI: PCL 2000: 1 BD			
Before molding		2	
After molding, unaged	2,2	75	
Aged wet	15,16	95	
Commercial Polyester Polyurethane			
Unaged	0,0	100	0.99
Aged wet	7.7,15	100	0.41
PU 13, 2 MDI: 1 PTMO; 0.95 BD			
Before molding		3.5	
After molding, unaged	0,0	74	
Aged wet	0,0	83	
Commercial Polyether Polyurethane			
Unaged	0,0	100	1.50
Aged wet	0,0	100	1.36

In Durability of Macromolecular Materials; Eby, R.;
ACS Symposium Series; American Chemical Society: Washington, DC, 1979.

Table II

Molecular Weight Effects in an MDI, PCL 1220, BD Polyurethane

MDI:PCL:BD	M_n	[η]	ΔH_F [a]	200% Strain	
mol ratio	g/mol	dl/g	J/g	MPa	
				25° C	60° C
2:1:2	1910	0.19	17	0	0
2:1:1.25	7370	0.28	2.1	b	0
2:1:0.95	36300	0.60	0,1.3	5.4	2.5
2:1:1	∞	2.1	0,0	6.0	4.3

a) Melting curve maxima at 41 - 43° C.
b) Broke at 2.1 MPa at less than 100% strain.

In Durability of Macromolecular Materials; Eby, R.;
ACS Symposium Series; American Chemical Society: Washington, DC, 1979.

Heats of fusion decrease as [η] increases, becoming zero for the polymers with the two highest [η]. However, of these the one with the lower [η] had slight residual crystallinity after being stretched 300% at 25° C and released. No crystallinity was detected in the sample of highest [η] after the same treatment. The stress values listed decrease more between 25 and 60° C for the polymer that crystallized on stretching at 25° C, showing that the crystallization influenced the stress at 25° C.

All hard segment (MDI+BD) and all soft segment (MDI+PCL 1200) polymers have melting peaks with maxima at about 200° C and at about 40° C respectively. Therefore the crystallinity observed in our specimens probably is due to the soft segment.

It is uncertain if earlier lifetime estimates [1] were affected by crystallization of the degraded specimens. An effect so large that the modulus was raised on aging, as found here, must not have occurred. However the data in Table 2 suggest that stretching might induce crystallinity more readily in aged than in unaged samples, and partially compensate for the molecular weight reduction in the former. This would have affected the lifetime estimates. By comparing moduli of aged and unaged material at high temperature one can detect this effect.

Polyester polyurethanes in service probably crystallize as they age, retaining their usual physical characteristics to casual examination. As the molecular weight decreases the melting temperature will eventually decrease also. Sorbed water may also affect the melting temperature. Eventually ambient temperature will exceed the melting temperature causing a relatively sudden loss of physical properties. Until a more certain lifetime estimate is available, test strips of the polyester polyurethane used might be located near critical applications. These could be tested at intervals, by modulus measurements at elevated temperature or perhaps by acid number determinations. Since each hydrolytic scission of an ester produces an acid group it is likely that the increase in acid content will equal the increase in the number of polymer molecules.

Acknowledgements

The work was supported in part by the Naval Air Systems Command and the Office of Naval Research.

Literature Cited

(1) G. Magnus, R. A. Dunleavy, and F. E. Critchfield, Rubber Chem and Tech., 39, 1328 (1965).
(2) Z. T. Ossefort and F. B. Testroet, Rubber Chem and Tech., 39, 1308 (1965).
(3) C. F. Bersch, Naval Air Systems Command, Private Communication.
(4) R. J. Athey, Rubber Age 96, 705 (1965).
(5) C. S. Shollenberger and F. D. Stewart, J. Elastoplastics, 3, 28 (1971).

RECEIVED December 8, 1978.

11

Effect of Hydrolytic Degradation on Compression-Deflection Characteristics and Hardness of Structured Polyurethane Castings

M. A. MENDELSOHN
Westinghouse Research Laboratories, Insulation Chemistry, Pittsburgh, PA 15235

G. B. ROSENBLATT
Westinghouse Marine Division, Missile Launching and Handling Dept., Sunnyvale, CA 94086

Polyurethane liner pads employed in naval missile launch systems are exposed to high humidities during storage and occasionally to sea water after their installation. In order to determine their durability towards water, a detailed study was made of their hydrolytic stability. Even though both polyether and polyester based urethanes can give the physical properties required for this application, only the polyether urethanes were studied since they display much superior resistance to hydrolysis (1, 2, 3, 4).

Accelerated testing was performed by immersing polyurethane liner specimens in water at several elevated temperatures. Periodically, the samples were removed from their respective water baths, dried and then subjected to hardness and compressive stress-strain measurements. An Arrhenius relationship was employed to estimate the expected life of the pads under the severe condition of being continually immersed in water at 35°C. The pads were considered to have failed when their compressive stress fell to 80 percent of the original value.

Experimental

Mechanical Tests. Hardness measurements taken with a Shore A durometer are reported every time a pad specimen has been removed from its water bath for compression-deflection tests. Separate flat slabs, 0.12 and 0.50 in. thick, of polyurethane elastomer, which were cast from the same batch of material and given identical exposure to water as the pads, were employed for the hardness tests.

The compressive stress-strain measurements are performed in an Instron Universal Test Machine. Pad specimens (Figure 1) are loaded to the bottomed deflection (Figure 2) at 1.1 in. and unloaded without pause. A cross-head rate of 2.0 in./min which is sufficiently slow as to give essentially a static loading condition is employed. Compressive stress data are reported for deflections of 0.2, 0.4 and 0.6 in.

For purposes of illustrating the data, measurements and calculations are presented for the 70°C immersion (Tables I-III).

0-8412-0485-3/79/47-095-155$05.00/0

In Durability of Macromolecular Materials; Eby, R.;
ACS Symposium Series; American Chemical Society: Washington, DC, 1979.

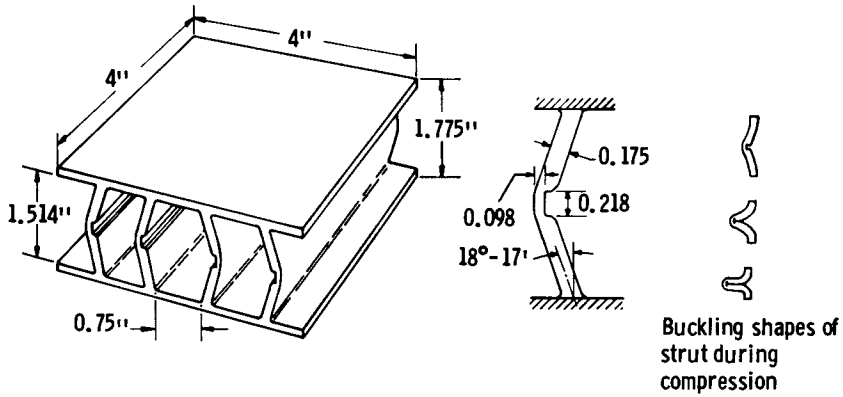

Figure 1. Test specimens of polyurethane linear pad

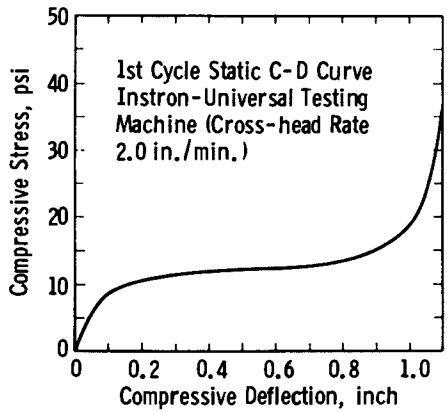

Figure 2. Typical compression–deflection curve

In Durability of Macromolecular Materials; Eby, R.;
ACS Symposium Series; American Chemical Society: Washington, DC, 1979.

TABLE I -- Effect of Water Immersion at 70°C on Retention of Hardness

Days	Hardness Readings[a] (Shore A)		% Retention of Original Hardness[b]
0	90	90	100
4	90	89	99
19	89	89	99
40	89	87	98
73	89	88	98
94	87	87	97
127	88	87	97
148	87	87	97
167	87	86	96
186	87	86	96
206	87	86	96
246	87	86	96
268	86	87	96
289	86	86	96
309	86	86	96
330	86	86	96
350	86	85	95
369	86	86	96
387	85	85	95
406	85	85	95
425	85	85	95
447	85	85	95
467	85	85	95
486	85	85	95
505	84	85	94
525	85	83	93

[a] Flat specimens having thicknesses of 0.50 in. and 0.12 in. were employed for the left and right columns respectively. These were cast from the same material and processed in an identical manner as the pad.

[b] The percent retention was calculated by dividing the average of the two hardness readings by the original hardness of 90.

In Durability of Macromolecular Materials; Eby, R.;
ACS Symposium Series; American Chemical Society: Washington, DC, 1979.

TABLE II -- Effect of Water Immersion at 70°C on Compression-Deflection Characteristics

Cumulative Days in Water	Compressive Stresa (psi) at Deflections (in.) of											
	Specimen A70			Specimen B70			Specimen C70			Blank		
	0.2	0.4	0.6	0.2	0.4	0.6	0.2	0.4	0.6	0.2	0.4	0.6
0	9.9	11.0	11.4	9.9	10.8	11.3	10.4	11.5	12.1	10.1	11.0	11.5
4	10.3	11.9	12.4	10.6	12.1	12.5	11.1	12.7	13.1	10.5	11.8	12.7
19	10.1	11.4	12.1	9.6	11.4	12.0	10.2	12.1	12.6	10.5	12.0	12.8
40	9.1	10.9	11.5	9.3	10.9	11.6	9.7	11.6	12.2	10.8	12.3	13.0
73	8.3	10.0	10.6	8.4	10.1	10.8	9.0	10.5	11.3	10.4	11.8	12.4
94	7.9	9.5	10.2	8.1	9.7	10.3	8.6	10.2	10.9	10.4	12.0	12.8
127	7.6	9.6	10.3	8.2	10.0	10.7	8.6	10.4	11.1	11.4	12.9	13.9
148	7.2	8.8	9.4	7.4	8.9	9.5	7.7	9.4	9.9	10.5	12.0	12.8
167	6.9	8.4	9.1	7.1	8.5	9.2	7.3	9.0	9.7	10.2	11.8	12.6
186	6.4	7.9	8.4	6.2	8.0	8.6	6.6	8.3	9.0	10.0	11.4	12.1
206	6.5	8.0	8.6	6.6	8.1	8.6	7.0	8.9	9.0	10.2	12.0	12.7
246	6.2	7.5	8.1	6.1	7.6	8.2	6.3	8.0	8.6	9.9	11.4	12.1
268	6.0	7.5	8.2	6.1	7.6	8.1	6.4	7.9	8.6	10.1	11.6	12.4
289	5.8	7.4	8.1	6.0	7.5	8.2	6.4	7.9	8.6	9.7	11.5	12.3
309	5.5	6.8	7.5	5.5	7.0	7.5	6.2	7.7	8.3	9.5	11.2	11.9
330	5.6	7.1	8.0	5.7	7.3	8.0	5.9	7.6	8.3	10.1	11.8	12.6
350	5.5	7.0	7.7	5.7	7.3	8.1	5.8	7.5	8.2	10.2	11.9	12.6
369	5.4	7.1	7.7	5.4	7.0	7.8	5.9	7.5	8.2	10.2	12.0	12.8
387	5.3	6.8	7.5	5.4	6.9	7.5	5.7	7.2	7.9	10.1	11.7	12.5
406	5.1	6.6	7.4	5.2	6.7	7.4	5.5	7.0	7.7	9.9	11.6	12.4
425	5.1	6.6	7.2	5.3	6.7	7.4	5.5	6.9	7.7	10.2	12.0	12.8
447	4.9	6.4	7.1	5.1	6.6	7.1	5.4	6.9	7.6	10.1	11.8	12.6
467	4.8	6.2	6.9	4.7	6.1	6.7	5.1	6.6	7.4	9.9	11.5	12.4
486	4.5	5.8	6.5	4.6	5.7	6.4	4.8	6.2	6.8	10.0	11.6	12.5
505	4.5	5.5	6.2	4.1	5.3	5.6	4.6	5.9	6.4	9.7	11.4	12.2
525	4.1	5.3	5.8	3.7	4.7	5.1	4.3	5.3	5.8	9.9	11.5	12.4

In Durability of Macromolecular Materials; Eby, R.; ACS Symposium Series; American Chemical Society: Washington, DC, 1979.

TABLE III. Effect of Water Immersion at 70°C on Retention of Compressive Stress

Cumulative Days in Water	0.2 in. deflection		0.4 in. deflection		0.6 in. deflection	
	100(S/Sb)[a]	% Relative Retention of Stress[b]	100(S/Sb)	% Relative Retention of Stress	100(S/Sb)	% Relative Retention of Stress
0	99.7	100.0	101.0	100.0	100.8	100.0
4	103.2	103.8	104.0	103.0	100.0	99.2
19	94.8	95.0	96.9	95.9	95.5	94.7
40	86.7	86.9	90.5	89.6	90.5	89.8
73	82.4	82.6	86.4	85.5	87.9	87.2
94	78.8	79.0	81.7	80.9	81.8	81.1
127	71.4	71.6	77.5	76.7	77.0	76.4
148	70.8	71.0	75.2	74.5	75.0	74.4
167	69.6	69.8	73.1	72.4	74.0	73.4
186	64.2	64.4	70.8	70.1	70.0	69.4
206	65.9	66.1	69.4	68.7	68.9	68.3
246	62.9	63.1	67.5	66.8	68.6	68.0
268	61.1	61.3	66.2	65.5	66.9	66.3
289	61.1	61.3	65.8	65.1	67.5	66.9
309	60.3	60.5	64.6	63.9	66.1	65.6
330	56.7	56.9	62.1	61.5	64.0	63.5
350	55.6	55.7	61.1	60.5	63.2	62.7
369	54.6	54.7	60.0	59.4	61.9	61.4
387	54.2	54.3	59.6	59.0	61.4	60.9
406	52.9	53.0	58.5	57.9	60.5	60.0
425	51.9	52.0	56.4	55.8	58.0	57.5
447	50.8	51.0	56.2	55.6	57.7	57.2
467	49.2	49.3	54.8	54.2	56.6	56.1
486	46.3	46.4	50.8	50.3	52.6	52.2
505	45.1	45.5	48.9	48.4	49.7	49.3
525	43.7	43.8	44.3	43.8	44.9	44.5

[a] S = average of the compressive stress values of the three specimens; Sb = compressive stress of corresponding blank.

[b] % relative retention of stress = 100 $(S/Sb)/(S/Sb)_o$, where subscript o refers to value of (S/Sb) at zero days in water.

In Durability of Macromolecular Materials; Eby, R.;
ACS Symposium Series; American Chemical Society: Washington, DC, 1979.

Results for the four test temperatures are shown in Figures 3 to 7.

Preparation of Cast Pads. One hundred parts Adiprene L100 (an isocyanate terminated prepolymer containing polyoxytetramethylene chain segments and having an equivalent weight of about 1025, manufactured by duPont) is heated to 87-88°C while 12.5 parts MOCA, 4,4'-methylenebis(2-chloroaniline), is brought to 124-126. Degassing of the Adiprene L100 and MOCA at a pressure of 1-2 Torr for about 5 and 1 minutes, respectively, follows. When the temperature of the prepolymer has dropped to 80 $\pm$ 2°C, it is stirred together with MOCA, which is at 122-124°C. After agitating for about two minutes, the resultant solution at a temperature of 87-88°C is poured into the mold which was preheated to the same temperature and then cured at that temperature for 6 hours.

Hydrolytic Aging of Specimens. The flat specimens and triplicate samples of four strut polyurethane pads (Figure 1) were immersed in water in constant temperature baths at 50 $\pm$ 0.5, 60 $\pm$ 0.5, 70 $\pm$ 0.5 and 98 $\pm$ 0.5°C. Periodically, the samples were removed from the water, dried by being baked for 24 hours at 50°C in a forced air circulating oven, permitted to cool in a desiccator over Drierite, subjected to mechanical testing within four hours of removal from the drying oven, and then returned to their respective water baths. The compression-deflection characteristics of the pads at each immersion temperature were compared with their corresponding standards (Tables II and III), i.e., pads which underwent identical treatment including oven drying and mechanical testing except that instead of being immersed in heated water, they were stored in air under normal room conditions.

Compressive stress values were recorded at deflections of 0.2, 0.4 and 0.6 in. for triplicate samples (Table II). The quantity (100 S/Sb) in Table III, S is the average stress value for the triplicate specimens at the same deflection, ε, immersion time, t, and temperature, T, and Sb is the stress for the corresponding blank or nonhydrolyzed specimen, provides a comparison between the immersed sample and respective blank. For example, the value of 86.7 for 100 S/Sb for pads immersed at 70°C for 40 days and deflected 0.2 in. (100[9.1+9.3+9.7]/3[10.8] = 86.7) indicates that the average compressive stress of the three aged samples is 86.7 percent as great as that of the corresponding nonhydrolyzed standard (Table III). Dividing the 100 S/Sb by its initial value (prior to immersion in water) gives the percent relative retention of original compressive stress, R. Thus,

In Durability of Macromolecular Materials; Eby, R.;
ACS Symposium Series; American Chemical Society: Washington, DC, 1979.

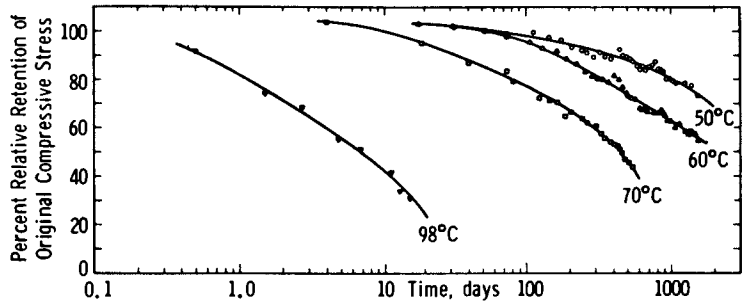

Figure 3. Effect of water immersion on retention of compressive strength at 0.2 in. deflection

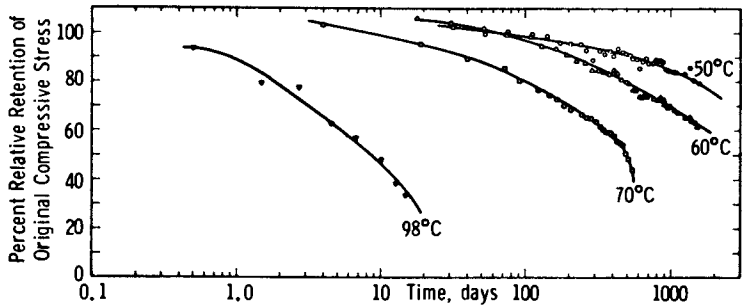

Figure 4. Effect of water immersion on retention of compressive strength at 0.4 in. deflection

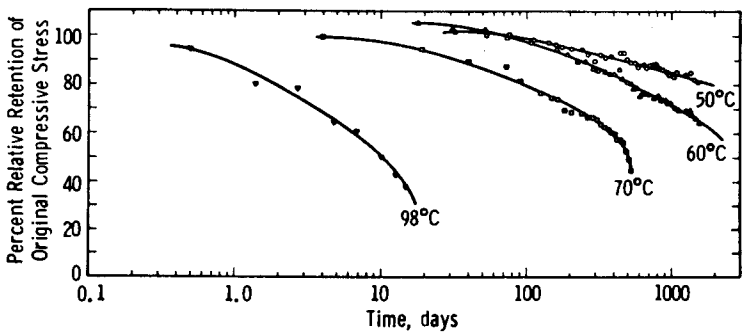

Figure 5. Effect of water immersion on retention of compressive strength at 0.6 in. deflection

In Durability of Macromolecular Materials; Eby, R.;
ACS Symposium Series; American Chemical Society: Washington, DC, 1979.

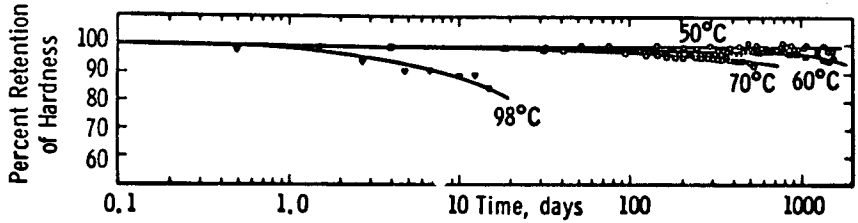

Figure 6. Effect of water immersion on retention of hardness

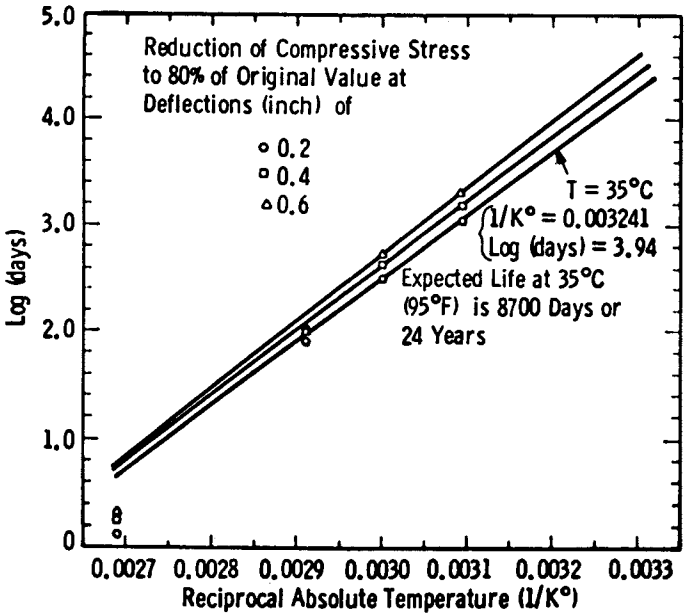

Figure 7. Arrhenius plot of hydrolytic stability compression–deflection data

In Durability of Macromolecular Materials; Eby, R.;
ACS Symposium Series; American Chemical Society: Washington, DC, 1979.

$$R_{T,\varepsilon,t} = \frac{100/n \sum_{i=1}^{n} (S_i/Sb)_{T,\varepsilon,t}}{1/n \sum_{i=1}^{n} (S_i/Sb)_{T,\varepsilon,0}}$$

where n = number of replicate specimens.

Utilizing the conditions of the above example, we have:

$$R_{70°C,0.2\ in.,40\ day} = \frac{100(9.1 + 9.3 + 9.7)/10.8}{(9.9 + 9.9 + 10.4)/10.1} = 87$$

The times required for the retention of original compressive stress at the three deflections to drop to 80 percent were obtained from the plots (Figures 3-5) of the effect of water immersion on retention of compressive strength. From an Arrhenius plot (Figure 7), log time versus the reciprocal of the absolute temperature, the extrapolated life expectancy of the pads was found to be 24 years. This value was obtained using the 0.2 in. deflection, since it gives the lowest value, an arbitrarily but conservatively selected temperature of 35°C, and the very conservative assumption of continuous exposure to total immersion conditions.

The concurrently recorded hardness readings (Table I) were employed in Figure 6. Since the retention of hardness appeared to be much less sensitive to the hydrolytic degradation than the compressive stress-strain properties, only the effect on the latter was employed in estimating the useful life of the material.

Error. Errors in these tests can result from the obvious sources; mechanical measurements, sample preparation, temperature variations in water baths, and absorption of atmospheric moisture during the time interval between removal from the desiccator and completion of testing.

From previous statistical studies on similar systems which include the combination of errors involved in sample preparation and measurement of static compressive stress-strain characteristics, the following reproducibility results were obtained (4,5,6):

Number of Determinations	Deflection* Percent	Compressive Stress (psi) Mean	Std. Dev.
9	30.0	5.90	0.272
21	23.3	5.24	0.229

*The above percent deflections are based on total pad heights of 1.775 and 4.30 in., respectively. Adjusted for strut height, they would correspond to deflections of about 0.5 and 0.35 in., respectively, which are well within the normal stress plateau.

In Durability of Macromolecular Materials; Eby, R.;
ACS Symposium Series; American Chemical Society: Washington, DC, 1979.

The quality of the sample preparation and physical tests in this study is comparable to the above reported work.

Error in the hydrolytic degradation studies is expected to be relatively small due to the use of blank or standard comparison specimens. The blanks, which are exposed to the same conditions except for hydrolysis and are tested within 2-10 minutes of the test specimen, should cancel much of the error caused by factors such as testing fatigue, absorption of atmospheric moisture after removal from drying and possible drifts in the characteristics of the testing machine or its operator. Besides employing more replicate samples and blanks, one could more rigorously equilibrate the moisture contents of the blank and samples, for example, by maintaining them at 50% R.H. for about two weeks after drying and then testing in a room having a controlled relative humidity of 50%. Since the undegraded blank exhibits greater differences from the specimens during the later stages of degradation, the accuracy of the data is expected to decrease as the process progresses. Being more resistant to fatigue and less hygroscopic, the blank will lose some of its effectiveness in neutralizing errors from these sources.

Error associated with temperature control in the water baths was limited to that caused by temperature variations of $\pm$ 0.5°C.

In performing accelerated degradation tests, there is indeterminate error inherent in the assumption that the mechanism and consequently the activation energy of the rate-limiting step will not change significantly over the explored temperature range and extrapolated end-point temperature. An additional complication is that the relationship between any physical measurement, especially one as complex as compression-deflection characteristics of the intricately designed structure employed in this study, and the extent and mode of the degradation process can be very complicated. Thus, it is not surprising that the points of the Arrhenius plot (Figure 7) do not fall on a perfectly straight line. As a result of the above consideration, we minimized the extent of extrapolation by testing at low temperatures and much more heavily weighted the lowest temperature points in the construction of the Arrhenius plot.

Degradation Phenomena

Even though the chemistry of urethane polymers has been described in the literature, a brief review of the more pertinent reactions and structures will be helpful to some readers.

An isocyanate terminated prepolymer such as Adiprene L100 has a chemical structure (R represents isomeric forms of the tolylene radical) of the type:

In Durability of Macromolecular Materials; Eby, R.;
ACS Symposium Series; American Chemical Society: Washington, DC, 1979.

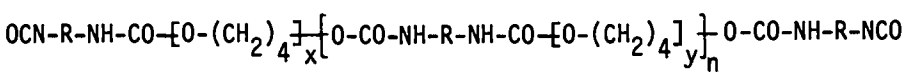

Similar prepolymers, having isocyanate equivalent weights of approximately 1025, have been prepared from 1.6 mole 2,4-tolylene diisocyanate and 1.0 mole of a polyoxytetramethylene glycol having an average molecular weight of approximately 950. Typical calculated average values of n, x and y for these prepolymers are 0.67, 13 and 13, respectively. Thus, they contain approximately 3.3 hydrolyzable urethane linkages per mole.

On treatment of the prepolymer with MOCA, chain extension results through formation of substituted urea groups which also provide sites for hydrolytic attack.

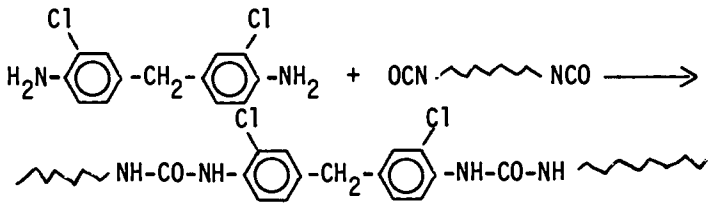

Substituted urea linkages also result from the presence of moisture which reacts with the isocyanate radical. (Subsequently, R can represent any portion of the system including polymer segments).

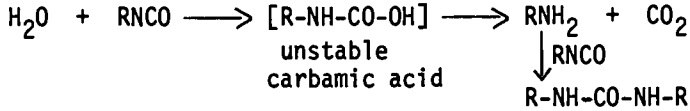

Other hydrolyzable groups consist of biuret and allophanate cross-links formed from the reaction of isocyanate radicals with active hydrogen atoms of the urea and urethane linkages, respectively.

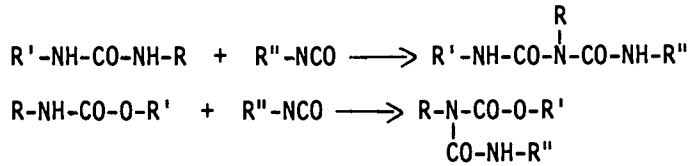

The above described adducts of the isocyanates are cleaved on reaction with water to give ultimately an amine, CO_2, and the active hydrogen containing progenitor. For example, the overall hydrolysis reactions of a urethane can be shown as:

In Durability of Macromolecular Materials; Eby, R.;
ACS Symposium Series; American Chemical Society: Washington, DC, 1979.

$$R''\text{-}NH\text{-}CO\text{-}O\text{-}R' + H_2O \longrightarrow R''NH_2 + CO_2 + R'OH$$

Similarly, the complete hydrolysis of an allophanate will yield the corresponding amines, an alcohol and CO_2.

$$R\text{-}\underset{\displaystyle CO\text{-}NH\text{-}R''}{\overset{\displaystyle |}{N}}\text{-}CO\text{-}O\text{-}R' + H_2O \longrightarrow R''NH_2 + RNH_2 + R'OH + CO_2$$

Substituted ureas and biurets undergo analogous reactions with water to yield amines and CO_2.

The initial reactions of polyurethane samples to immersion in heated water is their reversible absorption of water, often a slight advancement in the cure and concomitantly a slight degree of hydrolysis. Absorption of water results in plasticization of the material with an accompanying slight reduction in hardness and modulus. The short term immersion in hot water often furthers the polymerization of the polyurethane due to both the accelerating effects of the heat and the reactions between unreacted isocyanate groups and water, which provide chain extension through the resultant substituted urea linkages. These reactions proceed with great facility since the intermediate amines catalyze the reactions of the isocyanate radical with both water and themselves.

Thus, during the very early stages of exposure to water, the reactions that contribute to the extension of the polymer usually are considered to be more prominent than those involving hydrolysis. If the plasticizing water is removed by drying, the material will generally display a slightly greater modulus and strength than it had prior to its exposure to water. This is consistent with our results in which the compressive stiffness of the pads had risen slightly above the initial values during the early stages of immersion in water at 50°, 60° and 70°C. The first measurement at 98°C was taken after too long an immersion to show this effect.

However, another factor that could contribute to the initial improvement in physical properties of the polyurethanes is that the allophanate and biuret crosslinks, which are highly susceptible to hydrolysis, may be early victims of the degradation process. Even though crosslinks generally impart an increase in the modulus and rigidity of most polymers, the few allophanate and biuret crosslinks interfere with the spatial alignment of a vastly larger number of hydrogen bonds and thus can cause a net reduction of the intermolecular forces between the polymer chains. Elimination of some of these crosslinks through hydrolysis provides an arrangement of the polymer chain that more efficiently utilizes the hydrogen bonds.

As the hydrolysis proceeds further, it severs the urea and urethane linkages resulting in a dimunition in the size of the polymer chains. Increasing polymer degradation results in increased concentrations of absorbed water and the basic amino groups which cause an acceleration of the overall hydrolysis

In Durability of Macromolecular Materials; Eby, R.;
ACS Symposium Series; American Chemical Society: Washington, DC, 1979.

process. This manifests itself in a corresponding decline of the physical properties of the polymer.

Observations

The progress of the degradation was observed by monitoring the decay of compressive strength (Figures 3-5) and hardness (Figure 6). Particular attention was given to the compressive stresses over the early and middle portion of the stress-strain plateau. At deflections appreciably lower than 0.2 in. and above 0.8 in., the stress-strain curve rises too steeply for accurate monitoring (Figure 2). Thus, it was arbitrarily decided to monitor the stresses at deflections of 0.2, 0.4 and 0.6 in. As expected, the progress of the decay of the compressive strength of the pads was similar for the three deflections. The stress at 0.2 in. appeared to be somewhat more severely affected by the degradation process (Figures 3-5), and thus, was selected as the end-point criterion (Figure 7 , Table IV).

Results obtained by monitoring stresses at higher deflections near the end of the plateau would, in addition to being more difficult to read accurately, have less credence since the pads exhibit "bottoming" characteristics. By observing the buckling shapes of the strut during compression (Figure 1), it is apparent that at higher deflections the material surrounding both sides of the notch is pressed together. Under this "bottomed" condition, the compressive stress is expected to be less sensitive to small changes in the physical integrity of the polymer.

In addition to the compression-deflection measurements, the hardness of the specimens was monitored (Figure 6, Table I). Interestingly, the performance properties of the pads were affected considerably more than hardness by the progressive degradation. This is illustrated by the following data:

Immersion Time (Days)	Temp. (°C)	Percent Retention Hardness	Percent Retention Compressive Stress at 0.2 in.
1518	50	98	73
1538	60	96	55
525	70	93	41
13	98	89	33

Many investigators of hydrolytic stability of polymers utilize hardness measurements since the readings are very easy to take and the tests are essentially nondestructive, thus obviating the need for many test specimens. This work emphasizes that high retention of hardness does not prove that the material has displayed a good retention of other physical properties or withstood extensive degradation.

In Durability of Macromolecular Materials; Eby, R.;
ACS Symposium Series; American Chemical Society: Washington, DC, 1979.

TABLE IV -- Immersion Time Required for 20 Percent Loss of Compressive Strength[a]

Temperature[b] (°C)	Reciprocal Abs. Temp. (1/K°)	Time (days) (defl. = 0.2 in.)	Time (days) (defl. = 0.4 in.)	Time (days) (defl. = 0.6 in.)
98.0	0.002692	1.12	1.80	1.85
70.0	0.002914	80	99	99
60.0	0.003002	330	480	550
50.0	0.003094	1050	1480	2000

[a] Immersion times required for 20% loss of compressive strength were obtained from Figures 3, 4, and 5.

[b] Temperature variations during the immersion in water were ± 0.5°C.

In Durability of Macromolecular Materials; Eby, R.; ACS Symposium Series; American Chemical Society: Washington, DC, 1979.

Conclusions

Accelerated hydrolytic stability tests indicate that the polyether-based urethane employed in this study in the preparation of the liner pads can successfully withstand continuous immersion in water at 35°C for 24 years. Under such an exposure, the pads are expected to lose approximately 20 percent of their original compressive strength.

The percent retention of hardness has been found to be not nearly as sensitive an indicator of degradation of the polymer as the compression-deflection characteristics. Thus, it should not be assumed that materials which have displayed a good retention of their original hardness are stable.

Acknowledgment

The authors wish to express their appreciation to H. A. Steffey for diligently performing much of the experimental work of this study for a period of over four years.

Abstract

The hydrolytic degradation process of structural polyether-based urethane shock mitigating pads is described as beginning with reversible plasticization by water, a slight enhancement of the cure, hydrolysis of allophanate and biuret crosslinks and urea and urethane linkages in the backbone of the polymer chain. Degradation of pads immersed in water at a series of elevated temperatures was monitored by measurements of hardness and compression-deflection characteristics. Compressive strength was much more severely affected than hardness by hydrolysis. When the hardness decreased by 4 percent, the compressive strength had diminished by 45 percent. A decrease to 89 percent of the original hardness coincided with a catastrophic diminution of compressive strength to 33 percent of its original value. An Arrhenius relationship was applied to estimate the hydrolytic endurance of the tested substrate.

Literature Cited

1. Athey, R. V., Rubber Age, 705 (1965).
2. Gahimer, F. H. and Nieske, F. W., "Hydrolytic Stability of Urethane and Polyacrylate Elastomers in Humid Environments," Urethanes in Elastomers and Coatings (articles from the Journal of Elastoplastics), pp. 6-20, Technomic Publ. Co., Inc., Westport (1973).
3. Schollenberger, C. S. and Stewart, F. D., "Thermoplastic Polyurethane Hydrolysis Stability," Urethanes in Elastomers and Coatings (articles from the Journal of Elastoplastics) pp. 46-74, Technomic Publ. Co., Inc., Westport (1973).

In Durability of Macromolecular Materials; Eby, R.;
ACS Symposium Series; American Chemical Society: Washington, DC, 1979.

Literature Cited (Continued)

4. Mendelsohn, M. A., unpublished work.
5. Mendelsohn, M. A., Runk, R. H., Connors, H. J., and Rosenblatt, G. B., Ind. Eng. Chem. Prod. Res. Dev., 10, 14 (1971).
6. Mendelsohn, M. A., Rudd, G. E., and Rosenblatt, G. B., Ind. Eng. Chem. Prod. Res. Dev., 14, 181 (1975).

RECEIVED December 8, 1978.

12

Equilibrium Distribution of a Minor Constituent between a Polymer and Its Environment

ISAAC C. SANCHEZ

Polymer Science and Standards Division, National Bureau of Standards, Washington, DC 20234

A polymer's usefulness and lifetime are often determined by the rate at which a minor chemical constituent is released by the polymer. Obvious examples are the desorption of antioxidants and plasticizers. To quantitatively describe this phenomenon requires a knowledge of the diffusants' transport and thermodynamic properties within the polymer and in the environmental fluid phase. The main objective of this paper is to examine the thermodynamic or equilibrium aspect of this problem.

When the volume of the environmental fluid is finite, diffusion of a minor chemical species will proceed until equilibrium is attained. At equilibrium the diffusing species will partition itself between the polymer and environmental fluid phases defined by a partition coefficient K. The estimation of K is an importnat consideration in drug release from polymeric delivery devices (1) and in applications of polymers as food packaging materials (2).

We will consider the specific system of a non-ionic diffusant in an amorphous or semi-crystalline polymer (in contact with a liquid) at temperatures above the polymer glass temperature Tg. The liquid may be a good or poor solvent for the polymer. For this type of system a theoretical relation can be obtained for K by applying the Flory equation of state theory (3-6) or lattice fluid theory (7-10) of solutions. An important prerequisite for the application of these theories is for the polymer to behave as an equlibrium liquid. This condition is generally valid for a lightly crosslinked, amorphous polymer above its Tg or for the amorphous component of a semi-crystalline polymer above its Tg. The best example of the latter is polyethylene at room temperature.

THEORETICAL

Consider a polymer that initially contains M_0 grams of a diffusant in contact with a solvent of finite volume V_s. At long diffusion times, M_∞ grams of diffusant are transferred to the solvent. Using mass balance yields

In Durability of Macromolecular Materials; Eby, R.;
ACS Symposium Series; American Chemical Society: Washington, DC, 1979.

$$M_\infty/M_o = \alpha/(1+\alpha) \tag{1}$$

$$\alpha = (V_s/V_p)\,K \tag{2}$$

$$K = C^s/C^p \tag{3}$$

where C^s and C^p are the equilibrium concentrations (mass/unit volume) of the diffusant in solvent and polymer phases, respectively, and V_p is the polymer volume. For a semicrystalline polymer, V_p is the volume of the amorphous material (it is assumed that the diffusant is excluded from crystalline domains) and C^p refers to the diffusant concentration within the amorphous regions. (Superscripts s and p are used to designate solvent and polymer phases and subscripts are used, only when necessary, to designate species).

At equilibrium, the thermodynamic activity of the diffusant in the polymer a^p will equal the activity a^s of the diffusant in the solvent:

$$a^p = a^s \tag{4}$$

$$\gamma^p\phi^p = \gamma^s\phi^s \tag{5}$$

where γ^s and γ^p are the respective volume fraction activity coefficients. The partition coefficient is defined as

$$K \equiv \phi^s/\phi^p = \gamma^p/\gamma^s \tag{6}$$

Usually the diffusant will be present in low concentrations. In dilute solutions all concentration units (mole fractions, volume fraction, molarity, etc.) are proportional to one another, therefore

$$K = \phi^s/\phi^p = C^s/C^p = \gamma^p(\infty)/\gamma^s(\infty) \tag{7}$$

$$\gamma(\infty) \equiv \lim_{\phi \to 0} \gamma \tag{8}$$

In Durability of Macromolecular Materials; Eby, R.;
ACS Symposium Series; American Chemical Society: Washington, DC, 1979.

Partitioning with Negligible Solvent Absorption.

According to the well-known Flory-Huggins theory of solutions (11, 12), the activity and volume fraction activity coefficient of component 1 in a binary mixture of 1 and 2 are given by

$$\ln a_1 = \ln \phi_1 + (1 - r_1/r_2)\,\phi_2 + r_1 \chi_{12} \phi_2^2 \qquad (9)$$

$$\ln \gamma_1 = (1 - r_1/r_2)\,\phi_2 + r_1 \chi_{12} \phi_2^2 \qquad (10)$$

where $\phi_1 = 1-\phi_2$ is the site or volume fraction of component 1, r_1 and r_2 are the respective number of lattice sites occupied by the components, and χ_{12} is a dimensionless, symmetrical ($\chi_{12} \chi_{21}$) parameter that characterizes the interaction between the two components. Usually, r_1/r_2 is equated to the ratio of molar volumes and the product $r_1\chi_{12}$ (designated as χ_1 in reference 11) is treated as an empirical parameter.

For dilute solutions

$$\ln \gamma^p(\infty) = 1 + r_d \chi_p^\infty \qquad (11)$$

$$\ln \gamma^s(\infty) = 1 - r_d/r_s + r_d \chi_s^\infty \qquad (12)$$

where the subscripts p, s, and d refer to polymer, solvent, and diffusant, respectively; χ_p^∞ and χ_s^∞ are the infinite dilution values of polymer-diffusant and solvent-diffusant interaction parameters. The term r_d/r_p is absent in Eq. (11) because r_p, a parameter proportional to the molecular weight of the polymer, approaches infinity for a crosslinked polymer.

Combining Eqs. (7), (11), and (12) yields

$$\ln K_o = r_d (1/r_s + \chi_p^\infty - \chi_s^\infty) \qquad (13)$$

A zero subscript has been attached to K to remind us that Eq. (13) is only valid when solvent is not absorbed by the polymer.

Partitioning with Solvent Absorption

When solvent is absorbed by the polymer, the polymer phase becomes a ternary solution; the activity of the diffusant in the polymer phase can be written as (11, 12).

In Durability of Macromolecular Materials; Eby, R.;
ACS Symposium Series; American Chemical Society: Washington, DC, 1979.

$$\ln a^p = \ln \phi_d + (1 - r_d/r_s)\,\phi_s + \phi_p + r_d\,(\phi_s \chi_s + \phi_p \chi_p - \phi_s \phi_p \chi_{sp}) \qquad (14)$$

where, of course,

$$\phi_d + \phi_s + \phi_p = 1 \qquad (15)$$

and χ_{sp} is the solvent-polymer interaction parameter for a solvent concentration of ϕ_s. We will assume that the concentrations ϕ_s and ϕ_p are much larger than the diffusant concentration ϕ_d so that χ_s and χ_p can be replaced by χ_s^∞ and χ_p^∞. In this limit

$$\ln \gamma^p(\infty) = (1 - r_d/r_s)\,\phi_s + \phi_p + r_d\,(\phi_s \chi_s^\infty + \phi_p \chi_p^\infty - \phi_s \phi_p \chi_{sp}) \qquad (16)$$

Combining Eqs. (7), (12), and (16) yields

$$\ln K = (1 - \phi_s)\,[\ln K_o - \phi_s r_d \chi_{sp}] \qquad (17)$$

Absorption of solvent causes the polymer to swell. Within a swollen polymer, the pressure acting on the solvent is greater than the atmospheric pressure, P_o. The excess pressure π caused by the elastic forces of a crosslinked polymer (crystalline domains act as effective crosslinks) raises the chemical potential of the solvent μ_s within the polymer phase. The condition of equilibrium is

$$\mu_s^o = \mu_s(P_o + \pi) = \mu_s(P_o) + \int_{P_o}^{P_o + \pi} \frac{\partial \mu_s}{\partial P}\, dP \simeq \mu_s(P_o) + \pi \bar{V}_s \qquad (18)$$

where μ_s^o is the chemical potential of pure solvent at P_o and $\bar{V}_s$ is the partial molar volume of the solvent. Since, by definition

$$\ln a_s(P_o) \equiv [\mu_s(P_o) - \mu_s^o] / RT \qquad (19)$$

In Durability of Macromolecular Materials; Eby, R.;
ACS Symposium Series; American Chemical Society: Washington, DC, 1979.

we have by Eq. (9)

$$\ln \phi_s + \phi_p + r_s \chi_{sp} \phi_p^2 = -\pi \bar{V}_s / RT \qquad (20)$$

As can be seen from the derivation of Eq. (20), the swelling pressure π is equivalent to the osmotic pressure developed by a non-crosslinked polymer solution of the same concentration In the absence of significant swelling, this pressure will be relatively small and to a good approximation the right hand side of Eq. (20) can be set equal to zero. Thus, a measurement of the equilibrium absorption of solvent (ϕ_S) yields an approximate experimental value of χ_{sp}:

$$r_s \chi_{sp} \simeq -[\ln \phi_s + \phi_p] / \phi_p^2 \qquad (21)$$

If the swelling is appreciable, as it might be for a very good solvent, corrections can be made to Eq. (21) for both crosslinked amorphous polymers (13) and semi-crystalline polymers (14,15).

Substitution of Eq. (21) into (17) yields

$$\ln K = \ln K_o - \phi_s \left\{ \ln K_o + (r_d / r_s) \left[1 + \ln (1/\phi_s) / (1 - \phi_s) \right] \right\} \qquad (22)$$

where it is understood that ϕ_S is the equilibrium amount of absorbed solvent. Notice that $K \to K_o$ as $\phi_S \to 0$ and $K \to 1$ as $\phi_S \to 1$ as it should.

A further check of the self-consisting of Eq. (22) is obtained by considering the partitioning of a diffusant in which the diffusant is radiolabeled (RL) solvent. In this case $\chi_S^\infty = 0$, and $r_d = r_S$. Substituting these results into Eq. (22) or (17) yields

$$\ln K = -\ln \phi_s \qquad (23)$$

The RL solvent should partition exactly as the non-RL solvent. The partition coefficient for the non-RL solvent, K_S, is equal to the volume fraction of the bulk solvent in the solvent phase (unity) divided by the volume fraction of the solvent in the polymer phase (ϕ_S) or

$$K_s = 1/\phi_s \qquad (24)$$

In Durability of Macromolecular Materials; Eby, R.;
ACS Symposium Series; American Chemical Society: Washington, DC, 1979.

which agrees with the result obtained from Eq. (22) for the RL solvent.

Interaction Parameters

In the original formulation of the Flory-Huggins theory, χ_{ij} was strictly an energetic parameter that was proportional to the energy required to form an i-j bond from a i-i and j-j bond. It also had a simple 1/T temperature dependence and was independent of solution composition. Experimentally, χ_{ij} often has a large positive entropic component which arises, according to the Flory and lattice fluid (LF) theories, from differences in the equation of state properties of the pure components (6,10).

Both the Flory and LF theories require three equation of state parameters for each pure component which are determined from PVT data. Each component satisfies a theoretical equation of state; the LF equation of state is

$$\tilde{\rho}^2 + \tilde{P} + \tilde{T}\,[\ln(1-\tilde{\rho}) + (1 - 1/r)\,\tilde{\rho}\,] = 0 \qquad (25)$$

where $\tilde{T}$, $\tilde{P}$ and $\tilde{\rho}$ are the reduced temeperature, pressure, and density. Three equation of state parameter, T*, P*, and ρ*, are used to reduce the experimental temperature, pressure, and mass density of the fluid; r is the number of lattice sites occupied by a molecule and is proportional to its molecular weight, M:

$$r = (P^*/RT^*\rho^*)\,M \qquad (26)$$

For the LF, equation of state parameters have been tabulated for about 60 low molecular weight fluids (8) and ten different polymers (9).

From the LF theory, the interaction parameters χ_s^∞ and χ_p^∞ required in Eqs. (13) and (22) are given by (10)

$$\chi_s^\infty = \tilde{\rho}_s \Delta P_s^*/P_d^* \tilde{T}_d + (\tilde{\rho}_d - \tilde{\rho}_s)/\tilde{T}_d + \ln(\tilde{\rho}_s/\tilde{\rho}_d)/r_d \qquad (27)$$

$$+ (1 - \tilde{\rho}_s)\ln(1 - \tilde{\rho}_s)/\tilde{\rho}_s - (1 - \tilde{\rho}_d)\ln(1 - \tilde{\rho}_d)/\tilde{\rho}_d$$

and a similar expression holds for χ_p^∞ (replace s by p). The parameter ΔP_s^* which has units of pressure, is the only unknown parameter in Eq. (27). All other quantities are calculable from the equation of state properties of the pure components. The physical meaning of ΔP_s^* is that it is a measure of the net change

In Durability of Macromolecular Materials; Eby, R.;
ACS Symposium Series; American Chemical Society: Washington, DC, 1979.

in the energetics that occurs upon mixing solvent and diffusant at the absolute zero of temperature. At absolute zero, the sign of ΔP^* determines the sign of the heat of mixing. The analogous Flory equation for χ_s contains a parameter similar in meaning to ΔP^*as well as a second parameter that characterizes the relative surface/volume properties of the pure components (6).

In both the Flory and LF theories, the cohesive energy density of a fluid at absolute zero equals its characteristic pressure, P^*. It is, therefore, convenient to define a dimensionless parameter Δ_s in terms of the characteristic pressures of the pure components:

$$\Delta_s \equiv \Delta P_s^* / (P_s^* + P_d^*); \qquad \Delta_p \equiv \Delta P_p^* / (P_p^* + P_d^*) \tag{28}$$

Combining Eqs. (13), (27), and (28) yields

$$\ln K_o = r_d \left\{ \left[\tilde{\rho}_s [1 - \Delta_s (P_s^*/P_d^* + 1)] - \tilde{\rho}_p [1 - \Delta_p (P_p^*/P_d^* + 1)] \right] \tilde{T}_d^{-1} \right. \tag{29}$$
$$\left. + (1 - \tilde{\rho}_p) \ln (1 - \tilde{\rho}_p)/\tilde{\rho}_p - (1 - \tilde{\rho}_s) \ln (1 - \tilde{\rho}_s)/\tilde{\rho}_s + r_d^{-1} \ln (\tilde{\rho}_p/\tilde{\rho}_s) + r_s^{-1} \right\}$$

where r_d and r_s are defined by Eq. (26) and $\tilde{\rho}_s$ and $\tilde{\rho}_p$ are calculated from the equation of state (25).

RESULTS & DISCUSSION

In principle the diffusant-solvent or the diffusant-polymer interaction parameter can be empirically determined from a single solution datum such as a heat of mixing, a critical temperature, a solution density, etc. However, in some systems intelligent choices of Δ_s and Δ_p can be made from limited data. An example of this kind is the partitioning of the n-alkanes between linear polyethylene (PE) and n-heptane. In Table I, the partition coefficients K_o and K are calculated from Eqs. (29) and (22) for selected n-alkanes at 25°C. Equation of state parameters required in the calculations were obtained from references 8 and 9. For PE, the equilibrium amount of n-heptane absorbed is $\phi_s = 0.26$ (16). Entries enclosed within parentheses are K values and those without are K_o values. Entries that are crossed out with solid lines are considered unlikely values of the partition coefficient; those with broken lines are considered more probable than those crossed-out with solid lines, but less probable than the clear entries.

In Durability of Macromolecular Materials; Eby, R.;
ACS Symposium Series; American Chemical Society: Washington, DC, 1979.

$\Delta_s \rightarrow$	0	0	0	0	0	0.02	0.03
$\Delta_p \rightarrow$	0.04	0.03	0.02	0.01	0	0	0
n-pentane	9.1 (4.3)	7.0 (3.5)	5.3 (2.9)	4.1 (2.4)	3.1 (1.9)		
n-heptane	13.6 (5.6)	9.6 (4.3)	6.8 (3.3)	4.7 (2.6)	3.3 (2.0)		
n-decane	24.9 (8.3)	15.5 (6.1)	9.7 (4.3)	6.0 (3.0)	3.8 (2.2)		
n-heptadecane		40.4 (11.5)	19.2 (6.6)	9.2 (3.8)	4.4 (2.2)		
linear PE $M = 10^4$						1.3×10^3 (7.5×10^{-7})	6.7×10^{-10} (6.1×10^{-16})

Table I Calculated partition coefficients, K_0 and K, for selected n-alkanes between linear polyethylene and n-heptane at 25°C.

In Durability of Macromolecular Materials; Eby, R.;
ACS Symposium Series; American Chemical Society: Washington, DC, 1979.

The rational for selecting Δ_p in the range between 0.01 and 0.03 is based on the calculation of Δ_p for polyisobutylene (PIB) solutions of the n-alkanes from heats of mixing and the experimental result that $K=K_S = 1/0.26=3.8$ for n-heptane. For PIB, $\Delta_p=0.016$ for n-pentane and decreased monotonically with chain length to $\Delta_p=0.002$ for n-decane (10). Since PIB and PE are chemically very similar, it is not unreasonable to expect that Δ_p values in the PE/n-alkanes are similar to those in PIB/n-alkanes. Selection of $\Delta_S=0$ is certainly correct for n-heptane (assumed to be radiolabeled n-heptane) and is probably an excellent approximation for the n-alkanes between pentane and decane. Of course, as the chain length of the n-alkane increases, $\Delta_S \to \Delta_p$ and $\Delta_p \to 0$, which explains the choice of Δ_S and Δ_p values for the partitioning of PE of molecular weight 10^4. Because the partition coefficient is proportional to the chain length of the diffusant [see Eqs. (13) and (22)], the calculated values of the partition coefficient become more uncertain as chain length increases.

In Table II calculated values of K_0 are shown for the partitioning of some n-alkanes between linear PE and ethanol. Here the estimates of Δ_S, and consequently K_0, are much more uncertain. However, we have some crude guidelines to go by. We know that the n-alkanes exhibit limited miscibility in ethanol which is qualitatively indicative of a large, positive Δ_S value. Also, because ethanol is polar and PE and the diffusants are nonpolar, we can reasonably expect that $\Delta_p < \Delta_S$.

$\Delta_S \to$	0.1	0.075	0.05
$\Delta_p \to$	0.025	0.025	0.025
n-pentane	6.1×10^{-2}	1.8×10^{-1}	5.3×10^{-1}
n-heptane	1.8×10^{-2}	7.5×10^{-2}	3.1×10^{-1}
n-decane	3.1×10^{-3}	2.1×10^{-2}	1.5×10^{-1}
n-heptadecane	5.2×10^{-5}	1.1×10^{-3}	2.3×10^{-2}

Table II Calculated partition coefficients, K_0, for selected n-alkanes between linear polyethylene and ethanol at 25°C.

In Durability of Macromolecular Materials; Eby, R.;
ACS Symposium Series; American Chemical Society: Washington, DC, 1979.

Inspection of Eq. (22) reveals that if $K_0>1$; i.e., if partitioning favors the solvent phase, absorption of solvent lowers the partition coefficient ($K<K_0$) as is illustrated for the partitioning of the n-alkanes between PE and n-heptane in Table I. This effect on partitioning is best understood by imagining the partitioning to occur in two steps. In the first step the diffusant partitions in the absence of solvent absorption preferentially toward the solvent phase. In the second step, solvent containing some of the diffusant is absorbed by the polymer. Thus, the diffusant is reabsorbed literally on the "coattails" of the solvent.

When $K_0<1$, Eq. (22) suggests that it is possible for solvent absorption to increase the partition coefficient ($K>K_0$). The exact conditions for this to occur are

$$\chi_s^\infty > 1/r_s + \chi_p^\infty + \phi_p \chi_{sp} = \chi_p^\infty + \ln(1/\phi_s)/r_s(1-\phi_s) \qquad (30)$$

Under these conditions we have a reverse coattail effect. It can be understood as follows: A small K_0 implies a poor solvent-diffusant interaction (large positive χ_s^∞) and the diffusant prefers to remain in the polymer phase in the absence of solvent absorption. When solvent is absorbed, the diffusant now "sees" a thermodynamic environment in the polymer phase that is similar to the one in the solvent phase, neither of which it likes. Since the disparity in thermodynamic environments is reduced by solvent absorption, the diffusant tends to redistribute itself more evenly between the two phases.

LITERATURE CITED

1) Paul, D. R. and Harris, F. W., eds., "Controlled Release Polymeric Formulations", ACS Symposium Series 33, American Chemical Society, Wash. D. C., 1976.
2) Sanchez, I. C., Chang, S. S., McCrackin, F. L., and Smith, L.E., "An Evaluation of Existing Models Describing the Migration of Additives in Polymers", NBSIR 78-1499.
3) Flory, P. J., Orwoll, R. A., and Vrij, A., J. Amer. Chem. Soc., (1964), 86, 3515.
4) Flory, P. J., J. Amer. Chem. Soc., (1965), 87, 1833
5) Eichinger, B. E. and Flory, P. J., Trans. Faraday Soc., (1968), 64, 2035.
6) Flory, P. J., Discuss. Faraday Soc., (1970), 49, 7.
7) Sanchez, I. C. and Lacombe, R. H., Nature (London), (1974), 252, 381.
8) Sanchez, I. C. and Lacombe, R. H., J. Phys. Chem., (1976), 80, 2352, 2568.
9) Sanchez, I. C. and Lacombe, R. H., J. Poly. Sci., Polymer Letters Ed., (1977), 15, 71.

In Durability of Macromolecular Materials; Eby, R.;
ACS Symposium Series; American Chemical Society: Washington, DC, 1979.

10) Sanchez, I. C. and Lacombe, R. H., Macromolecules (accepted for pubilication, Dec. 1978).
11) Flory, P. J., "Principles of Polymer Chemistry", Cornell Univ. Press, Ithaca, N. Y., 1953.
12) Tompa, H., "Polymer Solutions", Academic Press, New York, 1956.
13) Flory, P. J. and Rehner, J., J. Chem. Phys., (1943), 11, 521.
14) Rogers, C. E., Stannett, V., and Szwarc, M., J. Phys. Chem., (1959), 63, 1406.
15) Kwei, K. P. and Kwei, T. K., J. Phys. Chem., (1962), 66, 2146.
16) Rogers, C. E., Stannett, V. and Szwarc, M., J. Poly. Sci., (1960), 45, 61.

RECEIVED December 8, 1978.

13

Polyphenylene Sulfide: Stability and Long-Term Behavior

H. WAYNE HILL, JR.

Phillips Petroleum Co., Bartlesville, OK 74004

Polyphenylene sulfide (PPS) is an engineering plastic prepared by the reaction of p-dichlorobenzene and sodium sulfide in a polar solvent.[1] As produced in the polymerization reaction, it is a linear polymer of modest molecular weight. However, heating this virgin resin below its melting point of 285°C in air yields products of substantially lower melt flow. The melt flow of these cured resins may be controlled by the specific choice of cure conditions. These cured polymers are much tougher than the virgin resin and provide the basis for a family of injection moldable engineering plastics that exhibit excellent affinity for pigments, glass fibers and mineral fillers. Polyphenylene sulfide resins are characterized by a combination of useful properties including good thermal stability, excellent chemical resistance, good mechanical properties, non-burning and non-dripping flammability behavior, and resistance to a wide variety of environmental conditions.

Polyphenylene sulfide resins have been produced commercially since 1973 by Phillips Petroleum Company and are sold under the trademark Ryton®.

Injection Molding Characteristics

This paper is concerned primarily with three basic grades of polyphenylene sulfide: (1) 40% glass-filled polymer (Grade R-4), (2) a glass- and mineral-filled polymer (Grade R-8), and (3) a glass- and mineral-filled color compound family (Grade R-10). While optimum injection molding conditions may vary slightly with mold design, part dimensions and resin grade, in general, a stock temperature of 315-330°C and a mold temperature of 120-130°C is preferred. Differential thermal analysis of unfilled PPS indicates a crystalline melting point of 285°C, a glass transition temperature (Tg) of 85°C, and a pre-melt crystallization temperature of about 130°C.[2]

Thermal history of a molded specimen determines the degree of crystallinity of the specimen and to some extent the mechanical

0-8412-0485-3/79/47-095-183$05.00/0

and thermal behavior of the molded part. When a part is molded in a mold below the Tg value of 85°C, it is substantially amorphous (less than 5% crystalline). On the other hand, when the mold temperature employed is about 130°C, a high crystallinity (ca. 60%) is obtained.[3] The amorphous part can be caused to crystallize by annealing in an oven at 200°C for about 30 minutes. In general, the optimum properties are realized when the crystallinity level is high. Unless otherwise stated, properties quoted in this paper were measured on well crystallized samples.

Mechanical Behavior

The mechanical properties of the three filled grades of polyphenylene sulfide are given in Table I. The 40% glass-filled material has the lowest density and the highest values for tensile strength, flexural strength, compressive strength, impact strength and hardness. The glass- and mineral-filled composition offers a good balance of properties at a substantial cost savings, and the glass- and mineral-filled color compounds offer competitive properties and attractive colors at an intermediate cost.

TABLE I

MECHANICAL PROPERTIES OF POLYPHENYLENE SULFIDE COMPOUNDS

	40% Glass Filled	Glass/Mineral Filled	Glass/Mineral Filled Color (Natural)
Density, g/cc	1.6	1.8	1.97
Tensile strength, MPa	135	92	69
Elongation, %	1.3	0.7	0.5
Flexural modulus, MPa	11,700	13,100	12,400
Flexural strength, MPa	200	141	121
Compressive strength, MPa	145	110	114
Izod impact strength, J/m			
Unnotched	430	117	91
Notched	75	27	37
Shore D hardness	92	88	90
Heat deflection temp. (264 psi), °C	>260	>260	>260

The retention of properties of 40% glass-filled PPS at temperatures of 93, 149 and 204°C as a per cent of the room temperature value are given in Figure 1.[4] In general, this material retains about 80% of the original property values at 93°C, 60 per cent at 149°C and 40 per cent at 204°C.

The flexural fatigue endurance limit (ASTM D671) provides information on the ability of a material to resist mechanical

In Durability of Macromolecular Materials; Eby, R.;
ACS Symposium Series; American Chemical Society: Washington, DC, 1979.

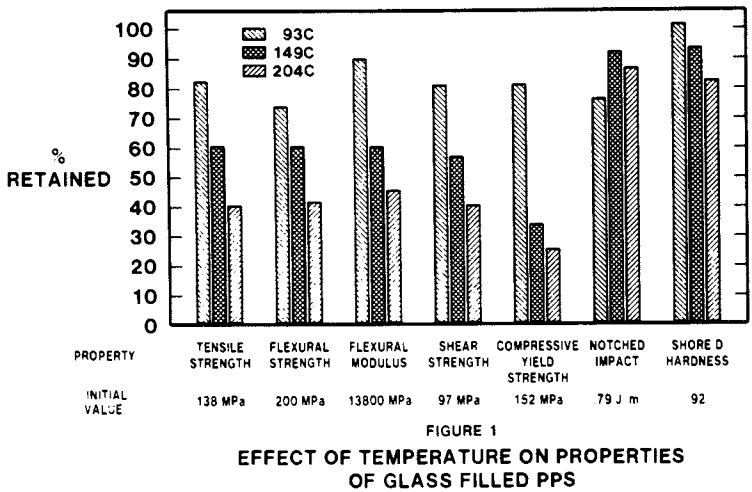

Figure 1. Effect of temperature on properties of glass-filled PPS

In Durability of Macromolecular Materials; Eby, R.;
ACS Symposium Series; American Chemical Society: Washington, DC, 1979.

deterioration as a result of a relatively large number of cycles of constant amplitude of force. This limit is reported as the stress level at which no failures occur at 10^7 cycles. The values for 40% glass-filled PPS and glass/mineral filled PPS are 45 MPa and 21 MPa respectively. The 40% glass-filled compound behaves similarly to other glass-filled engineering plastics in this test.

Thermal Stability

Thermogravimetric analysis of unfilled PPS in nitrogen or in air indicates no appreciable weight loss below about 500°C (Figure 2). In this analysis, degradation is essentially complete in air at 700°C, but in an inert atmosphere, approximately 40% of the polymer weight remains at 1,000°C. Thermogravimetric analysis is inherently a short-term, weight loss measurement and, as such, is only indicative of thermal stability in a practical sense.

Long term oven aging of the 40% glass-filled PPS in air was done at temperatures ranging from 204°C to 246°C. Figure 3 shows the retention of tensile strength (measured at room temperature) for times up to 9,500 hours (13 months). After an initial decrease during the first 4-5,000 hours, the tensile strength remains largely unchanged during the remainder of the exposure period. At the upper exposure temperature of 246°C, the initial drop in tensile strength is slower than at the lower exposure temperature. This is presumably due to some curing or crosslinking of the polymer at this temperature. At the end of the exposure period all three samples exhibited very similar tensile strengths.

Figure 4 shows similar oven aging data on glass- and mineral-filled polyphenylene sulfide at temperatures of 232°C, 260°C and 274°C. Again during the first 6-7,000 hours of exposure, the samples exposed at the higher temperatures retain higher tensile strengths. Again this is presumably due to crosslinking during exposure.

Underwriters Laboratories' has authorized temperature indices of 170°C for the 40% glass-filled PPS and 200°C for the glass- and mineral-filled resin. The glass- and mineral-filled color compounds have a provisional UL Temperature Index of 200°C.

When polyphenylene sulfide is heated in air at approximately 815°C, the major components of thermal degradation are: hydrogen, methane, carbon monoxide, carbon dioxide and carbonyl sulfide. In addition, minor amounts of sulfur dioxide and ethane or ethylene are also formed.

The creep behavior of 40% glass-filled polyphenylene sulfide is summarized in Figure 5 which plots creep modulus against time for three sets of experimental conditions: 23°C/5,000 psi, 66°C/5,000 psi, and 121°C/5,000 psi. Table II compares the per cent loss in apparent creep modulus at 1,000 hours and at 10,000

In Durability of Macromolecular Materials; Eby, R.;
ACS Symposium Series; American Chemical Society: Washington, DC, 1979.

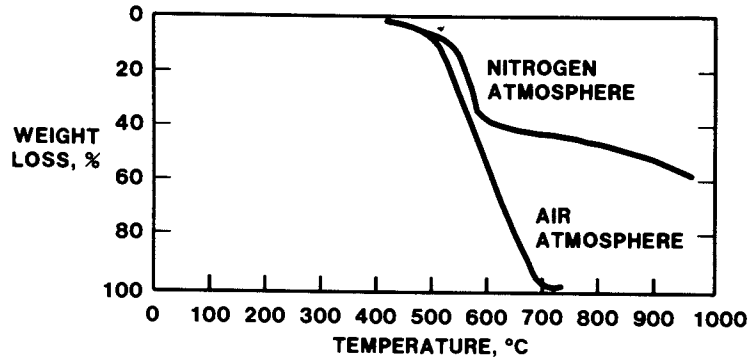

Figure 2. Polyphenylene sulfide–thermogravimetric analysis (DuPont 950 TGA instrument; heating rate, 15°C/min; atmosphere purge, 40 cc/min)

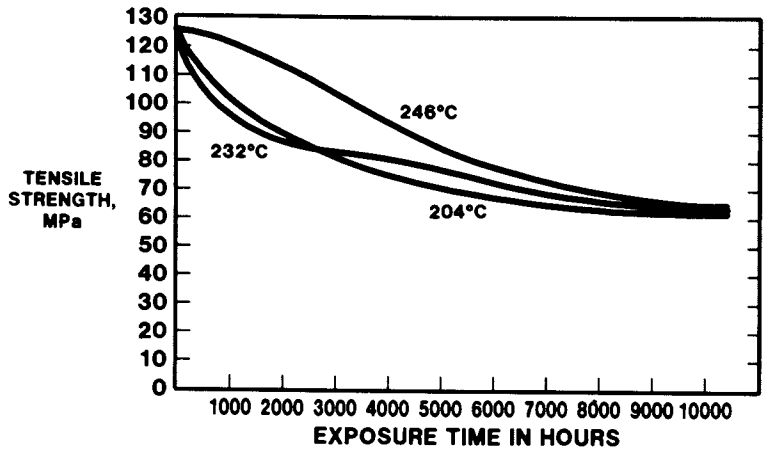

Figure 3. Oven aging of 40% glass-filled PPS in air

In Durability of Macromolecular Materials; Eby, R.;
ACS Symposium Series; American Chemical Society: Washington, DC, 1979.

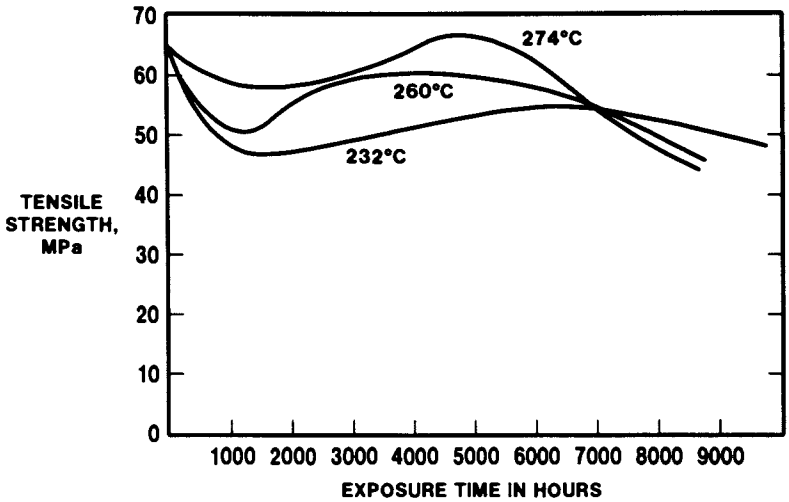

Figure 4. Oven aging of glass- and mineral-filled PPS in air

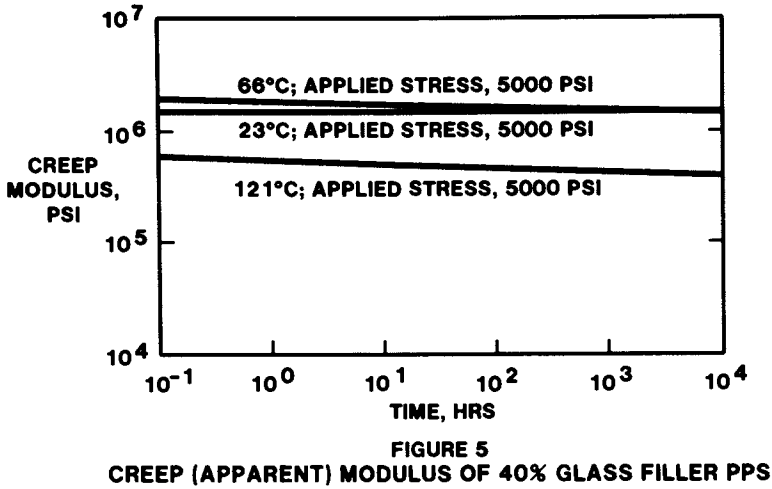

Figure 5. Creep (apparent) modulus of 40% glass-filled PPS

In Durability of Macromolecular Materials; Eby, R.;
ACS Symposium Series; American Chemical Society: Washington, DC, 1979.

hours for each of these conditions using the apparent creep modulus at one hour as a basis. These data indicate good creep resistance for a thermoplastic material with a glass transition of 85°C for the base polymer.

TABLE II

LOSS IN APPARENT CREEP MODULUS FOR 40% GLASS FILLED PPS

Test Condition		Loss in Apparent Creep Modulus, %[a]	
Temp., °C	Stress, psi	1,000 Hours	10,000 Hours
23	5,000	7.8	8.9
66	5,000	20.7	24.7
121	5,000	22.6	29.8

a - Per cent loss between one hour and indicated time.

Similarly, Figure 6 summarizes the creep behavior of glass- and mineral-filled polyphenylene sulfide under three sets of conditions: 24°C/5,000 psi flexural load, 66°C/5,000 psi, and 121°C/3,000 psi. Table III compares the per cent loss in apparent creep modulus at 1,000 hours and at 10,000 hours for each of these conditions using the apparent creep modulus at one hour as a basis. These data indicate that the creep resistance of the glass- and mineral-filled polymer is similar to that of the 40% glass-filled resin.

TABLE III

LOSS IN APPARENT CREEP MODULUS FOR GLASS- AND MINERAL-FILLED PPS

Test Conditions		Loss in Apparent Creep Modulus, %[a]	
Temp., °C	Stress, psi	1,000 Hours	10,000 Hours
24	5,000	8.2	11.6
66	5,000	20.0	25.6
121	3,000	16.0	21.4

a - Per cent loss between one hour and indicated time.

Electrical Behavior

The electrical properties of the three polyphenylene sulfide compounds are given in Table IV. The 40% glass-filled PPS is the best insulator as indicated by the dielectric constant of 3.8. The two compounds which contain glass- and mineral-fillers provide the best arc resistance and tracking index. All three materials provide a good balance of electrical properties.

In Durability of Macromolecular Materials; Eby, R.;
ACS Symposium Series; American Chemical Society: Washington, DC, 1979.

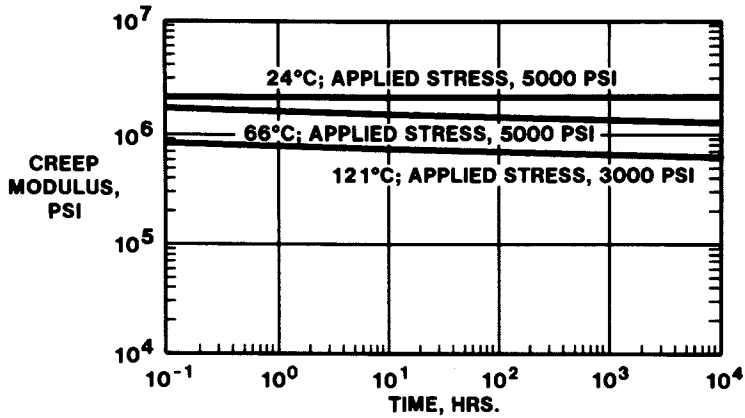

FIGURE 6
CREEP (APPARENT) MODULUS OF GLASS AND MINERAL FILLED PPS

Figure 6. Creep (apparent) modulus of glass- and mineral-filled PPS

In Durability of Macromolecular Materials; Eby, R.;
ACS Symposium Series; American Chemical Society: Washington, DC, 1979.

TABLE IV

ELECTRICAL PROPERTIES OF POLYPHENYLENE SULFIDE COMPOUNDS

Property	40% Glass Filled	Glass and Mineral-Filled	Glass and Mineral-filled Color (Black)
Dielectric strength, 1 kHz, volts/mil	350	340	324
Dielectric constant, 1 MHz	3.8	4.6	5.1
Dissipation factor, 1 MHz	0.0013	0.016	0.019
Volume resistivity, 2 min. Ohm-cm	4.5×10^{16}	2.0×10^{15}	1.3×10^{15}
Arc resistance, sec.	35	200	200
Comparative tracking index, volts	180	235	235

Table V indicates the good retention of electrical properties exhibited by the 40% glass-filled PPS at temperatures up to 147°C. In addition, exposure of test specimens to 50 per cent relative humidity for 5 days did not cause any appreciable change in either dielectric constant or dissipation factor. Thus, environmental factors do not have much effect upon the electrical behavior of polyphenylene sulfide resins.

TABLE V

ELECTRICAL PROPERTIES OF 40% GLASS-FILLED PPS AT ELEVATED TEMPERATURES

Property	Temperature 27°C	100°C	147°C
Dielectric Constant			
10^3 Hertz	3.9	3.9	4.0
10^6 Hertz	3.8	3.8	3.9
Dissipation Factor			
10^3 Hertz	0.0010	0.0016	0.0065
10^6 Hertz	0.0013	0.0015	0.0051

Flammability Behavior

Polyphenylene sulfide will not burn when tested by any of the common standard tests used for plastics, such as ASTM D635 and UL-94. However, when exposed in a fire, it will continue to burn until the externally applied flame is removed. It burns with a yellow-orange flame, producing gray smoke with traces of black. It does not drip and the char is black and glossy. The UL ignition temperature of the 40% glass-filled resin is 540°C.

In Durability of Macromolecular Materials; Eby, R.;
ACS Symposium Series; American Chemical Society: Washington, DC, 1979.

Table VI summarizes the flammability behavior of the three filled PPS resins by a variety of flammability tests.

TABLE VI

FLAMMABILITY OF FILLED PPS RESINS

Flammability Test	40% Glass-Filled PPS	Glass and Mineral-Filled PPS	Glass and Mineral-Filled Colored
ASTM D635	Non-burning	Non-burning	Non-burning
Oxygen index	46.5	53	50
UL-94	V-0	V-0	V-0

The smoke density test developed by the National Bureau of Standards employs a completely closed cabinet, measuring 3 feet wide, 3 feet high and 2 feet deep, in which a specimen 3 inches square is supported in a frame such that a surface area 2-9/16 inches square is exposed to heat under either flaming or non-flaming (smoldering) conditions. The heat source is a circular foil radiometer adjusted to give a heat flux of 2.5 watts per square centimeter at the specimen surface. The photometer path for measuring light absorption is vertical, to minimize measurement differences due to smoke stratification which could occur with a horizontal photometer path at a fixed height, and the full 3-foot height of the chamber is used to provide an overall average for the entire chamber. Smoke measurements are expressed in terms of specific optical density, which represents the optical density measured over unit path length within a chamber of unit volume produced from a specimen of unit surface area; since this value is dimensionless, it provides the advantage of presenting smoke density independent of chamber volume, specimen size or photometer path length, provided a consistent dimensional system is used.

The time to reach a critical smoke density, also called the obscuration time, is a measure of the time available before a typical occupant in a typical room would find his vision obscured by smoke sufficiently to hinder escape. The value of specific optical density describing this critical level is 16, based on 16 per cent light transmittance under certain specific conditions of room dimensions.

Results of smoke density measurements on 40% glass-filled polyphenylene sulfide are given in Table VII. These data indicate that PPS burns with the generation of a relatively small quantity of smoke.

In Durability of Macromolecular Materials; Eby, R.;
ACS Symposium Series; American Chemical Society: Washington, DC, 1979.

TABLE VII

SMOKE DENSITY OF RYTON PPS

Ryton	Max. Value of Specific Optical Density		Obscuration Time, minutes	
	Smoldering	Flaming	Smoldering	Flaming
40% Glass-filled PPS -				
125 mils thick	25	232	15.5	3.2
60 mils thick	23	171	15.5	2.7
Red oak (25 mils thick)[a]	393	75	4.1	8.0

a - Included for comparison purposes.

Chemical Resistance

Previous studies[5] comparing PPS to other engineering thermoplastics established the relative short term (24-hour) chemical resistance of PPS moldings to a wide variety of chemical environments at 93°C. A portion of these results are given in Table VIII.

More recent examinations have lengthened exposure time at this temperature to 12 months for the 40% glass-filled polyphenylene sulfide (Table IX). Even under these severe conditions under which most thermoplastic resins would fail catastrophically, the general chemical resistance of glass-filled PPS was again manifested. Resistance to phosphoric acid, water, alcohols, dibutyl ether, butylamine, gasoline, cresyldiphenyl phosphate, N-methyl pyrrolidone, and air was particularly favorable. Slight to moderate attack was noted by sulfuric acid, sodium hydroxide, sodium hypochlorite, methyl ethyl ketone, chloroform, ethyl acetate, dioxane, aniline, toluene, benzonitrile, phenol and benzaldehyde. Severe attack resulted upon exposure to concentrated hydrochloric acid, 10% nitric acid, carbon tetrachloride and nitrobenzene. This chemical resistance suggests the use of PPS moldings in many applications where harsh, corrosive or difficult to handle chemical environments are encountered.

In Durability of Macromolecular Materials; Eby, R.;
ACS Symposium Series; American Chemical Society: Washington, DC, 1979.

TABLE VIII

CHEMICAL RESISTANCE 93°C/24 hr

Chemical	Per cent tensile retained				
	Nylon 6-6	Polycar-bonate	Polysul-fone	Modified PPO	PPS
37% HCl	0	0	100	100	100
10% HNO_3	0	100	100	100	96
30% H_2SO_4	0	100	100	100	100
85% H_3PO_4	0	100	100	100	100
30% NaOH	89	7	100	100	100
28% NH_4OH	85	0	100	100	100
H_2O	66	100	100	100	100
$FeCl_3$	13	100	100	100	100
NaOCl	44	100	100	100	84
Br_2	8	48	92	87	64
Butyl alcohol	87	94	100	84	100
Phenol	0	0	0	0	100
Butylamine	90	0	0	0	50
Aniline	85	0	0	0	96
2-Butanone	87	0	0	0	100
Benzaldehyde	98	0	0	0	84
Chlorobenzene	73	0	0	0	100
Chloroform	57	0	0	0	87
Ethyl acetate	89	0	0	0	100
Butyl phthalate	90	46	63	19	100
p-Dioxane	96	0	0	0	88
Butyl ether	100	61	100	0	100
Gasoline	80	99	100	0	100
Diesel fuel	87	100	100	36	100
Toluene	76	0	0	0	98
Benzonitrile	88	0	0	0	100
Nitrobenzene	100	0	0	0	100

In Durability of Macromolecular Materials; Eby, R.;
ACS Symposium Series; American Chemical Society: Washington, DC, 1979.

TABLE IX

LONG TERM CHEMICAL RESISTANCE OF 40% GLASS-FILLED PPS

(Exposure Temperature, 93°C)

Chemical	Per cent Retention[a] of Tensile strength after 24 Hr.	3 Mo.	6 Mo.	12 Mo.
37% HCl	71	34	22	29
10% HNO_3	91	b	--	b
30% H_2SO_4	94	89	34	61
85% H_3PO_4	100	99	41	89
30% NaOH	100	89	44	63
Water	99	99	49	65
Clorox	94	77	54	61
n-Butyl alcohol	100	92	69	80
Cyclohexanol	100	91	69	86
Butylamine	96	46	58	85
Methyl ethyl ketone	100	100	57	61
Carbon tetrachloride	100	48	24	25
Chloroform	81	77	41	43
Ethyl acetate	100	88	46	58
Butyl ether	100	89	68	79
p-Dioxane	99	96	69	59
Gasoline	100	99	71	80
Aniline	100	86	60	42
Toluene	100	70	55	41
Benzonitrile	100	79	29	39
Nitrobenzene	100	63	53	31
Phenol	100	92	59	63
Benzaldehyde	97	47	27	42
Cresyl diphenyl phosphate	100	100	83	95
N-Methylpyrrolidone	100	92	84	80
Air	--	96	71	72

a - Compared to unannealed, unexposed tensile bars.
b - Specimens disintegrated.

In Durability of Macromolecular Materials; Eby, R.;
ACS Symposium Series; American Chemical Society: Washington, DC, 1979.

Additional Environmental Resistance Behavior

The effects of neutron and gamma radiation on the mechanical behavior of 40% glass-filled polyphenylene sulfide are summarized in Table X. These data indicate that this resin is quite stable to environments involving radiation.

TABLE X

EFFECT OF RADIATION ON PHYSICAL PROPERTIES OF 40% GLASS-FILLED PPS

Conditions	In Reactor Core	In Water Pool
Temperature	35°C	30°C
Radiation	Mainly neutrons	Mainly gamma
Intensity	10^8 rad	10^7 rad
Used particle detectors	Calorimeter and activation detectors	Ionization chamber
Radiation dose	Flexural strength, MPa	Modulus of Elasticity, MPa
0	198	13,091
A. Gamma		
5×10^8 rad	205	12,470
1×10^9 rad	208	12,670
5×10^9 rad	196	12,540
B. Neutron		
5×10^8 rad	200	13,160
1×10^9 rad	199	12,950

The 40% glass-filled PPS was aged in an Atlas Weather-Ometer for 10,000 hours. Changes in tensile strength and elongation were measured at specific time intervals. Tests were performed on a control resin with no UV inhibitor, one with 1% Tinuvin 327 and one with 1% UV 531. The results are shown in Table XI. These data indicate moderate stability to ultraviolet radiation without stabilizers and improved stability with stabilizers.

In Durability of Macromolecular Materials; Eby, R.;
ACS Symposium Series; American Chemical Society: Washington, DC, 1979.

TABLE XI

EFFECT OF WEATHER-OMETER EXPOSURE ON TENSILE PROPERTIES OF 40% GLASS-FILLED PPS

Hours Exposed	Resin Control Tensile, MPa	Resin Control Elong. %	Resin + 1% Tinuvin 327 Tensile, MPa	Resin + 1% Tinuvin 327 Elong. %	Resin + 1% UV 531 Tensile, MPa	Resin + 1% UV 531 Elong. %
0	115	1.10	113	1.20	115	1.35
2,000	105	1.20	109	1.30	103	1.15
6,000	106	1.38	104	1.23	100	1.15
8,000	98.9	1.23	97.8	1.15	93.7	1.05
10,000	72.7	0.60	103	0.95	88.5	1.00
% Tensile reduction	37	45	9	21	23	26
Erosion, mils	13		11		11	

Conclusions

Three filled injection molding grades of polyphenylene sulfide were described: (1) 40% glass-filled polymer, (2) a glass- and mineral-filled polymer and (3) a glass- and mineral-filled color compound family. Polyphenylene sulfide is a crystallizable polymer and optimum behavior is realized in well crystallized parts. These may be obtained by molding into a hot (120-130°C) mold or by annealing (200°C/30 minutes) the molded part. The filled resin compositions are strong, stiff and hard, and mechanical properties are retained well at temperatures up to about 200°C. Oven aging for 10,000 hours at temperatures from 204°C to 272°C indicate excellent retention of tensile strength. The filled polymers are also resistant to creep. A variety of electrical properties are available by appropriate choice of resin/filler composition and properties are retained at temperatures up to about 150°C. The various filled resins do not burn when tested by commonly used tests, but will burn as long as an externally applied flame is maintained. Smoke generation is low. Chemical resistance of the 40% glass-filled PPS is excellent in tests at 93°C for 1 year's exposure.

References

1. Edmonds, J. T., Jr. and Hill, H. W., Jr., U.S. 3,354,129 to Phillips Petroleum Company (November 21, 1967).
2. Short, J. N. and Hill, H. Wayne, Jr., Chemtech 2, 481 (1972).
3. Brady, D. G., J. Appl. Poly. Sci. 20, 2541 (1976).
4. Hill, H. Wayne, Jr. and Brady, D. G., Poly. Eng. and Sci. 16, 831 (1976).
5. Brady, D. G. and Hill, H. W., Jr., Mod. Plast., 51, No. 5, 60 (1974).

RECEIVED December 8, 1978.

14

Review of Experimental Investigations of Molecular Phenomena Associated with Fracture in Polymers

K. L. DE VRIES, DOUGLAS GUSTAVESON, and REDD SMITH
University of Utah, College of Engineering, Salt Lake City, UT 84112

Fracture is a phenomenon of considerable technical and scientific interest. In the relatively complex morphology of polymers some might envision different molecular mechanisms by which failure might occur. A complete understanding of fracture must involve a knowledge of occurrences on the molecular scale. Not only would information on the basic mechanisms responsible for failure be useful in establishing criteria for the prediction (or prevention) of failure but may also provide insight into means by which the structure of a material may be modified to enhance properties. We feel that it is particularly important to understand these fundamental mechanisms in order to predict long-term performance in service from short-term laboratory tests. Scientists and engineers have long theorized on the mechanisms involved in failure. Several intricate molecular models have been proposed to explain macroscopic phenomena. More recently several analytical techniques have become available and been adapted to make experimental observations of molecular occurrences during fracture that can be used to help verify these theories. These methods have included electron spin resonance (ESR), infrared spectroscopy (IR) and measurement of the change in molecular weight.

Most of the authors' experience has been with ESR. ESR is a form of microwave absorption spectroscopy which quantitatively detects the presence of unpaired electrons. When homolytic chain scission of a polymer chain takes place, the two electrons making up a covalent bond may be uncoupled forming two free radicals. If these free radicals are produced in sufficient number and are stable enough to produce a high enough concentration, they may be detected and their concentration measured by an ESR spectrometer. In a great many polymers, free radicals are either very unstable, (they may be annihilated through reaction with other radicals and/or impurities), or are produced in numbers too small for detection by currently available instruments. There are, however,

0-8412-0485-3/79/47-095-199$05.00/0

In Durability of Macromolecular Materials; Eby, R.;
ACS Symposium Series; American Chemical Society: Washington, DC, 1979.

some important systems where large, easily detectable concentrations are accumulated during the fracture process. Past work has been done on highly oriented polymer fibers and films [1-3]. There have also been several investigations on elastomers. Here we will primarily concentrate on these latter studies.

ESR has proven to be a very sensitive and informative means of monitoring bond rupture in rubbers under combined stress and exposure to ozone (4). Ozone attacks the unsaturated bonds in deformed rubber. Such carbon-carbon double bonds are of course found in natural rubber and many other elastomers. All of the gum rubbers that were susceptible to cracking when stressed and tested in an ozone atmosphere exhibited a strong distinct ESR signal.

The increase, with time of free radicals for gum acrylonitrile - butadiene rubber is indicated in Figure 1. The strongest signal shown in the figure is four orders of magnitude above the threshold sensitivity of the spectrometer. Detectable concentrations of free radicals were produced by exposure of natural rubber to an ozone concentration of 2.8 mg/l for less than 1 sec. under 35% strain. This was before microscope inspection (up to 400X) showed any evidence of damage.

Analysis of the change with time in load, strain, stored strain energy release rate, decrease in modulus, and ESR signal of ozone degraded rubber provides some insights into the failure processes. A comparison between the measured number of free radicals produced and the decrease in modulus indicates that bond rupture occurs selectively in the more effective load bearing molecules. A correlation has been established between atomic phenomena and the fracture mechanics for rubber under the combined effect of stress and ozone attack. The investigations indicate that cracks propagate, i.e. bonds rupture, only if sufficient strain energy is present. This observation made it possible to establish a quantitative bond rupture analysis to a macroscopic "Griffith" crack growth criteria. This microscopic criteria is somewhat analogous to the macroscopic criteria developed by Gent (5).

Generally, it is observed that elastomers at very low temperature become brittle and fracture with little detectable inelastic deformation. Andrews, Reed, and co-workers (5-6) have demonstrated that prestraining the rubber before cooling can drastically modify its fracture behavior. In their studies and subsequent studies by others (7-8) a variety of rubbers ranging from natural rubber to silicone were prestrained (~100% at room temperature) before reducing the temperature to -100°C or below. When further stressed at these low temperatures, the rubbers did

In Durability of Macromolecular Materials; Eby, R.;
ACS Symposium Series; American Chemical Society: Washington, DC, 1979.

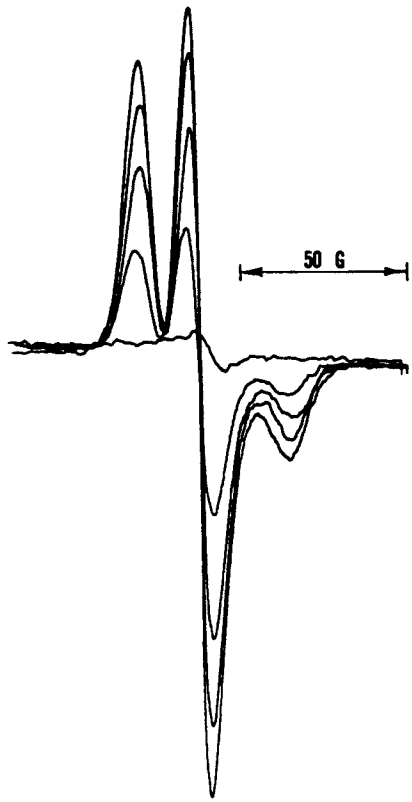

Figure 1. ESR spectra of ozone-degraded ANR (Hycar 1043) (ozone concentration, 2.8 mg/L). Lowest curve is residual signal; successively larger ones at 5-min intervals after application of 25% strain.

In Durability of Macromolecular Materials; Eby, R.;
ACS Symposium Series; American Chemical Society: Washington, DC, 1979.

not fracture in a brittle manner but exhibited a yield point followed by significant plastic deformation before ultimate failure. They also observed that samples that were prestrained and fractured at low temperatures exhibited strong ESR signals (see Figure 2), while samples that were fractured at the same temperatures but without prestrain showed little if any free radical production during the deformation process. These free radicals have been analyzed (the location of bond rupture identified) and the conditions for ductility and free radical production experimentally investigated.(8-9) The results of these studies in conjunction with X-ray studies of structure lead us to the hypothesis that the prestrain in conjunction with the decreases in temperature results in a molecular ordering of the rubber. Further loading at low temperatures eventually results in the production of microcracks. In the rubbers that had not been prestained these microcracks are sites of recipient failure. On the other hand, in the prestrained rubbers the microcracks hypothetically terminate when they intersect the ordered regions. The very large number of free radicals produced can only be interpreted as evidence that a great many microcracks are produced and subsequently arrested in materials treated in this manner. In fact it appears that under proper conditions in excess of 10^3 cm^2 of microcrack area are produced in a cm^3 of rubber. This, of course, results in large changes in strength, strain at fracture (ductility), and toughness (energy absorbed during deformation and failure). These are important properties. A better understanding and exploration of these phenomenon might well have technological importance.

In modern technological usage, elastomers are commonly filled with various granular materials. The presence of such fillers increases the complexity of the micromechanics of deformation and might modify the mode of fracture. At best polymeric fracture is quite complex; the addition of a filler increases the complexity in that it adds the possibility of separation between the matrix and filler, (i.e. dewetting), or failure of the filler and must result in local strain redistributions and very nonhomogeneous localized stress fields. The filler particles might also serve as crack arrestors and/or initiators and thereby modify the energy absorbed during crack growth.

ESR has been used to investigate the role of the filler-matrix interaction in filled rubbers at cryogenic temperatures (10). The breakdown in adhesion between filler and matrix results in vacuoles or voids in the material. Figures 3 and 4 show a contrast in behavior for 5μ glass spheres in rubber with and without a silicone coupling agent treatment. In the first case strength is low and very few free radicals are produced

In Durability of Macromolecular Materials; Eby, R.;
ACS Symposium Series; American Chemical Society: Washington, DC, 1979.

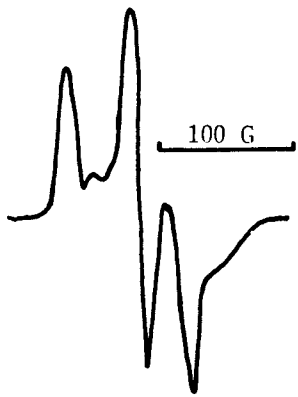

Figure 2. ESR spectrum resulting from deformation of natural rubber at −75°C and prestrain

In Durability of Macromolecular Materials; Eby, R.;
ACS Symposium Series; American Chemical Society: Washington, DC, 1979.

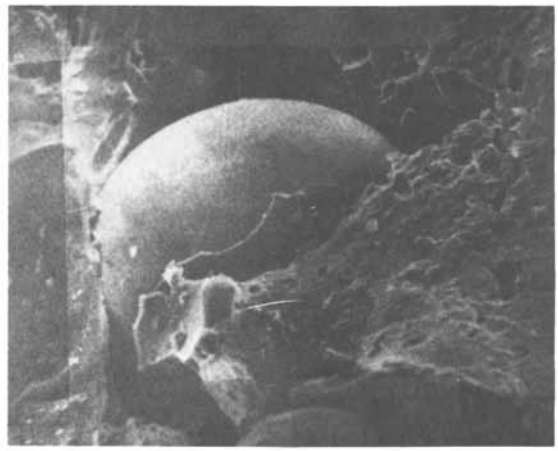

Figure 3. Dewetting in glass-filled EPDM subjected to 100% elongation (magnified 500×)

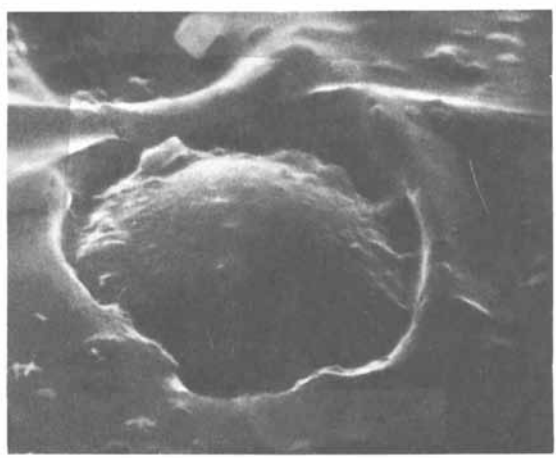

Figure 4. Treated glass-filled polyisoprene subjected to 50% elongation (magnified 500×)

In Durability of Macromolecular Materials; Eby, R.;
ACS Symposium Series; American Chemical Society: Washington, DC, 1979.

during deformation while materials of the second type exhibited high strength, toughness, and the production of relatively large numbers of free radicals during deformation. Quantitative correlations have been made between the amount of adhesion, the strength, toughness and the number of free radicals produced.

As noted above, most organic free radicals are inherently unstable entities. This is particularly true in polymers like rubbers where chain mobility is quite high. One known exception to this is the radicals produced during ozone degradation, where the oxygen present at the free radical produced appears to act as a stabilizer, yielding radicals with a half-life of approximately one hour. In other studies on rubbers, the radicals have been "trapped" by doing the studies at low temperature. For many studies a means is needed to detect more permanent changes in the polymer chains. End group analysis by IR spectroscopy has been proposed as just such a tool. Zhurkov and his associates in the USSR first proposed such studies (11) and Koenig, et al. (12-13) have pioneered its usage in the United States. Koenig has made use of Fourier Transform infrared spectroscopy (FTIR), which is more sensitive than dispersive IR and has the added advantage of having the spectra stored in a computer. It is possible to store the IR spectra from several samples and then, using the computer, make very accurate subtractions and other comparisons. Appropriate end groups once formed by chain scission should be very stable. ESR can only be used in restricted systems where the free radical produced by mechanical means are fairly stable. Even in these systems, free radical decay time has limited studies to an hour or so. If techniques using IR should prove sufficiently sensitive and accurate they should open a whole new range of molecular studies. This would open the way for long term fracture studies (e.g. fatigue and creep in materials with either "stable" or unstable radicals). The prerequisite here being that detectable new end groups must be formed.

Zhurkov, Novak and Vettegran have recently reported studies where IR was used to determine the formation of CH_3 and C=C bonds during deformation of polyethylene and polypropylene at room temperature and atmospheric conditions (11). In these studies, specimens of equal thickness, one unstrained, the other fractured, were interposed in the balanced light beams of double-beam spectrometer. In this mode the spectrometer reportedly records the difference in absorption ΔD, of the undeformed and fractured specimen. Strong absorption bonds were noted at 910, 965, 1379 and 1735 cm^{-1}. These were attributed respectively to ($RCH=CH_2$), ($RCH=CHR^1$), ($R-CH_3$), and (RCHO) groups.

Koenig, et al. have used FTIR to investigate chain scission due to γ-ray irradiation and mechanical stress (11-12).

In Durability of Macromolecular Materials; Eby, R.;
ACS Symposium Series; American Chemical Society: Washington, DC, 1979.

Exploratory studies of end group analysis by IR techniques have also been initiated in this laboratory. With the assistance of Bruno Fanconi of the National Bureau of Standards and L. D'Esposito of Digilabs we have made some Fourier transform IR measurements to complement those on our conventional equipment. These studies on polyethylene compare the bond rupture kinetics due to γ-ray damage and mechanical degradation at various temperatures as measured by ESR and IR spectroscopy. This study should be completed in the next few months and prepared for publication. Figures 5 and 6 show the typical IR absorption of samples degraded in air in the vicinity of 1700 cm^{-1}. More recently we have begun an IR investigation of stress-ozone cracking of rubber. Figure 7 is a difference spectrum of an ozone degraded isoprene rubber indicating some of the changes that occur.

The results of our IR studies are not yet complete and analysis of the spectra obtained to date is underway. However, it is appropriate to note that mechanical damage of polyethylene does indeed produce detectable changes in infrared absorption. However, the experiments and their analysis are not as straightforward as previously suggested [11]. Among other things, the changes in the absorption bands attributed to the end groups are very small and some of the apparent changes in these bands are not always even in the direction anticipated. IR absorption spectroscopy is highly dependent on such factors as sample surface condition, thickness, chain orientation, crystallinity, etc., all of which are apt to be altered by sample deformation and fracture. This has made accurate spectra comparison and analyses difficult to say the least. We have recently concentrated our efforts on techniques for reducing the effect of these parameters and comparing ESR (at low temperatures where radicals are very stable) and IR spectra.

In conclusion this paper has tried to focus on some of the analytical techniques which can be utilized in the study and correlation of molecular phenomena with material failure. An understanding which is important because of the inherent complexity of the molecular structure of polymers and the effect it has on material properties.

Through the use of ESR spectroscopy it has been possible to view immediate changes which occur during degradation. IR spectroscopy on the other hand has the potential of determining long-term effects which result from those initial changes. Establishing the exact relationship between these immediate (free radicals) and the ultimate changes (new end group) is at best a difficult task; however, there are indications that we will be able to establish a quantitative relationship by these means.

In Durability of Macromolecular Materials; Eby, R.;
ACS Symposium Series; American Chemical Society: Washington, DC, 1979.

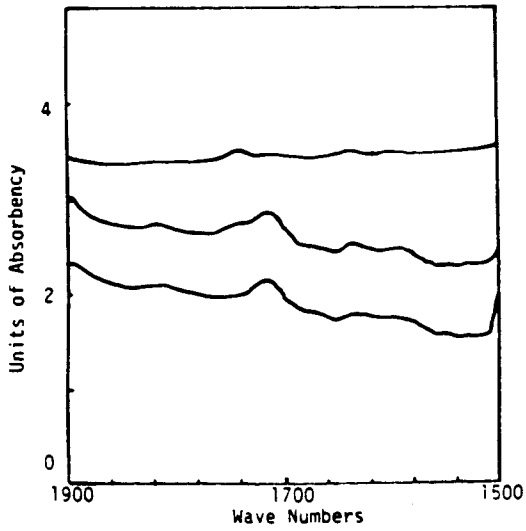

Figure 5. IR spectra for HDPE: upper curve, reference; middle curve, after 21 Mrad γ-irradiation; lower curve, the difference between the two above curves (horizontal position of base line is arbitrary).

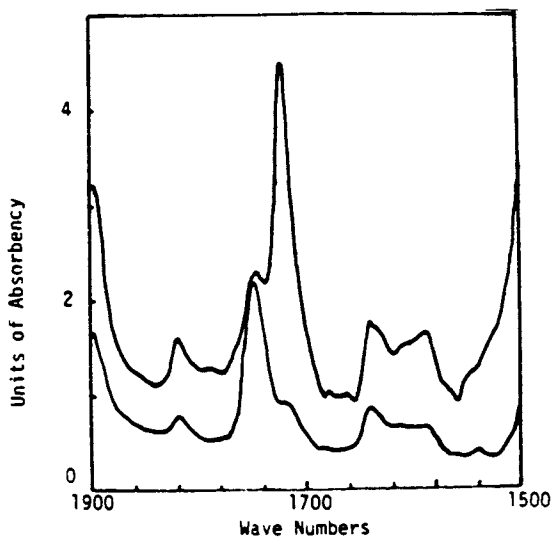

Figure 6. IR spectra for HDPE: upper curve, reference; lower curve, after tensile fracture (horizontal position of base line is arbitrary).

In Durability of Macromolecular Materials; Eby, R.;
ACS Symposium Series; American Chemical Society: Washington, DC, 1979.

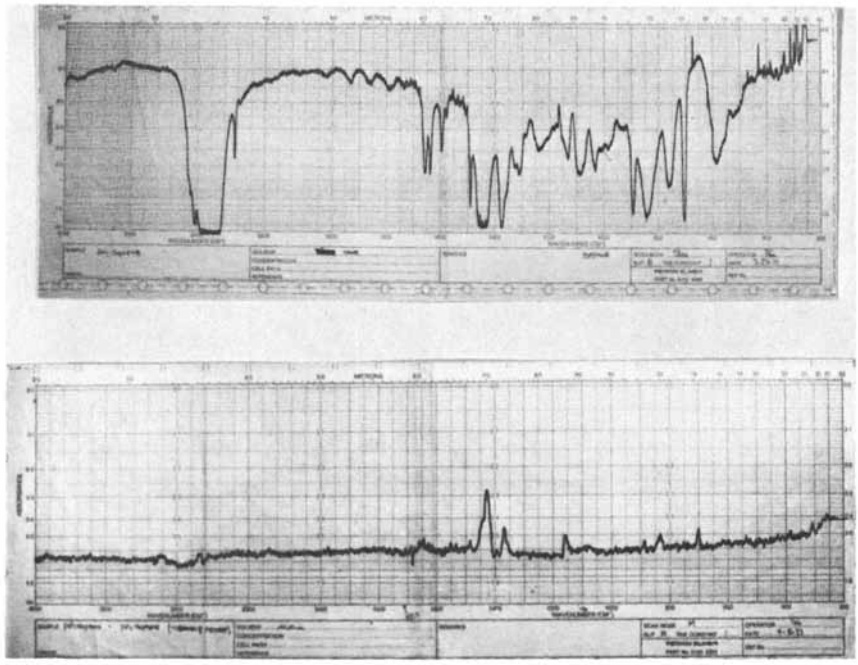

Figure 7. Upper curve, IR spectra of stress–ozone-degraded polyisoprene; lower curve, results from subtraction of reference polyisoprene curve from the upper curve.

In Durability of Macromolecular Materials; Eby, R.;
ACS Symposium Series; American Chemical Society: Washington, DC, 1979.

A basic understanding of molecular effects during failure aids in establishment of reliable failure criteria and predictions of material properties as well as providing an insight as to the means by which those properties could be tailored or enhanced.

ACKNOWLEDGMENT

Portions of this study were supported by the National Science Foundation under Grant #DMR 74-03271-A 01.

REFERENCES

1. Zhurkov, S. N., Intl. J. Fracture, 1, 311 (1965).

2. Lloyd, B. A., DeVries, K. L., and Williams, M. L., Rheol. Acta, 13, 352 (1974).

3. Kausch, H. and Becht, J., Rheol. Acta, 9, 137 (1970).

4. DeVries, K. L., Rubber Chem. & Tech., 48, 445 (1975).

5. Braden, M. and Gent, A. N., J. Appl. Polym. Sci., 2, 100 (1960).

6. Andrews, E. H. and Reed., J. Polym. Sci., Polym. Lett. Ed., 5, 317 (1967).

7. Mead, W. T. and Reed,P. E., Polym. Eng. Sci., 14, 22 (1974).

8. Brown, R. T., DeVries, K. L. and Williams, M. L., J. Polym. Sci., Polym. Lett. Ed., 10, 327 (1972).

9. Mead, M. T., Porter, R. S. and Reed, P. E., Org. Coatings and Plastics Chemistry, ACS, 38, 88 (1976).

10. DeVries, K. L., Wilde, T. B. and Williams, M. L., J. Macro. Sci. Phy., B7, 633 (1973).

11. Zhurkov, S. N., Zakrevskii, V. A., Korsukov, V. E. and Kuksenko, V. S., Sov. Phys. Solid State, 13:7, 1680 (1973).

12. Tabb, D. S., Sevcik, J. J. and Koenig, J. L., J. Polym Sci., 13, 815 (1975).

13. D'Esposito, L., and Koenig, J. L., Org. Coatings and Plastics Chemistry, ACS, 38, 306 (1978).

RECEIVED December 8, 1978.

15

The Application of Chemiluminescence for the Study of Polymer Mechanochemistry[1]

D. L. FANTER and R. L. LEVY

McDonnell Douglas Research Laboratories, McDonnell Douglas Corp., St. Louis, MO 63166

Stress is an important parameter in the service environment of loadbearing polymeric materials (1). The accelerating effect of stress on polymer-aging reactions is recognized; however, no experimental methods exist for direct determination of the effect of stress on the rates of real-time aging reactions. Chemiluminescence offers potential for direct determination of the rates of polymer aging reactions.

Exoergic chemical reactions that are accompanied by emission of electromagnetic radiation are called chemiluminescent (2). The chemiluminescence is proportional to the reaction rate, and the spectral distribution provides information on the reaction mechanism (2). The chemiluminescence of polymers observed during thermooxidative degradation is potentially a useful method to monitor polymer aging reactions at temperatures corresponding to the real service environment (3,4,5). However, the studies on chemiluminescence of polymers conducted to date (3,4,5) have been performed in the absence of stress. It was, therefore, necessary to design a special chemiluminescence system capable of studying stressed polymers. This paper describes the design of a stress-chemiluminescence system and discusses exploratory studies on stress-enhanced chemiluminescence of epoxies and nylon 66.

Experimental

A unique chemiluminescence photon-counting system, designed specifically for measurement of stress-enhanced polymer reactions, was used for the studies described here. This system includes a miniature tensile stress device, a controlled environment chamber and a luminescence detection system and associated optics integrated into a single unit.

[1]This research was conducted under the McDonnell Douglas Independent Research and Development Program.

0-8412-0485-3/79/47-095-211$05.00/0

The chemiluminescence instrument, shown schematically in Figure 1, measures the light emitted from polymers during exposure to selected combinations of stress, temperature and atmosphere. The system is designed to measure alternately the light generated by two different samples; therefore, two sample heaters and dual optical systems are required. The sample chamber, in addition to being light-tight, is also vacuum-tight to control the sample atmosphere. Sample temperatures are maintained by heater pads which are spring-loaded to provide uniform contact during tensile stress of the sample. The two heaters are controlled to within ± 1° and are housed in a ceramic block for thermal isolation.

Tensile loads are applied to one polymer sample by a stress apparatus which includes a small, synchronous gearmotor driving a wormgear attached to one of the tensile grips. A force transducer is mounted between a fixed framework and a second tensile grip. The tensile system is capable of exerting forces up to 800 N, sufficient to fracture the samples used in these studies.

The silica optical system conducts collected light through lenses and light pipes to a scanning mirror. The light from one of the optical channels passes through a filter wheel and is projected onto the photocathode of the photomultiplier tube (PMT). The PMT (EMI, 9829QA) was selected to maximize quantum efficiency over a broad spectral range.

The spectral distribution of the chemiluminescence can be measured using a series of wheel-mounted filters inserted in the optical path to determine the intensity of luminescence emitted at wavelengths above the cutoff wavelength of the individual filter. The filters used for this study are colored glass having sharp cut-offs at 300, 400, 500, 600, and 700 nm. The output from the PMT is processed by an amplifier/discriminator and photon counting system (Princeton Applied Research model 1112 and 1121).

Polymer samples were designed specifically for use in the chemiluminescence instrument. The samples are basically a tensile dogbone shape with cylindrical ends for insertion into the grips of the stress apparatus. Epoxy specimens were prepared from tetraglycidyl 4-4'diaminodiphenylmethane (TGDDM) cured at 170°C with 4-4'diaminodiphenylsulfone (DDS). Tensile samples were prepared by a special method based on curing the TGDDM-DDS resin mixture in silicone rubber molds. This method casts reproducible epoxy specimens free of contamination.(6)

Results and Discussion

Experiments on the stress-chemiluminescence (SCL) behavior of TGDDM/DDS epoxy and nylon 66 specimens were performed under various conditions to determine the potential of the technique to measure stress-induced and stress-accelerated aging processes. Representative results of typical SCL experiments with epoxy specimens are shown in Figures 2 and 3 where emitted light (photon counts/s) is plotted as a function of time and stress. In both

In Durability of Macromolecular Materials; Eby, R.;
ACS Symposium Series; American Chemical Society: Washington, DC, 1979.

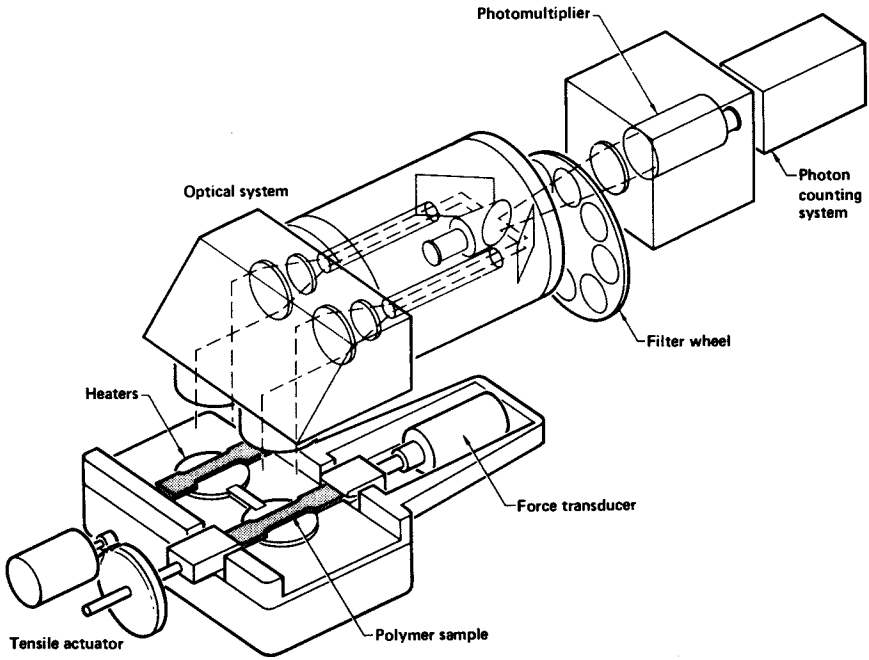

Figure 1. Stress chemiluminescence system

In Durability of Macromolecular Materials; Eby, R.;
ACS Symposium Series; American Chemical Society: Washington, DC, 1979.

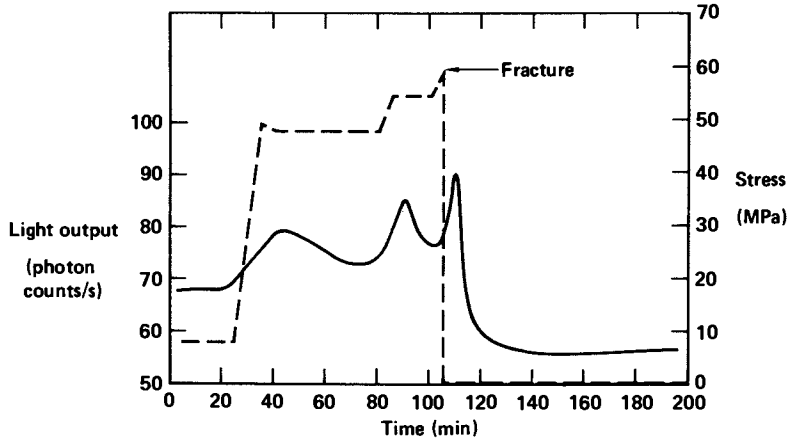

Figure 2. Stress chemiluminescence of epoxy resin (TGDDM/DDS) at 80°C in oxygen atmosphere

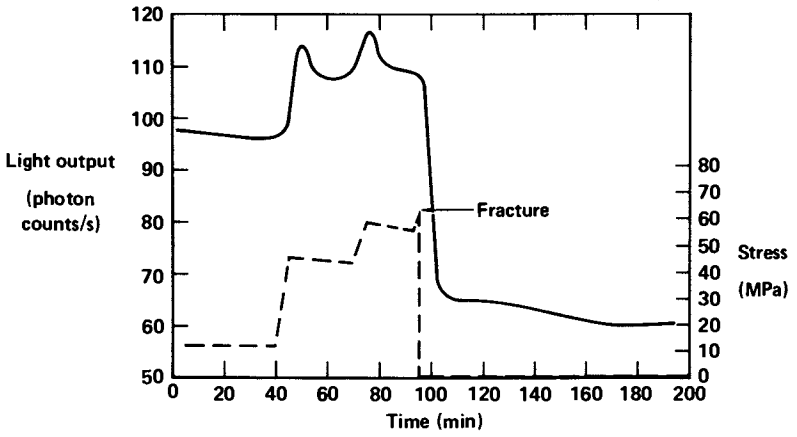

Figure 3. Stress chemiluminescence of epoxy resin (TGDDM/DDS) at 109°C in oxygen atmosphere

In Durability of Macromolecular Materials; Eby, R.;
ACS Symposium Series; American Chemical Society: Washington, DC, 1979.

cases a distinct pattern of stress-chemiluminescence is observed. Each increase in the stress level induces an increase in the light output. The stress-enhanced chemiluminescence then decays to a steady-state level which is 10-20% higher than the chemiluminescence of the unstressed state. A similar effect of tensile stress on the chemiluminescence of nylon 66 was observed and is shown in Figure 4.

The effect of stress at the molecular level must be considered to interpret the observed results. Two different mechanochemical phenomena can occur:

1) stress applied to the polymer chain produces an increase in the intramolecular and the interatomic distance plus a change in the bond angles without causing bond rupture;

2) stress-induced bond cleavage leads to formation of free radicals or other chemical species capable of further reaction.

The effect of both phenomena on potential chemiluminescent reactions must be considered.

An increase in the intramolecular/interatomic distances may be accompanied by redistribution of the potential energy between the polymer chains and the molecules of the reactant surrounding them (e.g., oxygen) leading to the formation of reaction intermediates (activated complexes) which enhance the probability of chemical reaction without free-radical formation. When the localized stress applied to a polymer chain exceeds a critical value, bond scission and free-radical formation occur. Under these conditions a different mechanism is involved; the newly formed macro-radicals undergo reactions which depend on the species present in their immediate environment (1). Based on these and other mechanochemical considerations and on the surrounding oxygen concentration, two different mechanisms responsible for the observed results are possible:

1) The recorded chemiluminescence originated from only a thin surface film. The thickness of this film depends on the extent of self-absorption of the emitted radiation and remains unknown at this time. The pseudo-first-order rate of thermo-oxidative reactions responsible for the chemiluminescence is not limited by oxygen concentration. The applied stress decreases the activation energy for thermooxidative reactions, resulting in the observed chemiluminescence increase. As stress-activated bonds in the surface film react, what can be called surface stress relaxation occurs resulting in the observed SCL decrease.

2) The recorded chemiluminescence originates not only from the surface but contains contributions from significant depths of the bulk material. When the initial stress-activation of bonds occurs, the expected increase in chemiluminescence is observed.

In Durability of Macromolecular Materials; Eby, R.;
ACS Symposium Series; American Chemical Society: Washington, DC, 1979.

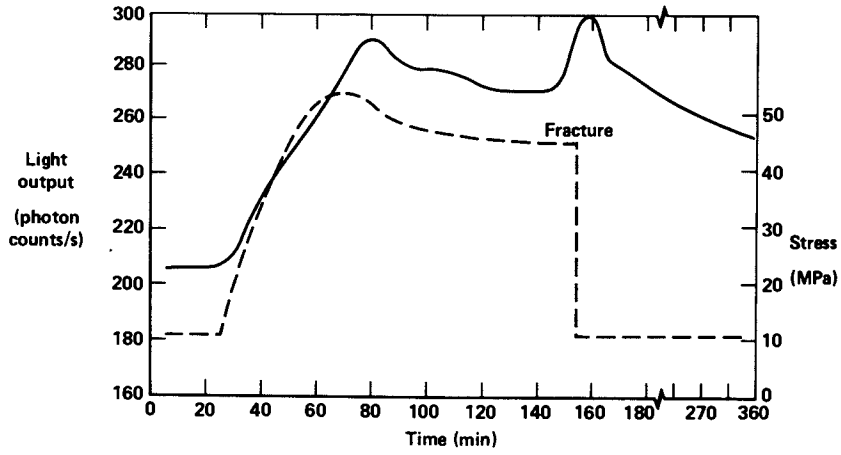

Figure 4. Stress chemiluminescence of Nylon 66 at 105°C in oxygen atmosphere

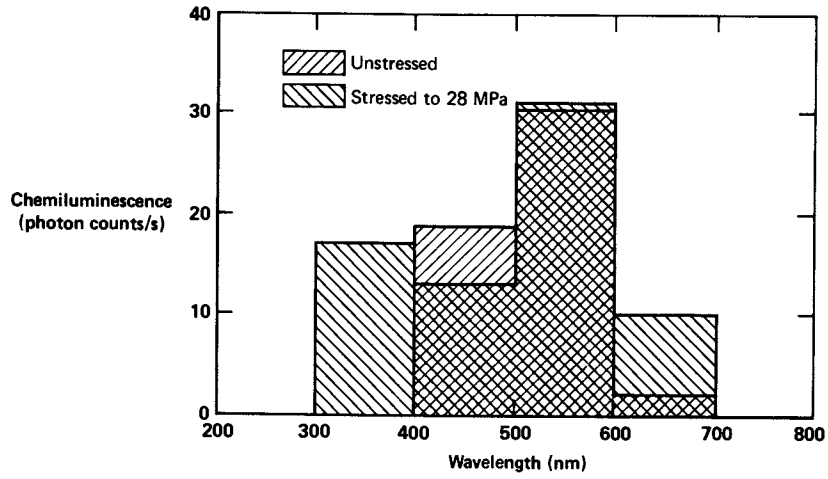

Figure 5. Spectral distribution of stressed and unstressed TGDDM/DDS epoxy at 140°C in oxygen atmosphere

In Durability of Macromolecular Materials; Eby, R.;
ACS Symposium Series; American Chemical Society: Washington, DC, 1979.

However, as the oxygen dissolved in the polymer is depleted and the thermooxidative reaction is limited by oxygen concentration, a SCL decrease is observed. Additional experiments are required to clarify the relative contribution of these and possible other mechanisms to the SCL process.

The spectral distributions of the chemiluminescence of stressed and unstressed TGDDM/DDS epoxy specimens are shown in Figure 5. The distinct difference in the spectral distributions of the chemiluminescence of stressed and unstressed states manifests itself in broadening of the CL spectral region for the stressed specimen. This suggests that thermooxidative reactions of stressed epoxy occur in a wider range of molecular sites than for unstressed specimens, or, alternatively, that the broadening of the spectral distribution represents a contribution from triboluminescence of the specimens.

Butyagin et al. (7) have studied the emission of light that accompanies deformation and rupture of polymers in nitrogen, i.e., triboluminescence. (8)

A fundamental difference between triboluminescence and the stress-enhanced chemiluminescence of polymers, i.e., stress chemiluminescence, should be distinguished. The triboluminescence phenomenon (8) is restricted to radiation emitted during mechanical deformation, independent of the oxygen concentration. Stress chemiluminescence is concerned with measurement of the stress acceleration of on-going chemiluminescent reactions such as thermooxidative aging occurring with or without mechanical deformation.

The preliminary results described here indicate that stress-chemiluminescence of polymers offers potential for direct measurement of mechanochemical contributions to the rates of certain polymer aging reactions.

Literature Cited

1. Barambiom, N. K., Mechanochemistry of Polymers, (MacLaren & Sons, London, 1964), pp. 5, 35.
2. Shlyapintokh, V. Ya., Chemiluminescence Techniques in Chemical Reactions, (Plenum Press, New York, 1968).
3. Schard, M. P. and Russell, C. A., J. Appl. Polymer Sci. 8, 985 (1964).
4. Allen, N. S., McKellar, J. F., and Phillips, G. O., J. Polymer Sci. 12, 2623 (1974).
5. Nathan, R. A., Mendenhall, G. D., Hassell, J. A., and J. D. Wallace, Ind. Res. December 62 (1975).
6. Fanter, D. L., Rev. Sci. Instrum. 49, 1005 (1978).
7. Butyagin, P. Yu., Yerofeyev, V. S., Musayelyan, I. N., Patrikeyev, G. A., Streletskii, A. N., and Shulyak, A. D., J. Polym. Sci. USSR 12 (2) 330 (1970).
8. Grabec, I., J. Polymer Sci. B 12, 573 (1974).

RECEIVED December 8, 1978.

16

Time-Cross-Link Density Reduction for Use in Long Time Behavior Prediction

C. YING-CHEUNG LEE and J. J. AKLONIS

Department of Chemistry, University of Southern California, Los Angeles, CA 90007

The possibility of predicting the long time behavior of polymeric materials based on short time laboratory tests is of great interest and practical importance. At first glance, one might attempt to couch such a prediction in terms of the time-temperature correspondence principle (1) which states that the viscoelastic spectrum shifts homogeneously along the log τ axis with temperature changes. Thus the results of high temperature experiments done at short times might be translated into predictions of lower temperature behavior over extended periods of time.

In actual long term applications of polymers, however, it is well known that chemical reactions occur which actually change the viscoelastic properties of the material while it is in use. In addition, environmental factors such as exposure to solvents or even water, while not always chemically modifying a material, can have a profound influence on its viscoelastic properties in much the same way as a true chemical transformation. If predictions based exclusively on time-temperature correspondence were to be successful, the rates of all of these processes would have to vary with temperature in exactly the same manner as does the viscoelastic spectrum. While this might be approximately true in certain special cases, it is usually not so. Thus, a more general theoretical framework is necessary to predict the properties of simultaneously chemically reacting and physically relaxing networks.

In developing such a scheme, it seems clear that at least three types of information concerning any specific polymer network are necessary: (a) a manifold of viscoelastic response curves of the polymers at well characterized states spanning all states which will be reached via the chemical reaction; (b) knowledge of the exact trajectory the system follows in going from one of these response curves to another as chemical changes proceed; (c) the time dependence of the chemical process involved; i.e. specific kinetic information concerning the interaction between the polymer

0-8412-0485-3/79/47-095-219$05.00/0

In Durability of Macromolecular Materials; Eby, R.;
ACS Symposium Series; American Chemical Society: Washington, DC, 1979.

and its environment. Here, the third type of information will depend strongly on the particular polymer environment combination. Thus we have concentrated our investigations on the first two areas with the hope of finding results of general applicability.

For a crosslinked rubber sample, one simple parameter which can be used to roughly characterize the material is the crosslink density (ν) or the average molecular weight between crosslinks ($M_c \propto 1/\nu$). It should be clear that this single parameter cannot completely represent a network in general. Nevertheless, it is well known that the viscoelastic behavior of a polymer network will vary with crosslink density as schematically depicted in Figure 1 for the creep behavior of a polymer at two crosslink densities $\nu_1 < \nu_0$. Here the kinetic theory of rubber elasticity (2) relates the equilibrium length to the crosslink density but there is, as yet, no completely satisfactory treatment of the time dependence of these length changes. The creep curves depicted are but two of a large number comprising a manifold of such curves, each one corresponding to the behavior of a network with a particular crosslink density reached via the chemical reaction. We will return to consider efficient methods to determine such manifolds below.

Now consider exactly what happens when the chemical reaction causes a crosslink density change during a viscoelastic experiment. Or, referring to Figure 1, suppose that the sample with crosslink density ν_0 is caused to creep through the application of a certain fixed stress so that it exhibits the behavior indicated by the ν_0 curve for $0 \leq t \leq t^*$. Furthermore at $t=t^*$, suppose that the crosslink density instantaneously changes from ν_0 to ν_1. For $t > t^*$, the ν_1 curve should give the sample behavior since this curve represents the total range of response of a sample with crosslink density ν_1 subjected to creep with this particular stress. The question is, from just what point on the ν_1 curve does this behavior commence?

There have been two different answers to this question given in the literature. One answer (3-5) is that point a is the starting point so that the strain is maintained continuous through the introduction of a linear time adjustment factor. The other (6) predicts that the past history under stress should be the controlling factor and that the response should start at point b.

To determine if either of these answers were correct, the properties of a series of polyurethane networks which contained photo labile disulfide bonds were studied (7). The creep curve of the sample in the initial crosslink density state (comparable to ν_0) was determined in the usual way. Then, after complete recovery, another creep experiment was started but, at time t^* during this run, the sample was subjected to ultraviolet irradiation which photochemically broke some of the network chains. After the irradiation was extinguished, the creep experiment was continued for the usual period. Finally, after complete recovery, the creep response of the network at the new crosslink density

In Durability of Macromolecular Materials; Eby, R.;
ACS Symposium Series; American Chemical Society: Washington, DC, 1979.

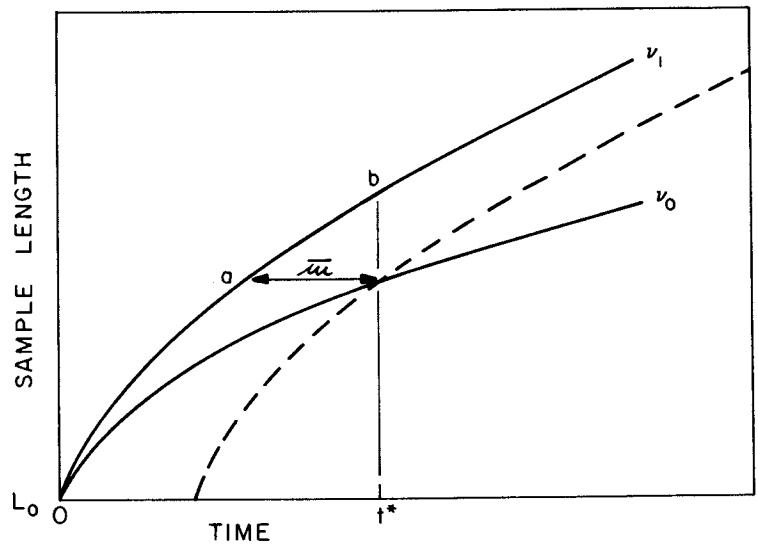

Figure 1. Schematic of the creep behavior of a polymer network at two cross-link densities $\nu_1 < \nu_0$. Points a and b denote two possible initial states immediately after a scission process which changes cross-link density ν_0 to ν_1 at time t: (– – –), ν_1 behavior shifted linearly by the time adjustment factor ω.*

In Durability of Macromolecular Materials; Eby, R.;
ACS Symposium Series; American Chemical Society: Washington, DC, 1979.

(corresponding to ν_1) was measured directly on the irradiated sample which was still held in the jaws of the extensometer. The results of such experiments showed that the strain was continuous during instantaneous chain scission and that the ν_1 response actually starts at point a appropriately time shifted in Figure 1.

So far then, if one knew the rates of the important chemical reactions involved and if one had the manifold of response curves, one could predict the behavior of simultaneously relaxing and reacting networks, presumably on any time scale. However, the direct measurement of the manifold of response curves is at best time consuming and almost always impractical. This is still true even though it has been shown that, in the case of a continuous chemical reaction, only the response at discrete crosslink densities must actually be known (7). Thus we are presently investigating indirect methods by which this information can be obtained.

The most attractive procedure for generating these curves involves use of a time crosslink density correspondence principle first suggested by Plazek (8). He observed that creep data for a series of networks at different crosslink densities could be shifted along the log time scale (after vertical adjustment to account for equilibrium compliance changes arising from the variation in crosslink density) to obtain a single creep master curve. Moreover, Plazek also observed that the horizontal shift factor (a_x) was related to the crosslink density ratio by the equation

$$a_x = \left(\frac{\nu_o}{\nu}\right)^b \qquad (1)$$

ν_o is the crosslink density of the reference network for which $a_x = 1$ and ν is the crosslink density of the network whose response curve is being shifted. He found that b was about 15 for natural rubber and SBR. To generate the manifold of response curves, then, one might merely measure the viscoelastic behavior of the material of interest at one crosslink density under nonreacting conditions and then shift this observed behavior vertically according to rubber elasticity theory (2) and horizontally according to eq. (1) to generate the individual curves of the manifold.

This situation becomes simplified even further if the creep behavior of the nonreacting network obeys the well known phenomenological equation (9-12) suggested by Thirion

$$D(t) = \frac{D_e(\nu)}{1 + ct^{-m}} \qquad (2)$$

where $D(t)$ and $D_e(\nu)$ are the compliance values at time t and at equilibrium respectively and a and m are adjustable parameters. In this case, if one knows $D_e(\nu)$, c and m values at any particular crosslink density along with the value of b, the complete manifold

In Durability of Macromolecular Materials; Eby, R.;
ACS Symposium Series; American Chemical Society: Washington, DC, 1979.

of response curves at all crosslink densities of interest can be easily generated.

Creep data gathered on the disulfide containing polyurethane samples discussed above were analyzed in terms of time crosslink density correspondence (13). The creep response followed Thirion's equation (eq. 2) and, furthermore, the data could be used to prepare a very acceptable master curve indicating that time crosslink density reduction is valid for this system. The values of b measured here, however, were between 3 and 4, much smaller than the values of 7.7 to 15.4 given in the literature (6, 8, 14). The probable cause of this discrepancy in b values is associated with the topological variations which accompany the crosslink density changes in each case. Usually crosslink density changes are brought about by varying cure conditions; in this situation decreasing crosslink density results in fewer network chains and an increasing average chain length. When the crosslink density is decreased photochemically through chain scission, however, the number of chains supporting stress decreases while the length of these chains remains roughly constant. Large variations in b would be expected under such conditions. Thus for reasonably short chain polyurethanes which undergo scission, experiment shows that both time crosslink density reduction and the Thirion equation are applicable.

The specific aim of the present work is to extend this investigation to a system where photochemical crosslinking is involved and the polymer chosen for this investigation was a MAPO crosslinked dicarboxylic acid terminated polybutadiene network.

Experimental

Crosslinked polymer networks were synthesized by mixing vacuum distilled tris (2-methyl-1-aziridinal) phosphine oxide (MAPO) (K&K Laboratories, Irvine, California) and carboxylic acid terminated polybutadiene with an M_n = 5500 from end group assay, (Butarez CTL II, Phillips Petroleum, Co., Phillips, Texas) in a one to one equivalent ratio of functional groups. The mixture was degassed overnight in a mold and then cured at 100°C for 24 hours. The resulting film was post cured at about 60°C for several days in vacuum. It is to be expected that these networks are far from ideal. In fact, Morton et al. (15) have carried out experiments with the same Butarez compound which indicate that a substantial fraction of the polybutadiene chains are not doubly carboxylic acid terminated, a feature which would insure many dangling chain ends in our preparation.

The extensometer used to measure creep compliance has been described previously (13). Some of the experiments were carried out on a newer piece of apparatus designed so that the center of gravity of the balance beam could be made coincident with the fulcrum point. The temperature of all experiments was controlled to ±0.1 C for the duration of the experiment. The

In Durability of Macromolecular Materials; Eby, R.;
ACS Symposium Series; American Chemical Society: Washington, DC, 1979.

sample extension was calculated from the change of the LVDT output voltage before and during the experiment. This voltage difference was converted to an extension via a predetermined calibration. The LVDT reading before extension was measured with a digital voltmeter to within $\pm$ .5 mV and the voltage during the experiment was recorded on a strip chart recorder with a precision of $\pm$0.2 mV. Since the voltage differences observed were in the range of 10^2 mV, these uncertainties cause the absolute values of D(t) to be accurate to .5% while the relative D(t) values as represented by the shape of any single curve are accurate to .2%.

Crosslink density changes were induced via ultraviolet irradiation as before (7, 13) with exposure times of 30 minutes. Relaxation periods of twenty-four hours between subsequent creep experiments were employed; in addition similar or longer periods separated irradiation and creep and vice versa.

Results and Discussion

Equation (2) can be rewritten in the form

$$\log \left(\frac{D_e(\nu)}{D(t)} - 1\right) = \log c - m \log t. \qquad (3)$$

In previous work on many materials, it has been shown that with a proper choice of a D_e value, a plot of the left hand side of equation (3) versus log t yields a very good straight line. Furthermore, from the slope and intercept of this plot, the parameters c and m can be evaluated. Thus with D_e as the variable and a straight line plot as the criteria for convergence of an iteration, the values of all three parameters can be determined. Several procedures to accomplish this are described in the literature (10, 16, 17). In Figure 2, the straight line is a computer fit of equation (3) to a set of experimental creep points for a polybutadiene sample. Although the agreement between the line and the data may seen acceptable, the plot of the residuals (Figure 3) clearly shows that the experimental scatter from the straight line is systematic rather than random. Such behavior was routinely found for our MAPO crosslinked polybutadiene networks and led us to conclude that equation 2 is not suitable for describing the creep of such materials.

This unusual feature of the behavior of our networks makes further investigations even more interesting and we continued by testing the applicability of time-crosslink density reduction to this system.

Creep behavior of a single sample at three different crosslink densities is depicted in Figure 4, ν_0 being the virgin network sample which was crosslinked by irradiating for 30 minutes to yield ν_1 which was further irradiated 30 minutes to yield ν_2. In the previous work on polyurethane samples, D_e values obtained from equation 3 were used to determine the rubber elasticity vertical

In Durability of Macromolecular Materials; Eby, R.;
ACS Symposium Series; American Chemical Society: Washington, DC, 1979.

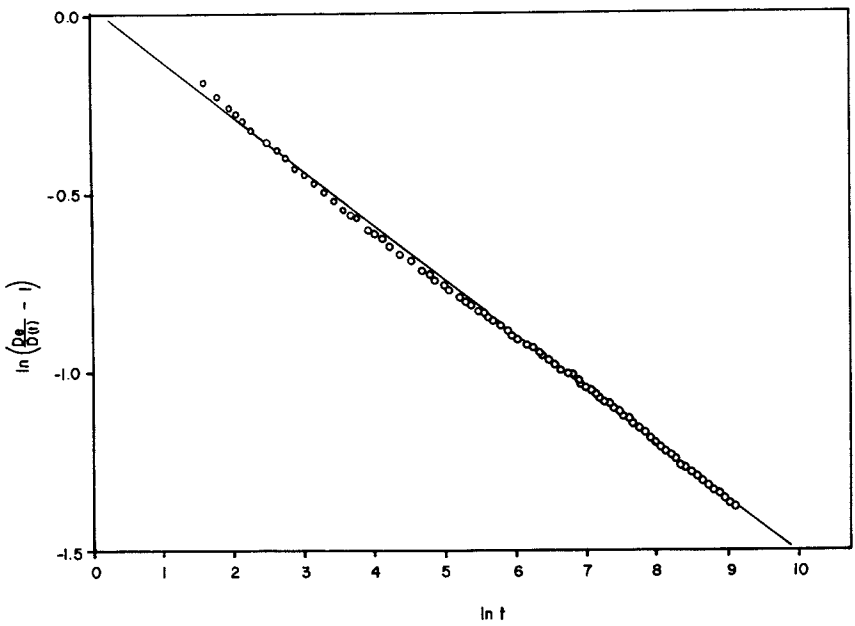

Figure 2. Plot of creep data according to Equation 3: (——), computer fitted equation.

In Durability of Macromolecular Materials; Eby, R.;
ACS Symposium Series; American Chemical Society: Washington, DC, 1979.

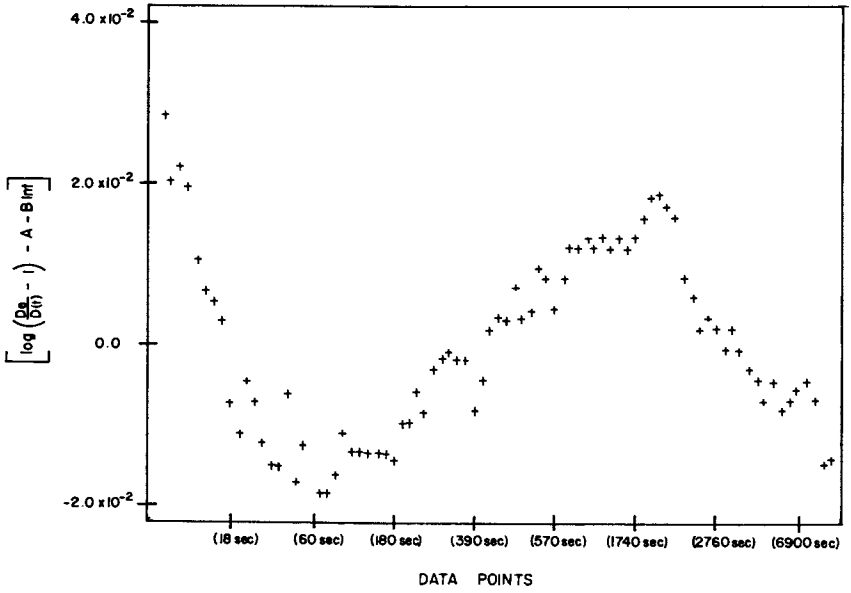

Figure 3. Plot of residues of Figure 1. The abscissa is nonlinear in time and the ordinate is the deviation from the best equation of the form log [($D_e(\nu)/D(t)$)] − 1 = A + B ln t.

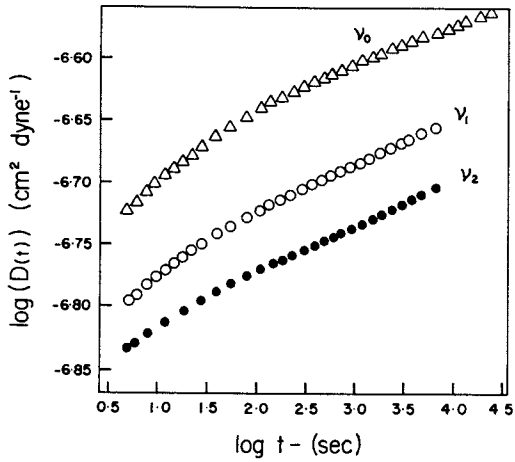

Figure 4. Plot of representative compliance curves for the sample at different cross-link densities

In Durability of Macromolecular Materials; Eby, R.;
ACS Symposium Series; American Chemical Society: Washington, DC, 1979.

shift (2) which was to be applied to the raw creep data before horizontal shifting resulted in a single master curve. Since equation 3 is inconsistent with the behavior of these polybutadiene networks, an alternate method must be used to access the applicability of time crosslink density reduction.

Differentiation of equation 2 yields

$$\ln\left(\frac{d(-1/D(t))}{d \ln t}\right) \equiv \ln\left(-\dot{E}(t)\right) = \ln \frac{mc}{D_e} - m \ln t \qquad (4)$$

which can be satisfactorily applied to short sections of creep curves. In Figure 5, we have plotted ln $(-\dot{E}(t))$ versus ln t for the single sample at the three different crosslink densities. According to equation 4, the effective value of m, the exponent in equation 2 at any time, t, is merely the slope of this plot at that particular time. In such a representation, a material which satisfies equation 2 with constant m would exhibit a straight line behavior. The fact that the behavior of our network viewed in this way is not linear, is further evidence that equation 2 is not applicable.

It is interesting to note that, at short times, the ln $(-\dot{E}(t))$ plot resembles a straight line with a slope of about -0.3. This value is close to the m value obtained previously on the polyurethane samples. It suggests that the system can be described by the Thirion equation at short times but deviates from it at larger times. From Figure 5, it can be seen that the onset of the deviation shifts to shorter times with increasing crosslink density.

For time-crosslink density reduction to be appropriate (even with variable m), a necessary but not sufficient condition is that the ln $(-\dot{E}(t))$ versus ln t curves for various crosslink densities be superposable. In Figure 5, it is clear that such is not the case, therefore, time crosslink density reduction is not possible with these particular samples.

This point is further demonstrated in Figure 6 where we have applied arbitrary vertical and horizontal shifts to the log D(t) curves for the MAPO crosslinked polybutadiene networks at the various crosslink densities. Superposition of all three curves along the entire time domain is clearly impossible. The short time parts, however, superposed very well.

In his work, Plazek (8) also observed behavior similar to this and found that the lack of superimposibility at long times could be ascribed to the onset of stress induced crystallization. This is probably not the reason for the deviation observed here since crystallization is expected to occur at lower crosslink densities. Nevertheless we have carried at several experiments to test this possibility.

A comparison of x-ray photographs of relaxed samples with highly strained samples (compared to the strain used in our experiments) gave no sign of crystallization. This evidence is not

In Durability of Macromolecular Materials; Eby, R.;
ACS Symposium Series; American Chemical Society: Washington, DC, 1979.

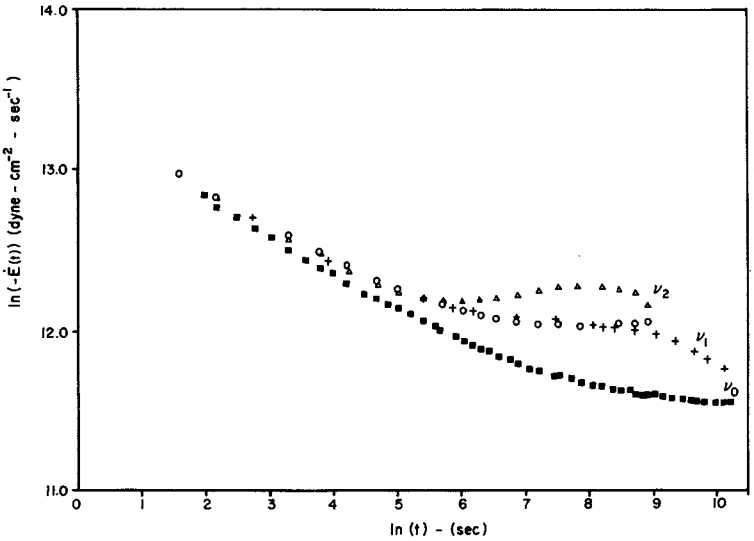

Figure 5. Computer calculated ln $(-\dot{E}(t))$ (Equation 4) vs. ln t. For cross-link density ν_1: (+) data at 42°C where the time scale is shifted by the factor log a_T = 0.565. All other data is at 28°C.

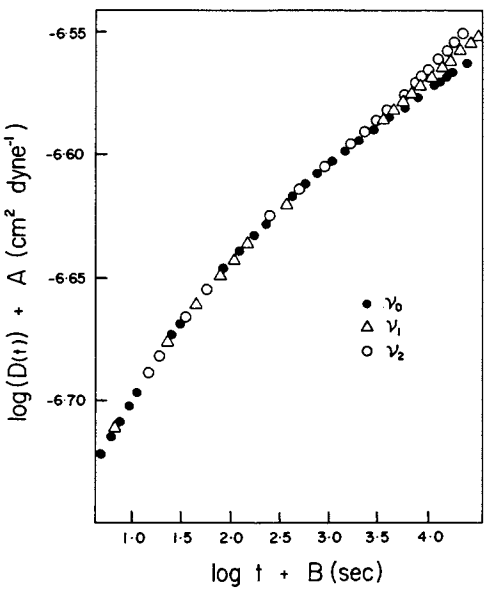

Figure 6. Shifted compliance curves at different cross-link densities. The shift factors are: log $a_x(\nu_0)$ = 0.0; log $a_x(\nu_1)$ = 0.304; log $a_x(\nu_2)$ = 0.630; $A(\nu_0)$ = 0.0; $A(\nu_1)$ = 0.0878; and $A(\nu_2)$ = 0.150.

In Durability of Macromolecular Materials; Eby, R.;
ACS Symposium Series; American Chemical Society: Washington, DC, 1979.

very conclusive, however, since slight, but viscoelastically significant, degrees of crystallization might not be observable in x-ray experiments. Additional measurements which we believe to be much more sensitive were also carried out. The sample, at experimental stage ν_1, was tested for linear viscoelastic behavior by carrying out creep experiments to long times under substantially different stresses. Figure 7 shows the result of such an experiment. The agreement of the D(t) data calculated from the two stress levels over the entire time range indicates that the response is linear and that the deviation from equation 2 is independent of stress. Furthermore, time-temperature correspondence was also used as a tool to investigate the possibility of stress induced crystallization by comparing the creep of this sample at 28°C and at 42°C (Figure 8). With an appropriate rubber elasticity vertical correction, the two creep curves superimposed well when shifted horizontally. The results of these experiments constitute strong evidence that the unexpected long time behavior observed here is due to viscoelastic effects and not to complications associated with crystallization or other sources.

Conclusions

Creep of MAPO crosslinked polybutadiene networks at various crosslink densities has been measured and we have shown that this behavior is inconsistent with the phenomenological equation (equation 2) which is usually used to analyze such data. The exact reason for this inconsistency is not clear at the moment but several factors which might contribute are: the particular chemical nature of this system is such as to give a distribution of retardation times which is qualitatively different from the distribution exhibited by most other polymer networks; the average chain length between corsslinks of samples used in this study is short compared with that of systems normally used in such investigations; the precision with which these experiments were carried out is particularly high and small discrepancies observed here might not have been discernable in some of the previous studies. We are continuing investigation on the last two possibilities.

In addition, we have found that time-crosslink density reduction is clearly not appropriate for this system. Here too there are several possible causes of this behavior. We suspect that the particular changes induced in network topology upon crosslinking are responsible for the lack of coincidence of the curves of various crosslink densities. Upon photochemical crosslinking, some of the chains of the previously existent network are replaced by shorter chains and this might even result in a bimodal distribution of chain lengths between crosslinks. It appears doubtful to us that the creep behavior of a sample with such a bimodal chain length distribution could be simply comparable to the behavior of a sample with an ordinary chain length distribution and this, we suspect, is the reason for the inapplicability of

In Durability of Macromolecular Materials; Eby, R.;
ACS Symposium Series; American Chemical Society: Washington, DC, 1979.

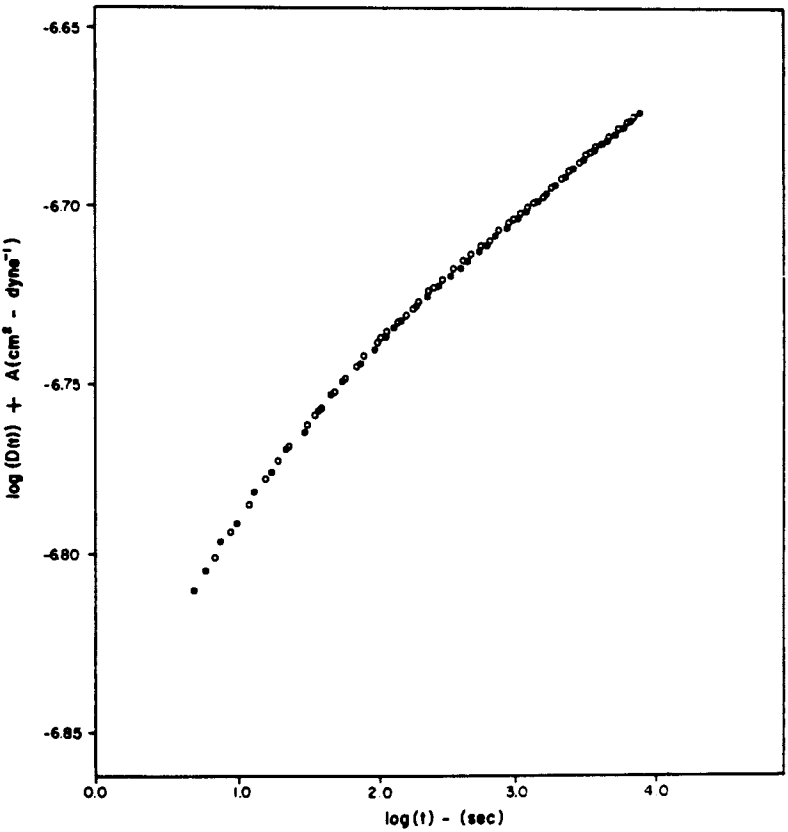

Figure 7. Verification of the linear stress–strain behavior of sample ν_1 at two different stress levels: (○), an experiment carried out at 60% of the stress used in the experiment shown as (■). A small vertical correction (within experiment error) was applied.

In Durability of Macromolecular Materials; Eby, R.;
ACS Symposium Series; American Chemical Society: Washington, DC, 1979.

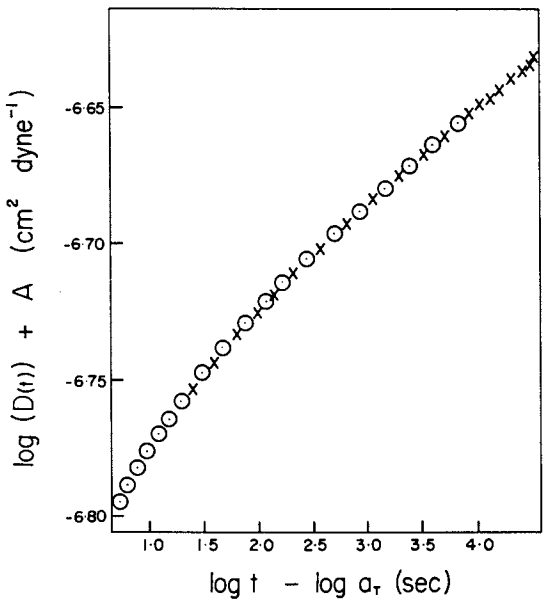

Figure 8. Verification of time–temperature correspondence for sample ν_1: (○), data at 28°C; (×), data at 42°C where the time scale has been shifted by log a_T = 0.565.

In Durability of Macromolecular Materials; Eby, R.;
ACS Symposium Series; American Chemical Society: Washington, DC, 1979.

time crosslink density reduction in this case.

Even though time crosslink density correspondence can be used very efficiently to generate viscoelastic response curves of some non-reacting polymer networks, our findings make it clear that this technique is not generally applicable to all systems even in the case of limited extents of chemical reaction.

In spite of the fact that the effects measured and discussed here are small and only discernable via very precise measurements, it must be remembered that we are interested in using this information as a base to support extensive extrapolation by which small effects can be considerably amplified.

Acknowledgements

This work was supported by the Army Research Office under grant number DAAG 29-76-C-0194 and by the California Institute of Technology President's Fund grant number PF-104.

Literature Cited

1. Tobolsky, A.V., "Properties and Structure of Polymers", 144-159, John Wiley and Sons, New York, 1960.
2. Ferry, J. D., "Viscoelastic Properties of Polymers", 2nd Edition, 296, John Wiley & Sons, New York, 1970.
3. J. Moacanin, J.J. Aklonis, and R.F. Landel, J. Macromol. Sci.-Phys., 1, 41 (1975).
4. J. Moacanin, J.J. Aklonis, and R.F. Landel, J. Chem. Phys., 64, 430 (1976).
5. J. Moacanin and J.J. Aklonis, J. Polym. Sci. C, 35, 71 (1971).
6. J.G. Curro and E.A. Salazar, J. Appl. Polym. Sci., 19, 2571 (1975).
7. Wu-Nan Huang and J.J. Aklonis, J. Macromol. Sci.-Phys., 15, 45 (1978).
8. D. Plazek, J. Polym. Sci. A-2, 4, 745 (1966).
9. P. Thirion and R. Chasset, Rubber Chem. Tech., 37, 617 (1964).
10. R.A. Dickie and J.D. Ferry, J. Phys. Chem., 70, 2594 (1966).
11. N.R. Langley and J.D. Ferry, Macromolecules, 1, 353 (1968).
12. R. Chasset and P. Thirion, Proceedings of Conference on Physics of Non-Crystalline Solids, J.A. Prins, Ed., North-Holland, Amsterdam, 1965, p. 345.
13. Wu-Nan Huang and J.J. Aklonis, J. Macrom. Sci.-Phys. B-13, 291 (1977).
14. R.F. Fedors, J. Polym. Sci. Polym. Phys. Ed., 12, 289 (1974).
15. M. Morton, L.J. Fetters, J. Inomata, D.C. Rubio, and R.N. Young, Rubber Chem. & Tech., 49, 303 (1976).
16. R.G. Mancke and J.D. Ferry, Trans. Soc. of Rheology, 12, 335 (1968).
17. Wu-Nan Huang, C. Ying-Cheung Lee, and J.J. Aklonis, Polym. Preprints, 19, 606 (1976).

RECEIVED December 8, 1978.

17

The Influence of Vacuole Formation and Growth on the Mechanical Behavior of Polymers

R. J. FARRIS, R. FALABELLA, and Y. D. TSAI

Polymer Science and Engineering Department, University of Massachusetts, Amherst, MA 01003

The mechanical behavior of phase separated polymer blends and composites is complicated by many factors of which the formation of crazes and vacuoles appears to be the dominant factor governing the stress-strain response (1-10). Crazes and vacuoles are the result of strong local variations in stress and strain at the microstructural level. When the material is subjected to high loads, vacuoles or crazes form in the high stress regions of the microstructure and upon doing so greatly relieve the local multiaxial state of stress. In systems where these crazes cannot readily propagate, crazing will occur throughout the microstructure. Generally speaking the onset of microstructural crazing causes a volume dilatation, a loss in modulus reinforcement, and an irreversible degradation of the microstructure due to mechanical loads (1,2,6,7).

It has been generally concluded that the mechanisms of craze formation and growth are the mechanisms which distinguish the energy absorption capabilities of phase separated polymeric systems. Since most very high impact polymers are of the crazing variety, there must be some truth to these arguments. It is important to note however that over a decade ago the same reasoning was being put forth with regard to the mechanical behavior of very highly filled elastomers. It was erroneously concluded that because of the large amounts of near rigid particulate filler that these systems contained, vacuole formation and growth was to be expected and was in fact the mechanism that permitted these systems to exhibit high elongations. Years later, when experiments were conducted under high superimposed pressure (1,2), it was found that pressure greatly suppressed vacuole formation and growth and generally resulted in a marked improvement in all mechanical properties, especially the stress and energy absorption characteristics. Interestingly, in the range of strain before vacuole formation, pressure had no influence on the mechanical properties.

The main purpose of this paper is to demonstrate the striking similarity between the behavior of particulate filled polymers and phase separated polymers. The changes in mechanical proper-

0-8412-0485-3/79/47-095-233$05.00/0

In Durability of Macromolecular Materials; Eby, R.;
ACS Symposium Series; American Chemical Society: Washington, DC, 1979.

ties of these materials with deformation is almost totally dependent upon the vacuole formation process and the factors controlling this process are not that well understood. The interesting conclusion one can draw from the experiences of researchers who work with highly filled polymers is that if craze formation could be suppressed, then the mechanical properties of high impact polymers could be improved. This observation is contrary to the thoughts of many in the polymer community who believe that craze formation and growth is one of the main mechanisms leading to very high impact characteristics.

Another interesting observation is that many thermal plastics that have been tested in a uniaxial tension mode in our laboratories exhibit negative volume changes in the strain region before yield. Others before have observed the same or equally confusing results and many researchers dismiss such observations as experimental errors. It is demonstrated that such observations can be real and are possible within the framework of linear elastic theory.

Experimental

All of the data discussed in this paper was obtained using a gas dilatometer (9) in conjunction with a standard tensile tester. These dilatometers yield simultaneous and continuous measurements of stress, strain and volume dilatation over a wide range of test conditions including strain rate, temperature and superimposed hydrostatic pressure. Stress and strain are measured in the usual manner within the dilatometer which is equipped with internal force transducers. Volume dilatation is assessed by measuring the change in pressure of the gas surrounding the uniaxial test specimen as it is deformed in a constant volume chamber. The instrument is quite accurate and only responds to changes in sample volume. Under normal operating conditions the instrument can detect changes in volume of ±.02 percent and greater accuracy can be achieved if measures are taken to control temperature and minimize the free air volume within the test cavity.

Filled Elastomers

The stress-strain dilatational response of filled polymers is very sensitive to material factors such as particle size, filler concentration, coupling agents to enhance adhesion and matrix modulus and strength (6). It is also sensitive to test conditions such as strain rate, temperature, and stress field. Generally speaking any modifications to the material that will reduce vacuole dilatation such as reducing the particle size, greatly improves the properties of these materials (6). Figure 1 illustrates the behavior of three highly filled elastomers. From this data it is clear that yielding or stress softening is a direct result of volume dilatation caused by the formation and growth of vacuoles. The effect of superimposed pressure on the stress-strain volume dilatation properties are shown in figure 2 and 3 for

In Durability of Macromolecular Materials; Eby, R.;
ACS Symposium Series; American Chemical Society: Washington, DC, 1979.

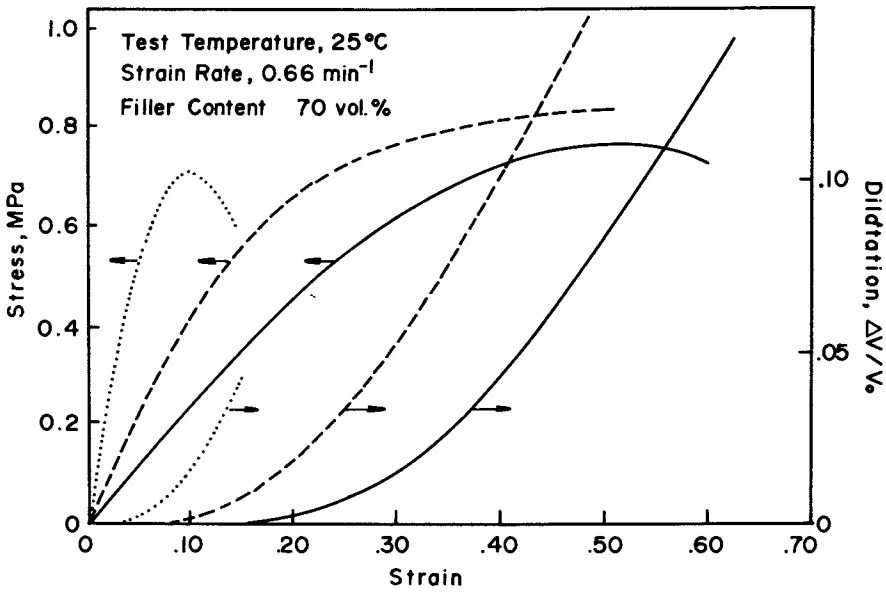

Figure 1. The stress–strain dilatational behavior of three highly filled elastomers

In Durability of Macromolecular Materials; Eby, R.;
ACS Symposium Series; American Chemical Society: Washington, DC, 1979.

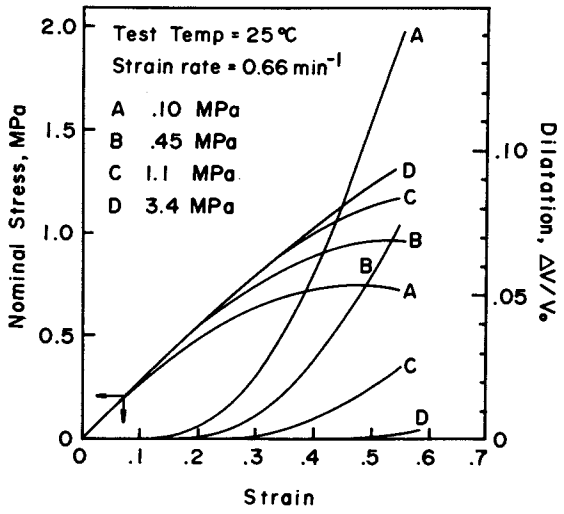

Figure 2. The stress–strain dilatational behavior of a 63.5 vol % filled elastomer at a series of hydrostatic pressures

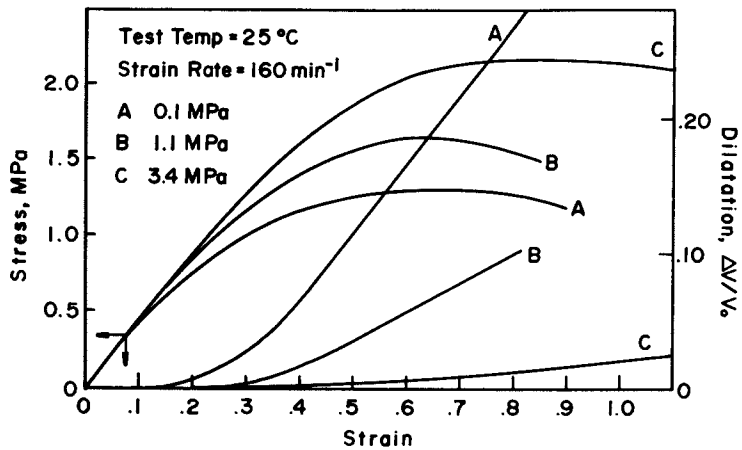

Figure 3. The stress–strain dilatational behavior of a 63.5 vol % filled elastomer at a series of hydrostatic pressures at a high strain rate

In Durability of Macromolecular Materials; Eby, R.;
ACS Symposium Series; American Chemical Society: Washington, DC, 1979.

another highly filled rubber based solid propellant for two different strain rates. These data clearly demonstrate that reduction in vacuole formation and growth via high pressure greatly improves their mechanical properties, especially strength and strain energy to rupture. With these low modulus composites high pressure acts like a super bonding agent and does not allow for much vacuole formation.

Vacuole dilatation information itself is not simply interpreted. The data instead are best understood through models of microstructural failure (1). Assuming a single size of spherical filler particles encompassed by elliptically shaped voids that form arbitrarily in strain, and once formed grow at a constant rate with further deformation, then one can readily separate vacuole growth from vacuole formation. Models such as the one described above have been substantiated by microscopic studies. The solution of such models (1) indicates that the first derivative of vacuole dilatation with respect to strain ε, is directly proportional to the cumulative number of vacuoles per unit volume,n, that exist at any strain. The second derivative is then directly proportional to the instantaneous frequency distribution of vacuole formation. These two results can be expressed mathematically as

$$n = c \frac{d(\Delta V/Vo)}{d\varepsilon} \quad (1)$$

$$\frac{dn}{d\varepsilon} = c \frac{d^2(\Delta V/Vo)}{d\varepsilon^2} \quad (2)$$

Figure 4 illustrates the typical volume dilatation-strain behavior along with its' first and second derivatives. Clearly these measures are realistic in that the derivatives do take on the character of cumulative and instantaneous frequency distributions. Similar models can be constructed to relate the loss in stiffness to the number of vacuoles that have formed resulting in very simple but accurate stress-strain relations (1).

Phase Separated and Filled Thermal Plastics

Data similar to that obtained on highly filled elastomers was recently taken on a variety of thermal plastics. These data are illustrated in figure 5 for a particulate filled polyethylene with and without a bonding agent. Figure 6 and 7 illustrate similar data for an ABS polymer with and without chopped glass fiber reinforcement. Additional data on nylon and polypropylene, figures 8 and 9, has been obtained and several other polymeric systems also show similar results in that yielding is caused by cavitation of the microstructure. These data were all obtained using injection molded samples provided by the polymer manufacturer. In every situation using these samples negative volume changes have been observed prior to yielding followed by a sudden increase in volume rate at yield. The instrument was checked several times and it demonstrated no sensitivity to load or stroke. After deter-

In Durability of Macromolecular Materials; Eby, R.;
ACS Symposium Series; American Chemical Society: Washington, DC, 1979.

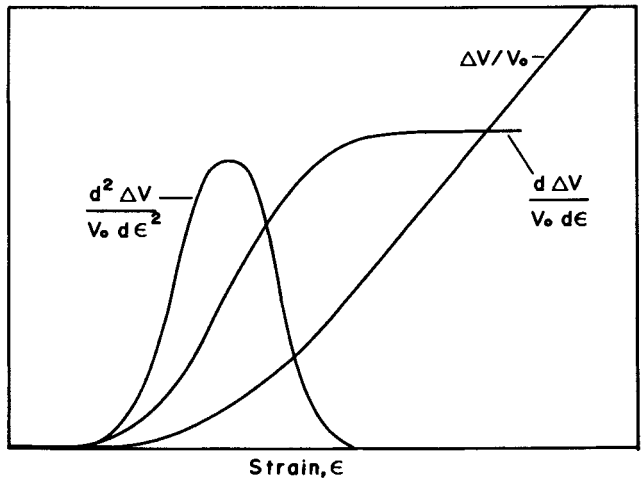

Figure 4. Schematic of the dilatation–strain relationship and its first and second derivatives

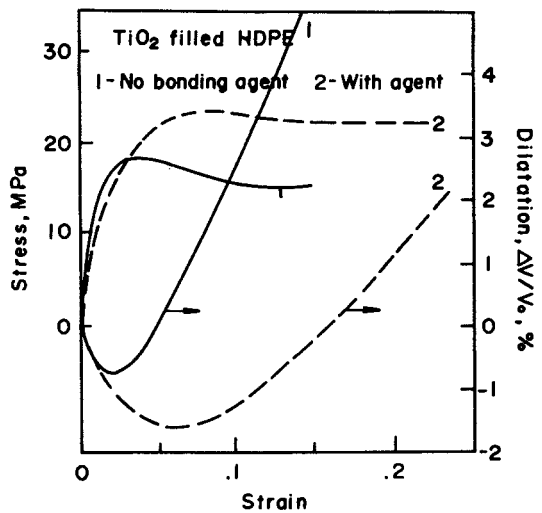

Figure 5. The stress–strain dilatational behavior of a filled high-density polyethylene with and without a coupling agent

In Durability of Macromolecular Materials; Eby, R.;
ACS Symposium Series; American Chemical Society: Washington, DC, 1979.

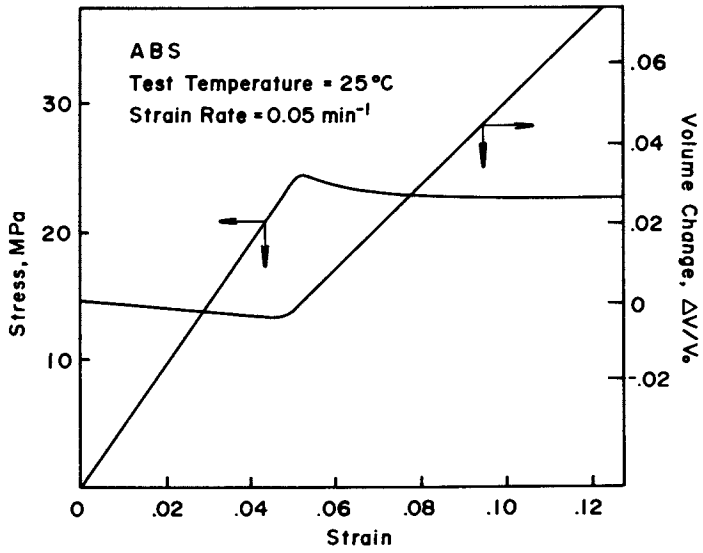

Figure 6. The stress–strain dilatational behavior of ABS

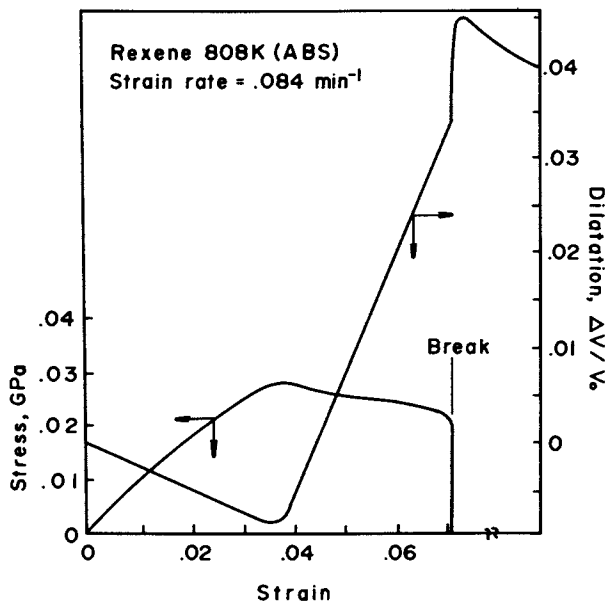

Figure 7. The stress–strain dilatational behavior of filled ABS

In Durability of Macromolecular Materials; Eby, R.;
ACS Symposium Series; American Chemical Society: Washington, DC, 1979.

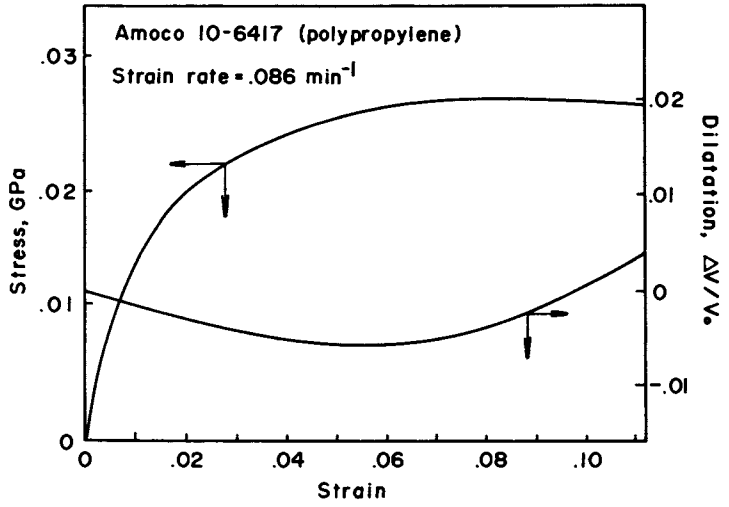

Figure 8. The stress–strain dilatational behavior of nylon

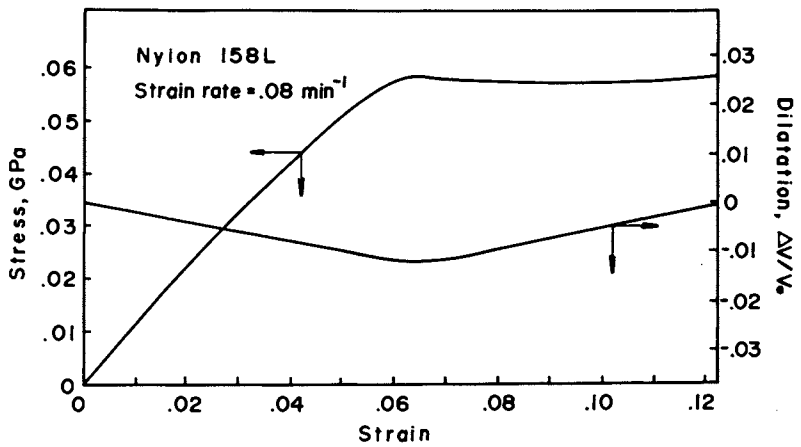

Figure 9. The stress–strain dilatational behavior of polypropylene

In Durability of Macromolecular Materials; Eby, R.;
ACS Symposium Series; American Chemical Society: Washington, DC, 1979.

mining that these negative volume changes were real it was thought that the effect could be induced by the method of gripping the samples. However, considerable variations in gripping methods showed no significant change in the observations. Consequently, the effect is considered real and a logical explanation must exist. The only possible explanation considered that is consistent with all of our observations is that of anisotropic behavior. The reason most people dismiss such observations to "poor experimental technique" is that they restrict their thinking to isotropic linear elasticity wherein such observations are impossible and a contradiction to theory. With that interpretation these data would yield a value for Poisson's ratio greater than 0.5 which is of course impossible for an isotropic linear solid. The restrictions on Poisson's ratio in elasticity theory come about by imposing a positive definite strain energy requirement, that is if the body is in a deformed state it must possess a finite positive strain energy density. For a linear elastic isotropic solid the constitutive equation can always be expressed as

$$\begin{bmatrix}\varepsilon_1\\ \varepsilon_2\\ \varepsilon_3\end{bmatrix} = \frac{1}{E}\begin{bmatrix}1 & -\nu & -\nu\\ -\nu & 1 & -\nu\\ -\nu & -\nu & 1\end{bmatrix}\begin{bmatrix}\sigma_1\\ \sigma_2\\ \sigma_3\end{bmatrix} \qquad (3)$$

where ε_i = principal strains
σ_i = principal stresses
E = Young's modulus
ν = Poisson's ratio

For the energy to be positive definite the compliance matrix must satisfy certain conditions which can be summarized as follows

(a) every diagonal element must be greater than zero
(b) the determinant of each submatrix remaining when the row and columns containing a diagonal element are deleted must be positive
(c) the determinant of the compliance matrix must be positive.

For an isotropic linear elastic solid the first condition is automatically satisfied since each diagonal element is unity. The second condition results in three identical equations

$$1 - \nu^2 > 0 \quad \text{or} \quad -1 < \nu < 1 \qquad (4)$$

The final condition yields a stronger constraint

$$1 - 3\nu^2 - 2\nu^3 > 0 \quad \text{or} \quad -1 < \nu < 1/2 \qquad (5)$$

In a uniaxial tensile test the volume dilatation simply becomes

$$\Delta V/Vo = \frac{\sigma}{E}(1 - 2\nu), \qquad (6)$$

which demands that the stress and dilatation have the same sign if ν is to be no larger than 0.5.

In Durability of Macromolecular Materials; Eby, R.;
ACS Symposium Series; American Chemical Society: Washington, DC, 1979.

Using identical methods one can write the stress-strain equation for an orthotropic linear elastic solid in terms of the principal values of stress and strain as

$$\begin{bmatrix}\varepsilon_1\\ \varepsilon_2\\ \varepsilon_3\end{bmatrix} = \begin{bmatrix}C_{11} & C_{12} & C_{13}\\ C_{12} & C_{22} & C_{23}\\ C_{13} & C_{23} & C_{33}\end{bmatrix}\begin{bmatrix}\sigma_1\\ \sigma_2\\ \sigma_3\end{bmatrix}, \qquad (7)$$

where the compliance matrix must be symmetric if the state of strain energy is to be unique and only a function of the final state of stress and strain.

In order to have a positive definite strain energy density the conditions cited above demand that

$$\begin{aligned}&(a)\ C_{11},\ C_{22},\ C_{33} > 0\\ &(b)\ C_{11}C_{22} - C_{12}^2 > 0\\ &(c)\ C_{11}C_{33} - C_{13}^2 > 0\\ &(d)\ C_{22}C_{33} - C_{23}^2 > 0\\ &(e)\ C_{11}C_{22}C_{33} + 2C_{12}C_{23}C_{13} - C_{22}C_{13}^2 - C_{33}C_{12}^2 - C_{11}C_{23}^2 > 0\end{aligned} \qquad (8)$$

The volume change in a uniaxial tensile test for the orthotropic case simply becomes

$$\frac{\Delta V}{Vo} = (C_{11} + C_{12} + C_{13})\,\sigma \qquad (9)$$

In order to have negative volume changes in a tensile test one must require that

$$C_{11} + C_{12} + C_{13} < 0 \text{ if } \frac{\Delta V}{Vo} < 0 \text{ when } \sigma > 0 \qquad (10)$$

Therefore equation 8 must be satisfied to yield a valid constitutive equation from an energy perspective and equation 10 must be satisfied to yield the experimental observations. It can be shown that the conditions of equations 8 and 10 can be met, however the proof is a tedious algebraic problem. An indirect proof by example is just as valid since if these conditions are met there are no other restrictions that can be imposed from a thermodynamic point of view. Consider the compliance matrix

$$C_{ij} = \begin{pmatrix} 1 & -.7 & -.7\\ -.7 & 3 & -.2\\ -.7 & -.2 & 3\end{pmatrix} \qquad (11)$$

This matrix clearly satisfies all our conditions yet yields a value of Poisson's ratio of 0.7 and strong negative volume changes in a tensile test. Consequently small amounts of anisotropy can result in negative dilatation. It is believed that the anisotropy is caused by the orientation of the melt and subsequent

In Durability of Macromolecular Materials; Eby, R.;
ACS Symposium Series; American Chemical Society: Washington, DC, 1979.

rapid cooling in these injection molded samples which are known to contain orientation and residual stress effects.

With the exception of the negative volume changes prior to cavitation the behavior illustrated in figures 5 through 9 for thermal plastics are remarkably similar to that observed in filled elastomers where vacuole dilatation is known to lower the properties of the composite material. These data indicate that if vacuole dilatation could be minimized the strain energy characteristics to rupture could be increased resulting in an improvement of impact properties. What factors control the vacuole process in incompatible polymer blends or semicrystalline polymers is not known however the effect should be strongly dependent upon the sizes and concentrations of each phase and the coupling between phases in a manner similar to that observed with filled elastomers. It would appear that systematic dilatational studies on these systems could shed considerable light on the mechanisms leading to high impact performance.

Acknowledgements

The authors wish to express their appreciation to the Materials Research Laboratory of the University of Massachusetts, Amherst, MA 01003.

References

1. R.J. Farris, Trans. Soc. Rheol. 12, 308 (1968).
2. R.J. Farris, Trans. Soc. Rheol. 12, 315 (1968).
3. T.L. Smith, Trans. Soc. Rheol. 3, 113 (1959).
4. F.R. Schwarzl, "On the Mechanical Properties of Unfilled and Filled Elastomers", MECH. AND CHEMISTRY OF SOLID PROPELLANTS, Proc. 4th. Symp. Naval Structural Mechanics, Pergamon Press, New York, 1965.
5. A.E. Oberth and R.S. Bruenner, Trans. Soc. Rheol. 9, 165 (1964).
6. A.E. Oberth, Rubber Chem. Technol. 40, 1337 (1967).
7. R.J. Farris, "The Stress-Strain Behavior of Mechanically Degradable Polymers," in POLYMER NETWORKS: STRUCTURAL AND MECHANICAL PROPERTIES, ed. A.J. Chompff and S. Newman, pp. 341-394, Plenum, New York, 1971.
8. W.M. Hess and F.P. Ford, Rubber Chem. Technol. 36, 1220 (1963).
9. R.J. Farris, J. Appl. Polym. Sci. 8, 25 (1964).
10. H.F. Schnippel, Ind. Eng. Chem. 12, 33 (1920).
11. L.C. Cessna, Polym. Eng. Sci. 14, 697 (1974).

RECEIVED December 8, 1978.

18

Physical Aging of Glassy Polymers: Effects of Subsidiary Relaxation Processes

A. S. MARSHALL and S. E. B. PETRIE

Research Laboratories, Eastman Kodak Company, Rochester, NY 14650

As discussed previously (1-8), glassy, or partially glassy, polymers prepared under normal conditions have excess thermodynamic properties because of the kinetic aspects of the glass transformation process. As a consequence of this thermodynamic potential, the physical properties of glassy polymers change with time and approach those of the corresponding equilibrium glassy state, the rate of change being commensurate with the level of segmental molecular mobility associated with the rigid matrix.

In parallel with small changes in the thermodynamic state of glassy polymers on aging or annealing, rather profound changes have been observed in some of the mechanical properties (8-17). Especially noteworthy is the loss of general ductile behavior that has been documented for many polymers on aging or annealing at temperatures below their respective glass-transition temperatures (8-17). Of particular concern in studies of processes, especially diffusion-controlled processes (18), taking place in rigid environments are matrix-viscosity effects attributable to changes in the thermodynamic state of glassy matrices (1). Consequently, the rates of these relaxation processes associated with the nonequilibrium nature of the glassy state, and the factors that influence them are of considerable technological importance as well as of academic interest.

To gain information concerning the rates of relaxation processes characteristic of the glassy state, and to project long-term aging effects, particularly for polymers, a general study was undertaken of relaxation rates and of the influential variables (2). The procedure adopted for following the progress of the relaxation processes at various temperatures for selected glassy materials was to monitor enthalpy relaxation.

In earlier investigations involving both polymeric and nonpolymeric compounds (1,2), it was established that the primary rate-controlling factor is the temperature, more precisely the temperature interval, of the glass transformation process. With decreasing temperature below T_g, the time required for the enthalpy of either polymeric or nonpolymeric glassy materials to decrease

0-8412-0485-3/79/47-095-245$05.00/0

by a specific amount becomes exceedingly long.

Of the secondary factors to be considered in a study of this nature, a fundamental variable is the molecular weight. Detailed studies (2) of relaxation rates for nearly monodisperse atactic polystyrenes (PS) of various molecular weights ranging from 2.0×10^3 to 811×10^3 have shown that the relaxation rate at comparable temperature intervals below T_g ($T_g - T_A$), where T_A denotes the annealing temperature, increased somewhat with decreasing molecular weight below a critical region corresponding to the critical molecular-weight range observed in the molecular-weight dependence of T_g (19). A slight dependence of relaxation rate on molecular-weight polydispersity involving low-molecular-weight polymer was also observed. Consistent with these observations, the relaxation rate of a nonpolymeric glass, Aroclor 5460, was somewhat faster than that of nearly monodisperse atactic PS having a similar T_g but higher molecular weight. All of these results suggest that molecular chain dimensions have a small effect, in addition to reducing T_g, on the limited segmental mobility occurring in the glassy state.

Other secondary factors that could influence the enthalpy-relaxation process are substantial subsidiary modes of motion and structure-forming capability. Enthalpy-relaxation rates for bisphenol-A polycarbonate (PC), which has substantial main-chain motion in the glassy states (8,10-17), and for poly(ethylene terephthalate) (PET), which in addition to having subsidiary modes of motion has significant crystal-ordering tendency (8,9), were studied in detail, and the results are reported here.

Experimental

Enthalpy Relaxation. It was established previously (1,20) through limited enthalpy-relaxation studies of a number of organic glasses, some having widely differing structure-forming characteristics, that it is possible to follow readily by differential scanning calorimetry (dsc) the enthalpy changes that occur in glassy materials as a consequence of the nonequilibrium nature of the glassy state. The procedure involves monitoring the absorption of thermal energy that is superposed on the specific-heat change associated with the glass transition observed during programmed heating cycles of aged or annealed glasses. Typical dsc traces are illustrated in Figure 1. For both PC and PET, significant increases were observed in T_g, as determined by the procedure adopted here, with increasing annealing time.

For samples prepared and programmed under the same conditions except for the annealing or aging step, the energy absorbed in the T_g region is related to the decrease in excess enthalpy that occurs during the annealing or aging process (1,20).

If the stability and reproducibility of the baselines in the dsc traces are adequate, the amount of energy absorbed in the T_g interval of a glassy material as a result of annealing processes

In Durability of Macromolecular Materials; Eby, R.;
ACS Symposium Series; American Chemical Society: Washington, DC, 1979.

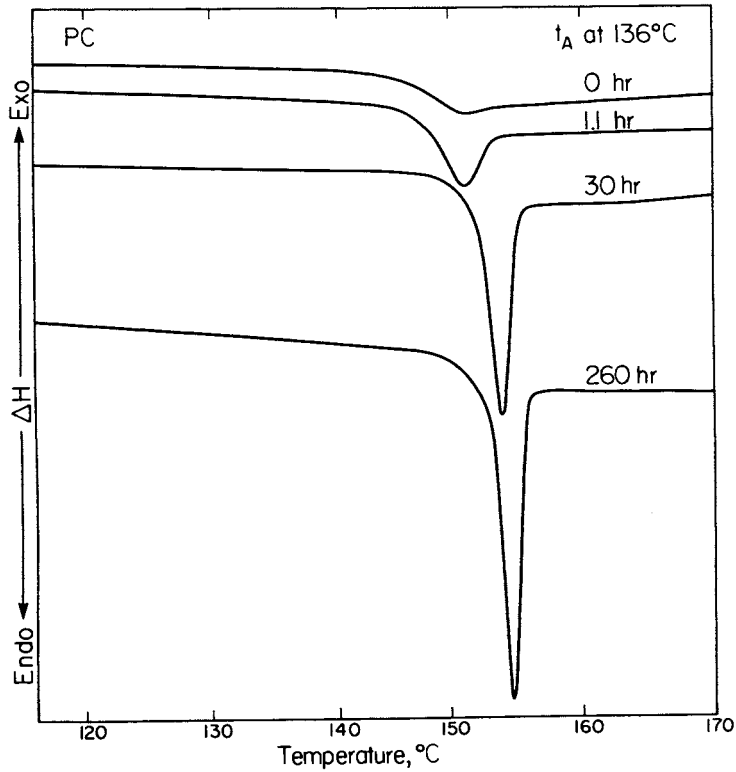

Figure 1. DSC scans at a heating rate of 5°C min^{-1} for PC after various annealing periods at 93°C following cooling from ca. 135°C

In Durability of Macromolecular Materials; Eby, R.;
ACS Symposium Series; American Chemical Society: Washington, DC, 1979.

can be determined merely by superposing the dsc curves, obtained under identical programming conditions, for the sample in the unannealed (quenched) and annealed states and evaluating the net energy absorption, $Q_t(\Delta H_{T_A}, T_A, r)$, where ΔH_{T_A} is the initial excess enthalpy at the annealing temperature T_A, and r is the programming rate.

Otherwise, a less direct, but equivalent, procedure is required that involves evaluating the magnitude of the endothermic peak and correcting it for enthalpy contributions associated with the increases in the T_g that occur as the relaxation process proceeds (1,2).

Generally, it is convenient to express the enthalpy changes that occur during isothermal annealing of a glass in terms of alterations in the enthalpy displacement from the equilibrium glassy state, i.e., alterations in the excess enthalpy $(H_t - H_E)$. Thus, a determination of the energy absorption in the T_g region for a corresponding sample in its equilibrium glassy state under the same programming conditions is necessary. From specific-heat data and a knowledge of the annealing and programming conditions, it is possible to estimate the maximum energy absorption $Q_E(\Delta H_{T_A}, T_A, r)$ if direct measurement is not readily attainable; that is,

$$Q_E(\Delta H_{T_A}, T_A, r_1) = (c_{p_f} - c_{p_g}) \left[T_g(r_1) - T_A\right] \tag{1}$$

where r_1 is the programming rate, and c_{p_f} and c_{p_g} are the specific heats of the fluid and glassy states, respectively. The excess enthalpy at the annealing temperature T_A after an annealing period t is related to Q_E and Q_t by

$$(H_t - H_E)_{T_A} = \left[Q_E(r_1) - Q_t(r_1)\right]_{T_A} \tag{2}$$

provided Q_E and Q_t are measured at the same programming rate r_1 (1).

The instrument employed was the Perkin-Elmer differential scanning calorimeter, Model DSC-2. The temperature scale was calibrated with the melting transitions of indium, tin, lead, and zinc. The energy input was calibrated with the heat of fusion of indium. The scanning rate used throughout this investigation was $5\,^{\circ}C\ min^{-1}$. In order to achieve the highest precision possible, the calibrations were checked frequently.

Since the stability of the baselines and the reproducibility of the dsc curves were adequate, the superposition procedure for evaluating the energy absorption at T_g of an annealed glass was adopted in these studies.

In Durability of Macromolecular Materials; Eby, R.;
ACS Symposium Series; American Chemical Society: Washington, DC, 1979.

Errors in the determination of $Q_t(\Delta H_{T_A}, T_A, r)$ were observed if the annealing temperature was not maintained precisely, and if the pans were not relocated exactly in the same position in the dsc holder. To minimize these errors, the samples were annealed directly in the holder. Under these conditions, the uncertainty in the enthalpy measurements was less than ± 0.02 cal g^{-1}. Specific heat was measured according to the procedures given in the instrument instruction manual. Data were reproducible to ± 0.001 cal $g^{-1}{}^{o}C^{-1}$.

Materials. The bisphenol-A polycarbonate used in this investigation was Lexan 145 as received from General Electric Co. ($\bar{M}_w \approx 3 \times 10^4$).

The amorphous poly(ethylene terephthalate) was prepared by quenching melt-cast polymer of molecular weight 2×10^4 to the amorphous state.

In order to eliminate the effects of previous thermal history, the approximately 10-mg, amorphous samples were heated to temperatures about 30°C above the corresponding T_g's observed for the unannealed materials at the selected heating rate of 5°C min^{-1}. Then, the samples were cooled to the annealing temperature at the fastest rate permitted by the instrument.

In these studies, T_g was taken as the temperature at which the specific heat reached a value that was midway between those corresponding to the fluid and glassy states.

Results and Discussion

Enthalpy-relaxation data obtained for glassy PC and PET during isothermal annealing at several temperatures below their respective T_g's are given in Figures 2 and 3, in which the excess enthalpy $[Q_E = Q_t]$ is plotted as a function of log t. The calculations of $Q_E(\Delta H_{T_A}, T_A, r)$ were based on $(c_{p_f} - c_{p_g})$ of 0.0778 cal $g^{-1}{}^{o}C^{-1}$ and 0.0855 cal $g^{-1}{}^{o}C^{-1}$ for PC and PET, respectively, as deduced from the specific-heat data obtained with the dsc.

For all of the polymers, the time required for relaxation of the enthalpy to that of the equilibrium glassy state at the various temperatures is extremely long, even at temperatures of the order of 15°C below the corresponding glass-transition temperatures. The principal rate-determining factor is the glass-transition temperature, as anticipated from previous studies (1,2).

Enthalpy relaxation for PC and PET proceeded almost comparably at corresponding temperature intervals below their respective T_g's ($T_g - T_A$). Furthermore, a comparison of these data with the PS results obtained previously (2) reveals no notable differences. The relaxation rates at comparable temperature intervals below T_g fall in the order PET > PS > PC -- an order

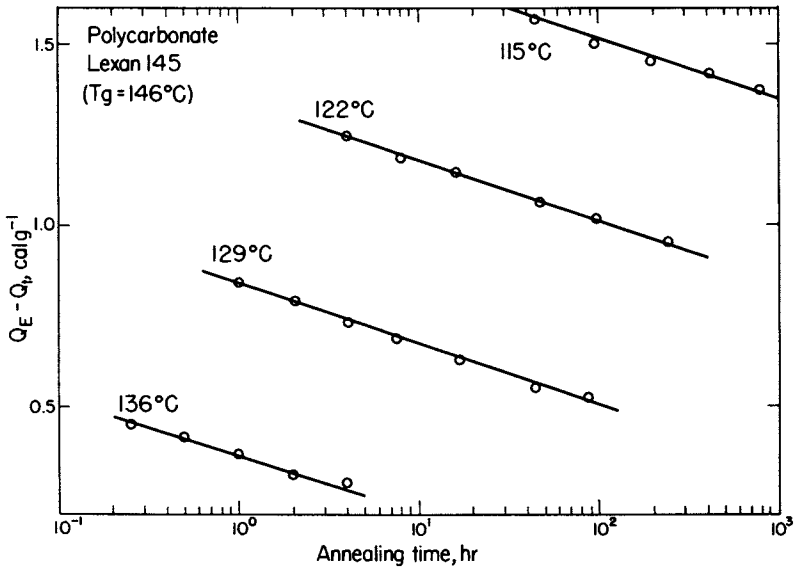

Figure 2. Enthalpy–relaxation data for PC at various temperatures

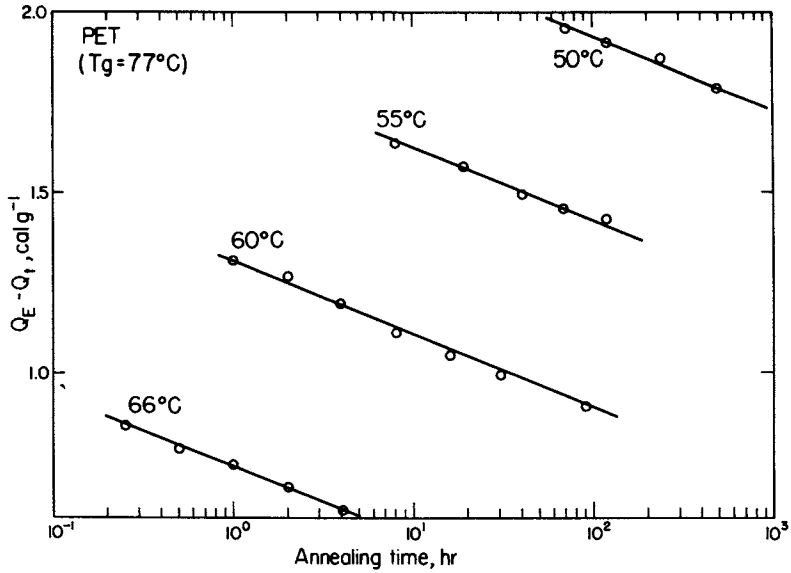

Figure 3. Enthalpy–relaxation data for PET at various temperatures

In Durability of Macromolecular Materials; Eby, R.;
ACS Symposium Series; American Chemical Society: Washington, DC, 1979.

reverse to that for T_g.

If it is assumed that the molecular weights of both PC and PET were above the critical molecular-weight region, as was the case for PS (2), and that the contributions of any low-molecular-weight fractions to the relaxation processes were not significant, the enthalpy-relaxation data suggest that molecular structure does not have a strong influence on relaxation processes associated with the nonequilibrium nature of the glassy state. Further, the data indicate that neither subsidiary modes of motion involving groups in the main chain nor the crystal-forming tendency of polymers has a significant effect on these relaxation processes.

The effect of molecular structure on the enthalpy-relaxation processes can be explored in greater detail by considering, as pointed out in previous studies of relaxation processes for glasses (1-6), that the rate of enthalpy relaxation is a function of the extent of the displacement of the system from its corresponding equilibrium state $(Q_E - Q_t)_{T_A}$ as well as a function of temperature, T_A.

At constant temperature, the relaxation time τ, $\{-d[\ln(Q_E - Q_t)]/dt\}^{-1}$, for each of the samples studied was found to be an exponential function of $[Q_E - Q_t]_{T_A}$. The data for PC and PET are plotted in Figures 4 and 5, respectively.

Also, at constant enthalpy displacement from the equilibrium glassy state, $(Q_E - Q_t)$, an Arrhenius temperature dependence was observed for the relaxation time for each polymer, as illustrated in Figures 6 and 7 for PC and PET, respectively. Some of the data plotted in Figures 6 and 7 correspond to extrapolated values of the enthalpy data in Figure 2, because of the exceedingly long relaxation times required to achieve a constant enthalpy displacement for the lower annealing temperatures.

Thus, the rate of enthalpy relaxation for each polymer can be expressed in terms of temperature and excess enthalpy according to a relationship of the form described previously (1), i.e.,

$$\frac{1}{\tau} = \frac{-d[\ln(Q_E - Q_t)]}{dt} = A \exp - (E_H/RT) \exp[C(Q_E - Q_t)] \qquad (3)$$

where E_H is the apparent activation energy of enthalpy relaxation, and A and C are constants. With the appropriate values for E_H, A, and C, for each polymer, equation (3) represents well the experimental data obtained. There is excellent agreement between $\ln\tau$ calculated from equation (3) as a function of $(Q_E - Q_t)$ and the experimental data obtained for PC and PET, as illustrated in Figures 4 and 5.

The values of E_H, A, and C of equation (3) for PC and PET varied little (Table I). The constant C, which reflects the dependence of the relaxation rate on the magnitude of the excess enthalpy, was larger for PC than for PET (the value for PS was

In Durability of Macromolecular Materials; Eby, R.;
ACS Symposium Series; American Chemical Society: Washington, DC, 1979.

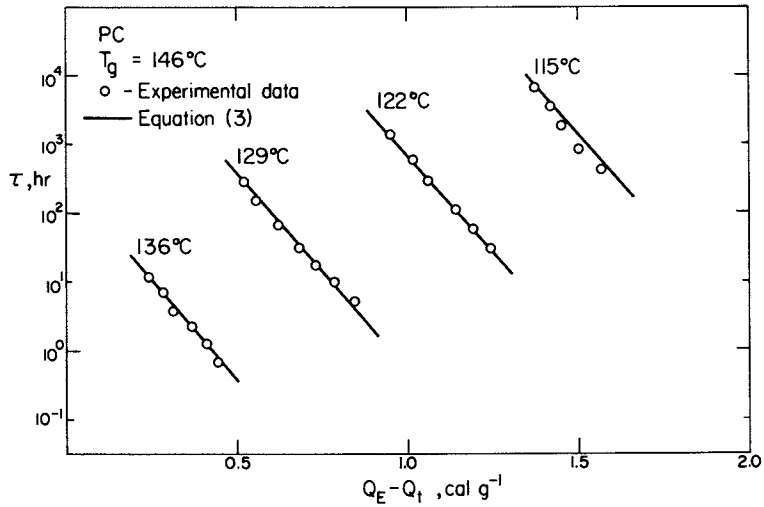

Figure 4. Relationship between the relaxation time, τ, and the enthalpy displacement from the equilibrium glassy state, ($Q_E - Q_t$), for PC at various temperatures

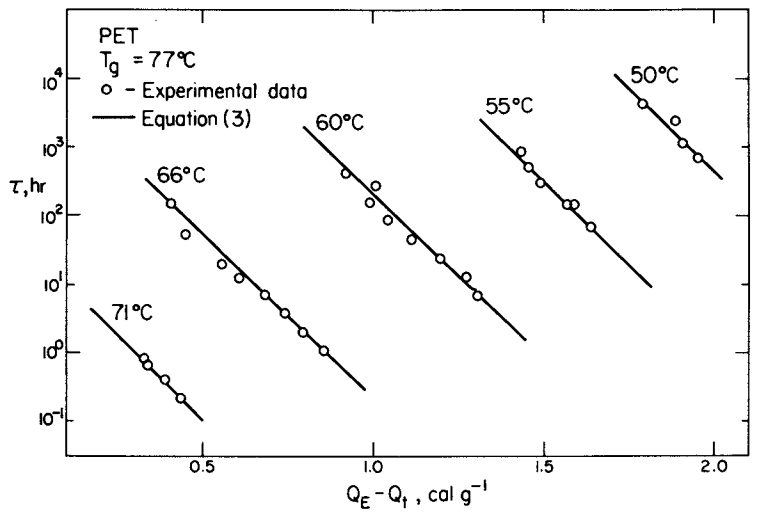

Figure 5. Relationship between the relaxation time, τ, and the enthalpy displacement from the equilibrium glassy state, ($Q_E - Q_t$), from PET at various temperatures

In Durability of Macromolecular Materials; Eby, R.;
ACS Symposium Series; American Chemical Society: Washington, DC, 1979.

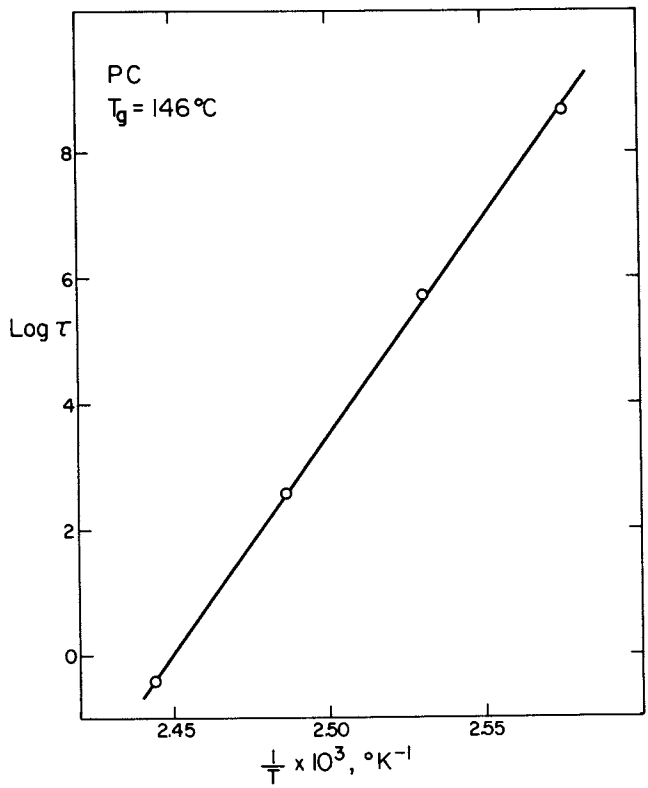

Figure 6. Arrhenius temperature plots for enthalpy–relaxation times at a constant excess enthalpy of 0.5 cal g^{-1} for PC

In Durability of Macromolecular Materials; Eby, R.;
ACS Symposium Series; American Chemical Society: Washington, DC, 1979.

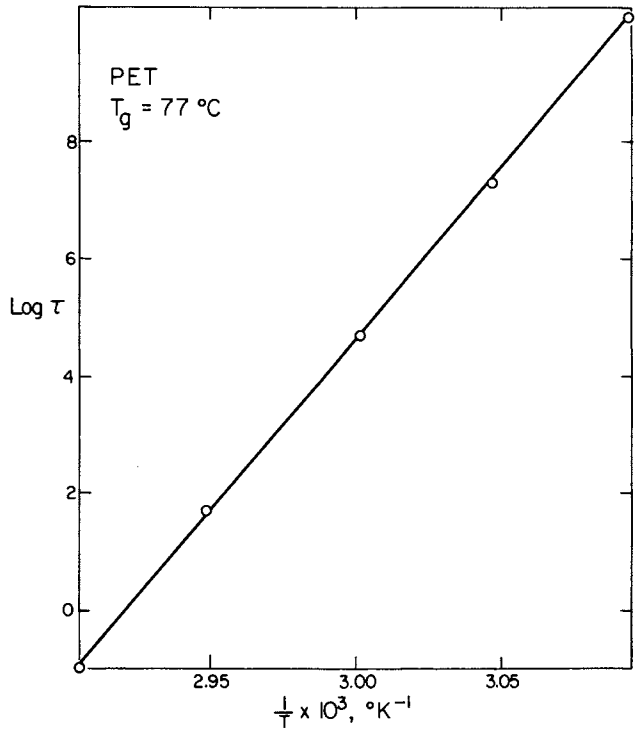

Figure 7. Arrhenius temperature plots for enthalpy–relaxation times at a constant excess enthalpy of 0.5 cal g^{-1} for PET

ENTHALPY-RELAXATION DATA FOR VARIOUS GLASSY POLYMERS

Polymer	$E_{H'}$ k cal mole^{-1}	C_1 g cal^{-1}
PC (Lexan 145)	317	13.1
PS (Koppers 8X)	292	12.2
PET	263	11.2

In Durability of Macromolecular Materials; Eby, R.;
ACS Symposium Series; American Chemical Society: Washington, DC, 1979.

intermediate between those for PC and PET). The apparent activation energy E_H in the temperature-dependent term also was slightly larger for PC than for PET (again the value for PS was intermediate between those for PC and PET).

These data concerning the molecular-structure dependency of the enthalpy-relaxation process suggest that the factors that influence the onset of segmental mobility influence enthalpy relaxation, but that the presence of mobile groups in the main chain or the crystal-ordering tendency of polymers does not seem to have a significant effect on the rate of enthalpy relaxation. These factors, however, are believed to influence the flexural properties of these polymers (8-17).

To summarize the effects of the molecular structural characteristics considered in this and the previous (1) investigation on the temperature dependence of the enthalpy-relaxation rate, the relaxation times at a constant excess enthalpy $(Q_E - Q_t) = 0.5$ cal g^{-1} are plotted in Figure 8 as a function of the corresponding temperature interval below T_g, i.e., at the same $(T_g - T_A)$, for the various organic glasses, Aroclor 5460 (2), PC, PET, and PS (2).

When the relaxation time τ determined for the glassy polymers after relaxing a specific increment in the level of the excess enthalpy, Q_t (0.5 cal g^{-1} for PS and corrected for differences in Δc_p for other materials), was plotted as a function of the reciprocal temperature, the data could be approximated over the limited temperature range by an Arrhenius relationship with an apparent activation energy of about 46 kcal $mole^{-1}$ for PET and 72 kcal $mole^{-1}$ for PC (61 kcal $mole^{-1}$ for PET and 72 kcal $mole^{-1}$ for PC (61 kcal $mole^{-1}$ was reported previously for PS (2)). The value for PET is consistent with that determined for the transition from ductile behavior to brittle fracture observed in the stress-strain data at room temperature upon different annealing times at the various temperatures (9), and is comparable to the values for polystyrene of molecular weight 2000 (44 kcal $mole^{-1}$) and Aroclor 5460 (43 kcal $mole^{-1}$). There is almost an order-of-magnitude difference between the apparent activation energies involving processes associated with constant displacements from the initial enthalpy states and those associated with constant displacements from the equilibrium enthalpy states.

Conclusions

From detailed studies of the effect of molecular structure on the rate of enthalpy relaxation for PC and PET, it is evident that the principal rate-determining factor in relaxation processes associated with the nonequilibrium nature of the glassy state is the glass-transition temperature.

The rates of enthalpy relaxation measured for the polymers can be expressed in terms of temperature and excess enthalpy according to relationships of the form described previously (1,2),

In Durability of Macromolecular Materials; Eby, R.;
ACS Symposium Series; American Chemical Society: Washington, DC, 1979.

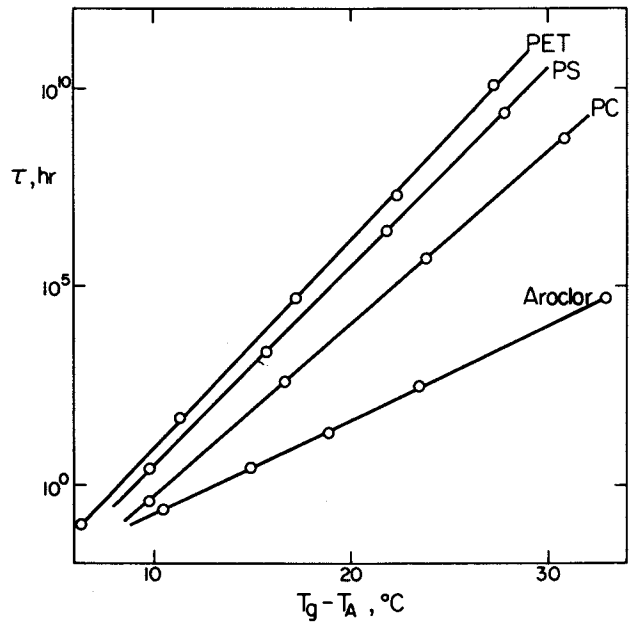

Figure 8. Normalized plots of enthalpy–relaxation times for PC, PET, polystyrene, and Aroclor 5460. Semilogarithmic plots of τ at a constant excess enthalpy of 0.5 cal g^{-1} vs. $(T_g - T_A)$.

In Durability of Macromolecular Materials; Eby, R.;
ACS Symposium Series; American Chemical Society: Washington, DC, 1979.

i.e., $\tau^{-1} = A \exp(-E_H/RT) \exp [C(Q_E - Q_t)]$, where τ is the relaxation time, E_H is the apparent activation energy of enthalpy relaxation, $(Q_E - Q_t)$ is the excess enthalpy, and A and C are constants. The values of E_H, A, and C of these relationships have been found to vary slightly with molecular structure in a manner similar to that observed for the molecular-structure dependence of the glass-transition temperature.

Neither the presence of mobile groups in the main chain nor the crystal-ordering tendency of polymers seems to have a significant effect, if any, on the rate of enthalpy relaxation of these polymers.

Thus, one could conclude that the molecular structure of glassy polymers has only a small effect on the relaxation processes associated with the nonequilibrium thermodynamic state of the glasses.

Acknowledgments

The authors are indebted to J. E. Fogg and W. W. Jacobe of the Manufacturing Technology Division, Kodak Park, Eastman Kodak Company, for the preparation of the amorphous PET film used in these studies.

Summary

In lifetime considerations for glassy or partially glassy polymeric materials, an important factor is the physical aging process associated with the nonequilibrium thermodynamic state of glasses. Because of the kinetic aspects associated with the transformation of a melt to a glass in the glass-transition temperature interval, the glassy states of materials prepared under normal cooling conditions have excess enthalpy and volume relative to those of the corresponding equilibrium states that can be achieved through slow cooling or annealing regimes. For glasses with excess thermodynamic properties, there is a thermodynamic potential for the properties to approach those of the equilibrium state, i.e., to decrease with time, the rate of decrease being commensurate with the level of molecular or segmental molecular mobility in the glassy state. Preliminary studies suggest that the rather substantial changes observed in some of the physical properties, particularly the flexural properties, of glassy or partially glassy polymers subjected to various annealing regimes at temperatures below their respective glass-transition temperatures are associated with the loss of excess thermodynamic properties that take place as a result of the annealing processes. To ascertain the effects of modes of motion involving groups in the polymer chain on the relaxation processes associated with this physical aging phenomenon, enthalpy relaxation studies were undertaken of two polymers having substantial main-chain motion in the glassy state--poly(ethylene terephthalate) and bisphenol-A poly-

In Durability of Macromolecular Materials; Eby, R.;
ACS Symposium Series; American Chemical Society: Washington, DC, 1979.

carbonate. The enthalpy relaxation data for the glassy polymers suggest that neither the presence of mobile groups in the main chain nor the crystal-forming tendency of polymers has a significant effect on the rate of enthalpy relaxation.

Literature Cited

1. Petrie, S.E.B., J. Polym. Sci. A-2, (1972) 10, 1255.

2. Marshall, A.S. and Petrie, S.E.B., J. Appl. Phys., (1975) 46, 4223.

3. Tool, A.Q. and Eichlin, C. G., J. Res. Nat. Bur. Stand., (1931) 6, 523.

4. Davies, R. O. and Jones, G. O., Adv. Phys., (1953) 2, 370.

5. Jones, G. O., "Glass," Methuen, London, 1956.

6. Kovacs, A. J., Fortschr. Hochpolym. Forsch., (1963) 3, 394.

7. Wunderlich, B., Bodily, D. M., and Kaplan, M. H., J. Appl. Phys., (1964) 35, 95.

8. Petrie, S.E.B., in "Polymeric Materials: Relationships Between Structure and Mechanical Behavior," edited by E. Baer and S. V. Radcliffe, Amer. Soc. Met., Metals Park, Ohio, 1975.

9. Mininni, R. M., Moore, R. S., Flick, J. R. and Petrie, S.E.B., J. Macromol. Sci.-Phys., (1973) B8, 343.

10. LeGrand, D. G., J. Appl. Polym. Sci., (1969) 13, 2129.

11. Flick, J. R. and Petrie, S.E.B., Bull. Amer. Phys. Soc., (1974) 19, 238.

12. Allen, G., Morley, D.C.W. and Williams, T., J. Mater. Sci., (1973) 8, 1449.

13. Sternstein, S. S. and Ho, T. C., J. Appl. Phys., (1972), 43, 4370.

14. Neki, K. and Geil, P. H., J. Macromol. Sci.-Phys., (1973), 8, 295.

15. Peilstöcker, G., Kunststoffe, (1961) 51, 509.

16. Schnell, H., "Chemistry and Physics of Polycarbonate," Interscience, New York, 1964.

In Durability of Macromolecular Materials; Eby, R.;
ACS Symposium Series; American Chemical Society: Washington, DC, 1979.

17. Golden, J. H., Hammant, B. L. and Hazell, E. A., J. Appl. Polym. Sci., (1967) 11, 1571.

18. Chen, S. P., Polym. Preprints, (1974) 15(2), 77.

19. Fox, T. G. and Flory, P. J., J. Polym. Sci., (1954) 14, 315.

20. Petrie, S.E.B., Polym. Preprints, (1974) 15(2), 336.

RECEIVED December 8, 1978.

19

Creep Failure of Rubbery Polymers

SUEO KAWABATA

Department of Polymer Chemistry, Kyoto University, Kyoto 606, Japan

The failure phenomena of viscoelastic materials consist of two factors. One is the time dependence of the bulk stress-strain relation of the material. For example, higher strain rate increases the stress level of the material and consequently the stress or the strain at break will be different from those of the case of the lower rate. The second factor is the time dependence of the failure mechanism itself, namely, the time dependence of the failure initiation mechanism.

In actuallity, both factors occur together and it is difficult to separate them. As shown later, this separation is possible by calculations based on the theory introduced here. However, it is not so simple and adds an extra factor to the analysis of the failure mechanism. In order to avoid confusion caused by the combined factors, it is advantageous to carry out the failure experiment under a simple stress state such as constant stress and so on.

Thus, it has been concluded that the creep process of elastomers is one of the suitable processes for separating the second factor from the combined state and that the creep failure experiment gives us a good information for estimating the failure mechanism of polymers.

It must be again noted that there are two classes in the creep failure phenomenon also. One of them is the creep failure where the creep proceeds with relatively high rate of strain and the body is deformed largely during the observation period. In uniaxial extension, for example, the cross-sectional area of the body becomes thiner and thiner with increasing creep strain and then the body is broken like the break down of a thread. This class is also a kind of the combined type of the first and the second factors. Another class of creep failure, which will be considered in this article is that in which the creep strain is not so large and the stress state is kept nearly constant and failure occurs suddenly at some time. The creep process of vulcanized rubbers is one of the processes closest to this second class. That is, both the strain rate and the creep strain are not so high in this creep process except at the moment just after

0-8412-0485-3/79/47-095-261$07.00/0

In Durability of Macromolecular Materials; Eby, R.;
ACS Symposium Series; American Chemical Society: Washington, DC, 1979.

loading. In the case of uniaxial extension, the stretch ratio is kept nearly constant and therefore the true stress in the body is also kept nearly constant.

The author's first research on creep failure to investigate the failure mechanism the view point was done in 1964 with P. J. Blatz (1) and this research was improved in 1970 (2). In this article, theories and the experiments will be introduced based on above researches adding new experimental data obtained recently by author.

Theoretical consideration

Let us consider a body under a homogeneous stressed state and define the stressed state of the body by ϕ such that ϕ takes zero value when the body is in undeformed state and the probability that the body fails is increased with increasing ϕ value. The relation between the usually defined stress, σ, and the ϕ will be discussed later. In a stressed state, rubbery polymers show creep behavior even though the creep strain is small compared with the initial strain at the moment of loading, and polymer chains flow slowly and continuously during the creep process. On the other hand, it is imagined that there are many defects inside the vulcanized rubber, each of them is probably a hole or a thin part of the chain assembly caused by the essentially statistical arrangement of the chains and their flow with time.

The assemblies of many separated short chains and many dangling chains with uncross-linked ends may form those defect parts and the size of those defects is therefore considered to be of the order of molecular size. During the creep process, that is, under a constant stress state, many of those defects will appear inside the body continuously and some of them will disappear with time. Assuming the above circumstances, consider a body having a unit volume and divide it into N cells with equal volume of the order that a few defect parts are contained in it during a unit time interval in average. The first assumption is made that if one of the cells falls into a critical state and produces a crack inside the cell, then the crack propagates through the body without delay and causes failure of the whole body.

Let us introduce a quantity m_c that is an expectation number of cells which fall in the critical state during a unit time interval and per unit volume of a body. Using this m_c, the probability that x cells fall in the critical state during a unit time interval is given by the following equation. Let P(x) be the probability then

$$P(x) = \frac{m_c{}^x}{x!} \exp(- m_c) \tag{1}$$

This type of distribution is called a Poisson's distribution

In Durability of Macromolecular Materials; Eby, R.;
ACS Symposium Series; American Chemical Society: Washington, DC, 1979.

and reduced from a binominal distribution when N, the number of cells, is a large number and m_c is small.

Let us now consider a body whose volume is V and placed in a constant and a homogeneous stress filed. The probability, Q_1, that the body is safe between the time interval from t=0 to $t=t_B$ is given by substituting x=0 into equation (1) considering that the mean number of x changes proportionally to the volume V and the time interval t_B.

$$Q_1 = exp(- m_c V t_B) \tag{2}$$

The probability Q_2 that failure occurs during the time interval between t_B and $t_B + \Delta t_B$ is given by

$$Q_2 = 1 - exp(- m_c V \Delta t_B) \tag{3}$$

Therefore, the probability that failure occurs first at between t_B and $t_B + \Delta t_B$ is given by a conditional probability such as

$$\begin{aligned} P(t_B)\Delta t_B &= Q_1 Q_2 \\ &= exp(- m_c V t_B)\{ 1 - exp(- m_c V \Delta t_B)\} \end{aligned} \tag{4}$$

where $P(t_B)\Delta t_B$ is the probability and $P(t_B)$ is the probability density function of the life time t_B. Putting $\Delta t_B \to dt$, Q_2 of eq(3) is written such that

$$Q_2 = m_c V dt \tag{5}$$

and substituting eq(5) into eq(4), we obtain

$$P(t_B) = m_c V exp(- m_c V t_B) \tag{6}$$

This is an exponential distribution, if m_c is kept constant with time, and the mean value of t_B in this case, is given by

$$< t_B > = \frac{1}{m_c V} \tag{7}$$

m_c is a function of the stressed state, but the stress is kept nearly constant during the creep process. Therefore, one may examine the relation given by eq(6) and eq(7) by creep failure experiment. This is the reason why the creep failure experiment makes the analysis of failure mechanism very simple.

In Durability of Macromolecular Materials; Eby, R.;
ACS Symposium Series; American Chemical Society: Washington, DC, 1979.

We can expand this theory to the more general cases as follows. Consider the case that the stress state of the body is not homogeneous and, therefore, each of cells is placed at different stress states according to its position in the body and more over, each of those stress states are varied also with time. For this case, divide the time into n of the short intervals. Then $P(t_B)$ can be obtained as follows applying the concept of conditional probability.

$$P(t_B)\ \Delta t_B = \sum_{j=1}^{n} m_{cij}\ \Delta V\ exp(-\sum_{i=1}^{k}\sum_{j=1}^{L} m_{cij}\ \Delta t\ \Delta V)\ \Delta t_B \qquad (8)$$

where m_{cij} is the value of m_c of the jth cell and the ith time interval, and ΔV is the volume of a cell.

This equation is reduced by multipling the two probabilities, the probability that no crack initiation occurs during t=0 to $t=t_B$ and the probability that one or more cracks occur between t_B and $t_B + dt_B$. In the case of homogeneous stress state through the body, and putting $\Delta t \to dt$, eq(8) becomes

$$P(t_B) = m_c\Big|_{t_B}\ V\ exp(-V\int_0^{t_B} m_c\ dt) \qquad (9)$$

In the case when m_c is constant with respect to time, eq(9) is conincident with eq(6), that is, the equation for constant stressed state process.

Interrelation between m_c and stress σ

As shown before, m_c is a function of stressed state ϕ and an important parameter for the failure process, and the functional form cannot be introduced from theoretical considerations in this stage. However, we can determine it by experiment, particularly by creep failure experiment because of a simple relation between $\langle t_B \rangle$ and m_c as shown in eq(7).

From a theoretical viewpoint, the only thing we can say about m_c is the following. Based on definition, ϕ expressed a stress state and the probability that a cell falls into critical state will be increased with increasing value of ϕ. On the other hand, the strength of each of the cells may be different. For example, if a cell contains a large number of defects, the cell will be weakened compared with the cell containing a small number of defects. Here we define ϕ_g with respect to the strength of a cell such that the cell will fall into the critical state when the cell is placed in stressed state of ϕ_g during a unit time interval. Let $\Psi(\phi_g)$ be the probability density function of ϕ_g and N is the number of cells in a unit volume, then $m_c(\phi)$ is given by

In Durability of Macromolecular Materials; Eby, R.;
ACS Symposium Series; American Chemical Society: Washington, DC, 1979.

$$m_c(\phi) = N \int_0^{\phi} \Psi(\phi_g)\, d\phi_g \tag{10}$$

The function $\Psi(\phi_g)$ is however an unknown function, and we can only say that $\Psi(\phi_g) = 0$ at $\phi_g = 0$. If we introduce the assumption that the number of defect parts in a cell is distributed obeying a Poisson's distribution and the strength of a cell is decreased in proportion to the number of the defects contained in the cell, then the following equation can be obtained assuming a Poisson's distribution of the number of the defects in a cell (3).

$$\Psi(\phi_g) = \frac{A}{k\,\Gamma(\mu)} \left(\frac{1 - \phi g/\phi g0}{k} \right)^{\mu-1} \exp\left(- \frac{1 - \phi q/\phi g0}{k} \right) \tag{11}$$

where ϕ_{g0} is the strength of cells when no defects exist in the cell, k is the proportional coefficient, μ is the mean value of defects contained in a cell, A is a constant and $\Gamma(\mu)$ is the gamma function. This functional form indicates that the function $\Psi(\phi_g)$ is not linear with respect to ϕ_g in small region of ϕ_g and can be expected as

$$\left. \frac{d\,\Psi(\phi_g)}{d\phi_g} \right|_{\phi_g \to 0} > 0$$

More over $\phi g/\phi g0$ should be small, therefore we can assume that

$$\Psi(\phi_g) = c_1\, \phi_g^{\,2} \tag{12}$$

where c_1 is a constant. Substituting eq(12) intl eq(10) we obtain

$$m_c(\phi) = c_2\, \phi^{3} \tag{13}$$

where c_2 is a constant.

Consider a uniaxial extension and assume that ϕ is related to the true stress σ_t such that

$$\phi = c_3\, \sigma_t^{\,n} \tag{14}$$

where c_3 and n are constants, then m_c is given as following.

$$m_c = c\, \sigma_t^{\,3n} \tag{15}$$

where c is a constant which is equal to $c_1 c_2/3$.

Substituting eq(15) into eq(6), we obtain the probability density function of t_B, time to break, in creep.

In Durability of Macromolecular Materials; Eby, R.;
ACS Symposium Series; American Chemical Society: Washington, DC, 1979.

$$P(t_B) = c\ \sigma_{t0}^{3n}\ V\ exp(-\ c\ \sigma_{t0}^{3n}\ V\ t_B) \tag{16}$$

where σ_{t0} is a constant true stress. The mean value of t_B is calculated from eq(16) as follows.

$$\langle t_B \rangle = \frac{1}{c\ V\ \sigma_{t0}^{3n}} \tag{17}$$

or

$$log\ \sigma_{t0} = -\ \frac{1}{3n}\ log\ c\ V - \frac{1}{3n}\ log\ \langle t_B \rangle \tag{18}$$

From the plot of $\log\langle t_B \rangle$ vs $\log\sigma_{to}$, the constants c and n are obtained from its slope and from the ordinate at $\log\langle t_B \rangle = 0$ respectively.

In the case when m_c is not constant in terms of time t because σ_t is varied with time, we can introduce the following from eq(9) and eq(15):

$$P(t_B) = c\ V\ \sigma_t^{3n}(t)\ exp(-\ c\ V \int_o^{t_B} \sigma_t^{3n}(t)\ dt) \tag{19}$$

where true stress $\sigma_t(t)$ is a function of t in general.

A different assumption

We have obtained an exponential distribution of t_B based on the first assumption where one crack leads the body to failure. Now examine another case under the assumption such that the second crack leads the body to failure and, in general, the ν th crack leads the body to failure. That is, the first, the second, and the ν-1 th crack do not lead the body to failure in this general case. These cases are understandable if we imagine the mechanism that the first, the second, . . . and the ν -1 th cracks are interrupted in their propagation through the body for some reason or other. For the case when the stressed state of the body is homogeneous through the body and is kept constant with time, then the distribution of t_B is calculated as follows. Let M_c be

$$M_c = V \int_0^{t_B} m_c\ dt = V\ m_c\ t_B \tag{20}$$

and the probability that the number of cells which fall into critical state is zero, 1, 2, . . ., ν-1 respectively is given by

$$Q_1 = \sum_{x=o}^{\nu-1} \frac{M_c^{\,x}}{x!}\ exp(\ -M_c\ ) \tag{21}$$

In Durability of Macromolecular Materials; Eby, R.;
ACS Symposium Series; American Chemical Society: Washington, DC, 1979.

Q_1 is the probability that no failure occurs during the time interval from t=0 to $t=t_B$. Then, the probability that failure occurs during the interval from t=0 to $t=t_B$ is given by

$$\int_0^{t_B} P(t_B)\, dt_B = 1 - Q_1 = 1 - \sum_{x=0}^{\nu-1} \frac{M_c^x}{x!} \exp(-M_c) \tag{22}$$

$$= 1 - \frac{1}{\Gamma(\nu)} \int_{M_c}^{\infty} x^{\nu-1} e^{-x}\, dx \tag{23}$$

where $\Gamma(\nu)$ is the gamma function. The derivation of eq(23) from eq(22) is given by the literature (3). From eq(23), we obtain the following equation as a probability density of t_B for this case.

$$P(t_B) = \frac{1}{\Gamma(\nu)} M_c^{\nu} t_B^{\nu-1} \exp(-M_c t_B) \tag{24}$$

and $\langle t_B \rangle$, the mean value of t_B, can be calculated from eq(24) such that

$$t_B = \frac{\nu}{M_c} = \frac{\nu}{m_c V} = \frac{\nu}{c V \sigma_t^{3n}} \tag{25}$$

where m_c is a constant with respect to t in this case. If we substitute $\nu=1$ into eq(24) and eq(25), then we have the same equation as eq(6) and eq(7) respectively. The distribution of eq(21) shows unimodal distribution of t_B when $\nu<2$. Those distributions are shown in Figure 1 together with the case of $\nu=1$, that is, the case of exponential distribution. In order to examine the type of distribution of t_B, define F as following.

$$F \equiv \int_{t_B}^{\infty} P(t_B)\, dt_B \tag{26}$$

In the case of $\nu=1$, that is, the case of exponential distribution we obtain a linear relation between F and $t_B/\langle t_B \rangle$:

$$\log F = -0.4343 \frac{t_B}{\langle t_B \rangle} \tag{27}$$

For cases when $\nu \leq 2$, log F vs $t_B/\langle t_B \rangle$ deviates from the linear relation and is shown in Figure 2 together with the case for $\nu=1$, obtained from eq 27).

Experiment

It has been observed that the exponential type of $P(t_B)$ is obtained for pure rubbers and the unimodal type for filled systems as shown below.

In Durability of Macromolecular Materials; Eby, R.;
ACS Symposium Series; American Chemical Society: Washington, DC, 1979.

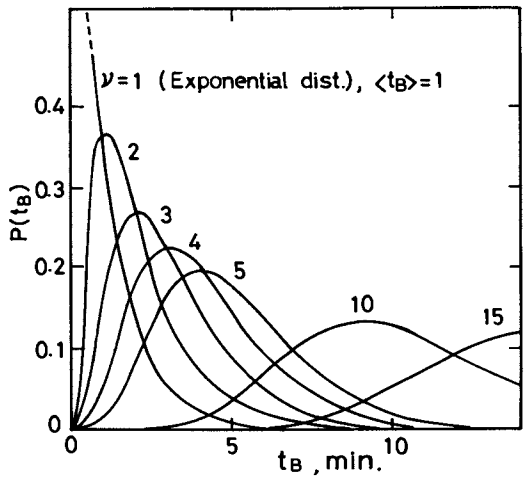

Figure 1. Distribution of t_B

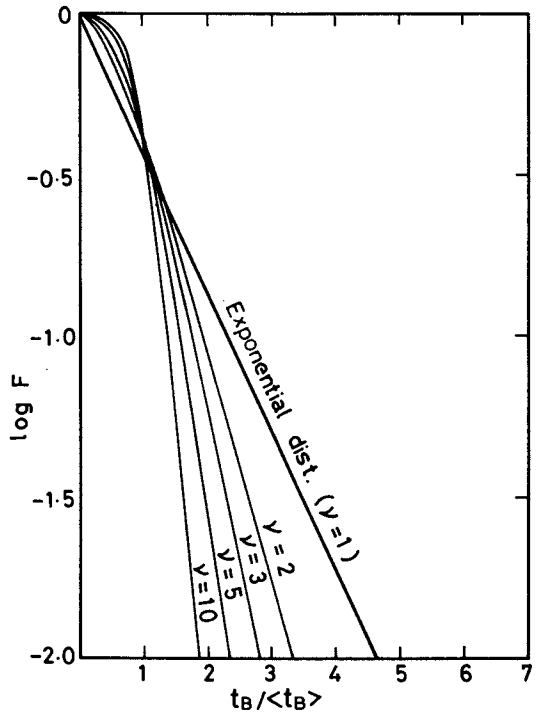

Figure 2. Plot of log F vs. $t_B/\langle t_B \rangle$

In Durability of Macromolecular Materials; Eby, R.;
ACS Symposium Series; American Chemical Society: Washington, DC, 1979.

Pure rubber system

The distributions of t_B are measured for vulcanized SBR and NR (Table 1) by creep experiment at 40°C in air. Figure 3(a) shows creep of SBR with time. A constant load is applied to a specimen of ring shape by a dead weight to stretch the specimen uniaxially. After loading, the creep continues normally and, at some time, the failure occurs suddenly, without any previous sign, at the moment indicated by "break" in the figure. Figure 3(b) is the close up figure just before the moment of break. This figure was recorded by an endless high speed recording system. Within the resolving time of 5-10μ sec, we can look for any sign of the failure occuring.

A relation between t_B and the applied true stress is shown in Figure 4 for NR specimen. Here, true stress σ_{to} is calculated by $\lambda_B \sigma_{eo}$ where λ_B is the stretch ratio of the specimen at failure and σ_{eo} is the constant engineering stress applied by a weight. The relation between $\langle t_B \rangle$ and σ_{to} reduced from the data of Figure 4 is shown in Figure 5 (plot of eq(18)) with the plot for SBR.

It was confirmed that the exponential distribution of t_B is obtained commonly for each of different stress levels. The examination of the type of distribution is shown in Figure 6 based on eq(27). In this figure the distribution obtained from the experiments for SBR are examined at the same time. The scattered data of t_B observed from both NR and SBR obey systematically the exponential distribution as expected by the theory based on the first assumption. The constants n and c are shown in Table 1.

The values of n are between about 2 and 4 and the values of c are very small and vary with the material. The value of c for NR is much smaller than that of SBR. This is caused by the higher strength of the NR than of the SBR.

From Figure 5, the temperature dependence of n and c for SBR can be estimated. As seen from the figure, n is independent of temperature and only c is dependent. That is, high temperature increases c and accelerates failure.

Filled rubber system

In order to examine the creep failure behavior of filled rubbers, a carbon filled SBR was examined. The distribution of t_B in this case becomes a unimodal distribution as shown in Figure 7. The exponential distribution obtained from pure SBR is also shown in the same figure in order to compare the change in the type of distribution from exponential to unimodal type. To examine this distribution type, the plot of log F vs $t_B/\langle t_B \rangle$ is shown in Figure 8 and some calculated curves for different values of ν are also overlapped on the data, and it is estimated that the case ν=4 provides a suitable description of this distribution.

In Durability of Macromolecular Materials; Eby, R.;
ACS Symposium Series; American Chemical Society: Washington, DC, 1979.

Table 1. Failure constants

Materials / Constants	SBR	Carbon filled SBR	NR	NBR *1	NBR,PVC blend *1	Plasticized PVC *2
n	1.94	2.00	3.62	3.60	1.04	2.28
$\sigma_{ts}^{3n} \equiv \nu/c\ V$	3.19×10^{10}	1.67×10^{19}	3.98×10^{34}	1.58×10^{16}	3.55×10^{7}	1.96×10^{21}
σ_{ts} (Kg/cm^2)	63.79	1598.77	1534.59	31.61	262.99	1296.89
ν	1	4	1	-	-	4
c *3	1.08×10^{-10}	8.32×10^{-18}	7.35×10^{-34}	3.00×10^{-16}	1.50×10^{-7}	2.72×10^{-19}
V (cm^3)	0.293	0.0287	0.0342	0.210	0.188	0.0075
Temp (°C)	40	40	40	23	23	23
Composition	SBR1500 100, ZnO 3, S.A 2, DPG 2, AO 1, S 2	SBR1502 100, HF 50, S.A 3, P.Oil 9, ZnO 3, S 2, D.M 1.8, AO 1	NR 70, IR 30, S 2.5, ZnO 1, AO 0.8, S.A 0.5	NBR(N 30%) 100, PMD 2.5	NBR(N 30%) 70, PVC 30 PMD 2.5 Stabilizer 1.5	PVC 100, DOP 41

*1 Prepared by Nippon Zeon Co, Kawasaki
*2 Prepared by Mitsubishi Monsanto Chemicals Co, Nagoya
*3 $\text{min}^{-1}\ \text{cm}^{-3}\ (\text{Kg/cm}^2)^{-3n}$

In Durability of Macromolecular Materials; Eby, R.; ACS Symposium Series; American Chemical Society: Washington, DC, 1979.

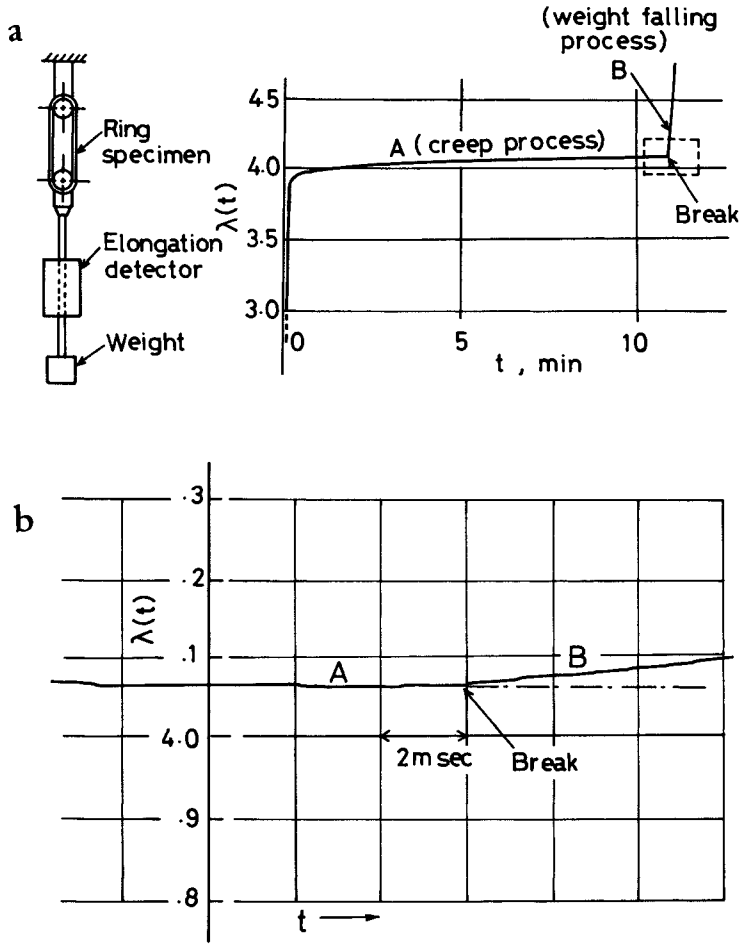

Figure 3. (a) Creep failure experiment and (b) close up of the creep curve at breaking. There are no previous signs for failure.

In Durability of Macromolecular Materials; Eby, R.;
ACS Symposium Series; American Chemical Society: Washington, DC, 1979.

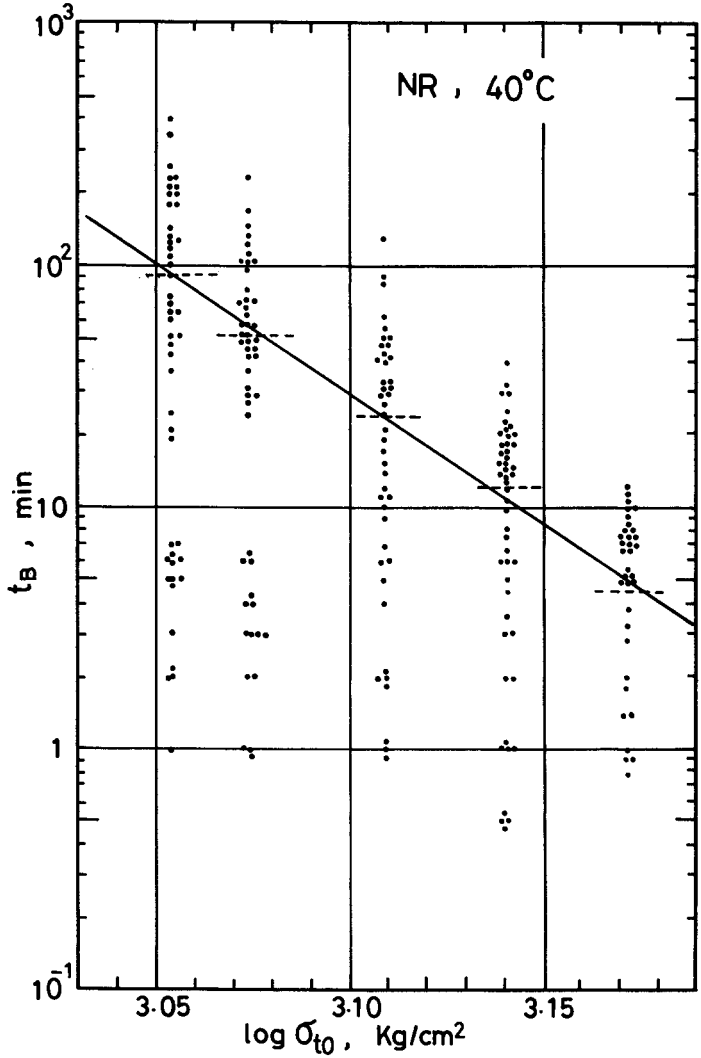

Figure 4. Plot of t_B vs. σ_{to}, t_B scatters over the three decades

In Durability of Macromolecular Materials; Eby, R.;
ACS Symposium Series; American Chemical Society: Washington, DC, 1979.

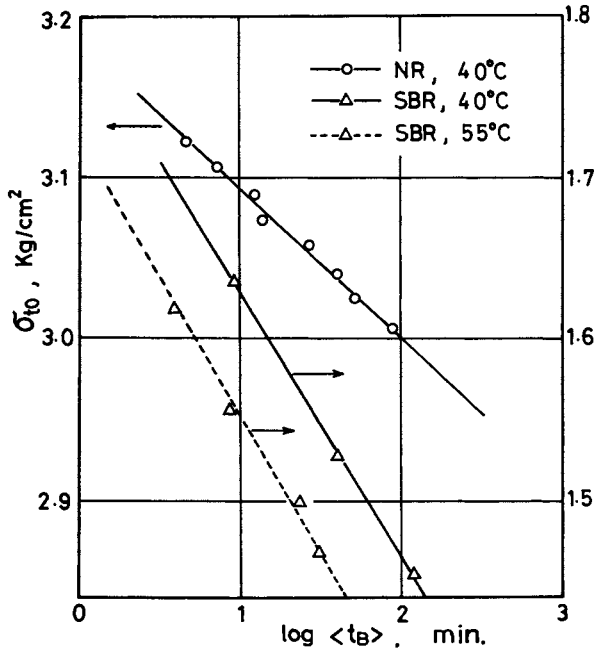

Figure 5. Plot of σ_{t_0} vs. log $\langle t_B \rangle$

In Durability of Macromolecular Materials; Eby, R.;
ACS Symposium Series; American Chemical Society: Washington, DC, 1979.

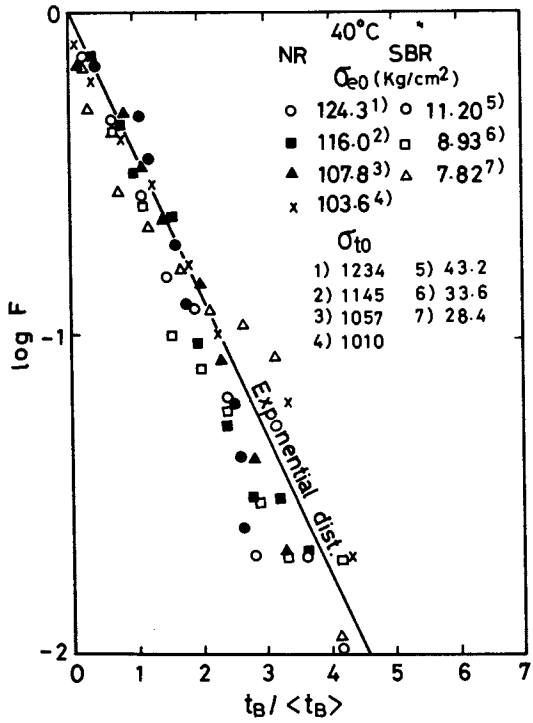

Figure 6. Plot of log F for NR and SBR

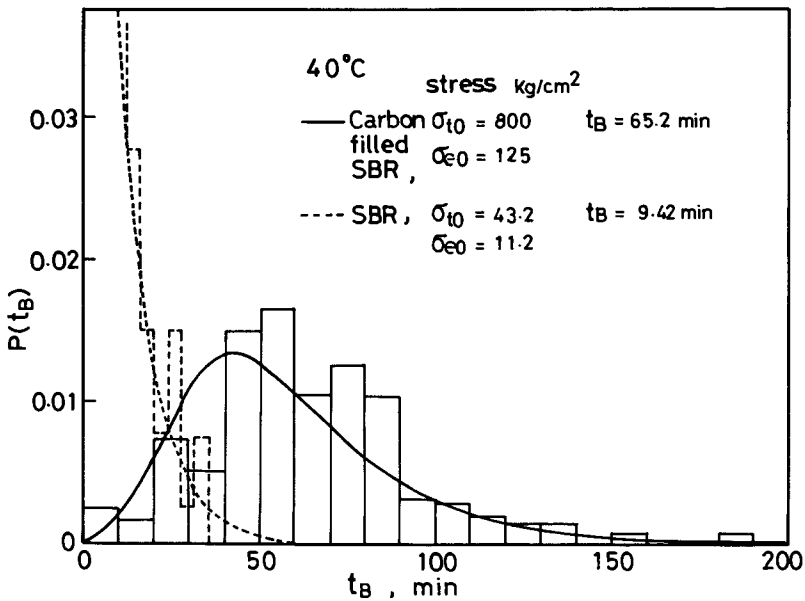

Figure 7. $P(t_B)$ for carbon-filled SBR

In Durability of Macromolecular Materials; Eby, R.;
ACS Symposium Series; American Chemical Society: Washington, DC, 1979.

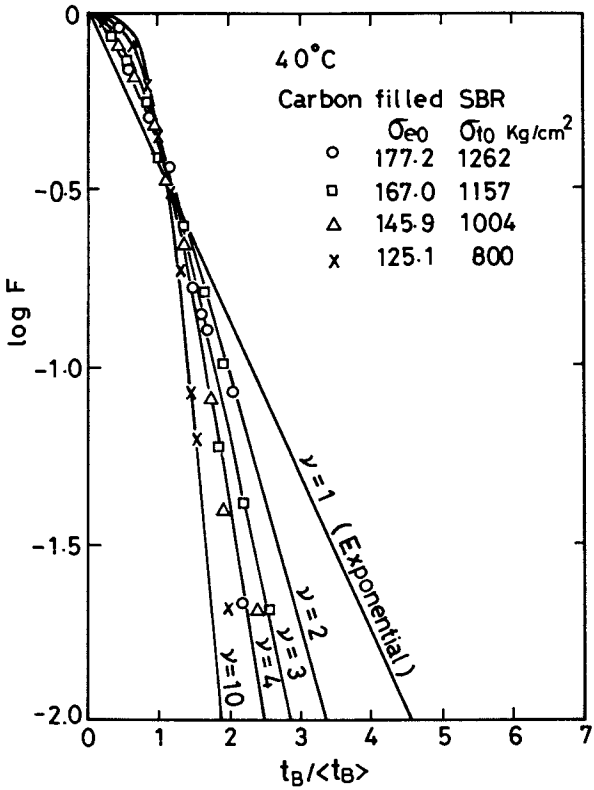

Figure 8. Plot of log F for carbon-filled SBR

In Durability of Macromolecular Materials; Eby, R.;
ACS Symposium Series; American Chemical Society: Washington, DC, 1979.

It is interesting that unimodal distributions are observed for the other filled systems. The distribution of t_B for pure NBR is shown in Figure 9 by dotted line, and the NBR PVC blend by solid line. The blend system shows clearly unimodal distribution. The type of the distribution of pure NBR, however, is biased from the exponential type as will be discussed later. It is seen that the distribution of t_B in the filled system shifts towards the unimodal.

Another example is the distribution of t_B for plasticized PVC (DOP 41 against PVC 100 pt), shown in Figure 10. This material is not filled, however, the distribution is clearly unimodal. The relation between t_B and log σ_{to} is still linear as shown in Figure 11 and $\nu=4$ is suitable for fitting the distribution as shown in Figure 10. In this case, however, we have to consider another factor affecting the t_B as shown by the dotted line in this figure, which will be discussed later.

Volume effect

According to eq(17), $\langle t_B \rangle$ is affected by the volume of the body such that $\langle t_B \rangle$ is reciprocally proportional to the volume. This effect was examined for only one case using SBR at 40°C and the result is shown in Figure 12. Line A is the relation of $\log\sigma_{to_3}$ vs $\langle t_B \rangle$ for the body of V_A=0.273 cm^3 and line B is for V_B=0.529 cm^3. The shifting of the curve on the t_B axis is nearly equal to the value estimated from eq(17),

$$shift\ on\ t_B\ axis = \frac{V_B}{V_A} = \frac{0.273}{0.529}$$

which is shown in Figure 12 by dotted line. In this experiment, the length of the specimen has changed with the cross-sectional area of specimen being constant. More experiments will be required where the different cross areas are examined for obtaining sufficient information about the volume effect.

Application of the theory to failure at constant rate extension

Based on the theory presented here, eq(9) is applicable not only to creep failure, but also to the other deformations where σ_t varies with time. If we substitute n and c which are obtained from creep failure experiments into eq(9), the $P(t_B)$ for the constant rate extension process must be described by this equation. To examine this, the constant rate extension experiment has been carried out. In constant rate uniaxial extension, stretch ratio λ is given by a function of time t as following.

$$\lambda(t) = 1 + u\,t \qquad (28)$$

where u is the strain rate. The $\sigma_t(t)$ at given $\lambda(t)$ can be measured by uniaxial constant rate extension experiment as a material property. By substituting this $\sigma_t(t)$ into eq(19), the

In Durability of Macromolecular Materials; Eby, R.;
ACS Symposium Series; American Chemical Society: Washington, DC, 1979.

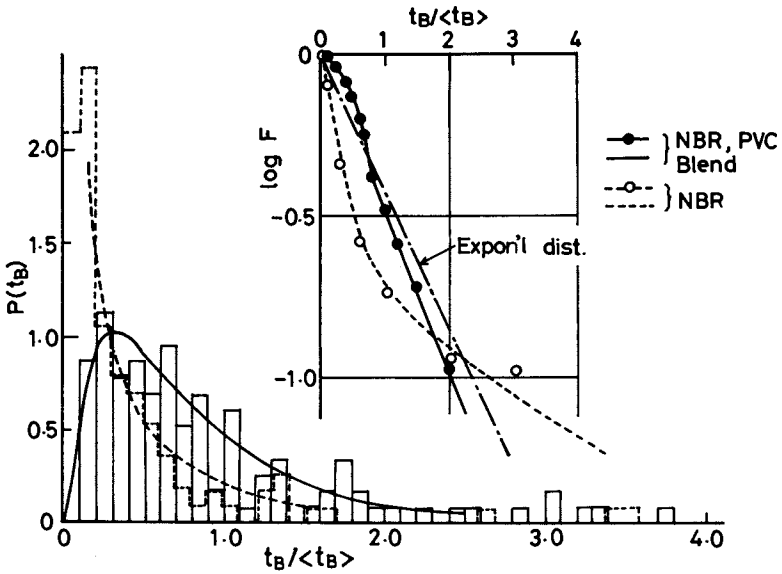

Figure 9. $P(t_B)$ and log F for each of NBR and NBR, PVC blend

In Durability of Macromolecular Materials; Eby, R.;
ACS Symposium Series; American Chemical Society: Washington, DC, 1979.

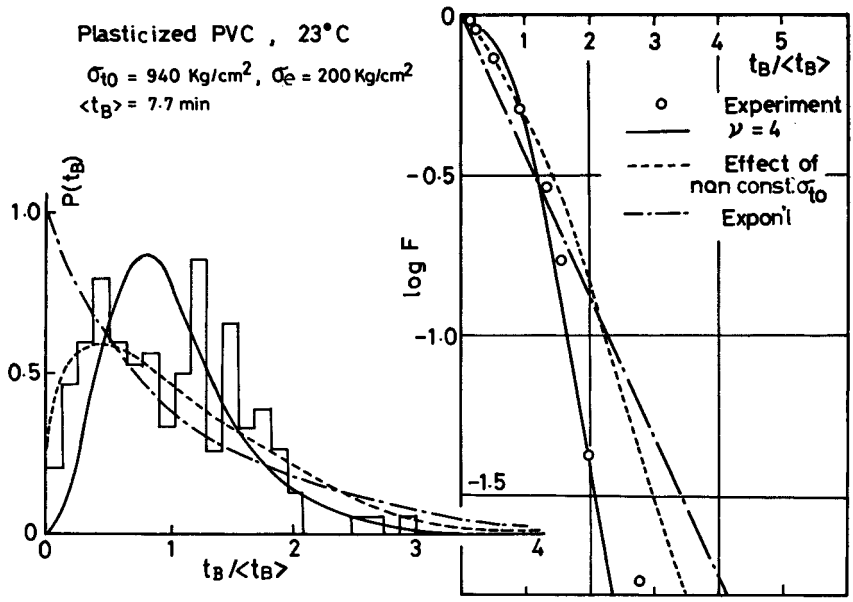

Figure 10. $P(t_B)$ and log F for plasticized PVC

In Durability of Macromolecular Materials; Eby, R.;
ACS Symposium Series; American Chemical Society: Washington, DC, 1979.

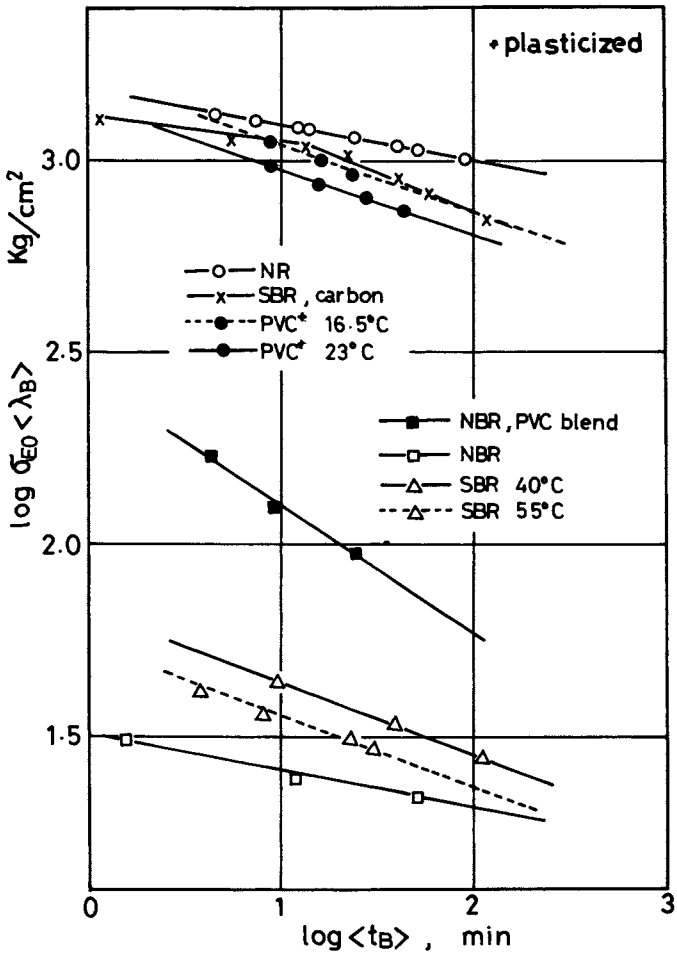

Figure 11. Plot of log σ_{t_0} vs. log $<t_B>$

In Durability of Macromolecular Materials; Eby, R.;
ACS Symposium Series; American Chemical Society: Washington, DC, 1979.

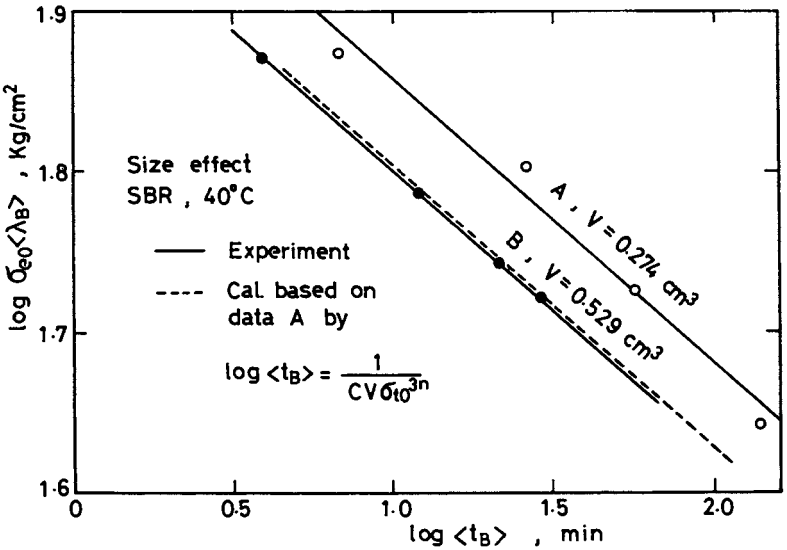

Figure 12. Size effect of specimen

In Durability of Macromolecular Materials; Eby, R.;
ACS Symposium Series; American Chemical Society: Washington, DC, 1979.

$P(t_B)$ in this case can be obtained, where the values of n and c should be known by creep failure experiments. Those constants are considered to be material parameters with respect to failure properties. We can replace the $P(t_B)$ with $P(\lambda_B)$ by using eq(28) where λ_B is the stretch ratio at failure, that is, the value of $\lambda(t)$ at $t=<t_B>$. The histogram shown in Figure 13 is the experimental result obtained for the same SBR which was used for the creep failure experiment shown already. n and c were obtained by the creep failure experiment and the distribution estimated for λ_B by eq(19) is shown by solid lines in this figure. From the figure, it is seen that good agreement is obtained. The effect of the viscoelasticity of this rubber on the stress-strain curves for those different extension rates are small in the range of the tensile rate examined in this experiment. The shifting of the distribution of λ_B by increasing rate of extension is considered to be caused by statistical reason which has been analyzed here.

Recently Shiokawa (4) traced and examined this experiment using plasticized PVC. He also has obtained good agreement between the experimental and estimated distributions of λ_B at relatively low rates of strain. At high rates of strain such as over 200% strain/sec, the experimental value of λ_B becomes smaller than the estimated one. However he compensated the temperature increase of the specimen caused by the high rate extension and tangent loss of the PVC. We again confirmed the agreement between the experiment and calculated results and found that the estimation by eq(19) is also valid for those extension rates.

Discussion

The creep experiments introduced here have been done under constant engineering stress where the stress has been translated into the true stress by multiplying λ_B by the engineering stress. We have not confirmed whether true stress used in eq(14) is warrantable or not for the expression of stressed state defined by ϕ for cross-linked materials. However we confirmed that the values of n are reduced to near 2 for many rubbery polymers except some polymers showing high molecular orientation at the critical extension. If we take true stress as the σ, then the relation $\phi \propto /\sigma_t^2$ is considered roughly to be the amount being proportional to strain energy. The particular behavior of the NR in its stress strain relation at near λ_B is the extreme orientation of molecular chains, and σ_t vs $\varepsilon(=\lambda-1)$ relation is biased from nearly linear relation as seen in the other rubbery polymers, which do not show so extreme orientation as NR. When we assume that true stress, σ_t, is a parameter which is related directly with the stressed state as used here in the theory, we have a problem that the creep experiments done here are not constant true stress creep but a constant engineering stress creep experiment, and this will disturb the simple stress history expected. That is, σ_t is not

In Durability of Macromolecular Materials; Eby, R.;
ACS Symposium Series; American Chemical Society: Washington, DC, 1979.

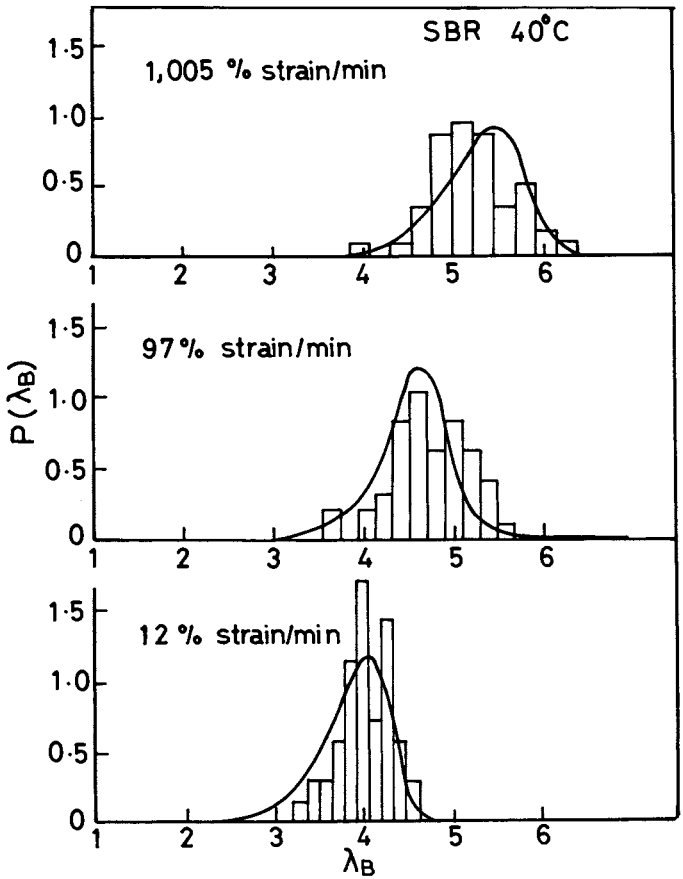

Figure 13. Distribution of breaking stretch ratio at constant rate of extension: (——), the calculated $P(\lambda_B)$ using parameters n *and* c *which were obtained by creep failure experiment.*

In Durability of Macromolecular Materials; Eby, R.;
ACS Symposium Series; American Chemical Society: Washington, DC, 1979.

constant although it changes only slowly with time. In order to examine this influence on the distribution of t_B, the effect of the movement of σ_t on $P(t_B)$ has been estimated by substituting the $\sigma_t(t)$, which is approximated as follows, into eq(19).

The creep behavior of the polymers used here is approximated by the following equations for the case of large λ. The stretch ratio λ (t) is given by

$$\lambda(t) = \lambda_o t^k \tag{29}$$

where k is a constant and, for example, k=0.0087 is obtained for SBR. $\sigma_t(t)$ is therefore given by

$$\left.\begin{aligned} \sigma_t(t) = \sigma_{eo}\,\lambda(t) &= \sigma_{eo}\lambda_o t^k \qquad \text{for } t \geq 0.1 \text{ min} \\ &= 10\,\sigma_{eo}\, t \qquad \text{for } t < 0.1 \text{ min} \end{aligned}\right\} \tag{30}$$

where σ_{eo} is a constant engineering stress and λ_o is taken as a stretch ratio at t=1 min. The σ_t before t=0.1 min is assumed to be a linearly increasing function with increasing time where σ_t=0 at t=0 from the consideration of actual experiment. Substituting eq(30) into eq(19), we can estimate the effect of the creep strain on $P(t_B)$. As seen from Figure 14, the deviation from the exponential distribution is relatively small and this deviation is within the experimental error. The value of k of filled SBR is also on the order of less than 0.02 and it is estimated that the clearly unimodal distribution obtained by the experiment as shown in Figure 7 is not caused by the effect above mentioned but by the other reasons.

Plasticized PVC, however, shows large creep strain during the observation of failure. The value of k is approximately 0.068. This value is relatively large and cannot be neglected. And it is estimated by the calculation using eq(19) that this creep strain deviates the $P(t_B)$ considerably from the exponential type to the unimodal type as shown in Figure 10 by dotted line. It is difficult to explain whether this unimodal distribution of t_B observed by the experiment depends on the non-true stress constant effect or on the crack interuption effect estimated from the theory. However the deviation observed is larger than the amount estimated from the former effect, probably, both effects may be expected. On the other hand, if we assume that engineering stress is related with the failure criterion directly instead of the true stress, the unimodal curve obtained from plasticized PVC maintains the later effect clearly.

The analysis of the difference in those $P(t_B)$ of NBR and NBR-PVC blended system shows that the effect of creep strain on $P(t_B)$ is also negligible and the difference between the distributions of t_B for those materials is considered to be the difference coming from the difference in their failure mechanisms.

In Durability of Macromolecular Materials; Eby, R.;
ACS Symposium Series; American Chemical Society: Washington, DC, 1979.

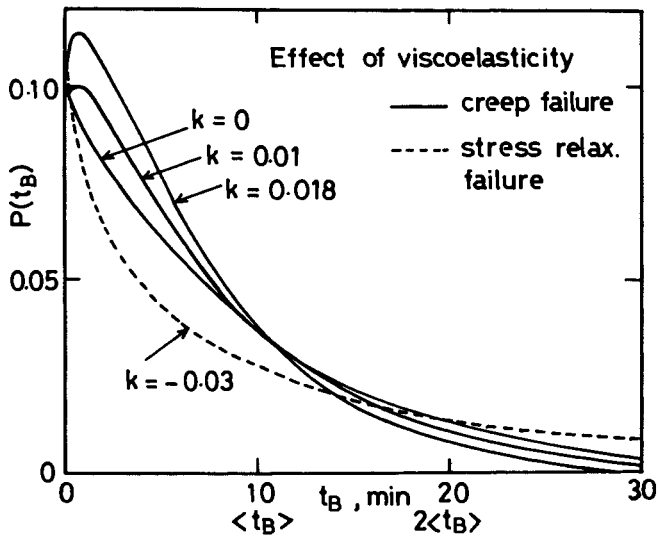

Figure 14. Effect of the increasing true stress during the creep of constant engineering stress on $P(t_B)$, which was estimated from theory

In Durability of Macromolecular Materials; Eby, R.;
ACS Symposium Series; American Chemical Society: Washington, DC, 1979.

Estimation of stress relaxation failure process

We can predict t_B for stress relaxation failure, where the failure occurs during stress relaxation process under a constant strain. From observation of rubbery polymers, we can approximate the stress relaxation behavior by following equation.

$$\sigma_t = \sigma_{to}\, t^{-k} \tag{31}$$

where k is a constant. Substituting eq(31) into eq(19) and we obtain following

$$P(t_B) = c\, V\, (\sigma_{to}\, t^{-k})^{3n} \exp\{ - c\, V \int_0^{t_B} (\sigma_{to}\, t^{-k})^{3n}\, dt\} \tag{32}$$

where σ_{to} is the true stress at t=1 min. The calculated results for k=-0.03 are shown in Figure 14 by a dotted line. In this calculation, σ_t is taken as following based on actual operation of the relaxation testing the same as in the calculation for the effect of non-true stress constant creep shown before.

$$\begin{aligned} \sigma_t &= \sigma_{to}\, t^{-k} && \text{for } t \geq 0.1 \text{ min} \\ &= 10\, \sigma_{to}\, t && \text{for } 0 < t < 0.1 \text{ min} \end{aligned} \tag{33}$$

The value of $P(t_B)$ decreases sharply with increasing t, however the probability density of long life is also increased.

Another factor deviating $P(t_B)$ from exponential type

Another factor which deviates the $P(t_B)$ from exponential distribution is the time dependence of c. For example, if the value of c depends on the creep rate, it causes the time dependence of c. If one assumes that,

$$c(t) = c_o\, (1 - e^{-\alpha t}) \tag{34}$$

then we obtain a unimodal distribution of t_B, which is very similar to the distributions obtained for the cases of $\nu > 2$ (2). We can obtain c(t) experimentally under the assumption of $\nu = 1$ from the unimodal distribution data. In another words, the case of $\nu > 2$ can be translated into the case of varing c with time under $\nu = 1$. The distribution of t_B for pure NBR obtained from the creep experiment (shown in Figure 9) suggests that there might be a possibility of decreasing c with time. This suggests that we have to consider the c(t) function as well as the crack interruption mechanism.

In Durability of Macromolecular Materials; Eby, R.;
ACS Symposium Series; American Chemical Society: Washington, DC, 1979.

Practical use of n and c

n and c introduced here are considered to be parameters which concerned with the failure property. However, from the practical point of view, the following relation is convenient to estimate the life time in creep. Eq(17) can be rewritten as

$$\langle t_B \rangle = \left(\frac{\sigma_{ts}}{\sigma_{to}} \right)^{3n} \times \min \tag{35}$$

where σ_{to} is the true stress applied in the creep process and σ_{ts} is given by

$$\sigma_{ts} = \left(\frac{1}{c\ V} \right)^{-3n} \tag{36}$$

σ_{ts} for the polymers used here are shown in Table 1 along with the parameters c and n.

Conclusion

It has been shown that the life time in the creep process of rubbery polymers scatters largeley but obeys the specified statistical distribution which are introduced theoretically based on some assumptions. Two assumptions are made here that "one crack leads the body to failure" and "the ν th crack leads the body to failure". The former assumption leads the exponential distribution of t_B, and the latter the unimodal distribution when $\nu > 2$. It has been explained from experiments that the distribution of t_B for pure rubbers of vulcanized SBR and NR are the exponential type and for filled systems the unimodal type. Theory introduced here can be applied not only to the creep failure but also to the failure process varing stress level such as uniaxial extension with constant strain rate. It has been demonstrated that the distribution of λ_B, the stretch ratio at break in the constant rate of extension, is well estimated by the theory substituting the parameters n and c which are obtained from creep failure experiment to eq(19).

The purpose of the research introduced here is to approach closely to the failure mechanism of rubbery polymers from a phenomenological view. Many of excellent observations on the time dependent failure behavior of rubbery polymers have been done by those scientists, T. L. Smith (5, 6, 7), F. Bueche (8), R. F. Landel (9), and so on during the past twenty years. The subject we have is to connect those phenomenological researches with molecular behavior or with the mechanism of failure initiation inside the materials. The author considers that the technique introduced here will be one of the useful tools for connecting those.

In Durability of Macromolecular Materials; Eby, R.;
ACS Symposium Series; American Chemical Society: Washington, DC, 1979.

Acknowledges

Author wishes to thank Mr. K. Fukumori, Mr. M. Yoneda and Mr. K. Tei, who are graduate students of Department of Polymer Chemistry, Kyoto University, for their assistance in the experiments of creep failure and the preparation of this manuscript, and also thank the Mitsubishi Monsanto Chemicals Co., Nagoya and the Nippon Zeon Co., for their assistance in preparing the samples used.

Literature cited

1. Kawabata, S. and Blatz, P. J., Rubber Chem. Technol., 39, 928 (1966)
2. Kawabata, S., Tatsuta, S. and Kawai, H., Proc. 5th Int. Congr. Rheol., 3, 111, Univ. Tokyo Press, Tokyo, 1970.
3. Wodsworth, G. P. and Bryan, G. P., "Introduction to Probability and Random Variables", MacGraw-Hill, New York, 1960.
4. Shiokawa, Y., Prepring of Ann. Meeting of Soc. Polymer Sci., Japan at Tokyo, 1974.
5. Smith, T. L., J. Polymer Sci., 32 99 (1958)
6. Smith, T. L., Trans. Soc. Rheol., 6, 61 (1962)
7. Smith, T. L., J. Polymer Sci., A1, 3597 (1963)
8. Bueche, F., J. Appl. Phys., 28, 784 (1957)
9. Landel, R. F. and Fedors, R. F., "Fracture Process in Polymeric Solids", Edited by Rosen, B., 361, John Wiley & Son, New York, 1964.

RECEIVED December 8, 1978.

Lifetime Behavior of Polyethylene Bars in Uniaxial Extension in Various Chemical Environments

J. M. CRISSMAN and L. J. ZAPAS

Polymer Science and Standards Division, National Bureau of Standards, Washington, DC 20234

In the study of the mechanical properties of amorphous materials the use of elevated temperature and solvents has provided one relatively successful means for obtaining long time behavior, i.e., long relaxation times, from short time experiments [1]. Provided the proper mechanisms can be specified, the same procedure should be applicable to semicrystalline polymers in cases where long times are required to fracture the material. In the work to be described here, fracture data will be presented for two types of polyethylene. The behavior in air at two different temperatures will be compared to that in solvent or stress-cracking agent at the same two temperatures. More specifically, creep data as a function of time up to the point of fracture were obtained under uniaxial loading for each combination of temperature and environment. We have attempted to separate out one failure mechanism arising from bond rupture which leads to crack propagation. The influence of environment on this mechanism will be demonstrated.

Experimental

Uniaxial creep experiments were carried out on two types of commercial polyethylene in the presence of various environments. One polymer, which will be designated hereafter as sample D, was a linear polyethylene having a weight-average molecular weight (M_W) of 99,000 and a nominal density of 0.966 g/cm^3. The second polymer (sample E) was an ethylene-hexene copolymer which is slightly branched, and had an M_W of 211,000 and a nominal density of 0.955 g/cm^3. Specimens approximately one millimeter thick were prepared from both polymers by molding flat sheets from which dumbbell-shaped bars were cut with a die. The sheets were molded by heating the polymer for ten minutes at 440K in a press at which time the heat was turned off and pressure applied. The polymer was then cooled in the press over

In Durability of Macromolecular Materials; Eby, R.;
ACS Symposium Series; American Chemical Society: Washington, DC, 1979.

a period of about two hours to a temperature of 360K at which time it was removed from the press.

For the creep experiments, deformation was obtained by measuring the distance between two fiducial marks placed on the straight portion of the specimen. Where the presence of an adverse environment was required, a method somewhat similar to that employed by Hittmair and Ullman [2] was used, except that no hole was introduced into the specimen, and in the present case the higher temperatures were achieved by circulating from a controlled temperature bath a mixture of ethylene glycol and water through a double walled jacket surrounding the specimen.

Two types of chemical environment were used, one was a ten percent solution in water of nonylphenoxypoly(ethyleneoxy) ethanol (hereafter to be designated as stress-cracking agent), and the other was solvent such as hexane, dodecane, or ortho-dichlorobenzene. This particular stress-cracking solution is generally regarded to be a highly aggressive surface active agent, whereas the solvents swell the polymer giving rise to triaxial stresses even in the absence of an externally applied stress. It was found that presoaking the specimens in the stress-cracking agent prior to loading had little or no influence on the time to fail, whereas in solvent a presoaking period of at least 16 hours was required in order for the time to failure to yield reproducible values. In reference [2] the results of several experiments on presoaking in the same stress-cracking agent were considered equivocal, since the data were not considered sufficiently reproducible to indicate whether or not a significant quantity of stress-cracking agent dissolved in the polymer.

Results and Discussion

Static fatigue in uniaxial loading depends highly on conditions of the ambient atmosphere. The total behavior is a summation of a variety of different mechanisms including flow, bond rupture, crack formation and propagation, which for a given material will depend upon load, temperature, and chemical environment. For simplicity, we distinguish that for a steady environment two modes of failure can occur, one as the result of an instability leading to necking, and the other arising mainly from crack growth. A possible mechanism for necking was presented in an earlier work [3,4] where it was shown that the failure envelope corresponding to necking could be predicted quantitatively. In accordance with that work, we shall refer to failure as the condition of necking and fracture as the condition where the specimen breaks into pieces. The following paper in this issue [4] describes a model which predicts necking as an instability. Based upon data obtained in our laboratory for a sample of linear polyethylene, some results will be shown which are consistent with such a model.

In Durability of Macromolecular Materials; Eby, R.;
ACS Symposium Series; American Chemical Society: Washington, DC, 1979.

In the present work, we wish to emphasize the region where brittle fracture occurs, and describe fatigue under static load conditions in uniaxial extension, both in air and other chemical environments.

As mentioned in Section II, we shall be concerned here with two samples of polyethylene, one a linear polymer, and the other an ethylene-hexene copolymer which is slightly branched and is considered to be a highly stress-crack resistant material. Presented in Figure 1 are data for log time to fail versus applied engineering stress for the linear polyethylene in air and in stress-cracking agent. In Figure 1, experimental results are shown for two temperatures. The solid lines without data points represent the behavior in air and the solid lines passing through the triangles correspond to the behavior in stress-cracking agent.

For the behavior in air, we distinguish two regions, one at stresses below about 12.5 MN/m^2, where the specimens cracked and broke, and the other at higher stresses corresponding to the regime where the specimens necked and then broke almost immediately in a ductile fashion. In a previous work [3] it was shown that, when the mechanism responsible for a viscous-like behavior is dominant, the material will enter into an unstable condition leading to neck formation and fracture. By monitoring the creep strain with respect to time, it was found that the specimens that failed by cracking cracked at strains of ten percent and below, whereas in the regime where necking is dominant, a creep strain of from 20 to 30 percent was required in order for necking to occur. It was observed that in the region where the specimens failed by cracking, the strain at fracture was nearly constant over 90 percent or more of the total time to failure. Therefore, at small loads, the material behaves for most of its lifetime as an elastic solid (strain independent of time). This behavior suggests that the mechanism of fracture can be treated in a manner similar to the behavior of glasses. Having in mind, also, the idea of additivity of damage, we found that the mechanism responsible for cracking could be represented by the relation suggested some thirty years ago by Glathart and Preston [6]. If f is the constant load and t_B is the time at which fracture occurs after loading, then the empirical relation given by them is

$$\frac{1}{f} = a + m \log t_B \qquad (1)$$

where a and m are constants which depend upon the material and temperature. With this expression, they were able to represent data covering the exceptionally large time range of 10^7 seconds. Taylor [7] attempted to derive a "mechanism of fracture of glass and similar brittle solids", which led also to equation (1). With equation (1) in mind as a possible representation of the mechanism, we have separated the total behavior into two regions by use of the relation

In Durability of Macromolecular Materials; Eby, R.;
ACS Symposium Series; American Chemical Society: Washington, DC, 1979.

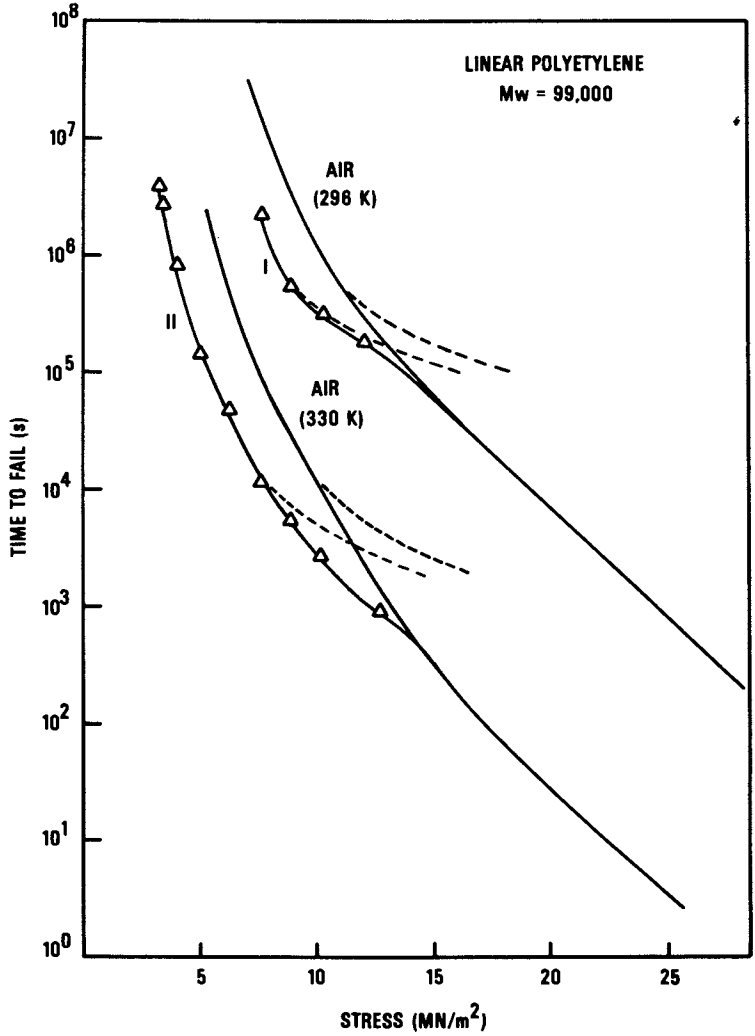

Figure 1. Log time to fail vs. applied stress for sample D: (——), time to fail in air; (—△—), time to fail in nonylphenoxypoly (ethyleneoxy) ethanol; (– – –), the extension to higher stresses of the crack growth mechanism which obeys Equation 1.

In Durability of Macromolecular Materials; Eby, R.;
ACS Symposium Series; American Chemical Society: Washington, DC, 1979.

$$1/t = \sum_j \frac{1}{t_j} \qquad (2)$$

where t is the total time for fracture or failure, and t_j is the time contributed from the j^{th} mechanism.

Since our main interest in this work lies in describing the behavior where the material fails by fracture, we choose to rewrite equation (2) as

$$\frac{1}{t} = \frac{1}{t_B} + \frac{1}{t_F},$$

where now t_B is the time contributed by the fracture mechanism, B, and t_F the time from one or more mechanisms [4] leading to necking and fracture. In Figure 1 the dotted lines represent the extension of mechanism B to higher stresses. In the absence of the other mechanisms and considering only the behavior in air it can be stated that the effect of temperature on mechanism B is simply one of translation along the time axis, equivalent to time-temperature superposition. The calculated activation energy is 124 KJ/mole. It is important to note, however, that the total time to fail curves do not superpose by simple translation along the time axis. Although not too pronounced for the data shown in Figure 1, the effect becomes more emphatic at higher temperatures. This is true, also, for other polyethylenes of different weight average molecular weight for which we have obtained data. In cases where more than one failure mechanism is present, a note of caution is appropriate with regard to using higher temperature as a means of accelerating failure. A proper lifetime prediction based on accelerated testing requires separating out each mechanism and determining their respective activation energies.

Having separated out mechanism B, our purpose was to determine the effects of various chemical environments on the total behavior. For that purpose, we have used a stress-cracking agent and also organic solvents which tend to swell the polymer. The results for the stress-cracking agent are indicated in Figure 1 as triangles. Data points obtained with stress-cracking agent at stresses higher than those shown with triangles have been omitted to avoid confusion. However, they fall on the same line as those for air indicating that at the higher stresses where the mechanism leading to necking is dominant the stress-cracking agent has no significant influence on the time to fail. For the linear polyethylene sample, the effect of stress-cracking agent at low stresses is one of a constant additive stress equal to about 2.1 MN/m^2 as shown in Figure 1. Because of this additive stress, there is no time-temperature superposition of the entire set of curves for time to fail. Due to the structure of these curves, the detrimental effect of the stress-cracking agent

In Durability of Macromolecular Materials; Eby, R.;
ACS Symposium Series; American Chemical Society: Washington, DC, 1979.

becomes more pronounced at the higher temperatures than is the case at room temperature.

If the separation into mechanisms is a valid representation, then, in the region where both are contributing equally, one would expect to see contributions from each. Experimentally, it was found that in this region, the specimens would tend to neck in one place and crack in another. Moreover, since mechanism B in the presence of stress-cracking agent is depressed in time relative to air, one would expect the specimens to crack into the region of higher stresses than is the case in air, a result that is observed experimentally.

In Figure 2 is shown the behavior of the same sample of linear polyethylene where now the specimens were obliged to creep immersed in the solvent dodecane. For the results shown, the stresses were calculated based on the dimension of the unswollen sample. In order to avoid time effects, the specimens were presoaked in the solvent for 16 hours prior to loading. Additional presoaking for longer periods of time had no appreciable influence on the final results. As can be observed, the behavior in solvent is markedly different than that in stress-cracking agent. Whereas in stress-cracking agent, only the region corresponding to mechanism B is influenced, in solvent the entire curve is significantly shifted. In solvent, the effect appears to be more nearly that of an increase in temperature. In the case of amorphous polymers, it is known [1] that a swelling agent shifts both the relaxation times and lowers the moduli. If this is true also of semicrystalline polymers, then one would expect a shift along both the time and stress axes for superposition. From Figure 2 it appears that this is the case, however, we have not attempted to superpose the curves since neither the amount of solvent present nor the values of the modulus which are needed for a quantitative test were determined. The observations here on the behavior in both stress-cracking agent and swelling agent are in agreement with the conclusions drawn previously by Suezawa et.al. [8], but in the present case, the differences in behavior stand out very clearly.

As in the case of the linear polyethylene, a quite similar behavior was found for the branched ethylene-hexene copolymer. In Figure 3 is shown a plot of log time to fail versus applied engineering stress for specimens tested in air and in stress-cracking agent. However, due to the very steep nature of the failure curve, it was not possible to separate out mechanism B at room temperature as in the case of the linear polymer. Even at times of 10^7 seconds and greater, the failure is not of the mechanism B type (cracking), and the specimens failed by necking. Since the stress-cracking agent effects mainly mechanism B, we do not expect to find significant differences in behavior in air and stress-cracking agent in the region where necking dominates, which is what is observed experimentally. It is largely this property which makes the branched polymer highly stress-crack resistant.

In Durability of Macromolecular Materials; Eby, R.;
ACS Symposium Series; American Chemical Society: Washington, DC, 1979.

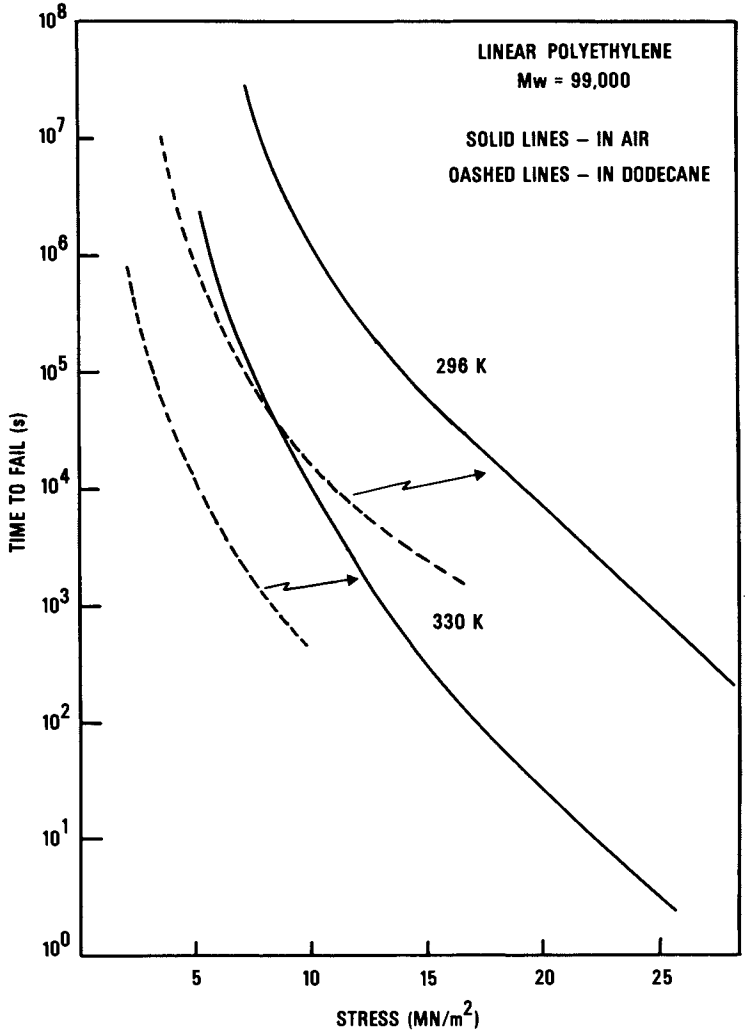

Figure 2. Log time to fail vs. applied stress for Sample D: (——), in air; (– – –), in the solvent dodecane.

In Durability of Macromolecular Materials; Eby, R.;
ACS Symposium Series; American Chemical Society: Washington, DC, 1979.

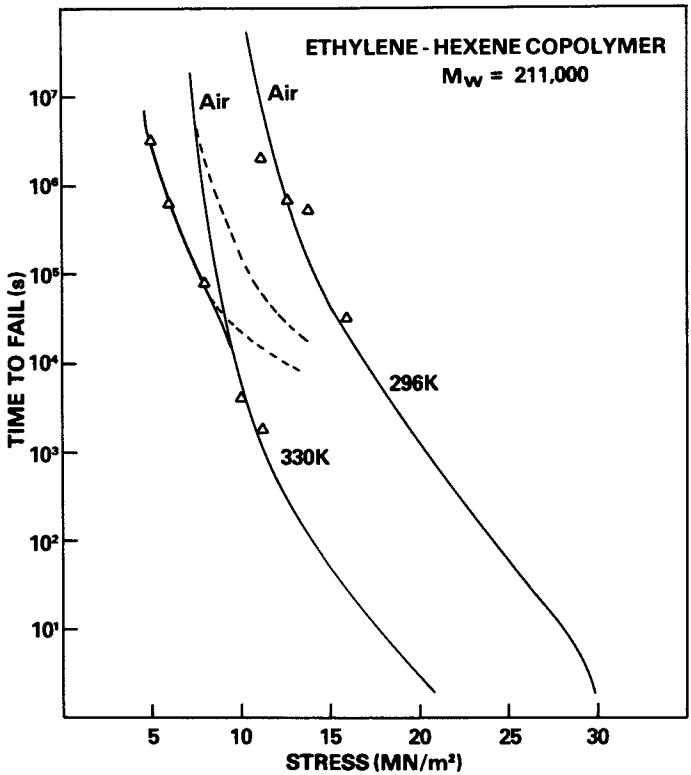

Figure 3. Log time to fail vs. applied stress for Sample E: (——), the time to fail in air; (—△—), the time to fail in stress-cracking agent; (– – –), the extension to higher stresses of the crack growth mechanism which obeys equation 1.

In Durability of Macromolecular Materials; Eby, R.;
ACS Symposium Series; American Chemical Society: Washington, DC, 1979.

However, at 330K, the region corresponding to mechanism B becomes somewhat accessible experimentally. As was true for the linear polymer, the presence of stress-cracking agent acts as an additive stress shifting the time to fail curve for mechanism B by about 2.2 MN/m^2. In Figure 3, we have indicated with dotted lines the extensions of mechanism B both in air and in stress-cracking agent. Although the data are not shown, the behavior of the branched copolymer in solvent was very much the same as for the linear polymer.

In Figure 4 is shown on a double-logarithmic plot the time to fail in solvent or stress-cracking agent versus the time to fail in air. The dashed line I with unity slope corresponds to behavior which is unaffected by the presence of either type of chemical environment. Deviations from this line represent, in some way, a relative measure of damage done due to the presence of the adverse environment. Line IV shows the behavior of the branched polymer in hexane at 296K. For this polymer, the effect of solvent is very pronounced. Lines II and III compare the behavior of the linear and branched material in stress-cracking agent at 330K. At times below about 10^4 seconds, the branched polymer shows no effect due to the presence of stress-cracking agent, while the lifetime of the linear polymer is shortened by about a factor of three at 10^4 sec. At the longer times it is interesting that the relative damage done to the branched polymer at 330K becomes much greater than for the linear polymer at the same temperature. However, this does not imply that the branched material will fail before the linear sample for the same stress, as can be seen by examination of Figures 1 and 3. The times to fail for the branched polymer in air are so much greater, for a given stress, than those for the linear polymer that even with much greater relative damage in the prsence of stress-cracking agent the branched material remains superior in terms of lifetime, at least under conditions of small loadings.

Conclusions

It has been shown for two different types of polyethylene under conditions of dead load fatigue in uniaxial extension that brittle fracture can be represented by a mechanism whose contributions become important at small loads, or very slow creep rates. This mechanism is also very much affected by the presence of stress-cracking agents. From experiments currently underway in our laboratory utilizing biaxial loading conditions, it is found that the adverse effect due to stress-cracking agent is much more emphatic than in the case of uniaxial extension. Since stress-cracking tests traditionally have been designated for short time testing, it becomes clear why the folklore came into being that stress-cracking occurred only under biaxial conditions. In solvents such as hexene or dodecane, the life-

In Durability of Macromolecular Materials; Eby, R.;
ACS Symposium Series; American Chemical Society: Washington, DC, 1979.

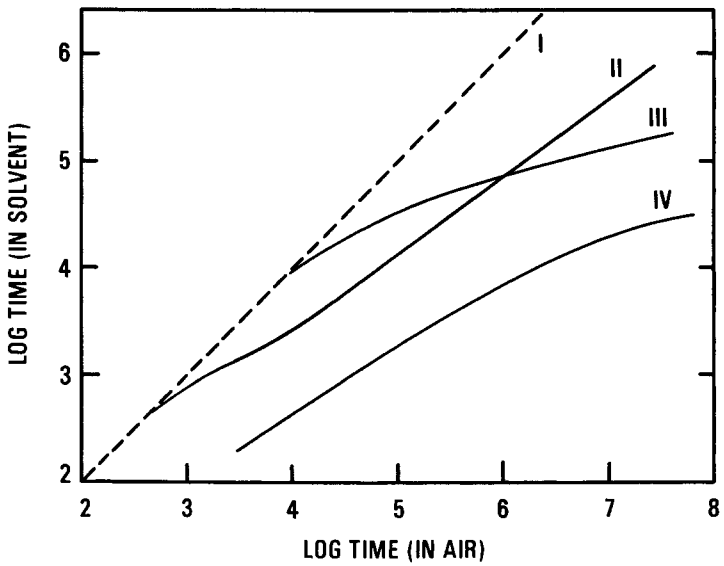

Figure 4. Log time to fail in air vs. log time to fail in the presence of chemical environment: (I) behavior equivalent to that in air; (II) linear polyethylene in nonylphenoxypoly (ethleneoxy) ethanol at 330 K; (III) branched polyethylene copolymer in nonylphenoxypoly(ethyleneoxy) ethanol at 330 K; (IV) copolymer in hexane at 296 K.

In Durability of Macromolecular Materials; Eby, R.;
ACS Symposium Series; American Chemical Society: Washington, DC, 1979.

time is shortened even more than is the case in stress-cracking liquid.

References

[1] J. D. Ferry, Viscoelastic Properties of Polymers, Chapter 17, Second Edition, John Wiley and Sons, New York, 1970.
[2] P. Hittmair and R. Ullman, J. Appl. Polymer Sci., 6, No. 19, 1 (1962).
[3] L. J. Zapas and J. M. Crissman, J. Engineering and Science, In Press.
[4] J. M. Crissman and L. J. Zapas, J. Engineering and Science, In Press.
[5] L. J. Zapas and J. M. Crissman, ACS Symposium Series: Symposium on Chemical and Physical Lifetime Limits of Macromolecular Materials. Miami, Florida, September, 1978.
[6] J. L. Glathart and F. W. Preston, J. Appl. Phys. 17, 189 (1946).
[7] N. W. Taylor, J. Appl. Phys. 18, 943 (1947).
[8] Y. Suezawa, H. Hoho, T. Ikeda, Y. Okamura, Mater. Res. Std. 5, 55 (1965).

RECEIVED December 8, 1978.

21

Stress-Strain-Time Diagrams, Including Failure Envelopes, for High-Density Polyethylenes of Different Molecular Weight

L. J. ZAPAS and J. M. CRISSMAN

Polymer Science and Standards Division, National Bureau of Standards, Washington, DC 20234

The creep behavior of polyethylene bars under uniaxial loading can be categorized as one of two types. One type occurs for relatively high stresses where after some time necking takes place as a result of plastic flow, and the other occurs for small stresses where the material fractures at small deformations due to crack formation and growth. The latter type of behavior has been discussed in the previous paper in this issue [1], where the influence of the ambient environment was also considered. In the present work, the emphasis will be on the first type of behavior, where now uniaxial creep data will be presented for several high density polyethylenes of different molecular weight. Depending upon the molecular weight, there exists a narrow region of stress for which one can obtain extension ratios of up to 25 (at 296K) before fracture occurs. The mechanical properties of the highly drawn material will also be discussed.

Experimental

High density linear polyethylenes of three different molecular weights were used in this study. Designated as samples D, A, and F, their weight average molecular weights (M_W) were 99,000, 160,000 and 192,000 respectively, while their number average molecular weights were very nearly the same, being between 15,000 and 16,000. Each polymer was molded in the form of sheets from which dumbbell-shaped specimens were cut with a die. The densities of the molded sheets, as determined with a density gradient column, were 0.969, 0.970, and 0.966 g/cm^3 respectively for samples D, A, and F. More information on the specimen preparation is given in the previous paper [1]. The creep measurements were obtained at room temperature (296 ± 1K) at constant load.

Specimens were also made by predrawing samples of polymers A and F to draw ratios between 10 and 20. The new dimensions

In Durability of Macromolecular Materials; Eby, R.;
ACS Symposium Series; American Chemical Society: Washington, DC, 1979.

were then measured and creep data obtained on the drawn material in air at temperatures ranging from 296 to 360K.

Theoretical Considerations

As mentioned already, the main consideration in this work will be the failure occurring as a result of necking during the uniaxial creep of polyethylene at relatively high loadings. Recently, Bernstein and Zapas [2] have extended the work of Ericksen [3] on the instability of elastic bars to the case of viscoelastic materials, more specifically to the class of materials which behave according to the BKZ theory [4].

Consider a bar which has a reference length L. For the case of an elastic bar, L will be taken to be the length when the bar is in a basic stress-free state. Let X be the lagrangian coordinate and x be the eulerian coordinate of each point along the bar. A motion is then stipulated by assigning the function $x = x(X,t)$ for $0 \leq X \leq L$ and for an interval of time t. The extension ratio λ is defined by $\lambda = \partial x/\partial X$. For an elastic bar, there is a strain energy density function $W(\lambda)$ giving the energy per unit length, so that pointwise the engineering stress σ is given by $\sigma = W'(\lambda)$, where the prime indicates differentiation with respect to the argument λ. In the case of a viscoelastic material which obeys the BKZ theory, the situation is similar, but with a time dependence such that the strain energy density function $w(\lambda,t)$ depends on both extension ratio and time.

Consider a viscoelastic bar which has been at rest at all times up to $t = 0$. The deformation history of a point X then can be represented by the function

$$\mu(X,\tau) = \frac{\partial x(X,\tau)}{dX}, \text{ for } \tau < t.$$

For convenience, we shall leave the dependence of μ on X understood and, following the BKZ theory, write the engineering stress at a time t as the following:

$$\sigma(X) = w'(\mu(t),t) - \int_0^t \frac{1}{\mu(\tau)} w_*' \left(\frac{\mu(t)}{\mu(\tau)}, t-\tau\right) d\tau, \qquad (1)$$

where $\mu(t) \equiv \lambda(t)$. In equation (1) the symbols prime and star now have the meaning of differentiation with respect to the first and second arguments respectively. Bernstein and Zapas introduced the quantity $\tilde{w}(\lambda,t;\mu(\tau))$ which at a given X is a function of λ and t as well as a functional of $\mu(\tau)$ for $\tau < t$. The derivative of $\tilde{w}$ with respect to λ at fixed t and $\mu(\tau)$, for $\tau < t$, gives according to the BKZ theory equation (1), where $\mu(t) = \lambda$. For values of λ which are different than $\mu(t)$ one obtains

In Durability of Macromolecular Materials; Eby, R.;
ACS Symposium Series; American Chemical Society: Washington, DC, 1979.

$$\sigma_J(\lambda,t) = w'(\lambda,t) - \int_0^t \frac{1}{\mu(\tau)}\, w_*'\left(\frac{\lambda}{\mu(\tau)},\, t-\tau\right) d\tau. \quad (2)$$

Equation (2) gives the stress to which the material will respond if, following a strain history $\mu(\tau)$, the strain was forced to take a value λ at a time t. For this reason, Bernstein and Zapas choose to refer to the curve $\sigma_J(\lambda,t)$ versus λ as the "jump curve" at time t.

For the case of creep in uniaxial loading, the material is at rest up to time $\tau = 0$ and then under constant load proceeds to deform, the deformation history being given by $\mu(\tau)$. At any time $t > \tau$ we can construct the jump curve $\sigma_J(\lambda,t)$. Consider the situation depicted in Figure 1. If σ_0 is the load divided by the undistorted (or initial) cross-sectional area, then the horizontal line passing through σ_0 will separate the jump curve into two sectional areas A_1 and A_2, as shown in Figure 1. Following Ericksen's work [3] Bernstein and Zapas have shown that if A_1 is larger than A_2, then the deformation at λ_1 is stable with respect to all disturbances. However, if A_1 is smaller than A_2, then λ_1 is unstable and part of the bar will have a stretch of λ_1 and the rest λ_2. The interesting point is when $A_1 = A_2$, since at that time and strain the material is at the insipient point of necking. For a viscoelastic material, it is easy to show that if the creep proceeds beyond the insipient point of necking, then A_2 becomes larger than A_1. A complete mathematical description of this work will appear in a forthcoming publication. As pointed out by Ericksen, this instability is analogous to that occurring on van der Waal's fluid. However, for viscoelastic materials, the instability depends not only on the stress, but also on the time.

Results and Discussion

As stated earlier, the emphasis of this work will be (1) on the instability occurring under uniaxial loading at relatively high stresses, and (2) the behavior after necking has started up until fracture occurs. In an earlier work [5] we had shown that one can obtain an instability using the BKZ theory, and further the failure envelope corresponding to necking could be described quantitatively. With the same data obtained from single step stress-relaxation experiments in uniaxial extension values of $w'(\lambda,t)$ were calculated for λ up to 1.08 and times up to 10^4 sec. This was accomplished by using equation (1) and the relation $w'(1,t) = 0$, which follows from the BKZ theory. From the single step stress-relaxation experiments, it was found that the function $w'(\lambda,t)$ could be separated into a product, $w'(\lambda,t) = f(\lambda)E(t)$. On the assumption that the

In Durability of Macromolecular Materials; Eby, R.;
ACS Symposium Series; American Chemical Society: Washington, DC, 1979.

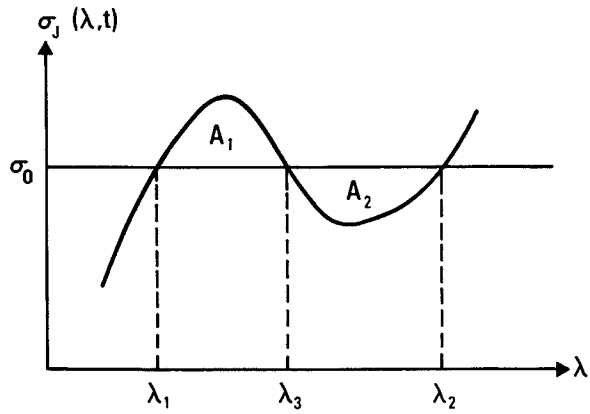

Figure 1. Schematic of a jump curve $\tilde{w}' = \sigma_J(\lambda,t)$ at time t: σ_0 is the engineering stress; λ_1 and λ_2 are possible equilibrium extension ratios corresponding to σ_0; and A_1 and A_2 are the areas of interest.

In Durability of Macromolecular Materials; Eby, R.;
ACS Symposium Series; American Chemical Society: Washington, DC, 1979.

function $w'(\lambda,t)$ can further be represented as

$$w'(\lambda,t) = f_1(\lambda)E_1(t) + f_2(\lambda)E_2(t), \quad (3)$$

where $E_1(t)$ is the modulus at small deformations and $E_2(t)$ that of the drawn phase, examples were constructed which led to the description of the necking process. Moreover, by using the inverse procedure, that is knowing the experimental values for the envelope of instability, we were able to construct the surface for $w'(\lambda,t)$ for values of λ up to 8. The above description led us to plot our creep data in terms of isochrones. Because of the high values of strain which the material achieves in the fully drawn state, the data are plotted semilogarithmically as shown in Figures 2, 3, and 4. Shown in Figure 2 is the behavior for sample A (M_W = 160,000). We distinguish three regions bounded by the lines α, β, and γ. Line γ represents the envelope for fracture. Below α is the region in which the material deforms homogeneously. Between lines α and β lies the region corresponding to the coexistence of the two phases (i.e., both necked and unnecked material), and above β is the third region where, again, the material deforms homogeneously as one phase until it breaks. It is interesting to point out that for this material there is a very narrow region of loads for which one can obtain highly strained material at room temperature. The maximum draw ratio obtained was 24. For engineering stresses below 10 MN/m^2 the specimens fracture without necking by a mechanism of crack formation and growth described in the previous paper. In Figure 3 is shown the behavior of sample F (M_W = 192,000). The main differences between this polymer and sample A are that the breadth of the highly drawn region becomes much greater, and the maximum extension ratio attainable at room temperature is slightly lower, (λ = 19).

In Figure 4 the behavior of sample D (M_W = 99,000) is shown, where now only one region exists. The reason is that at loads above 13.5 MN/m^2 the material necks and then breaks almost immediately. Below stresses of 12.5 MN/m^2 the material shows brittle fracture. It appears from these observations that the lack of a high molecular weight tail in the molecular weight distribution is responsible for the absence of the other two regions.

For sample A, after reaching the condition described by the region above line β (see Figure 2), the load was removed and the specimen allowed to relax. A recovery of about 3 percent of the final elongation was observed. Creep measurements were then made on this drawn material at room temperature and high temperatures. At 363K and a load of 88 MN/m^2 the elongation (ε) at 720 seconds was 0.83, so that the total elongation based on the initially undrawn material was 33 (λ = 34). Similar behavior was observed from experiments on sample F. This shows that at room temperature the specimens break considerably below the region where the

In Durability of Macromolecular Materials; Eby, R.;
ACS Symposium Series; American Chemical Society: Washington, DC, 1979.

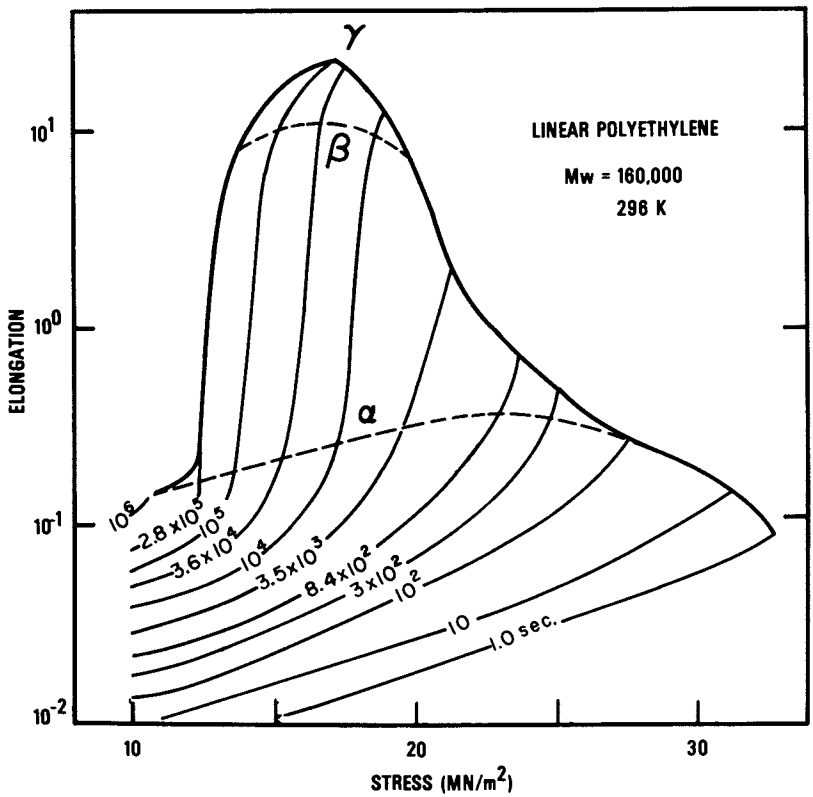

Figure 2. Failure envelope for Sample A. Log percent elongation vs. log stress (engineering) for various isochrones obtained from creep data. Line α corresponds to necking, line β to the fully necked condition, and line γ to fracture.

In Durability of Macromolecular Materials; Eby, R.;
ACS Symposium Series; American Chemical Society: Washington, DC, 1979.

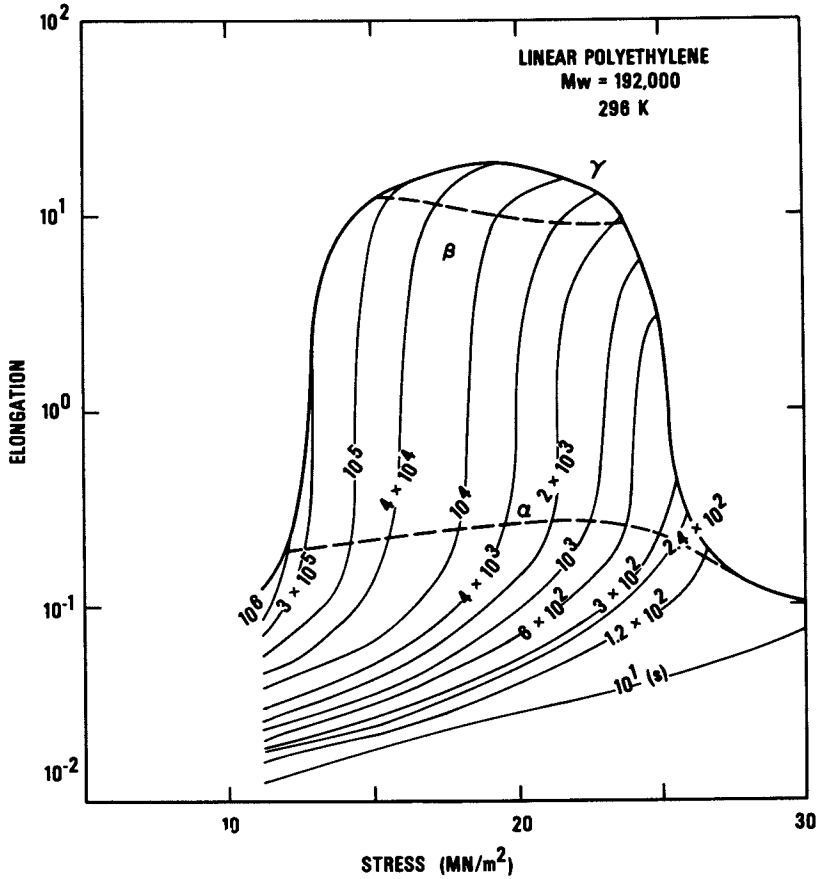

Figure 3. Failure envelope for Sample D. Log percent elongation vs. log stress (engineering) for various isochrones obtained from creep data. Symbols have the same meaning as in Figure 2.

In Durability of Macromolecular Materials; Eby, R.;
ACS Symposium Series; American Chemical Society: Washington, DC, 1979.

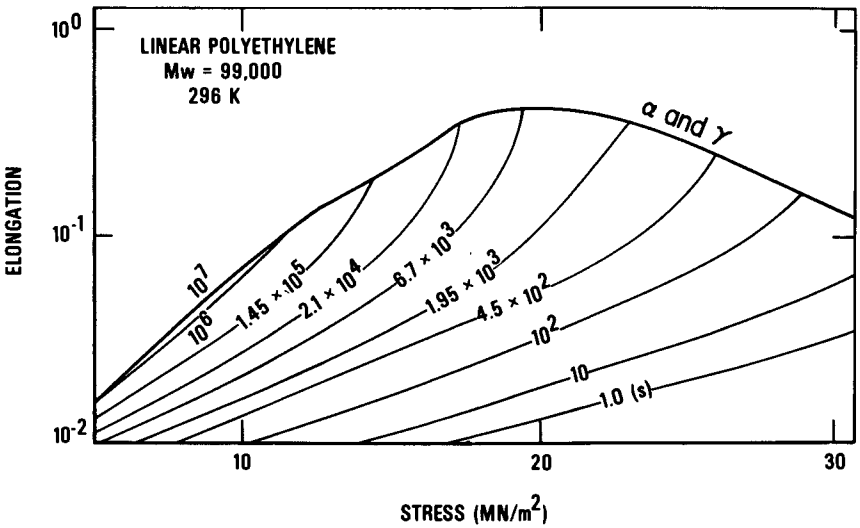

Figure 4. Failure envelope for Sample F. Log percent elongation vs. log stress (engineering) for various isochrones obtained from creep data. Symbols have the same meaning as in Figure 2.

In Durability of Macromolecular Materials; Eby, R.;
ACS Symposium Series; American Chemical Society: Washington, DC, 1979.

highest possible alignment of the tie molecules occurs. The above results appear to us to strengthen the validity of the model presented in section III. The idea of a multiplicity of moduli corresponding to the various states of deformation is a natural one. The existence of the two regions in which the material deforms homogeneously, though not shown explicitly in section III, is predicted from the model. Another interesting consequence of this model is that for small loads where the creep curves tend to level to a nearly constant deformation, the jump curve $\sigma_J(\lambda,t)$ shows that instability can not occur since the level of strain is very small. In this case, necking does not occur, however, the sample, given enough time, will fracture by the mechanism described in the previous paper [1].

It is not evident, without the proper biaxial data, that materials which show this instability in uniaxial extension, will also show a similar instability in biaxial deformation.

From experiments in our laboratory on biaxial deformations of thin sheets, it is found that in some materials cracks are formed without any evidence of necking, while at the same levels of strain in uniaxial extension necking had already occurred. This is not surprising since the potential function w depends on the strain invariants and for biaxial experiments, the solution given in section III has to be modified because the strain potential now has to be differentiated with respect to the first and second strain invariants. More work in biaxial deformations will lead to a better description of the failure mechanism in general.

References

[1] Preceding paper in this same issue.
[2] B. Bernstein and L. J. Zapas, unpublished result.
[3] J. L. Ericksen, J. Elasticity 5, Nos. 3 and 4, 191 (1975).
[4] B. Bernstein, E. A. Kearsley, and L. J. Zapas, Trans. Soc. Rheol. 7, 391 (1963).
[5] L. J. Zapas and J. M. Crissman, ACS Preprints, Symposium on Fracture Mechanics of Polymers, Anaheim, CA, March 1978.

RECEIVED December 8, 1978.

22

Fatigue Crack Propagation in PVC: Combined Effects of Rubbery Inclusions and Molecular Weight

M. D. SKIBO[1], J. A. MANSON, S. M. WEBLER, and R. W. HERTZBERG
Materials Research Center, Lehigh University, Bethlehem, PA 18015

E. A. COLLINS[2]
B. F. Goodrich Chemical Co., Avon Lake, OH 44012

This paper addresses three topics of current scientific and technological interest: poly(vinyl chloride) (PVC); toughening of brittle or ductile but notch-sensitive polymers by the inclusion of rubbery phases; and the kinetics of fatigue crack propagation (FCP).

The research described below is part of an extensive fundamental program on the effects of polymer structure, composition, and morphology on FCP in a wide range of polymers (1-11), from highly crystalline (e.g., polyamides) or mesomorphic (e.g., PVC) polymers, to typically glassy ones (e.g., acrylics). Within this program, PVC has been selected for special attention because of its interesting range of structural and compositional features (e.g., states of order, tacticity, and effects of second phases), and because of its technological importance.

The first paper in this series describes results of continued research on the effects of molecular weight (M) on FCP response (12). This paper describes and discusses results obtained in a study of the effects of a rubbery phase on the impact strength and FCP behavior of a series of PVC matrixes comprising a range of different molecular weights. It will be shown that combined effects of M with elastomer content — in this case, a methacrylate-butadiene-styrene (MBS) copolymer — lead to interesting FCP behavior. Additional results will be discussed in future papers, as well as results of current studies on the effects of other structural and compositional factors.

FCP in Polymers. Most, if not all, artifacts fabricated from plastics contain inherent flaws that may, if appropriate load criteria are met, propagate through the specimen and result in catastrophic failure (1,13,14), often at inconvenient times and places. Cyclic or repetitive loading (fatigue) can be especially insidious, for failure can occur at loads that are well

[1] Current address: Sandia Labs, Livermore, CA 94550
[2] Current address: Diamond Shamrock Corp., Painesville, OH 44077

0-8412-0485-3/79/47-095-311$05.00/0

In Durability of Macromolecular Materials; Eby, R.;
ACS Symposium Series; American Chemical Society: Washington, DC, 1979.

below those corresponding to the static yield or fracture stress. Since many polymers in service are in fact subjected to cyclic loads of some kind, fundamental understanding of the fatigue process is thus of engineering as well as scientific interest. In particular, it is beginning to be recognized that, contrary to earlier beliefs, much, and often most, of the fatigue life is spent in propagation of a preexistent flaw, rather than in the initiation of crack growth (15).

To characterize the rate of FCP, it is convenient to relate the rate of crack growth per cycle, da/dN, to ΔK, the range of the stress intensity factor at the crack tip. The following equation (16) has been found to be useful for many polymers (1):

$$\frac{da}{dN} = A\Delta K^n \tag{1}$$

When A and n are constants (at least over a range of ΔK). The stress intensity factor, ΔK, is itself a function of geometry, applied stress, Δσ, and crack length, a (17):

$$\Delta K = Y\Delta\sigma\sqrt{a} \tag{2}$$

where Y takes account of the specimen geometry (see below).

In previous studies by others (18,19) and by this group (8, 9) it was shown that equation 1 served well to describe the behavior of typical PVC's. Studies by this group also demonstrated a remarkable and unexpected effect of M on FCP, both in poly (methyl methacrylate) (PMMA) and PVC (2,3,9). It was also shown that PVC tended to fail by a discontinuous crack growth mechanism. This process comprises progressive growth, during many cycles, of a craze ahead of the crack to a characteristic length, followed by striking through of the crack in one cycle, and reinitiation of the progressive craze growth (4,8).

The question of toughening polymers (especially against impact loading) by the judicious incorporation of rubbery phases has also received much attention in recent years (see, for example, references 20, 21, and 22). Depending on the concentration, state of subdivision, and properties of the elastomer *per se*, various toughening mechanisms have been proposed and, in some cases, demonstrated. For example, the stimulation of localized crazing and shear yielding in the matrix, and the reduction of triaxiality at a crack tip, undoubtedly play significant roles in toughening, at least under many common loading conditions. However, much more attention has been given to the effects of static than to cyclic stresses. Also, perusal of the literature (see, for example, reference 20, pp. 313) reveals that few studies of the effects of rubber have involved the use of a constant-M matrix when the rubber concentration is varied. Our own earlier studies showing an apparently beneficial role of a rubbery phase (1,10,11) are no exception.

In Durability of Macromolecular Materials; Eby, R.;
ACS Symposium Series; American Chemical Society: Washington, DC, 1979.

Now the incorporation of rubbery phases in PVC is of particular interest, for, as pointed out by Bucknall (20, p. 299), maximum toughening by the addition of rubbery phases is obtained when the matrix is itself ductile, as is the case with PVC. Evidence suggests that the rubbery inclusions induce a high degree of shear yielding in the matrix, resulting in a lessening of notch sensitivity characteristic of such matrixes, and a dramatic increase in fracture energy. Certainly polyblending of elastomers with brittle polymers does seem to improve fatigue resistance to some degree, though not to as high a level as would be desirable (23); greater improvements are seen with crystalline and ductile polymers such as polyamides (24). This paper, then, addresses two specific questions: (1) are the dramatically high values of impact strength in toughened PVC carried over into fatigue? and (2) how does the M of the matrix interact with the rubber added? A third quesion, the mechanism of FCP in this system will be dealt with in detail separately.

Experimental

Materials. The PVC resins used were characterized by measurements of intrinsic viscosity ([η]) in cyclohexanone at 30°C. Values of [η] are given in Tables I and II, along with values of weight-average molecular weight, M_w, estimated from a calibration curve of [η] vs. M_w developed for an earlier series of PVC specimens (9). The methacrylate-butadiene-styrene (MBS) modifier used was grade BTA III N, supplied by the Mitsui Co., New York. Particle sizes ranged mainly between 500Å and 750Å (50 and 75 nm), with a fraction in the range of 2000Å to 2500Å (200 to 250 nm). Five different M's were selected for the matrix resins; each was blended with 0 parts per hundred of MBS (phr), 6 phr, 10 phr, and 14 phr. The two highest-M samples were milled at 340°F (171°C); the other samples were milled at 300°F (149°C). Stock temperatures ranged between 360°F (182°C) and 390°F (199°C), depending on the resin and modifier level. The milled samples were pressed at 400°F (204°C) [the highest-M samples] or 350°F (177°C) [the lower-M samples).

Characterization by DMS and DSC. Although characterization of small-strain viscoelastic and stress-strain behavior is not yet complete, preliminary dynamic mechanical spectroscopy (DMS) and differential scanning calorimetry (DSC) data were obtained for the blends having the highest and lowest molecular weights.

To obtain dynamic mechanical spectra, a Rheovibron unit (Toyo Instrument Co.), model DDV II, was used. The instrument was run at a frequency of 110 Hz. with a heating rate of one °C per minute. Glass transition temperatures, T_g, were determined by locating the maxima of the principal peaks in the loss modulus (E''_{max}) as a function of temperature. DSC curves were obtained using a Perkin Elmer instrument, model DSC 1B, at a heating rate

In Durability of Macromolecular Materials; Eby, R.;
ACS Symposium Series; American Chemical Society: Washington, DC, 1979.

Table I. Characteristics of the PVC Polyblends Studied

Specimen	$[\eta]^a$	$M_w{}^b$ x10^{-5}	phr MBS	Av. T_g, °C (by DMS)[c]	Av. T_g, °C (by DSC)[d]
131-1	0.54	0.67	0	101[e]	67
131-2	0.54	0.67	6	--	66
131-3	0.54	0.67	10	--	67
131-4	0.54	0.67	14	93	67
135-1	1.09	2.08	0	100(±3)	72
135-2	1.09	2.08	6	98(±3)	71
135-3	1.09	2.08	10	95	72
135-4	1.09	2.08	14	101(±7)	72

[a] Matrix resin in cyclohexanone at 30°C.

[b] From a calibration curve of $[\eta]$ vs. values of M_w obtained earlier (9).

[c] Dynamic mechanical spectroscopy, 110 Hz.

[d] Differential scanning calorimetry, at a rate of 10°C/min.

[e] Anomalously high.

of 10°C/min. The T_g values were taken to correspond to the mid-point of the transition in the curve.

Impact Strength. Values of notched impact strength were determined using notched specimens and an Izod tester following the ASTM procedure D256.

Fatigue Measurements. Specimens for determination of FCP behavior were cut in the form of compact tension (CT) coupons, with dimensions 0.64 cm x 7.5 cm x 7.5 cm. Specimens were cut in the machine direction, with the exception of one intermediate-M sample of unmodified PVC, 133-1. [The possible effect of this variation is under study, though the FCP rate was consistent with previous data (9).] Edge notches were introduced by first machining to a depth of ∿1.2 cm and then cutting with a razor blade. Testing was performed in the tension-tension mode as described previously (4) under ambient conditions at 10 Hz with a load ratio R of 0.1 (R = minimum load/maximum load). The progress of the crack was observed using a travelling microscope and the crack length was obtained as a function of load cycles ΔN. The FCP rate, da/dN, was then computed as a function of ΔK, using equation 2 and the following expression for the geometrical factor, Y:

$$Y = 29.6-185.5(a/w)+655.7(a/w)^2-1017(a/w)^3+638.9(a/w)^4 \quad (3)$$

Attempts were made to measure the fracture toughness, K_c (a measure of fracture energy), by determining ΔK_{max}, the maximum value

In Durability of Macromolecular Materials; Eby, R.;
ACS Symposium Series; American Chemical Society: Washington, DC, 1979.

Table II. Impact and FCP Response of PVC Polyblends

Specimen	[η]	Matrix M_w, x10^{-5}	phr MBS	$\frac{IS}{(IS_o)_o}$ [a]	$\left(\frac{IS}{IS_o}\right)$ [b]	$(\dot{a}_k/\dot{a}_{ko})$ [c]	K_c, MPa$\sqrt{m}$
131-1	0.54	0.67	0	1.0	1.0	1.0	1.0
131-2	0.54	0.67	6	1.2	1.2	2.5×10^{-2}	3.2
131-3	0.54	0.67	10	1.9	1.9	2.2×10^{-2}	---
131-4	0.54	0.67	14	4.4	4.4	2.5×10^{-2}	---
132-1	0.67	0.95	0	1.4	1.0	1.0	2.0
132-2	0.67	0.95	6	1.5	1.1	0.2	2.1
132-3	0.67	0.95	10	3.0	2.1	0.2	---
132-4	0.67	0.95	14	40	29	0.2	---
133-1	0.78	1.14	0	1.4	1.0	1.0	1.4
133-2	0.78	1.14	6	3.8	2.7	0.5	---
133-3	0.78	1.14	10	50	36	0.7	---
133-4	0.78	1.14	14	65	46	0.9	---
134-1	0.95	1.69	0	1.5	1.0	1.0	1.4
134-2	0.95	1.69	6	4.8	3.2	0.36	---
134-3	0.95	1.69	10	53	36	0.6	---
134-4	0.95	1.69	14	60	40	0.8	---
135-1	1.09	2.08	0	1.9	1.0	1.0	1.8
135-2	1.09	2.08	6	7.4	3.9	0.2	---
135-3	1.09	2.08	10	54	28	0.2	---
135-4	1.09	2.08	14	65	34	0.2	---

[a] Note that these values correct a numerical error in the data for the 131 series in ref. 10, and that values are taken as relative to the value for the lowest-M specimen, 131-1.

[b] Impact strength relative to the impact strength of the control specimen.

[c] Value of da/dN relative to da/dN for the control specimen; comparison at $\Delta K = 0.9$ times ΔK_{max} for the control specimen.

In Durability of Macromolecular Materials; Eby, R.;
ACS Symposium Series; American Chemical Society: Washington, DC, 1979.

observed for ΔK prior to catastrophic fracture, but except for the controls and for specimens having both low M's and low rubber contents (131-2 and 132-2) brittle failure was not observed. For the specimens that did exhibit brittle failure, K_c was estimated as before (2,9), by dividing ΔK_{max} by 0.9 (to account for the value of 0.1 selected for R).

Fracture Surface Morphology. Although full details will be published separately, preliminary observations of fracture surface morphology were made on an ETEC scanning electron microscope, using specimens that had been coated with gold and carbon prior to examination.

Results and Discussion

Characterization by DMS and DSC. Preliminary dynamic mechanical spectra for MBS rubber modified PVC samples showed no consistent dependence of T_g, or of the transition slope, on rubber content (Table I). Typical spectra for high-M PVC with 0 phr and 14 phr MBS modifier are shown in Fig. 1. It may be noted that, in contrast to prior experience with many polymers, reproducibility of spectra was not as good as expected, especially with specimens of sample 135-4, the sample having the highest molecular weight and the highest rubber content. This may reflect greater inhomogeneity in these specimens. Also, the T_g found for specimen 131-1 appears to be anomalous [higher than expected based on the value of M and, after allowance for differences in testing rate, on values of T_g found by DSC (see Table I)]. In general, each specimen exhibited a broad asymetrical secondary peak in E'' spanning the range from -100°C to 40°C. The shape of this peak and the slope of the T_g curve did not depend on rubber content. Since the percentage of butadiene in the MBS modifier is relatively low and since the T_g probably falls within the temperature range of the secondary transition for PVC (20, pp. 115 and 292), it is not surprising that no significant effect of MBS content is seen at the levels present in these specimens. Thus, so far these results are consistent with those expected for a relatively incompatible system (see references 24 and 25, Ch. 3) in which a modifier is present at relatively low concentration (i.e., relative to the concentrations of pure elastomer in the curves shown in reference 24) and in which a broad secondary transition is characteristic of the matrix.

The relative constancy of T_g was confirmed by the DSC measurements (see Table I and Fig. 2). The DSC measurements also indicated an expected slight dependence of T_g on molecular weight, with T_g increasing from ∿67°C for $M_w = 6.7 \times 10^4$ to ∿72°C for $M_w = 2.08 \times 10^5$. While these values are lower than values quoted for similar values of M (26), the heating rate was also lower (10°C/min instead of 32°C/min); the ∿5°C difference is consistent with results of other measurements (27).

In Durability of Macromolecular Materials; Eby, R.;
ACS Symposium Series; American Chemical Society: Washington, DC, 1979.

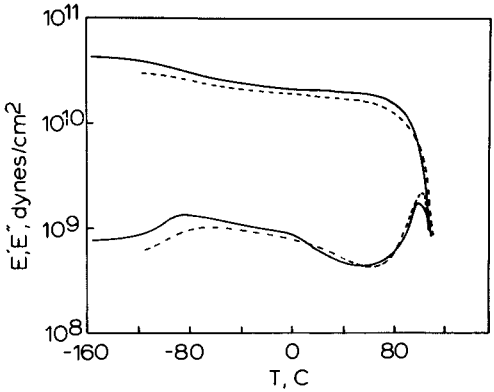

Figure 1. Dynamic mechanical spectra of (– – –), control and (——), MBS-modified PVC (M_w of matrix = 2.08 × 10^5; (– – –), phr MBS = 0 and (——), 14; frequency = 110 Hz)

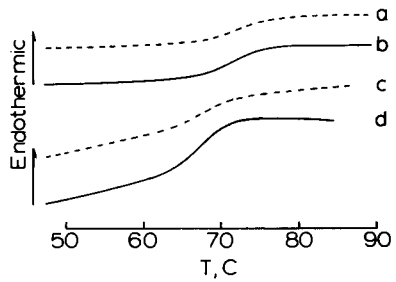

Figure 2. DSC traces for two pairs of control and MBS-modified PVC. Pair a and b displaced from pair c and d for better display. Compositions: (a) M_w = 2.08 × 10^5, 0 phr MBS; (b) M_w = 2.08 × 10^5, 14 phr MBS; (c) M_w = 6.7 × 10^4, 0 phr MBS; (d) M_w = 6.7 × 10^4, 14 phr MBS.

In Durability of Macromolecular Materials; Eby, R.;
ACS Symposium Series; American Chemical Society: Washington, DC, 1979.

Results of the more detailed characterization in progress will be reported separately, along with results of stress-strain and creep behavior.

Impact Strength. As shown in Fig. 3 and Table II, impact strength is increased by the incorporation of MBS at all levels of molecular weight. However, the relative effects depend strongly on both M and MBS content. Thus with 0 phr and 6 phr MBS, values of impact strength are increased twofold and sixfold, respectively as M increases from 0.67×10^5 to 2.08×10^5 (see values of $IS/(IS_o)_o$ in Table II). At higher MBS contents, the effects are much more dramatic, with values of impact strength for specimens containing 10 phr and 14 phr MBS increasing by factors of 28 and 34, respectively, over the same range of M. It is interesting that the general trend of impact strength with respect to modifier concentration is consistent with that noted by Petrich (28) for MBS-modified PVC as a function of temperature. In his case, the addition of modifier had the same effect as raising the temperature; the MBS induced a brittle-ductile transition. In our case, at a modifier level of 6 phr, the lower-M materials are brittle (cf. observations of K_c behavior noted above); as M is increased, failure becomes more ductile. At a modifier level of $\geq$10 phr, however, the temperature of the brittle-ductile transition is clearly >20°C (28) for all specimens, regardless of M.

At the same time (see Fig. 4), the impact strength (at a given M) relative to that of the unmodified control resin (IS/IS_o) appears to pass through a slight maximum at $1 \times 10^5 < M < \sim 1.5 \times 10^5$ for specimens with MBS contents $\geq$10 phr. (Values of IS/IS_o do, however, increase with modifier content at all values of M, as mentioned above.)

Thus at some critical value of MBS content (>6 phr), the impact strength exhibits a significant increase. This is consistent with arguments advanced by Petrich (28), Bucknall (20, ch. 10) and Deanin and Moshar (29): that the inclusion of an elastomeric phase in PVC reduces PVC's inherent notch sensitivity and permits the taking advantage of PVC's inherent ductility by stimulating a high degree of shear yielding. It is also suggested (20, ch. 10) that crazing is induced at the high rates of strain involved in impact loading, though crazing may not contribute much to deformation energies at lower strain rates (20, ch. 7; 28, 30, 31). With respect to the role of M, one would certainly expect that the impact fracture energy should rise as M is increased to a limiting value, as is the case with fracture energies determined under other conditions of loading (3). With respect to the small but apparent tendency for IS/IS_o to decrease slightly at high values of M, one may suppose that the highest-M molecules may be relatively less mobile at the high strain rates involved.

Fracture Toughness. Values of K_c for the neat resin agree reasonably well with those reported previously (9), though the

In Durability of Macromolecular Materials; Eby, R.;
ACS Symposium Series; American Chemical Society: Washington, DC, 1979.

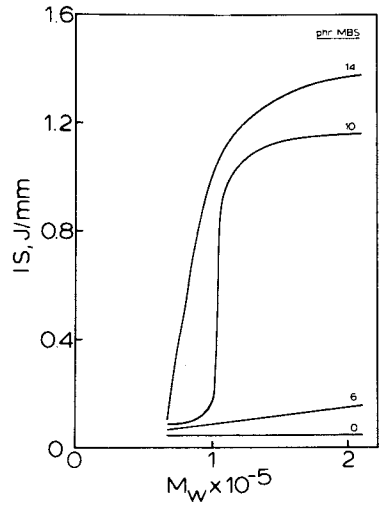

Figure 3. Effect of MBS content and M of matrix on notched impact strength of PVC blends

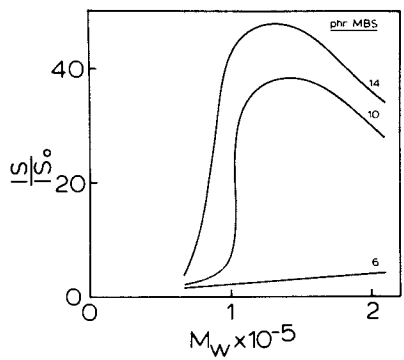

Figure 4. Effect of MBS content and M of matrix on notched impact strength of PVC blends relative to that of unmodified matrix

In Durability of Macromolecular Materials; Eby, R.;
ACS Symposium Series; American Chemical Society: Washington, DC, 1979.

values tend to be lower at high values of M. This lower trend is believed to be more realistic than the earlier one. In the earlier specimens intergranular fracture along PVC particle boundaries was observed at high values of ΔK; such a phenomenon would be expected to induce an increase in the apparent value of K_c in comparison to the case of intragranular (and hence relatively smooth) fracture. As mentioned above, however, values of K_c could only be estimated for specimens having both low M and low MBS content—namely, specimens 131-2 and 132-2. Clearly a brittle-ductile transition is involved (see also discussion above). In contrast to observations of impact strength, the addition of 6 phr MBS to the lowest-M resin increased the fracture energy (as implied by K_c) threefold; little effect was noted at the next level of M. Hence at the lower strain rates operative in FCP in comparison to impact fracture, the rubbery phase does significantly improve the ability to dissipate energy in low-M PVC, as reflected both in K_c and in the reduction in FCP rates (see below). As M is increased, failure becomes ductile at all levels of MBS; such specimens did not undergo rupture but rather became too compliant to continue testing. In this respect, the question of possible temperature rise would be worthy of investigation, though so far gross increases in temperature due to hysteretic heating have not been observed (see also discussion below).

Fatigue Crack Propagation Response. Typical FCP responses are summarized in Table II and in Figs. 5-9. As may be seen by comparison of the data with those reported in reference 9, the behavior of the control specimens agrees well with the behavior found with the earlier series. Although the curves exhibit some curvature not previously observed, the positions of the curves fit well with those of the previous ones, and the values of da/dN at $\Delta K = 0.6$ MPa$\sqrt{m}$ fall closely on the curve as a function of M (see Fig. 2, reference 9).

As shown in Table II and Fig. 5 (the curves in Fig. 5 also hold for 6 phr MBS), on adding 6 phr of MBS, FCP rates are significantly reduced. The effect is described quantitatively by the relative values of crack growth rates at constant ΔK (see Table II, in which $\dot{a}_K$ and $\dot{a}_{K_o}$ represent values of da/dN (at $\Delta K = 0.9\Delta K_{max}$ for the control) for modified and neat resins, respectively). Thus, with the lowest-M matrix, a striking reduction in da/dN is observed at all ΔK levels, accompanied by a threefold increase in K_c (Table II). Indeed, at a value of $\Delta K = 0.9\Delta K_{max}$ (of the control) da/dN is reduced 40-fold. On the other hand, with the highest-M matrix da/dN is reduced to a relatively lesser extent, only fivefold (the curves in Fig. 6 also hold for 6 phr MBS). At the same time, in the latter case, the failure becomes ductile in nature (see above). At intermediate values of M, reductions of da/dN at 6 phr of MBS range between twofold and fivefold. Thus in contrast to the case of impact strength, even a low concentration of MBS (6 phr) induces a significant toughening in fatigue even at a low

In Durability of Macromolecular Materials; Eby, R.;
ACS Symposium Series; American Chemical Society: Washington, DC, 1979.

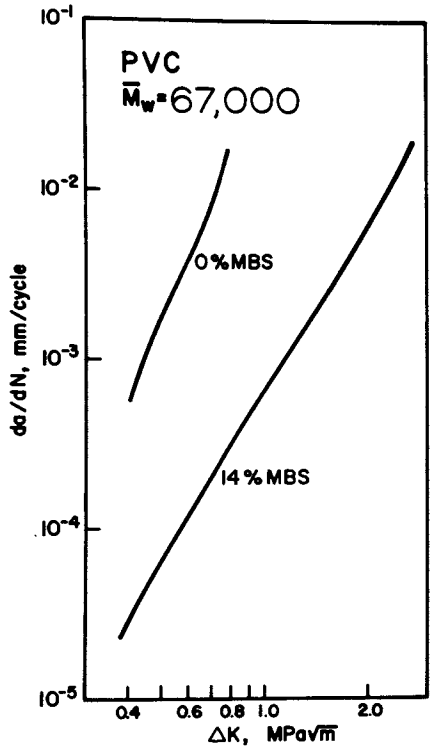

Figure 5. Effect of MBS addition (14 phr) on FCP behavior of PVC (M_w = 6.7 × 10^4). The curve for 14 phr also represents data for 6 phr and 10 phr of MBS.

In Durability of Macromolecular Materials; Eby, R.;
ACS Symposium Series; American Chemical Society: Washington, DC, 1979.

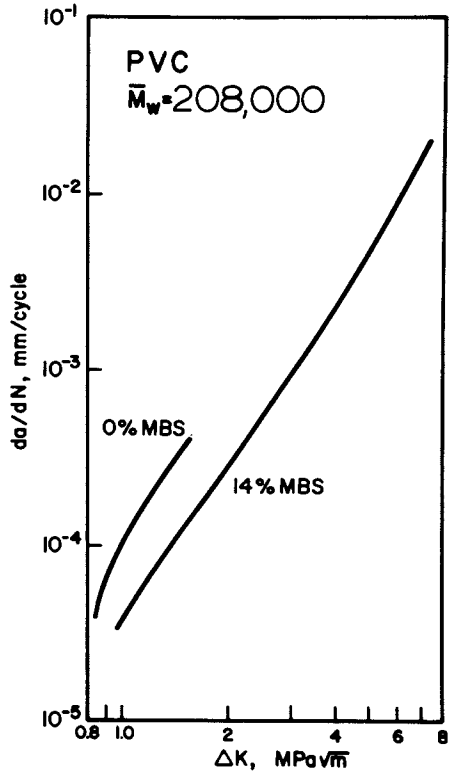

Figure 6. Effect of MBS addition (14 phr) on FCP behavior of PVC (M_w = 2.08 × 10^5). The curve for 14 phr also represents data for 6 phr and 10 phr of MBS.

In Durability of Macromolecular Materials; Eby, R.;
ACS Symposium Series; American Chemical Society: Washington, DC, 1979.

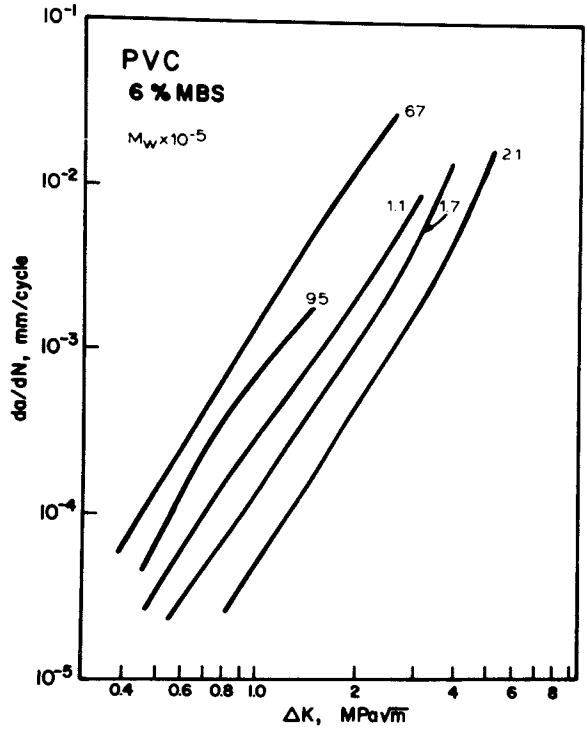

Figure 7. Effect of M on FCP behavior of PVC modified with 6 phr of MBS

In Durability of Macromolecular Materials; Eby, R.;
ACS Symposium Series; American Chemical Society: Washington, DC, 1979.

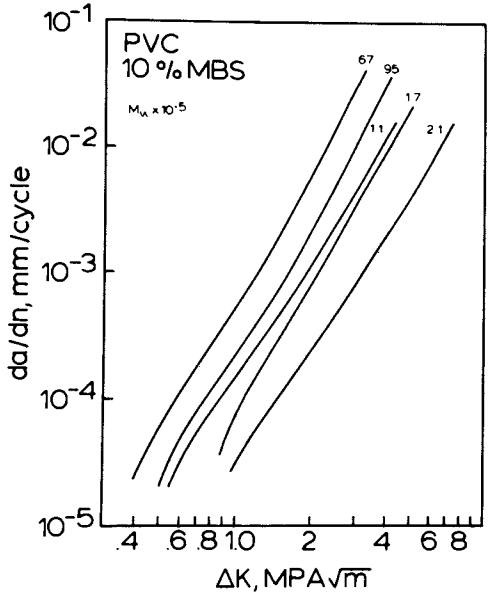

Figure 8. Effect of M on FCP behavior of PVC modified with 10 phr of MBS

In Durability of Macromolecular Materials; Eby, R.;
ACS Symposium Series; American Chemical Society: Washington, DC, 1979.

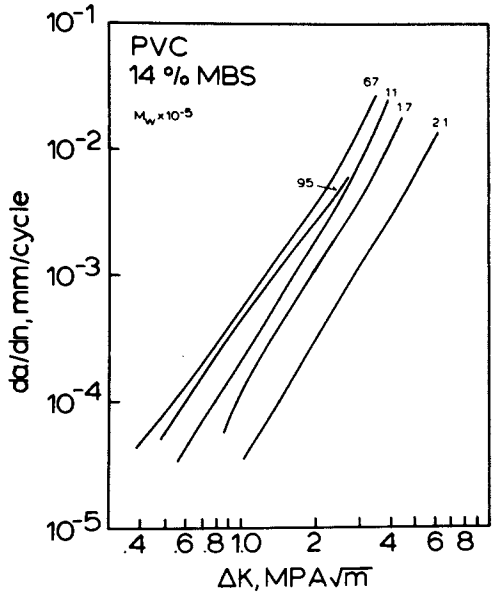

Figure 9. Effect of M on FCP behavior of PVC modified with 14 phr of MBS

In Durability of Macromolecular Materials; Eby, R.;
ACS Symposium Series; American Chemical Society: Washington, DC, 1979.

value of M (6.7×10^4). At higher values of M, the relative fatigue improvements at 6 phr of MBS are of the same order of magnitude as the improvements in impact strength (Table II).

Interestingly, with both the two lowest-M and the highest-M matrixes (specimens 131, 132, and 135, respectively), the addition of >6 phr of MBS has no significant effect on FCP rates. This behavior might speculatively be attributed to the consequences of a dynamic balance between (1) rubber-induced toughness due to the ability of the rubber to induce shear yielding and crazing and (2) rubber-induced softening (i.e., reduction in stiffness). Now stiffening can be reduced by two factors, acting alone or together: the presence of the rubber per se (see, for example, references 28 and 32), and by hysteretic heating due to inherent mechanical damping (1,6). While the present study cannot resolve these points, techniques are being developed in our laboratory to determine the value of E under actual test conditions, and an improved DMS instrument on order should permit more precise values of damping. (Note that, depending on the system and presumably frequency, E" or tan δ may increase (32) or show variable behavior (25) as the modifier content is increased.) It is interesting that the modified PVC's, but not the controls, tended to heat up to some degree during testing. Any such heating could have several possible and sometimes contradictory effects, e.g., increased creep and blunting of the crack tip (lower FCP rates), and reduced E (adding to the reduction due to the presence of the modifier, thus increasing FCP rates). In fact, with modified polyamides, da/dN-ΔK curves exhibit transitions to higher slopes at values of ΔK corresponding to the onset of palpable heating (24). One might speculate that when M is high the toughening effect due to crack blunting is relatively less prominent than in a lower-M material.

With intermediate values of M (specimens 133 and 134) behavior appears to be more complex; a decrease in toughening relative to other specimens, and a relative but consistent decrease in toughening as the modifier content is increased. However, since the data concerned are more preliminary in nature than the others, additional experiments in progress must be completed before definitive conclusions can be reached.

Thus it is clear that increases in both M and MBS content increase the resistance to FCP though the specific effect depends on the particular combination employed (see Figs. 7-9). One may conclude that by combining the inherent ability of a higher-M and ductile matrix to dissipate strain energy with the enhancement of highly delocalized deformations (probably mainly in shear at the strain rates involved here) by the rubber particles, one can obtain a much greater level of FCP resistance than is possible with, e.g., rubber-toughened polystyrene.

Finally, it is interesting to compare the FCP behavior of the rubber-modified PVC with that of other polymers. As mentioned above, the FCP curves for PVC tend to fall in between those for typically brittle polymers like poly(methyl methacrylate) and

In Durability of Macromolecular Materials; Eby, R.;
ACS Symposium Series; American Chemical Society: Washington, DC, 1979.

tough polymers such as polycarbonate. It was noted earlier that high-M PVC behaved rather like a typical commercial polycarbonate. With the incorporation of MBS, the behavior becomes significantly better than that of the same polycarbonate (see Fig. 10). In fact, MBS-modified high-M PVC (M_w ~$2x10^5$) is the most fatigue-resistant polymer examined to date, with the exception of highly crystalline polymers such as nylon, polyacetal or poly(vinylidene fluoride) (6). Even though the crystallinity of PVC is not high (~10%), the imperfect crystalline network evidently is able to confer a high level of shear yielding as opposed to crazing.

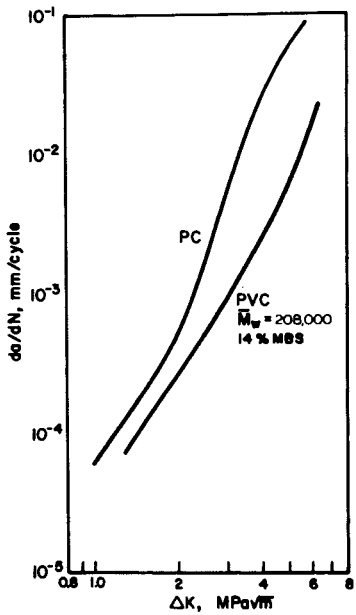

Figure 10. Comparison of FCP behavior of MBS-modified PVC (M_w = 2.08 × 10^5; 14 phr of MBS) with that of a typical commercial polycarbonate

Fracture Surface Morphology. While a complete study of fracture surface morphology and the micromechanisms of failure is still in progress, preliminary examination revealed major differences between the modified and neat PVC's. These are now being interpreted in order to elucidate the micromechanism of failure.

Conclusions

Several major conclusions may be made:

1. The inclusion of 6 to 14 phr of MBS in PVC enhances the FCP resistance of the matrix. At low and high values of matrix M, the degree of enhancement saturates at 6 phr of modifier; at intermediate values of M, the degree of enhancement exhibits complex behavior.
2. The FCP behavior does not correlate with the impact behavior, significant improvement of which requires the addition of 10 phr of MBS.
3. At a given level of modifier, the FCP resistance increases significantly with increasing M of the matrix. Indeed, a combination of high M with high MBS content leads to better FCP resistance than is observed with a typical commercial polycarbonate.

Acknowledgments

The authors wish to acknowledge financial support by the National Science Foundation through Grant No. DMR 77-10063. Assistance of P. Bretz, J. Janiszewski, and C. Rimnac with the testing and with the preparation of the manuscript is also very much appreciated.

Literature Cited

1. Manson, J. A. and Hertzberg, R. W., Crit. Rev. Macromol. Sci. (1973), 1, 433.
2. Kim, S. L., Skibo, M., Manson, J. A. and Hertzberg, R. W., Polym. Eng. Sci.(1977), 17(3), 194.
3. Kim, S. L., Skibo, M., Manson, J. A. and Hertzberg, R. W., accepted, Polym. Eng. Sci.(1978).
4. Skibo, M. D., Hertzberg, R. W., Manson, J.A., and Kim, S. L., J. Mater. Sci.(1977), 12, 531.
5. Hertzberg, R. W., Skibo, M. D. and Manson, J. A., Polymer (1978), 19(3), 58.
6. Hertzberg, R. W., Manson, J. A., and Skibo, M. D., Polym. Eng. Sci.(1975), 15, 252.
7. Skibo, M. D., Hertzberg, R. W., and Manson, J. A., Proceedings, 4th International Conference on Fracture(June 1977), Waterloo, Canada, p. 1127.
8. Hertzberg, R. W. and Manson, J. A., J. Mater. Sci.(1973), 8, 1554.

9. Skibo, M. D., Manson, J. A., Hertzberg, R. W., and Collins, E. A., J. Macromol. Sci.-Phys.(1977), B14(4), 525.
10. Skibo, M. D., Janiszewski, J., Hertzberg, R. W., and Manson J. A., Proceedings, International Conference on Toughening of Plastics(July 1978), the Plastics and Rubber Institute, London, paper 25.
11. Skibo, M. D., Janiszewski, J., Kim, S. L., Hertzberg, R. W., and Manson, J. A., Soc. Plast. Eng. Technical Papers(1978), 24, 304.
12. Paper for submission to J. Mater. Sci.(1978).
13. Andrews, E. H., "Fracture in Polymers", American Elsevier, New York, 1968.
14. Hertzberg, R. W., "Deformation and Fracture Mechanics of Engineering Materials", John Wiley & Sons, New York, 1976.
15. Hertzberg, R. W., Skibo, M. D., and Manson, J. A., in press, ASTM Spec. Tech. Publ.(1978).
16. Paris, P. C. and Erdogan, F., Trans. ASME D(1963), 85, 528.
17. Brown, Jr., W. F. and Srawley, J. E., ASTM STP(1966), 410.
18. Elinck, J. P., Bauwens, J. C., and Homès, G., Int. J. Frac. Mech.(1971), 7, 227.
19. Mills, N. J. and Walker, N., Polymer(1976), 17, 335.
20. Bucknall, C. B., "Toughened Plastics", Applied Science Publishers, Barking, UK, 1977.
21. Mann, J. and Williamson, G. R., in "The Physics of Glassy Polymers", Halstead Press, New York, 1973, Ch. 8.
22. Manson, J. A. and Sperling, L. H., "Polymer Blends and Composites", Plenum, New York, 1976.
23. Bucknall, Proceedings, International Conference on Toughened Polymers(July 1978), the Plastics and Rubber Institute, London, paper 24.
24. Skibo, M., Hertzberg, R. W., and Manson, J. A., Lehigh University, unpublished work, 1978.
25. Matsuo, M., Polym. Eng. Sci.(1969), 9, 206.
26. Ceccorulli, G., Piezzoli, M., and Pezzin, G., J. Macromol. Sci.-Phys.(1977), B14(4), 499.
27. Daniels, C. A. and Collins, E. A., submitted to Polym. Eng. Sci.(1978).
28. Petrich, R. G., Polym. Eng. Sci.(1973), 13, 248.
29. Deanin, R. D. and Moshar, C., ACS Polymer Preprints(1974), 15(1), 403.
30. Breuer, H., Stabenow, S. and Haaf, F., Proceedings, International Conferences on Toughened Polymers(July 1978), the Plastics and Rubber Institute, London, paper 13.
31. Breuer, H. Haaf, F. and Stabenow, J., J. Macromol. Sci.-Phys.(1977), B14(3), 387.

This is the second part of a series.

RECEIVED December 8, 1978.

23

Fatigue Effects in Poly(Methyl Methacrylate)

R. W. PENN and G. B. MC KENNA

Polymer Science and Standards Division, National Bureau of Standards, Washington, DC 20234

There has been much work reported recently dealing with failure in polymeric materials [1-9]. Many of the studies used pre-notched samples to study either time dependent crack propagation under dead load [1,2] or crack propagation under cyclic loading [3-7]. These studies provide information about the crack propagation process in polymers. However, their usefulness in predicting material failure is limited due to the fact that, in many polymers, crack propagation accounts for only a small portion of the material lifetime [8]. In addition, there is evidence that failure is a three stage process of crack initiation, arrest, and subsequent rapid propagation through a highly damaged "matrix" outside of the crack [9]. Our feeling is that a phenomenological approach, which implicitly includes these various aspects of failure, provides a better framework for studying failure than examining only one of the above processes individually. This is particularly so when one considers the difficulty of studying crack initiation.

We have chosen to study polymer failure in a framework which assumes that failure is the result of a cumulative damage process. When the damage reaches a critical value, then failure occurs. If the rate of damage accumulation is a function of only the current stress and not of stress rate or of the current state of damage, the simplest form of this concept is valid. This is the linear additivity of damage law. In the following paragraphs, we examine how well the failure and fatigue of Poly(methyl methacrylate) (PMMA) are described by this law.

Linear Additivity of Damage

For many polymeric materials, the lifetime of specimens is found to depend upon the stresses to which they are subjected. This fact in itself suggests that some kind of damage occurs in the material which accumulates to the point when failure occurs.

In Durability of Macromolecular Materials; Eby, R.;
ACS Symposium Series; American Chemical Society: Washington, DC, 1979.

When held at constant stress, specimens are found to have lifetimes (t_B) which depend on the level of the stress. For tests in other stress histories, if the rate at which the damage accumulates is dependent only on the current stress, the time for material failure, t_B, (i.e. the time to reach a critical value of damage) can be related to the stress history, $\sigma(\xi)$, by the following equation:

$$\int_0^{t_B} \frac{d\xi}{\tau(\sigma(\xi))} = 1 \tag{1}$$

where $\tau(\sigma)$ is the time to fail in constant stress experiments.

Thus, each increment of time, $d\xi$, during which the load is $\sigma(\xi)$, is weighted inversely as the lifetime $\tau(\sigma)$ which the specimen would have had under a constant load σ. This expression has been presented by Zhurkov [10] for the description of failure in polymeric materials.

Once $\tau(\sigma)$ is determined from constant stress experiments, equation (1) can be used to predict the time to fail under any stress history. The form of $\tau(\sigma)$ which we found describes our data is:

$$\tau(\sigma) = Ae^{-B\sigma} \tag{2}$$

where A and B are constants. For this form of $\tau(\sigma)$, the time to fail for a constant rate of stress experiment is obtained by integrating equation (1):

$$t_b = \frac{\ln(AB\dot{\sigma} + 1)}{B\dot{\sigma}} \tag{3}$$

where t_b is the time to fail and $\dot{\sigma}$ is the stress rate.

Similarly, if a sinusoidal stress

$$\sigma(t) = p + q \sin \omega t \tag{4}$$

is applied to the sample, the time to fail, t_b, is predicted to be:

$$t_b = \frac{\hat{t}_b(p)}{I_o(Bq)} \tag{5}$$

where $\hat{t}_b$ is the time to fail at the constant stress p and I_o is the zeroth order modified Bessel function. We note that the linear additivity of damage law predicts that fatigue life is independent of frequency.

Coleman [11] has exploited the additivity of damage concept to describe the failure of nylon fibers. He extended the concept by using the statistics of extreme values to describe the distribution of failure times in different loading conditions. His analysis demands that a material which obeys linear additivity of damage should have the same distribution of failure times independent of the type of stress history. A good measure of this is the coefficient of variation of the distribution of

In Durability of Macromolecular Materials; Eby, R.;
ACS Symposium Series; American Chemical Society: Washington, DC, 1979.

breaking times which is defined as the standard deviation divided by the mean.

In using the linear additivity of damage law as the framework for studying failure in PMMA, we will look for three things:

1. How well the time to break predictions for specific loading histories compare with the experimental results.

2. Whether or not the coefficient of variation for each loading history is the same.

3. Whether or not the fatigue lifetime is independent of frequency, as predicted by Eq. (5).

This we do, keeping in mind that deviations of experiment from the theoretical prediction ought to provide insight into the nature of the damage or failure process.

Experimental

A commercial grade PMMA was obtained in the form of a nominally 1.5 mm thick sheet. The sheet was machined into dumbbell specimens using a Tensil Kut* router. Specimens conformed to ASTM D 638 with the exception that the overall length was 150 mm instead of 165 mm. Each specimen's width and thickness were measured prior to testing. Mechanical testing was conducted using an Instron* servo-controlled hydraulic testing machine which is interfaced with a Hewlett-Packard* mini-computer for control and data acquisition.

The test machine is commanded by voltages generated by the computer. Dead load experiments were conducted by applying a single voltage and maintaining the voltage for the duration of the test. The tests were conducted at a predetermined voltage so that a given engineering stress was applied throughout the test. Constant rate of stress tests were conducted by commanding the machine from 0 to 10 Volts in 0.005 Volt increments. The stress at 10 Volts and the time between voltage increments were chosen to give the appropriate stress rates. The sinusoidal fatigue tests were run by generating a 200 point sinewave. The time between points was varied to obtain the desired frequencies.

*Certain commercial materials and equipment are identified in this paper in order to specify adequately the experimental procedure. In no case does such identification imply recommendation or endorsement by the National Bureau of Standards nor does it imply necessarily the best available for the purpose.

In Durability of Macromolecular Materials; Eby, R.;
ACS Symposium Series; American Chemical Society: Washington, DC, 1979.

The time to failure was recorded for each specimen. Constant load tests were conducted to provide a stress range of from 55 to 85 MPa. Rate of stress tests covered a range of from 0.0126 to 172.4 MPa/sec. The fatigue tests were conducted at peak stresses in the same range as the dead load tests and at frequencies from 0.002 to 0.164 Hz. Statistical analysis was performed on the constant load and fatigue experimental data.

Results and Discussion

For our constant stress tests on PMMA, we found that the average lifetime at the stress σ is represented by equation (2) with $A = 1.49 \times 10^{10}$ seconds and $B = 0.26$ MPa^{-1}. The agreement is within a few percent over the stress range covered. It is expected that at lower stresses, the form of $\tau(\sigma)$ would not be the same. The data are shown in Table I. The coefficients of variation are found to be about 0.3 with no apparent systematic variation with stress.

The first test of the applicability of linear damage additivity is from the constant rate of stress experiments. Equation (3) predicts the time to fail in a constant rate of stress test for PMMA. As can be seen in Figure 1, the agreement between the experimental values and the predicted values is very good. The agreement between experiment and prediction in the constant rate of stress test is, perhaps, not surprising. The nature of the test is such that the high stresses dominate the failure process and the monotonic loading, in some sense, assures that the damage mechanism doesn't change. Thus, while the agreement in this test is encouraging, it is by no means critical.

In order to obtain more definitive information about the failure of PMMA we conducted zero-tension sinusoidal fatigue tests at 0.164 Hz; i.e., $p + q$ in equation (4) and the peak stress is $p + q$. The results are shown in Table II. Figure 2 shows the comparison of the average times to break with those predicted from equation (5) and the value of B determined from constant stress tests. As can be seen, the predicted times to fail vs. peak stress form a line nearly parallel to the dead load data and at approximately seven fold greater failure times. The experimental results, however, are lower than the predicted values and show a concave deviation from the predicted values.

The second test of the applicability of linear damage additivity comes from the prediction that the coefficient of variation of failure times is independent of the stress and of the form of the stress history [11]. Tables I and II show the dead load and fatigue data obtained in this study with the coefficients of variation for the times to break. As can be seen from the tables, the coefficient of variation, C is approximately 0.20-0.45 for the dead load experiments, while in fatigue at 0.164 Hz it varies from 0.45 to 0.85. In the case of the constant stress data, there is no systematic variation of C with stress level

In Durability of Macromolecular Materials; Eby, R.;
ACS Symposium Series; American Chemical Society: Washington, DC, 1979.

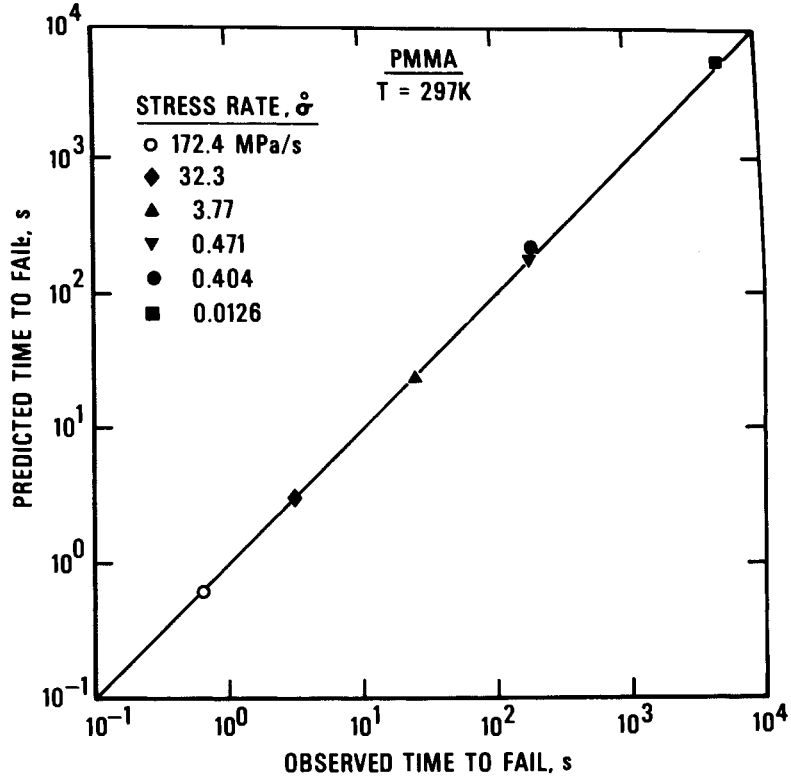

Figure 1. Time to fail for PMMA in constant rate of stress experiments. The points show experimental data at the stress rates shown. The line is predicted from Equation 3 applying constant stress data.

In Durability of Macromolecular Materials; Eby, R.;
ACS Symposium Series; American Chemical Society: Washington, DC, 1979.

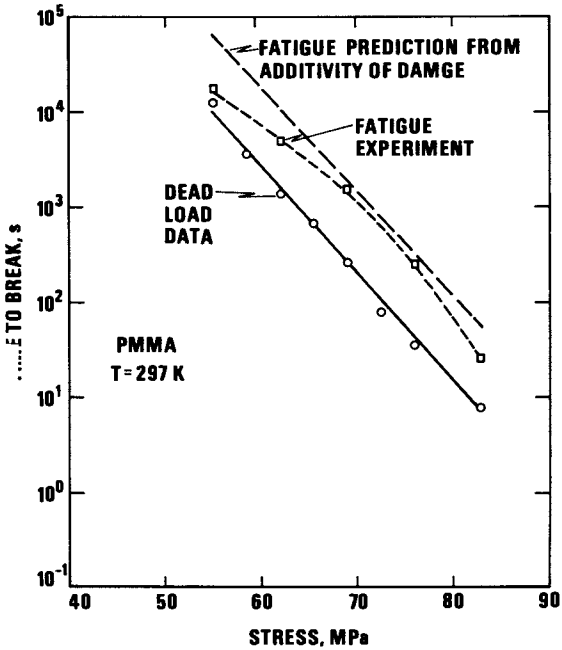

Figure 2. Time to fail vs. stress for PMMA in constant stress and sinusoidal stress experiments. The points show experimental data; (— —), the fatigue behavior predicted from Equation 5 applying constant stress data.

In Durability of Macromolecular Materials; Eby, R.;
ACS Symposium Series; American Chemical Society: Washington, DC, 1979.

while for the sinusoidal stress data C appears to increase with increasing stress. This suggests that the underlying processes which lead to failure in fatigue are different than those leading to failure under a static load. The result is a larger variability in the lifetime under sinusoidal loading than under constant loading conditions.

Table I

Time to Break for PMMA at Constant Stress

Stress (MPa)	Number of Specimens	Mean Time to Fail (seconds)	Coefficient of Variation (C)
55.2	10	12785	.353
58.6	9	3551	.233
62.1	10	1375	.364
65.5	10	670	.172
69.0	13	264	.239
72.4	15	78.9	.311
75.8	30	35.5	.456
82.7	3	.77	-

The third test of the applicability of linear damage additivity is the prediction that the time to fail should be independent of the frequency of the test. Within the constraints that the tests should include a large number of cycles and that they should be completed within an experimentally reasonable time, we were able to obtain data at three frequencies (0.164, 0.019, and 0.002 Hz) and the same peak stress of 55.2 MPa. Figure 3 shows the results of these tests in a plot of log time to fail vs. log frequency. Over the two orders of magnitude of frequency covered, the lifetimes vary by about one order of magnitude.

In other materials, fatigue has been successfully described as a cycle dependent process. In this case, the fatigue life would depend only on the number of cycles, and the data of Figure 3 would fall on a straight line with a slope of -1. As can be seen, the fatigue process is neither simply cycle dependent nor a linear additivity of damage process, but rather falls between the two.

Finally, the concept of linear additivity of damage serves as a useful framework for analyzing the failure behavior of polymeric materials. Examining the deviations of the experimental data from linear additivity behavior should provide a basis for expanding the concept to a more general damage law in which the

In Durability of Macromolecular Materials; Eby, R.;
ACS Symposium Series; American Chemical Society: Washington, DC, 1979.

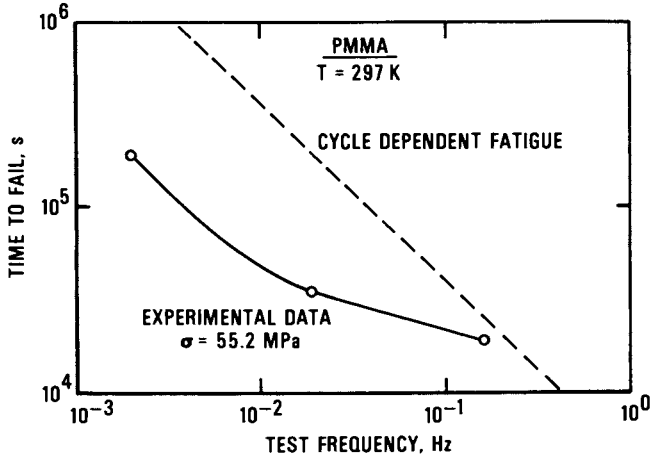

Figure 3. Time to fail vs. test frequency for PMMA in zero-tension and sinusoidal fatigue. The points show experimental data; (– – –), failure behavior of a material exhibiting cycle-dependent fatigue.

In Durability of Macromolecular Materials; Eby, R.;
ACS Symposium Series; American Chemical Society: Washington, DC, 1979.

rate of damage accumulation is a function, not only of the current stress, but also of other parameters such as current state of damage, the stress rate, etc. This work will be extended to develop such nonlinear damage laws.

Table II

Time to Break for PMMA Under Sinusoidal Stress (0.164 Hz)

Peak Stress (MPa)	Number of Specimens	Mean Time to Fail (seconds)	Coefficient of Variation (C)	Mean Number of Cycles to Failure
55.2	10	18026	.449	2956
62.1	19	5125	.579	840
69.0	17	1549	.783	254
75.8	14	257.9	.840	42
82.7	6	25.8	.868	4

Acknowledgements

The authors wish to thank L. J. Zapas and J. M. Crissman of the National Bureau of Standards for many fruitful discussions during the course of this work.

References

1. P. W. R. Beaumont and R. J. Young, J. Mater. Sci., 10, 1334-1342 (1975).
2. R. J. Young and P. W. R. Beaumont, Polymer, 17, 717-722 (1976).
3. B. Mukherjee and D. J. Burns, Eng. Fract. Mech., 4, 675-685 (1972).
4. R. W. Hertzberg, J. A. Manson and M. Skibo, Polymer Eng. and Sci., 15 252-260 (1975).
5. S. L. Kim, M. Skibo, J. A. Manson, and R. W. Hertzberg, Polymer Eng. and Sci., 17, 194-203 (1977).
6. S. Arad, J. C. Radon, and L. E. Culver, Eng. Fract. Mech., 4, 511-522 (1972).
7. J. C. Radon and L. E. Culver, Polymer Eng. and Science, 15, 500-506 (1975).
8. S. Rabinowitz and P. Beardmore, J. Mater. Sci., 9, 81-99 (1974).
9. Yu. G. Korabel'nokov and A. S. Freidin, Mekhanika Polymerov, No. 5, 904-911, Sept.-Oct. (1971).
10. S. N. Zhurkov, Int. J. Frac. Mech., 1, 311 (1965).
11. B. D. Coleman, J. Appl. Phys., 29, 968-983 (1957).

RECEIVED December 8, 1978.

24

The Effects of Temperature and Moisture on the Accelerated Aging of Paper

E. L. GRAMINSKI, E. J. PARKS, and E. E. TOTH

Center for Materials Science, National Bureau of Standards, Washington, DC 20234

The purpose of an accelerated aging test is to duplicate the physical and chemical changes occurring naturally in a material in a relatively short time frame so that the useful life of the material can be assessed. Therefore, the conditions of an accelerated test must be adequate for the satisfactory duplication of the degradative processes and not conducive to the initiation of degradative reactions that do not occur ordinarily at ambient conditions.

For over fifty years attempts have been made to predict the permanence of paper by means of accelerated aging. The earliest accelerated aging involved placing paper in an oven at 100-105°C for times ranging from 20 to 125 hours (1,2). The decline in physical properties resulting from exposure to elevated temperatures was considered a measure of paper permanence. The papers having a high retention of the original properties were considered to be permanent while those exhibiting an appreciable decline in properties were considered to be impermanent. The degree of impermanence was proportional to the extent of decline in properties. No attempt was made at predicting the service life of paper.

It was eventually recognized that the degradation rate for all papers might not remain constant and that the estimated permanence of paper could change with longer aging periods. This led to the practice of aging paper for longer periods of time with multiple withdrawals during the course of aging. The physical properties were plotted for the various time intervals. If necessary the

In Durability of Macromolecular Materials; Eby, R.;
ACS Symposium Series; American Chemical Society: Washington, DC, 1979.

data were suitably transformed in order to obtain straight lines. The slopes of these lines were considered to be a measure of the degradation rate and were used to assess the permanence of paper. The papers having the lowest degradation rates were judged to be the most permanent.

It became obvious that considerably more basic information had to be developed on the degradation process for paper. Too little was known about the effect of water on the degradation of paper and since accelerated aging involves exposing paper to higher than normal temperatures it would also be necessary to know whether the commonly used temperatures in laboratory aging were excessive.

A study was conducted to determine the effect of moisture and temperature on the degradation of paper in an accelerated aging test (6). The results of that study clearly demonstrated that moisture had a profound effect on the degradation rate of paper and that possibly the optimum temperature for an accelerated test for paper should be in the vicinity of 70°C. Unfortunately, the humidity range investigated in that study (0-50% R.H.) was too narrow to be able to specify the functionality of water in the degradation process or to be able to obtain adequate information on the existance of an upper temperature limit. It was decided to expand the study to include humidities up to 90% R.H. The results of both studies are reported below.

Experimental

Handsheets, prepared from a northeastern bleached kraft pulp containing approximately 85 percent alpha cellulose and 15 percent hemicellulose were used in this investigation. Six kilograms of the pulp were torn into pieces of approximately two square inches area and divided into three two-kilogram samples. Each sample was demineralized by soaking in 0.1N hydrochloric acid at a five percent consistency. After one hour the acid was drained and fresh acid was added to the pulp. After the fourth acid treatment the pulp was washed with distilled water on a larger Buchner funnel until the pH of the filtrate was identical to the pH of the distilled water and remained at that pH for an additional three to four rinses.

Following demineralization, the three two-kilogram samples were blended thoroughly, and washed four additional times with carbon dioxide-saturated distilled water. The bulk of the water was removed by filtration and the treated pulp was placed in a covered glass jar and stored at -18°C until used.

The pulp was beaten in a laboratory mill at 10 percent consistency with no clearance between bedplate and roll for 5,000 revolutions at 33.3N (3.4 kilograms force) and a relative velocity of roll to bedplate of 6m/s. The beating was done in distilled water using sufficient wet pulp to provide 40g of dry pulp for each charge. One kilogram of pulp was beaten (25 beater charges)

In Durability of Macromolecular Materials; Eby, R.;
ACS Symposium Series; American Chemical Society: Washington, DC, 1979.

and placed in a large stainless steel container, diluted to approximately one percent consistency and blended for approximately one hour prior to preparing handsheets.

Aliquots, containing sufficient pulp to make a 30.5 x 30.5 cm handsheets having a weight of 70 g/m^2 ± 5% were placed in a British Disintegrator, diluted with distilled water to a consistency of approximately 0.5 percent and disintegrated for 3000 revolutions. The disintegrated pulp was placed in a 30.5 x 30.5 cm deckle box containing approximately 28 liters of distilled water. The contents were agitated by moving a perforated place up and down five times followed by a pause of approximately 10 seconds then drained through a 100 mesh monel wire screen. The wire containing the formed sheet was placed on a blotter, covered with wool felt and consolidated by pressing with a 33 cm long roller weighing 22.5 kg. The sheet was carefully removed from the wire, placed between wool felts and passed through a roll press at a pressure of approximately 7 kg/per linear cm. The pressed sheet was then dried on a drum dryer at 95°C for approximately four minutes. The tension on the endless felt of the drum dryer was adjusted to restrict sheet shrinkage to a minimum. The sheets were stress relieved by suspending them in a humidity chamber at 30°C and 95% relative humidity for approximately 16 hours.

Accelerated Aging. All of the handsheets were randomized out of the order in which they were manufactured in order to obtain samples, representative of the lot, for the various combinations of aging time, temperature and relative humidity. All of the handsheets were randomized into sets of 12 handsheets. Six sets of 12 handsheets, selected at random, were designated for each of the four temperatures. Each sheet in the sets was cut into four quarters and each quarter was designated at random. The quarters from each sheet having the same designation were then grouped together and each set of quarters were then aged for the same time period at four different relative humidities. Following aging the specimens were conditioned according to TAPPI T402 OS-70 before testing.

Constant temperature oil baths of internal dimensions, 30 cm in width by 60 cm length and 37 cm in depth, were constructed of stainless steel. A heating coil, immersed in the bath, was an auxiliary source of heat, with current input controlled by a variable transformer. An immersion heater controlled by a relay box and thermoregulator was the principal source of heat and provided the desired temperature control with ± 0.1°C. The oil was continuously pumped in the bath with an immersion type pump to ensure uniform distribution of temperature.

Two baths were used in series. One bath (prehumidifer) was maintained at a temperature that would provide the desired partial pressure of water and the other (aging bath) was maintained at one of the four temperatures employed in this investigation. To provide a vented atmosphere at a specific relative humidity in the

In Durability of Macromolecular Materials; Eby, R.;
ACS Symposium Series; American Chemical Society: Washington, DC, 1979.

aging vessels, 50 cm^3 of air per minute was metered through water in the prehumidifier, passed through glass tubing surrounded by a heating jacket at a temperature somewhat higher than the prehumidifier bath to avoid condensation, then through coiled glass tubing immersed in the aging bath and finally through the aging vessel containing the suspended paper specimens. To provide dry air (0% RH), air was passed over silica gel through a flowmeter to the aging vessel. The baths were covered with black cloth to exclude light.

Properties Investigated. The following properties investigated along with the TAPPI test methods employed are as follows: Folding Endurance T511 Sn-69, Brightness T452 OS-58, Alkaline Solubility T212 OS-54, Copper Number T430 M-52, Tensile Stength T494 OS-70 using 1.5 cm wide specimens at a span of 10 cm and a rate of elongation of 1 cm/min, and pH by method T509 SU-68 with the exception that the pH measurement was made on the decantate (3).

Internal tear was performed on an Elmendorf tear tester having a 200 g capacity. A single ply was used unless the tear strength deteriorated considerably necessitating three or four piles in order to obtain a reading in the range suggested for the instrument.

Zero span tensile strength was determined on a commerically available zero-span tester. Sample size was 2 cm x 11 cm. The clamping pressure for each set of specimens was determined in advance to determine the minimum pressure at which slippage did not occur and the maximum pressure where fiber damage occurred. The clamping pressure chosen was midway between these two pressures.

Wet tensile strength was determined on a constant rate of elongation tensile tester using specimens 1.5 cm wide and a length of 10 cm. The samples were soaked for two hours in distilled water prior to testing.

Moisture regain specimens were first conditioned in a desiccator for 24 hours and the exposed to an atmosphere maintained at 23 $\pm$ 1°C and 50.0 $\pm$ 2.0% relative humidity for at least 24 hours. Specimens of approximately two grams were placed in weighting bottles and the total weight was determined to the nearest 0.1 mg. The sample was then dried in a vacuum oven at 105°C for one hour, covered immediately upon opening the oven, cooled in a desiccator for two hours and reweighed. This procedure was repeated until constant weight was obtained. The difference in weight between the conditioned and dried sample was due to the moisture in the specimen. The specimen was then removed from the weighing bottle, and the empty bottle was dried in the vacuum oven at 105°C for one hour, cooled in a desiccator for two hours and weighed. The difference between the weight of the bottle containing the dried specimen, and the empty weighing bottle was the weight of the

In Durability of Macromolecular Materials; Eby, R.;
ACS Symposium Series; American Chemical Society: Washington, DC, 1979.

of the anhydrous specimen. The weight of water divided by the weight of the anhydrous specimen multiplied by 100 was the percent moisture regain. The moisture isotherm given in Fig. 4 was obtained by making moisture regain measurements as described above but in a room capable of controlling relative humidities between 15 percent and 75 percent.

The results for folding endurance and zero span tensile strength are given in Tables 1 and 2 and are the averages of 12 specimens. The results of these two properties are representative of all the other properties investigated. The results for the remaining properties are not given.

Results and Discussion

The extent of paper degradation is generally determined by measuring the changes in physical properties with time. Apparently it is presumed that a direct relationship exists between the chemical changes in the cellulose and the physical properties of the paper. Most degradation processes are complex however, and it is very hazardous to make such an assumption.

Evidence exists that at least three reactions, hydrolysis, oxidation, and cross-linking, contribute to the deterioration of paper (4, 5, 6). The magnitude and rate of change of a specific physical property will depend on the extent one reaction proceeds relative to the others. It must also be recognized that each degradative reaction is affected differently by environmental variables and the results obtained from an accelerated aging test will depend on the selection of the environmental variables. It is therefore necessary to establish the relative importance of each environmental variable.

The rate of change for all the physical properties investigated in this study increased proportionately with the amount of moisture in the aging atmosphere at each of the temperatures studied. Unquestionably moisture has a profound affect on the degradation rate of paper and is perhaps the most important environmental variable to be considered in studies of paper permanence.

In an effort to obtain an estimate of the relative degree to which the three degradative reactions proceeded determinations of solubility in hot 1 percent alkali, copper number and wet strength were made during the course of aging. The bulk of material which dissolves in hot 1 percent alkali is low molecular weight carbohydrates consisting of hemicelluloses and degraded cellulose. Presumably any increase in alkali solubility is the result of degradation due to hydrolysis. The copper number indicates the relative number of reducing groups in paper and any increase in copper number should result from oxidation of the hydroxyl groups at either the 2, 3, or 6 positions of cellulose. Cross-linking should result in reduced swelling of the cellulose in water with an accompanying increase in wet strength. Therefore, increases

In Durability of Macromolecular Materials; Eby, R.;
ACS Symposium Series; American Chemical Society: Washington, DC, 1979.

Table 1. Effect of Aging on MIT Folding Endurance

AGING TEMP.	AGING TIME	RELATIVE HUMIDITY, % 0	10	25	50	60	75	80	90
°C	Days	Avg Double Folds	Avg Double Folds	Avg Double Folds	Avg Double Folds	Avg Double Folds	Avg Double Folds	Avg Double Folds	Avg Double Folds
90	0	1900	1900	1900	1900	2090	----	2090	2090
	1/2	----	----	----	----	1730	----	1270	1400
	1	1620	1730	1630	1270	1160	----	750	580
	2	----	----	----	----	570	----	68	58
	3	1730	1630	1030	270	70	----	2	1
	6	1640	1240	290	4	1	----	----	0
	12	1310	650	11	0	----	----	----	----
	18	1540	560	3	0	----	----	----	----
80	0	1830	1830	1830	1830	2040	1600	2040	2040
	3	1860	1630	1530	1240	1090	870	810	560
	6	1420	1430	1340	600	310	210	85	30
	9	----	----	----	----	62	24	21	1
	12	----	----	----	----	14	2	14	----
	15	----	----	----	----	1	0	0	----
	18	1500	1160	530	4	----	----	----	----
	30	1870	760	58	1	----	----	----	----
	42	1560	440	6	0	----	----	----	----
70	0	1590	1590	1590	1590	2110	----	2110	2100
	3	----	----	----	----	1600	----	1560	1390
	6	----	----	----	----	1360	----	1190	1240
	9	1750	1410	1330	1190	----	----	----	----
	12	----	----	----	----	1040	----	350	340
	15	----	----	----	----	850	----	240	170
	18	----	----	----	820	----	----	----	----
	24	----	----	----	----	300	----	34	18
	27	1600	1380	910	260	----	----	----	----
	54	1560	1250	503	10	----	----	----	----
	72	----	----	----	4	----	----	----	----
	90	1510	930	75	----	----	----	----	----
	126	1660	540	26	----	----	----	----	----
60	0	1690	----	1690	1690	1900	1690	1900	1900
	12	----	----	----	----	1450	----	1370	1310
	24	1580	----	1490	1470	1520	1180	1240	1120
	36	----	----	----	----	----	920	----	----
	42	----	----	----	----	900	----	530	490
	48	1880	----	1550	1220	----	520	----	----
	60	----	----	----	----	----	460	----	----
	72	1800	----	1180	190	390	240	17	32
	96	----	----	----	----	1	----	----	19
	117	1560	----	740	95	----	----	----	----
	162	1660	----	440	7	----	----	----	----

In Durability of Macromolecular Materials; Eby, R.;
ACS Symposium Series; American Chemical Society: Washington, DC, 1979.

Table 2. Effect of Aging on Zero Span Breaking Length

AGING TEMP.	AGING TIME	RELATIVE HUMIDITY, %							
		0	10	25	50	60	75	80	90
°C	Days	Breaking Length Km	Breaking Length Km	Breaking Length Km	Breaking Length Km	Breaking Length Km	Breaking Length Km	Breaking Length Km	Breaking Length Km
90	0	14.62	14.62	14.62	14.62	14.27	---	14.27	14.27
	1/2	---	---	---	---	13.39	---	12.64	12.49
	1	15.05	15.00	14.73	13.99	13.67	---	12.90	12.78
	2	---	---	---	---	12.83	---	10.17	10.16
	3	14.88	14.71	13.71	11.86	10.71	---	7.92	7.36
	6	14.56	14.31	12.01	8.83	8.30	---	---	4.34
	12	14.20	12.69	9.25	5.62	---	---	---	---
	18	15.62	12.67	8.20	4.71	---	---	---	---
80	0	14.44	14.44	14.44	14.44	14.92	14.62	14.92	14.92
	3	14.13	14.44	14.32	13.74	13.40	12.89	12.65	12.14
	6	14.01	13.63	13.59	12.15	11.70	11.55	10.27	9.69
	9	---	---	---	---	10.74	9.11	10.20	7.70
	12	---	---	---	---	9.72	7.36	8.46	---
	15	---	---	---	---	7.50	6.41	5.90	5.00
	18	14.49	13.32	12.15	8.45	---	---	---	---
	30	14.38	13.55	10.08	5.96	---	---	---	---
	42	14.04	12.61	9.20	5.56	---	---	---	---
70	0	15.22	15.22	15.22	15.22	14.40	---	14.40	14.40
	3	---	---	---	---	14.20	---	13.60	13.23
	6	---	---	---	---	---	---	13.08	12.90
	9	14.87	14.87	14.35	14.57	---	---	---	---
	12	---	---	---	---	13.11	---	11.93	11.58
	15	---	---	---	---	12.95	---	11.68	11.26
	18	---	---	---	12.69	---	---	---	---
	21	---	---	---	---	11.55	---	10.19	---
	27	15.24	14.45	13.39	11.86	---	---	---	---
	54	14.37	13.54	12.18	9.53	---	---	---	---
	72	---	---	---	8.92	---	---	---	---
	90	13.72	13.09	10.51	---	---	---	---	---
	126	13.83	12.53	9.70	---	---	---	---	---
60	0	14.48	---	14.48	14.48	14.76	14.48	14.76	14.76
	12	---	---	---	---	14.13	---	13.76	14.05
	24	14.84	---	14.66	13.87	13.30	14.09	12.90	13.25
	36	---	---	---	---	---	12.03	---	---
	42	---	---	---	---	13.69	---	12.54	12.89
	48	14.10	---	14.00	13.10	---	12.12	---	---
	60	---	---	---	---	---	13.49	---	---
	72	15.03	---	13.86	11.14	12.35	11.10	9.10	9.68
	96	---	---	---	---	9.73	---	---	7.39
	117	14.57	---	12.82	10.62	---	---	---	---
	162	14.37	---	12.61	9.02	---	---	---	---

In Durability of Macromolecular Materials; Eby, R.;
ACS Symposium Series; American Chemical Society: Washington, DC, 1979.

in wet strength should be related directly to the amount of cross-linking.

Both alkali solubility and copper number increased with time and the rate of increase was proportional to the amount of moisture in the aging atmosphere. It appeared that the alkali solubility reached a maximum in the neighborhood of 34 percent solubility. No maximum was detected for copper number, although it appeared that the rate of increase in copper number decreased somewhat at the time alkali solubility reached a maximum.

Reactions in cellulose occur primarily in the amorphous regions. Each wood pulp contains a specific amount of amorphous material so that at some point in the degradative process maxima in property changes can be expected to occur.

At the maximum alkali solubility the paper still retains appreciable physical strength. A possible explanation for this behavior may stem from the reactivity of oxidized cellulose in alkali. Oxidation of cellulose generally results in the formation of β-alkoxyl groups. The β-alkoxycarbonyl grouping occurs in all possible situations where a carbonyl is introduced into a cellulose molecule. Whenever a β-alkoxycarbonyl groups is present in alkali, a rapid elimination of the alkoxyl group occurs (7) resulting in chain scission, generating substantial quantities of alkali soluble material. This would explain the reasons for a high alkali solubility without a complete loss of physical strength. It further indicates that the extraction in 1 percent alkali is not a reliable means for assessing the extent of hydrolysis in paper degradation since considerable hydrolysis of cellulose occurs during the extraction process itself.

While the β—elimination reaction is detrimental in alkali solubility for estimating the extent of hydrolysis, it is favorable for assessing the extent of oxidation by following the change in copper number. Oxidation of cellulose may result in some ketone formation but ketones do not reduce copper. However, ketones do undergo the β-elimination reaction and in the process form reducing end groups which do reduce copper. Therefore, it would appear that the increase in copper number during accelerated aging gives a reasonable estimate of oxidation of cellulose.

The one property which perhaps demonstrates the complexity of paper degradation most is wet strength. In desiccated air and at very low relative humidities wet strength increases during the duration of accelerated aging. As the humidity is increased, the rate of increase in wet strength also increases; however, at some combination of temperature and humidity, wet strength reaches an optimum and then declines (Fig. 1). It is apparent that more than one reaction affects wet strength.

Presumably, the rate of oxidation increases as the amount of atmospheric moisture increases. The resulting functional groups produced by oxidation can enter into cross-linking reactions which lead to increased wet strength. However, oxidation can also facilitate hydrolysis since it has been shown that the rate of

In Durability of Macromolecular Materials; Eby, R.;
ACS Symposium Series; American Chemical Society: Washington, DC, 1979.

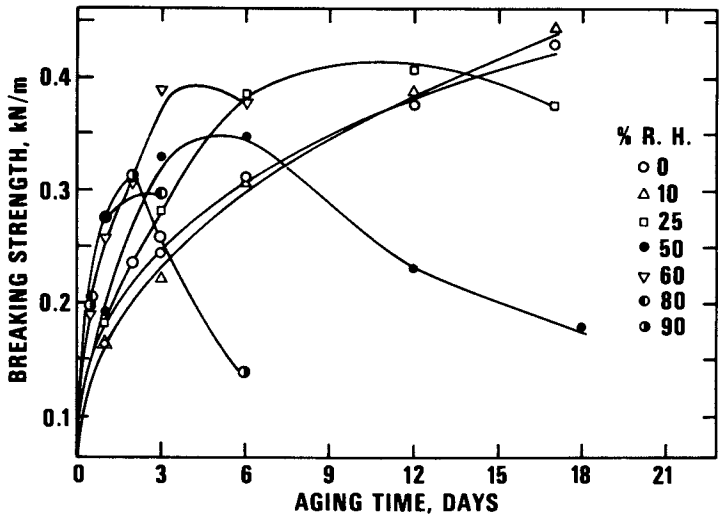

Figure 1. Change in wet breaking strength of paper with time when aged at 90°C and various relative humidities

In Durability of Macromolecular Materials; Eby, R.;
ACS Symposium Series; American Chemical Society: Washington, DC, 1979.

hydrolysis can increase by as much as 20 to 70 times the normal rate by the introduction of a carbonyl group in the 6 position (8). In essence the changes in wet strength occuring during accelerated aging are dependent on the proportion of at least three reactions occurring simultaneously.

Good linear relationships were obtained by plotting the log of the property in question as a function of time for all the properties investigated in the study except for alkali solubility, copper number, hydrogen ion cconcentration and wet strength. Better linear relationships were obtained for these four properties when plotted on linear coordinates. The slopes of the various plots were considered to be a measure of the degradation rates.

Typical plots of the degradation rate as a function of relative humidity are shown in Figs. 2 and 3. These plots strongly resemble the moisture adsorption isotherm (Fig. 4) for the handsheets used in this investigation especially for the 80° and 90°C plots. This suggests a linear relationship between the degradation rate and the moisture content.

Unfortunately the moisture contents of paper were not determined for any of the experimental conditions employed in this study and the only moisture contents measured were at ambient temperature (Fig. 4). Since the moisture content decreases with increasing temperatures by some constant factor (9) it would be appropriate to use the ambient moisture contents to verify whether a direct relationship exists between bound water and degradation rate.

Good linear plots were obtained when the degradation rates were plotted against the ambient temperature moisture contents (Fig. 5). It was interesting to note that the plots intersected the X axis substantially above the origin which indicates a portion of the bound water is "inactive". The fact that all four plots intersect the X axis at approximately the same point is probably an artifact caused by assuming the moisture content was identical for all the experimental conditions.

In an earlier study it was found that the moisture content for a sulfite pulp decreased by 20% at 60°C and by 40% at 90°C relative to the moisture content of ambient temperature(10). In an effort to obtain a more realistic depiction of the actual plots shown in Fig. 5 the 60° and 90°C data was replotted after the moisture contents were decreased by 20% and 60°C and by 40% at 90°C (Fig. 6). There was a substantial increase in the slope of the 90°C plot and only a small change in the 60°C plot. Once again there is an indication that a fraction of the bound water is "inactive". The amount of "inactive" water apparently decreases as the temperature increases.

Since the slope of the degradation rate-moisture content plot is so high it is apparent that control of environmental conditions must be very precise to obtain reliable results. Small changes in partial pressure of water or in temperature can

In Durability of Macromolecular Materials; Eby, R.;
ACS Symposium Series; American Chemical Society: Washington, DC, 1979.

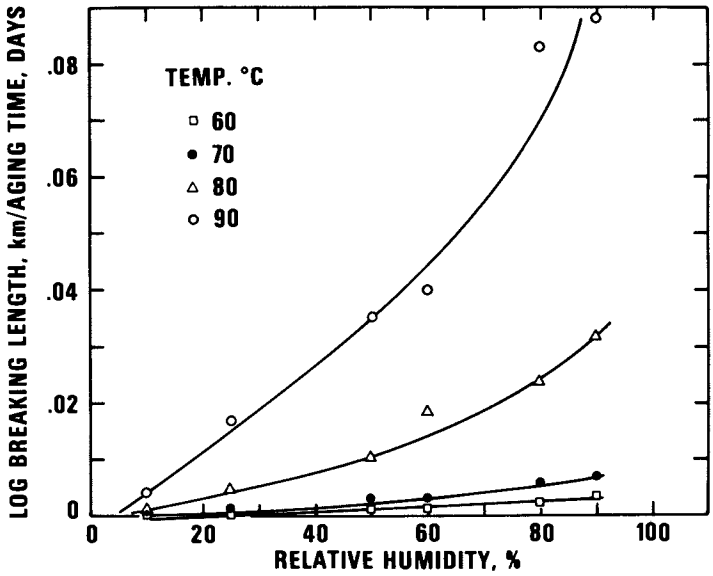

Figure 2. Change in degradation rate of zero span tensile strength of paper with relative humidity when aged at various elevated temperatures

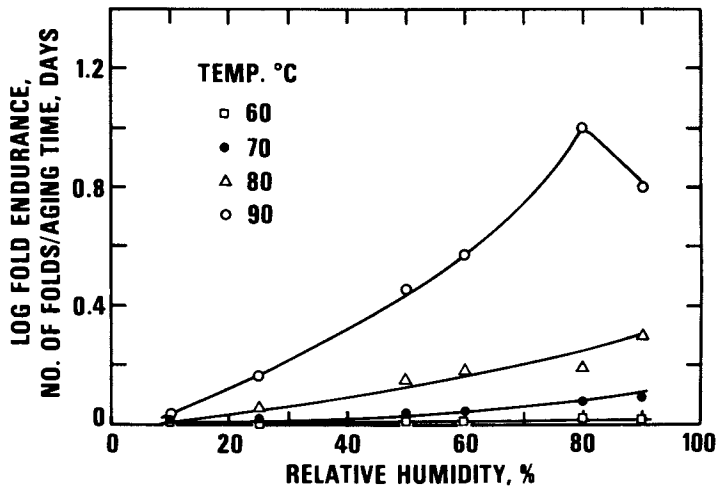

Figure 3. Change in degradation rate of paper folding endurance with relative humidity when aged at various elevated temperatures

In Durability of Macromolecular Materials; Eby, R.;
ACS Symposium Series; American Chemical Society: Washington, DC, 1979.

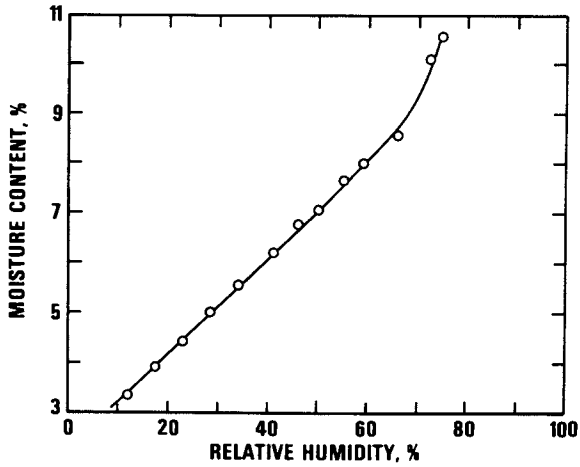

Figure 4. Moisture isotherm at 23°C for the paper used in this degradation study

In Durability of Macromolecular Materials; Eby, R.;
ACS Symposium Series; American Chemical Society: Washington, DC, 1979.

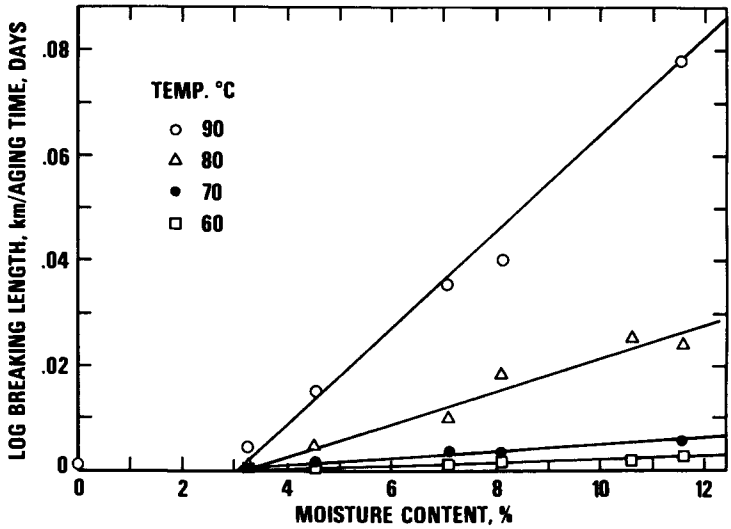

Figure 5. Change in degradation rate of zero span tensile strength with moisture content for various temperature moisture contents for all relative humidities were measured at 23°C

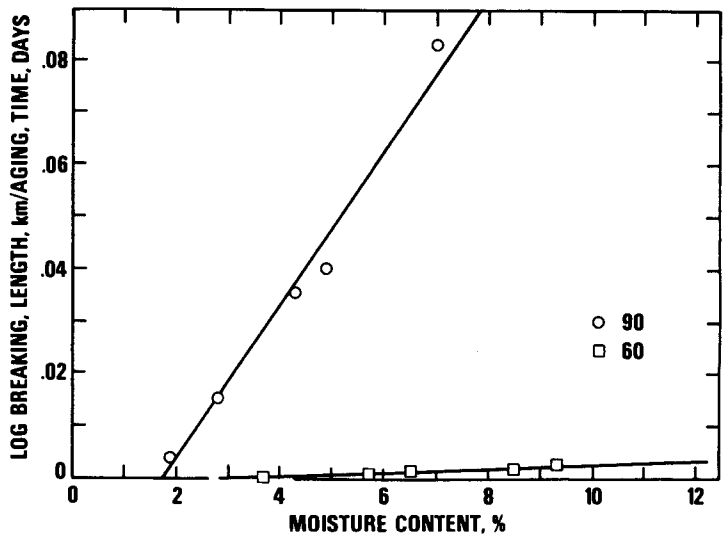

Figure 6. Change in degradation rate of zero span tensile strength with moisture content at 60° and 90°C. Moisture contents corrected for increased temperature

In Durability of Macromolecular Materials; Eby, R.;
ACS Symposium Series; American Chemical Society: Washington, DC, 1979.

result in large changes in degradation rate. In fact it is quite possible that most of the disagreement between earlier investigators of paper permanence may have originated in poor environmental control.

The results of this investigation also indicate that simple oven aging will eventuate in illusory results. The water bound to cellulose in an oven at 100°-105° is very low and quite likely "inactive."

There is no clear cut indication from the results that temperatures up to 90°C are excessive for paper permanence studies. Many of the problems in accelerated aging studies of paper, previously associated with higher temperatures and humidities, were apparently caused by improper control of the environment. It is very difficult to control relative humidity precisely at high temperatures and for that reason 80° and 90°C may be considered excessive.

Conclusions

The degradation rate of paper at elevated temperatures is dependent on the amount of water bound to cellulose. A fraction of the bound water appears to be "inactive" with the amount of "inactive" water decreasing with increasing temperatures. In assessing paper permanence it will be necessary to determine the effect of both temperature and humidity on the degradation rate of paper since it cannot be assumed the one or both variables will have the same effect on all papers. None of the results of this investigation give a clear indication that temperatures up to 90°C are excessive in degradation studies for paper. Temperature and moisture content will both have to be controlled very precisely at 80°C and higher in order to obtain reliable data.

In Durability of Macromolecular Materials; Eby, R.;
ACS Symposium Series; American Chemical Society: Washington, DC, 1979.

Bibliography

1. Hall, G., Paper Trade Journal, 82 (1926) TAPPI Section 185.

2. Rasch, R.H., J. Res. Nat. Bur. Std., 3:469 (1929).

3. Parks, E.J. and Hebert, R.L., "A Source of Error in Paper, Extract pH Determination. Contact between Paper and References Electrodes." NBSIR 74-915, January 31, 1976, NTIS PB 2490775.

4. Parks, E.J. and Hebert, R.L., "Accelerated Aging of Laboratory Handsheets; Changes in Acidity, Fiber Strength and Wet Strength," NBS Report 10-627, Dec. 27, 1971, NTIS COM 75 10164.

5. Parks, E.J. and Hebert, R.L., "Accelerated Aging of Laboratory Handsheets: Retention of Folding Endurance, Internal Tear, Bursting Strength, and Tensile Strength," NBS Report 10,628, Dec. 1, 1971, NTIS COM 75 10165.

6. Parks, E.J. and Hebert, R.L., "Accelerated Aging of Laboratory Handsheets: Reflectance, Moisture Retain, Sonic Modulus and Differential Thermal Analysis, NBS Report 10-687, Feb. 22, 1972, NTIS COM 75 10602.

7. Isbell, H.S.J. Res. Natl. Bur Std. 32, 45 (1944).

8. Lindberg, B. Chim, Biochem. Linguine, Cellulose Hemicelluloses, Acto. Lymp. Inter., Grenoble, France, 303 (1964).

9. Unquhart, A.R. and Williams, A.M., J. Textile Research 15, T559 (1924).

10. Jeffries, R.J., Text. Inst. 51, No. 9 T339 (1960).

RECEIVED December 8, 1978.

25

Reinforcing Degraded Textiles: Effect of Deacidification on Fabric Deterioration[1]

N. KERR, S. P. HERSH, P. A. TUCKER, and G. M. BERRY

School of Textiles, North Carolina State University, Raleigh, NC 27650

Textiles which have deteriorated with age are frequently weak, brittle and powdery and often require treatment to prevent further damage. However, there is a lack of understanding of both the mechanisms of degradation and techniques for preserving historic textiles. For these reasons studies were initiated about three years ago to examine new approaches to textile conservation. Part of this program involved the characterization of naturally degraded historic textiles and the development of model degraded fabrics by means of artificial aging (1) and the use of textile finishing resins as consolidants (2).

The naturally degraded archaeological fabrics examined were obtained from two locations in Peru. The first group of samples dated from about 1200 A.D. and came from a Chancay Valley grave site. The others dated from about 1000 B.C. and were obtained from the Gramalote site in northern Peru. The model degraded fabrics were prepared from a contemporary cotton print cloth by irradiation with high voltage electrons, exposure to dry heat and hydrolysis with mineral acids.

The fabrics were characterized by measuring their tensile and tear strengths, extent of oxidation via Turnbull's blue test and infrared spectroscopy, infrared crystallinity index and molecular weight.

A comparison of the properties of the artificially degraded fabrics with those of the Pre-Columbian cottons indicated that none of the artificially degraded fabrics duplicated the ancient samples in all properties. For example, none of the aging techniques produced the severe powdering evident in naturally degraded samples. The strength levels of laboratory degraded samples, however, could be controlled to match those of the archaeological cottons. Both types of samples, whatever the degradation process, showed a sharp drop in DP and an

[1]Project supported by the National Museum Act, which is administered by the Smithsonian Institution.

0-8412-0485-3/79/47-095-357$05.00/0

accompanying strength loss. However, the degree of crystallinity, actual DP and extent of oxidation depended on the mode of degradation.

The research to be reported here concerns efforts to prevent or retard degradation of cotton textiles by applying various deacidifying agents.

Prevention of Deterioration

The deterioration of paper in books and documents has been a concern for many years. Research by paper conservators indicates that books and manuscripts may be protected from aging by treatment with alkaline agents which neutralize the acidity of the paper as it develops (3,4,5,6,7). The deacidification process not only neutralizes the acidity of the oxidized cellulose, but also leaves an "alkaline reserve" in the paper to retard future deterioration.

Textiles made from cellulose fibers such as cotton, flax and rayon are subject to tendering with age just as paper weakens and yellows with age. As a conservation measure, textiles may be washed and rinsed thoroughly to remove oxidation byproducts and neutralize the fabric. Yet historic textiles are rarely treated with alkaline agents to neutralize them and reduce the rate of degradation. There is a reluctance among conservators to leave on a fabric any substance which was not originally present in the fabric. However, if a fabric is likely to become acidic from oxidation or exposure to atmospheric pollutants, the presence of an alkaline buffer would be expected to reduce future tendering of the fabric. There might be some historic textiles which would benefit from the presence of an alkaline reserve, provided the buffer had no deleterious effect on the physical properties of the textile. If a fabric could not be neutralized by wet cleaning, a vapor phase treatment might serve to remove the acidity of the textile.

The objective of the present study was to determine whether cotton fabrics treated with alkaline agents can be protected from degradation during accelerated oven aging. The buffers selected were ones which have been used in paper conservation. Morpholine was of particular interest because it can be applied from the vapor phase.

Experimental

Fabric. The fabric used for the accelerated aging tests was a 78 x 76 count 3.5 oz/yd^2 unbleached scoured print cloth. Before use, it was machine washed twice, once in Triton® X-100 nonionic detergent and once in hot water.

Reagents. Cotton fabrics were treated with three alkaline agents, $Ca(OH)_2$, $MgCO_3$ and morpholine, before

In Durability of Macromolecular Materials; Eby, R.;
ACS Symposium Series; American Chemical Society: Washington, DC, 1979.

artificially aging in an oven. Solutions of $Ca(OH)_2$ and $MgCO_3$ were prepared for wet treating the cotton by shaking one gram of reagent in 500 ml distilled water for two minutes. The mixture was then allowed to settle for 24 hours before decanting the clear supernatant liquid. The cotton was exposed to morpholine vapor from a solution prepared by combining 50 ml morpholine with 50 ml distilled water.

Application Procedures. All fabric samples were cut to 4 x 6 inch (W x F) rectangles. Three replicate specimens were processed for each treatment to be subjected to each of the artificial aging experiments described below. For the comparison samples which were not to be artificially aged, six replicate specimens were treated either with water or one of the alkaline agents.

The control fabric was wet out for 10 minutes with distilled water at 24°C, drained for 10 seconds, then dried flat on glass. To treat samples with $MgCO_3$ and $Ca(OH)_2$, the samples were immersed in the solution at 24°C for 10 minutes (liquor to fabric ratio of 50:1), drained 10 seconds then laid flat on glass to dry. $Ca(OH)_2$ treatment gave a weight gain of approximately 2%. For the 360 and 600 hour aging experiments, the samples to be treated with $MgCO_3$ were immersed, dried and then immersed and dried a second time to obtain an add-on of approximately 2%. Samples were exposed to morpholine vapor by hanging for 1 hour at 24°C from a rack in a desiccator containing 100 ml of the aqueous morpholine solution. A partial vacuum was drawn to encourage the penetration of morpholine vapor into the cotton fabric. Other conditions for exposing to morpholine were investigated.

Artificial Aging. Samples were artificially aged by exposure either to dry or moist heat in an oven. All except the 600 hour exposures were conducted in a Fisher Isotemp forced draft oven. The 600 hour exposure was carried out in a Grieve Industrial forced draft oven. Dry aging was accomplished by hanging samples in the oven and heating at 100°C or 170°C for 50, 116, 120 or 600 hours. A relative humidity of approximately 50% was achieved by placing the samples in desiccators containing sufficient water to half saturate the atmosphere within the container. An earlier attempt to obtain a closed system with a relative humidity of 50% using a saturated solution of NaI was not successful. A saturated solution of NaI should maintain a relative humidity of 50.4% at 100°C in a closed container (8). When a desiccator containing 145 ml of saturated NaI solution was heated in the oven at 100°C, the colorless solution gradually turned dark brown as iodine was released. In addition, a layer of crystals formed on the surface of the salt solution thus preventing the evaporation of water and control of relative humidity.

In Durability of Macromolecular Materials; Eby, R.;
ACS Symposium Series; American Chemical Society: Washington, DC, 1979.

To obtain a relative humidity of 100% at 100°C, 10 ml of water was added to each desiccator. This quantity of water was approximately three times that needed to saturate the atmosphere within the container. Each set of treated samples was hung on a glass rod in the desiccator, a partial vacuum was drawn, then the container was placed in the oven. Samples were heated for 120, 360 and 600 hours.

Test Methods. Fabric Tensile Strength: Samples were conditioned at 21 ± 2°C and 65 ± 2% relative humidity. Tensile strength was measured on an Instron CRE machine according to ASTM method D-1628 (Breaking load and elongation of textiles - grab test) (9).

Fabric pH: The pH of one or two samples from each treatment and aging period was measured using the following adaptation of the Barrow method (6): ten square inches of fabric (0.9 g) was cut into 1/8 inch squares, added to 50 ml water at 47°C and stirred vigorously to facilitate wetting out of the fabric. After steeping for one hour at room temperature, the fabric was removed, and the pH of the liquid was measured. The pH of five samples of the original untreated fabric as well as the $Ca(OH)_2$ and $MgCO_3$ buffer solutions were also measured.

In order to determine whether the alkaline treatments would effectively neutralize acidic cotton, fabric exposed to 50 Mrads of ionizing radiation was treated in the following manner before measuring pH:

(a) Two 2 gram samples of 50 Mrad coton were immersed in 400 ml distilled water at 25°C for 15 minutes, the process was repeated and then the samples were dried flat on glass.

(b) After rinsing and drying additional samples as described above, two samples were immersed in either $MgCO_3$ or $Ca(OH)_2$ solution (liquor to fabric ratio of 90:1) for 10 minutes at 24°C and then dried flat on glass. The alkaline liquors were prepared as described previously.

Fabric Color Change: The color of the aged samples was assessed with a General Electric Recording Spectrophotometer which measures tristimulus values X, Y and Z and reflectance. Color difference ΔE in NBS units (AN 40 units) was calculated using the Adams-Nickerson color difference formula (10, 11):

$$\Delta E = 40 \{(0.23\Delta V_y)^2 + [\Delta(V_x - V_y)]^2 + [0.4\Delta(V_y - V_z)]^2\}^{1/2}$$

The terms V_x, V_y and V_z are modified Munsell X, Y and Z values (11).

In Durability of Macromolecular Materials; Eby, R.;
ACS Symposium Series; American Chemical Society: Washington, DC, 1979.

Results and Discussion

Fabric Properties after Treatment. None of the treatments altered fabric color, and only $Ca(OH)_2$ harshened the fabric hand. The samples exposed to morpholine vapor were significantly weaker (87% of the original strength) than fabric treated with water.

Fabric Strength. The strength retention of treated cotton aged under various conditions is given in Table 1. The values reported are an average of six breaks for unaged samples (5 breaks for water treated) and at least three breaks for artificially aged samples. The standard deviation and the coefficient of variation for each treatment and aging period was calculated. A pooled standard deviation, σ_p, for all treatments and aging conditions was also calculated. Within each aging period, the strength of alkaline treated samples was compared with that of the water treated and aged control using a Student's-t test for significant differences between means based on the pooled standard deviation.

$$t = (\bar{X}_1 - \bar{X}_2)/\sigma_p(1/n_1 + 1/n_2)^{1/2}$$

No significant differences between treatments were evident when samples were heated in a dry oven. At temperatures of 100°C, strength losses occurred at a very slow rate. After 600 hours (25 days) all samples retained more than 80% of their original strength. The slow degradation of cotton aged under dry conditions at low temperatures has been reported by others (12, 13). Heating at 170°C accelerated the strength loss considerably and reduced the strength of all fabrics to about 20% of the original. In most experiments, samples exposed to morpholine vapor lost strength more rapidly than the cotton treated only with water. This result is surprising since morpholine vapor is recommended for the deacidification of ancient books and manuscripts and is not considered detrimental to the strength of paper (5, 6, 7).

Table I also shows that when moisture is present during oven aging, the degradation rate is accelerated. Spinner confirms this finding in a review article on the aging of paper (13). The strength loss of fabrics heated at 100°C and 100% R.H. as a function of time are shown in Figures 1, 2, and 3 for $Ca(OH)_2$, $MgCO_3$ and morpholine, respectively. Only $Ca(OH)_2$ significantly decreases the rate of degradation. After 600 hours heating, the fabric treated with $Ca(OH)_2$ retained 49% of its original strength while all other samples retained only approximately 10% of their original strength. High humidity appears to be necessary to enable the anions to diffuse into the cotton fibers and reduce fabric acidity. Aging at 50% relative humidity did not appear to provide sufficient

In Durability of Macromolecular Materials; Eby, R.;
ACS Symposium Series; American Chemical Society: Washington, DC, 1979.

Table I. Strength Retention (%) of Treated Fabrics After Heating[a]

Heating Conditions	Treatment			
	Water	$MgCO_3$	$Ca(OH)_2$	Morpholine
None	100	101	102	87*
Dry, 100°C, 50 hours	96[b]	102	100	94
Dry, 100°C, 120 hours	93[b]	93	96	85*
Dry, 100°C, 600 hours	84	91	87	85
Dry, 170°C, 116 hours	20	19	18	18
50% RH, 100°C, 50 hours	97	93	93	94
50% RH, 100°C, 120 hours	84	71*	84	75*
100% RH, 100°C, 120 hours	75	79	93*	77
100% RH, 100°C, 360 hours	42	49*	69*	38
100% RH, 100°C, 600 hours	10	9	49*	8

[a]Average of six breaks for unheated samples and three breaks for heated samples (except as noted).
[b]Average of 7 breaks
*Significantly different at the 95% confidence level from aged water-treated samples based on pooled standard deviation σ_p = 4.7%.

In Durability of Macromolecular Materials; Eby, R.; ACS Symposium Series; American Chemical Society: Washington, DC, 1979.

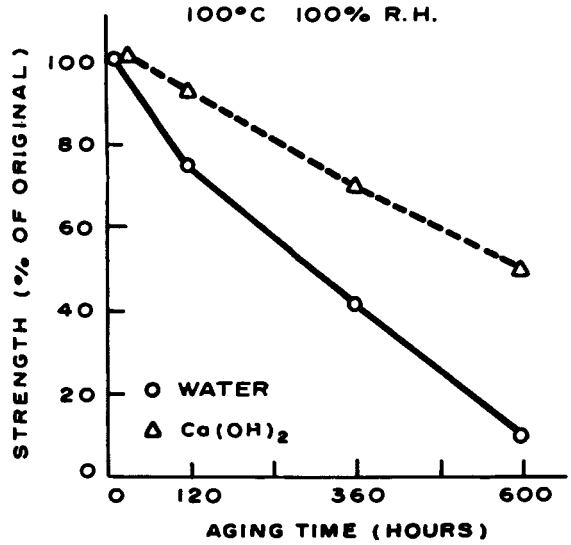

Figure 1. Strength of cotton print cloth pretreated with $Ca(OH)_2$ or water as a function of time of heating at 100°C and 100% R.H.

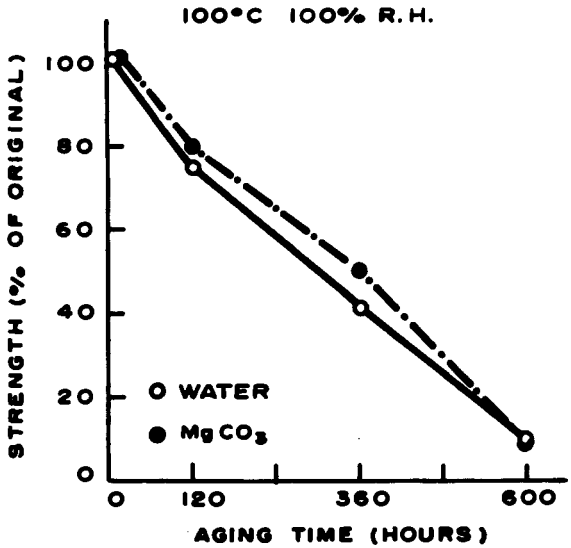

Figure 3. Strength of cotton print cloth pretreated with morpholine vapor or water as a function of time of heating at 100°C and 100% R.H.

In Durability of Macromolecular Materials; Eby, R.;
ACS Symposium Series; American Chemical Society: Washington, DC, 1979.

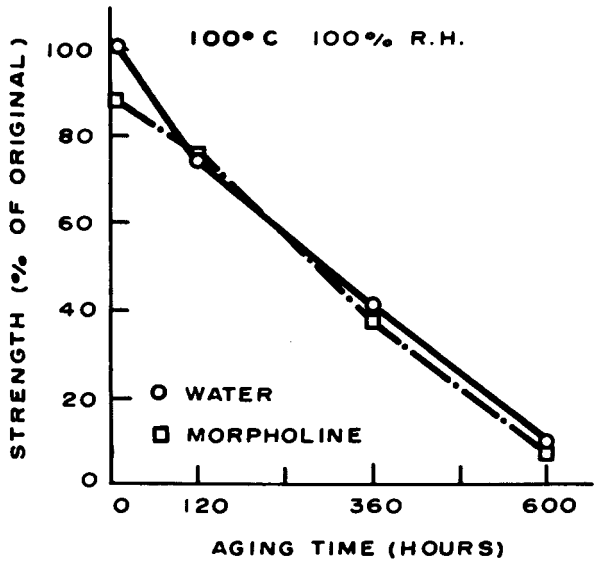

Figure 2. Strength of cotton print cloth pretreated with $MgCO_3$ or water as a function of time of heating at 100°C and 100% R.H.

In Durability of Macromolecular Materials; Eby, R.;
ACS Symposium Series; American Chemical Society: Washington, DC, 1979.

moisture to mobilize the anions as treated samples were not significantly stronger than the water treated controls.

Fabric pH. The pH of samples treated with various alkaline agents and then aged is reported in Table II. Both exposure to high heat (170°C) and long term heating at 100°C cause cotton to become acidic. The presence of an alkaline buffer such as $Ca(OH)_2$ or $MgCO_3$ on the cotton while it ages assists in reducing the development of acidity. The $Ca(OH)_2$ treatment was most effective in maintaining an alkaline pH. Samples treated with this agent remained alkaline during all of the aging experiments, and these samples exhibited the least loss in strength.

The pH of 50 Mrad cotton treated with distilled water, $MgCO_3$ and $Ca(OH)_2$ is reported in Table II. Simply rinsing the 50 Mrad cotton with distilled water for 30 minutes raised the pH from 4.3 to 5.5. Rinsing with water and then treating with $MgCO_3$ did not neutralize the fabric. Because of the low solubility of $MgCO_3$ in water and the fact that this buffer solution had a pH of 8.5 compared with 12.4 for the $Ca(OH)_2$ solution, it is likely that repeated application of $MgCO_3$ would be necessary to neutralize an acidic fabric. The $Ca(OH)_2$ treatment raised the fabric pH to 9.0 but also yellowed the 50 Mrad degraded fabric. Hey (3) reports that paper is occasionally yellowed by immersion in $Ca(OH)_2$, and the yellow color developed during extraction in sodium bicarbonate has been used to determine the C_1 aldehyde content in oxidized cotton (14).

Fabric Yellowing. The color change (in NBS Units) of fabrics treated with alkaline agents and exposed to heat is reported in Table III. A color change of 4 NBS units represents a "slight change" in color or a rating of 4 on the AATCC Grey Scale for Evaluating Color Change, while a difference of 12 NBS units is equivalent to a Grey Scale rating of 2 (10). Exposure of cotton to heat causes it to change from a creamy white to a yellow brown color. The color which develops depends on the alkaline treatment and the conditions of aging including temperature, humidity and time. Both high temperatures (>100°C) and high humidity accelerate the yellowing of cellulose. These findings agree with the work of other researchers (13). However, it is interesting to note that less yellowing occurs during moist aging when samples are pretreated with $Ca(OH)_2$ than when pretreated with $MgCO_3$, morpholine or water. In fact, pretreatment with morpholine accelerates yellowing during exposure to heat although no color change occurred when these samples were first treated with morpholine vapor. Walker reports that fewer than one percent of the 3000 books treated with morpholine at the Barrow laboratory showed an initial color change (7). He made no comments concerning color changes

In Durability of Macromolecular Materials; Eby, R.;
ACS Symposium Series; American Chemical Society: Washington, DC, 1979.

Table II. pH of Treated Fabrics After Heating

Heating Conditions	Treatment				
	None	Water	$MgCO_3$	$Ca(OH)_2$	Morpholine
None		6.8	7.1	9.1	7.3
Dry, 100°C, 50 hours		7.0	8.0	8.7	8.0
Dry, 100°C, 120 hours		7.2	7.8	8.4	7.8
Dry, 100°C, 600 hours		6.0	7.8	8.5	7.4
Dry, 170°C, 116 hours		5.4	5.7	7.4	5.3
50% RH, 100°C, 50 hours		7.1	7.6	8.4	7.1
50% RH, 100°C, 120 hours		6.7	6.8	8.0	6.7
100% RH, 100°C, 360 hours		5.7	6.3	8.2	5.4
100% RH, 100°C, 600 hours		4.3	4.5	7.7	4.2
50 Mrad Cotton	4.3	5.5	6.5	9.0	-

In Durability of Macromolecular Materials; Eby, R.;
ACS Symposium Series; American Chemical Society: Washington, DC, 1979.

Table III. Color Change (in NBS units) of Treated Fabrics After Heating

Heating Conditions	Treatment			
	Water	$MgCO_3$	$Ca(OH)_2$	Morpholine
None	0.0	0.4	0.3	0.2
Dry, 100°C, 50 hours	1.7	2.1	1.5	3.6
Dry, 100°C, 120 hours	3.0	3.0	2.2	5.4
Dry, 100°C, 600 hours	2.2	2.1	3.5	6.0
50% RH, 100°C, 50 hours	6.0	4.4	2.9	8.3
50% RH, 100°C, 120 hours	10.6	11.6	10.5	11.1
100% RH, 100°C, 120 hours*	19.2	20.4	16.8	19.2
100% RH, 100°C, 360 hours*	31.5	24.8	27.4	34.1
100% RH, 100°C, 600 hours	38.7	43.1	33.2	43.9

*Average of two replicate experiments

In Durability of Macromolecular Materials; Eby, R.; ACS Symposium Series; American Chemical Society: Washington, DC, 1979.

during heating. In a review article on the yellowing of paper, Spinner (13) reports that a number of researchers have associated yellowing of cellulose with the presence of aldehyde groups at carbons two and three. Later work by Albeck, Ben-Basset and Lewin, attribute the yellow color of hot alkaline extracts from modified cotton primarily to the C_1 aldehyde content (14).

Summary and Conclusions

The ability of three alkaline agents to retard the degradation of cotton exposed to heat has been investigated. The effectiveness of each agent is summarized in Table IV. Measurement of pH after aging indicates that $Ca(OH)_2$ is able to deposit an alkaline reserve on cotton. This alkalinity will protect cotton from strength loss if there is sufficient moisture present during aging to mobilize the hydroxyl ions and enable them to diffuse into the cotton fibers. The disadvantages associated with the use of $Ca(OH)_2$, namely a harshening of fabric hand and yellowing if used to deacidify degraded cotton, must also be considered. However, since treatment with $Ca(OH)_2$ is reversible, the original hand of a fabric should be restored by washing with distilled water.

Table IV. Effect of Deacidifying Agents on Properties of Heated Cotton Fabrics

Characteristic	Agent		
	$Ca(OH)_2$	$MgCO_3$	Morpholine
Reduces strength loss, moist heating	yes	no	no
Reduces strength loss, dry heating	no	no	no
Extent of yellowing, moist heating	less	varies	greater
Extent of yellowing, dry heating	varies	same	greater
Maintains pH >7.0	yes	no	no

Magnesium carbonate is less effective than $Ca(OH)_2$ in preventing strength loss during aging. Because of its low solubility in water, it is difficult to deposit sufficient $MgCO_3$ on a fabric to provide a good alkaline reserve. It is likely that more than one application of a saturated solution would be necessary to neutralize acidic cotton.

Although morpholine is frequently used in deacidifying paper and has a distinct advantage in that it can be applied from the vapor phase, it has not proven to be suitable for use on cotton fabrics. Even a short exposure to morpholine enhances yellowing during aging and accelerates loss in strength.

In Durability of Macromolecular Materials; Eby, R.;
ACS Symposium Series; American Chemical Society: Washington, DC, 1979.

Literature Cited

1. Berry, G. M., Hersh, S. P., Tucker, P. A., Walsh, W. K., "Reinforcing Degraded Textiles Part I: Properties of Naturally and Artificially Aged Cotton Textiles," Adv. Chem. (1977) 164, 228-248.
2. Berry, G. M., Hersh, S. P., Tucker, P. A., Walsh, W. K., "Reinforcing Degraded Textiles Part II: Properties of Resin Treated Artificially Aged Cotton Textiles," Adv. Chem. (1977) 104, 249-260.
3. Hey, Margaret, "The Deacidification and Stabilization of Iron Gall Inks - Cellulose Combinations on Paper," a paper delivered at the A.I.C. 5th Annual Meeting, Boston, Mass., May 30 - June 2, 1977.
4. Kelly, George B., "Practical Aspects of Deacidification," IIC-AG Paper, Conference at the American Philosophical Society, Philadelphia, Penn., 1972.
5. Kusterer, J. K. and Sproull, R. C., "Gaseous Diffusion Paper Deacidification," U.S. Patent 3,771,958, Nov. 13, 1973.
6. Walker, B. F. and Kusterer, J. K., "Process for Deacidifying a Book which Has a Pyroxylin-containing Cover," U.S. Patent 3,837,804, Sept. 24, 1974.
7. Walker, B. F., "Morpholine Deacidification of Whole Books," Adv. Chem. (1977) 164, 72-78.
8. Weast, R. C., "Handbook of Chemistry and Physics," CRC Press, Cleveland, Ohio, 1974, E-46.
9. "1977 Annual Book of ASTM Standards, Part 24," American Society for Testing and Materials, Philadelphia, 1977.
10. AATCC Technical Manual, Vol. 53, AATCC, Research Triangle Park, 1977, 103.
11. McLaren, K. "Adams-Nickerson Color Difference Formula," J. Soc. Dyers and Colorists (1970) 86, 354-366.
12. Morris, M. A. "Effect of Weathering on Cotton Fabrics," California Agricultural Experiment Station Bulletin 823, Davis, 1966.
13. Spinner, I. H., "Brightness Reversion," TAPPI (1962) 45, 495-513.
14. Albeck, M., Ben-Bassat, A. and Lewin, M., "The Yellowing of Cotton Cellulose Part II: The Influence of Functional Groups and the Nature of Yellowing," Textile Research J. (1965) 35, 935-942.

This is the third part of a series.

RECEIVED December 8, 1978.

Factors Affecting Adhesion of Lithographic Materials

K. L. MITTAL

IBM Data Systems Division, E. Fishkill, Hopewell Jct., NY 12533

The lithographic technique is used extensively for the fabrication of semiconductor devices and large scale integrated circuits by planar technology. The present and future demands for extremely small pattern dimensions put more stringent requirements on all the materials and processes involved in the lithographic technique. Typical processing steps used for delineating patterns using resists are shown pictorially in Figure 1. Figure 1 shows line pattern generation in SiO_2 insulator film but the same steps are also used for making patterns in metal and alloy films. It should be noted that the cleaning and preparation (for example, use of adhesion promoters) of the substrate (e.g. SiO_2) and application of a resist layer precede the process of exposure to radiation. Different resists are sensitive to different sources of radiation: UV light, X-ray, E-beam, ion beam or laser. If the resist is sensitive to UV light, then it is termed a photoresist and the technique is called photolithography. In the case of E-beam lithography, the resist is sensitive to E-beam and so on.

The resist composition consists essentially of three components: polymeric resin, photoactive compound or sensitizer, and solvent. Sometimes a surfactant is also added to enhance its wettability characteristics. There are two kinds of resists: negative and positive. In the case of negative resists, the polymeric resin gets crosslinked on exposure to radiation, thereby rendering it insoluble in the developer, whereas a positive resist on exposure to radiation undergoes chemical transformation that increases its solubility in subsequent developing solutions. It is the differential solubility of the exposed and the unexposed regions that allows the development of high-resolution chemically resistant patterns.

Early materials which showed changes in solubility upon UV exposure were: Fish glue, asphalt, sugars, gelatins sensitized with

0-8412-0485-3/79/47-095-371$05.25/0

In Durability of Macromolecular Materials; Eby, R.;
ACS Symposium Series; American Chemical Society: Washington, DC, 1979.

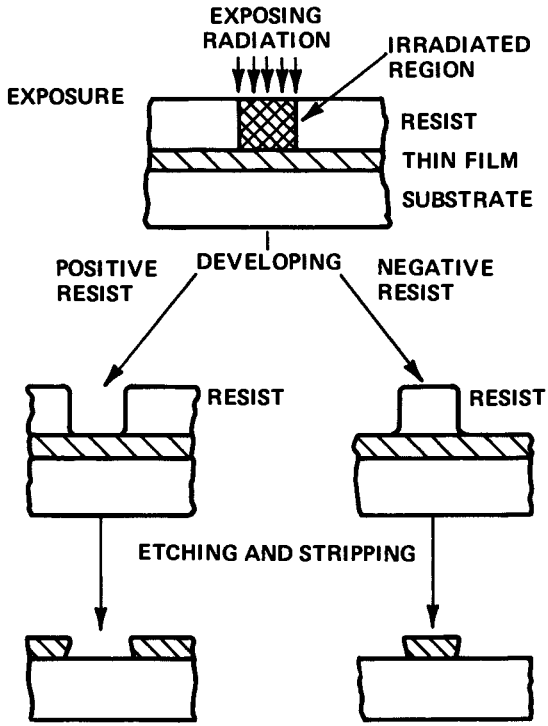

Figure 1. Pattern delineation sequences for positive and negative resists (1)

dichromates. In 1953, Kodak introduced the commercially available negative photoresists. Positive photoresists were developed at a later date, and the E-beam, X-ray or laser-resists became available relatively recently. The latest developments in resist materials and processes and future requirements are discussed in references 1, 2, 3.

The purpose of the resist is to protect the desired areas from the attack of the chemical etchants while the exposed portions of the substrate are being dissolved, and the importance of the adhesion of the resist material to the substrate is quite obvious. Lack or inadequency of adhesion culminates in undercutting which limits the pattern resolution and consequently the device yield. Ideally, one would like to have patterns with vertical walls and the phenomenon of undercutting results in slanted patterns.

Also during the developing stage, the resist patterns should adhere very well to the substrate, otherwise they will be lifted off by the action of the developer. So it is quite clear that the adhesion of the resist is important both during the developing and the etching steps. It should be noted that it is the wet chemical etching process which causes concern about adhesion of resists, and there is an increasing interest in going to the dry etching or RIE* process which alleviates such concern, but it requires special resists which do not degrade when exposed to RIE. In any case, all of the processing steps and the materials (resist, developing medium, etchant) can influence the adhesion of a resist and the effects of these on the resist adhesion will be analyzed. As most of the work has been done using photolithography in making patterns in the SiO_2 film, I will concentrate in this paper on the factors affecting adhesion of photoresists on SiO_2 surfaces.

What is Photoresist Adhesion and How is it Monitored?

Before defining and discussing photoresist adhesion, it is in order to discuss briefly the concept of adhesion of films and coatings as practiced in other areas of human endeavor. The word "adhesion" simply signifies sticking together of two similar or dissimilar materials. In the case of thin films or thick deposits (e.g., electrodeposits) one is more concerned with what has been termed "practical adhesion" (4,5). Practical adhesion represents the forces or the work required to effect separation of the adhering phases and depends upon the intermolecular interactions at the interface (termed as "basic" or "fundamental" adhesion) and "other factors". These "other factors" include stresses in the film, sites of easy fracture mode, and the method of applying external stresses to disrupt the adhering system. There are a legion of methods for measuring practical adhesion of thin films (6) and thick deposits (7).

* Reactive ion etching.

In Durability of Macromolecular Materials; Eby, R.;
ACS Symposium Series; American Chemical Society: Washington, DC, 1979.

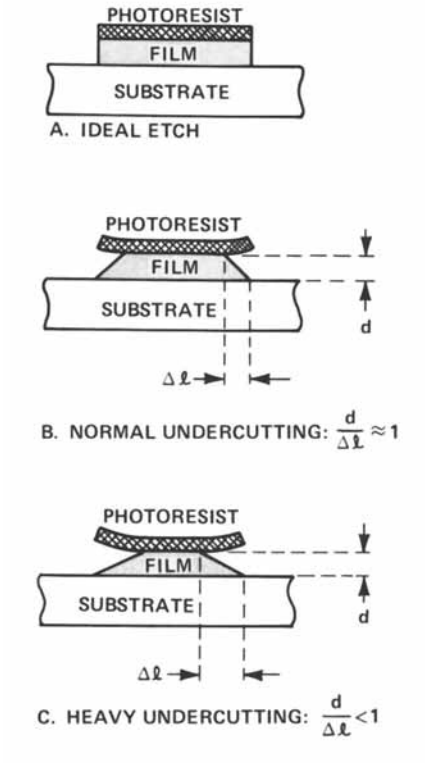

Figure 2. Etched thin film line profiles: (A) without; (B) with normal; and (C) with heavy undercutting

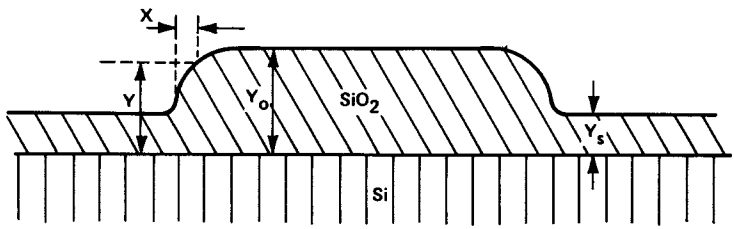

American Society for Testing and Materials

Figure 3. Schematic of a patterned SiO_2/silicon specimen after being subjected to the undercutting test and stripped of photoresist. The parameters of equation for K_u are illustrated. (8)

However, in the case of resists the adhesion or rather the lack of it is expressed in terms of "floating images" observed during developing and "undercutting" observed during chemical etching as shown in Figure 2. It should be noted that there is always a natural degree of undercut as the etchant penetrates in all directions, but the lack of adhesion exaggerates the undercutting. The undercutting is caused by the penetration of the etchant along the substrate-resist interface.
So in the case of photoresist adhesion, one is primarily concerned with the events at the photoresist-substrate interface and how these are affected by the developer and the etchant.
The relationship between the conventional practical adhesion (in terms of peel, pull, shear, scratch) and floating images and/or undercutting behavior has not been investigated. It is quite possible that the photoresist has very poor practical adhesion (as defined above) but is quite acceptable in terms of resistance to etchant penetration. Conversely, there could be very high practical adhesion but extremely poor resistance to the etchant. This will become clearer when the role of the hexamethyl disilazane (HMDS) as an adhesion promoter for photoresists is discussed.

Apropos of monitoring adhesion of photoresists, there are three techniques discussed in the literature. The extent of undercutting has been used for a long time to monitor adhesion of photoresists on a relative basis; but recently (8,9) this technique has been used to describe the adhesion behavior in terms of undercutting constant, K_u. The technique is based upon the use of a fluoride - containing etchant which exaggerates the rate of undercutting of photoresist on SiO_2 surfaces. An empirical equation $K_u = r_o \ln (x+1)/y-y_s$ is given which approximately describes the shape of the undercut oxide edges, thus allowing a numerical measure of the relative adhesion in terms of K_u. The various parameters used in the above equation are shown in Figure 3; r_o is the rate of oxide undercut. The large values for the undercutting constant correspond to poor photoresist/SiO_2 adhesion. Some of the results from this study are shown in Table I.
Another technique described by Klem and Lussow (10) is based upon the ion migration principle. Figure 4 is a schematic of the experimental set up. Test samples consist of SiO_2 substrates overcoated with photoresist in which windows to the SiO_2 are developed out. It should be pointed out that this technique is not restricted to SiO_2 substrate, rather the technique is applicable to all dielectric or insulating substrates. Individual test sites on a wafer consist of two identical windows separated by a photoresist land of known width. A calibrated amount of ionic solution deposited in each window results in direct contact with the SiO_2/photoresist interface as in the substrate etching process. Any electronic flow between the two solutions caused

In Durability of Macromolecular Materials; Eby, R.;
ACS Symposium Series; American Chemical Society: Washington, DC, 1979.

Table I. Values of $1/K_u$ Obtained in Undercutting Tests

Specimen	HMDS	$1/K_u$ Relative Adhesion
KTFR/Aged SiO_2	-	0.25
	+	0.29
KTFR/New SiO_2	-	0.18
	+	0.23
WAYCOAT IC/Aged SiO_2	-	0.20
	+	0.27
AZ-1350B/Aged SiO_2	-	0.16
	+	0.28
Ideal Specimen	' ' '	∿ 3

[A] Based on theoretical specimen having perfect photoresist adhesion, in which lateral distance undercut equals thickness of SiO_2 etched away (∿0.4 μm in a test of 1-min duration).

American Society for Testing and Materials

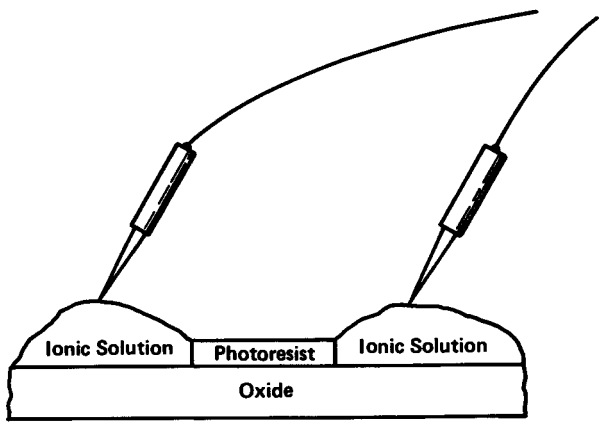

IBM

Figure 4. Principle of the ion migration test for monitroing photoresist adhesion (10)

by ionic migration through the resist, the SiO_2 or along the interface is detected by contacting these solutions with the two platinum probes in the test circuit and applying a potential across them. Independent experiments confirmed (11) that the flow was along the interface and not through the resist layer. The time interval between deposition of ionic solution to detection of current (1 microamp threshold) is indicative of ionic migration time across the resist barrier. The time required for a solution of specified composition to penetrate a fixed distance, t, along the interface would be a measure of the strength of interaction between the substrate (SiO_2) and the photoresist layer. The larger the t, the higher the adhesion, and thus this technique offers a method for comparing adhesion for differe photoresists and dielectric substrates.

The third technique described by Yanazawa et al, (12) is based upon calculating the thermodynamic work of adhesion; W_A, between the dry photoresist and the substrate (SiO_2, Si_3N_4 with and without various surface treatments) and W_A based upon the penetration of the liquid, e.g., water, as shown in Figure 5. They used water as the liquid because they used positive photoresists in their study and an aqueous medium is used as the developer for such resists. Based upon the concept of W_A in the dry and wet state, they defined wet adhesion factor, f^{wet} as $f^{wet} = W_A(wet)/W_A(dry)$. Subsequently they correlated f^{wet} with N^{wet} which signifies the number of patterns lifted. The experiment involved making photoresist (+ve) patterns and counting how many were lifted off after ultrasonic agitation in water. Their results are shown in Figures 6 and 7. Figure 7 shows the correlation between f^{wet} and adhesion of photoresist on a variety of substrate materials.

Although they have made a number of assumptions in calculating W_A's but still their results are interesting. It will be further interesting to apply this approach in the case of other developing media as well as etchants.

What is Dewetting and what Factors Influence it?

Another related phenomena to adhesion of photoresists is that of dewetting. The dewetting signifies retraction of a uniformly spread layer of photoresist. It should be added that quite often dewetting and non-wetting are used synonymously, but there is a fundamental difference between the two. Non-wetting means that the SiO_2 surface is not wetted anytime by the photoresist, whereas dewetting means that the photoresist no longer spreads (on the total surface or on a selected spot) where it spread earlier.

In Durability of Macromolecular Materials; Eby, R.;
ACS Symposium Series; American Chemical Society: Washington, DC, 1979.

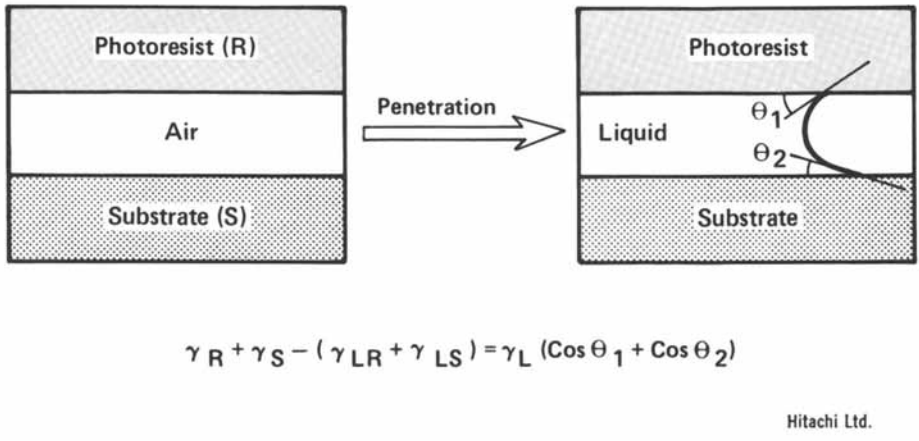

Figure 5. Schematic of adhesion tension in photoresist-liquid–substrate system (12)

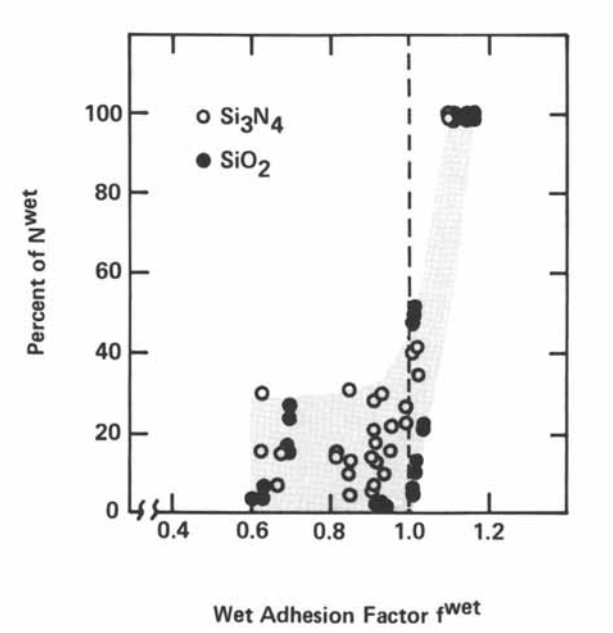

Figure 6. Wet adhesion test for positive working photoresist and SiO_2 or Si_3N_4 system (12)

In Durability of Macromolecular Materials; Eby, R.;
ACS Symposium Series; American Chemical Society: Washington, DC, 1979.

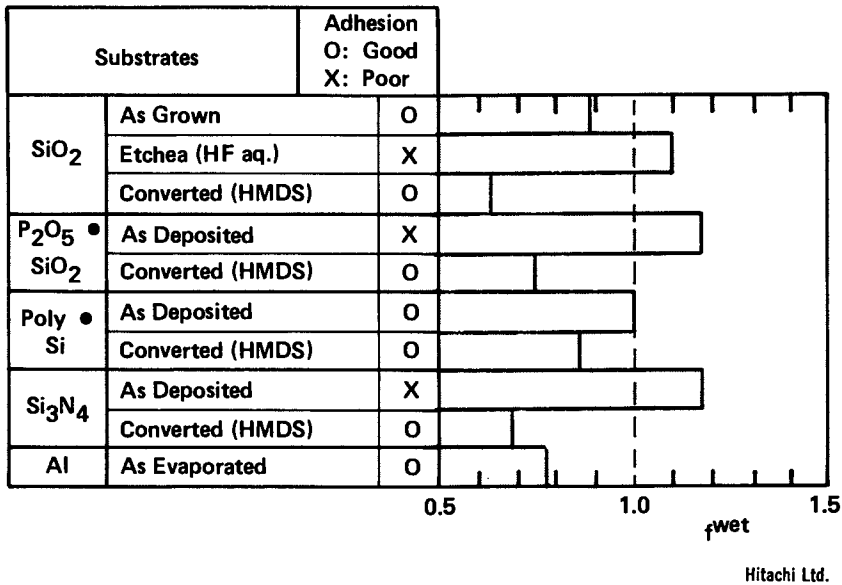

Figure 7. Obtained f^{wet} values for various materials common to silicon integrated circuit processes (12)

For complete wetting (or contact angle, θ, to be zero) it is axiomatic in surface chemistry that $\gamma_{lv} \leq \gamma_{sv}$ where γ_{lv} and γ_{sv} represent the surface free energies of the liquid and solid surface respectively. If this condition is not fulfilled, then there will be a positive θ. This is a thermodynamic requirement and one must also consider the kinetic aspects of spreading. Even if this condition is satisfied, the liquid may not spread to form $\theta = 0°$ because the liquid is too viscous and adequate time was not allowed to let it spread on the solid. So the viscosity of and spinning speed for photoresist solutions are quite important.

If the condition for setting is theoretically satisfied, then the prime cause of non-wetting is the presence of contaminant layers or particles (these lead to non-wetting in spots) which render the surface nonwettable by reducing its surface free energy. However, the main causes of dewetting are: (i) Autophobic nature of the surface. Autophobicity means that the liquid does not spread on its own layer and is caused by the presence of a layer whose surface free energy is less than the surface free energy of the spreading liquid. Such layers could be due to certain reaction products of the liquid with the solid surface or in the case of two components spreading liquid, one of the components may selectively adsorb at the solid surface giving rise to these relatively low surface free energy layers. (ii) Stresses in the solidified film or layer. The internal stresses (caused by evaporating solvent) in the photoresist film can be a source of dewetting. As a corollary to this discussion one should be able to eliminate the problem of non-wetting and/or dewetting by a proper choice of photoresist components.

Before closing this section, it is proper and important to discuss the relationship between wetting and adhesion of photoresists. The adhesion of a layer depends upon the quality and quantity of its intimacy with the substrate. Quality refers to the nature of bonding (van der Waals) acid-base, electrostatic) and quantity signifies the area of intimate contact. Complete wetting (θ=0°) simply signifies the increase in the area of intimacy; however, if the quality of bonding is poor then the net result would be poor adhesion. On the other hand, if there is no wetting, there is no adhesion. In other words, wetting is necessary but not sufficient for good adhesion. So three cases are possible: (i) poor wetting, poor adhesion; (ii) good wetting, poor adhesion; (iii) good wetting, good adhesion. Recently it has been emphasized that the van der Waals)and the acid-base are the only interactions which are important in adhesion (13).

It should be added that adhesion is used here to represent interfacial interactions, and if the interface is susceptible to the attack of the etchant, then it may very well result into poor photoresist adhesion.

In Durability of Macromolecular Materials; Eby, R.;
ACS Symposium Series; American Chemical Society: Washington, DC, 1979.

Effects of Processing Steps and Materials on the Adhesion of a Resist Material.

Effect of Substrate. In the area of conventional adhesion, some correlation has been found between the joint strength and the surface energetics of the substrate material (14). The surface energetics has been expressed in terms of wetting of the substrate by the liquid adhesive and in many cases simply by the contact angle of water, θ_{H_2O}, on the substrate. Similar attempts have been made to correlate water wettability of variously treated SiO_2 surfaces and the adhesion of photoresists in terms of undercut. Thermal SiO_2 is the commonly used substrate so we will concentrate on this material. SiO_2 surface has been characterized by water contact angle (15,16,17,18,19) and its water wettability depends upon its method of preparation, storage conditions, relative humidity, etc., and can be further modified by various treatments. (See Figure 8 and Table II). Also it has been shown that water wettability of SiO_2 depends upon its thickness and after a certain thickness it has no effect (See Figure 9).

Bergh (16) found that the lower the θ_{H_2O}, the lower was the adhesion of KPR*; however, Lussow (18) concluded that not only the θ_{H_2O} but also the surface structure of SiO_2 is important in dictating the adhesion behavior of a photoresist. He deduced three types of SiO_2 surface structures from wettability changes caused by various surface treatments as shown in Figure 10. The wettability of these surfaces as measured by the contact angle of water droplets increases in the order: siloxane < silanol < hydrated form whereas negative photoresist adhesion is in the reverse order. According to Lussow's work, the adhesion of KTFR* is most sensitive to the surface composition and only satisfactory on the siloxane type, whereas KPR* adheres well on silanol surfaces too. Hydrated surfaces yield poor adhesion with both resists. KMER* coatings are relatively unaffected by the surface constitution. It can be concluded from this discussion that adsorbed water on the SiO_2 surface is undesirable for photoresist adhesion. In order to avoid the unpleasant effect of the adsorbed water, coupling agents or adhesion promoters (HMDS, silanes, etc.) are commonly used. These coupling agents react so as to form a siloxane bond with the SiO_2 surface and the organic moiety (for example, $-NH_2$, $-CH_3$) is turned outwards as shown in Figure 11. Once the SiO_2 surface is covered with adhesion promoter layers, the interactions between these organic layers and the photoresist should dictate its adhesion behavior. It is interesting to note that the HMDS is the workhorse of the photoresist industry, but it can not be recommended as an adhesion promoter for promoting adhesion in the mechanical (peel, pull, etc.) sense, because after reaction with SiO_2, the HMDS leaves a bed of $-CH_3$ groups on the outside which are quite inert chemically

* These represent Eastman Kodak resists.

In Durability of Macromolecular Materials; Eby, R.;
ACS Symposium Series; American Chemical Society: Washington, DC, 1979.

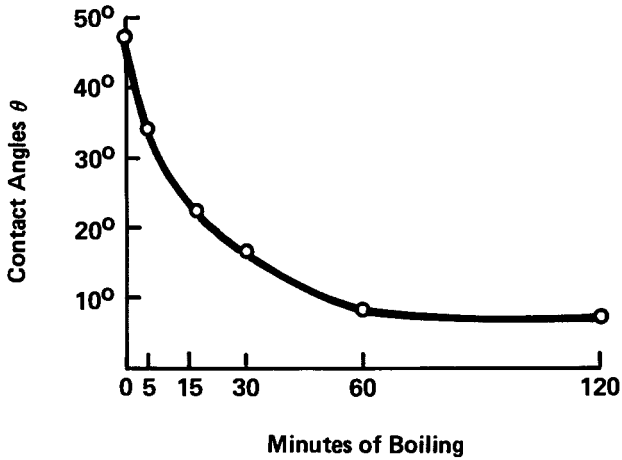

Figure 8. Water contact angle on boiled SiO_2 (15)

Table II Contact Angles of Water on Si After Oxidation and After Rinsing

	θ After Oxidation		θ After Rinse		After Rinse
Type of Oxide	Average Value	Range	Average Value	Range	KPR Adherence
1050 °C-Oxide	32	26-36	24	18-32	Good
650°C -Oxide	3	0-8	3	0-8	Poor
CO_2-Oxide	21	11-38	4	3-12	Poor
RPS-Oxide	32	19-38	7	5-12	Poor

Journal of the Electrochemical Society

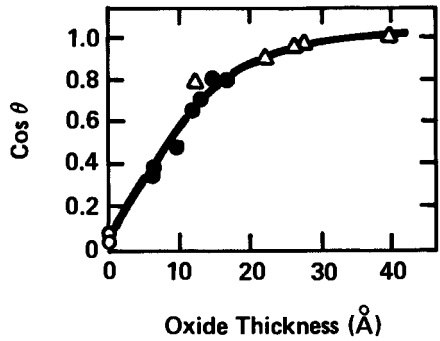

Applied Physics Letters

Figure 9. Cos θ as a function of the oxide thickness: (●), oxide grown at room temperature; (△), oxide grown at 600°C; (○) no oxide (19)

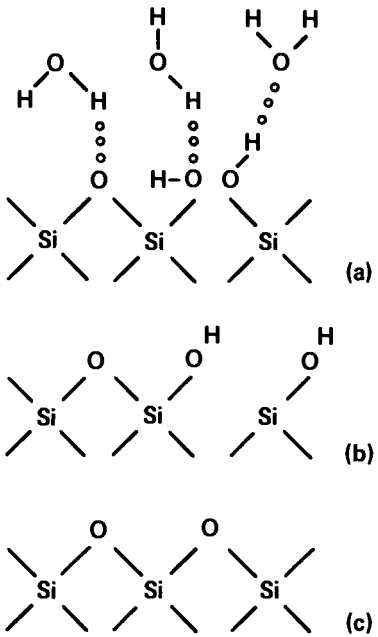

Journal of the Electrochemical Society

Figure 10. Schematic of thermal SiO_2 surface structures: (a) Type 1, with adsorbed molecular water, referred to as hydrated; (b) Type 2, containing silanol groups with no adsorbed molecular water; (c) Type 3, predominantly siloxane structure, no adsorbed molecular water (18)

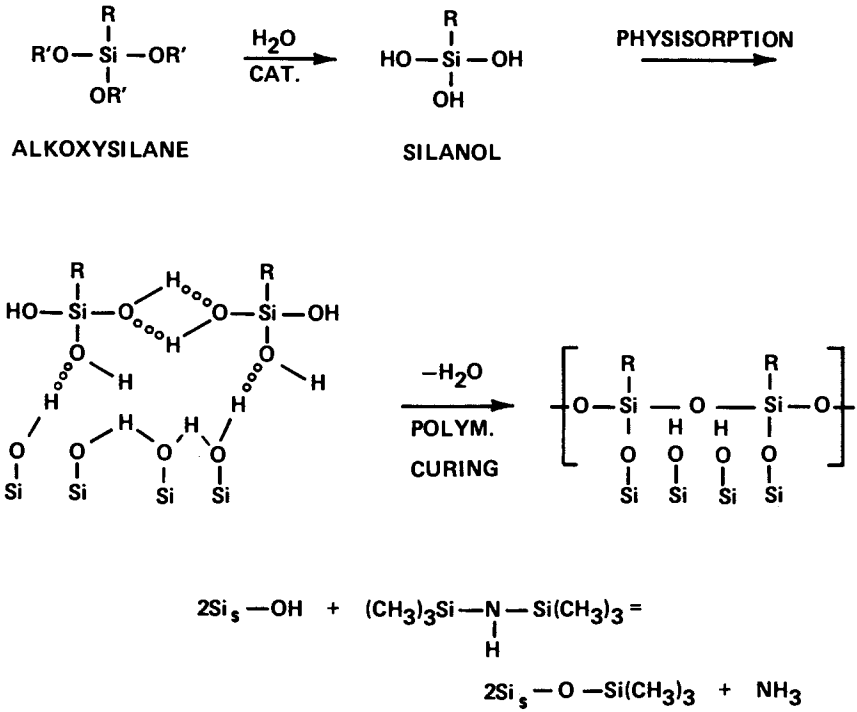

Figure 11. Schematic of: (Top) *reaction of alkoxysilanes with a highly hydroxylated* SiO_2*;* (Bottom) *reaction of hexamethyldisilazane (HMDS) with hydroxylated* SiO_2*. R group contains* $—NH_2$*,* $—CH_3$*,* $—CH_2{=}CH$*, etc. moieties.*

In Durability of Macromolecular Materials; Eby, R.;
ACS Symposium Series; American Chemical Society: Washington, DC, 1979.

(and hydrophobic in nature) and would not react with any adhesive or coating. However, it is the lack of reactivity or hydrophobicity of these $-CH_3$ groups which prevents or curtails the penetration of the etchant along the interface with the result that photoresist adhesion is enhanced. This example is a good illustration of the fact that the factors affecting mechanical adhesion and the photoresist adhesion can be discordant with each other.

So in summary, for good photoresist adhesion, the following conditions are important. (i) With bare SiO_2 surface, the adsorbed water should be removed (e.g., by heating) so that the polymeric component of the photoresist can come in intimate contact with the surface. (ii) The condition for wetting of bare or treated SiO_2 with the liquid photoresist should be satisfied and the kinetics of wetting should be favorable. (iii) As SiO_2 is acidic in character, a basic polymer would culminate in better adhesion provided the interface can be made resistant to etchant penetration. Under certain conditions, acid-base combinations can be made resistant to hydrolysis (20) and it is worth investigating how these could be profitably utilized to improve photoresist adhesion. Also using Fowkes approach (21), the acid-base characteristics of the SiO_2 treated with adhesion promoters should be investigated. Apropos, it will be an interesting study to correlate the surface energetics of the SiO_2 treated with HMDS or silanes with the photoresist adhesion on such surfaces. (iv) The solvent should have less interaction with SiO_2 (bare or treated) than the the polymeric component. This is amplified in the following paragraphs.

Effect of Polymer and Solvent. For good adhesion, there should be maximum contact between the polymer and the substrate and if the solvent has greater affinity for the surface than the polymer, this would prevent the polymer from coming into contact with the surface. The compatibility between polymers and solvents is described in terms of the solubility parameter, δ, and for a given polymer a "good" solvent is the one whose δ matches with that of the polymer. The δ's of various polymers are listed in reference 22, whereas δ's for solvents are compiled in numerous places, see, e.g., reference 23. In a good solvent the polymer is extended permitting large degree of contact between the polymer and the solvent; whereas in a "bad" solvent the polymer is tightly coiled. The role of the solvent is very important in the adsorption of polymers on solid substrates, and the importance of the acid-base considerations in polymer adsorption from solvents has been emphasized recently (24). So for good adhesion, the polymer should have the right acid-base characteristics with respect to the substrate, and should cover the maximum area of the substrate. The solvent should have minimum interaction with the substrate, should evaporate fast, and should not be trapped. Furthermore, the solvent should be free from any impurity which can adsorb selectively on the substrate. For example, even a trace amount

In Durability of Macromolecular Materials; Eby, R.;
ACS Symposium Series; American Chemical Society: Washington, DC, 1979.

of water in an organic solvent is extremely undesirable as water has great affinity for the SiO_2 surface.

Effect of Pre-Bake. The purpose of the pre-exposure baking is to dry the resist film (i.e., to remove the solvents), prevent tackiness and improve adhesion to the substrate. However, the pre-baking step should not destroy the photoactive compound, so the pre-baking temperature and time are important. Pre-baking can relieve the internal stresses in the resist film thereby improving the adhesion of the dry resist film to the substrate. If the prebake is done at higher than the desired temperature, it could lead to "fogging" due to thermal crosslinking (negative resists) or melting or decomposition in the case of positive resists.

Effect of Exposure. The purpose of the exposure is to cause certain chemical changes in the polymer resin and this causes differential solubility behavior in the developing medium. For a negative resist, the exposure step causes crosslinking and renders the polymer resist insoluble in the developer. The larger the number of crosslinks, the greater will be the rigidity of the structure; however, too high rigidity may not be desirable. If the polymer is not properly exposed, it will cause undesirable swelling in contact with the developer as discussed below. Underexposure results into crosslinking only near the surface. Also the effect of gaseous environment is important. The presence of oxygen is considered bad as it prevents crosslinking by destroying the sensitizer, which could lead to floating image behavior or thinning of resist pattern during developing.

Effect of Development. The phenomenon of "floating image" is attributed to the interaction of the developer with the polymeric resin and the substrate. The developer should not cause swelling of the resist pattern, as the swelling is resolution limiting (see Figure 12). In the case of positive resist, the unexposed regions remain quite hydrophobic and thus do not interact rapidly with the developing solvent and are not subject to swelling. A good developer should be a poor solvent for the exposed ($-v_e$) resist, and should possess minimal interaction with the substrate. For minimum swelling, the initial molecular weight of the polymer should be high, the molecular weight between crosslinks should be low (many crosslinks) and the solvent should be poor (26). Also the wetting behavior of the exposed resist ($-v_e$) pattern by the developer should be important. The critical surface tension of wetting, γ_c, of some resist materials are given in Table III as determined by Davidson and Levi (27), but no attempts have been made to correlate γ_c of the resist with its floating image behavior.

In Durability of Macromolecular Materials; Eby, R.;
ACS Symposium Series; American Chemical Society: Washington, DC, 1979.

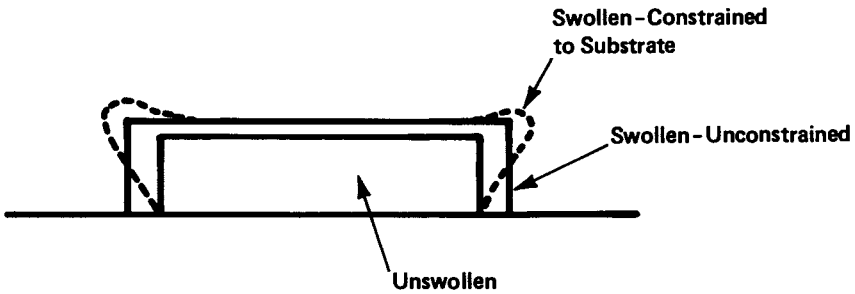

$$q^{5/3} \cong \frac{\bar{v} M_c}{V_1} \left[1 - 2 \frac{M_c}{M}\right]^{-1} (1/2 - X)$$

Where q = The Ratio of the Volumes In the Swollen and Dry States

$\bar{v}$ = The Specific Volume of the Polymer

V_1 = The Molar Volume of the Solvent

M_c = The Molecular Weight Between Crosslinks

M = The Molecular Weight of the Polymer

X = Polymer-Solvent Interaction Parameter

Figure 12. Swelling of the resist layer

In Durability of Macromolecular Materials; Eby, R.;
ACS Symposium Series; American Chemical Society: Washington, DC, 1979.

Table III. Critical Surface Tension of Wetting (γ_c) for some Photoresists (from Ref. 27, reprinted by permission of the publisher, The Electrochemical Society, Inc.)

PHOTORESIST	(γ_c)
Cartesian - C^2LSP	29.9 ± 1.7
Dynachem - CMR-5000	33.7 ± 1.4
- DC31400P	38.5 ± 0.3
Hunt - IC	33.3 ± 1.2
Kodak - KMER	33.7 ± 1.3
- KPR 4	40.0 ± 0.5
- KTFR	32.0 ± 1.0

The Electrochemical Society, Inc.

Table IV. Effect of Etch Rate On the Adherence of KPR

(from Ref. 16, reprinted by permission of the publisher, The Electrochemical Society, Inc.)

Etch Rate, Å/Min.	Etching Time(min)	Hydrophobic Oxide	Hydrophilic Oxide
4000	2.5	Not Undercut	Slight Undercut
1000	10	Not Undercut	Undercut
330	32	Not Undercut	Heavy Undercut
140	70	Undercut	All Oxide Removed

Journal of the Electrochemical Society

In Durability of Macromolecular Materials; Eby, R.;
ACS Symposium Series; American Chemical Society: Washington, DC, 1979.

Effect of Postbake. Postbaking is commonly done to improve the resistance of photoresists to etchants and plating solutions. The temperature of postbaking is important; too high a temperature will render the photoresist difficult to remove later on.

Effect of Etching. The phenomenon of undercutting, as shown in Figure 2, is commonly observed during the chemical etch step. As pointed out earlier this may not be a problem in the case of dry etching. The undercutting is caused by the lateral movement of the etchant, so the interfacial bonds between the resist and the substrate should be resistant to the attack by the etchant. Here, the right kind of acid-base considerations should be very helpful in alleviating the undercutting problem. The chemical nature, concentration, and the time of etching all are important in undercutting. Slower etch rate produces more undercutting as shown in Table IV; furthermore, the etching behavior depends upon the hydrophobicity or hydrophilicity of the SiO_2 surface.

The last step involves the removal of the photoresist layer using chemical strippers or by volatilizing it. If the photoresist adheres too well, then it can pose a problem in its removal.

SUMMARY

It is shown that the adhesion of a resist to a substrate depends upon the chemical composition of the resist, the surface characteristics of the substrate, and the various processing steps. How photoresist adhesion is influenced by these materials and processing parameters is analyzed. It is emphasized that certain surface treatments can influence the photoresist adhesion and mechanical adhesion (in terms of peel, pull, scratch, etc.) in different ways, and commonly used techniques to improve mechanical adhesion of films and coatings may be fruitless, or even harmful, so far as photoresist adhesion is concerned. By a proper understanding of the factors affecting photoresist adhesion, one should be able to control it.

In Durability of Macromolecular Materials; Eby, R.;
ACS Symposium Series; American Chemical Society: Washington, DC, 1979.

Literature Cited

1. Thompson, L.F., Kerwin, R. E., Ann. Rev. Materials Sci. (1976), 6, 267-301.
2. International Conference on Microlithography, Paris, France, June 21-24, 1977.
3. Symposium on Polymeric Materials for Electronic Applications, held at the American Chemical Society meeting, Chicago, Aug. 29-Sept. 2, 1977.
4. Mittal, K.L., Polymer Eng. Sci. (1977), 17 467-473.
5. Mittal, K. L., in "Adhesion Measurement of Thin Films, Thick Films and Bulk Coatings", K. L. Mittal, Editor, pp. 1-17, American Society for Testing and Materials, Philadelphia, March 1978.
6. Mittal, K. L. Electrocomponent Sci. Technol. (1976), 3, 21-42.
7. Mittal, K. L., in "Properties of Electrodeposits", pp. 273-306, Electrochemical Society, Princeton, N.J., 1975.
8. Deckert, C. A., in "Adhesion Measurement of Thin Films, Thick Films and Bulk Coatings", K. L. Mittal, Editor, pp. 327-341, American Society for Testing and Materials, Philadelphia, March 1978.
9. Deckert, C. A., and Peters, D. A., in "Proceedings of the 1977 Kodak Microelectronics Seminar", pp. 13-25, 1977.
10. Klem, C. G., and Lussow, R. O, IBM Tech. Disc. Bull (June 1970), 13, No. 1, 35.
11. Lussow, R. O., (1978), private communication.
12. Yanazawa, H., Matsuzawa, T. and Hashimoto, N. in "Proceedings of the 1977 Kodak Microelectronics Seminar", pp. 153-160, 1977.
13. Fowkes, F. M., J. Adhesion (1972), 4, 155-
14. Mittal, K. L., in "Adhesion Science and Technology", L. H. Lee, Editor, Vol. 9A, pp. 129-168, Plenum Press, New York, 1975.
15. Frieser, R. G., J. Electrochem. Soc. (1974), 121 669-672.
16. Bergh, A. A., J. Electrochem. Soc. (1965), 112, 457-458.
17. Lussow, R. O., Wirtz, L. H., and Levine, H. A., J. Electrochem. Soc. (1967), 114 877-879.
18. Lussow, R. O., J. Electrochem Soc. (1968), 115, 660-664.
19. Williams, R., and Goodman, A. M., Appl. Phys. Lett. (1974), 25, 531-532.
20. Bolger, J.C., and Michaels, A.S., in "Interface Conversion" P. Weiss, Editor, Elsevier, Amsterdam, 1968.

In Durability of Macromolecular Materials; Eby, R.;
ACS Symposium Series; American Chemical Society: Washington, DC, 1979.

21. Fowkes, F.M., and Maruchi, S., ACS Organic Coatings Preprints, Vol. 37, No. 1, pp 605-610, March 1977.

22. Brandrup, J, and Immergut, E. H., Editor, "Polymer Handbook", John Wiley and Sons, New York, 1975.

23. Barton, A.F.M., Chem. Rev. (1975), 75, No. 6, 731-753.

24. Fowkes, F. M., and Mostafa, M.A., ACS Organic Coatings Preprints, Vol. 37, No. 1, pp. 142-145, March 1977.

25. Hughes, H.G., Paper presented at the Nepcon West 1976, Anaheim, CA, Feb. 26, 1976.

26. Davidson, E.B., Preprints of the Mid-Hudson Conference on Photoresist Materials, pp. 141-148, 1970.

27. Davidson, E.B. and Levi, G, Extended Abstract of the Electrochemical Society meeting, Spring 1971.

RECEIVED December 8, 1978.

27

Durability of the Bond between Mineralized Tissues and Potential Adhesives

G. M. BRAUER, D. J. TERMINI, and J. A. JACKSON

National Bureau of Standards, Washington, DC 20234

A major shortcoming of bone cements and dental restorations is the lack of chemical bonding between the currently used synthetic materials and the hard tissues, i.e. bone and tooth, in the humid environment encountered under clinical conditions. Thus, orthopaedic implants or dental restoratives are kept in place by mechanical interlocking to the bone or tooth substrate. A truly adhesive dental cement may be expected to have the following properties, for instance: (1) inhibit the formation of secondary caries since it would prevent percolation of microorganisms, liquids and foreign matter into the marginal area of the restoration, (2) lead to simpler cavity preparations resulting in a decreased loss of non-carious tooth substance, (3) be especially advantageous in the repair of incisal fractures since it would avoid the cutting of healthy tissue, (4) make it possible to obtain leakproof cementation of cast fixed prostheses, (5) allow the attachment of orthodontic appliances directly to the teeth without the need for placing bands on each tooth, (6) be used as a sealant for pits and fissures and incipient carious lesions and (7) serve as an adhesive coating which acts as a barrier to the formation of plaque or deposition of calculus and which may inhibit the formation of caries.

Many problems are encountered in obtaining strong, permanent bonding between an adhesive and hard tissue. Bone and dental tissues are not homogeneous, but have variable physical and chemical properties. The inorganic apatite crystals of enamel change directions at prism boundaries and also contain 1% organic portion of proteins and lipids. The wettability of bone, enamel and dentin varies according to their contamination with low energy organic films. The collagen of the dentin matrix provides hydroxyl, carboxyl and amino groups which may be utilized in securing chemical bonding to this substrate. The odontoblast protoplasm comprising 10% of the dentin surface precludes adhesion, but may allow adhesive penetration for mechanical interlocking. For a dental restoration to fill a cavity and retain close adaptation to the cavity walls, the bond strength between restorative and the tooth surface

In Durability of Macromolecular Materials; Eby, R.;
ACS Symposium Series; American Chemical Society: Washington, DC, 1979.

must at all times be as great as the tensile and shearing stresses tending to separate these materials.

A cavity surface from which decayed material has been removed and which has been rinsed and dried resembles a loosely held brush-heap of debris held electrostatically to sound tooth structure. This is especially true for enamel where details of the prepared surface are masked by debris. A smear layer often covers the dentin surface. Complete drying of the surface cannot be accomplished under *in vivo* conditions, since fluid seeps rapidly from the dentinal tubules. Thus the tooth surface is highly heterogeneous and bonding is only accomplished at localized active sites.

Without pretreatment an adhesive will set the flat tissue surface and will flow into surface voids. On curing, contraction of the resin occurs and stresses are set up which will reduce bond strength. The high modulus tooth substrate in contact with a relatively brittle resin adhesive (which has a 20-times lower modulus) produces a condition that enhances failure close to the interface. Stresses caused by aging of the adhesive or changes at the substrate surface may also result in failure. Good *in vitro* bonding of hard tissues is often obtained in air. The adhesive joints may be expected to suffer at least some loss of strength and durability in the hostile, humid *in vivo* environment because of the diffusion and the displacement of adhesive at the interface by water as can be predicted from thermodynamic considerations (1). The rate of water diffusion to the interface effects the decrease in bond strength (2). Undoubtedly, the kinetics of this phenomena will depend on the kind of substrate and adhesive employed as well as on the geometry of the joint. Where hydrogen bonding is the source of adhesion, debonding is likely to take place fairly rapidly. When a boundary region rich in polar forces is formed prior to curing, this region will be highly oriented and very susceptible to interaction with water molecules (3). Adhesion under clinical conditions may not only be subject to the hydrolytic reaction by water or aqueous systems (blood, saliva, food) but can also be reduced by bacteria or enzymatic systems as well as by the mechanical stresses caused by mastication.

The adhesive-substrate bond may also be subject to thermal stresses resulting from differences in the coefficients of thermal expansion of the hard tissue and the resin. Ideally the values of these two coefficients should be the same (in practice the coefficient of thermal expansion of the adhesive is usually much higher) to avoid the build-up of stresses which eventually may lead to bond failure. This is especially important for dental adhesives since the temperature range in the mouth may vary from 2°C to 55°C.

Acid etching pretreatment of enamel, such as the use of buffered 50% phosphoric acid solutions, has found clinical applications to bond enamel to restorative materials, sealants and orthodontic brackets (4,5). The etching creates an increased enamel surface area and opens pores into which the resin can flow. Greater porosity of the substrate allows an easier ingress of un-

In Durability of Macromolecular Materials; Eby, R.;
ACS Symposium Series; American Chemical Society: Washington, DC, 1979.

cured resin and therefore better mechanical interlocking of the hardened resin into the enamel phase. Enhanced bonding to acid-conditioned surfaces has been demonstrated by the penetration of composites and unfilled resins into the etched enamel pores (6) and by the absence of dye or radioisotope penetration at the resin-enamel interface (7). Such penetration results in the encapsulation of the crystallite components of the enamel providing a clinical effective permanent bond.

Acid etching pretreatment of dentin prior to application of a resin restorative leaves the collagenous component of this substrate substantially untouched. The collagen at the dentin surface interferes with the mechanical adhesion of the hydroxyapatite, (the inorganic constituent of dentin) to the adhesive. Thus, in contrast to its successful use with enamel, etching pretreatment produces a bond between dentin and restorative resin that is too weak to withstand the forces encountered at the interface under clinical conditions.

Many potential ways have been suggested to obtain adhesion to dentin. Complexation of polycarboxylates with the hydroxyapatite component gives some adhesion (8,9,10). Probably because of the lower calcium content of the dentin the resulting bonds are much weaker than those formed with enamel. A similar effect is obtained with vinylbenzyl phosphonic acid (11,12). Under carefully controlled conditions a monomer such as N-(2-hydroxy-3-methacryloxypropyl)-N-phenylglycine (NPG-GMA) enhance adhesion to dentin (13,14,15,16,17). Another means of attachment to dentin is through interaction of reactive organic compounds with functional groups present in the collagen, e.g. tri-n-butyl borane-cured poly(methyl methacrylate) (18), the nitrene produced by the photolysis of p-azidobenzoyloxyethyl methacrylate (19) or alkyl-dichlorotriazine derivatives, or for example, the reaction product of 3-hydroxypropyl methacrylate and trichlorotriazine (20,21). Many reactions involving a variety of functional groups which can be utilized in chemically bonding to collagen have been summarized by Glenn (22). Grafting of polymers onto the collagenous component of hard tissue is possible under experimental conditions which might be tolerated clinically (23, 24). However, nearly instantaneous grafting procedures which can be employed in dental practice have not been developed. Most adhesive systems used so far to bond substrates to hard tissues are composed of 2-cyano-acrylate esters (25,35) or contain isocyanate-urethane polymers (36,37,38).

The objective of this study was to determine (1) which 2-cyanoacrylate or isocyanate-urethane methacrylates adhere to bone or dentin, (2) what is the durability of the resulting bond and (3) how to improve long-term stability of the bond.

The requirements for acceptable hard tissue adhesives include room temperature cure, fast setting, and high, durable bond strength combined with excellent biocompatibility. No such material is available at the present time.

In Durability of Macromolecular Materials; Eby, R.;
ACS Symposium Series; American Chemical Society: Washington, DC, 1979.

Materials and Methods

Cyanoacrylates were obtained from commercial sources and from the U. S. Army Medical Research and Development Laboratory. Urethane-methacrylates containing residual isocyanate groups were

Flat bovine bond cylinders, 5 mm in width, 8 mm in diameter, with a groove approximately 2 mm in width and depth, about 2 mm above the base of the bone, were cut from the forequarter shin by a procedure previously described (39). Specimens were stored in water before use.

The bone specimens were patted dry and pretreated if desired. A small drop of the adhesive was then placed on a bone surface. The specimen was placed into the groove of a rectangular aluminum block and the surface was butted with another bone cylinder. Finger pressure was applied for 1 or 3 minutes respectively, depending on the curing time of the adhesive, to 2 brass rods which had been placed in the groove on opposite ends of the bonded bone specimens. The joined specimens were immediately placed in water at 37°C or thermocycled at 5° and 55°C with 70 sec. at each temperature and 10 sec. for each transfer; a total of 540 cycles per day, for the desired length of time. Before measuring the bond strength, the specimens were removed from the bath, and the ends were placed into split cylindrical adapters with slip rings designed to lock into the groove for each bone cylinder. The jaws of a universal testing machine gripped metal strips to which adapters for holding the specimen were attached by means of pins. Tensile alignment was abetted by the use of a gimbal in the upper jaw assembly. Stress was applied at a loading rate of 5 mm/min. To obtain statistically valid results the strength of at least 5 joints was determined for each adhesive treatment.

The bond strength of bovine dentin cemented to poly(methyl methacrylate) was determined using mandibular anterior teeth of yearling calves embedded in resin. Flat dentin surfaces were cut with a diamond wheel employing a water spray. Prior to testing, the specimens were stored in water, then blotted dry, pretreated if desired (swabbing the surface for 30 sec. with a cotton pladget saturated with the respective solution, rinsing the surface with distilled water one minute after starting the treatment and blotting the surface dry before applying the adhesive) and a drop of adhesive was placed on the dentin surface. An approximately 4 cm long acrylic rod of 0.32 cm diameter was positioned on top of the dentin surface. To obtain vertical alignment the rod was guided onto the surface through a 0.34 cm hole in an acrylic cylinder. A 200 g weight was placed on top of the rod for 3 min and the excess adhesive was wiped off the dentin surface.

Some dentin-acrylic resin joints were covered with a thin film by brushing a hydrophobic coating of monomeric liquid around the interface. The film was cured by irradiation for one minute with a UV light source which was moved circularly at a distance of 2 mm around the joint.

In Durability of Macromolecular Materials; Eby, R.;
ACS Symposium Series; American Chemical Society: Washington, DC, 1979.

The specimens were immediately placed in water at 37°C or thermocycled for the desired length of time. Adhesion of the dentin to the acrylic rod was measured by using a modified procedure of the tensile test of Lee, Swartz and Culp (40). A stainless steel washer was slipped over the rod and the assembly was positioned into the gripper attached to the lower jaw of the universal testing machine. To align the assembly a pin was placed through a hole near the top of the acrylic rod and through holes in a gimbal. The top jaws of the testing machine gripped a metal strip which supported the gimbal. Stress was applied at a loading rate of 5 mm/min.

Results and Discussion

Adhesion to bone: Curing of the cyanoacrylates cemented to bone varied from a few seconds to less than 3 minutes. An exception is n-hexyl 2-cyanoacrylate (and probably most other cyanoacrylates with six or more carbon atoms in the side chain) which does not cure between bone surfaces in this time period. Curing is speeded up by pretreating one or both of the bone surfaces with a nucleophilic agent such as a 1% alcoholic dimethyl-p-toluidine solution. Even after acid etch of the bone surface little or no adhesion was observed for controls in which the bone cylinders were joined by a composite resin. No bonding was obtained when the 2-cyanoacrylate adhesive was placed on dried bone kept in a dessicator over phosphorous pentoxide prior to application of the adhesive. Thus traces of water in the substrate are necessary for successful bonding with cyanaoacrylates. Immediate placement of the joined bone specimens into the 37°C water did not reduce the bond strength when compared to bonded specimens which, after cementation were kept for 3 min. at 22°C prior to water immersion. The one-day bond strength of ethyl, isobutyl, n- and isoamyl cyanoacrylates showed excellent adhesion after one day water storage (Table I). Mean maximum 1 day tensile strength of smooth surface bone cemented together with these adhesives was 7.2 MPa for the viscous isoamyl homologue. However, a commercial ethyl-, and the n-amyl and non-viscous isoamyl, and the isobutyl cyanoacrylates also adhere well to bone. The hydrophilic ethyl-cellosolve and a fluorinated 2-cyanoacrylate yielded bonds that rapidly degraded in water. No clear-cut correlation between length of the alkyl chain and 1-day bond strength could be established.

Any bond strength achieved with ethyl 2-cyanoacrylates rapidly decreased on prolonged water storage with nearly complete destruction of the bond occurring within thirty days (Table I).

Although hydrolytic stability of the higher alkyl 2-cyanoacrylate-cemented specimens increased with the length of the ester chain, all bond strengths were observed to decrease as a function of the time specimens were stored in water. Results of these tests with specimens stored up to 6 months are given in Table I and Fig. 1. The smallest decrease in bond strength was observed for the isomeric, amyl cyanoacrylates. After the six month storage in

In Durability of Macromolecular Materials; Eby, R.;
ACS Symposium Series; American Chemical Society: Washington, DC, 1979.

Table I
TENSILE STRENGTH OF ALKYL CYANOACRYLATES BONDED BONE SPECIMENS

2-Cyanoacrylate	Tensile Strength in MPa After H_2O Storage at 37°C 1 day	1 month	3 months	6 months
Ethyl	6.60(1.13)[a]	0.16(0.19)	-	-
n-Butyl	2.86(1.75)	-	-	-
Isobutyl	6.62(1.73)	4.65(1.51)	4.62(1.02)	2.01(0.27)
n-Amyl	6.62(1.75)	-	3.80(0.37)	4.84(0.88)
Isoamyl	6.27(0.94)	-	4.98(1.00)	4.39(0.71)
Isoamyl, viscous	7.18(1.47)	-	6.33(0.38)	5.14(1.17)
Ethyl cellosolve	0 (0)	-	-	-
Fluorinated	1.31(1.04)	-	-	-

[a] Standard deviation shown in parentheses

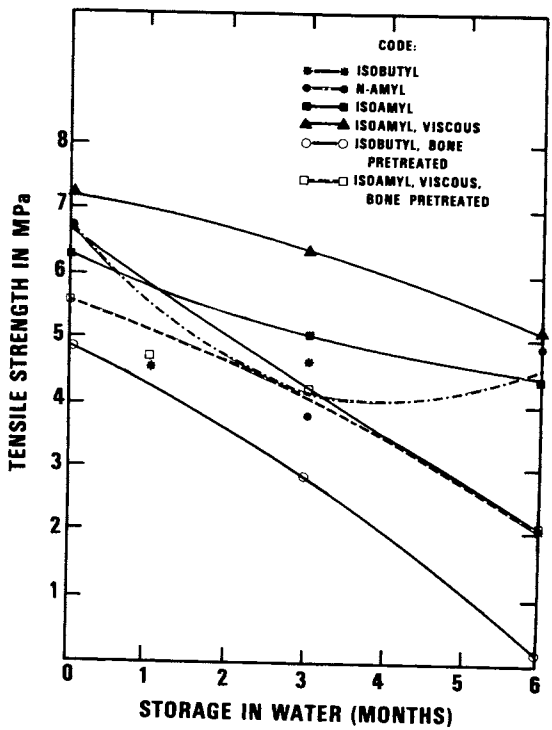

Figure 1. Tensile strength of cyanoacrylate–bone bond after storage in water

In Durability of Macromolecular Materials; Eby, R.;
ACS Symposium Series; American Chemical Society: Washington, DC, 1979.

water the n-amyl, isoamyl and viscous isoamyl 2-cyanoacrylate retained respectively 73%, 70% and 72% of their 1 day bond strength.

Pretreatment of the bond surfaces with 1% alcoholic dimethyl-p-toluidine lowered the one-day bond strength somewhat, but had a very deleterious effect on long term adhesion (Fig. 1). The treated surfaces gave much lower tensile adhesion values than the untreated substrate after one and 3 month water storage and retained only a small percentage of the original strength after a 6 month observation period. Again the n-amyl (1.6 MPa) and the viscous isoamyl (2.1 MPa), homologues had the best 6 month adhesive strength.

Temperature cycling experiments were conducted to determine (1) how the bond strength is affected by temperature changes and (2) if a correlation exists with the long-term (isothermal) studies. As indicated in Table II the results correlate well with the long-term behavior as obtained from the long-term storage tests at 37°C. Isobutyl, n- and viscous isoamyl-2-cyanoacrylates have the highest one-day tensile strength values. However, all values for thermocycled specimens were much lower than for those stored isothermally at 37°C for the same length of time. Again amine pretreatment lowered the tensile strength of the bone joints. Viscous isoamyl cyanoacrylate is the most hydrolytically stable material. However, the bond strength for this adhesive is greatly reduced (by 67% of the 1-day strength at 37°C of 7.18 MPa) after cycling for 30 days and additional storage in 37°C water for 39 days. The results of the cycling test give the same ranking for the decrease in strength of the adhesive bond as those of long-term isothermal storage studies. Thus, the former test is valuable as an accelerated procedure to predict long-term performance of adhesive joints.

The viscous isoamyl cyanoacrylate shows the least deterioration of bond strength to bone in an aqueous environment. This material has the further advantage that (1) it may be more suitable for applications where some filling of a gap by the adhesive is required and (2) it is considered to be less toxic than the lower homologues of the 2-cyanoacrylate series.

The adhesion tests were conducted with flat, well-mated substrate specimens to minimize the effect of mechanical interlocking of the adhesive to the substrate. However, with bone containing surface pits, greater tensile adhesion values were obtained. Bone etched with 37% phosphoric acid prior to applying the adhesive did not improve joint strength.

Experiments were performed to determine if monomers containing 2-cyanoacrylates were grafted, that is bonded covalently, to bone. Bone slabs were primed with 1% solution of triethylamine in n-hexane, and an ethyl cyanoacrylate was spread on the treated bone. Two hours after application of the adhesive, the attenuated total reflectance infrared spectrum showed clearly the presence of 2-cyanoacrylate on the coated surface. This coating was not removed on prolonged water exposure. After placing the treated bone

In Durability of Macromolecular Materials; Eby, R.;
ACS Symposium Series; American Chemical Society: Washington, DC, 1979.

Table II

TENSILE STRENGTH OF ADHESIVE-BONE BOND AFTER TEMPERATURE CYCLING

Temperature of Water Bath 5° & 55°C; Number of Cycles Per Day: 540

	Tensile Strength in MPa After Cycling		
Cyanoacrylate	1 day	12 days	30 days[c]
Ethyl	3.90(.81)[b]	0 (0)	-
Isobutyl	4.52(.46)	4.06(1.66)	1.61(.43)
Isobutyl[a]	3.36(.88)	3.19(1.54)	-
n-Amyl	4.59(1.27)	2.92(.35)	0.59(.52)
n-Amyl[a]	4.47(1.41)	2.55(.84)	-
Isoamyl	-	1.64(.91)	-
Isoamyl[a]	3.15(.55)	2.70(.72)	-
Isoamyl, viscous	4.40(.87)	2.73(.42)	2.32(.29)
Isoamyl, viscous[a]	3.97(.93)	2.37(1.38)	-

[a] Bone pretreated with 1% alc. dimethyl-p-toluidine.
[b] Standard deviations are given in parentheses.
[c] Total time in water: 30 days cycled + 39 days at 37°C.

In Durability of Macromolecular Materials; Eby, R.;
ACS Symposium Series; American Chemical Society: Washington, DC, 1979.

for 1 hour in acetone with stirring, then for 1 day in dimethylsulfoxide and finally drying in air, the infrared spectrum was identical to that of untreated bone. Similar results were obtained on exposure of bone treated with the viscous isoamyl cyanoacrylate to the same solvents. The complete removal of the 2-cyanoacrylate adhesive indicates that no bond formation occured. Thus, contrary to the reaction of collagen or amino acids the collagenous component of the bone surface does not bond covalently to the cyanoacrylate (41).

An exploratory study was also conducted to evaluate urethane-methacrylates containing pendant isocyanate groups as bone adhesives. The following adducts were studied:

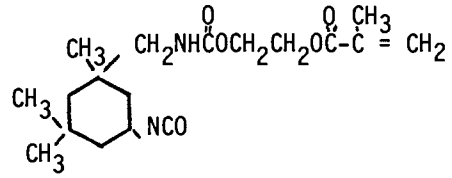

Isophorone diisocyanate-hydroxyethyl methacrylate (IPDI-HEMA)

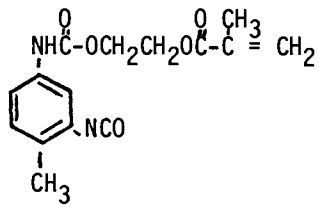

Toluene diisocyanate-hydroxyethyl methacrylate (TDI-HEMA)

and 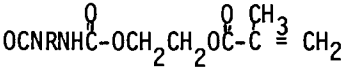

where R = $(CH_2)_6$: HDI-HEMA

R = 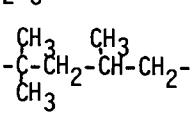 : TMDI-HEMA

R = C_{36} hydrocarbon: DDI-HEMA

The isocyanate-HEMA adduct was diluted with 33% triethylene glycol dimethacrylate. A mix prepared from two equal volumes of this solution, one portion containing 2% benzoyl peroxide and the other containing 1% dimethyl-p-toluidine was applied to the bone. Only the IPDI-HEMA adduct cured rapidly and gave a weak, but statistically significant bond after one-day thermocycling. Bond strength was not improved by acid-etch pretreatment. However, application of 1% NAOH to the bone prior to application of the adhesive yielded bond strengths of 2.6 MPa, 1.9 MPa and 1.2 MPa after thermocycling the specimens for 1, 7 and 30 days respectively. These values are considerably lower than those obtained with isobutyl- and amyl 2-cyanoacrylate adhesives.

The urethane-methacrylates may be useful, however, as adhesive coatings to hard tissues. The IPDI-HEMA liquid containing 2% methyl ether of benzoin, when placed on bone surface cured within 30 seconds after exposure

In Durability of Macromolecular Materials; Eby, R.;
ACS Symposium Series; American Chemical Society: Washington, DC, 1979.

to a UV source. The coating adhered to bone specimens stored in water during the period of observation (12 months). The treated bone surface gave an ATR infrared spectrum showing the presence of isocyanate and methacrylate groups. Extraction of the bone with acetone and dimethylsulfoxide for 1 week did not change the infrared spectrum. Although the film obtained on curing IPDI-HEMA is not soluble in any of a number of common solvents studied, it is not possible to state if the IPDI-HEMA film is bonded covalently to bone or if the attachment to this substrate occurs by formation of a interpenetrating network.

Adhesion to Dentin: Results of the strength of dentin bonded to acrylic rod are given in Table III. Only the ethyl-, isobutyl- and viscous isoamyl 2-cyanoacrylates cure within the 3 minute period that a force is applied to the assembly. The best bond strength (5.5 MPa) is obtained with the commercial isobutyl 2-cyanoacrylate. Pretreatment with N,N-dimethyl-p-toluidine (DMPT) which speeds up curing of the adhesive, sometimes lowers the bond strength (Table 3). Acid-etch pretreatment of the dentin surface with 37% phosphoric acid greatly increases adhesion, giving a one-day tensile strength of 7.23 MPa (1080 PSI). This bond strength rapidly decreases with storage time. After 90 days the tensile adhesion of the joint cemented with isobutyl- and viscous isoamyl-2-cyanoacrylates is reduced to 1.89 and 0.25 MPa, respectively.

Table III

Tensile Strength of the Dentin-Acrylic Joint Bonded with Various Cyanoacrylates

2-Cyanoacrylate	Treatment	Days in H_2O at 37°C	Tensile Strength MPa *
Ethyl	-	1	2.80 (0.34)
Ethyl	DMPT	1	1.67 (0.97)
n-Butyl	-	1	did not cure
Isobutyl	-	1	5.54 (2.29)
Isobutyl	DMPT	1	3.50 (2.65)
Isobutyl	37% H_3PO_4	1	7.23 (2.86)
Isobutyl	37% H_3PO_4	90	1.89 (0.56)
n-Amyl	-	-	did not cure
n-Amyl	DMPT	-	did not cure
Isoamyl	-	-	did not cure
Isoamyl	DMPT	1	3.22 (0.39)
Isoamyl, viscous	-	1	2.29 (1.21)
Isoamyl, viscous	DMPT	1	2.65 (0.70)
Isoamyl, viscous	37% H_3PO_4	1	3.00 (1.09)
Isoamyl, viscous	37% H_3PO_4	90	0.25 (0.38)

* Standard deviations are given in parentheses.

In Durability of Macromolecular Materials; Eby, R.;
ACS Symposium Series; American Chemical Society: Washington, DC, 1979.

One-day thermocycling also reduces the bond strength (Table IV). Thus the phosphoric acid-etched dentin adhesive bond has a one day bond strength of 7.2 MPa after storage in water at 37°C. This value is reduced to 5.7 MPa after thermocycling for the same time period. Even the acid-etched specimens show minimal adhesion or completely destroyed bonds after 30 days of thermocycling.

The results of the cycling test again give the same ranking for the decrease in the adhesive bond strength as those of the long term isothermal storage studies. Therefore, all subsequent tensile adhesion tests were performed using the accelerated aging thermocycling test.

Table IV

Tensile Strength of the Dentin-Acrylic Joint Bonded with Various Cyanoacrylates

Temperature of water: 5°C and 55°C; Frequency of cycles: 540/day

2-Cyanoacrylate	Surface Treatment	Tensile Strength in MPa after cycling		
		1 day	7 days	30 days
Isobutyl	--	--	0.12(0.27)	--
Isobutyl	37% H_3PO_4	5.65(2.40)	3.32(2.71)	0.25(0.56)
Isoamyl	37% H_3PO_4	--	--	0.00
Isoamyl, viscous	--	--	0.00	0.00
Isoamyl, viscous	37% H_3PO_4	2.38(0.68)	2.53(0.43)	0.00

* Standard Deviations are given in parentheses

Addition of typical crosslinking agents, such as 20% diallyl phthalate, 10% ethylene glycol dimethacrylate, 1% maleic anhydride or 1% itaconic anhydride, to the isobutyl 2-cyanoacrylate so that after curing a more rigid, insoluble, hydrolytically stable polymeric adhesive might be formed, does not increase the strength of the dentin-poly(methyl methacrylate) joint. Perhaps the crosslinked adhesive possesses decreased resistance to the thermal shock encountered by the test specimens.

Thirty second pretreatments of the dentin with very dilute acid solutions are more promising to improve bond strength than the incorporation of crosslinking agents into the monomer adhesive. Results of these tensile adhesion measurements for treated dentin surfaces are given in Table V. Swabbing the dentin surface with diluted ethanol prior to bonding increases adhesion, due to the cleansing action of this pretreatment. Etching pretreatment of dentin with 1% phosphoric acid prior to bonding yields a bond strength of 12.4 MPa (1800 PSI). Etching the dentin with 1% succinic, methacrylic or aconitic acid or maleic anhydride does not improve tensile adhesion. Best results are obtained using a 1% solution of citric acid in dilute alcohol (1:2 ETOH/H_2O by volume). The bond strength after pretreatment of the dentin with this solution and after curing and thermocycling for one day is 14.10 MPa (2050 PSI).

In Durability of Macromolecular Materials; Eby, R.;
ACS Symposium Series; American Chemical Society: Washington, DC, 1979.

Table V
Strength of Pretreated Dentin-Acrylic Resin
Bond After Thermocycling for One Day

Adhesive: Isobutyl 2-Cyanoacrylate

Dentin Pretreatment*	Tensile Strength, MPa Mean	Stand. Dev.
Aq. Ethanol (2:1)	7.79	1.97
1% Phosphoric Acid	12.38	2.75
1% Alc. (1:2) Succinic Acid	2.83	3.89
1% Alc. (1:2) Methacrylic Acid	3.68	1.59
1% Alc. (1:2) Aconitic Acid	2.75	2.57
1% Alc. Maleic Anhydride	4.94	1.61
1% Alc. Abietic Acid	4.28	2.36
1% Aq. Citric Acid	12.60	3.62
1% Alc. (1:2) Citric Acid	14.10	4.46
0.5% Alc. (1:2) Citric Acid	13.44	3.91
0.1% Alc (1:2) Citric Acid	10.68	3.89
1% Alc. (1:2) Itaconic Acid	8.29	3.25
1% Alc (1:2) Itaconic Anhydride	5.80	2.42
1% Alc. (1:2) Citraconic Anhydride	11.13	2.83
1% Alc. (1:2) Tetrahydrofuran 2,3,4,5-tetracarboxylic acid	10.22	2.75
1% Alc. Triallyl Phosphate	2.51	2.84
1% Alc. Triallyl Cyanurate	4.25	4.31
0.5% Alc. Triallyl Cyanurate	1.17	1.69
0.2% Alc. Triallyl Cyanurate	2.51	2.84
1% Aq. Calcium Hydroxide	0.12	0.18
1% EDTA Tetrasodium salt	11.66	2.54

* Percentages given are weights of solids or volumes of liquids dissolved in volume of ethanol (1:2) or water

In Durability of Macromolecular Materials; Eby, R.;
ACS Symposium Series; American Chemical Society: Washington, DC, 1979.

This bond strength is considerably higher than any value for the adhesion to smooth dentin surfaces which has been previously reported. The bond strength is slightly decreased when more dilute citric acid solutions are used. Other pretreatments yielding tensile adhesion values above 10 MPa include solutions of 1% alcoholic (1:2) citraconic anhydride, 1% alcoholic tetrahydrofuran -2,3,4,5-tetracarboxylic acid, and 1% aqueous ethylenediaminetetraacetic acid tetrasodium salt.

Increasing the length of storage of the joined (citric acid pretreated) specimens in the thermocycled water bath considerably decreases the tensile adhesion. Seven-day bond strength values of 2.6 to 4.9 MPa are obtained with the pretreated specimens using the unmodified isobutyl 2-cyanoacrylate adhesive (Table VI). Addition of 2-5% cross-linking monomer such as diallyl maleate, triallyl phosphate or triallyl cyanurate does not appreciably increase the hydrolytic stability. Addition of from 3% to 30% poly(ethyl 2-cyanoacrylate) to the isobutyl 2-cyanoacrylate monomer, however, yields a bond with greater resistance to water. Thus, the seven-day bond strength of adhesive containing 5% poly-(ethyl 2-cyanoacrylate) is 8.7 MPa compared to 3.9 MPa for the unmodified adhesive. Formulations containing more than 30% of dissolved polymer become quite viscous and their bond strength is quite low. Results of 30-day thermocycling tests employing isobutyl 2-cyanoacrylate with or without 5% allyl methacrylate are disappointing giving a bond strength of 0.1 MPa for the unmodified adhesive.

To reduce or eliminate debonding, a UV-polymerized, hydrophobic sealant was painted around the dentin-methacrylate interface. Thus, it was hoped that hydrolytic degradation of the bond would be minimized. The rationale for this procedure is that the coating would seal off the adhesive from contact with water, or at least the water permeation through the protective film to the adhesive surface would be reduced. Suitable protective formulations should (1) cure within 1 minute, (2) be hydrophobic, (3) be compatible with the etched dentin and the cured cyanoacrylate adhesive, and (4) be storage stable for at least 24 hours. A number of compositions (Table VII) polymerize after 30 sec-irradiation with the UV light source. Contact angles of the cured resins varied from 54 degrees to 80 degrees. A significant improvement in the shorter term stabilization of the bond was obtained with a composition containing 43% hexamethylene glycol dimethacrylate, 41% Bis-GMA, 12% 1H,1H,5H-octafluoropentyl acrylate, 2% benzoin ethyl ether UV initiator and 2% of a UV photocrosslinking agent (1 oxa-5-acryloxymethyl-3,7-dioxabicyclo[3,3,0]octane. After seven days of thermocycling the bond strength of dentin-resin joints coated with a protective film of this composition averaged 8.9 MPa (1340 PSI). However, after 30 days of thermocycling the adhesive strength was reduced to 1 MPa. The other formulations containing a urethane dimethacrylate or the most hydrophobic composition, which contained a fluoropoly-

In Durability of Macromolecular Materials; Eby, R.;
ACS Symposium Series; American Chemical Society: Washington, DC, 1979.

Table VI
Strength of Dentin-Acrylic Resin Joint Bonded With Isobutyl 2-Cyanoacrylate After Thermocycling

Dentin pretreated with alc (1:2) citric acid.

Adhesive Modifier[1]	No. of Days	Tensile Strength, MPa Mean	Std. Dev.
-[2]	7	2.57	1.73
-[3]	7	3.71	1.34
-[4]	30	0.12	0.25
-	7	3.87	1.78
-	7	2.98	1.72
-	7	4.88	1.98
5% Allyl methacrylate	7	3.72	2.05
5% Allyl methacrylate	30	0	--
5% Triallyl phosphate	7	2.89	1.35
5% Diallyl maleate	7	3.18	2.61
2% Triallyl cyanurate	7	4.35	2.34
3% Poly(ethyl 2-cyanoacrylate)	7	5.84	1.47
5% Poly(ethyl 2-cyanoacrylate)	7	8.67	1.68
12% Poly(ethyl 2-cyanoacrylate)	7	6.59	1.12
20% Poly(ethyl 2-cyanoacrylate)	7	6.77	1.92
30% Poly(ethyl 2-cyanoacrylate)	7	6.28	2.69
40% Poly(ethyl 2-cyanoacrylate)	7	1.51	0.82
50% Poly(ethyl 2-cyanoacrylate)	7	1.18	0.88

[1]Percentages are given as weight of solids dissolved in volume of liquid and volume of liquid dissolved in liquid
[2]Dentin pretreatment: 0.5% alc. (1:2) citric acid
[3]Dentin pretreatment: 1% alc. (1:2) itaconic acid
[4]Dentin pretreatment: 1% alc. (1:2) citraconic acid

In Durability of Macromolecular Materials; Eby, R.;
ACS Symposium Series; American Chemical Society: Washington, DC, 1979.

Table VII

Strength of Dentin-Acrylic Resin Joint Covered with a Protective Coating After Thermocycling

Adhesive: Isobutyl 2-Cyanoacrylate

Dentin pretreated with 1% alcohol (1:2) citric acid

Protective Coating			Adhesive Tensile Strength, MPa	
Composition	Curing Time Sec	H_2O Contact Angle	7 day	30 day
60% Bis-GMA 25% Trimethylolpropane trimethacrylate 10% 2,2,2-Trifluoroethyl methacrylate 2% UV initiator; 3% photocrosslinking agent	30	59°	5.11(2.00)	0.98(0.68)
Same as above but adhesive containing 5% poly(ethyl 2-cyanoacrylate)	30	-	5.27(2.77)	
41% Bis-GMA 43% Hexamethylene glycol dimethacrylate 12% 1H,1H,5H-Octafluoropentyl acrylate 2% UV initiator, 2% photocrosslinking agent	30	60°	8.92(3.88)	0.59(0.63)
43% Urethane dimethacrylate 43% Hexamethylene glycol dimethacrylate 10% Pentadecafluorooctyl methacrylate 2% UV initiator; 2% photocrosslinking agent	30	54°	3.58(1.06)	
70% Polyfluoropolyacrylate 30% Pentadecafluorooctyl methacrylate 2% UV initiator 0.3% Dimethylaminophenyl acetic acid	30	80°	4.40(1.64)	

In Durability of Macromolecular Materials; Eby, R.; ACS Symposium Series; American Chemical Society: Washington, DC, 1979.

acrylate, gave coatings that resulted in only marginal improvement.

The accelerated thermocycling test was by necessity used to evaluate promising new adhesives. The objective of this test was to predict long-term performance and reliability based upon short term tests involving thermal and environmental stress under intensified conditions. The many abrupt temperature changes during the cycling procedure also resulted in considerable mechanical stress formation in the joints because of the expansion and contraction of the adherents. Simultaneous stress and environmental exposures have a drastic effect on bond durability. A stress hydrolysis reaction may have occured that may not be encountered clinically, i.e. the accelerated test may be so excessively severe as not to be predictive of the clinical long-term applicability of this procedure. Thus, if the biocompatibility of these compositions has been established long term *in vivo* studies of promising formulations should be conducted to determine the service life under clinical conditions.

Conclusions

The strength of adhesive joints between bone-bone and dentin-poly(methyl methacrylate) decreases on prolonged storage in water. With 2-cyanoacrylate esters debonding is greatly reduced by increasing the length of the ester group. Thermocycling tests give the same rankings for the decrease in the adhesive bond. strength as those of the long-term isothermal storage studies.

The bonding of 2-cyanoacrylates to mineralized tissues in an aqueous environment appears to be superior to that of other adhesives. The higher homologues of 2-cyanoacrylates may be useful clinically where an intermediate-term bone adhesive is desired. The isobutyl ester is the most effective 2-cyanoacrylate for bonding dentin to acrylic resin. Pretreatment of the dentin with dilute acid, addition of 2-cyanoacrylate polymer to the adhesive or application of a protective coating to the bonded surface increases the hydrolytic stability of the bond.

This work was supported by the National Institute of Dental Research, Interagency Agreement #Y01-DE-4001.

In Durability of Macromolecular Materials; Eby, R.;
ACS Symposium Series; American Chemical Society: Washington, DC, 1979.

Literature Cited

1. Kinloch, A. J., Dukes, W. A., Gledhill, R. A., "Adhesion Science and Technology," Lee, L. H., Ed., Polymer Sci. and Tech. (1975) 9B, 597.
2. Gledhill, R. A., Kinloch, A. J., J. Adhesion (1974) 6, 315.
3. MacDonald, N. C. in "Aspects of Adhesion," Alner, D.J., Ed., (1969) 5, 121.
4. Simonsen, R. J. "Clinical Applications of the Acid Etch Technique," Quintessence Publishing Co., Chicago, 1978.
5. Silverstone, L. M., Dogon, I. L., Eds., "The Acid Etch Technique," North Central Pub. Co., St. Paul, MN, 1975.
6. Sharp, E. C., Grenoble, D. E., J. S. Calif. State Dent. Assn. (1971) 39, 741.
7. Buonocore, M. G., Matsui, A., Gwinnett, A., Archs Oral Biol. (1968) 13, 61.
8. Smith, D. C., Brit. Dent. J. (1968) 125, 381.
9. Smith, D. C., Dent. Clins. N. Am. (1971) 15, 3.
10. Smith, D. C., J. Can. Dent. Assn. (1971) 37, 22.
11. Anbar, M., St. John, G. A., Edward, T. E., J. Dent. Res. (1974) 53, 1240.
12. Farley, E. P., Jones, R. L. and Anbar, M., J. Dent. Res. (1977) 56, 943.
13. Bowen, R. L., J. Dent. Res. (1965) 44, 895.
14. Bowen, R. L., J. Dent. Res. (1965) 44, 903.
15. Bowen, R. L., J. Dent. Res. (1965) 44, 906.
16. Bowen, R. L., J. Dent. Res. (1965) 44, 1369.
17. Chandler, H. H., Bowen, R. L., Paffenbarger, G. C. and Mullineaux, A. L., J. Am. Dent. Assn. (1974) 88, 114.
18. Masuhara, E., Dtsch Zahnärzt Z. (1969) 24, 620.
19. Nakabayashi, N., Hayata, S. and Masuhara, E., J. Biomed. Matls. Res. (1977) 11, 395.
20. Cranfield, P. J., Ger. Offen. 2,630,745, 9 July 1975.
21. Smith, D. C., Microfilm of papers presented before Dental Materials Group, Int. Assn. Dent. Res., Washington, DC, March 1978, No. 1062.
22, Glenn, J.F. in "Adhesive Restorative Dental Materials" Phillips, R. W. and Ryge, J. Eds. p. 67, Owen Litho Service (Indiana), 1961.
23 Brauer, G. M., Termini, D. J., in "Applied Chemistry at Interfaces," Baier, R. E., Ed., Advan. Chem. Ser. (1975) 145, 175.
24. Brauer, G. M., Termini, D. J., Levy. S. M., J. Dent. Res. (1977) 56, 646.
25. Leonard, F., in "Adhesion in Biological Systems," Manly, R. S. Ed., p. 185, Academic Press, New York, NY, 1970.
26. Beech, D. R., J. Dent. Res. (1972) 51, 1438.
27. Stanford, J. S., J. Am. Dent. Assn. (1975) 90, 727.
28. Lambert, R. L., J. Prosthet. Dent. (1975) 34, 187.
29. Baum, L., Gen. Dent. (July-Aug 1976), 24, 32.

In Durability of Macromolecular Materials; Eby, R.;
ACS Symposium Series; American Chemical Society: Washington, DC, 1979.

30. Buck, C. J., U.S. Patent 4,041,061, Aug. 9, 1977.
31. Buck, C. J., U.S. Patent 4,041,063, Aug. 9, 1977.
32. Buck, C. J., U.S. Patent 4,003,942, Jan. 18, 1977.
33. Aleksieva, K., Chakmakov, D., Probl. Stomatol. (1974) 2, 109; through Chem. Abst. 1977, 86, No. 16 1266.
34. Takeuchi, M. Otsuki, A., U.S. Patent 4,012,840, March 22, 1977.
35. Otsuki, A., Takeuchi, M., Caries Res.(1976), 10, 463.
36. Alter, H., Fookson, A., J. Adhesion (1971) 3, 35.
37. Lee, H., Cupples, A. L., Schubert, R. J. and Swartz, M. L., J. Dent. Res. (1971) 50, 125.
38. Antonucci, J. M., Brauer, G. M. and Termini, D. J., J. Dent. Res. (1977) 56B No. 658 (Abstract).
39. Brauer, G. M., Termini, D. J., and Davidson, K., Microfilm of papers presented before the Dental Materials Group, Int. Assn. Dent. Res., Las Vegas, Nev., June 1977, No. 786.
40. Lee, H. L., Swartz, M. L., and Culp, G., J. Dent. Res. (1969), 48, 211.
41. Kulkarni, R. K., Bartok, D. E. and Leonard, F., J. Poly. Sci. (1971) 9, 2977.

RECEIVED December 8, 1978.

Surface Degradation of E-Glass and S-Glass in the Presence of Water

ANDREW C. T. HSU and JAMES R. SCHAFNER

Department of Chemical Engineering, Auburn University, Auburn, AL 36830

ABSTRACT

E-Glass and S-glass fibers have been used in the fabrication of high-strength reinforced plastics composites. The composites are noted for their resistance to moisture and weathering, however, they are susceptible to strength degradation in the presence of high humidity and elevated temperature. This report presents the dissolution of magnesium and silicon in water from E-glass and S-glass rovings (fiber strands) at 40°, 50°, and 60°, and from E-glass powders at 40°C. The concentrations of dissolved magnesium and silicon from both E-glass and S-glass increased with temperature and time. The results show that more Mg than Si was leached out of these two types of glass. Less dissolution of Mg and Si from S-glass than from E-glass indicates that S-glass is not only a stronger glass, but is also a more stable one in the presence of water. The concentration of leached-out magnesium from S-glass in water is approximately proportional to the square root of contact time, indicating that diffusion in the solid surface layer is rate-controlling.

E-glass and S-glass fibers are both used in the fabrication of high-strength reinforced plastics composites. E-glass is less strong than S-glass, but its cost is only a fraction of that of S-glass; the former is therefore more widely utilized in less demanding applications.

Glass reinforced composites are noted for their resistance to moisture and weathering, but they tend to lost their strength in the presence of high humidity and elevated temperatures (1,2,3). Water is apparently able to attack, to different extents, the glass filaments, resin matrix, and coupling agent and sizing between them. Because several ingredients and their interplays are involved, there have been various theories on the mechanism of strength degradation of these composites.

0-8412-0485-3/79/47-095-411$05.00/0

In previous articles (4,5), results on the solvent effect of water on S-glass fibers and powders at temperatures between 30°-50°C were presented and discussed. This paper reports the solvent effect of water on E-glass at 40°, 50°, and 60°C. The following are compositions of S-glass (6,7) and E-glass (1,6,8) in weight percent of their respective components given in the literature.

	S-glass	E-glass
SiO_2	65 wt.%	54.5 wt.%
Al_2O_3	25	14.5
MgO	10	4.5
CaO	--	17.0
B_2O_3	--	8.5
Na_2O, K_2O, TiO_2, Fe_2O_3	--	1.0

EXPERIMENTAL

E-glass rovings and powders and Type S-1014 S-glass rovings, all from Ferro Corporation, were used in the surface dissolution studies. There are 204 filaments in each strand of the rovings, and the filaments have an average diameter of approximately 10 microns. As described in the previous paper (4), the strands were made into coils about one and one-half inches in diameter to facilitate weighing and transferring.

Degradation of E-glass and S-glass in water between 40°-60°C was determined in terms of the amounts of magnesium, aluminium, and silicon dissolved in water from these glasses. For the E-glass rovings, approximately 10 grams of the coils were weighed into 250 ml. wide-mouth polypropylene bottles. To each bottle 150 ml. of distilled water were added and the bottles were tightly capped. The bottles were placed in a constant-temperature bath maintained at 40°C. After different time periods, the bottles were separately removed from the bath and the water in the bottles decanted into 150 ml. polypropylene sample bottles. The water samples from each of the bottles were analyzed for their Mg, Al, and Si contents. Atomic absorption spectroscopy, the Aluminon colorimetric method, and the heteropoly blue colorimetric method were used, respectively, to determine the low concentrations of Mg, Al, and Si. (4).

Additional runs were made for E-glass rovings at 50°C and 60°C, and for S-glass rovings at 60°C.

E-glass powders were obtained by crushing E-glass marbles. The powders were screened and the portions retained on 48-, 65-,

In Durability of Macromolecular Materials; Eby, R.;
ACS Symposium Series; American Chemical Society: Washington, DC, 1979.

and 100-mesh screens were mixed and used in this series of runs. Two grams of the glass powders and 50 ml. of distilled water were placed in each of five 3-0z. polypropylene bottles and maintained at 40°C. The bottles, which were gently shaken a few times a day, were removed from the temperature bath after different time periods. The water in each bottle was filtered and its Mg, Al, and Si contents determined.

RESULTS AND DISCUSSION

Dissolution of magnesium and silicon in water from E-glass rovings at 40°, 50°, and 60°C after different time periods is shown in Figures 1 and 2, in which the dissolved amounts are in milligrams of these components per liter (equivalent to parts per million by weight). The dissolutions were relatively rapid in the early stage, but the rate tapered off with time. As with S-glass rovings, Mg (or MgO) was more readily leached out than Si from E-glass, i.e., the relative amounts of Mg and Si dissolved in water were higher than those of the solid phase. For instance, after 200 hours at 50°C, the Mg/Si weight ratio in the water is approximately 0.37 against a Mg/Si weight ratio of 0.107 in the solid phase.

Figures 3 and 4 show the concentration changes of Mg and Si, respectively, in water with time at 40°C for E-glass powders. As comparisons, the corresponding Mg and Si concentration changes for S-glass powders obtained earlier (4) are also plotted in Figures 3 and 4. It may be noted that between S-glass and E-glass the former yielded more Mg to the water phase than E-glass, perhaps reflecting the higher fraction of Mg in S-glass (10 weight%) than in E-glass (4.5 weight%). On the otherhand, water dissolved more Si from E-glass than from S-glass, even though in the solid phase the former contains less Si than the latter (54.5% in E-glass vs. 65% by weight in S-glass). Apparently, the presence of considerable amounts of CaO, and alkali oxides, especially the alkali oxides, enhances the dissolution of Si from E-glass.

Dissolution of magnesium and silicon in water from S-glass rovings at 60°C is shown in Figures 5 and 6. The results reported earlier (4) for S-glass rovings at 30, 40, and 50°C are replotted in these two figures, which show that dissolution of Mg and Si increased rapidly with increasing temperature in the range 30 - 60°C. The activation energy E_a for magnesium dissolution is calculated from Figure 5 and the relation.

$$\frac{d\ln(1/\theta)}{d(1/T)} = \frac{-E_a}{R} \qquad (1).$$

in equation 1, θ is time in hours and T temperature in °K. The average activation energy for early-stage magnesium dissolution in the temperature range is 2.4×10^4 calories per gram mole.

In Durability of Macromolecular Materials; Eby, R.;
ACS Symposium Series; American Chemical Society: Washington, DC, 1979.

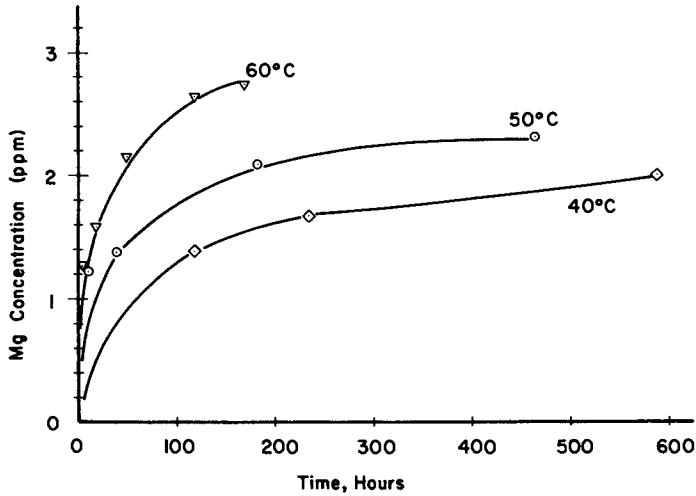

Figure 1. Dissolution of magnesium from E-glass rovings in water (temperature: 40°, 50°, 60°C)

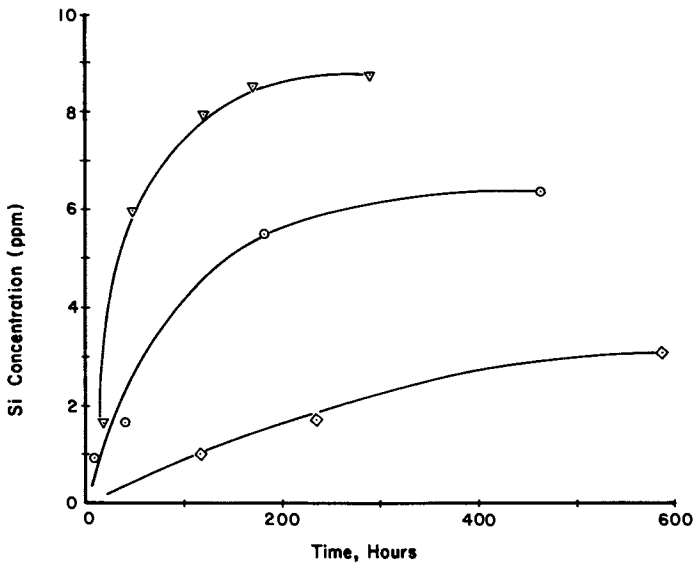

Figure 2. Dissolution of silicon from E-glass rovings in water (temperature: 40°, 50°, 60°C)

In Durability of Macromolecular Materials; Eby, R.;
ACS Symposium Series; American Chemical Society: Washington, DC, 1979.

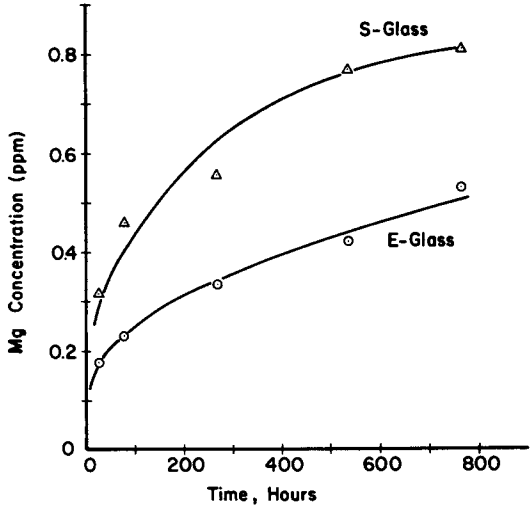

Figure 3. Dissolution of magnesium from E-glass and S-glass powders in water (temperature: 40°C)

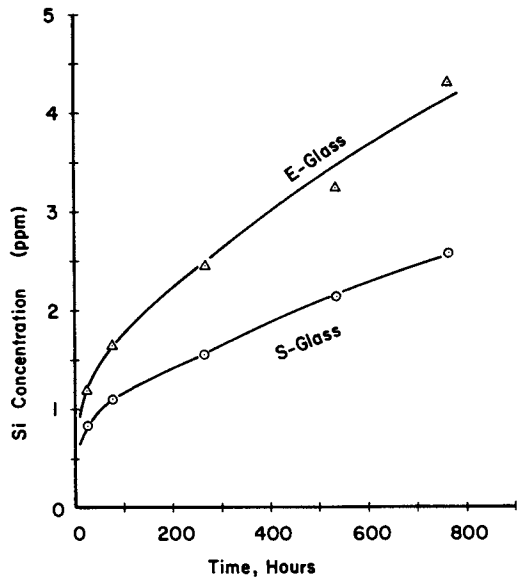

Figure 4. Dissolution of silicon from E-glass and S-glass powders in water (temperature: 40°C)

In Durability of Macromolecular Materials; Eby, R.;
ACS Symposium Series; American Chemical Society: Washington, DC, 1979.

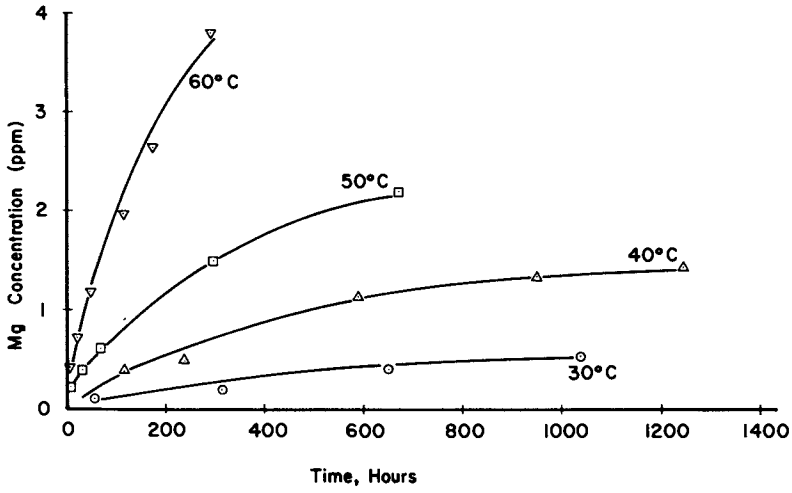

Figure 5. Dissolution of magnesium from S-glass rovings in water (Temperature: 30°, 40°, 50°, 60°C)

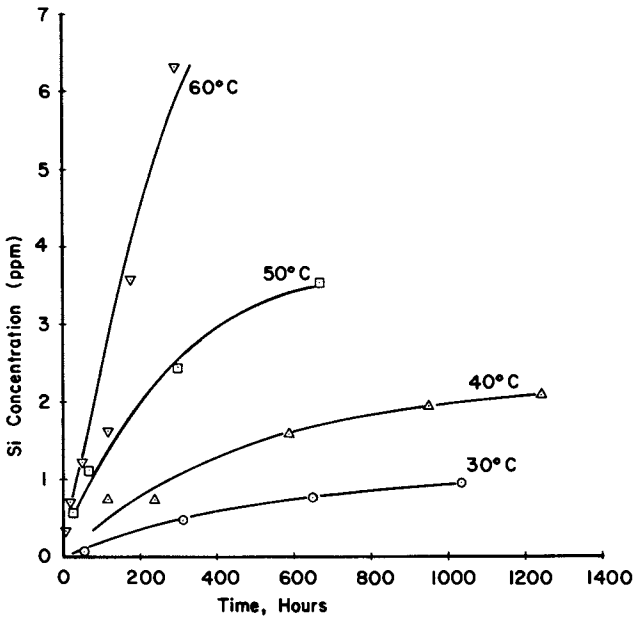

Figure 6. Dissolution of silicon from S-glass rovings in water (temperature: 30°, 40°, 50°, 60°C)

In Durability of Macromolecular Materials; Eby, R.;
ACS Symposium Series; American Chemical Society: Washington, DC, 1979.

In the case of S-glass in water, magnesium in the form of hydroxide is the most soluble compared to SiO_2 and Al_2O_3 (9). So, magnesium (as MgO or $Mg(OH)_2$) is preferentially leached out of S-glass.

In alkali glasses, the slow loss of alkali has been ascribed to three possible mechanisms which may be extended to the loss of magnesium from S-glass.

(1) The action of water on alkali glasses is attributed to an ion exchange process, in which hydrogen ions replace sodium ions on the surface of the glass (10).

(2) A hydrated layer formed on the glass surface acts as a barrier (controlling resistance) through which leachable matter has to diffuse (11).

(3) Sodium ions are leached out as sodium hydroxide, while SiO_2 is left behind as a porous matrix. (12,13).

These possible mechanisms can all be treated in terms of unsteady-state mass diffusion and result in an equation of the following general form.

$$C_b = \frac{M}{V_b} = K\sqrt{\theta} \qquad (2).$$

In equation 2, M is the total amount of Mg leached out, V_b volume of the bulk liquid phase, θ time, and K a characteristic constant which is dependent on the concentration of magnesium at the solid surface, total surface area of glass, temperature, and diffusivity of magnesium ion in water. In logarithmic form, Equation 2 becomes (C_b=Mg concentration in bulk liquid phase.)

$$\log C_b = \log K + \tfrac{1}{2} \log \theta \qquad (3).$$

The data for magnesium dissolution from S-glass in Figure 5 are replotted as log C_b versus log θ as shown in Figure 7. The average slope of the lines for 30, 40, 50, and 60°C. is 0.55 (ranging between 0.51 and 0.61) which is in fair agreement with that predicted by the above equations. Here, diffusion in the bulk liquid phase is fast relative to that in the solid phase, i.e., the rate of loss of Mg from the solid phase is controlled by mass transfer resistance in the solid phase. Further work is, however, needed to resolve the exact mechanism involved in the dissolution process.

The results in Figure 6 for magnesium dissolution from E-glass, when replotted in the log-log scale, give lines with slopes considerably lower than 0.50. Apparently, interactions in the presence of water among CaO, Na_2O, MgO, B_2O_3 and other oxides in E-glass make E-glass-water a more complicated system than S-glass-water.

In Durability of Macromolecular Materials; Eby, R.;
ACS Symposium Series; American Chemical Society: Washington, DC, 1979.

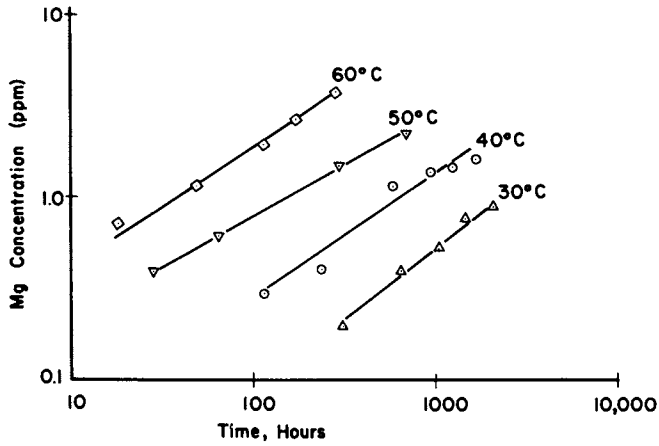

Figure 7. Magnesium concentration changes in water vs. time (log — log plot); S-glass rovings (temperature: 30°, 40°, 50°, 60°C).

In Durability of Macromolecular Materials; Eby, R.;
ACS Symposium Series; American Chemical Society: Washington, DC, 1979.

SUMMARY AND CONCLUSION

1. In the presence of water, magnesium is preferentially leached out from both S-glass and E-glass rovings (compared to silicon and aluminium).

2. Between S-glass and E-glass, E-glass is more susceptible to the action of water as indicated by its losing a higher proportion of silicon and magnesium, and losing them more rapidly, from the solid phase. Thus, S-glass is not only the stronger glass and is also the more stable one against degradation by water.

3. The amount of magnesium dissolution in water from S-glass is proportional to the square root of the S-glass-water contact time in the temperature range 30 - 60°C and contact time up to 2000 hours covered in this work.

4. The results signify that even with a stationary liquid phase the controlling resistance to the overall dissolution process in water lies in the surface layer of the solid phase.

ACKNOWLEDGEMENT

The authors wish to acknowledge the financial support of the US Army Missile Command, Huntsville, Alabama under the research contract No. DAAH01-73-C-0466 and of the Research Grant-in-Aid, Auburn University, Auburn, Alabama.

REFERENCES

1. Schmitz, G. K. and A. G. Metcalfe, IEC Prod. R&D, 5, 1 (1966).

2. Parham, J. L., Report No. RS-TR-70-8, US Army Missile Command, Redstone Arsenal, October, 1970.

3. Jemian, W. A. and Wilcox, R. C., Stability of Glass-Fiber Glass Plastics Composites, Final Report, Contract DAAH01-72-C-0294, School of Engineering, Department of Mechanical Engineering, Auburn University, Auburn, Alabama, October, 1973.

4. Hsu, A. C. T., Jemian, W. A., Wilcox, R. C., J. Materials Sci., 11, 2099 (1976).

5. Hsu, A. C. T., Jemian, W. A., and Wilcox, R. C., AIChE Symposium Series 170, Vol. 73, 146 (1977).

6. Lowrie, R. E., in "Modern Composite Materials", edited by L. J. Broutman and Krock, R. H. (Addison-Wesley), Reading, Mass., (1967) p. 307.

7. Romans, J. R., Sands A. G., and Cowling, J. E., NRL Report No. 7246, April 5, 1971.

8. Guzzetta, F. H., in "Fundamental Aspects of Fiber Reinforced Plastic Composites", edited by R. T. Schwartz and H. S. Schwartz (Interscience Pub., New York, 1968) p. 219.

9. "Landolt-Bornstein Physikalisch-Chemische Tabellen", 2nd supplement, (Springer, Berlin, 1931) p. 343.

10. Douglas, R. W. And J. O. Isard, J. Soc. Glass Tech., 33, 289 (1949)

11. Lyle, A. K., J. Am. Ceramic Soc., 26, 201 (1943).

12. Hubbard, D. and Rynders, G. F., J. Res. Nat. Bur. Standards, 41, 477 (1948).

13. Schroeder, H., Z. Naturforschung, 4a, 515 (1949).

14. Rana, M. A. and Douglas, R. W., Phys. and Chem. of Glass, 2, 179-96, (1969).

RECEIVED December 8, 1978.

Molecular Weight Distribution Studies of Electrically Stressed Polyethylene

JOHN A. CROWTHER, JULIAN F. JOHNSON, and JOHN TANAKA

Institute of Materials Science and Department of Chemistry,
University of Connecticut, Storrs, CT 06268

Polyethylene has become one of the most widely used materials for electrical insulation due to its excellent dielectric properties and low cost. Original estimates of its probable lifetime using Arrhenius type extrapolation led to lifetime predictions of the order of forty years or more and yet a substantial number of failures in transmission and distribution cables have been observed at times under ten years. For 1977 failures on HMW URD cable totalled 1697 a failure rate of 3,08 per 100 miles while XLP cables were 0.53 per 100 miles and increasing (5). This work was undertaken to find out the role played by the polymer molecule under separate thermal and electrical stress.

Experimental

All measurements of molecular weight distribution were made on a specially constructed high temperature size exclusion chromatograph. This instrument has been described in detail elsewhere(1). Basically chromatographic conditions were: temperature 140°C, solvent o-dichlorobenzene chromatographic column 21 foot 3/8" O.D. is packed with varying grades of controlled pore glass, detector infra-red operating at the C-H stretching frequency. The amount of eluent was recorded on an automatic recording balance.

Samples were prepared from a commercially available DuPont Alathon high density polyethylene resin. This resin was hot pressed at 180°C between two sheets of aluminum foil. The pressing operation was conducted twice to insure uniform films.

Thermal and Electrical Stressing

The thermal stressing was carried out on thin films, approximately 50μm thick, to insure a large surface area and adequate oxygen permeability. Small samples, approximately 25 mg in weight, were placed on microscope slides for support. These samples were then thermally stressed in a small laboratory oven which maintained the desired temperature, to ±1°C.

0-8412-0485-3/79/47-095-421$05.00/0

In Durability of Macromolecular Materials; Eby, R.;
ACS Symposium Series; American Chemical Society: Washington, DC, 1979.

Five temperatures were used in the thermal stressing experiments. These temperatures were 60°C, 90°C, 130°C, 150°C, and 170°C. Samples were introduced into the oven as quickly as possible to minimize the thermal loss. The samples were then withdrawn at timed intervals and allowed to cool to room temperature.

Electrical stressing was accomplished with an electrical stresser built for this purpose. An Allanson luminous tube transformer, North Tonawanda, N.Y., was used to obtain the desired stress levels. This transformer is capable of producing stress levels of up to 15,000 A.C. volts at 60 cycles when supplied to its primary with 120 volt 60 cycle A.C.. The stress level was easily changed by means of a variable transformer placed in the primary circuit and the resulting secondary voltage was calibrated using a high voltage voltmeter.

The sample cell was constructed of Plexiglass which enclosed three sides of a rectangular box arrangement. The sample cell assembly was fitted with contacts which could be slid on and off the secondary voltage terminals. The two secondary voltage contacts were connected to two square aluminum electrodes with copper wire. The bottom electrode was 2" x 2" and secured to the bottom of the cell assembly. The upper electrode was 1" by 1" and contact was made with a spring loaded copper strip. In this fashion a sample may be placed between the electrodes and contact maintained by the spring, with minimal sample distortion.

Samples for electrical stressing were compression molded, as discussed previously, into films approximately 100 μm thick. The films were visually inspected and squares approximately 2" x 2" were cut out of the region with the least visible flaws. The squares were then placed between two parallel plates attached to a micrometer dial and the thickness was recorded. These samples of known thickness were then placed between the electrodes and the voltage level raised to result in a stress of approximately 15 kv/mm. It should be noted, at this point, that the stress levels used in this work are well above that ordinarily found in commercial cables.

Molecular Weight Distribution Analysis

(a) Effects of Thermal Stressing and Oxidative Degradation

Analysis of thermal degradation has been performed on electrical insulating materials extensively. These experiments have, for the most part, been conducted to extrapolate lifetimes at service temperatures from experimental data obtained at elevated temperatures. One of the problems is that it is possible that the degradation mechanism may change between the elevated test temperatures and the service temperatures encountered. Polyethylene melts between 100°C and 135°C, and therefore the accelerated thermal tests have almost exclusively been on the

In Durability of Macromolecular Materials; Eby, R.;
ACS Symposium Series; American Chemical Society: Washington, DC, 1979.

polymer in the melt phase. A change in degradation mechanism is a very real possibility in this case because most properties of a system may not be extrapolated through a phase transition in a continuous, linear fashion.

In an attempt to detect subtle changes in the molecular weight distribution of polyethylene at temperatures below the melting point, the precise high temperature SEC previously described was utilized.

To obtain an estimate of the magnitude of the changes expected at temperatures below the melt using an Arrhenius extrapolation, the data of Holmström and Sörvik (2) was used. In this work a low density polyethylene was subjected to thermal stresses from 280°C to 355°C in atmospheres containing less than 1.2% oxygen. The samples were then analyzed using various techniques including SEC measurements on molecular weight distributions. The data contained in table 1 in the work by Holmström and Sörvik gives the temperature, oxygen content, time of stressing, limiting solution viscosity, $\bar{M}_w$, and $\bar{M}_w/\bar{M}_n$. The data chosen to do the Arrhenius extrapolation was that pertaining to an oxygen content of 1.160%. As the mole fraction of oxygen in air under standard conditions is 0.2095, the data taken at 1.160% should give a slower rate of degradation than that obtained under atmospheric conditions.

The model chosen to describe the degradation of polyethylene was random chain scission. Lenz (3) in his section on degradation reactions of polymers cites work which supports the contention that polyethylene does thermally degrade in a random chain scission manner as opposed to depolymerization. For this model a statistical treatment has been developed by Montroll and Simha (4). The extent of reaction may be related to the number average molecular weight by:

$$\bar{M}_n = M_o/(1-p)$$

where

$\bar{M}_n$ = number average molecular weight

M_o = molecular weight of each repeating segment

p = extent of reaction

If the condition $p = p_o$ at zero time is imposed, the following relationship can be developed:

In Durability of Macromolecular Materials; Eby, R.;
ACS Symposium Series; American Chemical Society: Washington, DC, 1979.

Table I

Specific Rate Constants (min^{-1})

Temp. (°C)	K	Source
	Measured	
130	$5.94 \pm 0.89 \times 10^{-6}$	This work
150	$1.74 \pm 0.19 \times 10^{-5}$	"
170	$4.23 \pm 0.89 \times 10^{-5}$	"
284	$7.02 \pm 1.98 \times 10^{-6}$	Ref. 2
333	$2.17 \pm 0.65 \times 10^{-5}$	"
355	$2.00 \pm 0.60 \times 10^{-5}$	"
	Calculated	
60	1.29×10^{-9}	Ref. 2
90	7.61×10^{-9}	"
60	6.21×10^{-8}	This work
90	5.48×10^{-7}	This work

In Durability of Macromolecular Materials; Eby, R.;
ACS Symposium Series; American Chemical Society: Washington, DC, 1979.

$$p = p_o \exp - kt$$

where

p = extent of reaction at time t

p_o = extent of reaction time o

k = rate constant

t = time

With this equation the extent of reaction may be calculated at any time, t, as long as the initial molecular weight and specific rate constant are known.

The data from Holmström and Sörvik for polyethylene in 1.160% oxygen atmospheres were treated by the use of these equations to calculate rate constants as given in table 1 at 284°C, 333°C and 355°C. From this, using the Arrhenius relationship, constants for the system can be calculated with A = 2.632 and the activation energy 14.13 ± 1.20 Kcal/mol. Using these constants rate equations were calculated at 60°C and 90°C.

Additionally, using the technique described previously, we made measurements at 60°C, 90°C, 130°C, 150°C, and 170°C. The data from the three higher temperatures were used to calculate rate constants and in turn Arrhenius extrapolations for air containing the normal amount of oxygen yielding $A = 1.713 \times 10^4$ and an activation energy of 17.43 ± 0.49 Kcal/mol.

Table 2 gives the calculated weight average molecular weights for the samples run at 60°C bracketed between samples run without stressing. Similar data are given at 90°C in table 3. There appeared to be no detectable difference between the molecular weight distributions run at 60°C and those run at 90°C. Statistical analysis of the unstressed runs yielded the following values for molecular weight and 95% confidence limits. $M_n = 2.057 \pm 0.39 \times 10^4$ and $M_w = 6.620 \pm 0.226 \times 10^4$. The calculated rate constants from the two sets of experimental data were used to predict the number average molecular weight that should be observed after various periods of stressing at 60°C and 90°C. Table 4 shows a summary of the end points. Changes at 90°C of at least 80% should have been observed compared with the actual observation of no change detected within the limits of experimental error. Although not as dramatic for the data from reference 3 with a much lower oxygen content the changes would have still been observed as they are far in excess of the uncertaincies in the method.

The results just discussed indicate that the degradation rate is definitely changing between the high temperature stressing, $\geq$130°C, and the low temperature stressing, $\leq$90°C.

In Durability of Macromolecular Materials; Eby, R.;
ACS Symposium Series; American Chemical Society: Washington, DC, 1979.

Table II

Sample	$Mn \times 10^{-4}$	$Mw \times 10^{-4}$
Unstressed	2.108	6.719
24 hrs. @ 60	1.980	6.431
Unstressed	2.043	6.771
Unstressed	1.996	6.267
51 hrs. @ 60	2.028	6.601
Unstressed	2.027	6.554
Unstressed	2.041	6.348
117 hrs. @ 60	2.053	6.395
Unstressed	2.084	6.728
Unstressed	2.102	6.954
169 hrs. @ 60	2.112	6.992

Table III

Sample	$Mn \times 10^{-4}$	$Mw \times 10^{-4}$
Unstressed	2.027	6.414
24 hrs. @ 90	2.061	6.443
Unstressed	2.091	6.659
Unstressed	2.026	6.428
48 hrs. @ 90	2.027	6.514
Unstressed	2.033	6.388
96 hrs. @ 90	2.104	6.572

In Durability of Macromolecular Materials; Eby, R.;
ACS Symposium Series; American Chemical Society: Washington, DC, 1979.

Table IV

Temp.	Time	$M_n \times 10^{-4}$ Observed	Calc. [Ref. 3]	Calc. This Work
60	169 hrs.	2.11	2.01	1.07
90	96 hrs.	2.10	1.93	0.37

Table V

Sample	$M_n \times 10^{-4}$	$M_w \times 10^{-4}$
Unstressed	2.049	6.302
3 hrs. @ 15 kV/mm halo	2.039	6.621
3 hrs. @ 15 kV/mm center	2.028	6.330

Table VI

Sample	$M_n \times 10^{-4}$	$M_w \times 10^{-4}$
Unstressed	1.996	6.379
24 hrs. @ 15 kV/mm halo	1.994	6.133
24 hrs. @ 15 kV/mm center	1.980	6.223

In Durability of Macromolecular Materials; Eby, R.;
ACS Symposium Series; American Chemical Society: Washington, DC, 1979.

The essentially linear Arrhenius plot for the temperatures 130°, 150°, and 170°C demonstrates that random chain scission for polyethylene in the melt does behave in an Arrhenius manner. While we are not able to determine if the degradation behaves Arrheniusly in the solid state, we can conclude that there is a definite discontinuity in the linear behavior between the two states. This discontinuity precludes the use of high temperature melt experiments to determine rate constants at temperatures below 90°C.

As mentioned previously, lifetimes of more than 40 years have been predicted for polyethylene used for electrical insulation where electrical, thermal, mechanical and environmental stresses exist. The fact that cables are failing in a much shorter time period than predicted seems to point to an acceleration in rate of degradation over that assumed. This is directly opposite the results for thermal degradation obtained in this work where the rate of thermal degradation was found to be much slower than that predicted from high temperature experiments.

The following conclusions may now be drawn for random chain scission degradation of polyethylene with the obvious qualifications that only limited data are reported herein.

1) Random chain scission appears to follow an Arrhenius plot in the temperature region of at 130° - 170°C.
2) Extrapolations to determine rate constants at temperatures of 90°C below do not agree with experimentally observed results.
3) The behavior of polyethylene at temperatures of 90°C and below may be Arrhenius, but a discontinuity in the linear behavior takes place somewhere in the 90°C - 130°C range.
4) Extrapolated lifetimes for polyethylene cables have proven to be greater than those actually observed yet these data indicate that the material is in fact thermally more stable than the original tests indicate.
5) Random chain scission due to thermal or oxidative degradation with the resulting lowering of molecular weight may not be the breakdown precurser to eventual failure of cables in the absence of other stresses.

These conclusions essentially prevent the use of changes in polymer molecular weight brought about by thermally accelerated tests above 130°C to predict the thermo-oxidative stability of polyethylene at operating temperatures.

(b) Effects of Electrical Stressing

Electrical tests were conducted to evaluate the effect of electrical stresses on the molecular weight distribution of polyethylene. The electrical stress apparatus discussed previously was used to electrically age polyethylene at room

In Durability of Macromolecular Materials; Eby, R.;
ACS Symposium Series; American Chemical Society: Washington, DC, 1979.

temperature. Polyethylene sheets were compression molded as discussed previously and square samples about 2" by 2" were prepared. The thicknesses of the resulting films were determined by placing the films between two parallel plates attached to a micrometer dial. All films were found to be between 90 and 120 μm in thickness. The exact thickness of each sample was recorded. The sample was placed between the electrodes and stressed at a level of ∿15 kv/mm. As any surface features of the electrodes may cause distortion of the stress fields, great care was taken to minimize any irregularities. The aluminum electrodes used were ground down to insure a parallel contact. The electrodes were then smoothed with the abrasive paper used for preparing metallurgical samples for microscopic examination. Finally the surfaces were ground and polished using polishing wheels and small diameter abrasive materials. The resulting electrode surfaces were found to have mirror-like qualities with no microscopic defects. This procedure was followed before each sample was stressed to remove any breakdown products and washed with acetone just prior to the actual stressing.

The actual voltage applied to the films was varied according to the films thickness to obtain the desired stress level of 15 kv/mm. Stress levels higher than this were attempted but these tests resulted in almost instantaneous breakdown and resulting arcing.

A stress of 15 kv/mm is well above the normal operating stress levels for cables. This may be observed by looking at a typical 115 kv electrical cable. These cables have an inner copper conductor surrounded by at least 25 mm of insulation. This results in a calculated stress level of about 4.6 kv/mm if the cable is used at its maximum rated voltage. The stress level of 15 kv/mm used in this work also proved to be more than enough to cause electrical breakdown of the samples used. Most of the samples stressed even at this level broke down in short periods of time with the resulting arcing and carbonization of the sample. As this research was interested in the prebreakdown processes, and not the products formed after breakdown, the samples which failed were not used.

The first sample evaluated was allowed to remain under a stress of 15 kv/mm for three hours. Upon visual examination a halo could be observed of slightly more opaque material where the edges of the electrode were positioned. The location of this halo came as no surprise since it is well established that there is an edge effect associated with any electrode system. This edge

In Durability of Macromolecular Materials; Eby, R.;
ACS Symposium Series; American Chemical Society: Washington, DC, 1979.

effect results in an increase in the actual stress level encountered at the edges of an electrode. As the electrodes used in this work were rectangular in shape, the abruptness of the transition results in truly enhanced fields above the imposed 15 kv/mm at the edges. The appearance of this halo also demonstrated that a stress level of this magnitude, when maintained for three hours, was enough to change the appearance of the sample.

Molecular weight distribution analyses were conducted on portions of the stressed material using the high temperature gel permeation chromatograph and techniques discussed earlier. A sample of the unstressed material was run and the molecular weight distribution observed, and molecular weight averages calculated as in previous experiments. A sample of the polyethylene making up the halo was dissolved and run on the HTGPC. This halo sample was obtained by cutting out strips of the material showing greater opaqueness which was about 1 mm wide. The resulting chromatogram was then reduced to molecular weight averages and a molecular weight distribution curve. Additionally a sample was obtained from the center of the stressed sample and its data evaluated to obtain a molecular weight characterization. The results of these runs may be found in table 5. These calculated molecular weight averages along with visual inspection of the molecular weight distributions demonstrated no significant variance between stressed and unstressed samples within the experimental error.

An attempt was made to stress a sample for longer periods of time at 15 kv/mm. After many unsuccessful attempts a sample which had been stressed for 24 hours at 15 kv/mm without breakdown was obtained. This sample also exhibited the halo phenomena but but it could not be determined if the capacity of this halo was greater than that of the previous sample. Samples were again taken from the halo and center of the stressed sample. Molecular weight distributions and averages were obtained for these samples as well as for an unstressed sample using the previously mentioned procedure. The results of these experiments may be found in table 6. Once again there was no detectable change in either the molecular weight distribution or calculated molecular weight averages between the stressed and unstressed samples.

Several attempts were made to obtain samples stressed for longer periods of time without success. These failures, while disappointing, did serve to reinforce the position that the stress levels imposed were, in fact, great enough to cause breakdown in the periods of time used for these experiments.

In Durability of Macromolecular Materials; Eby, R.;
ACS Symposium Series; American Chemical Society: Washington, DC, 1979.

The results just discussed indicate that when stressed electrically the molecular weight distribution remains unchanged. This evidence leads one to the conclusion that electrical breakdown of polyethylene is probably not preceded by a gradual deterioration throughout the polymer through chain cleavage and resulting decrease in molecular weight. The data presented cannot exclude the possibility of localized degradation producing changes in the molecular weight distribution which would be too small to be detected in the bulk polymer.

Acknowledgements

This work was supported in part by grants from the National Science Foundation and Northeast Utilities Service Company. Part XVII of a series on Lifetime Prediction of Electrical Insulating Materials.

Literature Cited

1. Crowther, J. A., and Johnson, J. F., J. Appl. Polym. Sci. submitted.
2. Holmström, A., and Sörvik, E. M., J. Appl. Polym. Sci. (1974), 18, 779.
3. Lenz, R. W., Organic Chemistry of Synthetic High Polymers, (1967) Interscience, New York.
4. Montroll, E. W., and Simha, R., J. Chem. Phys. (1940) 8, 721.
5. R. Luther, Presented at the Electric Council of New England Transmission and Distribution Committee Meeting #54, White River Junction, Vermont, September 21-22, 1978.

RECEIVED December 8, 1978.

Aging of Polyolefin Electrical Insulation

K. D. KISS, H. C. DOEPKEN, JR., and N. SRINIVAS
Phelps Dodge Cable and Wire Company, Yonkers, NY 10702
B. S. BERNSTEIN
Electric Power Research Institute, Washington, DC 20006

Polyolefins are the preferred insulating materials due to a fortuitous combination of their properties: high resistivity and dielectric strength, low dielectric constant and dissipation factor, low specific gravity, moderate melting range and good processability, adaptability to stabilization and compatability with additives and fillers and economy and availability on large scale.

In power transmission and distribution cables rated 5 kV and above low density polyethylene (PE), cross-linked low density polyethylene (XLPE) and ethylene-propylene rubbers (EPR) are used in large quantities. A recent survey (1) shows that the combined length of underground power cables exceeds 190,000 miles in the U.S.A. Field data covering over 25% of this total reveals dielectric failures attributable to premature ageing beginning approximately 3 to 8 years after the installation (Figure 1). This is considered a serious indicator of potential hazard and has precipitated a major effort to define the problem areas, understand the causes with a view of eliminating or at least minimizing them.

Background

Ageing Process in Solid Dielectrics. "Ageing" and life time" are terms based on biological analogies, and, though widely used describe the investigated phenomena with limited accuracy. Kelen (2) suggests the use of the term "endurance", which is the opposite though not the exact reverse of ageing.

0-8412-0485-3/79/47-095-433$08.50/0

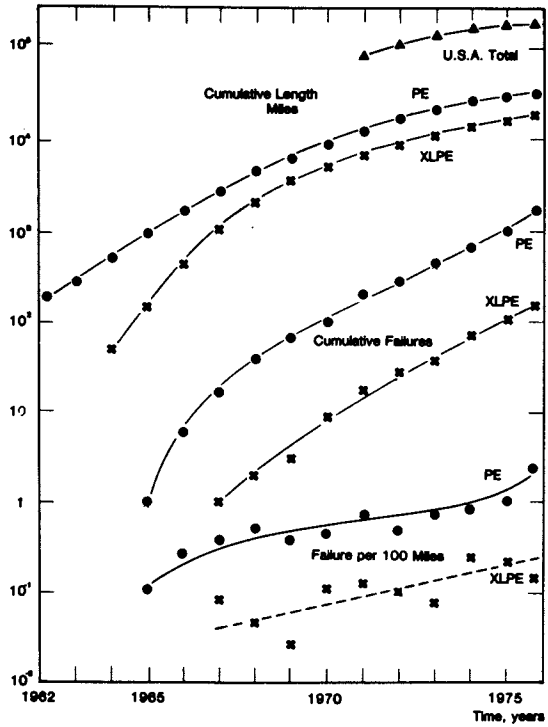

Figure 1. Field performance of high voltage cables

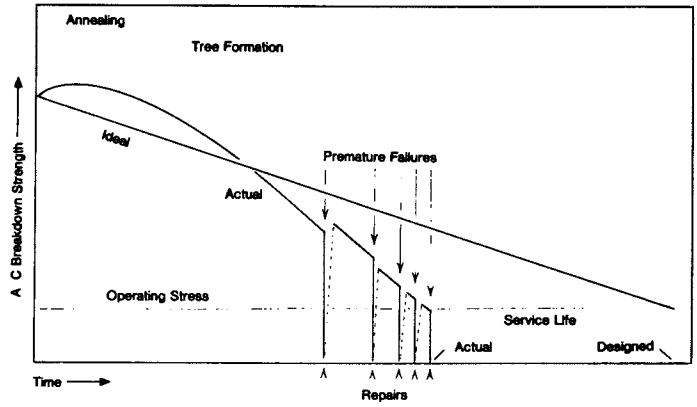

Figure 2. Schematic life curve

In Durability of Macromolecular Materials; Eby, R.;
ACS Symposium Series; American Chemical Society: Washington, DC, 1979.

The inherent dielectric strength of polyethylene measured on thin films is estimated as 600 to 800 kV/mm. This value decreases with increasing thickness. Prolonged exposure to high electric stress gradually decreases the dielectric strength of solid dielectrics, measured as AC breakdown strength, according to the so-called "life equation" which in its simplest form correlates the stress with time at constant temperature:

$$t_c = A.E_c^{-n} \qquad (1)$$

where t_c = time at constant stress
A = constant
E_c = constant stress
n = exponent, empirically found as 9 to 12 for XLPE (3)

This empirical correlation is widely used to predict life expectation through accelerated tests by exposing the dielectric to constant high stress and measuring the time to failure. A logarithmic plot of the results produces a linear correlation with a slope of $-1/n$ which can be extrapolated to the operating stress. When applied to progressive tests where stress is increased in discrete steps the life equation can be written as:

$$t_1E_1^n = t_2E_2^n \qquad (2)$$

where E_1 and E_2 represent different stresses t_1 and t_2 represent the corresponding life times.

Field data (1, 4, 5) reveal that predictions based on these equations are often optimistic and failure rates exist considerably higher than those attributable to the factors considered in the life equation. The schematic life of a high voltage cable, Figure 2 shows the "ideal" lifeline based on Equations (1) and (2) as a straight line of negative slope.

It has been reported (6) that XLPE cable preheated to a temperature just below the insulation melting point (by conductor heating) leads to a 6% higher breakdown voltage. This phenomenon could lead to a minor initial upward trend in the cable life - breakdown strength relationship shown in Figure 2. This may result from a relieving of mechanical stresses and/or

In Durability of Macromolecular Materials; Eby, R.;
ACS Symposium Series; American Chemical Society: Washington, DC, 1979.

morphological changes. Beyond the cresting point the expected life line declines at a slope comparable to or steeper than that predicted from Equation (1). The possibility exists that this decline may be interrupted prior to reaching the operating stress level by a catastrophic breakdown possibly due to a lightning surge or increased localized stress due to a large imperfection in the cable. This point may represent the end of service life, or, after suitable repair, the beginning of a second phase. Since the breakdown eliminated the weakest point of the system, the predicted life value after repair may be somewhat higher than it was before the breakdown. The gradual deterioration continues through one or more breakdowns until further repairs become not feasible.

Factors other than the stress induced ageing also play an important role in cable failure. Thorough investigation (7, 8) has revealed that imperfections present in the cable are responsible for premature failures and also indirectly for the gradual deterioration.

Cable Construction. A typical power cable consists of several concentric layers:

- metallic conductor, solid or stranded,
- conductor shield, usually carbon containing extruded polymer,
- insulation, extruded over the conductor shield, usually high purity polyolefin, (PE, XLPE, or EPR). Other polymers are also used and the composition may contain additives, by-products of crosslinking agents and fillers,
- insulation shield, carbon containing polymer similar to the conductor shield,
- wire or metallic tape shield,
- jacket (optional)

The typical manufacturing process (Figure 3) applies the 3 polymeric layers over the conductor sequentially in 3 extruders through corsshead dies in a continuous process. Two or all three dies may be combined into a "common head" die. Cables with thermoplastic insulation and shields are cooled after extrusion.

In Durability of Macromolecular Materials; Eby, R.;
ACS Symposium Series; American Chemical Society: Washington, DC, 1979.

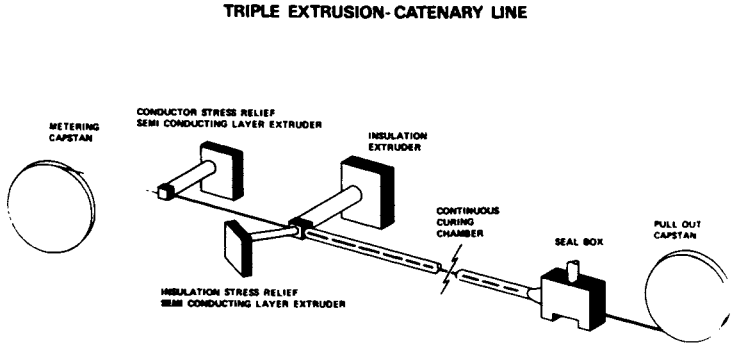

Figure 3. Manufacturing process

In Durability of Macromolecular Materials; Eby, R.;
ACS Symposium Series; American Chemical Society: Washington, DC, 1979.

Crosslinking is commonly effected by passing the extruded cable through a catenary tube and heating it directly with high pressure steam. Modifications of this process include the use of a vertical line instead of the catenary tube and the use of heat transfer media other than steam.

These cables are designed to carry the specified current load and to provide adequate electrical insulation with a wide margin of safety. Present requirements for XLPE (9) specify a 90°C maximum operating and a 130°C maximum emergency temperature at the conductor and a minimum of 0.016 mil/V insulation thickness. Other countries' specifications vary, especially the emergency temperature.

Imperfections. A schematic view of the potential imperfections (Figure 4) depicts those occurring in the freshly prepared cable. Others that may develop during the service life will be discussed later.

Flow marks develop during the extrusion process due to the velocity gradient in the melt flow. Various levels of orientation result in internal stresses when the extrudate is cooled below its melting range. Crosslinking in the melt phase restricts the molecular movement on cooling, thus altering the mode of crystallization. A special case of flow marks is the cusp or coalescence line of the two branches of melt flowing around the conductor in the crosshead.

Protrusions are surface imperfections of the conductor shield or of the insulation shield ingressing into the insulation. Die drool, foreign matter in the semiconductive material, uneven heat causing "cold pellets" are a few of the possible causes. Their effect is enhanced when their location is at the point of highest electrical stress, at the conductor shield - insulation interface. This enhancement is given by Bahder (10) and Bateman (11) assuming ellipsoid shape:

$$\frac{E_{max}}{E_{avg}} \cong \frac{2n^3}{m \ln\left(\frac{m+n}{m-n}\right) - 2n} \qquad (3)$$

where:

$m = \frac{c}{a}$ ratio $\frac{\text{major}}{\text{minor}}$ axes

$n = \sqrt{m^2 - 1}$

In Durability of Macromolecular Materials; Eby, R.;
ACS Symposium Series; American Chemical Society: Washington, DC, 1979.

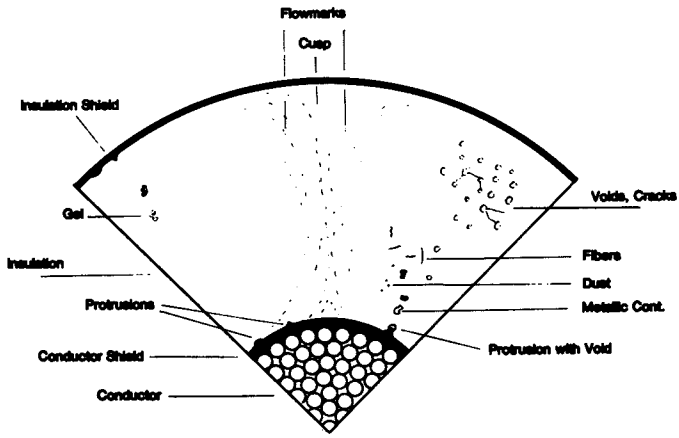

Figure 4. Imperfections in high voltage insulation

In Durability of Macromolecular Materials; Eby, R.;
ACS Symposium Series; American Chemical Society: Washington, DC, 1979.

For hyperboloid to plane geometry Mason defines the stress enhancement as:

$$\frac{E\ max}{E\ avg} \cong \frac{2\ d}{r\ \ell n\left(1 + \frac{4d}{r}\right)} \qquad (4)$$

where:

r = radius conductive point
d = point to plane dist.
d>= 10 r

Whelan (12) presents the equation for two hyperboloidal points:

$$\frac{E\ max}{E\ avg} \cong \frac{\ell\left(1 + \frac{2r}{\ell}\right)^{1/2}}{r\ \tanh^{-1}\left(\frac{\ell}{\ell + 2r}\right)^{1/2}} \qquad (5)$$

where:

r = radius conductive point
ℓ = point to point dist.

This correlation was adopted by Aschcraft (13) for the calculation of stress enhancement at the tip of the electrodes in the double needle test used in some laboratories in treeing studies. Depending on the radius at the tip of the protrusion or on the ratio of axes in the ellipsoid, the stress enhancement may amount to several hundred fold compared to the smooth, protrusion free surface (14). This level of stress increase in turn may trigger immediate dielectric breakdown or initiate gradual deterioration.

Though polymers made specifically for high voltage insulation are remarkably clean, occasional contaminants occur and contribute to the deterioration of dielectric properties. Some of these are polymeric in nature such as gels or prematurely corsslinked polyethylene particles which may appear amber to dark brown in color depending on heat history. Figure 5 shows one

In Durability of Macromolecular Materials; Eby, R.;
ACS Symposium Series; American Chemical Society: Washington, DC, 1979.

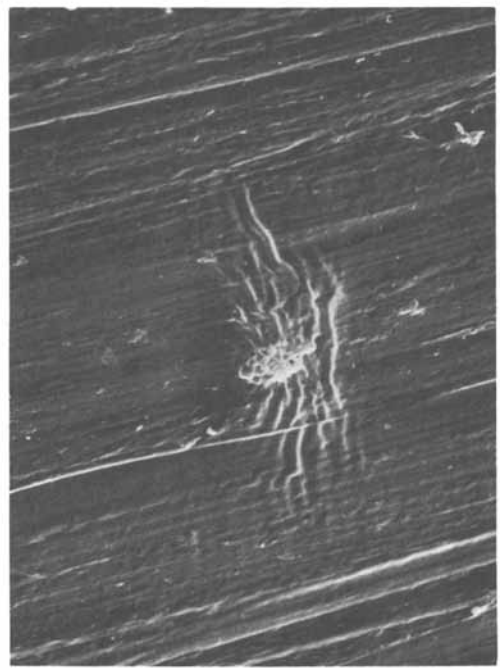

Figure 5. Gel particle in XLPE (10 μm)

In Durability of Macromolecular Materials; Eby, R.;
ACS Symposium Series; American Chemical Society: Washington, DC, 1979.

of these in the center, the vertical ripples are artifacts caused by the cutting blade forcing the resisting gel forward. Inorganic particles (Fig. 6) such as metallic filings contribute to tree initiation and hence gradual deterioration. Along with contaminant nature, their shape, direction and location may amplify their detrimental effect. Those imbedded at the conductor shield - insulation interface (Figure 8) may act as protrusions and cause localized stress enhancement. Cellulosic fibrous particles (Figure 7) (15-20 mils, 0.38 to 0.51 mm) at about 10 per linear foot of cable were shown by Bahder (15) to lower the average AC breakdown strength by 40%.

Existing specifications for 5 to 69 kV cables prohibit "any translucent material that is larger than 50 mil (2 mm) in its radial vector projection" and "any contaminant larger than 10 mils (0.4 mm) in its largest dimension" and limits those 2 to 5 mils (0.08 to 0.2 mm) to 15 per cubic inch (0.92 per ccm) (9).

Part of the contaminants may be present in the pelletized raw materials, another part originates from material handling and processing. The extrusion process and the application of screens removes the larger particles or breaks them down.

Ionic contamination may occur during the service life due to corrosion products of the conductor or of the metallic shields entering the insulation.

Voids or cavities are the most numerous of the imperfections. Their number in steam cured XLPE is estimated as 10^6 per cubic cm. (16) Their combined volume amounts to less than 1% of the total, which computes as about 30 μm average diameter assuming spherical shape. This spherical shape probably applies to the majority of them though ovaloid shapes, roundish ones with irregular corners, polygonals with slightly rounded corners and long, narrow cracks have also been found (Fig. 9); the latter ones may originate from round voids.

Void distribution is not uniform (15, 17). In the radial direction of the cable relatively few are located at the conductor side and at the outside surface, and the distribution curve peaks between the midpoint and the outer surface (18). This distribution is associated with the effect of steam used to cure XLPE.

The solubility of water is very low (50 to 70 ppm)

In Durability of Macromolecular Materials; Eby, R.;
ACS Symposium Series; American Chemical Society: Washington, DC, 1979.

Figure 6. Contamination in XLPE (600 μm)

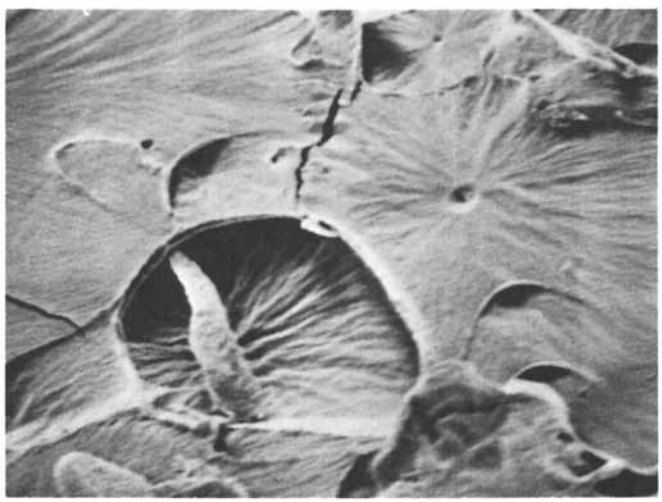

Figure 7. Fibrous contamination (25 μm)

In Durability of Macromolecular Materials; Eby, R.;
ACS Symposium Series; American Chemical Society: Washington, DC, 1979.

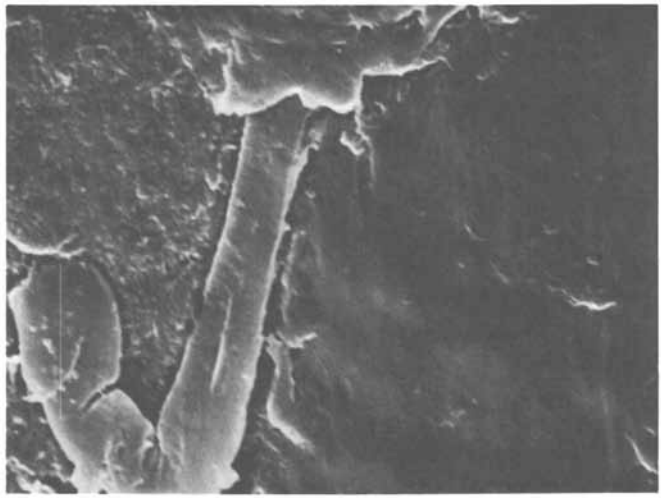

Figure 8. Contamination at conductor shield–insulation interface (15 μm)

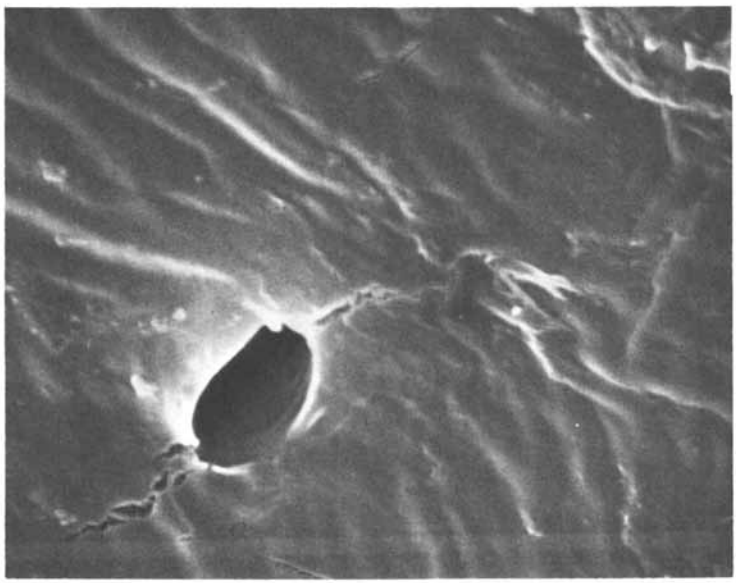

Figure 9. Void (5 μm) and cracks

In Durability of Macromolecular Materials; Eby, R.;
ACS Symposium Series; American Chemical Society: Washington, DC, 1979.

(19) in polyethylene at room temperature, but reaches 4000 - 5000 ppm under the conditions prevailing in the steam tube. Thus, most of this absorbed water forms a distinct separate phase when the crosslinked cable is cooled and is probably responsible for the majority of the voids. Especially harmful are the voids at the conductor shield-insulation interface (Figure 10) which, when filled with a conductive liquid, may act as protrusions.

Even in XLPE cables cured under dry conditions some voids exist. These are thought to be due to the coalescence of catalyst by-products or interspherulitic space caused by crystallization of the cooling polyethylene.

Relative to the morphological structure, the larger voids were shown by Phillips (17) to occur at the interstices of spherulites, and the smaller ones along the spherulitic dividers. Similar views were presented by Patsch (20). An opposing view (16, 21) places them in the center of the spherulite like structures (Figure 11).

In the freshly made XLPE cable the cavities are filled with either a gas (water vapor, air, nitrogen, methane, low molecular weight hydrocarbons) or a liquid (water or organic liquids from the by-products of the decomposed curing agent). Even radiation crosslinked polyethylene contains voids, presumably caused by the evolution of hydrogen or low molecular weight hydrocarbons (22) (Figure 12). Both the gaseous and the liquid by-products may escape gradually.

Thermal treatment was shown to diminish void number and size (18). This would necessitate an increase in density and such an increase was reported by Nitta and al (6). Electric stress and dielectric heating among other factors could result in a rearrangement of void distribution, shape, size and number, and is a possible cause of some slowly occurring changes during service.

Ageing Parameters

Several of the typical factors effecting service life or ageing of polymers in other applications can be eliminated on the basis that either by themselves or in combination they appear to cause less damage than

In Durability of Macromolecular Materials; Eby, R.;
ACS Symposium Series; American Chemical Society: Washington, DC, 1979.

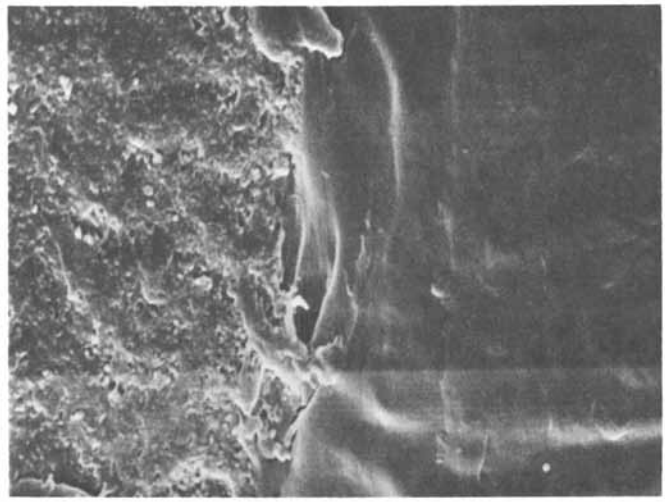

Figure 10. Void at conductor shield–insulation interface (4 μm)

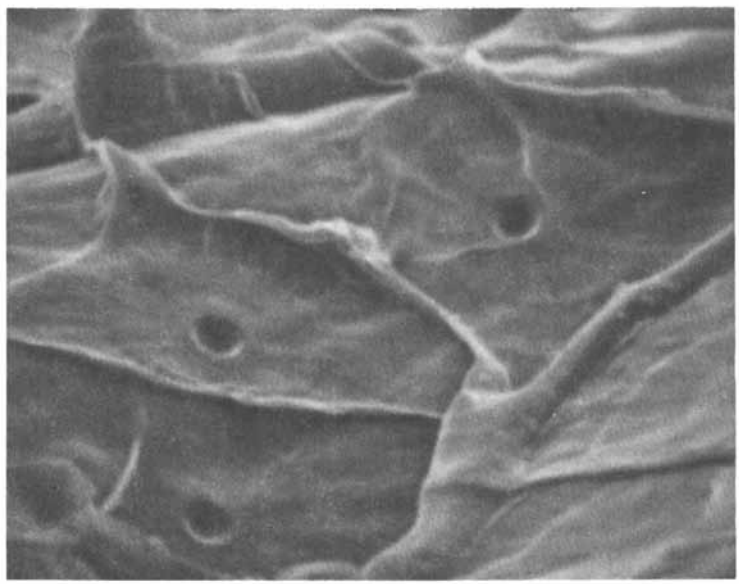

Figure 11. Voids in center of spherulitic structures (5 μm)

In Durability of Macromolecular Materials; Eby, R.;
ACS Symposium Series; American Chemical Society: Washington, DC, 1979.

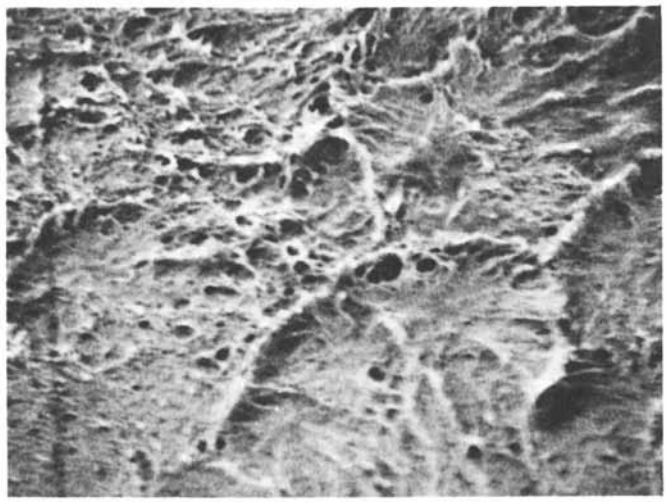

Figure 12. Voids in radiation cross-linked polyethylene (1–8 μm)

In Durability of Macromolecular Materials; Eby, R.;
ACS Symposium Series; American Chemical Society: Washington, DC, 1979.

others, therefore not playing a determining role in the ageing process.

Effect of Environment. Exposure of the insulation to ultraviolet light is very limited, since the overwhelming majority of cables is buried. The outer jacket contains carbon black thus providing adequate protection in this respect. Gilroy (23) presented data on carbon black containing PE surviving 32 years of outdoor exposure at a Florida site.

Oxidative stability of the insulation is enhanced by the protective covering and by the limited availability of oxygen in underground application. The most commonly used antioxidant systems are based on the derivatives of paraphenylene diamine or on thiophenols, the same general types found highly efficient in telecommunication applications (25). A complicating factor in XLPE cables is the potential interaction of antioxidants with free radicals generated during the crosslinking process. Specific oxidative stabilizer systems are being employed and appear to provide satisfactory protection (24). A point of interest is the reported beneficial effect of the aromatic amines on preventing electrical treeing (14).

The effect of temperature on the insulation is complex. The fact of elevated conductor temperature would imply a major concern for potential limitation due to thermal degradation. Obviously, the temperature was a key variable considered in a variety of investigations dealing directly or indirectly with performance, stability or endurance. No major deleterious effect is apparent up to allowed operating and emergency conductor temperatures, either in field performance or in comprehensive laboratory investigations. Beneficial effect of heat treatment per se was noted by Nitta (6) and Mangaraj (16) among others. Most of the work in this area combines the temperature effect with that of other parameters such as antioxidant concentration (24) or frequency acceleration (26).

Mechanical and Electrical Stress. With reference to mechanical stress, axial and radial deformations are of potential concern. Excessive axial elongation is largely prevented by the conductor which serves as an

In Durability of Macromolecular Materials; Eby, R.;
ACS Symposium Series; American Chemical Society: Washington, DC, 1979.

internal support. Radial deformation may occur at the high end of the allowed temperature range due to poorly designed shields or at cross supports especially when the weight of a long section is applied at one point. However, these problems are not inherent material limitations and can be solved by other means such as design changes.

The internal stress whether initially present in the freshly made cable or developed during service life could have deleterious effects. Patsch (20) shows no effect of either the cusp or of areas with distinct flow pattern on the dielectric strength in high voltage insulation beyond the 95% confidence limit.

The development of internal stress during service life has been reported by Tanaka (27) to be associated with tree formation. Electrical stress by itself and in combination with other contributing factors referred to above is considered the key ageing parameter. Its effect as a single variable under controlled conditions is characterized by the life equation (2) presented earlier. This correlation is widely used in generating life projections from accelerated test data, despite the fact that it lacks theoretical basis and its validity is questionable without postulating restrictive assumptions (28). Similarly, using set stress levels as test criteria to project service life, could result in questionable conclusions. At present, acceptance criteria (9) include a 5 minute withstand at 150 V/mil (6 kV/mm) level, although a voluntary limit of 200 V/mil (8 kV/mm) is applied by some manufacturers. This test and other acceptance tests are suitable to pinpoint major deficiencies in the cable and prevent the "infant mortality" type failures which would occur after a relatively short time at operating stress, but do not necessarily predict the long term performance under field conditions.

Higher frequency testing accelerates certain types of processes leading to premature failure, and is a useful tool to study tree formation (29).

Treeing

When field performance indicated lower than anticipated lifetime in solid dielectric insulation, close

In Durability of Macromolecular Materials; Eby, R.;
ACS Symposium Series; American Chemical Society: Washington, DC, 1979.

inspection of recovered cables revealed the presence of dendritic structures or "trees" (Figure 13) near the site of dielectric failures (30). Correlation was established between the presence of certain types of trees and the breakdown strength of partially aged cables. These observations initiated a major effort to understand the nature of these phenomena with a view of assessing their effect on the ageing process and possibly minimizing it to a practically tolerable level.

The generally accepted view is that excessive treeing lowers the breakdown strength to the point where the longest tree causes the catastrophic failure. Since this tree is usually destroyed in the breakdown process, only nearby trees can be examined and it is assumed that the tree that caused the failure had to be longer than the longest remaining nearby tree to be the first to fail.

Types of Trees. The word "tree" is descriptive of the appearance of some of the structures (Figures 13 to 16). Other structures are adequately described by terms like broccoli, plume, bow tie, streamer, delta, dendrite, etc (7). Another way to describe them is by origin. Though no uniform nomenclature is accepted, and some overlapping and controversy still exists, the four types of trees are classified as electrical and electrochemical trees, water trees, and chemical trees.

The chemical tree is described by Lanctoe (5) as a short, very dense, dark colored, broccoli type tree, which is unique to cables with a tape conductor shield. Since this is not a frequently used design, the chemical tree is considered as of limited importance.

Electrical trees are easy to observe without staining. They are caused by electrical discharge initiated at imperfections in the insulation at stresses higher than the corona inception voltage. They consist of hollow connected channels lined with decomposed polymer. They can be filled through a fine hypodermic syringe (14). Their rate of propagation at high stress may be extremely fast resulting in immediate insulation breakdown. In actual service they can be initiated at the interface of insulation with conductor shield or insulation shield or within the insulation and take days, weeks or months to cause a failure. Under laboratory

In Durability of Macromolecular Materials; Eby, R.;
ACS Symposium Series; American Chemical Society: Washington, DC, 1979.

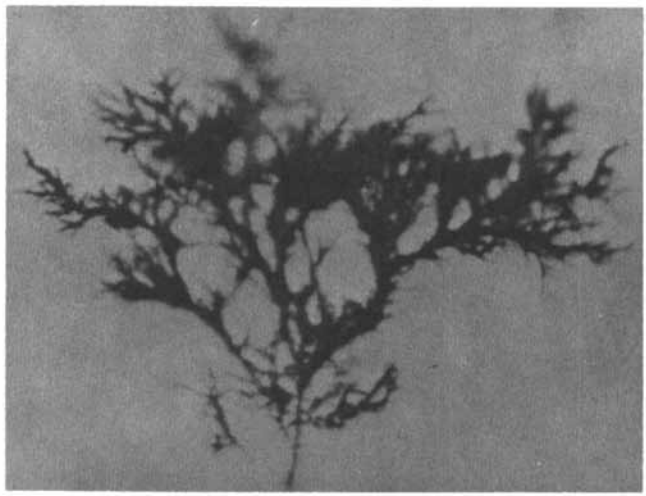

Figure 13. Dendritic tree

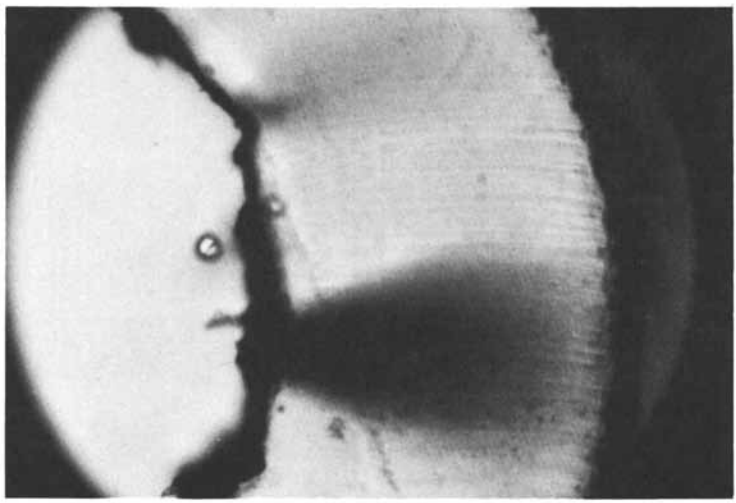

Figure 14. Electrochemical tree

In Durability of Macromolecular Materials; Eby, R.;
ACS Symposium Series; American Chemical Society: Washington, DC, 1979.

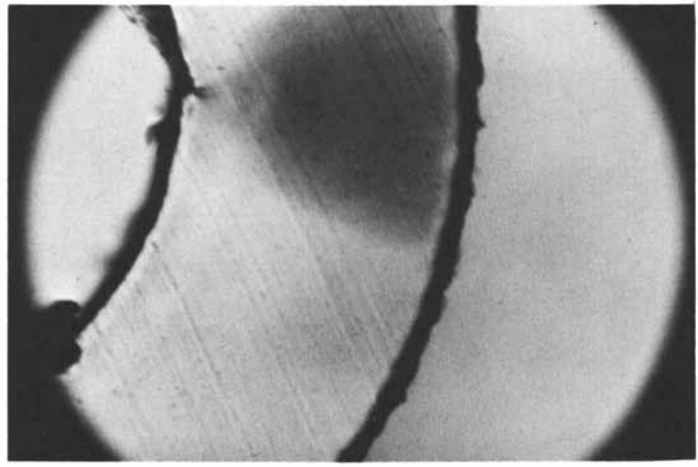

Figure 15. Water tree

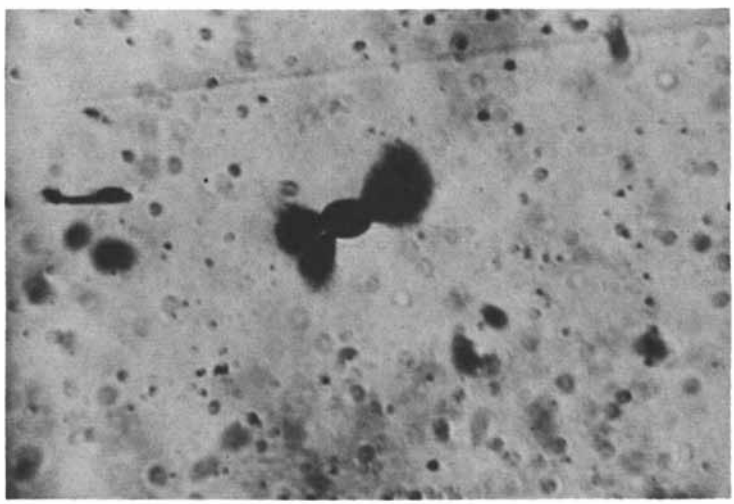

Figure 16. Bowtie tree (40 μm)

In Durability of Macromolecular Materials; Eby, R.;
ACS Symposium Series; American Chemical Society: Washington, DC, 1979.

conditions high stress is used to accelerate their formation.

Electrochemical (or water) trees appear to consist of water-filled voids which may or may not be connected by very fine channels. They can be initiated at stresses significantly below the corona inception voltage, i.e., in the absence of measurable partial discharge. The presence of a liquid phase (not necessarily water) (29) is a prerequisite. They propagate slowly and evidence exists that they do not necessarily cause breakdown even when bridging the full insulation thickness. They are more diffuse in appearance than electrical trees. Dissolved chemicals such as copper or iron salts may stain them (5) or they can be stained by methylene blue (31) in alkaline solution. Electrochemical trees have been referred to as water trees, containing chemicals, though the two terms are often used interchangeably.

Bow tie trees (Figure 16) can be of either electrical or electrochemical nature in origin. They are initiated at voids or contaminants not connected to either the conductor shield or to the insulation shield. They are aligned parallel to the electrical field direction.

The relative effect of electrical and electrochemical trees on ageing, and hence their contribution to premature failure depends on the quality of insulation and on the service conditions. Electrical trees, when initiated, can propagate fast and cause failure directly. However, their formation requires that stress in a void be above the corona inception level. It is possible to calculate the minimum stress level to initiate partial discharges in spherical voids (32). According to this widely used correlation (Figure 17) 3.8 kV/mm stress is necessary to induce partial discharge in voids of 250 μm diameter, and no partial discharge takes place below 12 kV/mm in voids less than 25 μm in diameter. In practice it is possible to keep the voids small enough to avoid partial discharges in voids at operating stress.

Electrochemical trees form at relatively low stress levels, propagate slowly but do cause deterioration. Even if not immediately causing the failure they may weaken the insulation and may sire electrical trees which in turn cause failures. The increasing rate of

In Durability of Macromolecular Materials; Eby, R.;
ACS Symposium Series; American Chemical Society: Washington, DC, 1979.

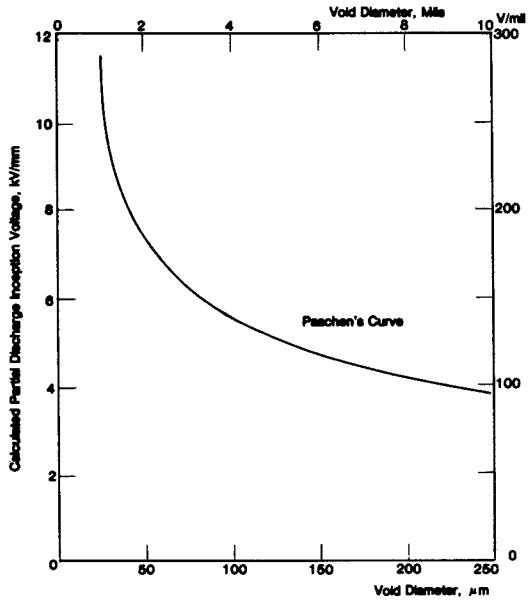

Figure 17. Calculated partial discharge inception voltage

In Durability of Macromolecular Materials; Eby, R.;
ACS Symposium Series; American Chemical Society: Washington, DC, 1979.

failures with increasing service life could reflect the slow deterioration due to electrochemical treeing. Though subject to qualifications, it is believed that the major contribution to dielectric ageing in real life results from electrochemical treeing.

A major study was funded by the Electric Power Research Institute to evaluate the effects of electrochemical trees in extruded cable materials (29). The primary objective of this work was to quantify the major parameters responsible for their formation. Using coated wires with #14 AWG solid round or square conductors and with 0.75 mm insulation, accelerated experiments were performed under aqueous conditions. Over 300,000 trees were observed and measured during the course of the project, and statistical methods were applied to analyze the data obtained.

Accelerating Parameters. Voltage stress emerged as the condition most influential in accelerating tree growth. Average voltage stresses of 2, 3.4, 5.0 and 6.8 kV/mm were applied at 70°C temperature and at 8.0 kHz frequency and treeing observations were made of average and of maximum tree length up to 70 days. The initiation of trees was induced by scratching the inner insulation surface. The results, summarized in Figure 18, show that the applied stress correlates exponentially with the time required to penetrate the 0.75 mm insulation. Tree growth rate in PE appears to be at least twice as high as in XLPE.

The effect of frequency as an accelerating factor was studied in the range of 60 to 8000 Hz. At 70°C temperature and 3.4 kV/mm applied stress the number of trees, their average length and the length of the longest trees increased with time. Large scatter of data mandated the use of a high number of specimens and of statistical methods in the evaluation to establish trends. Obviously, both the initiation and the propagation of the trees progresses simultaneously. The summary in Figure 19 for various lengths of trees shows a drastic increase from 60 to about 600 Hz, but minor effect from 600 to 8000 Hz.

In actual service, the frequency is constant, therefore it is not a contributor to ageing. The significance of this correlation is its applicability to accel-

In Durability of Macromolecular Materials; Eby, R.;
ACS Symposium Series; American Chemical Society: Washington, DC, 1979.

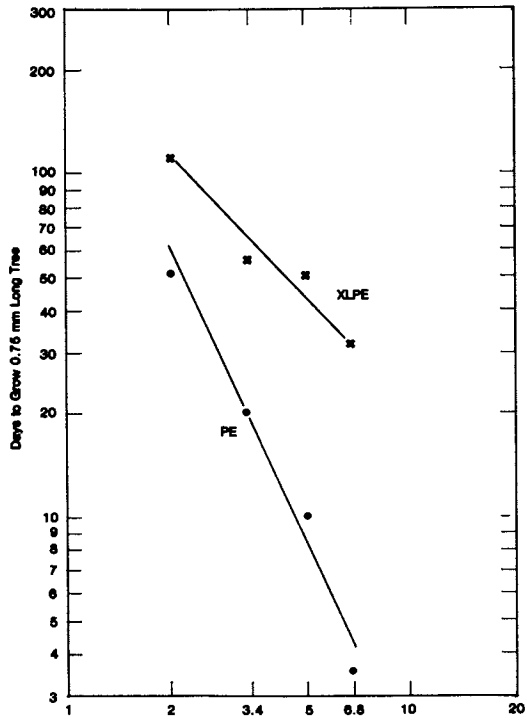

Figure 18. Effect of applied stress on tree growth

In Durability of Macromolecular Materials; Eby, R.;
ACS Symposium Series; American Chemical Society: Washington, DC, 1979.

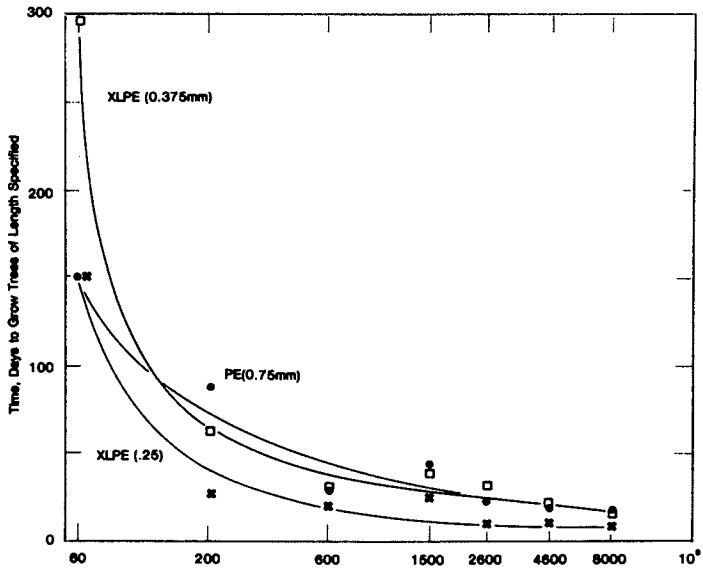

Figure 19. Effect of frequency on tree growth

In Durability of Macromolecular Materials; Eby, R.;
ACS Symposium Series; American Chemical Society: Washington, DC, 1979.

erate ageing in laboratory investigations, and possibly to serve as a quality control technique.

The effect of temperature on tree growth is complex and required statistical evaluation of a large number of samples. At 4600 Hz and 30°C, 3.4 kV/mm stress the growth rate was 5 to 8 times higher for PE than for XLPE. Increasing the temperature to 90°C lowered the rate for both insulations by a factor of about 2. In both cases 0.1 N$CuSO_4$ increased the rate obtained with local (Yonkers) tap water. Figure 20 presents the trend as days to penetrate the 0.75 mm insulation by the longest tree. Similar trends were found for average tree lengths. EPR, on the other hand, shows slightly increasing rates with higher temperatures.

Organic chemicals as additives to either PE or XLPE influence tree growth. The comparison of antioxidants, peroxides, and their decomposition products was revealing. The most commonly used crosslinking agent, dicumyl peroxide (dicup), is typically applied at about 2% level in the crosslinkable polymer. In the crosslinking process, decomposition products are generated and amount to the same 2% or slightly less. Their relative ratios vary somewhat according to the reported values (33).

The bulk appear to be cumyl alcohol, with lesser amounts of acetophenone and traces of ∝ methyl styrene. Stochiometric considerations postulate the formation of methane and water. Data presented in Figure 21 shows 0.054% methane, which was detected but not quantitatively measured. This trace amount could be soluble in the polymer matrix without forming voids. Similarily the 0.0062% water is at its solubility level at ambient temperature and does not necessitate void formation. Its presence, however, shows that even in the absence of steam and water in the manufacturing process the insulation still contains catalytic amounts of water. Hydrogen can be found in trace quantities and would originate from the polymer matrix through a free radical attack by the peroxy radical. All these compounds are volatile and are known to disappear from the insulation with time.

The effect of some of these compounds on treeing varies. Small amounts of acetophenone cause improvement. PE and radiation crosslinked PE are comparable

In Durability of Macromolecular Materials; Eby, R.;
ACS Symposium Series; American Chemical Society: Washington, DC, 1979.

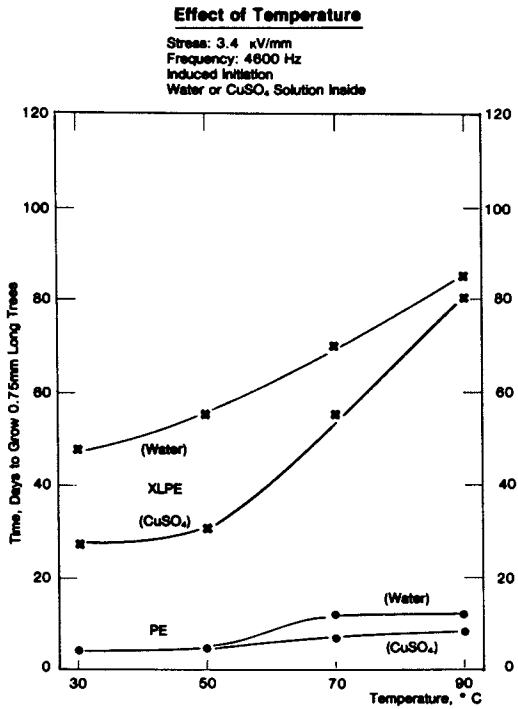

Figure 20. Effect of temperature

In Durability of Macromolecular Materials; Eby, R.;
ACS Symposium Series; American Chemical Society: Washington, DC, 1979.

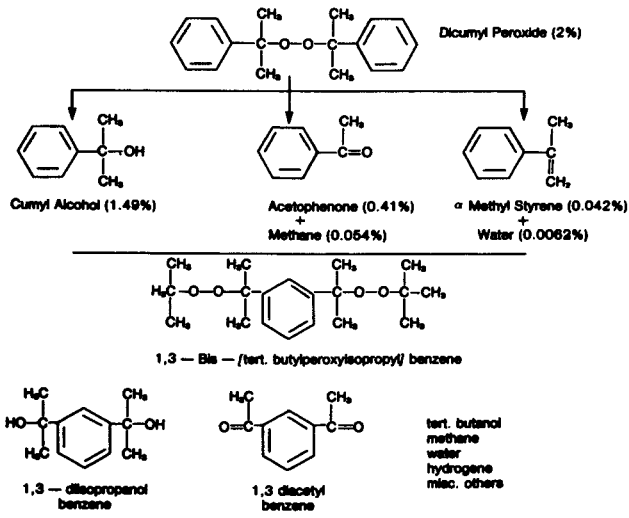

Figure 21. Decomposition of organic peroxides

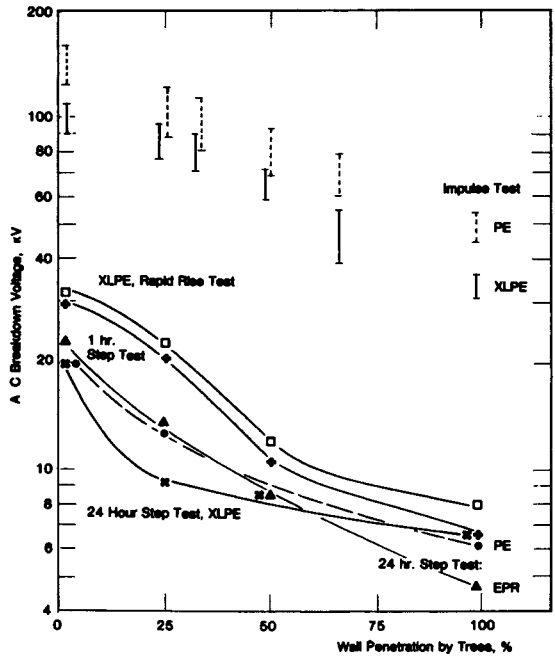

Figure 22. Effect of tree length on AC breakdown voltage

In Durability of Macromolecular Materials; Eby, R.;
ACS Symposium Series; American Chemical Society: Washington, DC, 1979.

to the crosslinkable PE when the latter is extruded below the decomposition temperature for dicup. In other words, dicup in its original form has no beneficial effect on suppressing tree growth as noted by Eichhorn (38).

The use of a different peroxide, Vulcup R, provides results comparable to dicumyl peroxide, a fact which can be interpreted as an indication of beneficial effects from its decomposition products also, in suppressing tree growth.

The effect of the decomposition products could be reason for the increase in tree growth rate in dicup cured coated wires after vacuum drying. In two separate sets of experiments the vacuum dried wire compared favorably with PE but less than favorably with XLPE; more extensive vacuum drying appears to have a more deleterious effect. The decrease in the AC breakdown strength after vacuum drying on slabs machined from the insulation of a 138 kV rated cable has previously been reported (16).

Effect of Treeing on Performance. Electrochemical treeing does not result directly in catastrophic breakdown, but lowers the breakdown strength significantly (34). The effect of tree length on AC, and impulse strength is summarized in Figure 22. Trees were developed at 4600 Hz, 50°C and 3.4 kV/mm stress for various periods, and their lengths measured after the appropriate breakdown test.

In the impulse test (35) a wave shape of 1.2 x 50 μ sec. and negative polarity was applied immediately after the samples were removed from the treeing bath. The first two shots were at 25 kV and subsequent two impulses were applied at 5 kV increments until breakdown. The measured tree lengths were in line with values expected on basis of previous results. Figure 22 shows a gradual decrease with tree lengths for both PE and XLPE from 145 to 60 kV and from 100 to 40 kV respectively.

The AC rapid rise test was performed at 0.5 kV per second stress rate on similarly treated samples, and resulted in a decrease from 32 to 8 kV breakdown voltage for XLPE with tree penetration progressing from 0 to 100% of the insulation (Figure 22). Comparably shaped curves represent the performance of XLPE in

In Durability of Macromolecular Materials; Eby, R.;
ACS Symposium Series; American Chemical Society: Washington, DC, 1979.

tests where stress was applied at 5 kV for one hour and raised by 2.5 kV in one hour intervals until breakdown occurred, and in another experiment where the time periods were 24 hours for each step. In both cases gradual deterioration was found with increased tree length, and generally lower resistance at comparable tree lengths progressing from the rapid rise test to 1 and then to 24 hour step tests. The difference between the three tests diminishes at 100% penetration. PE and EPR in the 24 hour step test exhibit gradual deterioration with tree penetration, generally comparable to that for XLPE.

The fact that a significant percentage of the original breakdown strength is retained after complete penetration through the coated wires indicates that electrochemical trees per se do not cause catastrophic breakdown.

The DC breakdown strength was determined under conditions applied in the rapid rise AC breakdown test, but with direct current. In the absence of trees, both PE and XLPE exhibited DC breakdown strengths in excess of 50 kV, and flashovers at this stress prevented the determination of exact values. About 33% wall penetration lowered this value to 15 kV for XLPE and it remained approximately constant at higher penetration.

Attempts to Increase Life Time

Attempts to increase the useful life of cables and to combat premature failure has resulted in a variety of approaches. They cover improvements in design, processing and in materials and include post extrusion treatments.

Major improvement is expected by the prevention of water ingress during service life. The application of a water impermeable jacket is an obvious possibility, and lead jackets can be used but at a major increase in cost.

Systematic optimization of processing conditions seeks to continuously lower the levels of mechanical stresses, protrusions and contaminants. Attempts at void elimination lead to a variety of steam free processes, using radiant heat, hot gas, molten salt or simply an elongated die to achieve crosslinking. These

In Durability of Macromolecular Materials; Eby, R.;
ACS Symposium Series; American Chemical Society: Washington, DC, 1979.

processes could be combined with dry cooling of the extrudate reducing still further the opportunity of water penetration. Radiation crosslinking with electron beams is under scrutiny. Though major reduction in water content and in the number of voids was demonstrated in these dry cure processes, cables still may contain voids (Figure 23) and water trees can still initiate at the remaining voids (36).

Material improvement is concentrated on the development of additives which minimize tree growth. Recently, two major suppliers introduced "stabilized" PE insulating compounds, and the appearance of comparable crosslinkable compounds is expected. Work is also in progress to improve cable quality by removing contaminated pellets from a moving stream prior to their entrance into the extruder (37).

Improvement due to heat treatment was reported (6). An interesting possibility to improve extrudate quality is the impregnation of the insulation, and work in this area, impregnation with hydrocarbons was reported (16).

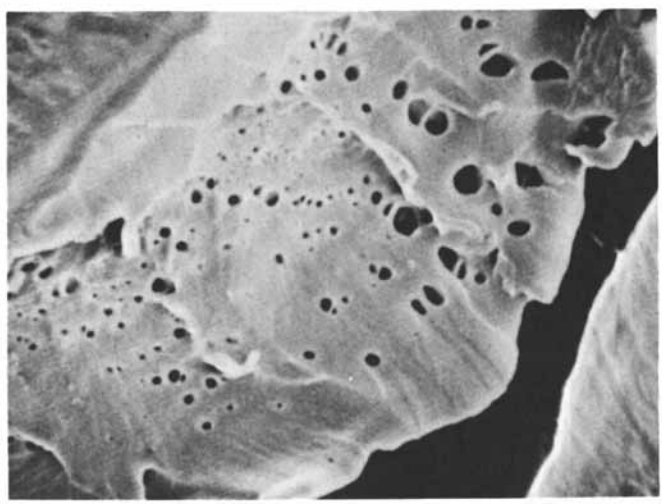

Figure 23. Voids in dry cured XLPE (1–5 μm)

In Durability of Macromolecular Materials; Eby, R.;
ACS Symposium Series; American Chemical Society: Washington, DC, 1979.

Literature Cited

1. Thue, W.A., Insulated Conductors Committee Open Forum-Richmond, Virginia (1977).

2. Kelen, A., IEEE Trans. on Electrical Insulation (1977). EI-12 (1).

3. McKean, A.L., IEEE Trans. (1976) PAS-95(1.)

4. Vahlstrom, W., IEEE Conference on Underground Distribution, Detroit, Michigan (1971). C 42 PWR.

5. Lanctoe, T.P., Lawson, J.H., McVey, W.L., IEEE PES Summer Meeting, Los Angeles, CA (1978) A 78 509-2.

6. Nitta, Y., Fukagawa, H., Takashima, H. (1975) Central Research Institute of Electric Power Industry, Tokyo, Japan, D-9.

7. Bahder, G., Katz, C., Lawson, J., Vahlstrom, W., IEEE Trans. (1974) PAS-93.

8. Katz, C., Srinivas, N., Bernstein, B.S., Conference on Electrical Insulation and Dielectric Phenomena (1975) Annual Report.

9. Association of Edison Illuminating Companies, (1975) AEIC No. 5-75.

10. Bahder, G., Dakin, T.W., Lawson, J.H., (1974) CIGRE Paper 15-05.

11. Bateman, H., "Partial Differential Equations of Mathematical Physics", P. 436, Dover Publications New York (1944).

12. Whelan, J.M., "Conference Record of 1976 IEEE International Symposium on Electrical Insulation" Montreal, p. 218.

13. Aschcraft, A.C., Eichhorn, R.M., Shaw, R.G., ibid p. 213.

14. Eichhorn, R.M., IEEE Trans. (1977) E 1-12 (1).

In Durability of Macromolecular Materials; Eby, R.;
ACS Symposium Series; American Chemical Society: Washington, DC, 1979.

15. Bahder, G., Katz, C., Eager Jr., G.S. Silver, D.A. IEEE Trans. (1977) PAS 96-6.

16. Mangaraj, D., Kiss, K.D., Malawer, E., Doepken, Jr., H.C., ACS Annual Meeting, Anaheim, CA. (1978) Organic Coatings and Plastics Chemistry Division Reprints, 38.

17. Mucigrosso, J., Phillips, P.J., IEEE Trans. (1978) EI-13-3.

18. Augood, D.R., IEEE PES Summer Meeting, Portland, Oregon (1976) A 76 360-8.

19. Soma, K., Hitachi Review (1976) 25.

20. Patsch, R., Wagner, H., Heumann, H., (1976) CIGRE Paper No. 15-11.

21. Mizukami, T., Takashaki, C., Ikeda, N., Kato, B., IEEE Transactions on Power Systems (1976) 95.

22. Bernstein, B.S., (1974) Society of Plastics Engineers Regional Technical Conference, Boston, Mass.

23. Gilroy, H.M., Macromolecular Symposium on Chemical and Physical Lifetime Limits of Macromolecular Materials, Miami Beach, Florida (1978) 30.

24. Matsubara, H., Miyauchi, H., Sumitomo Electric Technical Review (1970) 47.

25. Winslow, F.H., Macromolecular Symposium on Chemical and Physical Lifetime Limits of Macromolecular Materials, Miami Beach, Florida (1978) 2.

26. Johnston, D.R., La Forte, J.T., Podhorez, P.E., IEEE Trans. (1978) CHI 287.

27. Tanaka, T., Fukuda, T., Suzuki, S., IEEE PES Winter Meeting, New York, (1976) F 76 178-4.

28. Augood, D.R., IEEE Trans. (1978) CH 1287.

29. Phelps Dodge Cable and Wire Company, "Electro-

In Durability of Macromolecular Materials; Eby, R.;
ACS Symposium Series; American Chemical Society: Washington, DC, 1979.

chemical Treeing in Cable", Electric Power Research Institute Report EL-647. (1978).

30. Vahlstrom, W., IEEE Conference on Underground Distribution, Detroit, Michigan (1971) C 42 PWR.

31. Matsubara, H., Yamanouchi, S., CEIDP Annual Report (1974).

32. Timpe, N.B., Heyer, D.V. LEEE Trans. (1977) EI-12.

33. Wagner, H., Wartusch, J., IEEE Trans. (1977) EI-12 6.

34. Bernstein, B.S., Srinivas, N., Lee, P.N., (1975) CEIDP Annual Report.

35. Srinivas, N., Doepken, Jr., H.C., (1978) Conference Record of IEEE International Symposium on Electrical Insulation.

36. Kawasaki, Y., Otani, K., Miyauchi, H., "Radiant Curing Process for Manufacturing HV and EHV XLPE Cables" Wire Association, Guilford, Connecticut, p. 5.

37. Reynolds Metal Company, Food Technology Corporation. Electric Power Research Institute Project RP-7865.

38. Eichhorn, R.M., IEEE Underground T. and D. Conference, Pittsburgh, PA. (1972).

RECEIVED January 5, 1979.

31

Concluding Remarks

F. E. BAILEY, JR.

Union Carbide Corporation, Chemicals and Plastics, South Charleston, WV 25303

First, I want to thank those who participated in and those who helped to organize this very fine symposium. When I first became involved in the organization of the Macromolecular Secretariat in 1975, I suggested to Otto Vogl, then Secretary General, that a very suitable topic for a symposium would involve materials science aspects of macromolecular systems for the highly interdisciplinary character of the symposia sponsored by the Secretariat. Such a topic would touch not only on the most fundamental structure-property relationships, but also use of such relationships in real systems.

Professor Vogl saw such a symposium topic as a means of involving research beyond the usual perimeters of an American Chemical Society meeting even of national scope and discussed the question further at our National Bureau of Standards, particularly with Dr. R. K. Eby. Dr. Eby graciously accepted the task of organizing the general program for this symposium, obtaining the participation of five Divisions of the American Chemical Society, each of which accepted responsibility for one of the sessions: the Polymer Chemistry Division, Rubber Division, Organic Coatings and Plastics Chemistry Division, the Colloid and Surface Chemistry Division and the Cellulose, Paper and Textile Division. We have also been joined in the Symposium by the High Polymer Physics Division of the American Physical Society and the Division of Engineering Structures and Properties of the Society of Plastics Engineers as well as two exceptional keynote speakers: Dr. John D. Hoffman of the National Bureau of Standards and Dr. Field Winslow of Bell Telephone Laboratories.

As plastics materials are ever more widely used, the necessity of knowing the use-life relationships has grown in importance. Most commonly, these relationships are thought of in terms of service for long periods of time. Rapid expansion of use and need for use has required the development of means of predictative testing of materials durability. I recall the impatience of one of our Marketing personnel some years ago when a house we had painted had withstood five years of New Jersey weather and he was developing sales literature to emphasize the

0-8412-0485-3/79/47-095-467$05.00/0

In Durability of Macromolecular Materials; Eby, R.;
ACS Symposium Series; American Chemical Society: Washington, DC, 1979.

the endurance of this particular vinyl coating: "Do I have to wait another 20 years to write this brochure?"

The work discussed here has related not only to structure relationships but also to means of protection of the macromolecular material and the protective functions of these materials. There are many modes of failure, by chemical reaction, failure by fracture, environmental stress cracking and creep. Further there are complicating interactions arising from chemical reaction during relaxation of polymer networks, and in multiphase polymer systems and composites, failure at interfaces by adhesive failure or stress-stress dilation.

Modes of accelerated testing have led to the development of expression lifetime limits in terms of failure envelopes within which confidence levels of use can be given. In addition to modes of testing quite long in use such as testing of wear, abrasion and exposure, data can now be expressed in terms of molecular relaxation processes and kinetics of failure and time dependence of strength, i.e., fatigue testing. Means have been developed to measure very low reaction rates of the order of 10^{-12} mol/year as well as the subtle effects of changes in molecular weight distribution and "stress memory" especially in reinforced polymer systems.

Interest in predicative testing extends not only to long periods of service but to relatively short time periods as well when biodegradability is concerned or in biocompatible systems in medical use whether it be in adhesion of bone or prosthesis or packaging is concerned, and in food additives when for example a species may be of consequence when present in the polymer and potentially extracted or present as a delicate flavor or color and absorbed by the macromolecular system.

In summary, this has been a most worthwhile symposium from both the topical and interdisciplinary views. I want to again thank the organizers, the participants and especially our sister Societies in making this Symposium a success.

RECEIVED December 8, 1978.

INDEX

In Durability of Macromolecular Materials; Eby, R.;
ACS Symposium Series; American Chemical Society: Washington, DC, 1979.

D

In Durability of Macromolecular Materials; Eby, R.;
ACS Symposium Series; American Chemical Society: Washington, DC, 1979.

In Durability of Macromolecular Materials; Eby, R.;
ACS Symposium Series; American Chemical Society: Washington, DC, 1979.

O

P

In Durability of Macromolecular Materials; Eby, R.;
ACS Symposium Series; American Chemical Society: Washington, DC, 1979.

R

S

T

U

V

W

X

Z

In Durability of Macromolecular Materials; Eby, R.;
ACS Symposium Series; American Chemical Society: Washington, DC, 1979.